LEABHARLANN CHOLÁISTE NA TRÍONÓIDE, BAILE ÁTHA CLIATH | TRINITY COLLEGE LIBRARY DUBLIN
Ollscoil Átha Cliath | The University of Dublin

Terms and Conditions of Use of Digitised Theses from Trinity College Library Dublin

Copyright statement

All material supplied by Trinity College Library is protected by copyright (under the Copyright and Related Rights Act, 2000 as amended) and other relevant Intellectual Property Rights. By accessing and using a Digitised Thesis from Trinity College Library you acknowledge that all Intellectual Property Rights in any Works supplied are the sole and exclusive property of the copyright and/or other IPR holder. Specific copyright holders may not be explicitly identified. Use of materials from other sources within a thesis should not be construed as a claim over them.

A non-exclusive, non-transferable licence is hereby granted to those using or reproducing, in whole or in part, the material for valid purposes, providing the copyright owners are acknowledged using the normal conventions. Where specific permission to use material is required, this is identified and such permission must be sought from the copyright holder or agency cited.

Liability statement

By using a Digitised Thesis, I accept that Trinity College Dublin bears no legal responsibility for the accuracy, legality or comprehensiveness of materials contained within the thesis, and that Trinity College Dublin accepts no liability for indirect, consequential, or incidental, damages or losses arising from use of the thesis for whatever reason. Information located in a thesis may be subject to specific use constraints, details of which may not be explicitly described. It is the responsibility of potential and actual users to be aware of such constraints and to abide by them. By making use of material from a digitised thesis, you accept these copyright and disclaimer provisions. Where it is brought to the attention of Trinity College Library that there may be a breach of copyright or other restraint, it is the policy to withdraw or take down access to a thesis while the issue is being resolved.

Access Agreement

By using a Digitised Thesis from Trinity College Library you are bound by the following Terms & Conditions. Please read them carefully.

I have read and I understand the following statement: All material supplied via a Digitised Thesis from Trinity College Library is protected by copyright and other intellectual property rights, and duplication or sale of all or part of any of a thesis is not permitted, except that material may be duplicated by you for your research use or for educational purposes in electronic or print form providing the copyright owners are acknowledged using the normal conventions. You must obtain permission for any other use. Electronic or print copies may not be offered, whether for sale or otherwise to anyone. This copy has been supplied on the understanding that it is copyright material and that no quotation from the thesis may be published without proper acknowledgement.

Bound By:
THE
THESIS CENTRE
65 Camden St. Lwr.,
Dublin 2. Ph: 475 3616
www.thesiscentre.com

TRINITY COLLEGE DUBLIN
09 MAR 2016
ACADEMIC REGISTRY

PhD
Natural Science

Ammonoid Biostratigraphy of the Shannon Basin, western Ireland

A thesis submitted for the degree of Doctor of Philosophy

2016

Anthea R. Lacchia

Declaration of authorship:

I declare that this thesis has not been submitted as an exercise for a degree at this or any other university and it is entirely my own work.

I agree to deposit this thesis in the University's open access institutional repository or allow the Library to do so on my behalf, subject to Irish Copyright Legislation and Trinity College Library conditions of use and acknowledgement.

Anthea Lacchia

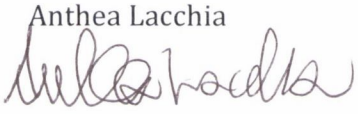

TRINITY LIBRARY
27 JUL 2016
DUBLIN

Thesis 11042

Broken Shell

By Anne Morrow Lindbergh

After "The Unicorn and other poems 1935-1955", Pantheon Books.

Cease searching for the perfect shell, the whole

Inviolate form no tooth of time has cracked;

The alabaster armor still intact

From sand's erosion and the breaker's roll.

What can we salvage from ocean's strife

More lovely than these skeletons that lie

Like scattered flowers open to the sky,

Yet not despoiled by their consent to life?

The pattern on creation morning laid,

By softened lip and hollow, unbetrayed;

The gutted frame endures, a testament,

Even in fragment, to that first intent.

Look at this spiral, stripped to polished nerve

Of growth. Erect as compass in its curve,

It swings forever to the absolute,

Crying out beauty like a silver flute.

Table of Contents

Declaration of authorship	i
Summary	vii
Abstract	ix
Acknowledgements	x
List of abbreviations	xiii
List of figures	xv
List of tables	xxxi
Chapter 1 Introduction	1
1.1 Introduction to the project	1
1.2 Ammonoids	1
1.2.1 Shell structure	2
1.2.2 Ontogeny	5
1.2.3 Mode of life	6
1.3 The Carboniferous	10
1.3.1 Global and regional context	10
1.3.2 The Shannon Basin	11
1.3.3 Carboniferous ammonoid biostratigraphy	22
1.3.4 Previous correlation schemes	27
1.4 Project aims	33
1.5 Material and methods	35
1.6 Thesis plan	37
Chapter 2 Ammonoid Localities	38
2.1 Sampled fossiliferous localities	38
2.2 Locality Details	40
2.2.1 Clare Shale Formation	40
2.2.1.1 Fisherstreet Bay	40
2.2.1.2 Aille River	47
2.2.1.3 Inishcorker	49
2.2.1.4 Foynes Island	54
2.2.1.5 Foynes Harbour	57
2.2.1.6 Roadford	60
2.2.1.7 Spectacle Bridge	62
2.2.1.8 Slieve Elva	62
2.2.1.9 Gowlaun River	64
2.2.2 Ross Sansdstone Formation	66

	2.2.2.1 Ballybunion Waterfall Band	66
	2.2.2.2 Canal Band (Reading Room)	70
	2.2.2.3 Castle Band	73
	2.2.2.4 Ballybunion "*Ph. circumplicatile*" band	75
	2.2.2.5 Ballybunion "*Ph. paucicrenulatum* band"	79
	2.2.2.6 Reading Room band	83
	2.2.2.7 Dunmore west band	87
	2.2.2.8 Rehy Hill band	91
	2.2.2.9 Senan's Beach band	94
	2.2.2.10 West Senan's Beach band	97
	2.2.2.11 Lighthouse band	101
	2.2.2.12 Toorkeal band	104
	2.2.2.13 Rinevella	107
	2.2.2.14 Holy Well band	110
	2.2.2.15 Cloonoconeen Lower	113
	2.2.2.16 Blackrock west band	116
	2.2.2.17 Blackrock	119
	2.2.2.18 Ross Bay east	121
	2.2.2.19 Cloonconeen Top	124
	2.2.2.20 Kilcredaun Top band	127
	2.2.2.21 Quilty Band	131
	2.2.2.22 Cloghaunsavaun band	135
	2.2.2.23 Ross Slump	138
	2.2.2.24 Ross Bay west	140
	2.2.2.25 Bridges of Ross band	143
	2.2.2.26 Cross band	148
2.2.3 Other Irish localities		152
	2.2.3.1 Leinster Coalfiled: Killeshin Glen and Luggacurren	152
Chapter 3 Palaeontology		153
3.1 Typical Faunal Assemblages		153
3.2 Ammonoids		155
3.2.1 Preservation		155
3.2.2 Pseudo-ammonoids		156
3.2.3 Ammonoid taxonomy		158

	3.2.4. Issues in the taxonomy of crushed material		160
	3.2.5 Tackling taxonomical Issues		162
3.3 Systematic palaeontology			164
	3.3.1 Thick-shelled ammonoids		164
	3.3.2 Discussion		217
	3.3.3 Thin-shelled ammonoids		222
		3.3.3.1 Notes on systematics	222
		3.3.3.2 Occurrence	223
3.4 Bivalves			224
	3.4.1 Notes on systematics		224
	3.4.2 Occurrence		225
3.5 Palaeoecology			228
	3.5.1 Ammonoid basinal communities		228
	3.5.2 Thin-shelled ammonoids		229
	3.5.3 Bivalves		229
	3.5.4 Benthic fauna (crinoids, corals and trilobites)		230
Chapter 4 Ammonoid Distribution and Salinity Implications			232
4.1 Introduction			232
4.2 Highstand-lowstand model			233
4.3 Ammonoid distribution in the Shannon Basin			236
4.4 Discussion			245
4.5 Conclusions			250
Chapter 5 Biostratigraphy			251
5.1 Introduction			251
5.2 Ammonoid biostratigraphy in context			252
5.3 Lithostratigraphic correlations			254
		5.3.1 Results of current study	254
		5.3.2 Discussion	259
5.4 Ammonoid biostratigraphy			261
		5.4.1 Material	261
		5.4.2 Rationale and methods	261
		5.4.3 Results	263
		5.4.4 Summary of results	274
		5.4.5 Discussion	275
5.5 Palynology			278

5.5.1 Methods 278
5.5.2 Results 278
5.5.3 Discussion 279
5.6 Biostratigraphy: summary and discussion 280
5.7 Analytical techniques 283
5.7.1 QEMSCAN analysis 283
5.7.1.1 Further work 298
5.7.2 XRD analysis 299
5.7.3 Further work: trace element analysis 302
Chapter 6 Conclusions and Further Work 303
6.1 Taxonomy of crushed ammonoids 303
6.1.1 Main findings 303
6.1.2 Further work 304
6.2 Palaeosalinity in the Shannon Basin 306
6.2.1 Main findings 306
6.2.2 Further work 308
6.3 Biostratigraphy 309
6.3.1 Main findings 309
6.3.2 Further work 311
Reference List 313
Appendix A (Tables) 336
Appendix B (Borehole graphic logs) 352
Appendix C (Palynology Data) 369
Appendix D (XRD results) 371

Summary

This thesis deals with ammonoids from the Carboniferous Shannon Basin, western Ireland, with a focus on the ammonoid biostratigraphy of the Ross Sandstone Formation, a classic turbidite succession. Within the Ross Sandstone Formation, ammonoids are concentrated in laterally extensive black shale bands, which are taken to represent intervals of sediment starvation and are often referred to as "condensed sections" or "ammonoid bands". Early biostratigraphic work in the basin, done in the 1950s and 1960s, recognized the presence of four ammonoid bands within the Ross Sandstone Formation.

During the course of this study and in conjunction with research at University College Dublin, ten ammonoid-rich horizons (including eight condensed sections) have been identified within the Ross Sandstone. In addition to coastal exposures, a set of 12 behind-outcrop wells, which were drilled by a consortium consisting of Statoil and University College Dublin, were examined and sampled for biostratigraphy. Several seasons of fieldwork were undertaken to this end. More than 3,000 fossil specimens from the Clare Shale Formation and Ross Sandstone Formation were investigated and specimens from various European museum collections were also examined in order to strengthen identifications. Given current lack of published information on the taxonomy of crushed ammonoid material, new systematic data on 14 Serpukhovian-Bashkirian ammonoids for which ontogenetic information was previously incomplete or lacking are presented here (Chapter 2). This information not only furthers knowledge of the ontogeny of these ammonoids in general, but leads to more confident identifications of ammonoids preserved as flattened external moulds.

Faunal assemblages from the five main highly-condensed sections in the Ross Sandstone Formation are described in detail in this study (Chapter 5), which is also the first to present details of abundance and proportion of ammonoid taxa (beyond recording the presence of a given ammonoid band) at localities within the Ross Sandstone Formation. These new biostratigraphic data, coupled with

lithostratigraphical correlations, provide the most detailed dataset for the Ross Sandstone Formation to date, also allowing biostratigraphy to be cross-checked against lithostratigraphical correlations.
Statistical analysis of the faunal assemblages was not always found to confirm that bands which are known to correlate by physical means are indeed indistinguishable.
While some assemblages in condensed sections proved to be globally distinctive (namely those indicative of the "*Hud. proteus-Ho.smithii* band" and the "*Ht. prereticulatus* band"), most were not, and some were only locally distinctive (that of the "*Ph. paucicrenulatum* band"); therefore most bands in the Ross Sandstone Formation cannot be confidently linked to a given ammonoid band in the Western European framework. This puts the validity of ammonoid-bearing condensed sections both in intrabasinal and extrabasinal correlation into question.

In addition to these results, despite marine fossils being commonly reported as confined to thin ammonoid-rich layers ("marine bands") bounded by barren strata, several new ammonoid-bearing horizons have been found in between the "marine bands" in the Shannon Basin (Chapter 4). The presence of ammonoids at various intervals outside the condensed sections was not recognized before and is taken as good evidence for normal marine salinity throughout deposition of the Ross Sandstone and Clare Shale Formations. The presence of normal marine faunas outside the traditional "marine bands" suggests that salinity values of the Shannon Basin and, by implication, other deep-water basins may well have been normal between periods of sediment starvation.

Abstract
Title: Ammonoid Biostratigraphy of the Shannon Basin, western Ireland
Author: Anthea Rosa Lacchia

This study concerns ammonoid faunas from a classic turbidite succession, the Ross Sandstone Formation (Serpukhovian-Bashkirian) of the Shannon Basin, western Ireland. In addition to coastal exposures, a set of 12 behind-outcrop wells were examined and sampled for biostratigraphy. More than 3,000 fossil specimens from the Clare Shale Formation and Ross Sandstone Formation were investigated. Given current lack of published information on the taxonomy of crushed ammonoid material, new systematic data on 14 Serpukhovian-Bashkirian ammonoids for which ontogenetic information was previously incomplete or lacking are presented. This information furthers knowledge of ammonoid ontogeny and also leads to more confident identification of ammonoids preserved as flattened external moulds. Marine fossils were commonly reported as confined to thin ammonoid-rich layers ("marine bands") bounded by barren strata, leading to a suggestion, based on examples from the Pennines, that fossil occurrence may be controlled by variations in salinity. While ammonoids are indeed concentrated in laterally extensive black shale bands, taken to represent intervals of sediment starvation, several new ammonoid-bearing horizons have been found in between the "marine bands" in the Shannon Basin, which are therefore better referred to as "condensed sections" or "ammonoid bands". The presence of ammonoids at various intervals outside the condensed sections is good evidence for normal marine salinity in the Ross Sandstone and associated Clare Shale Formation. The presence of normal marine faunas outside the traditional "marine bands" suggests that salinity values of the Shannon Basin and, by implication, other deep-water basins may well have been normal between periods of sediment starvation. Early biostratigraphic work in the basin recognized the presence of four ammonoid bands within the Ross Sandstone Formation. During the course of this study and in conjunction with research at University College Dublin, ten ammonoid-rich horizons (including eight condensed sections) have been identified within the Ross Sandstone. Faunal assemblages from the five main highly-condensed sections in the Ross Sandstone Formation are described in detail in this study, which is also the first to present details of abundance and proportion of ammonoid taxa at localities within the Ross Sandstone Formation. These new biostratigraphic data, coupled with the lithostratigraphical correlations, provide the most detailed dataset for the Ross Sandstone Formation to date, also allowing biostratigraphy to be cross-checked against lithostratigraphical correlations. Overall, biostratigraphy was not as high-resolution as one might have hoped, in the sense that statistical analysis of the faunal assemblages does not always confirm that bands which are known to correlate by physical means are indeed indistinguishable. While some assemblages in condensed sections proved to be globally distinctive, most were not, and some were only locally distinctive; therefore most bands in the Ross Sandstone Formation cannot be confidently linked to a given ammonoid band in the Western European framework. This puts the validity of ammonoid-bearing condensed sections both in intrabasinal and extrabasinal correlation into question.

Acknowledgements

The list of people that have helped me in different ways over the past four years is a long one. First of all, I would like to thank my parents. Without their support, none of this would have been possible and I'd like to dedicate this thesis to them. I know that, deep down, they enjoyed hopping over electric fences and running away from bulls while accompanying me on fieldwork!

I would like to sincerely thank my supervisors at Trinity, Dr John Graham, Prof George Sevastopulo and Dr Patrick Wyse Jackson for their constant support, guidance, discussion and words of encouragement along the way. I feel very lucky to have had the opportunity to learn from each of you. Thank you also for supporting me through difficult situations that stretched beyond the academic realm.

I would also like to express my gratitude to Prof Peter Haughton at UCD and Dr Ole Martinsen at Statoil, who both advised me during the course of this project and generously shared their time and ideas.

This project was entirely funded by Statoil and I would like to gratefully acknowledge their support.

Thank you to Gillian Lewarne who helped me get started in the world of ammonoids. Her enthusiasm for the project was unfailing and my work was very much a continuation of what she started.

Thank you to Colm Pierce and Arnau Obradors Latre, for their help and advice throughout the project, as well as for being great fieldwork companions. Their help with fossil hunting in some of the less accessible sections is greatly appreciated.

I am also grateful to Maura and Sean Keating, who helped make fieldwork on Loop Head a memorable and enjoyable experience. I would also like to thank

John Shaughnessy for generously offering to assist me with fieldwork in the Leinster Coalfield.

From the Statoil team, I would like to thank Dr Simon Barker, Kristin Walderhaug Porten, Dr Kristina Bakke, Frode Hadler-Jacobsen for their advice and help with the project. I am also grateful to Lisbet Søyset, Ørjan Bjorøy, Rannveig Litlabø and Jan Inge for their help and assistance with core sampling, palynology and QEMSCAN analysis.

I am grateful to Dr Mike Reich (formerly at University of Göttingen Museum), Dr Matthew Parkes (National Museum of Ireland), Eliza Howlett (Oxford University Natural History Museum), Dr Svetlana Nikolaeva and Zoe Forde (Natural History Museum, London), Paul Shepherd (British Geological Survey) for helping me access ammonoid collections. A special thanks to Svetlana Nikolaeva for all her support and words of advice.

Thank you to Sarah Gatley at the GSI for her help with geological maps towards the very end of my corrections.

My sincere thanks go to Dr Dieter Korn for advising me during the course of the project and during my visit to the Berlin Natural History Museum. Thank you also to Dr Nick Riley and Dr Colin Waters at the British Geological Survey for their help with ammonoid identification and Carboniferous-related questions.

Thank you to Peter Fallon and Dr John Murray (National University of Ireland Galway) for their assistance in the field, advice throughout the project and for loaning me ammonoid material.

I would also like to thank Prof Celia Holland for generously helping me with statistics at the very end of my project (one week from submitting my thesis!). Your help was greatly appreciated.

Sincere thanks go to Dr Robbie Goodhue (TCD) for his help with XRD. Thank you also to Mags, Maura, Noel, Neil and Frank, who were always available to help and give words of encouragement when needed.

A huge thank you to Frank for his generosity in times of need, for introducing me to mindfulness meditation and for fuelling my appreciation for Tom Petty. *Yeah runnin' down a dream...*

Thank you to all the postgrads. I will miss the card games in the coffee room! Special thanks to Vincent, Mike, Ann-Kristin, Sam and Meabh for enduring an invasion of ammonoids in our office! Vincent, Teresa and Ann-Kristin: your support and encouragement meant a lot.

Finally, I would like to thank my family as a whole and especially my aunt Celine, for being there and supporting me over the past four years (and more). Gavin, thank you for making the load much lighter to bear. And a special thanks to Pedro too (*fiesta ole'*).

A sincere thank you to my external and internal examiners, Dr John Murray and Dr Robbie Goodhue, for their very helpful comments that have greatly improved this work.

List of Abbreviations

Ammonoid abbreviations:

A. = *Anthracoceras*

Basch. = *Baschkirites*

C. = *Cravenoceras*

Ct. = *Cravenoceratoides*

D. = *Dimorphoceras*

E. or *Eu.* = *Eumorphoceras*

Ho. = *Homoceras*

Hod. or *Hd.* = *Hodsonites*

Ht. = *Homoceratoides*

Hud. = *Hudsonoceras*

Iso. or *Isoh.* = *Isohomoceras*

N. = *Nuculoceras*

Ph. = *Phillipsoceras*

R. = *Reticuloceras*

V. = *Vallites*

Other abbreviations related to ammonoids/palaeontology:

sp. = species

spp. = more than one species of a given genus

cf. = confer

aff. = affinis

pc. = paucicrenulatum

cp. = circumplicatile

wh = whorl height

ww = whorl width

uw = umbilical width

Borehole names:

09-CE-UCD-01

09-CE-UCD-02

10-CE-UCD-03

10-CE-UCD-04

10-CE-UCD-05

11-CE-UCD-06

11-CE-UCD-07

11-CE-UCD-08

12-KY-UCD-09

GSI 09/05 = Geological Survey of Ireland borehole drilled at Ballybunion, Co. Kerry

GSI 09/04= Geological Survey of Ireland borehole drilled at Kildysart, Co. Clare

Other:

Fm. = Formation

Irish Grid References are given as [xxxxx/xxxxx].

List of Figures

Chapter 1 Introduction

Fig. 1.1. Basic conch parameters for Palaeozoic ammonoids (after Korn 2010).

Fig. 1.2. Generalized terminology of the suture line (modified after Korn 2010).

Fig. 1.3. Rib shape, spacing and course (after Arkell 1957; Klug et al. 2015).

Fig. 1.4. Ammonoid developmental stages and associated changes in shape and suture, showing increasing complexity in suture line during an individual's lifetime (after Bisat 1924).

Fig. 1.5. Phylogenetic change in orientation of the conchs and swimming velocity of Bactritida and primitive Ammonoidea. Outlines of the conchs of one bactritid and nine ammonoids from the Early and Middle Devonian with body chamber lengths (BCL), orientation of the aperture (OA), and relative swimming speed. Centre of gravity is indicated by a cross and the centre of buoyancy by a circle (Klug & Korn 2004).

Fig. 1.6. Westermann morphospace. Three components of shell shape (exposure of the umbilicus, overall inflation, and whorl expansion) dictate data placement within this ternary diagram (Ritterbush & Bottjer 2012).

Fig. 1.7. Pennsylvanian paleogeography (based on Ron Blakey, University of Arizona - http://jan.ucc.nau.edu/~rcb7/mollglobe.html, reproduced with permission). Note glaciation in the southern hemisphere. Location of the Shannon Basin is shown by the black dot.

Fig. 1.8. Map showing location of the Shannon Basin and schematic stratigraphy through the basin axis (modified after GSI Datasets Public Viewer: http://spatial.dcenr.gov.ie/imf/imf.jsp?site=GSI_Simple).

Fig. 1.9. View of the Ross Sandstone Formation on the north coast of Loop Head looking NE from Toorkeal. Recessed interval corresponds to a condensed section.

Fig. 1.10. Photo of sand volcano on top of Ross Slump, Bridges of Ross, Co. Clare. Hammer is 35 cm long.

Fig. 1.11. *Phillipsoceras circumplicatile* (Foord, 1903) preserved as a 2D mould (bottom centre of photo), Dunmore West band, (see Ch. 3 for locality details). Coin diameter is 23.25 mm.

Fig. 1.12. Typical highly-condensed section, "*Ph. circumplicatile* band", Quilty, [77281/51701].

Fig. 1.13. Lesser condensed section (RVM) at Rinevella, [81840/49106] (see Ch. 2 for locality details) (a) frontal view, (b) view looking west.

Fig. 1.14. Simplified stratigraphic column through the Ross Sandstone Formation, showing the three main previously-recognized ammonoid bands.

Fig . 1.15. Summary of ammonoid zones and subzones of the Serpukhovian-Bashkirian (therefore pertinent to the Shannon Basin) with diagnostic ammonoids and conodonts (after Fallon & Murray 2015).

Fig. 1.16. Ammonoid-based correlation of the Serpukhovian and Bashkirian (after Nikolaeva & Kullmann 1998).

Fig. 1.17. Ammonoid zones and subzones in the Serpukhovian and Bashkirian with diagnostic ammonoids, indices and associated ammonoids (after Riley *et al.* 1995; Waters & Condon 2012). For a list of abbreviations, see p. xvi.

Fig. 1.18. Stratigraphy of the Shannon Basin from North Clare, through the Shannon Estuary to North Cork (after Martinsen & Collinson 2002; Collinson *et al.* 1991).

Fig. 1. 19. Summary and comparison of lithostratigraphy and biostratigraphy of the outcrops of northern county Clare ad along the Shannon Estuary, showing ammonoid bands in the Ross Sandstone Formation (after Wignall & Best 2000; p. 62).

Chapter 2 Ammonoid Localities

Fig. 2.1. Location map showing Fisherstreet Bay sampling locality [06640/96316] and geological map of the Shannon Basin showing the locality and regional geology (Google Earth map).

Fig. 2.2. Fisherstreet Bay sampling site, looking towards the Fisherstreet Slide [06640/96316]. Hammer for scale.

Fig. 2.3. Sedimentary log legend (valid for all sedimentary logs in this chapter).

Fig. 2.4. Sedimentary log of Fisherstreet Bay section showing location of samples.

Fig. 2.5. Aille River exposure [13619/97982]. Hammer for scale.

Fig. 2.6. Location map showing Aille River sampling locations at Twin Wells near Lisdoonvarna and further east at [13791/97993] and geological map of the Shannon Basin showing the locality and regional geology (Google Earth map).

Fig. 2.7. Location map showing Inishcorker sampling area of south coast and geological map of the Shannon Basin showing the locality and regional geology (Google Earth map).

Fig. 2.8. Sedimentary log of Inishcorker section ("*Nu. nuculum* band" to "*Ho. beyrichianum* band" showing location of samples.

Fig. 2.9. Bullion, Foynes Island, south coast [25099/52196].

Fig. 2.10. Roadside exposure at Foynes Harbour, showing contact between shale and silststone deposits and mass transport deposits [24686/51862].

Fig. 2.11. Location map showing Foynes Island and Foynes Harbour sampling areas and geological map of the Shannon Basin showing the locality and regional geology (Google Earth map).

Fig. 2.12. Location map showing Slieve Elva sampling areas and geological map of the Shannon Basin showing the locality and regional geology (Google Earth map).

Fig. 2.13. Location map showing Gowlaun River sampling site at /13678/98119] and geological map of the Shannon Basin showing the locality and regional geology (Google Earth map).

Fig. 2.14. Ballybunion Waterfall band (thickness in between dashed yellow lines) [86837/44563].

Fig. 2.15. Location map showing Ballybunion Waterfall band sampling locality [86837/44563] and geological map of the Shannon Basin showing the locality and regional geology (Google Earth map).

Fig. 2.16. Sedimentary log of "Waterfall Band" showing location of samples.

Fig. 2.17. Canal Band, Ballybunion [86644/44765].

Fig. 2.18. Location map showing Ballybunion Canal band sampling locality at [86644/44765] and geological map of the Shannon Basin showing the locality and regional geology (Google Earth map).

Fig. 2.19. Sedimentary log of "Canal Band" showing location of samples.

Fig. 2.20. Location map showing Ballybunion Castle band sampling locality at [86189/45046], and geological map of the Shannon Basin showing the locality and regional geology (Google Earth map).

Fig. 2.21. Location map showing Ballybunion *Ph. circumplicatile* band sampling locality at [86354/45441], and geological map of the Shannon Basin showing the locality and regional geology (Google Earth map).

Fig. 2.22. Décollement horizon in Ballybunion *Ph. circumplicatile*" condensed section [86354/45441].

Fig. 2.23. Sedimentary log of "Ballybunion *Ph. circumplicatile*" band showing location of sampled horizons.

Fig. 2.24. Location map showing Ballybunion *Ph. paucicrenulatum* band sampling locality at [86574/45666] and geological map of the Shannon Basin showing the locality and regional geology (Google Earth map).

Fig. 2.25. Sedimentary log through "Ballybunion *Ph. paucicrenulatum*" band showing sample location.

Fig. 2.26. Ballybunion *Ph. paucicrenulatum* band [86574/45666]. Hammer for scale.

Fig. 2.27. Location map showing Reading Room sampling locality at [73846/47687] and geological map of the Shannon Basin showing the locality and regional geology (OSI rural place maps: http://maps.osi.ie/publicviewer).

Fig. 2.28. Sedimentary log of "Reading Room" band showing sampled horizons (R03-6 were sampled from the section further west and are not shown here).

Fig. 2.29. Reading Room band exposure, looking towards Kilbaha Bay at [73846/47687].

Fig. 2.30. "Dunmore West" band at [70494/46845].

Fig. 2.31. Location map showing Dunmore West sampling locality at [70494/46845] and geological map of the Shannon Basin showing the locality and regional geology (OSI rural place maps: http://maps.osi.ie/publicviewer).

Fig. 2.32. Sedimentary log of "Dunmore West" band showing ammonoid-bearing horizons.

Fig. 2.33. Location map showing Rehy Hill sampling locality at [80776/48616] and geological map of the Shannon Basin showing the locality and regional geology (OSI rural place maps: http://maps.osi.ie/publicviewer).

Fig. 2.34. Senan's Beach condensed section offset by a small fault, [76725/47707].

Fig. 2.35. Location map showing Senan's Beach band sampling locality at [76725/47707] and geological map of the Shannon Basin showing the locality and regional geology (OSI rural place maps: http://maps.osi.ie/publicviewer).

Fig. 2.36 Sedimentary log of "Senan's Beach" band.

Fig. 2.37. West Senan's Beach band at [76525/47887].

Fig. 2.38. Location map showing West Senan's Beach band sampling locality at [76525/47887] and geological map of the Shannon Basin showing the locality and regional geology (OSI rural place maps: http://maps.osi.ie/publicviewer).

Fig. 2.39. Sedimentary log of "West Senan's Beach" band showing sampled horizons.

Fig. 2.40. Lighthouse band outcrop at tip of Loop Head at [70420/48683].

Fig. 2.41. Location map showing Lighthouse sampling locality at [70420/48683] and geological map of the Shannon Basin showing the locality and regional geology (OSI rural place maps: http://maps.osi.ie/publicviewer).

Fig. 2.42. Sedimentary log of "Lighthouse band", showing sample location.

Fig. 2.43. Toorkeal Band, north coast of Loop Head at [76635/51342].

Fig. 2.44. Location map showing Toorkeal sampling locality at [76635/51342] and geological map of the Shannon Basin showing the locality and regional geology (Google Earth map).

Fig. 2.45. Sedimentary log of "Toorkeal band", showing sample location.

Fig. 2.46. Location map showing Rinevella sampling localities at [81692/49008] and geological map of the Shannon Basin showing the locality and regional geology (OSI rural place maps: http://maps.osi.ie/publicviewer).

Fig. 2.47. Lowest of two sampled horizons (RVW), close to Rinevella Point at [81692/49008]. Hammer for scale.

Fig. 2.48. Location map showing Holy Well sampling locality at [84922/49205] and geological map of the Shannon Basin showing the locality and regional geology (OSI rural place maps: http://maps.osi.ie/publicviewer).

Fig. 2.49. Sedimentary log of "Holy Well band", showing sample locations.

Fig. 2.50. Cloonconeen Lower band, [82829/49445]. Ruler is 30 cm long. Pen also for scale.

Fig. 2.51. Location map showing Cloonconeen Lower sampling locality at [82829/49445] and geological map of the Shannon Basin showing the locality and regional geology (OSI rural place maps: http://maps.osi.ie/publicviewer).

Fig. 2.52. Sedimentary log of "Cloonconeen Lower band", showing sampled horizons.

Fig. 2.53. Blackrock West band at [70419/48692]. Ruler is 30 cm long.

Fig. 2.54. Location map showing Blackrock West sampling locality at [70419/48692] and geological map of the Shannon Basin showing the locality and regional geology (Google Earth map).

Fig. 2.55. Sedimentary log of "Blackrock west band", showing sample location.

Fig. 2.56. Location map showing Blackrock West sampling locality at [70419/48692] and geological map of the Shannon Basin showing the locality and regional geology (Google Earth map).

Fig. 2.57. Location map showing Ross Bay east sampling locality at [72841/49714] and geological map of the Shannon Basin showing the locality and regional geology (OSI rural place maps: http://maps.osi.ie/publicviewer).

Fig. 2.58. Sedimentary log of Ross Bay east band, showing sampled horizons.

Fig. 2.59. Ross Bay East band at [72841/49714]. Ruler is 30 cm long.

Fig. 2.60. Location map showing Cloonconeen Top sampling locality at [82774/49551] and geological map of the Shannon Basin showing the locality and regional geology (OSI rural place maps: http://maps.osi.ie/publicviewer).

Fig. 2.61. Sedimentary log of "Cloonconeen Top band".

Fig. 2.62. "Cloonconeen Top Band" exposed in gully at [82774/49551].

Fig. 2.63. Seven sampled horizons at "Kilcredaun Top band" at [85029/49504].

Fig. 2.64. Location map showing Klcredaun Top sampling locality at [85029/49504] and geological map of the Shannon Basin showing the locality and regional geology (OSI rural place maps: http://maps.osi.ie/publicviewer).

Fig. 2.65. Sedimentary log of "Kilcredaun Top band", showing sampled horizons.

Fig. 2.66. Location map showing Quilty sampling locality at [77281/51701] and geological map of the Shannon Basin showing the locality and regional geology (Google Earth map).

Fig. 2.67. Sedimentary log of "Quilty band", showing sampled horizons.

Fig. 2.68. Location map showing Cloghaunsavaun sampling locality, at [75298/51003], and geological map of the Shannon Basin showing the locality and regional geology (OSI rural place maps: http://maps.osi.ie/publicviewer).

Fig. 2.69. Sedimentary log of "Cloghaunsavaun band", showing sampled horizons.

Fig. 2.70. "Cloghaunsavaun band" at [75298/51003].

Fig. 2.71. Location map showing Ross Slump sampling locality close to Fishermans's Point, at [74624/50910], and geological map of the Shannon Basin showing the locality and regional geology (OSI rural place maps: http://maps.osi.ie/publicviewer).

Fig. 2.72. Ross Bay West band at [70991/49071]. Ruler is 30 cm long.

Fig. 2.73. Location map showing Blackrock West sampling locality at [70419/48692] and geological map of the Shannon Basin showing the locality and regional geology (Google Earth map).

Fig. 2.74. Sedimentary log of "Ross Bay west band", showing sampled horizons.

Fig. 2.75. "Bridges of Ross" band at [72732/50231]. Sandstone injection visible.

Fig. 2.76. Solid ammonoid in sandstone at "Bridges of Ross" band at [72732/50231].

Fig. 2.77. Location map showing Bridges of Ross sampling locality at [72732/50231] and geological map of the Shannon Basin showing the locality and regional geology (OSI rural place maps: http://maps.osi.ie/publicviewer).

Fig. 2.78. Sedimentary log of Bridges of Ross band showing sampled horizons.

Fig. 2.79. Location map showing Cross sampling locality at [77499/51786] and geological map of the Shannon Basin showing the locality and regional geology (Google Earth map).

Fig. 2.80. Sedimentary log of Cross band, showing location of sampled horizons.

Fig. 2.81. Cross band in gully at [77499/51786].

Chapter 3 Palaeontology

Fig. 3.1 Typical faunal assemblage in Shannon Basin condensed sections: an example from Fisherstreet Bay, Doolin, Co. Clare, [Irish Grid 06640/96316], with *Dunbarella* sp. and ammonoid moulds. Scale is 1 cm.

Fig. 3.2. Orthoconic nautiloid (black arrow) and mouldic ammonoids (light arrow), shale bedding surface, "*Phillipsoceras circumplicatile* band", Cloghaunsavaun [75298/51003], north coast Loop Head, Co. Clare. Scale is 1 cm.

Fig. 3.3. Close-up view of a polished section through a concretion. 3D ammonoids are found in cross sectional view, showing inner whorls, St. Brendan's Well, Lisdoonvarna, Co. Clare, Ireland. Scale is 1 cm.

Fig. 3.4. Solid (3D) pyritized ammonoid, "*Ph. paucicrenulatum* band" on shale bedding surface, Bridges of Ross, north coast of Loop Head, Co. Clare. Scale is 1 cm.

Fig. 3.5. Solid (3D) pyritized ammonoids (most are highlighted by circles), "*Ph. paucicrenulatum* band" on shale bedding surface, Bridges of Ross, north coast of Loop Head, Co. Clare. Scale is 1 cm.

Fig. 3.6. Pseudo-ammonoids on sandstone surface, east of Senan's Beach, [76727/47705].

Fig. 3.7. Pseudo-ammonoids on sandstone surface, east of Senan's Beach, [76727/47705].

Fig. 3.8. Pseudo-ammonoid on sandstone surface, east of Senan's Beach, [76727/47705].

Fig. 3.9. *Phillipsoceras circumplicatile* (Foord, 1903) syntypes and traces of the ornament, (a) Paralectotype (NMING : F23969), (b) Lectotype (NMING : F23968), (c) Syntype (NMING : F23972, *partim*). Note that specimen c is probably not attributable to this species (see text for discussion) but it is included as it is one of the syntypes designated by Foord. Specimens are from Lisdoonvarna, Co. Clare, Ireland. Scale is 10 mm.

Fig. 3.10. Changes in ornament in *Phillipsoceras circumplicatile* (Foord, 1903) (a) Paralectotype (NMING : F23972 *partim*), Lisdoonvarna, Ireland, (b) TCD.60601, Murphy's Bridge, Ireland, (c) GSM 86917, Neheim, Germany, (d) Lectotype (NMING : F23968), Lisdoonvarna, Ireland. Scale is 10 mm long. (e) Growth lines in paralectotype (NMING : F23972 *partim*) at 4 mm diameter with shaded ventral sulcus, (f) Growth lines in TCD.60601 at 9 mm diameter, (g) Growth lines in lectotype (NMING : F23968). Scale bars are 2 mm long.

Fig. 3.11. *Phillipsoceras circumplicatile* lectotype (NMING : F23968), Lisdoonvarna area, Co. Clare, (a-b-c) side, dorsal and ventral view. Scale is 20 mm.

Fig 3.12. Ontogenetic study of the ornament for *Phillipsoceras circumplicatile* (Foord, 1903) (a) Specimen associated with syntypes (NMING : F23972 *partim*); (b) TCD.60601, Murphy's Bridge, Ireland; (c) GSM 86917, Neheim; (d) Lectotype (NMING : F23968). Scale is 20 mm.

Fig. 3.13. Unpublished note in the Manchester Museum written by R.G.S. Hudson mentioning W.S. Bisat (c. 1940).

Fig. 3.14. *Phillipsoceras paucicrenulatum* type material. All specimens from Lumbutts Clough, Todmorden, Yorkshire. (a) GSM 71076, paratype, (b) GSM 71075, paratype (c) GSM 71078, paratype, (d) unlabelled specimen associated with type material, (e) GSM 71074, holotype, (f) GSM 71077, paratype. Scale is 10 mm.

Fig. 3.15. Ammonoids which occur in the Shannon Basin, Ireland. 1 *Phillipsoceras paucicrenulatum* (a-b) zi 7097 (BGS), Fisherstreet Bay, Co. Clare, side and dorsal view; (c-d) zi 7098 (BGS), Fisherstreet Bay, Co. Clare, side and ventral view; (e) zi 7100 (BGS), Fisherstreet Bay, Co. Clare; (f) TCD.61064, Luggacurren section, Co. Laois; (g) zi 7096, Fisherstreet Bay, Co. Clare, side view. Scale is 10 mm.

Fig. 3.16. Ontogenetic study of the ornament for *Phillipsoceras paucicrenulatum* (Bisat & Hudson, 1943) (a) zi 7095 (BGS), Fisherstreet Bay, Co. Clare, (b) zi 7097 (BGS), Fisherstreet Bay, Co. Clare, (c) zi 7096 (BGS), Fisherstreet Bay, Co. Clare, scale is 10 mm.

Fig. 3.17. *Reticuloceras pulchellum* holotype (NMING specimen, unlabelled). Scale is 20 mm.

Fig. 3.18. Changes in ornament in *Reticuloceras subreticulatum* (Foord, 1903) (a) TCD.60602, Blake's Bridge, (b) TCD.60603, Blake's Bridge, (c) TCD.60604, Blake's Bridge, (d) Lectotype (NMING : F23964), Foynes Island, Co. Limerick, Ireland, (e) TCD.60605, Blake's Bridge. Scale bar is 10 mm long. (f) Growth lines of TCD.60602, Blake's Bridge, and shaded constriction, (g) Growth lines in lectotype (NMING : F23964), Foynes Island, Co. Limerick, Ireland. Scale bars are 2 mm long.

Fig. 3.19. Ontogenetic study of the ornament for *Reticuloceras subreticulatum* (Foord, 1903) (a) TCD.60602, Blake's Bridge; (b) TCD.60603, Blake's Bridge; (c) TCD.60604, Blake's Bridge; (d) Lectotype (NMING : F23964); (e) TCD.60605, Blake's Bridge. Scale is 20 mm.

Fig. 3.20. *Reticuloceras subreticulatum* lectotype (NMING : F23964), Foynes Island, Co. Clare, (a-b) side and ventral view. Scale on top left is 20 mm.

Fig. 3.21. Suture line, *R. subreticulatum* Foord lectotype (NMING : F23964), at 11 mm diameter.

Fig. 3.22. Changes in ornament in *Homoceras beyrichianum* (de Koninck, 1843) (a) TCD.61003, Lisdoonvarna district, Co. Clare (b) TCD.61004, Lisdoonvarna district, Co. Clare, (c) TCD. 61000, Coolagh River, Co. Clare, scale is 10 mm.

Fig. 3.23 *Homoceras beyrichianum* (a-b) TCD.61000, Coolagh River, Co. Clare, side and ventral view; (c-d) TCD.61003, Lisdoonvarna district, Co. Clare, side and ventral view; (e-f) TCD.61004, Lisdoonvarna district, Co. Clare, side and ventral view. Scale on top left is 20 mm.

Fig. 3.24. Changes in ornament in *Homoceras smithii* (Brown, 1841) (a) TCD.61002, Lisdoonvarna, Co. Clare, (b) TCD.61005, Lisdoonvarna, Co. Clare, (c) TCD.61006, Lisdoonvarna, Co. Clare, scale is 10 mm.

Fig. 3.25. *Homoceras smithii* (a-b) TCD.61002, Lisdoonvarna, Co. Clare, side and ventral view; (c-d) TCD.61005, Lisdoonvarna, Co. Clare, side and ventral view; (e-f) TCD.61006, Lisdoonvarna, Co. Clare, side and ventral view. Scale on top left is 20 mm.

Fig. 3.26. *Homoceras undulatum* (a-b) zi 4534 (BGS), Kilmoon Stream, Lisdoonvarna, Co. Clare, side and ventral view; (c-d) F24480/3, Roadford, Co. Clare, side and ventral view; (e) F24480/6, Roadford, Co. Clare, side view; (f) F24480/5, Roadford, Co. Clare, side view. Scale is 20 mm.

Fig. 3.27. *Isohomoceras subglobosum* (a) TCD.61021, Inishcorker, Co. Clare, side view; (b-c) TCD.61022, Inishcorker, Co. Clare, side and ventral view. Scale is 10 mm.

Fig. 3.28. Changes in ornament in *Vallites henkei* (Schmidt, 1925) (a) Syntype GZG.INV.48185, (b) Syntype GZG.INV.48186, (c) Syntype GZG.I NV.48184. Specimens are from Neheim, Germany. Scale bar is 10 mm long. (d) Growth lines (NMING : F23971) at 7 mm with dashed lines at edges of umbilical wall, (e) Growth lines of TCD.60608 at 10 mm diameter, (f) Growth lines of TCD.60608 at 15 mm diameter. Specimens are from Lisdoonvarna, Ireland. Scale bars are 2 mm long.

Fig. 3.29. Ontogenetic study of the ornament for *Vallites henkei* (Schmidt, 1934) (a) GZG.INV.48185; (b) GZG.INV.48186; (c) GZG.INV.48184. Specimens are from Neheim, Germany. Scale is 20 mm.

Fig. 3.30. *Vallites henkei* (a-b) NMING : F13974, Lisdoonvarna area, Co. Clare, side and dorsal view; (c) TCD.61030, Aille River, Co. Clare; (d-e) TCD.60608, Lisdoonvarna, Co. Clare, side and ventral view; (f) NMING : F23971, Lisdoonvarna area, Co. Clare, side view. (g) Corofin, Co. Clare, enlarged x 5, after Lewarne (1959). Scale bar on top left is 20 mm.

Fig. 3.31. *Homoceratoides prereticulatus* (a) TCD.61028, below Blakes Bridge, Co. Clare; (b) C25749, Lectotype, Holden Beck, Silsden, Yorkshire, UK; Scale is 20 mm.

Fig. 3.32. Ontogenetic study of the ornament for *Homoceratoides varicatus* Schmidt, 1934 (a) GZG.INV.48188, paratypoid, Neheim, (b) TCD. 61007, Loose bullion, Kilmoon River, (c) TCD.61008, Loose bullion, Kilmoon River, (d) GZG.INV.48187, holotype, Neheim. Scale is 10 mm.

Fig. 3.33. *Hodsonites magistrorum* (a) NMING : F2028, River Aille, Phosphate Mine, Roadford, Co. Clare; (b-c) GSM.86913, River Aille, Phosphate Mine, Roadford, Co. Clare, side and ventral view. Scale is 20 mm.

Fig. 3.34. *Hudsonoceras proteus* (a-b) TCD.61050, Coolagh River, Co. Clare, side and ventral; (c-d) TCD.61051, Coolagh River, Co. Clare, side and ventral; Scale is 20 mm.

Fig 3.35. *Hudsonoceras ornatus/Baschkirites ornatus* type material. British Museum of Natural History, London. (a) c5279, syntype, Halifax, Yorkshire, side, ventral and dorsal views; (b) c70994, syntype, Halifax, Yorkshire, side, ventral and dorsal views; (c) c70995, syntype, Halifax, Yorkshire, side, ventral and dorsal views. Photographs were taken by Svetlana V. Nikolaeva.

Fig. 3.36. Irish ammonoids preserved in 2D. (a) *Ph. circumplicatile* (TCD.60606) (b) *V. henkei* (TCD.60607). Specimens are from Loop Head, Co. Clare, Ireland. Scale bars are 5 mm long.

Fig. 3.37. Number of growth lines per diameter (mm) in the species *R. subreticulatum*, *Ph. circumplicatile* and *Ph. paucicrenulatum.* A representative solid specimen is shown next to each trend line.

Fig. 3.38. Number of growth lines per diameter in *Ho. beyrichianum*, *Iso. subglobosum*, *Ho. smithii*, *V. henkei*, *Ho. undulatum* and *Hod. magistrorum.* A representative solid specimen is shown next to each trend line.

Fig 3.39. Number of growth lines per diameter plotted for *Ht. prereticulatus* and *Ht. varicatus.* A representative solid specimen is shown next to each trend line.

Fig. 3.40. Paper pecten morphotypes (after Wignall 1994, p. 35).

Fig 3.41. First occurrences of taxa and stratigraphic ranges through the Ross Sandstone Formation. Number of specimens in each locality is shown. Ranges of bivalves are highlighted in red. Ranges of thin-shelled ammonoids are highlighted in green.

Fig. 3.42. Serpukhovian-Bashkirian ammonoid community (after Ramsbottom 1978). (a) *Hudsonoceras* (ammonoid), (b) *Reticuloceras* (ammonoid), (c) *Posidonia* (bivalve), (d) *Dunbarella* (bivalve).

Fig. 3.43. Trilobite pygidium from "Dunmore Head west band" sample (Chapter 2, section 2.2.2.8). Pencil for scale.

Chapter 4 Ammonoid Distribution and Salinity Implications

Fig. 4.1. Ideal faunal and salinity cycles in the Serpukhovian and Bashkirian of Britain, after Ramsbottom (1962), Holdsworth & Collinson (1988) and Martinsen *et al.* (1995). (a) Eustatic

sea level curve varying from highstand to lowstand and its probable relation to the faunal changes through the cycle in (b).

Fig. 4.2. Schematic representation of the "highstand-lowstand" model for sedimentation in Late Mississippian and Pennsylvanian basins in north-west Europe (based on Holdsworth & Collinson 1988). (a) At times of sea level highstand fully marine conditions are established (b) At times of lower sea level, basins become restricted and there is fresh water influx, resulting in salinity decrease.

Fig. 4.3. (a) Field photo and sedimentary log through a highly-condensed section in the Shannon Basin, located west of Dunmore Head, Loop Head, Ireland, Irish Grid coordinates [70494/46845], showing both (b) mouldic (2D) preservation and (c) solid (3D) preservation of ammonoids. (d) Summary stratigraphic log of the Ross Sandstone Formation, showing the stratigraphic position of the consensed section shown in (a).

Fig. 4.4. (a) Field photo and stratigraphic log of low-density turbidite sequence in northern Senan's Bay, south coast of Loop Head (Irish Grid Coordinates [76525/47887]) from which ammonoids have been recovered. (b) Location of ammonoids found in shale veneers in borehole 10-CE-UCD-04 (1 m-long core intervals from borehole 10-CE-UCD-04 were chosen as a representative example). (c) *Vallites henkei* (Schmidt, 1925), an ammonoid preserved in borehole material. (d) Summary stratigraphic log of the Ross Sandstone Formation, showing the stratigraphic position of the section shown in (a).

Fig. 4.5. (a) Field photo and sedimentary log of Kilbaha Bay locality (Irish Grid Reference [75394/48264]) showing position of ammonoid-bearing siltstone shown in (b). (c) Ammonoids found in silt-rich mudstones, showing internal chambers in the shell. (d) Summary stratigraphic log of Ross Sandstone Formation, showing the stratigraphic position of the locality shown in (a).

Fig. 4.6. (a) Stratigraphic position within the Ross Sandstone Formation of massive sandstone on the south coast of Loop Head, west of Dunmore Head, Irish Grid Coordinates [70662/46893]). Here, ammonoid casts shown in (c) are preserved on the underside of the sandstone bed indicated by the arrow in (b).

Fig. 4.7. Summary log of the Ross Sandstone Formation, Shannon Basin, with the stratigraphic position of ammonoid-bearing horizons (indicated by arrows) in and between the main highly-condensed sections. Stars show approximate (within 10 m of stratigraphic thickness) positions of ammonoids on selected shale horizons within low-density turbidite sequences, which are too many to show on this scale.

Fig. 4.8. (a) Schematic representation of emerging model for sedimentation in the Shannon Basin, western Ireland. (b) Concentration of ammonoids in the Shannon Basin visualized in an idealized log through the basin fill, showing greater numbers of ammonoids corresponding to times of lower sedimentation rate and fewer at times of higher sedimentation rate.

Chapter 5 Correlations within the Ross Sandstone Formation

Fig. 5.1. A compilation of ammonoid taxa recoded by Gillian Lewarne for localities in stratigraphic order within the Ross Sandstone Formation (from unpublished notes). Locality names have been updated to reflect locality names in Chapter 3. Ticks indicated presence of a given taxon in a locality. Number of ticks indicate abundance, as recorded by Lewarne: ✓= rare to very rare, ✓✓= frequent to rare, ✓✓✓= frequent, ✓✓✓✓= abundant. Where this occurrence has been confirmed in the present study (not necessarily in the same abundance), the box is shaded. Boxes were shaded whether or not specimens were identified confidently or were prefixed with cf (confer).

Fig. 5.2. Lithostratigraphic correlation panel of core and outcrop sections of the Ross Sandstone Formation (modified after Pierce 2015). Taxa that were also identified by Gillian Lewarne are underlined (cf Fig. 5.1). Logs that are measured by Pierce (2015) are grey, while sections measured in this work are black. For detailed logs, see relevant Figs. in Chapter 2 and Appendix B.

Fig. 5.3. Geological map of the Shannon Basin, showing localities mentioned in the text.

Fig. 5.4. Range chart for ammonoids and thin-shelled bivalves in the Ross Sandstone Formation, western Ireland.

Fig. 5.5. Comparison of ammonoid assemblages in the "*Hud. proteus-Ho.smithii* band" at different localities. The vertical axis shows the number of specimens on a log scale.

Fig. 5.6. Comparison of ammonoid assemblages in the "*Ht. prereticulatus* band" at different localities. The vertical axis shows the number of specimens on a log scale.

Fig. 5.7. Comparison of ammonoid assemblages in the "Dunmore Head west band" at different localities. The vertical axis shows the number of specimens on a log scale.

Fig. 5.8. Proportion of *Reticuloceras/Phillipsoceras* spp. compared to all other taxa at the Dunmore Head west locality, where the "Dunmore Head west band" crops out.

Fig. 5.9. Comparison of ammonoid assemblages in the "*Ph. circumplicatile* band" at different localities. The vertical axis shows the number of specimens on a log scale.

Fig. 5.10. Proportion of *Reticuloceras/Phillipsoceras* spp. compared to all other taxa at the Quilty locality where the "*Ph. circumplicatile* band" crops out.

Fig. 5.11. Comparison of ammonoid assemblages in the "*Ph. paucicrenulatum* band" at different localities. The vertical axis shows the number of specimens on a log scale.

Fig. 5.12. Magnitude and duration of sea-level oscillations (after Waters & Condon 2012: Fig. 8). Sea-level maxima are estimated through the determination of maximum areal extent of acme ammonoid facies. For marine bands lacking ammonoid fauna the magnitude of sea level is determined through the acme marine fauna, ranging from *Estheria* to brachiopod–bivalve facies. Sea-level minima are determined through the presence of incised valleys, with the magnitude recorded by the number of underlying marine bands removed beneath the sequence boundary. The proposed four main glaciations are highlighted as grey bands. The Ross Sandstone Formation is shown straddling a glacial-interglacial boundary.

Fig. 5.13. Comparison of Shannon Basin ammonoid bands (the five main highly-condensed sections are shown in the Ross Sandstone Formation schematic architecture) with Pennine Basin ammonoid bands (modified after Waters & Condon 2012).

Fig. 5.14. Mineralogical composition of Phase 1 samples (volume %) with relative core depth of each sample (Samples 1 to 4).

Fig. 5.15. Volume % mineralogy for Phase 1 samples.

Fig. 5.16. Normalized values of volume % mineralogy for Phase 1 samples.

Fig. 5.17. Sample 1 normalized mineralogy (20.20 m depth in borehole 10-CE-UCD-05, sampled from the "Reading Room band").

Fig. 5.18. Sample 2 normalized mineralogy (47.73 m depth in borehole 09-CE-UCD-01, from the *"Ph. circumplicatile* band".

Fig. 5.19. Sample 3 normalized mineralogy (73.92 m depth in borehole 09-CE-UCD-02, from the "*Ph. paucicrenulatum* band".

Fig. 5.20. Sample 4 normalized mineralogy (82.7 m depth from borehole 10-CE-UCD-05 part of the "*Hud. proteus-Ho. smithii* band".

Fig. 5.21. Phase 2 samples from "*Hud. proteus-Ho. smithii* band" in boreholes 10-CD-UCD-03 and 10-CE-UCD-05.

Fig. 5.22 (a) Mineralogy of samples taken from borehole 10-CD-UCD-03; (b) Mineralogy of samples taken from borehole 10-CD-UCD-05.

Fig. 5.23. Normalized results of Phase 2 samples from borehole 10-CE-UCD-03.

Fig. 5.24. Normalized results of Phase 2 samples from borehole 10-CD-UCD-05.

Fig. 5.25. Samples included in Phase 3, with sample name (including core number and depth), description and source (core or outcrop).

Fig. 5.26. QEMSCAN Phase 3 mineralogy results visualised in a ternary diagram with the three axes showing carbonate, sand and clay/mica. Results are normalized with respect to pyrite.

Fig. 5.27. (a) QEMSCAN Phase 3 results; (b) Results once normalized with respect to pyrite.

Fig. 5.28. Carbonate (dolomite, calcite and others) content (volume %) across Phase 3 samples.

Fig. 5.29. Apatite content (volume %) across Phase 3 samples.

Fig. 5.30. Sphalerite concentration (volume %) across Phase 3 samples.

Fig. 5.31. Sphalerite concentration (volume %) across QEMSCAN Phase 2 samples from boreholes 10-CE-UCD-03 and 10-CE-UCD-05.

Fig. 5.32. Plot of angle (°2Θ) versus Intensity (Counts) for sample X05PROT-89.84, from the "*Hud. proteus-Ho. smithii* band" after XRD analysis. Peak positions and intensities are matched to lines from the ICDD database.

List of Tables

Chapter 1 Introduction

Table 1.1. Hodson's faunal band scheme for the lower Clare Shales, (after Hodson, 1954a, p. 265). Original measurements in feet/inches have been converted to metric values and taxonomic details have been updated.

Table 1.2. Simplified succession showing the four condensed sections ("marine bands") identified by Dr Gillian Lewarne (modified from unpublished notes). Succession nomenclature is presented as mapped by Lewarne.

Chapter 2 Ammonoid Localities

Table 2.1. Summary of Hodson's log for Fisherstreet Bay (after Hodson & Lewarne 1961). Original measurements in feet/inches have been converted to metric values.

Table 2.2. Aille River faunal content.

Table 2.3. Foynes Island faunal content.

Table 2.4. Foynes Harbour faunal content.

Table 2.5. Taxa present in National Museum of Ireland collection samples.

Table 2.6. Spectacle Bridge faunal content.

Table 2.7. Slieve Elva faunal content.

Table 2.8. "Castle Band" faunal content.

Table 2.9. "Rehy Hill" band faunal content.

Table 2.10. Rinevella faunal content.

Table 2.11. Blackrock locality faunal content.

Table 2.12. Kilcredaun faunal content in Lewarne (unpublished notes).

Table 2.13. Ross Slump faunal content.

Table 2.14. Leinster Coalfield faunal content.

Chapter 3 Palaeontology

Table 3.1. Diagnostic features in *Ho. beyrichianum*, *Ho. smithii* and *Ho. undulatum*.

Table. 3.2. Summary of differences in diagnostic characters between *Hod. magistrorum*, *Ht. varicatus* and *V. henkei*.

Table 3.3. Systematics of thin-shelled ammonoid genera *Anthracoceras* and *Dimorphoceras*.

Chapter 5 Correlations within the Ross Sandstone Formation

Table. 5.1. Summary of high-resolution stratigraphic subdivision of the Ross Sandstone Formation with unit-bounding condensed sections/slump horizons/fossiliferous intervals and main core and outcrop localities (after Pierce 2015).

Table 5.2. Contingency table and Chi-square test results for the "*Hud. proteus- Ho. smithii*" band using PAST software.

Table 5.3. Observed frequencies for the "*Ht. prereticulatus*" band and results from the Chi-square test using PAST software.

Table 5.4. Observed frequencies for the "Dunmore Head West" highly-condensed section and results from the Chi-square test using PAST software.

Table 5.5. Observed frequencies for the "*Ph. circumplicatile*" highly-condensed section and results from the Chi-square test using PAST software.

Table 5.6. Observed frequencies for the "*Ph. paucicrenulatum*" highly-condensed section and results from the Chi-square test using PAST software.

Table 5.7. Observed frequencies for the Toorkeal condensed section and results from the Chi-square test using PAST software.

Table 5.8. Chi-square test for ammonoid assemblage at Quilty and Cross, Loop Head.

Table 5.9. Chi-square test for ammonoid assemblage at Quilty and Dunmore W, Loop Head.

Table 5.10. QEMSCAN Phase 1 samples with associated borehole depths and descriptions.

Table 5.11. Samples analysed by XRD and description of sample location.

Table 5.12. Summary table of sample and mineral presence based on XRD analysis.

Chapter 1 Introduction

1.1 Introduction to the project

This study presents the results of a reinvestigation of the ammonoid fossil faunas preserved in the Serpukhovian-Bashkirian strata of the Shannon Basin, western Ireland. It focuses in particular on the Ross Sandstone Formation, a classic turbidite succession that provides an important analogue for deep-water sequences elsewhere which contain hydrocarbons. Over 3,000 specimens were studied during the course of the project: having reinvestigated their taxonomy and palaeoenvironmental significance, their true biostratigraphic potential is assessed.

1.2 Ammonoids

Goniatites are extinct, externally-shelled cephalopods that, together with ammonites and ceratites, form the subclass Ammonoidea. They range from the middle of the Devonian to the end of the Cretaceous. Because of their high evolutionary rates, their broad geographic distribution and relatively easy recognition, ammonoids are an excellent tool in biostratigraphy (Ramsbottom & Saunders 1985). The term "goniatite" is commonly used as a synonym for all Palaeozoic ammonoids even though, in the strictest definition, goniatites are those ammonoids that belong to the order Goniatitida (Lehmann 1981).
After a severe decline in number of taxa at the end of the Devonian period, the Carboniferous period saw the proliferation and diversification of ammonoids up until the Mid Carboniferous Boundary (Kullmann 1980), when another crisis in ammonoid evolution took place. Notwithstanding these two crises, an unusually rapid evolutionary rate allowed Carboniferous goniatites to become the richest and most diverse of all Palaeozoic ammonoid faunas (Ramsbottom & Saunders 1985). While goniatites proliferated during the Carboniferous, ammonites thrived in Mesozoic times, probably to occupy similar ecological

niches. There is general agreement that ammonoids evolved from bactritids (Engeser 1996), another cephalopod subclass with small, orthoconic (straight) to cyrtoconic (slightly curved) shells. Bactritids were themselves derived from orthoconic nautiloids (Lehmann 1981). A brief account of salient topics related to ammonoids is given below, as this aids interpretation in later chapters.

1.2.1 Shell structure

Ammonoids were very diverse in terms of size, shape and sculpturing. They possessed an external shell, also known as conch, made of aragonite, but this mineral is rarely preserved since it is readily soluble in the pore fluids in a rock. The mould left by solution is commonly filled by calcite (Lehmann 1981). The shell consisted of three main layers: periostracum, the outer prismatic layer and the inner prismatic layer (Kulicki 1996). The shell was divided internally into several chambers, whose chamber walls were secreted sequentially by the organism as it grew. The animal itself resided in the last formed chamber, the body chamber. As the animal grew, it vacated the previously formed body chamber, or camera, and secreted a chamber-dividing wall, or septum, behind it. The body chamber is always the largest and it is located in the anterior of the shell. The remaining chambers contained fluid and gas, which are thought to have served a function in buoyancy control (Taylor & Lewis 2005). The open end of the body chamber is termed aperture and the mouth border, or peristome, is located at the edge of the aperture. Goniatite shells are always coiled in a single horizontal plane (planispirally), with each complete coil of 360° being termed a whorl or volution. The initial chamber is known as the protoconch and the portion of shell divided into camerae is known as the phragmocone (Lehmann 1981). Ammonoid shells can be evolute, where the whorls overlap little or not at all, or involute, where the whorls overlap considerably (Teichert 1964). In general, involute forms were prevalent and most Palaeozoic ammonoids had a globose (roughly spherical or globular) shell. In apertural view (viewed facing the aperture) shells vary from narrow discs to broad, globose shapes (Fig. 1.1). A membranous tube, called the siphuncle, extended back through all the chambers of the shell, from the

protoconch to the body chamber. It originated as a small bulb, known as the caecum, within the protoconch, and consisted of organic and mineral components (Lehmann 1981). The siphuncle was used to regulate fluid levels in the chambers (Westermann 1996).

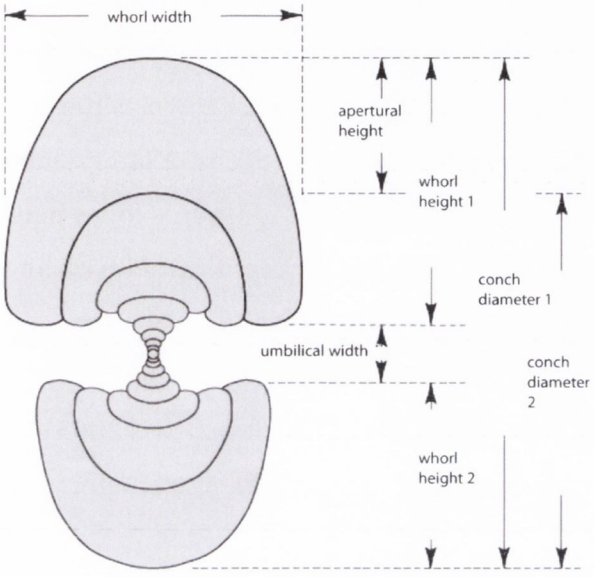

Fig. 1.1. Basic conch parameters for Palaeozoic ammonoids (after Korn 2010).

The outer surface of ammonoids, where the external shell has been removed, commonly displays zig-zag lines: these are known as suture lines. It is the angular pattern of these lines that gives goniatites their name: in fact, the Greek word γωνία means angle. Suture lines mark the position where the internal chamber-dividing walls (septa) join to the inner side of the external shell. Hence they are only visible once the external shell has been removed (Lehmann 1981) (Fig. 1.2).

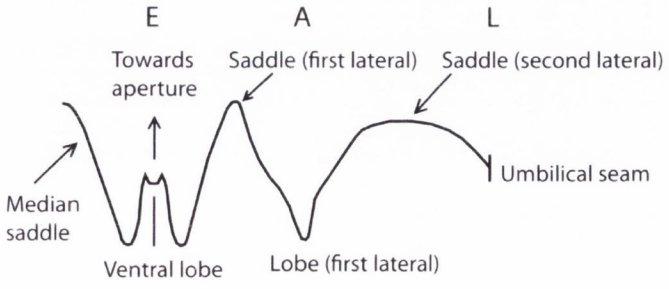

Fig. 1.2. Generalized terminology of the suture line (modified after Korn 2010).

There are several terms associated with the description of suture lines (see Lehmann 1981; Teichert 1964). For example, saddles are deflections of the suture line in the adoral direction (towards the aperture), whereas lobes are deflections in the adapical direction (away from the aperture). The oldest suture line is called prosuture and it is defined as the part of the septum that partitions off the protoconch. The next suture to be formed is the primary suture, which is generally regarded as the first true suture. Within the suture line, external (ventral), lateral and internal (dorsal) lobes are known as the primary lobes, since they appear first in ontogeny and phylogeny. A lateral lobe is nearly always present on the flank of ammonoid shells. Additional lobes may form by division of the saddles. Suture lines are generally represented with an arrow pointing in the direction of growth and, when illustrated, they are projected as a line on a plane, although usually only half is represented. Ammonoids are typically less than 20 cm in diameter (Taylor & Lewis 2005); most ammonoids investigated in herein were less than 20 mm in diameter.

Ammonoid shells can be smooth or can present varying degrees of ornamentation (Taylor & Lewis 2005). Examples of ornamentation include ribs, which are radially directed ridges, sometimes referred to as costae or pilae, riblets, which are small ribs, furrows or depressions, and growth lines, which are minute lines on the shell surface marking its gradual increase in size (Teichert 1964). In addition to these, constrictions, defined as coarse radial grooves encircling the whorl, and plications, defined as coarse radial folds, are common examples of ornamentation (Fig. 1.3).

Ammonoid taxonomy is based on knowledge of the morphology of the conch, and generally involves the study of conch shape and size, suture line outline and shell ornament. While ammonoid generic determinations mainly rely on suture line description, ornament is the main tool in specific identification. Knowledge of the ornament is essential in the taxonomy of 2D ammonoids, because it is often the only shell feature that is preserved.

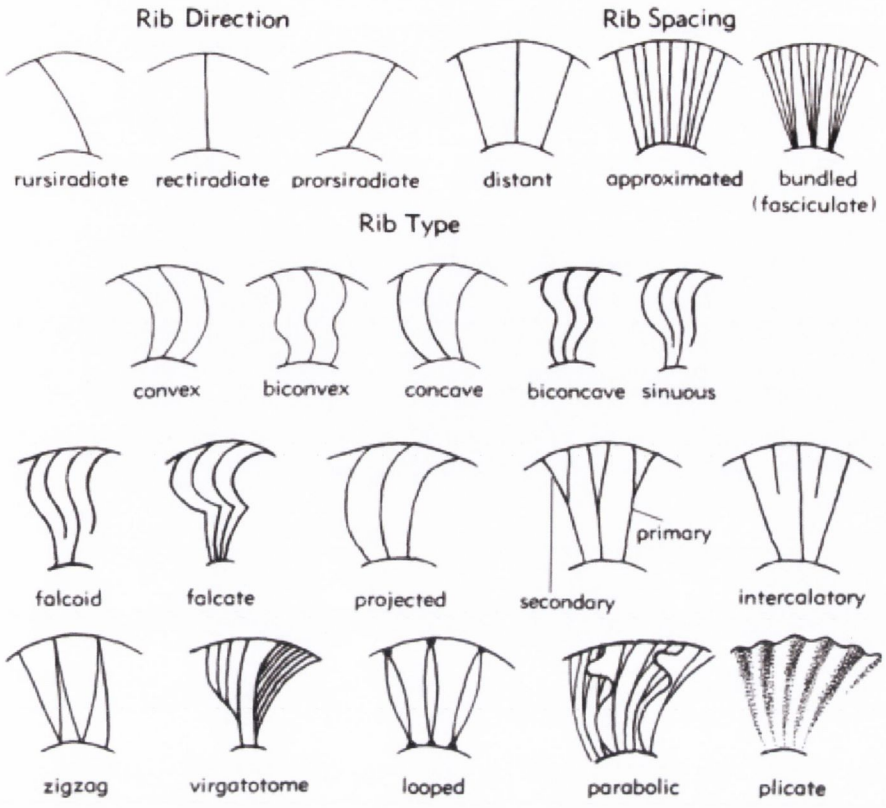

Fig. 1.3. Rib shape, spacing and course (after Arkell 1957; Klug et al. 2015).

1.2.2 Ontogeny

Ammonoids grew incrementally, via periodical secretion of new septa. A record of their growth is thus retained in their shells, facilitating ontogenetic studies. The following growth stages have been recognised: ammonitella, which is essentially the embryo; neanoconch, or early juvenile (shell diameter is 3-5 mm); juvenile (taken here to correspond to less than a 10 mm shell diameter) and adult (Bucher *et al.* 1996; Westermann 1996). The term adolescent is taken as equivalent to a late juvenile stage (Bucher *et al.* 1996) and is here defined as the growth stage of shells between 10 and 18 mm diameter. In the course of this study, adulthood is defined by shell diameters greater than 18 mm diameter (cf. Hodson 1957).

If one traces the ontogenetic development of the suture line in a single shell, it is clear that it becomes more complex during the individual's life (Fig. 1. 4). In

turn, this is paralleled in the phylogenetic development of ammonoids as a whole: while goniatites had relatively simple suture lines, ammonites evolved complex patterns.

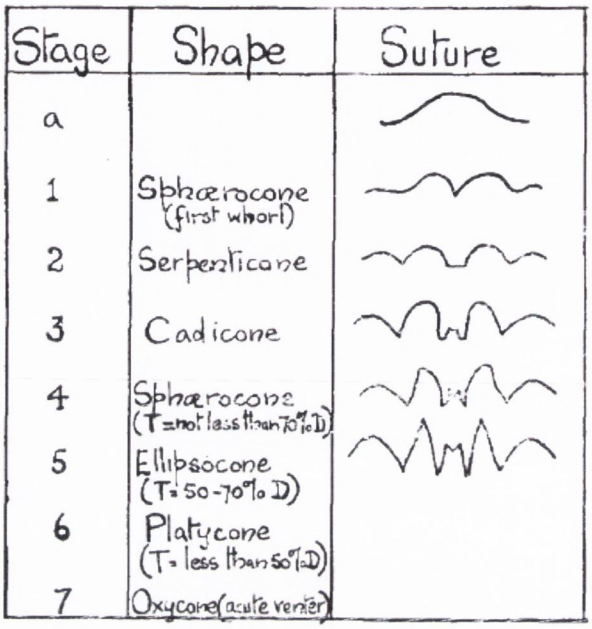

Fig. 1.4. Ammonoid developmental stages and associated changes in shape and suture, showing increasing complexity in suture line during an individual's lifetime (after Bisat 1924).

1.2.3 Mode of life

Ammonoids are extinct, so any interpretation of their mode of life is by inference. Indeed, the distribution of ammonoids in space and time is much better known than their biology (Landman *et al.* 1996; Taylor & Lewis 2005). The Pearly Nautilus is one of two living descendants of externally shelled cephalopods (including the Paper Nautilus, which is a coleoid). But, however tempting it may be to draw palaeoecological inferences from *Nautilus*, it must be noted that it is not phylogenetically closely related to ammonoids (Engeser 1996).

Nevertheless various approaches can be used, from synecological studies, which look at the associations and occurrences of ammonoids in the field, to autoecological studies, which focus on the morphology of the individual shell in

order to obtain physical constraints on the living organism (Westermann 1996).

Ammonoids are confined to strata of marine origin (see Ch. 4 for a discussion on palaeosalinity) and it is thought that they were generally pelagic, the remainder being demersal (inhabitants of the water column just above the benthic zone) (Westermann 1996). Of course, post-mortem drift can affect fossil assemblages and must be taken into account. In general, assemblages containing various growth stages of the same species are likely to have accumulated *in situ*. Concentrations of mature individuals may reflect habitat change during lifetime, while concentrations of small individuals may be the result of mechanical sorting. The worldwide distribution of ammonoids indicates a nekto-pelagic habit (Riley 1993) and the ability to invade various habitats. While neanic and most small juveniles were quasiplanktic, at maturity they became more mobile. Having said this, swimming ability remains controversial in ammonoids and the drag associated with the shell would certainly hinder high-speed swimming (e.g. Jacobs 1992). Klug & Korn (2004) studied changes in aperture position in several Devonian ammonoids (Fig. 1.5) and derived inferences on the locomotion ability of the ammonoids from the orientation of the shell. They showed that evolution of a coiled conch from the uncoiled bactritid conch was probably coupled with changes in swimming ability and velocity.

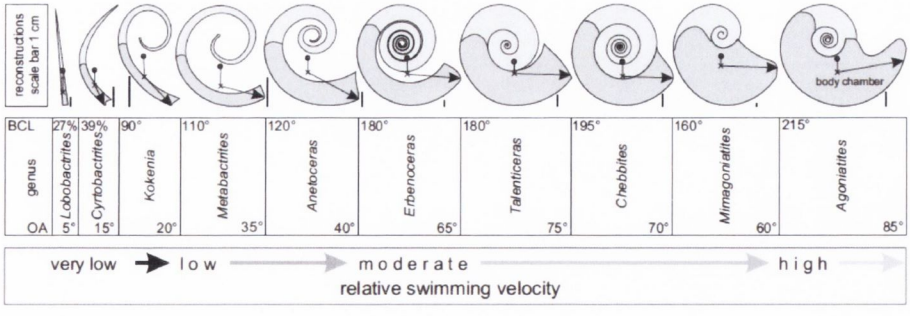

Fig. 1.5. Phylogenetic change in orientation of the conchs and swimming velocity of Bactritida and primitive Ammonoidea. Outlines of the conchs of one bactritid and nine ammonoids from the Early and Middle Devonian with body chamber lengths (BCL), orientation of the aperture (OA), and relative swimming speed. Centre of gravity is indicated by a cross and the centre of buoyancy by a circle (Klug & Korn 2004).

Studies that focus on ammonoid palaeoecology are mostly concerned with shell architecture (e.g. Swan & Saunders 1987). For example, the presence of a hyponomic sinus, or sinus marking the location of the hyponome, is thought to be a sign of greater flexibility of the hyponome, which in turn suggests greater swimming ability. In fact, it is generally thought that movement was achieved via jet propulsion: water was drawn in, passed over the gills and then was directed out through the hyponome. The shell functioned in protecting and supporting the animal. Furthermore, the chambered construction probably allowed buoyancy control by trapping fluids. It is thought that ammonoids could migrate vertically through the water column. Lenticular shells with bilateral symmetry are generally associated with mobility, while prominent ornamentation is associated with reduced locomotion. In Palaeozoic ammonoids, the growth lines are generally fine and not very prominent, which is consistent with a nektonic habit. However, the globose shape of most goniatites suggests they were poor swimmers.

Ritterbush & Bottjer (2012) linked shell measurements to hypothesized ammonoid life modes in a ternary diagram known as "Westermann Morphospace" (Fig. 1.6). In this diagram, shell shapes grade between serpenticone (evolute with much of the umbilicus exposed), sphaerocone (overall inflated with most or all of the umbilicus covered) and oxycone (compressed forms, with no exposure of the umbilicus). They hypothesize that oxycone shapes facilitated swimming, while sphaerocone shapes may have facilitated vertical migration through the water column, and serpenticone shapes may have been associated with very poor swimming ability and planktonic mode of life.

Modifications of the shell at maturity include the formation of lappets, which are projections of the peristome in the ventral area (e.g. in *Eumorphoceras*): this particular modification may have served to streamline the shell and facilitate swimming.

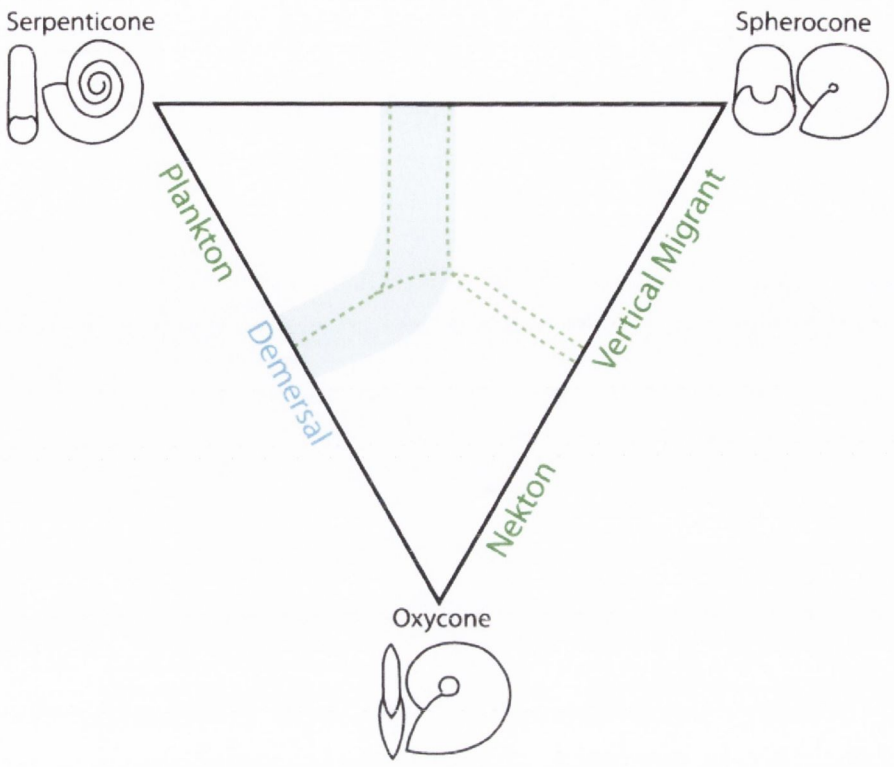

Fig. 1.6. Westermann morphospace. Three components of shell shape (exposure of the umbilicus, overall inflation, and whorl expansion) dictate data placement within this ternary diagram (Ritterbush & Bottjer 2012).

The genus *Entogonites* is characterised by a tetrangular coiling of its inner whorls, a unique feature in Palaeozoic ammonoids. Even though it is unclear what the functional properties of this type of coiling were, the horizontally orientated aperture (calculated from the opening rate of the whorl spiral) in *Entogonites* suggests a planktonic lifestyle (Korn *et al.* 2005).

It is likely that ammonoids grew rapidly and were characterised by short life spans (Taylor & Lewis 2005). Even though gut contents in fossil forms are rare, it is thought that the main food item was zooplankton, such as crustaceans and ostracods. The main predators were larger ammonoids, fish, reptiles and teuthoids (an order of coleoids) (Westermann 1996). In general, a combination of autoecological and synecological approaches is best in any comprehensive palaeoecological study (Lacchia 2012).

1.3 The Carboniferous

1.3.1 Global and regional context

During the Carboniferous, the final assembly of the Pangaea, which was underway as Gondwana collided with Laurussia, fundamentally changed global oceanic circulation patterns (Mii *et al.* 1999; Fallon & Murray 2015). This resulted in the Variscan Orogeny in Western Europe (Davies *et al.* 2012).

During this time, early Palaeozoic greenhouse conditions were broadly replaced by icehouse conditions (see glaciation in Fig. 1.7), leading to pronounced sea-level fluctuations (Davies 2008; Fielding *et al.* 2008). Several glacial episodes occurred during Serpukhovian and Bashkirian time and the presence of eustatic sea level fluctuations related to the Gondwanan ice sheet is now well established (Davies 2008; Holdsworth & Collinson 1988; Maynard & Leeder 1992; Waters & Condon 2012). Ice-melting occurred every 100 ka (Pointon *et al.* 2012b), suggesting a link to the Milankovitch 100 ka "short" eccentricity cycle (Pointon *et al.* 2012b; 2014) and brought with it potentially wetter atmospheric conditions and major eustatic sea-level transgressions.

A series of small, intracratonic basins is thought to have developed in northwestern Europe as a result of crustal extension in the latest Devonian and Mississippian time (Leeder 1976; Leeder & McMahon 1988). The "block and basin" topography generated during Late Devonian to Mid-Mississippian rifting (Leeder 1982) was gradually infilled by fluvio-deltaic sediments during Serpukhovian and Bashkirian times. The Shannon Basin is part of this series of intracratonic basins.

By the end of the Mississippian and into the Pennsylvanian, Ireland was located a few degrees north of the equator, based on palaeomagnetic evidence (Scotese & McKerrow 1990), and the Shannon Basin would have experienced a humid-tropical climate at this time, with some seasonal drying (Davies 2008). The

Shannon Basin basin fill succession is a far field (i.e. distant from polar ice sheets) record of glacio-eustatic sea level changes (see Ch. 5).

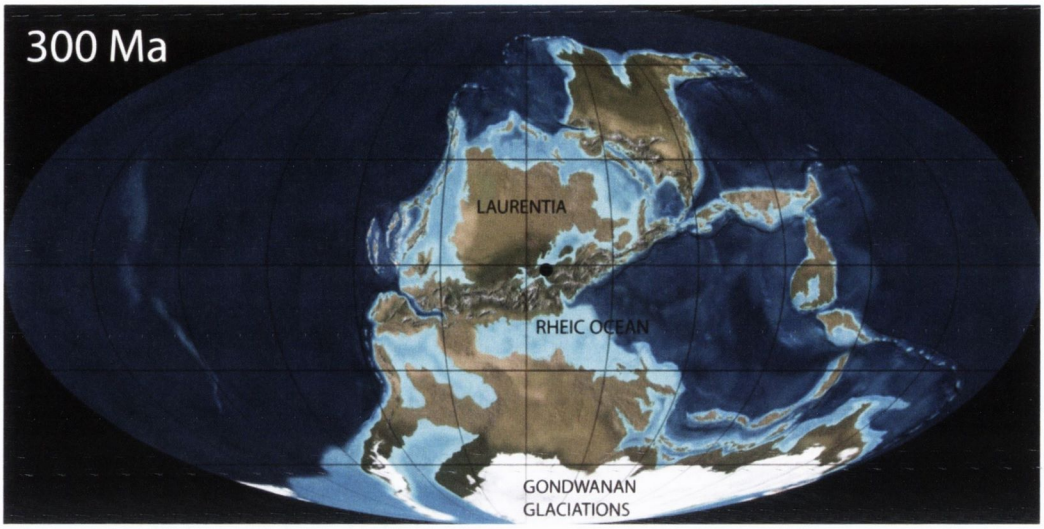

Fig. 1.7. Pennsylvanian paleogeography (based on Ron Blakey, University of Arizona - http://jan.ucc.nau.edu/~rcb7/mollglobe.html, reproduced with permission). Note glaciation in the southern hemisphere. Location of the Shannon Basin is shown by the black dot.

1.3.2 The Shannon Basin

Geological history and basin fill succession

The Shannon Basin (Fig. 1.8), which has also been variously termed the West Clare Basin (Gill 1979), Western Irish Namurian Basin (Martinsen 1989) and Clare Basin (e.g. Haughton *et al.* 2009), is located in Western Ireland. The basin developed during latest Devonian and early Carboniferous times as a result of crustal extension (Collinson *et al.* 1991). The basin centre is located above the Iapetus Suture, which is generally thought to follow the line of the present day Shannon Estuary (Martinsen & Collinson 2002). There is still some debate regarding basin orientation, lateral extent, and the location of sediment sources (see discussion in Wignall & Best 2000; Martinsen & Collinson 2002; Pointon *et al.* 2012a).

The basin fill succession consists of a shallowing-upward sequence of deep-water shales and siltstones (Clare Shale Formation) overlain by, and in part

laterally equivalent to, deep-water, sand-rich fan deposits (Ross Sandstone Formation), in turn succeeded by muddy slope (Gull Island Formation) and deltaic (Central Clare Group) deposits.

Carbonate production, which was extensive during the Tournaisian and Visean, ceased at approximately the beginning of the Serpukhovian (Late Mississippian), when it gave way to widespread deposition of non-calcareous, organic, dark shales (Clare Shale Formation). In the Bashkirian (Early Pennsylvanian), a thick (about 500 m) sequence of turbiditic siltstones and sandstones (Ross Sandstone Formation) was deposited in the central axis of the basin, with the Clare Shale Formation continuing to be deposited around the margins (Rider 1974; Barham et al. 2015; Fallon & Murray 2015).

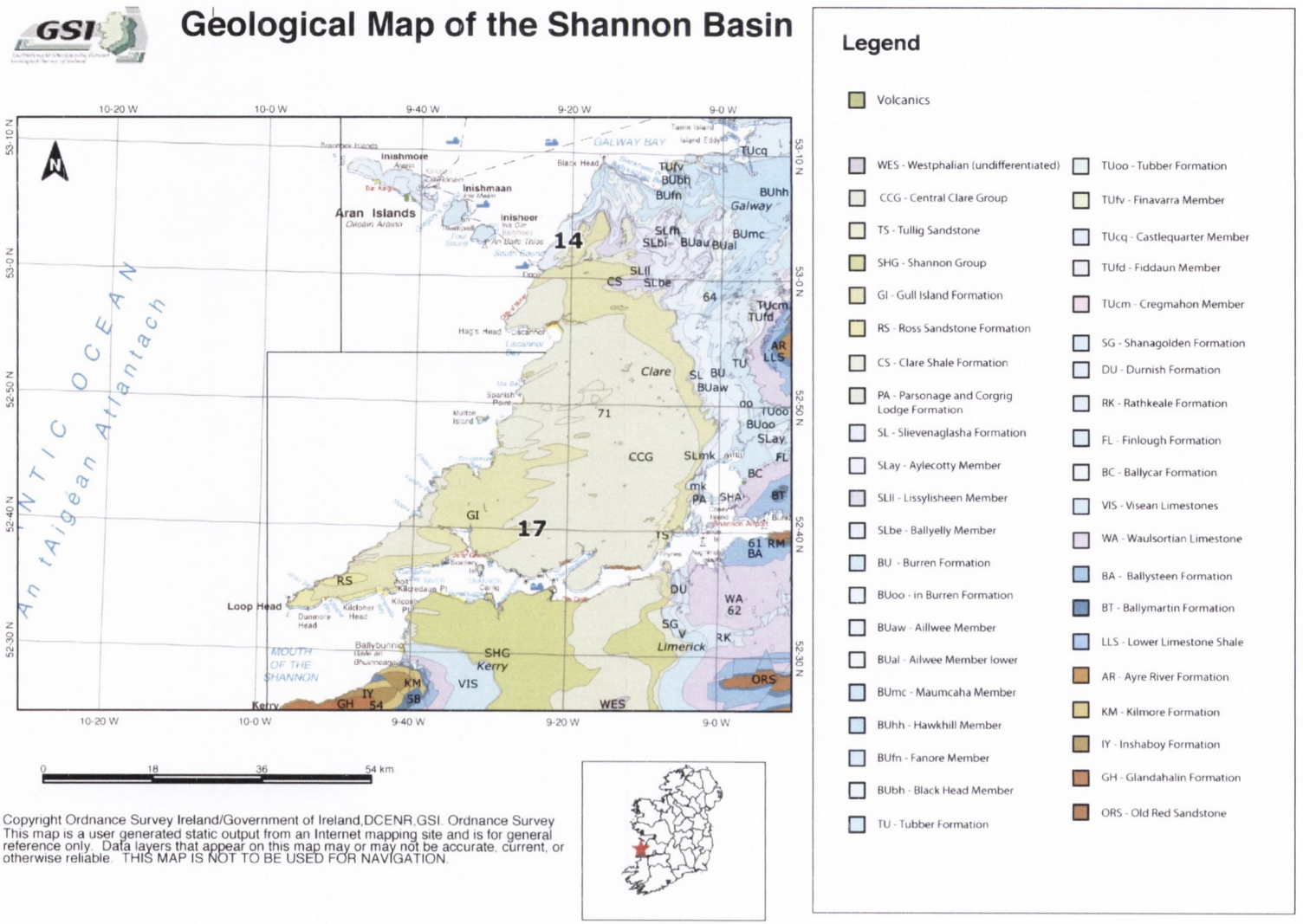

Fig. 1.8. Map showing location of the Shannon Basin and schematic stratigraphy through the basin axis (modified after GSI Datasets Public Viewer: http://spatial.dcenr.gov.ie/imf/imf.jsp?site=GSI_Simple).

The switch from carbonate production to terrigenous sedimentation, which occurred in Britain and Ireland, is thought to be related to very large river systems encroaching on the British Isles at this time mainly as a result of tectonic uplift (Sevastopulo 2009).

The lithostratigraphy of the upper part of the Shannon Basin succession was first established by Rider (1974). Pioneering biostratigraphic work by Hodson (1954a,b) and Hodson & Lewarne (1961) was fundamental in proving the existence of a mid-Carboniferous trough, with an axis roughly aligned with the present-day Shannon estuary. While this early biostratigraphic work focused mainly on the Clare Shale Formation, the present study is based on data recovered both from the Clare Shale Formation and from the Ross Sandstone Formation (Rider 1974; Collinson *et al.* 1991; Elliot 2000a,b; Lien *et al.* 2003; Pulham *et al.* 2014).

The Ross Sandstone Formation (Figs. 1.8-1.9) consists predominantly of deep-water turbiditic sandstone that prograded north-eastward over dark muds of the Clare Shale Formation. During deposition of the Ross Sandstone Formation, these muds continued to be deposited around the basin margins, to the north and to the east, where they replace and are coeval to the Ross Sandstone Formation.

In addition to coastal exposures, a set of 12 behind-outcrop wells, which were drilled by a consortium consisting of Statoil and University College Dublin (UCD) to target the sand-rich Ross Sandstone Formation, were examined during the course of this study.

The lithostratigraphic base of the Ross Sandstone Formation is defined at the entry of the first significant (over 5 cm thick) sandstone bed (at 183.2 m depth in borehole 10-CE-UCD-03 and 131.4 m depth in borehole 10-CE-UCD-05) (Pierce 2015). Many authors have informally taken the top of the Ross Sandstone Formation (boundary with overlying Gull Island Formation) to be at

a biostratigraphic boundary, namely the "*Phillipsoceras paucicrenulatum* band" (see Sevastopulo 2009, p. 279).

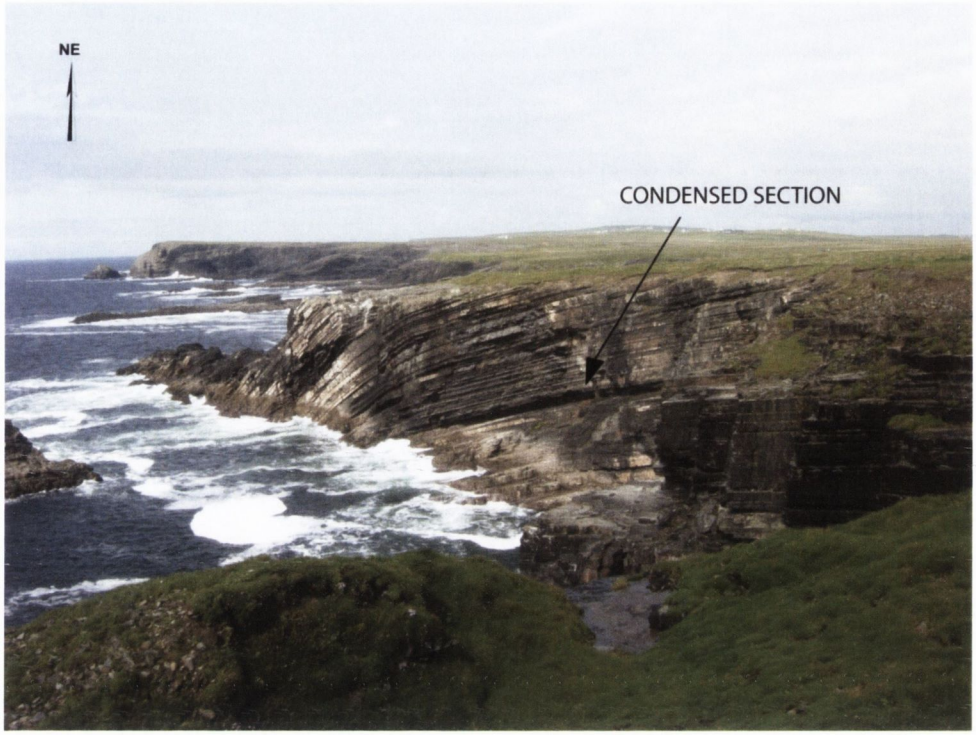

Fig. 1.9. View of the Ross Sandstone Formation on the north coast of Loop Head looking NE from Toorkeal. Recessed interval corresponds to a condensed section.

However, recent work at University College Dublin (UCD) has provided a lithostratigraphic definition for the base of the Gull Island Formation: it is now defined as the base of the first mass transport deposit above the topmost condensed section in the Ross Sandstone Formation (which is the "*Ph. paucicrenulatum* band") (Obradors-Latre pers. comm., 4 Nov 2014); this boundary corresponds to a change to a dominance of silty slumps over in-situ sandstones with the latter continuing to occur in the lower part of the Gull Island Formation (Pierce 2015).

Fig. 1.10. Photo of sand volcano on top of Ross Slump, Bridges of Ross, Co. Clare. Hammer is 35 cm long.

The Ross Sandstone Formation is a 500 m thick succession consisting mostly of sandstones (65% net clean sand: Pulham *et al.* 2014), with interbedded shales and slumped horizons. Channelized sandstones and slumped horizons become more common towards the top of the formation (Haughton 2009). Slumping occurs at several horizons within the Ross Sandstone Formation, with the most famous example being the Ross Slump (Gill 1979; Martinsen & Bakken 1990; Strachan 2002; Lien *et al.* 2003), which is well exposed near Bridges of Ross, on the north coast Loop Head (Fig. 1.8). Sand volcanoes (Fig. 1.10) are developed on the upper surface of the slump as a result of sediment-rich fluid extrusion and sandstone dykes are another common feature. The movement of the slump is thought to be to the north-east (Strachan 2002). The Ross Sandstone Formation is thought to have been deposited over a timespan of about 1.5 million years (Pulham *et al.* 2014).

The Gull Island Formation (Fig. 1.8) consists of extensively slumped slope deposits. It thins on the northern margin of the basin, where it was described by Hodson and Lewarne (1961) as the Ribbed Beds, the Cronagort Sandstone,

and the Doonagore Shale. The youngest part of the succession in the Shannon Basin (the Central Clare Group; R_{1b}-R_{2c}; Fig. 1.8) consists of five (and part of a sixth) cyclothems, each containing a unit of ammonoid-bearing black shale interpreted as a maximum flooding surface, overlain by complexes of deltaic siltstones and sandstones (Rider 1974; Pulham 1989).

The global significance of the Shannon Basin lies in its value as an analogue for deep-water reservoirs elsewhere (Martinsen & Collinson 2002). As such, it is often visited by representatives of industry and academia, who choose it as a popular site for field-courses each year. In particular, the deep-water turbidites of the Ross Sandstone Formation, which are beautifully exposed in the cliffs and foreshore of the Loop Head Peninsula, Co. Clare, Ireland (e.g. in Fig. 1.9), have proven to be an instructive analogue for deep-water sequences elsewhere which contain hydrocarbons (e.g. Gulf of Mexico: see Pyles 2008).

Thermal history and deformation

All rocks in the Shannon Basin have been affected by Variscan deformation, even though Ireland lies near the northern limits of the Variscan orogenic belt (Graham 2009). East-west trending Variscan cleavage is common on bedding surfaces (Haughton 2009).

The thermal history of the Shannon Basin has been investigated by examining the maturation of organic matter (Goodhue & Clayton 1999), conodont alteration indices (Clayton *et al.* 1989) and crystallinity of white mica and chlorite (Graham 2015). Maturation levels in the Shannon Basin are exceptionally high (e.g. vitrinite reflectance values of 4.5-6.5%; see Goodhue and Clayton 1999). Conodonts from limestone concretions have conodont alteration indices (CAI) of 5 (Clayton *et al.* 1989). These data suggest peak palaeotemperatures of 340-370°C (Fitzgerald *et al.* 1994), which are higher than expected (but consistent with development of pressure solution cleavage) and difficult to explain by tectonic overburden (Graham 2015). It is instead

attributed to fluid advective heating (the expulsion of hot fluids) from the Munster Basin to the south (Fitzgerald *et al.* 1994; Clayton & Baily 1999).

Condensed sections

In the Shannon Basin, ammonoids are concentrated in laterally extensive black shale bands, which are taken to represent intervals of sediment starvation and are often referred to as "condensed sections" or "ammonoid bands". These bands display small-scale variations in lithology from paper shale to clay-rich, resistant shale, to clay-rich siltstone. Within the assemblages in the condensed sections, ammonoids are the dominant faunal component and are accompanied by bivalves, orthoconic nautiloids, conodonts and plant material (see Ch. 2). While most condensed sections are thick (up to c.8 m) intervals of black shale, no condensed section is composed entirely of shale: in fact, lithological variation from shale to siltstone to sandstone is always observed at varying scales.

Ammonoids (Fig. 1.11) are usually preserved both as crushed external moulds (2D ammonoids), and occasionally as 3D shells within concretions, often referred to as "bullions" in Carboniferous sections (see e.g. Hodson 1954a,b).

Fig. 1.11. *Phillipsoceras circumplicatile* (Foord, 1903) preserved as a 2D mould (bottom centre of photo), Dunmore West band, (see Ch. 3 for locality details). Coin diameter is 23.25 mm.

The areal extent of condensed sections is primarily a function of the magnitude of eustatic sea-level rise, influenced by basin topography and subsidence or uplift rates (Waters & Condon 2012). The condensed sections are thought to record significant water depth increase (Davies 2008) and are have been interpreted as maximum flooding surfaces driven by eustatic rises in sea level (e.g. Martinsen *et al.* 1995; Hampson *et al.* 1997; Davies 2008).

A hierarchy of condensed sections was recognized in the Shannon Basin during the course of this study, leading to a broad subdivision into highly- and lesser-condensed sections:

- Highly-condensed sections are generally thick (c.1-8 m), dark in colour, shale-dominated, with several ammonoid-bearing horizons and ammonoids present throughout in varying abundance (see Fig. 1.12).
- Lesser-condensed sections are generally thinner, not as well-expressed, less distinctive in terms of colour (lighter), lithology (not as shale dominated, and tend to split laterally (see Fig. 1.13).

Fig. 1.12. Typical highly-condensed section, "*Ph. circumplicatile* band", Quilty, [77281/51701].

Fig. 1.13. Lesser condensed section (RVM) at Rinevella, [81840/49106] (see Ch. 2 for locality details) (a) frontal view, (b) view looking west.

The pioneering biostratigraphic work of Gillian Lewarne and Frank Hodson in the 1950s and 60s (1954a,b; 1961) recognized three main "ammonoid-bands" in the Ross Sandstone Formation. These are: "the *Homoceratoides prereticulatus* band", "the *Phillipsoceras circumplicatile* band" and "the *Phillipsoceras paucicrenulatum* band", each named after its most abundant taxon (Fig. 1.14).

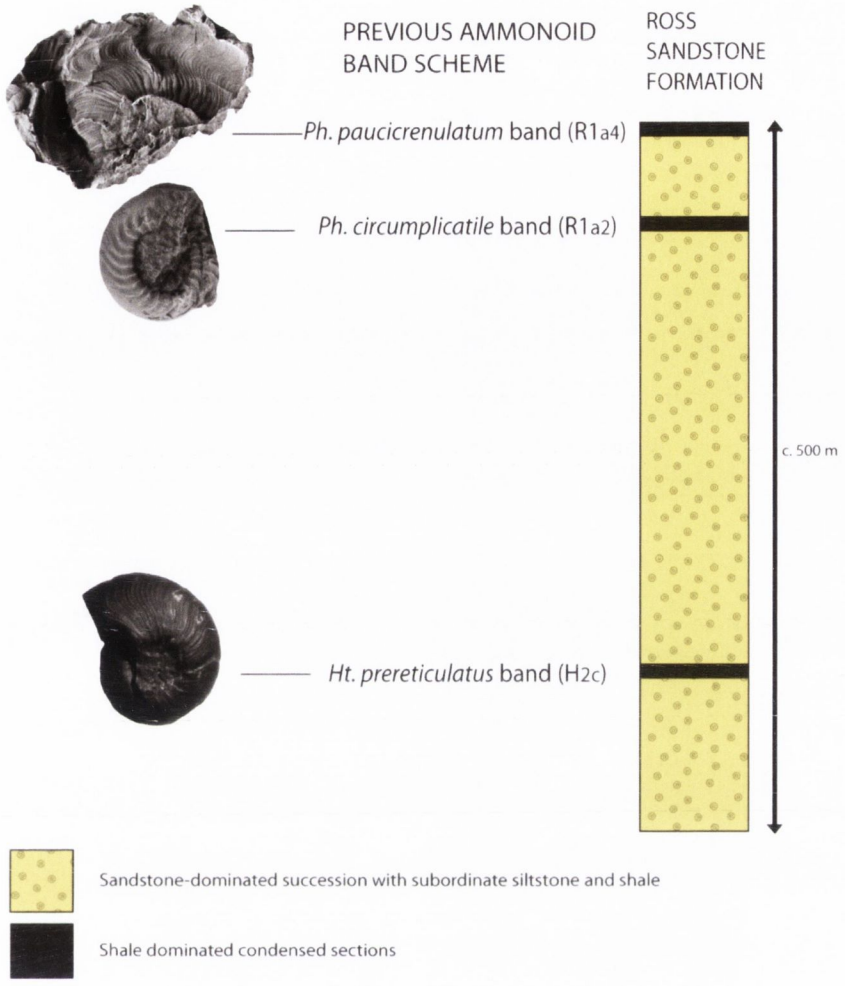

Fig. 1.14. Simplified stratigraphic column through the Ross Sandstone Formation, showing the three main previously-recognized ammonoid bands.

Several new condensed sections have since been recognized during the course of this study, in conjunction with detailed analysis of outcrop and borehole material undertaken by Colm Pierce and Arnau Obradors Latre at University College Dublin (UCD). At least ten ammonoid-rich shale intervals outside of condensed sections, as well as eight condensed sections, have been identified within the Ross Sandstone Formation. The new biostratigraphic data, coupled with the lithostratigraphical (i.e. physical) correlations, allow a very detailed dataset for the Ross Sandstone Formation to be described in Chapter 5.

At least eight condensed sections are now recognised within the Ross Sandstone Formation (see Ch. 5), resulting in duration of c.200 ka for each (see Ch. 5 for discussion).

1.3.3 Carboniferous ammonoid biostratigraphy

Alongside the key role of conodonts as biostratigraphic tools for identifying the Mid-Carboniferous boundary (Richards *et al.* 2011; Sevastopulo & Barham 2014; Barham *et al.* 2015; Fallon & Murray 2015), thick-shelled ammonoids (Fig. 1.15), plant spores and thin-shelled bivalves (Sevastopulo 2009) have been used to subdivide and zone the Carboniferous Period. Thick-shelled ammonoids are particularly useful in providing a high-resolution biostratigraphic framework for the late Mississippian to Pennsylvanian Subsystems (Waters *et al.* 2011).

System	Subsystem	Stage	Regional Substage	Ammonoid Biozone		Conodont Biozone	
				Index	Ammonoid	Shelf	Basin
Carboniferous (part)	Pennsylvanian (part)	Baschkirian (part)	Kinderscoutian	R1c	*Reticuloceras reticulatum*	*Idiognathoides corrugatus-Idiognathoides sulcatus*	
				R1b	*Retculoceras eoreticulatum*		
				R1a	*Hodsonites magistrorum*	*Declinognathodus noduliferous*	
			Alportian	H2c	*Vallites eostriolatus*		
				H2b	*Homoceras undulatum*		
				H2a	*Husdsonoceras proteus*		
			Chokierian	H1b	*Homoceras beyrichianum*		
				H1a	*Isohomoceras subglobosum*		
	Mississippian (part)	Serpukhovian	Arnsbergian	E2c	*Nuculoceras stellarum*	*Gnathodus postbilineatus*	
				E2b	*Cravenoceratoides edalensis*		
				E2a	*Cravenoceras cowlingense*	*Gnathodus bilineatus bollandensis*	
			Pendleian	E1c	*Cravenoceras malhamense*	*Kladognatus-Gnathodus girty simplex*	
				E1b	*Cravenoceras brandoni*		
				E1a	*Cravenoceras leion*		
			Brigantian	P2c	*Lyrogoniatites georgiensis*	*Gnathodus girty collinsoni*	*Gnathodus bilineatus*
				P2b	*Neoglyphioceras subcirculare*	*Lochriea nodosa*	
				P2a	*Lusitanoceras granosus*		
				P1d	*Paraglyphioceras koboldi*		
		?		P1c	*Paraglyphioceras elegans*		
		Visean (part)		P1b	*Arnsbergites falcatus*	*Mestognathus bipluti*	
			Asbian	P1a	*Goniatites crenistria*		
				B2b	*Goniatites globostriatus*	*Gnathodus bilineatus*	
				B2a	*Goniatites hudsoni*		
				B1	*Beyrichioceras*	*Lochriea commutata (part)*	
			Holkerian	BB	*Bollandites-Bollandoceras (part)*		

Fig . 1.15. Summary of ammonoid zones and subzones of the Serpukhovian-Bashkirian (therefore pertinent to the Shannon Basin) with diagnostic ammonoids and conodonts (after Fallon & Murray 2015).

Having said this, ammonoid faunas become more provincial during the Mississippian Subsystem of the Carboniferous. In fact, Korn *et al.* (2012) showed that middle and early-late Tournaisian faunas from Morocco closely resemble time-equivalent faunas from the United States, Europe, the Urals and Central Asia, but, later during the Late Visean, ammonoid provinces were formed. The genera *Entogonites* and *Goniatites* have wide palaeogeographical distribution, indicating cosmopolitism at the genus level at least until the end of the middle Visean (Korn *et al.* 2005; 2012). Even when provincial, ammonoids are extremely useful in more local studies (Lacchia 2012).

Western European ammonoid bands in the Serpukhovian/Bashkirian have been summarized several times in the literature, resulting in different classification schemes ranging from the simplest ones with only zonal index ammonoids listed (e.g. Riley *et al.* 1993; Wignall & Best 2000), to more complex ones, where index ammonoids are presented alongside diagnostic ammonoids and associated ammonoids (e.g. Waters & Condon 2012).

Thick-shelled ammonoids are particularly useful in providing a high-resolution biostratigraphic framework for the late Mississippian to Pennsylvanian Subsystems (Waters *et al.* 2011). Nikolaeva & Kullmann (1998) summarized ammonoid biostratigraphic schemes in the Serpukhovian and Bashkirian worldwide (Fig. 1.16).

Serpukhovian and Bashkirian ammonoid biostratigraphy for Northwestern Europe was first set up by Bisat (1924; 1928) and Bisat and Hudson (1943), and later developed by Ramsbottom (1969; 1971), largely resulting from work in the Central Pennine Basin of northern England (Waters *et al.* 2011). It is usually assumed that UK biostratigraphy is the most complete record of ammonid bands with diagnostic thick-shelled ammonoids (Ramsbottom *et al.* 1979; Davies *et al.* 1999).

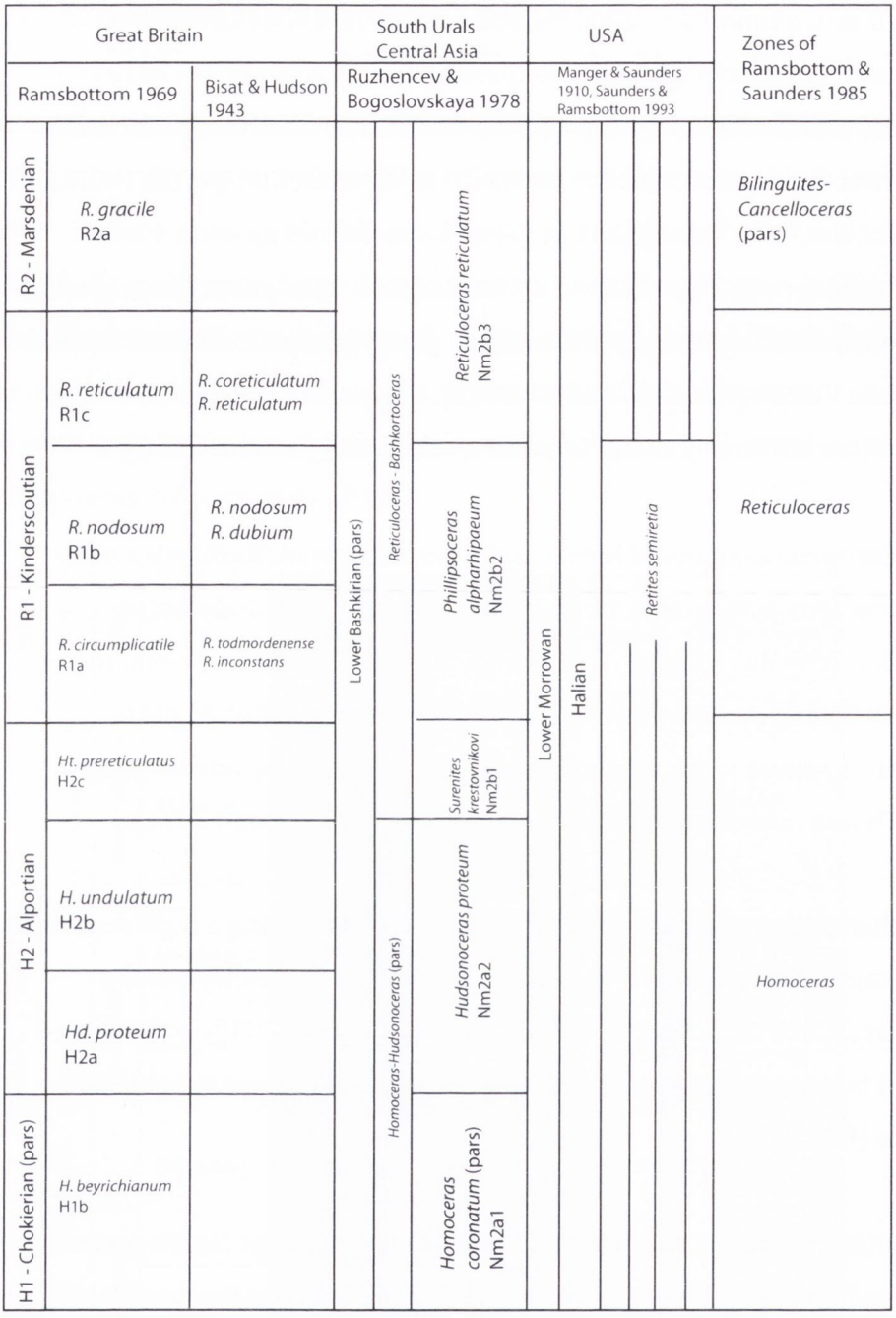

Fig. 1.16. Ammonoid-based correlation of the Serpukhovian and Bashkirian (after Nikolaeva & Kullmann 1998).

In a recent study, Fallon & Murray (2015) showed the biostratigraphic ranges of Irish conodonts sampled from two sections in the Clare Shale Formation spanning the mid-Carboniferous boundary. Their work suggested that the current definition of the mid-Carboniferous boundary (based on *D. noduliferus s.l.* first occurrence) and the suitability of the Arrow Canyon section as a Global

Boundary Stratotype Section and Point (GSSP) need to be reassessed because the evolutionary history of *D. noduliferus s.l.* on which the boundary is based is not applicable to Europe.

The biostratigraphic framework allows coeval basins to be compared (Davies *et al.* 1999). During the Serpukhovian and Bashkirian, at least 46 ammonoid-bearing bands (Fig. 1.17) are known from the Pennine Basin, UK (Riley *et al.* 1995; Davies *et al.* 1999), providing a framework that the Shannon Basin biostratigraphy results can be compared to (see Chapter 5). Ammonoid bands in the Lublin Coal Basin, Poland, which were described by Dzik (1997, p. 148) were seen to be only partly similar to those in the Pennine Basin (Davies *et al.* 1999).

In summary, ammonoids are the organism of choice for several biostratigraphic studies and the obvious choice in the Shannon Basin, where they dominate the faunal assemblages.

Regional Substage	ZONES			WESTERN EUROPEAN MARINE BANDS	
	Index	Ammonoid	Index	Diagnostic ammonoid	Associated ammonoids
KINDERSCOUTIAN	R1c	*Reticuloceras reticulatum*	R1c5		Butterly MB- Lingula
			R1c4	*R. coreticulatum*	*Anthracoceratites sp., Homoceratoides divaricatus, Hudsonoceras ornatum, R. reticulatum (late form), V. striolatus*
			R1c3	*R. reticulatum*	*Homoceratoides prereticulatus, R. davisi, R. regularum, Vallites sp., V. striolatus*
			R1c2	*R. reticulatum*	
			R1c1	*R. reticulatum*	
	R1b	*Reticuloceras eoreticulatum*	R1b3	*R. stubblefieldi*	*Vallites striolatus, Hudsonoceras ornatum, R. moorei, R. regularum*
			R1b2	*R. nodosum*	*Homoceras spiraloides, Vallites striolatus*
			R1b1	*R. eoreticulatum*	*Reticuloceras sp.*
	R1a	*Hodsonites magistrorum*	R1a5	*R. dubium*	*Reticuloceras sp., R. adpressum*
			R1a4	*R. todmordenense*	*Homoceras sp., Reticuloceras sp., Ph. (R.) paucicrenulatum, R. adpressum*
			R1a3	*Ph. (R.) subreticulatum*	*Homoceratoides sp., Reticuloceras pulchellum*
			R1a2	*Ph. (R.) circumplicatile*	*Homoceratoides sp., Vallites henkei*
			R1a1	*Hod. magistrorum*	*R. compressum*
ALPORTIAN	H2c	*Vallites eostriolatus*	H2c2	*Ht. prereticulatus*	*Homoceras sp.*
			H2c1	*V. eostriolatus*	*Ho. undulatum*
	H2b	*Homoceras undulatum*	H2b1	*Ho. undulatum*	*Ho. beyrichianum, Ho. smithii*
	H2a	*Hudsonoceras proteus*	H2a1	*Hud. proteus a,b & c*	*Homoceras smithii*
CHOKIERIAN	H1b	*Homoceras beyrichianum*	H1b2	*Isohomoceras sp. nov.*	*Homoceras sp.*
			H1b1 a & b	*Ho. beyrichianum*	*Ho. diadema, Iso. subglobosum, Isohomoceras sp.*
	H1a	*Isohomoceras subglobosum*	H1a3	*I. subglobosum*	
			H1a2	*I. subglobosum*	
			H1a1	*I. subglobosum*	
ARNSBERGIAN	E2c	*Nuculoceras stellarum*	E2c4	*N. nuculum*	*C. darwenense, Ct. fragile, E. bisulcatum, Kazakhoceras hawkinsi*
			E2c3	*N. nuculum*	
			E2c2	*N. nuculum*	
			E2c1	*N. stellarum*	*Fayettevillea holmesi*
	E2b	*Cravenoceratoides edalensis*	E2b3	*Ct. nitidoides*	*Cravenoceras sp., Eu. rostratum*
			E2b2a-c	*Ct. nitidus*	*Cravenoceras sp., C. subplicatum, Crevenoceratoides sp., Eumorphoceras sp., E. bisulcatum, E. leitrimense, Fay. holmesi, Glaphyrites sp., Gl. kettlesingense*
			E2b1a-c	*Ct. edalensis*	*Cravenoceras sp., C. subplicatum, Fay. cf. holmesi*
	E2a	*Cravenoceratoides cowlingense*	E2a3	*Eumorphoceras yatesae*	*Cravenoceras sp., C. gairense, Eumorphoceras sp.*
			E2a2beta	*Anthracoceras*	Saleswheel Marine Band
			E2a2alpha	*C. gressinghamense*	*C. cf. gairense, Eumorphoceras sp.*
			E2a2	*Eu. ferrimontanum*	*Cravenoceras sp., C. gairense, E. erinense, Kazakhoceras scaliger*
			E2a1a-c	*C. cowlingense*	*Cravenoceras sp., E. grassingtonense*
PENDLEIAN	E1c	*Cravenoceratoides malhamense*	E1c2		Blacko Marine Band- Sanguinolites
			E1c1	*C. malhamense*	*Cravenoceras sp., Eumorphoceras sp.*
	E1b	*Cravenoceratoides brandoni*	E1b2 a & b	*Tumulites pseudobilinguis*	*Edmooroceras angustum, Ed. hudsoni, Ed. stubblefieldi, Eumorphoceras sp., Tumulites sp.*
			E1b1	*C. brandoni*	*Edmooroceras stubblefieldi*
	E1a	*Cravenoceras leion*	E1a1 a-c	*C. leion*	*Cravenoceras sp., Cousteauceras rota, Eumorphoceras sp., E. involutum, Ed. bisati, Ed. medusa, Ed. pseudocoronula, Ed. tornquinsti*

Fig. 1.17. Ammonoid zones and subzones in the Serpukhovian and Bashkirian with diagnostic ammonoids, indices and associated ammonoids (after Riley *et al.* 1995; Waters & Condon 2012). For a list of abbreviations, see p. 26i.

1.3.4 Previous correlation schemes

Ammonoid biostratigraphy in the Shannon Basin has been studied before and a summary of attempts previous to this study is presented here.

Hodson (1954a,b) and Hodson & Lewarne (1961) were the first to publish detailed records of ammonoids in the Clare Shale Formation (Table 1.1).

Dr Gillian Lewarne was the first to investigate the ammonoid biostratigraphy of the Ross Sandstone Formation in the 1950s and recorded her findings in unpublished notes, which were kindly made available at the start of the present project. Her stratigraphic framework, in which she recognizes four condensed sections, is summarized in Table 1.2 and the assemblages found in various Loop Head localities are detailed later (Chapter 5).

Faunal Band	Fauna and Lithology
I	*Reticuloceras subreticulatum, Vallites (Homoceras) henkei, Dimorphoceras* sp. Shale, about 4.6 m
H	*Phillipsoceras (Reticuloceras) circumplicatile, V. (Homoceras) henkei* Shale, 1.4 m
G	*Phillipsoceras (Reticuloceras) circumplicatile, Homoceratoides varicatus, V. (Homoceras) henkei* Shale, 0.30 m
F	*R.* aff. *compressum, R.* sp., *V. (Homoceras) henkei, Hod. magistrorum (Ho.* sp. nov. *A), Dimorphoceras* cf. *looneyi* Shale, 0.30 m
E	*Ht.* aff. *prereticulatus, Ho.* sp. nov., *Dimorphoceras* sp. nov. Shale, 0.30 m
D	*Ho. undulatum, Dimorphoceras* sp. nov. Shale, 0.30 m
C	*Hudsonoceras proteus, Ho. smithii, Dimorphoceras* sp. nov. Shale, 1.22 m
B	*Ho. beyrichianum* group Shale, 2.13 m
A	*Ho. beyrichianum* group, *Isohomoceras (Homoceras)* aff. *subglobosum*

Table 1.1. Hodson's faunal band scheme for the lower Clare Shales, (after Hodson, 1954a, p. 265). Original measurements in feet/inches have been converted to metric values and taxonomic details have been updated.

Name of condensed section ("marine band") (also see Fig. 5.4 for stratigraphical position of these condensed sections)	Condensed section localities /name of succession in between the bands (for locality names see Ch. 3, Fig. 3.1)	Main faunal components
	TULLIG SANDSTONE GROUP	
MB4	OUGHTERARD-ROSS-MONEEN-FODRY MB (i.e. marine band)	*Phillipsoceras (Reticuloceras) paucicrenulatum, Dunbarella*
	ROSS SLUMP GROUP CARRIGAHOLT SUCCESSION	
MB3	QUILTY-CLOGHUANSAVAUN MB AND KILCREDAUN MB	*Phillipsoceras (Reticuloceras) circumplicatile, Phillipsoceras (Reticuloceras) paucicrenulatum, Caneyella*
	LOOP HEAD SUCCESSION, KILCREDAUN SUCCESSION	
MB2	LISDOONDALHEN MB & LIGHTHOUSE MB	*Phillipsoceras (Reticuloceras) circumplicatile, V. (H.) henkei*
	DUNMORE HEAD-KILTRELLIG STRAND-REHY HILL SUCCESSION	
MB1	DOONDALHEN MB- READING ROOM	*Homoceratoides prereticulatus*

Table 1.2. Simplified succession showing the four condensed sections ("marine bands") identified by Dr Gillian Lewarne (modified from unpublished notes). Succession nomenclature is presented as mapped by Lewarne.

The presence of four condensed sections has been confirmed in the present study, with additional assemblage data, as well as new localities and condensed sections being recognized.

Following on from the work of Hodson and Lewarne (Hodson 1954a,b; Hodson & Lewarne 1961), Rider (1974) was responsible for establishing the lithostratigraphy of the upper part of the basin fill (three-part division into Ross Sandstone Formation, Gull Island Formation and Central Clare Group). He recorded three condensed sections, or ammonoid bands, in the Ross Sandstone Formation on Loop Head: the *Ht. prereticulatus* band, the *Ph. (R.) circumplicatile* band and the *Ph. (R.) paucicrenulatum* band. Rider (1974) also states that these bands can be used in correlation with the Clare Shale Formation further north. Gill (1979) took up Rider's (1974) correlation scheme

in his seminal work on slumping and sliding in the Shannon Basin (his "West Clare Namurian Basin").

Since then, several other correlation schemes have been presented in the literature using both condensed horizons and slumped horizons. The regional cross section for the Ross Sandstone Formation in Collinson *et al.* (1991) (see Fig. 1.18) includes five ammonoid bands, namely, in stratigraphical order:

- "*Ho. smithii/Hud. proteus* band"
- "*Ht. prereticulatus* band"
- "*Ph. (R.) circumplicatile* band"
- "*Ph. (R.) paucicrenulatum-R. subreticulatum* band"
- "*R. dubium* band"

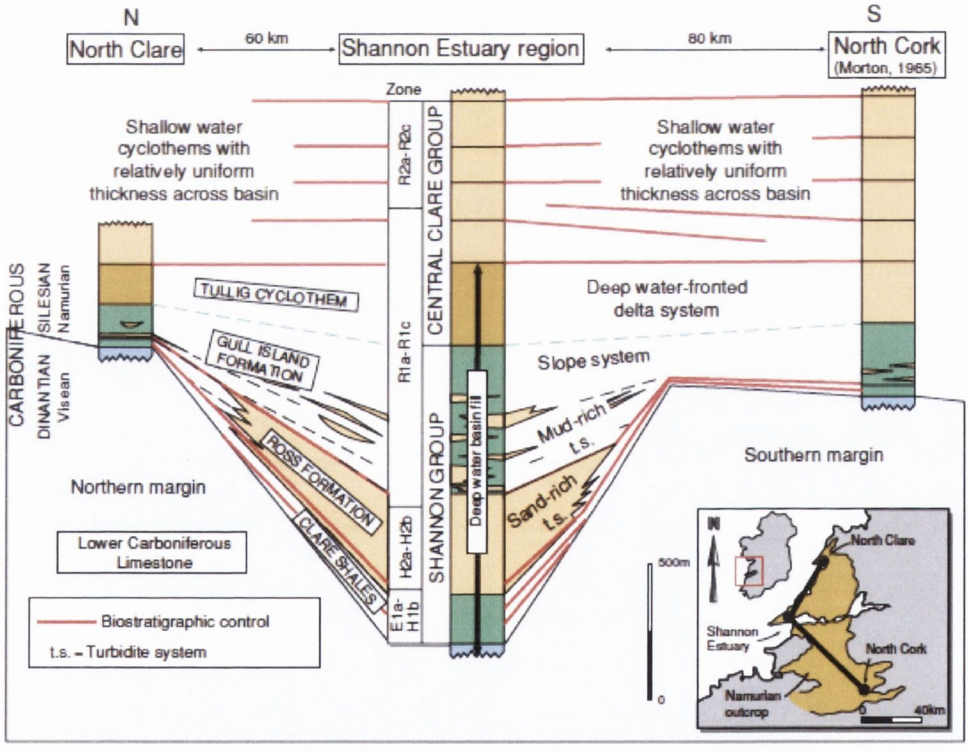

Fig. 1.18. Stratigraphy of the Shannon Basin from North Clare, through the Shannon Estuary to North Cork (after Martinsen & Collinson 2002; Collinson *et al.* 1991).

Wignall & Best (2000; p. 62) illustrate a similar correlation scheme (Fig. 1.19), where the bands in the Ross Sandstone Formation in stratigraphical order are:

- "?*Ho. undulatum* band"
- "*Ht. prereticulatus* band"
- "?*Ph. circumplicatile* band"
- "*R. subreticulatum* band"
- "*R. dubium* band"

The question marks before the "*Ho. undulatum* band" and the "*Ph. circumplicatile* band" denote uncertainty in recognition of the bands.

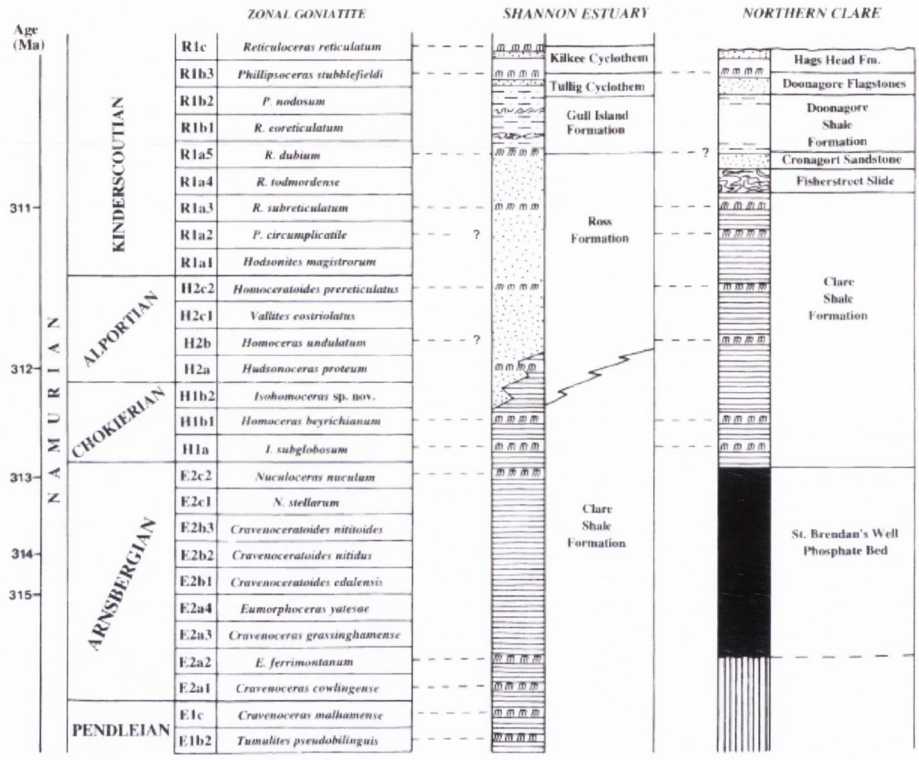

Fig. 1. 19. Summary and comparison of lithostratigraphy and biostratigraphy of the outcrops of northern county Clare ad along the Shannon Estuary, showing ammonoid bands in the Ross Sandstone Formation (after Wignall & Best 2000; p. 62).

Chapin *et al.* (1994) provided a detailed correlation of the Ross Sandstone across various outcrop localities. They include four condensed section in the Ross Sandstone Formation: these are the "*Ho. smithii/Hud. proteus* band", the "*Ht. prereticulatus* band", the "*Ph. (R.) circumplicatile* band" and the "*Ph. (R.) paucicrenulatum* band".

Kelk (1960) studied the Clare Shale Formation sections in Ballybunion, Co. Kerry, and also included details of the lowermost Ross Sandstone Formation at Ballybunion: he recorded the "*Hud. proteus* band" at the waterfall produced by Glenachoor Stream [86837/44563], although he did not record the presence of *Ho. smithii* at this locality. He placed the "*Ht. prereticulatus* band" 6.4 m above the "*Hud. proteus* band" (Kelk 1960; p. 34), although these two bands were found to be separated by at least 50 m of succession in the present study (see section 5.4).

Lien *et al.* (2003) also provided detailed correlations within the Ross Sandstone Formation based on 13 measured sections both on Loop Head and Ballybunion. He included, in stratigraphic order:

- "*Ho. smithii* band"
- An unidentified "marine band"
- "*Ht. prereticulatus* band"
- "*Ph. (R.) circumplicatile* band"
- "*Ph. (R.) paucicrenulatum* band"
- "*Ph. (R.) paucicrenulatum/R. dubium* band"
- "*R. dubium*" band

More recently, Pyles (2008) constructed a correlation panel for the Ross Sandstone Formation with the following six condensed sections in stratigraphic order:

- "*Ho. smithii/Hud. proteus* band"
- "*Ho. undulatum* band"
- "*Ht. prereticulatus* band"
- "*Ph. (R.) circumplicatile* band"
- *Ph. (R.) paucicrenulatum* band"
- "*R. dubium* band"

However, the presence of a "*Ho. undulatum* band" was not confirmed in the present study nor is it recorded in other studies.

The top of the Ross Sandstone Formation is usually taken at the "*R. dubium*" band (Collinson *et al.* 2001; Lien *et al.* 2003; Pyles 2008), but this was not confirmed in the present study (see Chapter 5, section 5.4), which did not find *R. dubium* on the Loop Head sections (see Chapter 2).

As well as working on the Ross Sandstone Formation, Lewarne, together with Hodson, mapped the Clare Shale Formation in the north Clare exposures (Hodson 1954a,b; Hodson & Lewarne 1961). Their ammonoid band scheme is presented in Chapter 2, Table 2.1.

Braithwaite (1993; 1995), during her investigation of the stratigraphy of the mid-Carboniferous boundary, reassessed the biostratigraphy of the Clare Shale Formation at Inishcorker (see Chapter 2 for locality and ammonoid assemblage details): she recorded the lowest ammonoid band at Inishcorker as *Nuculoceras nuculum* (E_2c_2) and the topmost ammonoid band as *Hudsonoceras proteus* (H_2a_1). However, the present study found that the succession in Inishcorker ranges in age from Pendleian at its base (E_1) to Kinderscoutian at the top (R_{1a} ammonoid biozone).

There are clear inconsistencies in the ammonoid data presented above concerning the Shannon Basin biostratigraphy, warranting further investigation.

1.4 Project aims

Major project aims were:

- To develop a detailed biostratigraphic framework for the Ross Sandstone Formation, both reassessing and building on previous biostratigraphic work by Lewarne and Hodson (1954a,b; 1961).
- Despite the numerous existing correlation schemes detailed in Section 1.3, since the fundamental work of Hodson and Lewarne (1954a,b; 1961), no additional details of faunas at a given locality, such as numbers and proportions of taxa, have been provided in previous studies (except Kelk's 1960 thesis which contains details of faunas in the Clare Shale Formation). This means that it is altogether unclear how a certain band acquired a particular name, resulting in turn in uncertainty in biostratigraphic frameworks and poor reproducibility of results. A major aim of this work has been to make this information available.
- To integrate and collaborate with parallel doctoral research at UCD, which used both outcrop data and behind-outcrop drilling data to establish detailed sedimentological and lithostratigraphical correlations within the Ross Sandstone Formation, thereby allowing biostratigraphy to be cross-checked against lithostratigraphical correlations.
- To provide an integrated high-resolution subdivision of the Ross Sandstone Formation, stemming from this collaborative approach. This would then underpin applied research of direct relevance to subsurface reservoir description (see Chapter 5 for further details).
- To further the understanding of the genesis and significance of ammonoid-bearing condensed sections in the Shannon Basin and, by extension, in other coeval basins.
- To examine ammonoids in the Clare Shale Formation and build an overall picture of ammonoid occurrence in the Shannon Basin.
- To assess the significance of ammonoid occurrences in terms of previous palaeosalinity models (see Chapter 4 for further details).

Additional, more specific aims that emerged during the course of the project were:

- To clarify the stratigraphic position and context of key exposures visited on training courses (e.g. Rehy Cliff on the south coast of Loop Head).
- To test the lateral continuity of slumped horizons in the Ross Sandstone Formation by high-resolution correlation of sections on the north and south Loop and across the Shannon estuary.
- To investigate lateral changes in the character of some of the condensed horizons, in particular:
  - Lateral continuity and changes in expression of the Dunmore Head band, which is provisionally correlated with the Senan's Beach band, as it is traced westwards from Aillnagreagh (see Ch. 2 for locality details).
  - Further fieldwork in Ballybunion, Co. Kerry, will confirm whether the *R. dubium* band is present at the top of the Ross Sandstone Formation and whether *Ph. paucicrenulatum* and *R. dubium* are separated by 60 m of sediment, as suggested by various authors (e.g. Collinson *et al.* 1991) (i.e. is there major lateral offset of sandstone packages in the uppermost Ross Sandstone Formation).
- To examine sections at Inishcorker and Foynes Island. Because of their palaeogeographic location on the eastern part of the Shannon Basin, these sections provide important information on the diachroneity in the onset, lateral extent and larger scale overall architecture of the Ross Sandstone Formation and of the basin fill succession in general.

1.5 Material and methods

Training

Following literature review, the first stages of the project involved locating ammonoid type specimens and key reference material from museum collections. Travel to museums allowed description and photography of key ammonoid taxa. Study of reference material in the following museum collections was made: the Geological Museum, Trinity College Dublin (catalogue numbers prefixed TCD); the National Museum of Ireland (catalogue numbers prefixed NMING); the British Geological Survey, Keyworth, UK (catalogue numbers prefixed GSM); the Manchester Museum (catalogue numbers prefixed MANCH) and the Geological Sciences Museum of the University of Göttingen (catalogue numbers prefixed GZG.INV).

Training on species recognition was obtained during a three-day course led by Dr Nick Riley at British Geological Survey, Keyworth, UK. Further training and consultation with ammonoid experts (mainly Dr Dieter Korn, Museum für Naturkunde, Berlin, and Svetlana V. Nikolaeva, Natural History Museum, London) was made during the course of the project.

Sampling

The project involved sampling from both outcrop sections and borehole material. Samples were collected over several seasons of fieldwork (2012-2014). When sampling outcrop, a sedimentary log was produced for each condensed section (see Chapter 2 for sedimentary logs at each locality): this was then used as an additional tool for correlation (see Appendix B for borehole logs). In the case of delicate specimens, photographs were taken in the field prior to sampling. Details of each field locality are presented in Chapter 2.

Boreholes from behind-outcrop drilling were split so that one half (held in UCD) will be preserved for future reference and study, and the remaining half (held in Statoil Headquarters, Bergen, Norway) could be sampled for biostratigraphy and other analytical studies such as QEMSCAN (see Chapter 5). Sedimentary logging of condensed sections in the borehole material was undertaken prior to core sampling.

Sample analysis

Sampled specimens from both borehole and outcrop material were described and identified in Trinity College Dublin. A stereo-microscope was used to view the specimens and cameral lucida drawing was used to produce diagrammatic tracings of ammonoid ornament (see Ch. 3). Samples taken from borehole material held at Statoil headquarters in Bergen, Norway, were shipped to Trinity College Dublin for analysis. Once specimens were identified, they were labelled and deposited in the Geological Museum, Trinity College Dublin.

1.6 Thesis plan

Following a broad introduction to the contents of the thesis in the present chapter, a description of the assemblages of different taxa at each condensed section is given in Chapter 2, which also contains locality details. The systematic palaeontology of ammonoids and bivalves is dealt with in Chapter 3, which also contains details of palaeoecology. Chapter 4 concerns the distribution of ammonoids in the Shannon Basin and the implications for palaeosalinity. Chapter 5 contains details of first occurrences of taxa and results of biostratigraphic analysis. This chapter also contains details of sample analysis via analytical techniques such as Quantitative Evaluation of Materials by Scanning Electron Microscopy (QEMSCAN) and X-ray Diffraction Analysis (XRD). A summary of conclusions is presented in Chapter 6. The Appendices contain: ammonoid conch parameter measurements (Appendix A), sedimentary logs of boreholes (Appendix B), palynological analysis results (Appendix C) and XRD analysis results (Appendix D).

Chapter 2 Ammonoid Localities

2.1 Sampled fossiliferous localities

Detailed sampling of ammonoids and other faunas was undertaken during several seasons of fieldwork in the Shannon Basin, Western Ireland, targeting all known and several new fossiliferous localities within the Ross Sandstone Formation, as well key localities within the Clare Shale Formation, which are thought to be time equivalents to the Ross Sandstone Formation.

Most localities were located on the Loop Head Peninsula (Fig. 1.8), where the Ross Sandstone Formation crops out in spectacular coastal exposures. Fieldwork was also undertaken south of the basin axis, north of Ballybunion, Co. Kerry, where the Clare Shale and Ross Sandstone Formations are both exposed in dramatic coastal sections. Within the Ross Sandstone Formation, ammonoid-bearing, highly condensed sections were the main target of sampling, but lesser-condensed (*sensu* Chapter 1) ammonoid-bearing silt and sand-prone sections were also examined (also see Chapter 4). For each locality, geographic location, lithological details and faunal content are presented, along with sedimentary logs (a legend valid for all sedimentary logs is presented in Fig. 2.3). All faunal tables show the oldest levels at the bottom and the youngest at the top. Gillian Lewarne's unpublished data on the faunal composition of localities sampled during her PhD research are also included, where available. Faunal details can be compared to Hodson's (1954a) generalized succession of faunal bands for the H_1 to R_1 biozone interval (corresponding to the lower Clare Shales in North Clare) (Chapter 1, Table 1.1). Whenever a given locality could be correlated with confidence with a section from the core material, this was noted (for full details of correlation, see Chapter 5). More general details are presented for classic localities in north Co. Clare, located north of the basin axis, which were visited and sampled mainly

to further knowledge of ammonoid taxonomy through the study of 3D ammonoids.

Localities close to the basin axis in the Shannon Estuary (namely Inishcorker and Foynes Island) were included in order to obtain a more complete biostratigraphic framework for the basin. Lastly, Irish localities with age-equivalent ammonoids in the Leinster Coalfield (Luggacurren and Killeshin Glen, Co. Laois) were investigated. It is recognized that localities under the Clare Shale Formation heading are often coeval with Ross Sandstone Formation deposits on Loop Head; localities are presented in broad stratigraphic order where possible.

Firstly, localities where the Clare Shale Formation was sampled are presented. In the case of Ross Sandstone Formation localities, those in Co. Kerry are listed before those in County Clare.

2.2 Locality details

2.2.1 Clare Shale Formation

2.2.1.1 Fisherstreet Bay

Fisherstreet Bay, Doolin, North Co. Clare, is located where the Aille River reaches the Atlantic Ocean [06640/96316] (Fig. 2.1); it can be reached by walking along the shoreline south from Doolin pier. The section was described by Hodson & Lewarne (1961) and encompasses shale beds that are part of the top of the Clare Shale Formation, and overlying siltstones and sandstones, previously referred to as "Ribbed Beds" (Hodson & Lewarne 1961), which record the transition of Clare Shale Formation to coarser grained strata that have been assigned to the Gull Island Formation by Rider (1974). When traced in a south-westward direction along the shoreline, these topmost sandstones and siltstones beds are overlain by the Fisherstreet Slide, a c.20 m-thick slump unit accessible from the track running from the village of Fisherstreet towards the Cliffs of Moher (Gill 1979).

The Clare Shale section at Fisherstreet (Fig. 2.2) is c.20 m-thick and it consists of alternating black and grey shales, with frequent mm-scale horizons with evenly disseminated, mm-scale pyrite crystals that are continuous along bedding, as well as silt-rich shales with muddier intercalations.

Only the lowest 6 m of section are accessible and these were sampled and measured in this study. The basal part of the section, at beach level, has a brecciated horizon, with black shale clasts and sandy matrix, for which reference could not be found in past studies. This particular horizon is interpreted as having formed much later than the rest of the section, and being Quaternary in age.

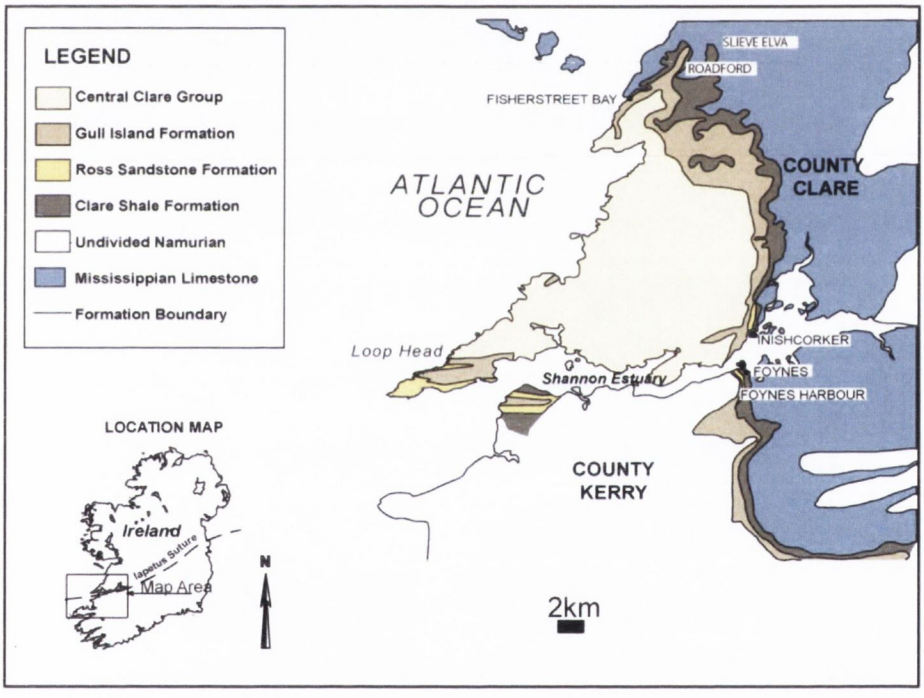

Fig. 2.1. Location map showing Fisherstreet Bay sampling locality [06640/96316] and geological map of the Shannon Basin showing the locality and regional geology (Google Earth map).

Faunal Composition

Hodson & Lewarne (1961) recorded ammonoids of *Reticuloceras* age, crinoid ossicles and *Dunbarella* sp. bivalves from the Fisherstreet section (see Table 2.1). While present sampling confirmed the presence of these taxa, it was found that ammonoids were far more abundant than previously thought: several shale beds where no fossils had been recorded in Hodson & Lewarne (1961, p. 312) were instead found to contain abundant faunas and, furthermore, the assemblages were found to be more diverse than previously thought. The same observation is true for other localities in the basin (see Chapter 4, for details on ammonoid distribution in the basin).

Ammonoid bed-by-bed abundance counts broadly range from abundant to frequent, to rare, to very rare, and this is sometimes independent of lithology: in fact, it is usually but not always true that the darkest (inferred to be most condensed) shale contains the most specimens.

Fig. 2.2. Fisherstreet Bay sampling site, looking towards the Fisherstreet Slide [06640/96316]. Hammer for scale.

Overall, ammonoid taxa at Fisherstreet Bay span the H_{2c} to R_{1a} biozones (Alportian and Kinderscoutian substages). A typical fauna of ammonoids, bivalves, nautiloids and plant material is present throughout the section, concentrated in several mm-scale horizons. Plant fragments are often pyritized and reach large sizes, up to 30 cm in length. The basal bullions (F02; see Fig. 2.4) are large (up to 1 m in length of the long axis) and contain abundant, high-quality *Ht. prereticulatus* solid specimens. Interestingly, towards the top of the section, *Dunbarella* sp. (with minor *Caneyella* sp.) becomes the dominant element of the fauna and ammonoids are rare.

Crinoid stems were found to be abundant in one horizon c.1 m from the base of the section (around F06) along with a crinoid calyx; the crinoid could be identified as *Rhabdocrinus*, which is thought to be a deep-water crinoid (Prof Sevastopulo, pers. comm. 2014). Crinoid ossicles are also reported from a "hard shale" towards the top of the section (Hodson & Lewarne 1961) and a loose block with two zaphrentid-type corals and crinoid material was found in this area (Dr John Murray, pers. comm., 2014): this block also contains the ammonoids *R.* cf. *subreticulatum* and *Reticuloceras/Phillipsoceras* sp., and is therefore thought to have detached from the "hard shale" horizon mentioned in Hodson & Lewarne (1961, p. 312): "*hard shale with crinoid ossicles and R. cf. paucicrenulatum.*" What appears to be the same horizon is also apparently present at Foynes Island (see section 2.2.1.4).

Lithological and faunal description	Thickness (m)
Fisherstreet slumped beds	9.14m
Ribbed Beds: finely-bedded black shales with hard ribs and rows of small nodules	12.19m
Bullions with *Reticuloceras* sp.	-
Shales	0.102m
Hard shale with crinoid ossicles and *Ph. (R.)* cf. *paucicrenulatum*	-
Shales	0.051m
Bullions with *Ph. (R.)* cf. *paucicrenulatum*, *R. subreticulatum* and abundant *Dunbarella* cf. *rhythmica*	-
Shale	0.610m
Flat Bullions with *Ph. (R.)* cf. *paucicrenulatum*	-
Shales	0.305m
Occasional small nodules	-
Shales	1.83m
Layer of small flat nodules	-
Shales to beach level	2.44m
Shales at lowest level containing *Reticuloceras* sp.	Base

Table 2.1. Summary of Hodson's log for Fisherstreet Bay (after Hodson & Lewarne 1961). Original measurements in feet/inches have been converted to metric values.

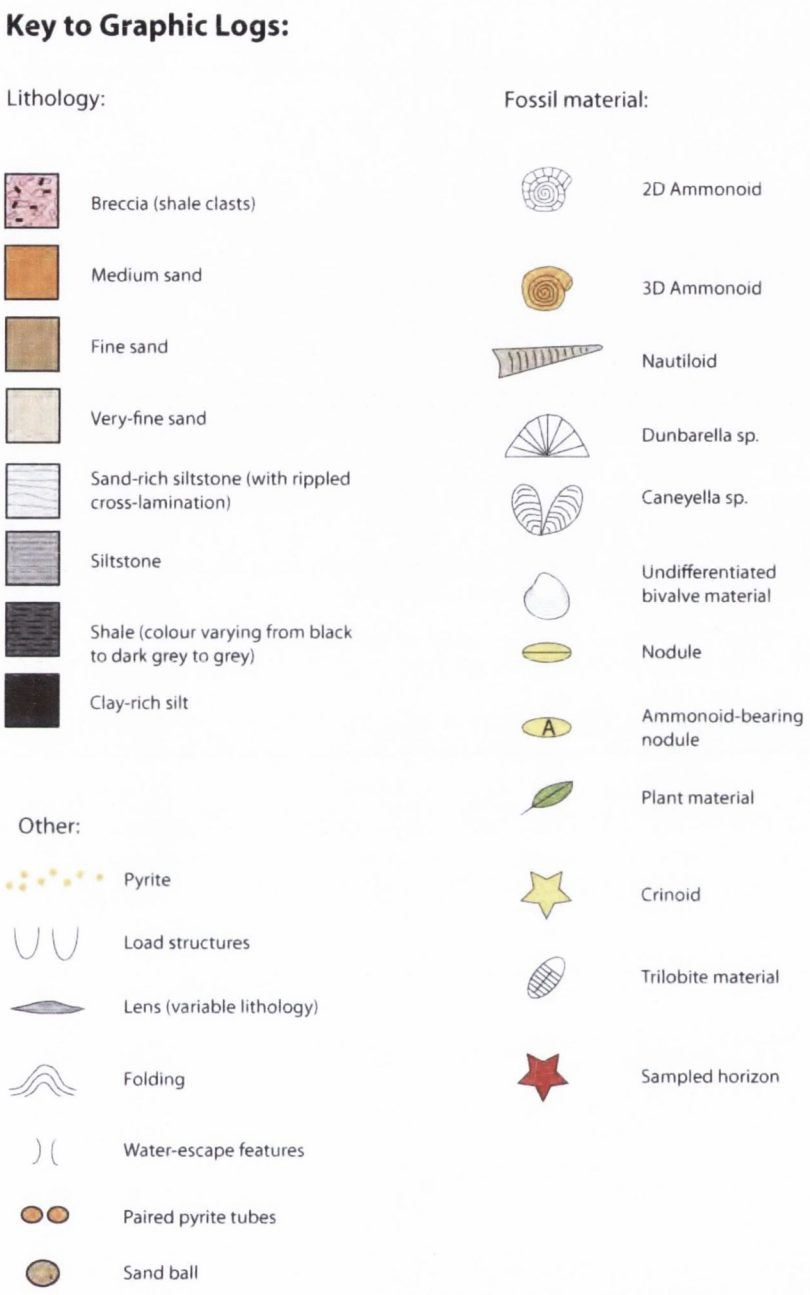

Fig. 2.3. Sedimentary log legend (valid for all sedimentary logs in this chapter).

Graphic log with lithological descriptions:
Location: Fisherstreet Bay, Doolin
Grid Ref: 06640/96316

Scale: 15mm=30cm
Log prefix=F01

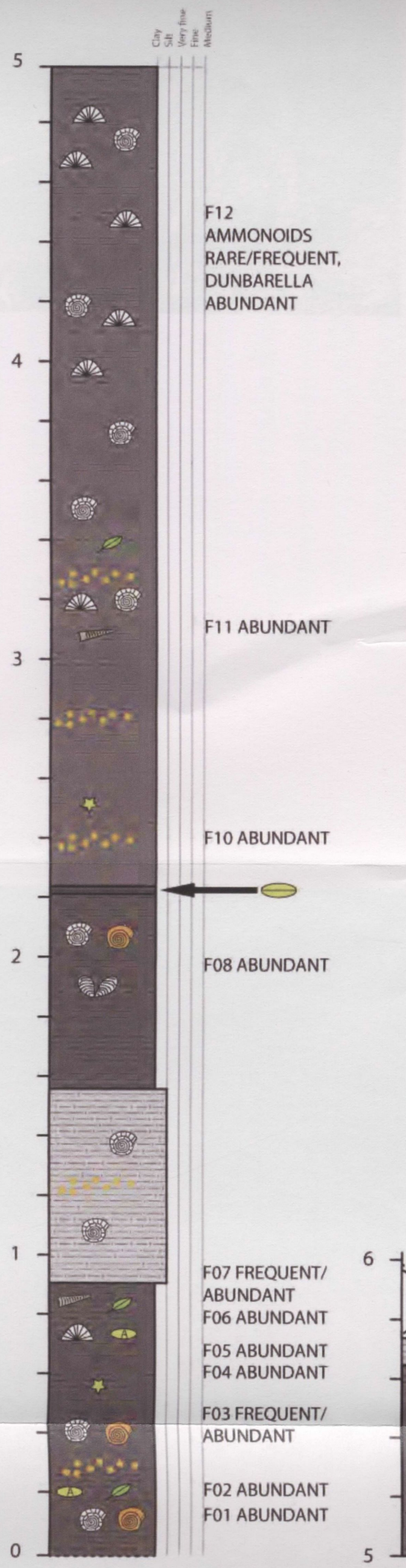

Fisherstreet Sampling Site [06640/96316]	Description	Fossil Content (taxa in a given horizon are ordered by abundance)
FIU	Ammonoid-bearing shale	*R./Ph.* sp., *Ph.* cf. *pc.*, *Ph.* cf. *cp.*, *Ph. paucicrenulatum*, *Ph. circumplicatile*, *Anthracoceras/Dimorphoceras* sp., Bivalve material
FILOBU	Ammonoid-bearing bullion	*Ht.* cf. *prereticulatus*
F14	Ammonoid-bearing shale	*Dunbarella* sp., *Basch.* cf. *ornatus*, *V.* cf. *henkei*, *Posidonia/ella* sp.
F13	Ammonoid-bearing shale	*Dunbarella* sp., *V.* cf. *henkei*, *R./Ph.* sp.
F12	Ammonoid-bearing shale	Family *Ph.cp.-pc.*, *Caneyella* sp., *R./Ph.* sp., *Ph. cf. pc.*, *Ph. pc.*, *R.* cf. *pulchellum*
F11	Ammonoid-bearing shale	*Dunbarella* sp., *R./Ph.* sp., *R.* cf. *subreticulatum*, *R.* cf. *pulchellum*, *Basch.* cf. *ornatus*, *Ph.* cf. *cp.*
F10	Ammonoid-bearing shale	*R.* cf. *subreticulatum*, *Ph. pc.*, *R.* cf. *pulchellum*, *Ph.* cf. *pc.*, *R./Ph.* sp., *Ph.* aff. *cp.*, *Basch.* cf. *ornatus*, *V.* cf. *henkei*, *Dunbarella* sp., *R.* cf. *todmordenense*, *Ph.* cf. *cp.*, Bivalve material
F09	Bullion, no ammonoids	Bullion material
F08	Ammonoid-bearing shale	*R./Ph.* sp., *Homoceras sp.*, *R.* cf. *pulchellum*, *Caneyella sp.*, *Ht.* cf. *varicatus*, *V. henkei*
F07	Ammonoid-bearing shale	*R./Ph.* sp., *V.* cf. *henkei*, *Homoceras* sp.
F06	Ammonoid-bearing shale	*Ph. pc.*, *R./Ph.* sp., *Dunbarella* sp.
F05	Ammonoid-bearing bullion material	*Ph. cp.*, *Ht.* cf. *prereticulatus*, *Ph.* cf. *cp.*, *V.* cf. *henkei*
F04	Ammonoid-bearing shale	*R./Ph.* sp., *V. henkei*, *V.* cf. *henkei*, *R.* cf. *subreticulatum*, *Ph. cp.*, *Ph.* cf. *cp.*, *Anthracoceras/Dimorphoceras* sp., *Ht.* cf. *varicatus*, Bivalve material, Nautiloid, *Homoceras* sp.
F03	Ammonoid-bearing shale	*V. henkei*, *V.* cf. *henkei*, Nautiloid
F02	Ammonoid-bearing bullion material	*Ht. prereticulatus*, *Ht.* cf. *prereticulatus*, *Ph.* cf. *cp.*, *Ht.* aff. *varicatum*, *R./Ph.* sp.
F01	Ammonoid-bearing shale	*V. henkei*
FBR	Breccia	None present; Rock sample

Fig. 2.4. Sedimentary log of Fisherstreet Bay section showing location of samples.

2.2.1.2 Aille River

The Aille River, Co. Clare, flows from Slieve Elva through Lisdoonvarna and Doolin, finally entering the Atlantic Ocean at Fisherstreet Bay. The river flows over a riverbed of Visean limestone and cuts through the overlying Namurian siliciclastic succession, which is often exposed on its banks. A thin bed of pebbly-phosphate is locally developed on top of the Visean limestone. Various Aille River sections were inspected and sampled by Hodson (1954a).
The river was visited during a day-trip with the aim of targeting bullions for 3D ammonoids. Unfortunately, many of the sections mentioned in Hodson (1954a) proved to be inaccessible due to heavy vegetation cover, which has significantly altered the landscape in the past 50 years. However, two loose bullions with long axis c.50 cm in length were collected just east of the Twin Wells Spa, Lisdoonvarna (Fig. 2.5; Table 2.2). Further east towards Ballyteighe Bridge, [13791/97993], two *in situ* bullions were sampled in the shale section 1.30 m above the Visean limestone (Fig. 2.6). This exposure can only be reached by wading through the river and the waters become inaccessible further east towards Ballyteighe Bridge.

Fig. 2.5. Aille River exposure [13619/97982]. Hammer for scale.

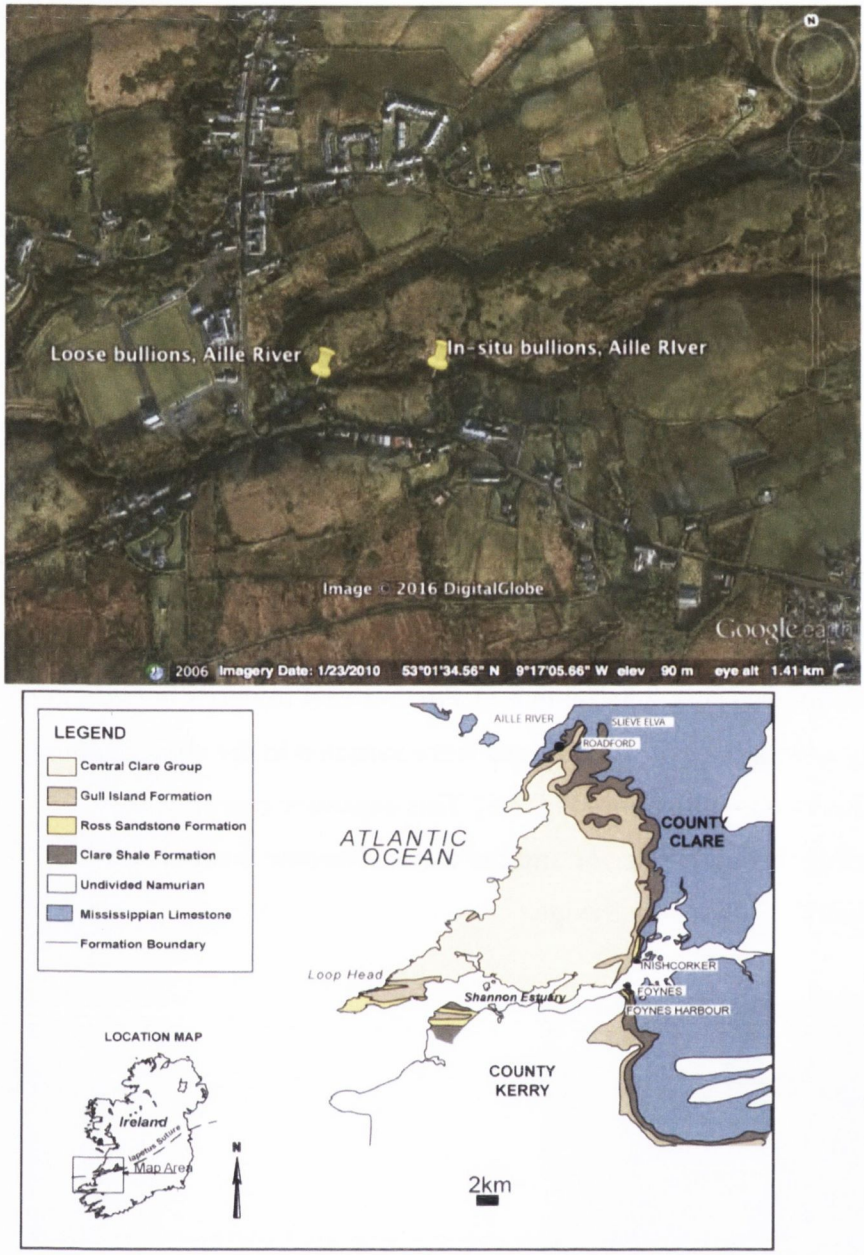

Fig. 2.6. Location map showing Aille River sampling locations at Twin Wells near Lisdoonvarna and further east at [13791/97993] and geological map of the Shannon Basin showing the locality and regional geology (Google Earth map).

Aille River Sampling Sites	Irish Grid Reference	Description	Fossil Content(taxa in a given horizon are ordered by abundance)
AILL01	13619/97982	Loose ammonoid-bearing bullion	*Homoceras smithii*
AILL02	13619/97982	Loose ammonoid-bearing bullion	*Vallites henkei, Hod. magistrorum*
AILL03	13791/97993	In situ ammonoid-bearing bullion	*Hod.* cf. *magistrorum*
AILL04	13791/97993	In situ ammonoid-bearing bullion	Weathered ammonoids

Table 2.2. Aille River faunal content.

Faunal Composition

The bullions yielded the following taxa preserved as solid specimens: *Ho. smithii*, *V. henkei*, *Hod. magistrorum* and *Hod.* cf. *magistrorum*. Each bullion either contained one or two species. Specimens of each taxon were abundant with all major growth stages represented.

2.2.1.3 Inishcorker

Inishcorker, Co. Clare, is a small island in the eastern reaches of the Shannon Estuary, close to the mainland village of Kildysart (Fig. 2.7). It is situated south of the confluence of the River Fergus into the River Shannon and is accessible from the mainland at low tide via a gravel road-bridge.

The island is located close to the basin axis, east of the main basin depocentre (Collinson *et al.* 1991) and it has good coastal exposure, comprising a c.200 m-thick succession (Fallon & Murray 2015) of black and dark grey shale sediments, which display small-scale (cm and mm-scale) variations in lithology from paper shale to clay-rich, resistant shale, to clay-rich siltstone. The shales are overlain by c.300 m-thick (Philcox 2007) mass transport deposits, with minor, interbedded turbidite deposits. Details of the faunal succession are found in Hodson & Lewarne (1961; p. 320) and Braithwaite (1993). More

recently, the facies associations of the sediments were studied in Pyles & Jennette (2009).

Faunal Composition

A mixed fauna of ammonoids, bivalves and plant material constitutes the make-up of the fossil assemblages on Inishcorker. Fossils were restricted to the shale-dominated unit, with none being found in the mass transport deposit-dominated unit. Ammonoid-bearing bullions are rare, with most ammonoids preserved as moulds on shale, sometimes pyritized.

While the presence of all the "ammonoid bands" recorded by Hodson & Lewarne (1961) was confirmed upon inspection of the section, the pattern of ammonoid occurrence was found to be quite different to what is apparent from their paper: rather than being restricted to a number of bands, ammonoids were found to be present in varying abundances throughout the succession. The section between Hodson & Lewarne's (1961) "*Nu. nuculum* faunal band" and "*Ho. beyrichianum* faunal band" was measured and sampled in detail in order to show this pattern of occurrence (see Fig. 2.8 for the sedimentary log). Hodson & Lewarne (1961) record the oldest ammonoid taxon as *Tumulites pseudobilingue* (E_1). From here, the section can be continuously traced upwards to a horizon containing *Ho. undulatum* (H_{2b} ammonoid biozone), when there is a gap at beach level (Fig. 2.8). The beds missing in the field due to this gap have been recognized, thanks to lithostratigraphical correlations, in a borehole (GSI 09/04) drilled in Kildysart (Obradors Latre, pers. comm. 4 Nov. 2014) on the mainland close to Inishcorker: the core is 152 m long and was sampled during this study. At 90 to 100 m depth, (see Appendix B) the borehole contains a mixed assemblage of ammonoids of Kinderscoutian age (R_1 biozone), with abundant *Reticuloceras/Phillipsoceras* sp. and associated *Basch. ornatus*- a typical assemblage for the upper Ross Sandstone Formation.
In summary, the shale-dominated succession ranges in age from Pendleian at its base (E_1) to Kinderscoutian at the top (R_{1a} ammonoid biozone).

Biostratigraphic evidence therefore indicates that the succession comprises 165 m of Clare Shale Formation-age deposits and c.40 m (Obradors Latre, pers. comm., 4 Nov. 2014) of shale deposits that are coeval to the Ross Sandstone Formation elsewhere, based on their fossil content. The overlying mass transport deposits with interbedded turbidites are thus coeval to the Gull Island Formation of the Loop Head Peninsula whose base is Kinderscoutian in age. Interestingly, paired pyrite tubes were found in the section [26318/57533]. These structures have already been recorded by Braithwaite (1993) and could occur as a result of bioturbation, although their origin is still enigmatic and could also be a result of diagenesis. Furthermore crinoid ossicle moulds are abundant in a poorly-cemented shale bed at [26526/57552]. These two observations indicate oxic to dysoxic bottom water conditions (see discussion on paleoecology in Chapter 3, Section 3.5).

In contrast to the present findings, Braithwaite (1993) recorded the lowest ammonoid band at Inishcorker as the "*Nuculoceras nuculum* band" (E_2c_2) and the topmost ammonoid band as the "*Hudsonoceras proteus* band" (H_2a_1).

a

b

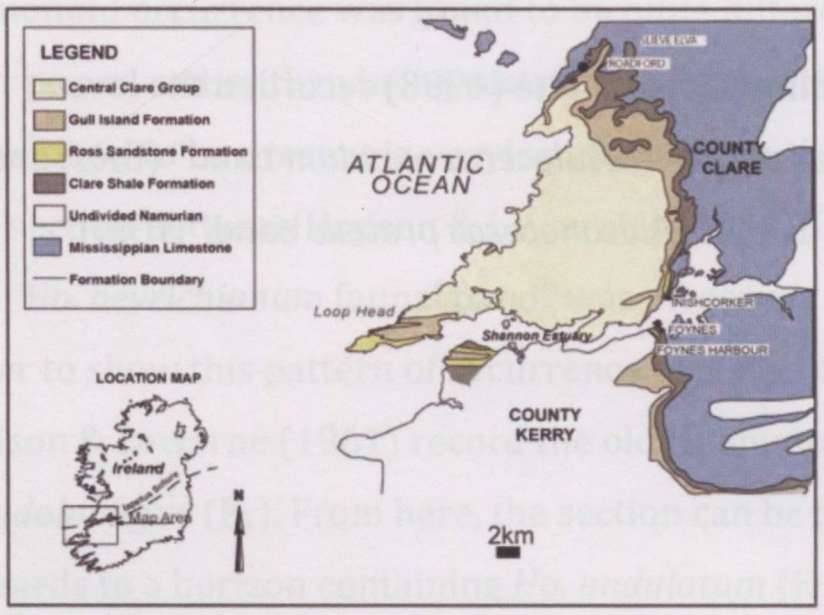

C

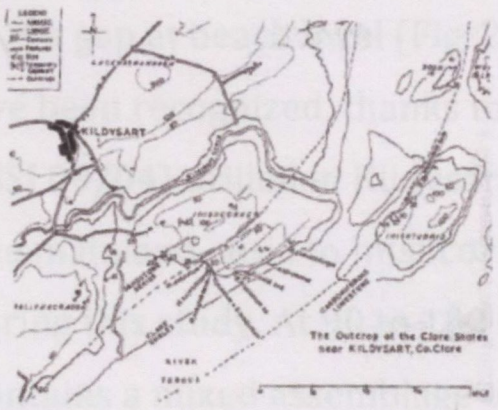

Fig. 2.7. Location map showing (a) Inishcorker sampling area on south coast of the island (highlighted by yellow line) and (b) geological map of the Shannon Basin showing the locality and regional geology (Google Earth map); (c) is a map of Inishcorker after Hodson and Lewarne (1961) showing his mapped ammonoid bands.

Graphic log with lithological descriptions:
Location: Inishcorker, "Nu. nuculum" to "Ho. beyrichianum" bands
Grid Ref: 26247/57582

Scale: 1:50
Log prefix=INI

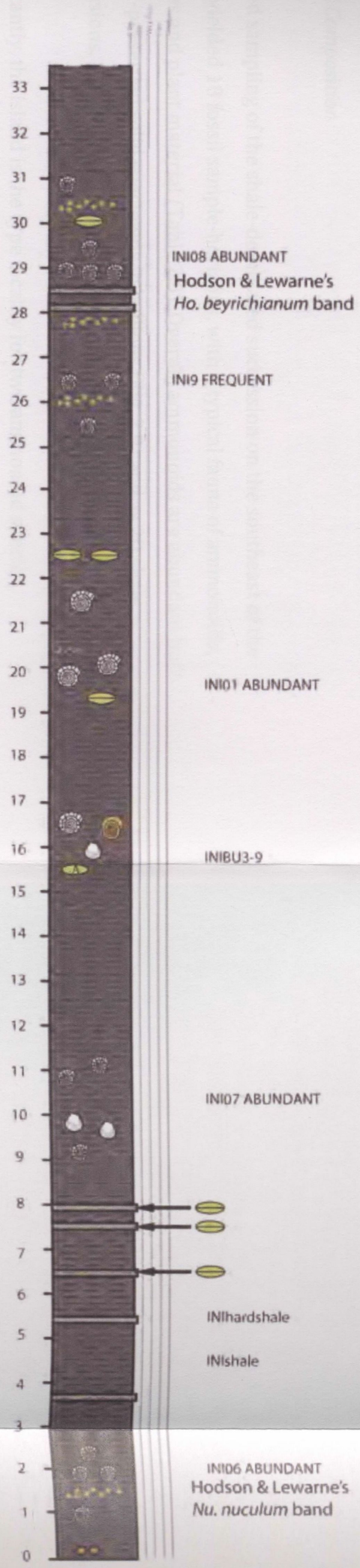

Inishcorker Sampling Sites	Irish Grid Reference	Description	Fossil Content (taxa in a given horizon are ordered by abundance)
INICR	**26526/57552**	**Crinoidal shale**	**Crinoid stems/ossicles, *Dunbarella* sp., Ammonoid material**
INIBU12	26463/57562	Bullion, no ammonoids	None
IN1BU11	26463/57562	Bullion, no ammonoids	None
INI10	26211/57628	Ammonoid-bearing shale	*Ho. undulatum*, *Ho.* cf. *undulatum*, *A./D.* sp.
INI09	26234/57614	Ammonoid-bearing shale	*Ho.* cf. *beyrichianum*, *Homoceras* sp., *Caneyella* sp.
INI08	26234/57614	Ammonoid-bearing shale	*Ho. beyrichianum*
INI05	26312/57535	Ammonoid-bearing shale	*Nu.* cf. *nuculum*, bivalve material
INI04	26318/57533	Pyrite burrows	N/A
INI03	26404/57526	Ammonoid-bearing shale	*?Eumorphoceras ?bisulcatum*
IN02	26424/57545	Ammonoid-bearing shale	*Eu. bisulcatum*, *Posidonia/Posidoniella*, Plant material
IN01	26247/57582	Ammonoid-bearing shale	*Ho.* cf. *beyrichianum*, Bivalve material
INIBU9	26247/57582	Ammonoid-bearing bullion material	*Isoh. subglobosum*
INIBU8	26247/57582	Ammonoid-bearing bullion material	*Isoh. subglobosum*
INIBU7	26247/57582	Ammonoid-bearing bullion material	*Isoh. subglobosum*
INIBU6	26247/57582	Ammonoid-bearing bullion material	*Isoh. subglobosum*
INIBU5	26247/57582	Ammonoid-bearing bullion material	*Isoh. subglobosum*
INIBU4	26247/57582	3D ammonoid from bullion	*Isoh. subglobosum*
INIBU3	26247/57582	3D ammonoid from bullion	*Isoh. subglobosum*
INI07	26248/57569	Ammonoid-bearing shale	Ammonoid and bivalve material
INI06	26272/57545	Ammonoid-bearing shale	*Nu. nuculum*, *Eu. bisulcatum*, Bivalve material

Fig. 2.8. Sedimentary log of Inishcorker section ("*Nu. nuculum* band" to "*Ho. beyrichianum* band" showing location of samples.

2.2.1.4 Foynes Island

Foynes Island is located on the southern side of the Shannon Estuary in Co. Limerick, c.300 m from the mainland (Fig. 2.11). Here, a c.92 m-thick succession of fine-grained lithologies (mostly shale with subordinate siltstone) crops out on the south-eastern and eastern shorelines. This is succeeded by a c.393 m succession of mass transport deposits, with minor interbedded turbidite deposits, which are exposed along the northern and southern shorelines. No inland exposure is present due to heavy vegetation cover. The shale-dominated succession is exposed on the south-eastern shoreline and consists of alternating black and grey shale beds, which display small-scale (cm and mm scale) variations in lithology from paper shale to clay-rich, resistant shale, to clay-rich siltstone. Bullion bands are a noticeable feature of the succession, whereby large (from 50 cm to c.1 m in length of the long axis) bullions can be traced along bedding. Sometimes, when there is no foreshore exposure of shale due to beach cover, bullions are the only element of the geology remaining and they act as a useful marker for bedding. The lithological and faunal succession of Foynes Island was described in detail by Hodson (1954b) and Hodson & Lewarne (1961, p. 324).

Faunal Composition

Detailed sampling of the shale-dominated succession on the southeast of the island yielded 18 fossil sample-horizons, with a typical fauna of ammonoids, bivalves and plant material (Table 2.3). Overall, ammonoids are abundant both as well-preserved solid specimens in bullions (Fig. 2.9) and as 2D shale impressions.

Importantly, the island is the type locality for two ammonoid species, *Reticuloceras subreticulatum* (Foord, 1903) and *Ramosites divaricatus* (Hind, 1905). Examination of the faunal succession confirmed the location of the horizon yielding *Reticuloceras subreticulatum*, [25099/52196], while *Ramosites divaricatus* was not present among the samples collected in this present study.

Determination of the ammonoids revealed that the succession ranges in age from Arnsbergian at its base (E_2) to Kinderscoutian at the top (R_{1a} ammonoid biozone). In fact, the oldest zonally indicative ammonoids are identified as *Eumorphoceras* sp. (sample FOY13) and the youngest (zonally-indicative), sampled c.2 m below the start of the sandstone and siltstone succession, are identified as *Reticuloceras/Phillipsoceras* spp. (sample FOY1). These biostratigraphic results conform to Hodson's (1954b) detailed analysis of the Clare Shale succession on Foynes Island.

Particularly noteworthy are the large (largest has long axis more than 1 m in length) ammonoid-bearing bullions with well-preserved *Hudsonoceras proteus* and *Homoceratoides prereticulatus* solid ammonoids.

Ammonoids are present throughout the succession and tend to be concentrated in thin horizons, which are darker in colour and interpreted as highly condensed. However, rare intervals yielded no fossils, despite being the same in lithology (when hand specimens are examined using a hand lens) as the ones with abundant ammonoids.

A zaphrentid-type solitary coral specimen was found in the uppermost part of the section, in the type locality for *R. subreticulatum* (FOY14). In this particular horizon, crinoid ossicle and stem moulds are also abundant, as well as ammonoids, plant and bivalve material. The coral is preserved as a 3D external mould with details of the ornament. Notably, this is not the only occurrence of a coral in the basin: two other coral specimens, with accompanying crinoid and ammonoid material, were found in a loose block at Fisherstreet Bay, Doolin. The presence of *R.* cf. *subreticulatum* in association with the coral indicates that the block probably fell from a horizon located towards the top of the shale-dominated succession, which correlates with the one at Foynes. Therefore this horizon is a useful correlation marker, but it also has significant ecological implications (see Ch. 3).

Foynes Sampling sites	Irish Grid Reference	Description	Fossil content (taxa in a given horizon are ordered by abundance)
FOY1	25083/52204	Ammonoid-bearing shale	*R./Ph.* spp., plant, crinoid moulds.
FOY2	25099/52196	Ammonoid-bearing shale	*Ph. circumplicatile*, *Ph.* cf. *cp.*, *Dunbarella* sp., *V.* cf. *henkei*, *R./Ph.* sp.
FOY3	25112/52214	Ammonoid-bearing bullion material	*Ht. prereticulatus*
FOY4	25112/52214	Ammonoid-bearing bullion material	*Ht. prereticulatus*
FOY5	25112/52214	Ammonoid-bearing bullion material	*Ht. prereticulatus*
FOY6	25112/52214	Ammonoid-bearing bullion material	*Ht. prereticulatus*
FOY7	25112/52214	Ammonoid-bearing bullion material	*Ht. prereticulatus*
FOY8	25129/52222	Ammonoid-bearing bullion material	*Ht. prereticulatus*
FOY9	25129/52222	Ammonoid-bearing bullion material	*Hud. proteus*
FOY10	25248/52264	Possible pyrite burrows	None
FOY11	25254/52261	Ammonoid-bearing shale	*?Posidonia*
FOY12	25266/52263	Ammonoid-bearing shale	*Eumorphoceras* sp., *Cravenoceratoides* sp.
FOY13	25318/52282	Ammonoid-bearing shale	*Eumorphoceras* sp.
FOY14	25099/52196	Ammonoid (and crinoid and coral)-bearing shale	*Basch. ornatus*, *R. subreticulatum*, *R./Ph.* sp., Zaphrentid-type coral, crinoids, *V.* cf. *henkei*, nautiloid, bivalve material.
FOY15	N/A	Ammonoid-bearing shale	*Ho.* cf. *beyrichianum*
FOY16	N/A	Ammonoid-bearing shale	*Isoh.* cf. *subglobosum*, *Anthracoceras/Dimorphoceras* sp.
FOY17	N/A	Ammonoid-bearing shale	*Nu. nuculum*
FOYUN	N/A	Ammonoid-bearing shale	*Ho. beyrichianum*, *Basch.* cf. *ornatus*

Table 2.3. Foynes Island faunal content.

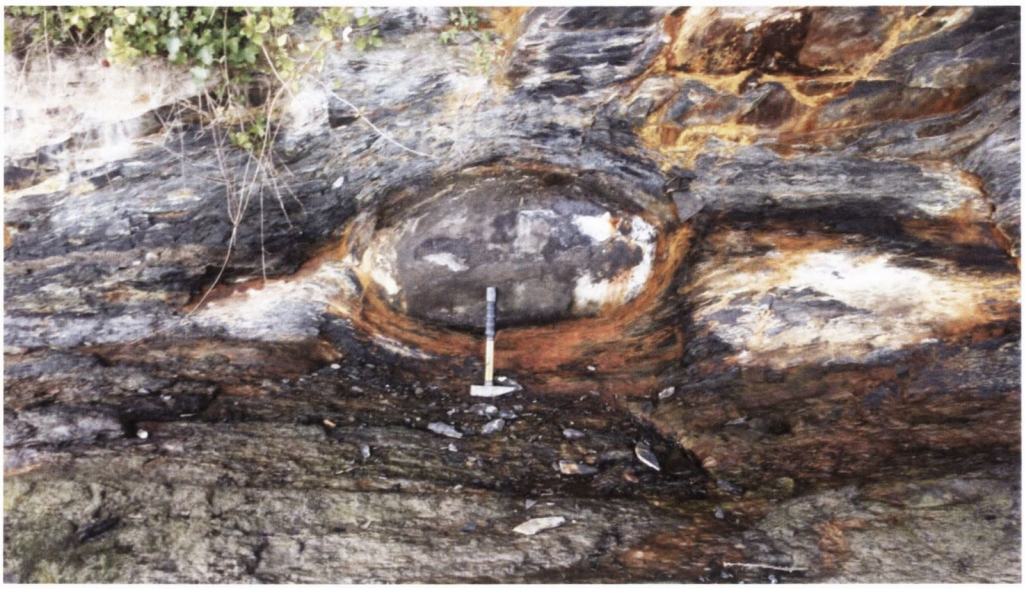

Fig. 2.9. Bullion, Foynes Island, south coast [25099/52196].

2.2.1.5 Foynes Harbour

Two localities were sampled on the mainland at Foynes, close to Foynes Harbour, Co. Limerick (Fig. 2.11). The first locality is a roadside exposure near the entrance of the Foynes Yacht Club, [24686/51862]. The exposure consists of tabular shales and interbedded thin siltstone-horizons, conformably overlain by mass transport deposits (Fig. 2.10). At this locality, a recent small landslide provided plenty of freshly-exposed shale rubble and, based on the morphology of the beds still in place, most of the fallen material was thought to have come from a horizon just below the mass transport deposits. The same interval can be sampled a little further east behind the Foynes Flying Boat Museum, [24720/51806], where the shale is more weathered and the specimens are of lower quality.

Fig. 2.10. Roadside exposure at Foynes Harbour, showing contact between shale and silststone deposits and mass transport deposits [24686/51862].

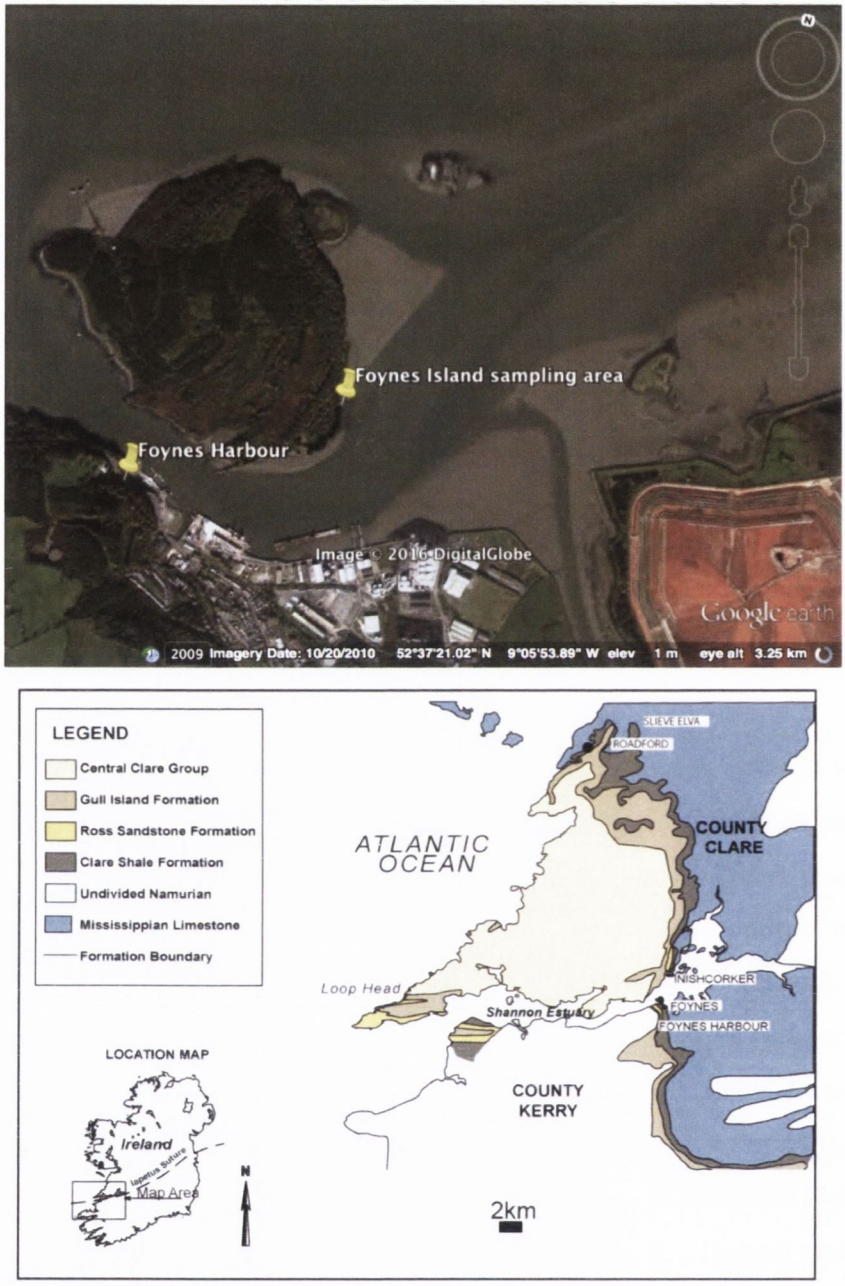

Fig. 2.11. Location map showing Foynes Island and Foynes Harbour sampling areas and geological map of the Shannon Basin showing the locality and regional geology (Google Earth map).

Faunal Composition

The faunal assemblage consists of ammonoids typical of the R_{1a} biozone (Kinderscoutian) (Table 2.4), as well as crinoid stems and bivalve material. The section is thus correlated both biostratigraphically and lithostratigraphy with the topmost shale-dominated section on Foynes Island. Biostratigraphy suggests that this shale rich succession is coeval both with the Clare Shale Formation in North and central Clare and the Ross Sandstone Formation on Loop Head. Thus the overlying mass transport deposits are here deemed to be part of the Gull Island Formation and the Ross Sandstone Formation is not present.

Foynes Harbour Samples	Irish Grid Reference	Description	Fossil Content (taxa in a given horizon are ordered by abundance)
FOR1	24686/51862	Ammonoid-bearing shale	*R./Ph.* sp, *R. subreticulatum*, crinoid stems, *V. henkei*, *V.* cf. *henkei*, *Ph.* cf. *cp.*, bivalve material
FOR2	24720/51806	Ammonoid-bearing shale	*Ht.* cf. *varicatus*, *R./Ph.* sp.

Table 2.4. Foynes Harbour faunal content.

2.2.1.6 Roadford

Roadford, also known as the Phosphate mine, is located in the townland of Toomullun, Co. Clare, near Doolin. Here, an outcrop of rock phosphate occurring at the base of the shale beds overlying Visean limestone was locally mined. The mine was in operation from 1924 to 1947 and its workings provided artificial exposures of the lower portion of the shale succession. Hodson (1954a) measured sections on both banks of the River Aille at this locality and recognised several faunal bands here.

Faunal Composition

Roadford specimens on loan from the National Museum of Ireland collections were studied in order to strengthen current understanding of 3D ammonoid taxonomy (Table 2.5). Most of these were identified by J. Bouckaert (unpublished note); a few were collected by Nigel Monaghan (National Museum of Ireland) and identified by the author of the present study. Most of the bullion material contained one, or at most two ammonoid taxa, with many growth stages represented. The ammonoids present were: *Ho. beyrichianum*, *Hud. proteus*, *Ho. undulatum*, *Ht. prereticulatus* and *Hod. magistrorum* (typical of the Alportian and Early Kinderscoutian regional stages). All taxa had previously been recorded at this locality by Hodson (1954a, p. 268). The specimens have proven useful in advancing the understanding of the ontogenetic development and taxonomy of ammonoids (see Chapter 3).

GSI Roadford Samples used to study given taxa	Irish Grid Reference	Description	Fossil content (taxa in a given horizon are ordered by abundance)
F24480	N/A	Ammonoid-bearing bullion material	*Homoceras undulatum*
F24478, F24477, F24475	N/A	Ammonoid-bearing bullion material	*Hudsonoceras proteus*
F24472, F24477 F0210, F026, F0220, F025	N/A	Ammonoid-bearing bullion material	*Homoceratoides prereticulatus*
F24476	N/A	Ammonoid-bearing bullion material	*Hodsonites magistrorum*
Unlabelled	N/A (Roadford or Spectacle Bridge)	Ammonoid-bearing bullion material	*Homoceras beyrichianum*
F20264, F20263	N/A	Ammonoid-bearing bullion material	*Homoceras beyrichianum*

Table 2.5. Taxa present in National Museum of Ireland collection samples.

2.2.1.7 Spectacle Bridge

Spectacle Bridge, north Co. Clare, is located where an unnamed tributary joins the River Aille, west of Lisdoonvarna. Hodson (1954a, p. 268) measured the shale section that crops out on the left bank of the tributary, above Visean Limestone.

Faunal Composition

Ammonoid-bearing bullion material from Spectacle Bridge, collected by Nigel Monaghan, was examined thanks to a loan from the National Museum of Ireland. The specimens were processed in Trinity College Dublin and most of the ammonoids were identified as *Hod. magistrorum*, with some associated *Ht.* cf. *varicatus* (Table 2.6). These taxa were not recorded by Hodson (1954a) at this locality, but elsewhere they are a typical component of the faunal bands present at this locality (see Hodson's faunal band scheme, p. 265, Hodson, 1954a: Table 3.1).

GSI Specimens used to study given taxa	Irish Grid Reference	Description	Fossil content(taxa in a given horizon are ordered by abundance)
F20280, F20282, F20275-6	N/A	Ammonoid-bearing bullion material	*Hodsonites magistrorum*
F20273-F20281	N/A	Ammonoid-bearing bullion material	*Homoceratoides* cf. *varicatus*

Table 2.6. Spectacle Bridge faunal content.

2.2.1.8 Slieve Elva

Slieve Elva is a 344 m-high hill in the Burren region, North Co. Clare. It provides some relatively good sections through the shale beds deposited above the Visean limestone. These sections were studied by Hodson (1954a), who also

described the faunal succession. Two sections were inspected during the course of this study with the intention of locating ammonoid-bearing bullions.

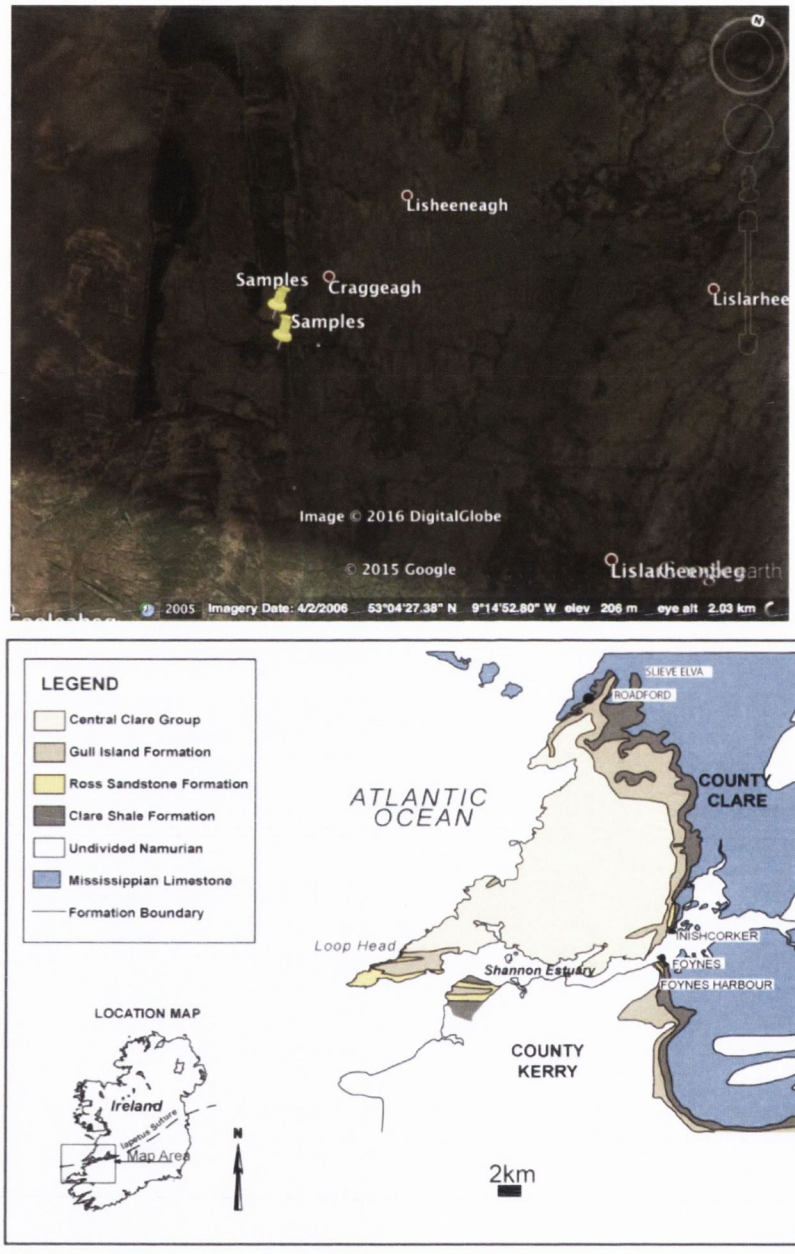

Fig. 2.12. Location map showing Slieve Elva sampling areas and geological map of the Shannon Basin showing the locality and regional geology (Google Earth map).

Faunal Composition

Samples (Table 2.7) were collected from two localities at the foot of Slieve Elva, starting with a small stream at Cragreagh - Hodson's (1954a) locality 46 - north-northeast of Lisdoonvarna. Despite Hodson's record of ammonoid-bearing bullions at this locality, only 2D ammonoid material on shale could be found during the present study. Sampled ammonoids are Kinderscoutian (R_1 ammonoid biozone) in age. Secondly, a narrow stream section at Lismorahaun, Hodson's (1954a) locality 51, on the eastern side of Slieve Elva, was sampled. Once again, none of Hodson's bullion bands could be located, but 2D ammonoid moulds were sampled nonetheless, yielding Kindercoutian-age specimens (R_1 ammonoid biozone).

Slieve Elva Samples	Irish Grid Reference	Description	Fossil content (taxa in a given horizon are ordered by abundance)
SLI01	16053/01781	Ammonoid-bearing shale	*R./Ph.* sp., *A./D.* sp., *Dunbarella* sp., *R.* cf. *subreticulatum, Family Ph. cp.-pc., Ht.* cf. *varicatus,* Bivalve material
SLI02	16222/02079	Ammonoid-bearing shale	*Dunbarella* sp., *R.* cf. *subreticulatum, R./Ph.* sp., *R. cf. pulchellum*

Table 2.7. Slieve Elva faunal content.

2.2.1.9 Gowlaun River

The Gowlaun River, Co. Clare, which runs through St. Brendan's Well, meets the Aille River at the Twin Wells in Lisdoonvarna. Only a small bullion (20 cm in length of long axis) with rare, unextractable juvenile ammonoids was collected from the left bank of the river, [13678/98119], 1.60 m stratigraphically above the Visean limestone (Fig. 2.13).

Faunal Composition

Specimens from St. Brendan's Well on loan from the National Museum of Ireland collected by Nigel Monaghan (National Museum of Ireland) were identified as *Ht.* cf. *varicatus.*

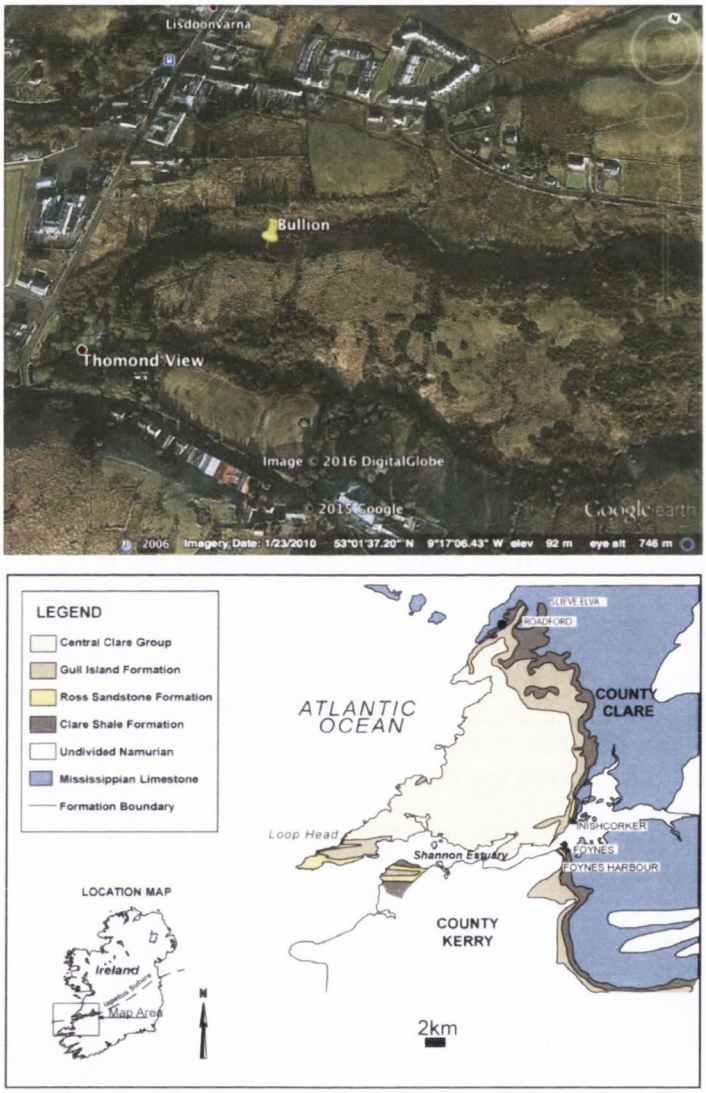

Fig. 2.13. Location map showing Gowlaun River sampling site at [13678/98119] and geological map of the Shannon Basin showing the locality and regional geology (Google Earth map).

2.2.2 Ross Sandstone Formation

Co. Kerry Localities

The cliffs at Ballybunion provide exceptional exposure through the Clare Shale Formation, into the Ross Sandstone Formation and the overlying Gull Island Formation. Indeed, the boundary between the Clare Shale Formation and the Ross Sandstone Formation is only visible at outcrop level in Ballybunion, Co. Kerry, where a series of coastal bays provide superb cliff sections.

2.2.2.1 Ballybunion Waterfall Band

The lowest ammonoid band in the Ross Sandstone Formation, often referred to as "*Hudsonoceras proteus-Homoceras smithii*" band (Collinson, 1991; Hodson & Leckwijck 1958), is herein referred to as "Waterfall Band" and it crops out in Ballybunion, just below the large waterfall of Glenachoor Stream [86837/44563] (Fig. 2.15). It can also be confidently picked out in core material, specifically in the following cores: 10-CE-UCD-03, 10-CE-UCD-05 and 12-KY-UCD-09 (Appendix B).

In the field, it is c.8 m-thick (Fig. 2.14), with a base at the top of a sandstone bed with rippled surface, which can be traced all along the cliff face to the south. The condensed section starts off with c.50 cm of sand-rich silt, with micaceous flakes that catch the light, and it fines upwards into dark grey and black shale. A sequence of more or less uninterrupted black shale with pyrite-rich horizons (mm-scale and laterally continuous along bedding) makes up the main thickness of the condensed section. Occasional sandy intercalations with wavy bedding and irregular bases are also present and these sometimes appear to be replaced laterally by pyrite. Towards the top of the condensed section, at c.7.5 m, the shale becomes more silt-rich and, at c.8 m, the incidence of a siltstone bed greater than 25 cm in thickness is taken to coincide with the end of the condensed section. Bullions are frequent throughout the condensed section,

with several large (up to 80 cm in length of long axis) *Hud. proteus*-bearing bullions found spaced along bedding c.60 cm from the base of the section.

Faunal Composition

The condensed section at Ballybunion has a simple assemblage, dominated by *Hud. proteus* and *Ho. smithii,* so it is a very useful marker in local correlation (see Chapter 5).

The faunal composition of this band (Fig. 2.16) was already studied by Hodson and Leckwijck (1958), and is known across Britain, Ireland, France, Germany, Belgium, south Urals and central Asia (Hodson 1957; Hodson & Leckwijck 1958). Although *Hud. proteus* and *Ho. smithii* were not found together in the outcrop section, but it is likely that they co-occur, based on the fact that they do so in the core samples.

Fig. 2.14. Ballybunion Waterfall band (thickness in between dashed yellow lines) [86837/44563].

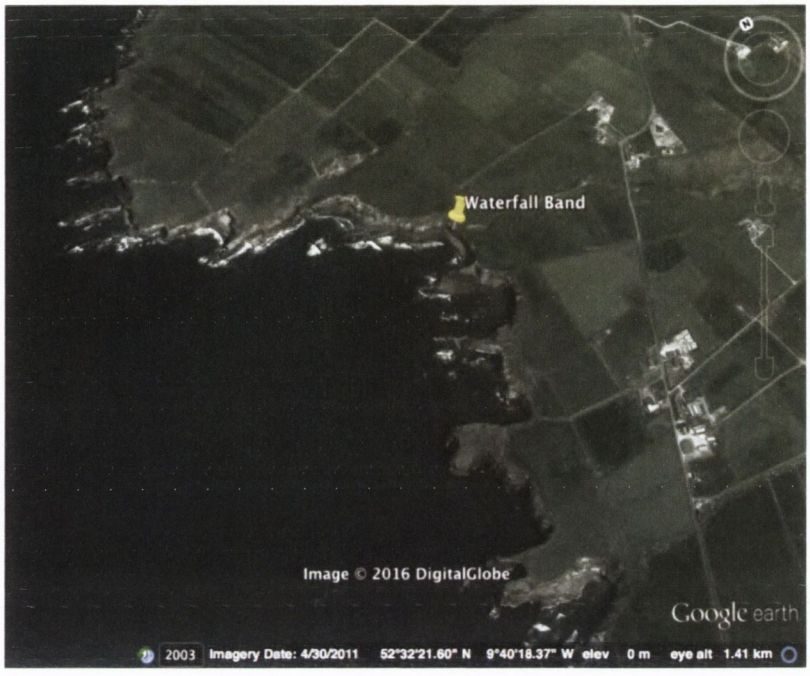

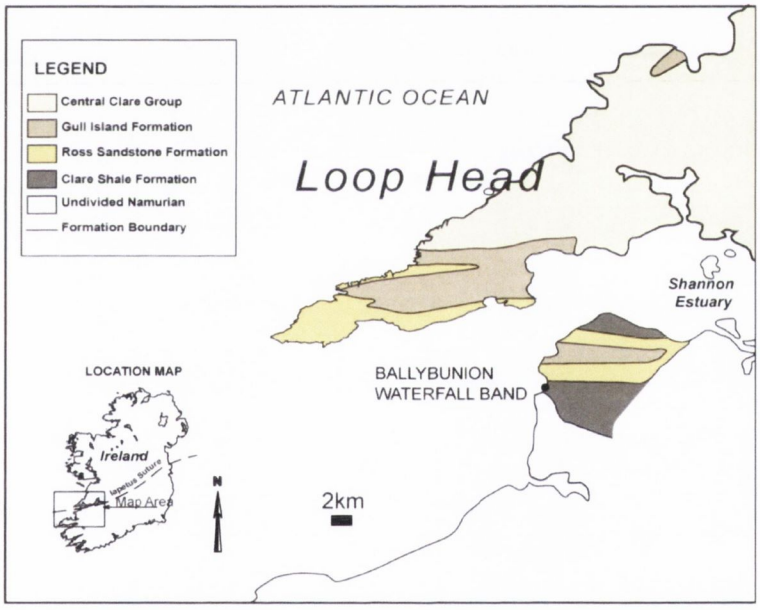

Fig. 2.15. Location map showing Ballybunion Waterfall band sampling locality [86837/44563] and geological map of the Shannon Basin showing the locality and regional geology (Google Earth map).

Graphic log with lithological descriptions:
Location: *Hud. proteus-Ho. smithii* band Ballybunnion/ Waterfall Band
Grid Ref: 850261/49505

Scale: 15mm=30cm
Log prefix=BA02

Sample	Irish Grid Reference	Description	Fossil content (taxa in a given horizon are ordered by abundance)
BA025	86837/44563	Ammonoid-bearing shale	*Ho. cf. smithii, A./D.* sp.
BA024	86837/44563	Ammonoid-bearing shale	*Ho. smithii, Ho. cf. smithii, Ho. undulatum?, A./D.* sp.
BA023	86837/44563	Ammonoid-bearing shale	Ammonoid Material
BA022	86837/44563	Ammonoid-bearing shale	*Ho. smithii, Ho. cf. smithii, A./D.* sp., Bivalve Material
BA02N02a,b,c	86837/44563	Ammonoid-bearing nodule material	*Hud. proteus*
BA02b	86837/44563	Ammonoid-bearing shale	*Hud. proteus*, Bivalve and Plant Material.
BA02a	86837/44563	Ammonoid-bearing shale	*Caneyella* sp.
BA02N01	86837/44563	Ammonoid-bearing nodule material	*Hud. proteus*

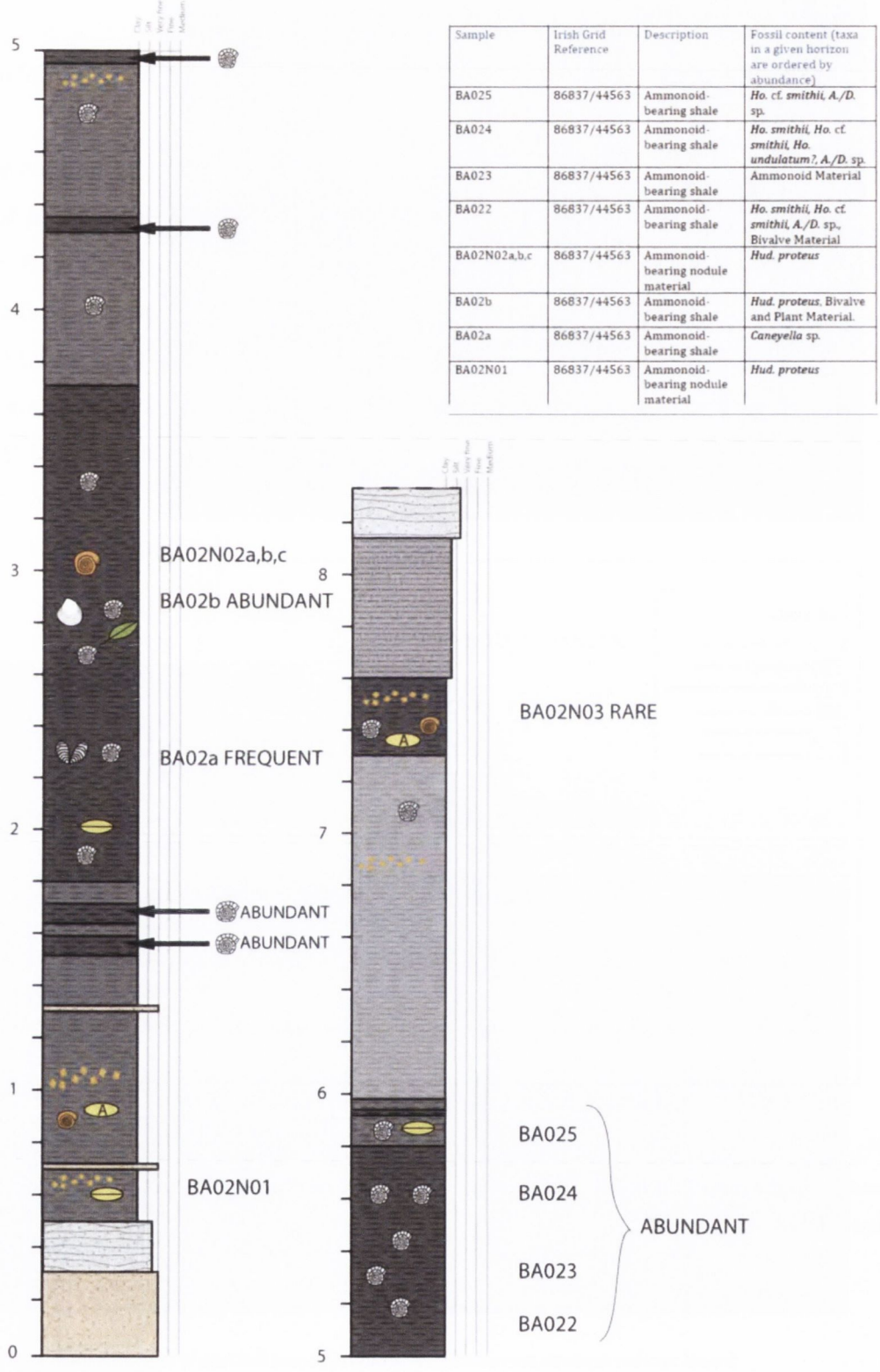

Fig. 2.16. Sedimentary log of "Waterfall Band" showing location of samples.

2.2.2.2 Canal Band (Reading Room)

The "Canal Band", which is here also referred to as "Ballybunion Reading Room Band", crops out at [86644/44765] (Fig. 2.18). Here, the Ross Sandstone Formation beds are folded and tectonized (Fig. 2.17). The condensed section consists of c.2.30 m of shale (Fig. 2.19), with thin siltstone interbeds and common mm-scale silicified plant horizons. The condensed section starts at the top of the last sand thicker than 20 cm and ends with the first sand thicker than 20 cm, which also shows load structures at its base. No bullions were recovered. This condensed section can also be confidently picked out in core material, specifically in the following cores: 10-CE-UCD-03 and 10-CE-UCD-05.

Faunal Composition

This condensed section is monospecific, *Ht. prereticulatus* being the sole taxon present. Thus it is a very useful marker in correlation (for correlations, see Chapter 5). Ammonoids are abundant to the point that several moulds are found overlapping each other on the shale. All ammonoids are preserved as 2D moulds and they are concentrated in four horizons.

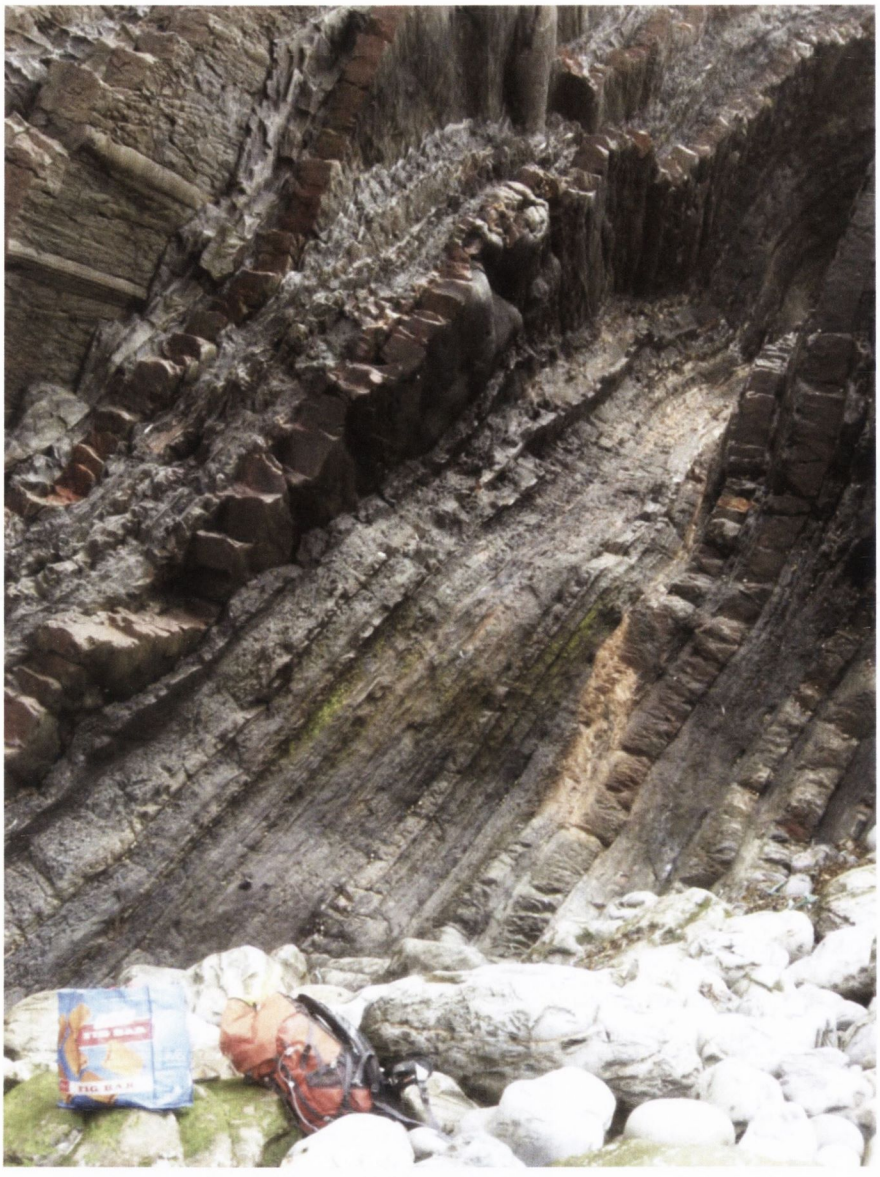

Fig. 2.17. Canal Band, Ballybunion [86644/44765].

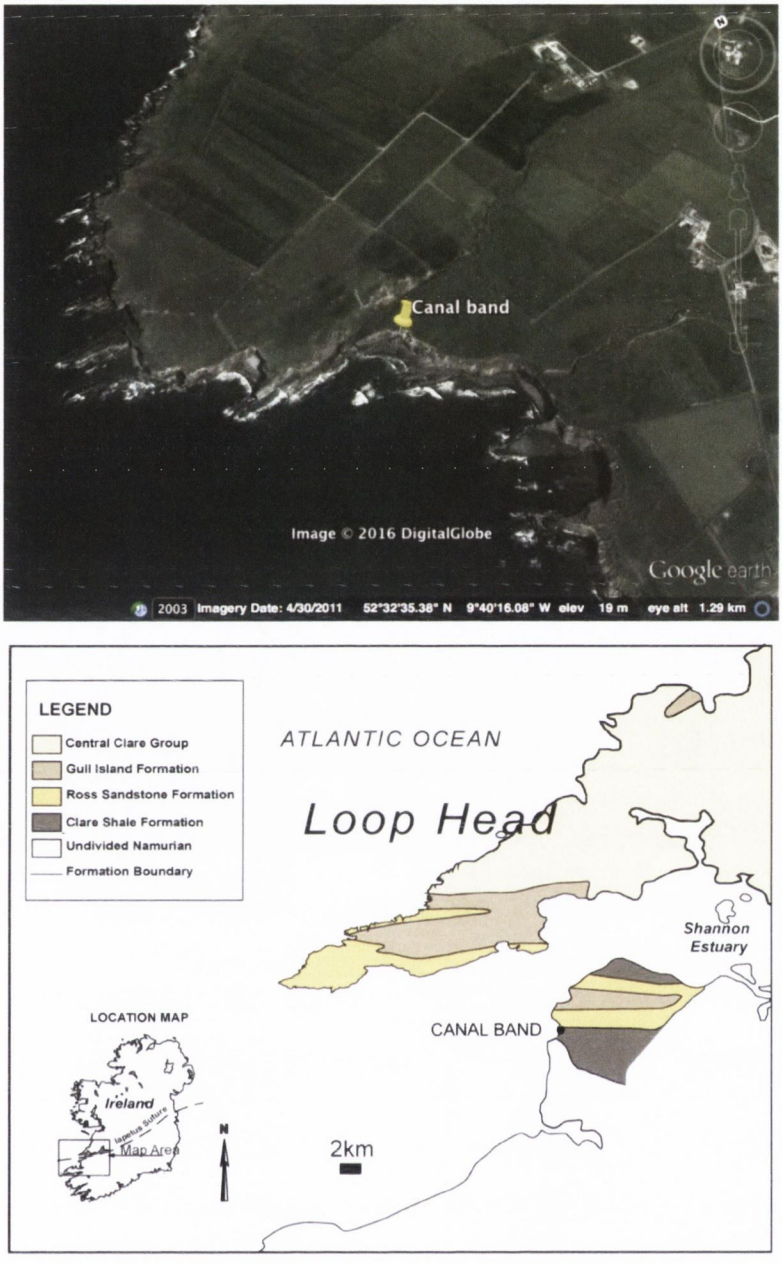

Fig. 2.18. Location map showing Ballybunion Canal band sampling locality at [86644/44765] and geological map of the Shannon Basin showing the locality and regional geology (Google Earth map).

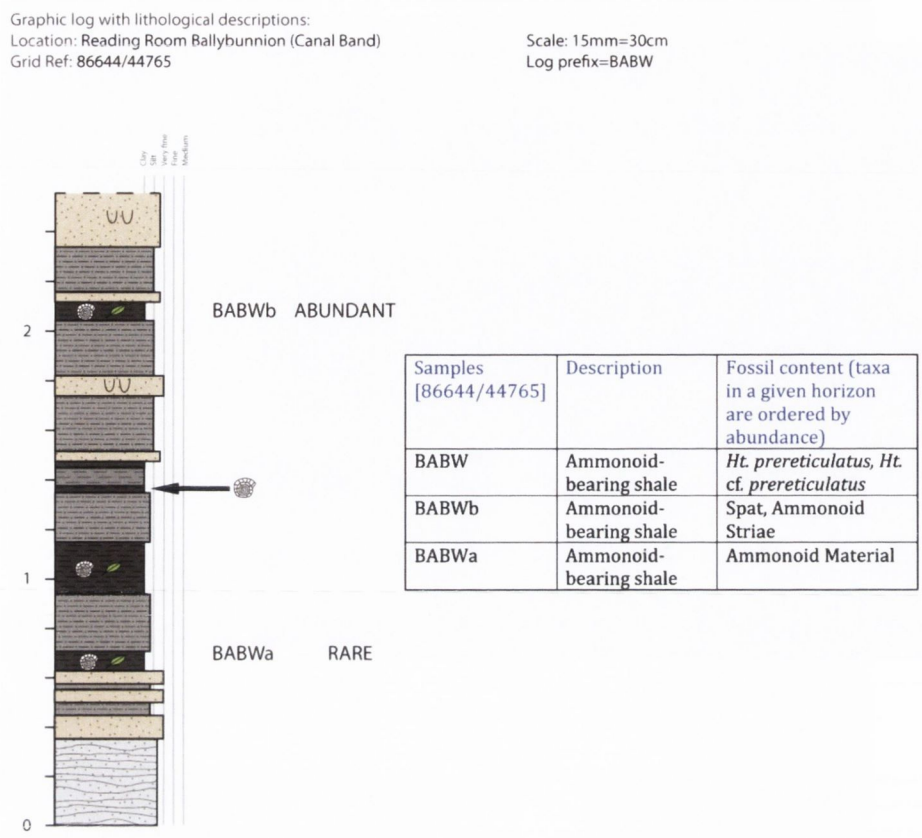

Fig. 2.19. Sedimentary log of "Canal Band" showing location of samples.

2.2.2.3 Castle Band

Looking at the cliff-face north-east from the ruined castle at Leck Point, north of Ballybunion along the Co. Kerry coastline, [86189/45046], there is a c.2.50 m-thick condensed section, named "Castle Band" which is dominated by grey silt-rich shale and also contains two thin sandstone interbeds (Fig. 2.20). The exposure is on a ledge that is difficult to access safely and was not measured and logged for this reason (Arnau Obradors Latre is thanked for sampling this band).

Faunal Composition

The ammonoid assemblage is typical of the Mid- to Upper Ross Sandstone Formation, featuring a mixture of *Phillipsoceras/Reticuloceras* sp. and other

species, such as *V.* cf. *henkei* (Table 2.8). The overall appearance is not of a highly condensed section; rather, it appears quite silt-rich when viewed from the ruined castle.

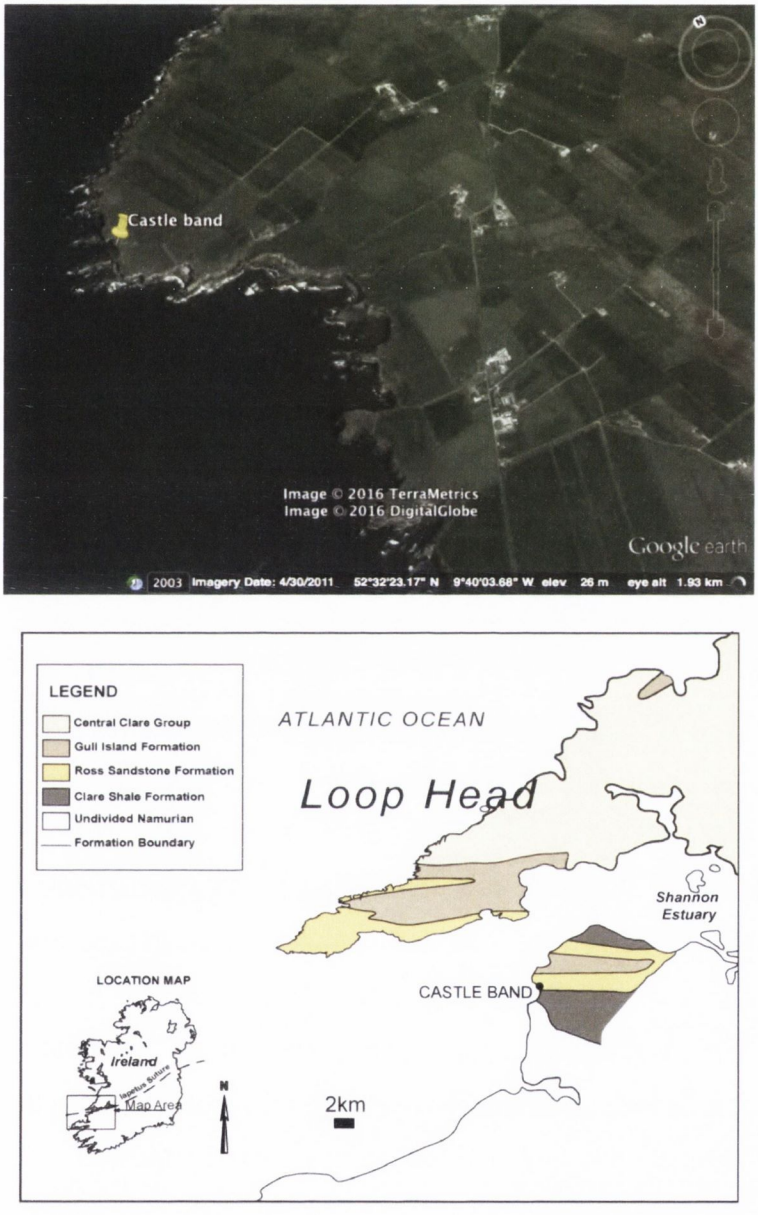

Fig. 2.20. Location map showing Ballybunion Castle band sampling locality at [86189/45046], and geological map of the Shannon Basin showing the locality and regional geology (Google Earth map).

Samples [86189/45046]	Description	Fossil content (taxa in a given horizon are ordered by abundance)
BACA	Ammonoid-bearing shale	*Phillipsoceras/ Reticuloceras* sp., *V.* cf. *henkei,* spat

Table 2.8. "Castle Band" faunal content.

2.2.2.4 "Ballybunion *Ph. circumplicatile*" band

The "Ballybunion *Ph. circumplicatile*" condensed section is accessible at low tide in an exposure along the Co. Kerry coastline, north of the ruined castle at Leck Point, [86354/45441] (Fig. 2.21). Here, a 3 m-thick condensed section lies above a large mass transport deposit. The section is taken to start right above a 5 cm-thick sandstone bed. Above this, lies a 15 cm-thick siltstone with ripple-cross lamination, which is in turn overlain by the shale constituting the main part of the condensed section. A décollement horizon (or slip surface), thought to be Quaternary in age, is present 25 cm into the shale beds: it consists of brecciated mud-clasts up to 10 cm in length (Fig. 2.22), in a matrix of grey, clay-like cement and it varies in thickness from less than a cm to c.20 cm. The first ammonoids were seen to occur just above this distinctive horizon. The shale is black in colour and varies from fissile, papery-shale to clay-rich, non-fissile shale. Occasional thin sandstone and siltstone interbedded horizons, are laterally traceable within the section. Silicified plant material commonly occurs as thin mm-scale layers within the section. The shale is overlain by c.90 cm of clay-rich siltstone, with sandy intercalations. The condensed section is taken to end at the junction between this siltstone and the overlying sandstone bed, which is over 5 cm-thick. Above it, sand packages thicken upwards, giving way to a sequence of turbidite deposits. No bullions were found. This condensed section can also be picked out in core 09-CE-UCD-01 (Appendix B).

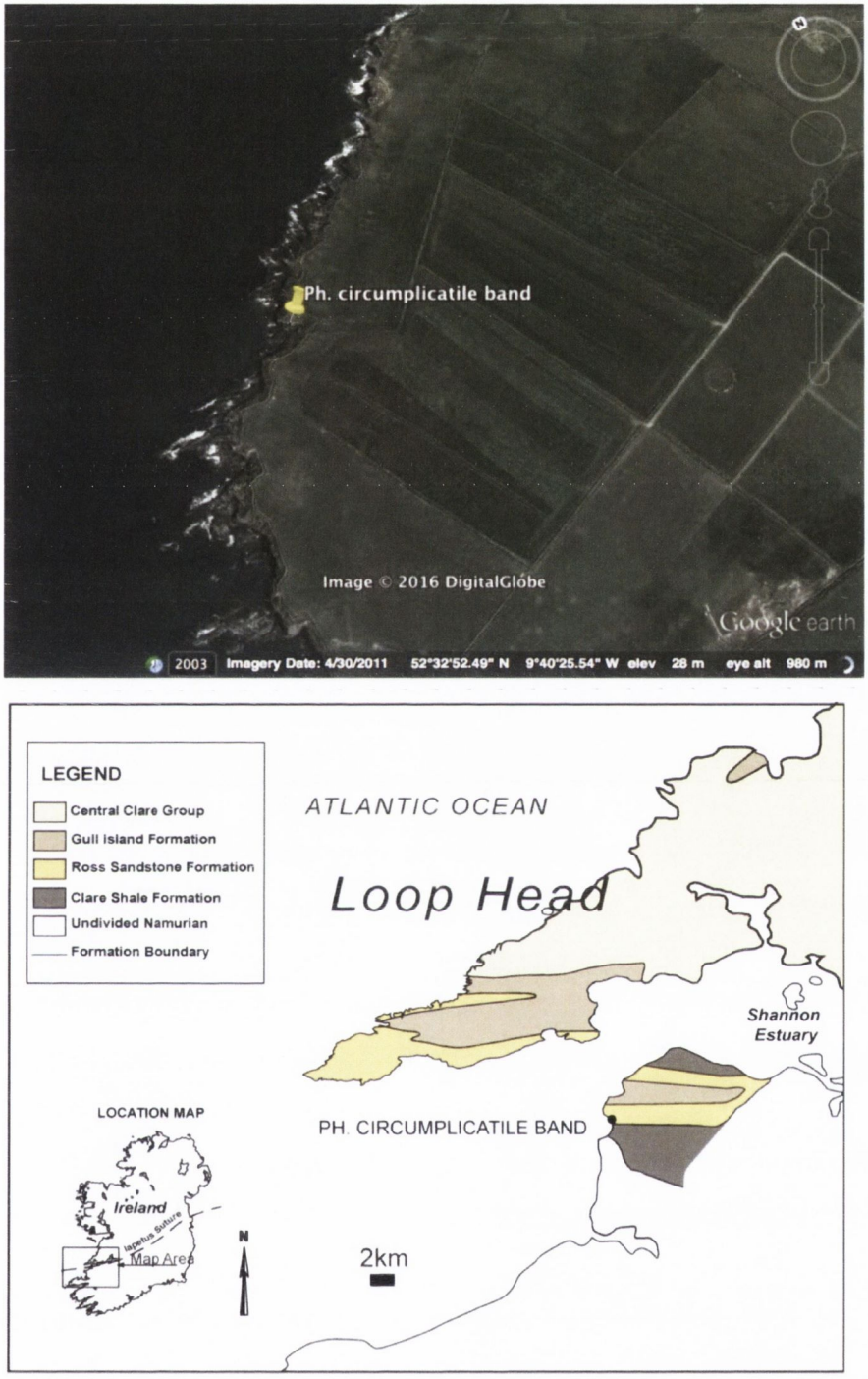

Fig. 2.21. Location map showing Ballybunion *Ph. circumplicatile* band sampling locality at [86354/45441], and geological map of the Shannon Basin showing the locality and regional geology (Google Earth map).

Fig. 2.22. Décollement horizon in Ballybunion *Ph. circumplicatile*" condensed section [86354/45441].

Faunal Composition

Three highly fossiliferous horizons (Fig. 2.23) could be recognized. They contain mixed assemblages of ammonoids preserved as 2D moulds and often partially pyritized. The lowest horizon contains a mixed assemblage, mainly composed of *Reticuloceras/Phillipsoceras* spp., with associated *Phillipsoceras* cf. *paucicrenulatum* and *Basch.* cf. *ornatus.* The middle horizon contains a mixed assemblage composed of *Reticuloceras/Phillipsoceras* spp., *Phillipsoceras* cf. *paucicrenulatum* and *Phillipsoceras* cf. *circumplicatile.* The upper horizon contains a mixed assemblage dominated by *Reticuloceras/Phillipsoceras* sp. Plant material is present throughout. Ammonoids were also found on sand-rich silt horizons towards the top of the condensed section, but no complete specimen could be found suggesting they had been fragmented during transport in the sandy flow.

Graphic log with lithological descriptions:
Location: Ballybunnion "*Ph. circumplicatile* band"
Grid Ref: 86354/45441

Scale: 15mm=30cm
Log prefix=BAM

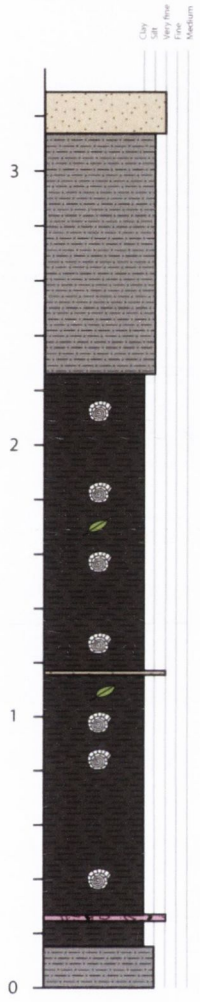

Samples [86354/45441]	Description	Fossil content (taxa in a given horizon are ordered by abundance)
BAMSAND	Ammonoid-bearing sandy silt	Ammonoid striae
BAMU	Ammonoid-bearing shale	*R./Ph.* sp., *Ph.* cf. *cp., Ph.* cf. *pc.*, Weathered ammonoids
BAMM	Ammonoid-bearing shale	*R./Ph.* sp., *Ph.* cf. *cp., Ph.* cf. *pc, Ph. cp., V.* cf. *henkei,* Plant Material
BAML	Ammonoid-bearing shale	*R./ Ph.* sp., Family cp.-pc., *Ph. pc., Ph.* cf. *pc., Ph.* cf. *cp., Ph. cp., Basch.* cf. *ornatus, A./D.* sp., *Dunbarella* sp.

BAMU ABUNDANT

BAMM ABUNDANT

BAML FREQUENT/RARE

Fig. 2.23. Sedimentary log of "Ballybunion *Ph. circumplicatile*" band showing location of sampled horizons.

2.2.2.5 "Ballybunion *Ph. paucicrenulatum*" band

The topmost condensed section in the Ross Sandstone Formation, here named "Ballybunion *Ph. paucicrenulatum*" band, [86574/45666], can be reached by following the coastline north from the "Ballybunion *Ph. circumplicatile*" condensed section (Fig. 2.24). Here, the condensed section, which is strikingly obvious due to its thickness and colour, lies above a prominent mass transport deposit (slump) (see Fig. 2.25 for a sedimentary log).

It is 3 m-thick, starting at the top of a sandstone bed (less than 20 cm-thick), which can be traced along the cliff face to the north, where the condensed section rapidly becomes inaccessible. The lowermost 50 cm consists of grey clay-rich silt. This is overlain by black shale and a laminated, 10 cm-thick very fine sand, which gives way once again to clay-rich siltstone fining-upwards to shale. Overall there are c.1.50 m of black shale with occasional sand-rich silt interbeds (Fig. 2.26). The shale coarsens upwards to siltstone towards the top of the condensed section, where it is overlain by thinly bedded sandstones with cross lamination. The contact between the siltstone and sandstone above is taken to represent the top of the condensed section. The sandstone packages then thicken upwards away from the section. No bullions could be found. This condensed section can be picked out in core 09-CE-UCD-02 (see Appendix B).

Faunal Composition

Ammonoids are rare but present in the lowermost siltstone, while three highly fossiliferous horizons could be recognized in the main shale section. They contain mixed assemblages of ammonoids preserved as 2D moulds.
The lowest horizon contains a mixed assemblage of ammonoids dominated by *Phillipsoceras/Reticuloceras* sp. and *Ph.* cf. *paucicrenulatum*, as well as abundant specimens of *Dunbarella* sp. The middle horizon contains a mixed assemblage dominated by *Phillipsoceras/Reticuloceras* sp., *Ph.* cf. *paucicrenulatum* and *R. dubium. Dunbarella* sp. is again abundant in the faunal assemblage. The upper horizon contains a mixed assemblage dominated by

Phillipsoceras/Reticuloceras sp., with associated *Ph. paucicrenulatum* and *V.* cf. *henkei*. Plant material (impressions) is present throughout and it should be noted that none of the ammonoids were pyritized.

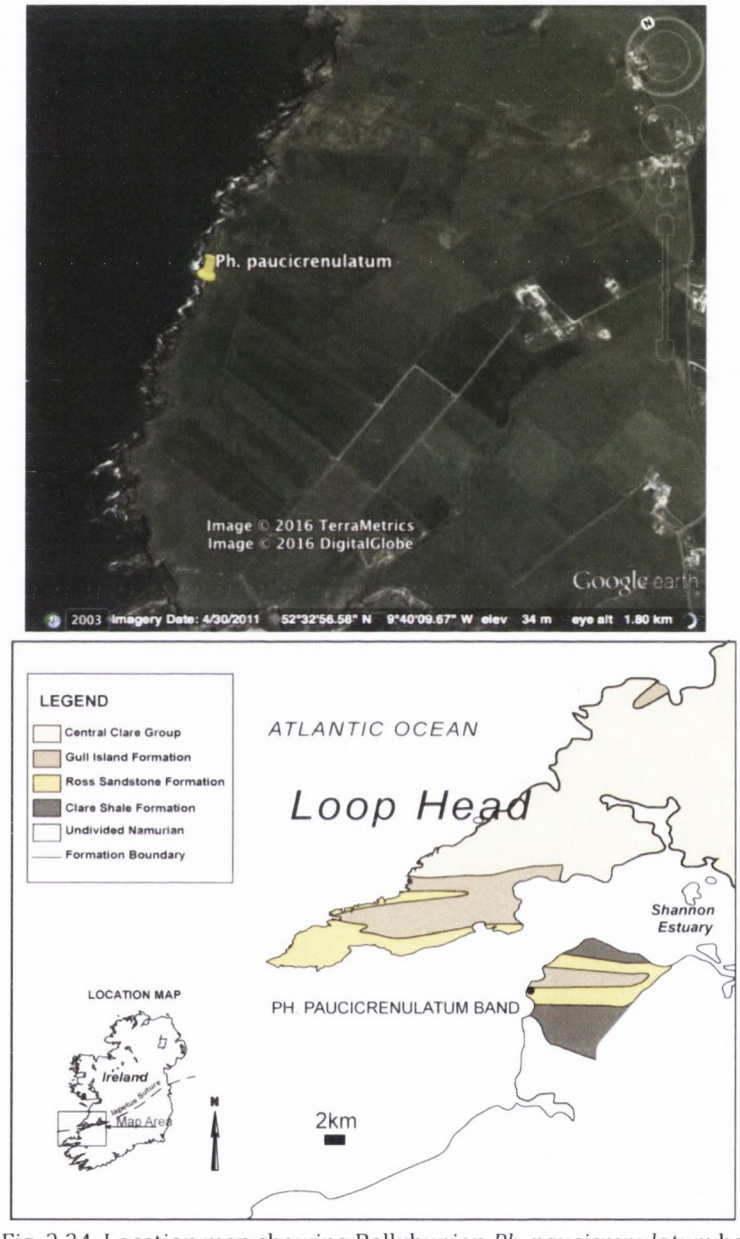

Fig. 2.24. Location map showing Ballybunion *Ph. paucicrenulatum* band sampling locality at [86574/45666] and geological map of the Shannon Basin showing the locality and regional geology (Google Earth map).

Graphic log with lithological descriptions:
Location: Ballybunnion *"Ph. paucicrenulatum"*
Grid Ref: 86574/45666

Scale: 15mm=30cm
Log prefix=BAT

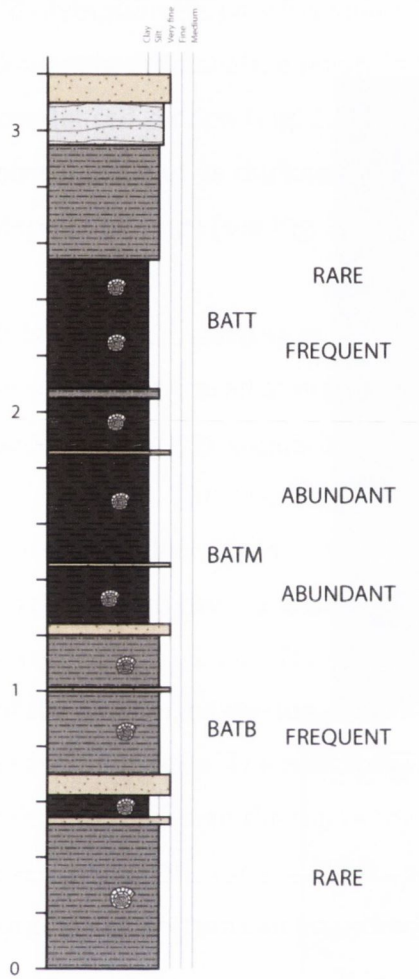

Samples [86574/45666]	Description	Fossil content (taxa in a given horizon are ordered by abundance)
BATT	Ammonoid-bearing shale	*Phillipsoceras/Reticuloceras* sp., *Dunbarella* sp., *V.* cf. *henkei*, *Ph. paucicrenulatum*, Plant Material
BATM	Ammonoid-bearing shale	*Phillipsoceras/Reticuloceras* sp., *Ph.* cf. *paucicrenulatum*, *R.* cf. *dubium*, *Dunbarella* sp., *V.* cf. *henkei*, *R. dubium*, Plant Material, *A./D.* sp.
BATB	Ammonoid-bearing shale	*Phillipsoceras/Reticuloceras* sp., *Dunbarella* sp., *V.* cf. *henkei*, *Ph.* cf. *paucicrenulatum*, *Ph. paucicrenulatum*, *R. ?todmordenense*

Fig. 2.25. Sedimentary log through "Ballybunion *Ph. paucicrenulatum*" band showing sample location.

Fig. 2.26. Ballybunion *Ph. paucicrenulatum* band [86574/45666]. Hammer for scale.

Despite several mentions in the literature (Collinson *et al.* 1991; Lien 2003) of a supposed "*R. dubium*" band above the "Ballybunion *Ph. paucicrenulatum*" band, no condensed section is present above the latter. Rather, *R. dubium* is a component of the faunal assemblage in the middle horizon of the "Ballybunion *paucicrenulatum*" band. This could have led to confusion in past studies (see also Chapter 5).

Co. Clare Localities

The Ross Sandstone Formation crops out on the Loop Head Peninsula, Co. Clare, where condensed sections were sampled at the following localities. Where possible, localities are treated in lithostratigraphic order.

2.2.2.6 "Reading Room" Band

On the south coast of Loop Head just west of Kilbaha Bay, at a locality just east of Doondalden House, also known locally as the "Reading Room", a condensed section crops out [73846/47687] (Fig. 2.27). The mass transport deposit beds are steeply folded into a monocline, which brings the condensed section to just above sea level just below Doondalden House. This condensed section is c.1.20 m-thick (Fig. 2.28-29) and it is taken to start with the first recessed siltstones and shales above a prominent sandstone bed. The section starts off with sand-rich siltstone beds with ammonoid-bearing bullions (the largest observed bullion is up to 50 cm in long axis length). Lamination in the surrounding silt and shale envelops the bullion, which is routed in the sandstone bed below, implying that it formed pre-compaction. These are overlain by siltstone with occasional sandier interbeds, which are lighter grey in colour and c.10 cm of black, paper shale with small concretions and a cm-scale coaly layer. Above this, a 40 cm-thick sequence of interbedded siltstones with sandy intercalations and sandstones with ripple cross-lamination is separating the next dark shale package from the underlying one. This next black shale package is c.15 cm in thickness and contains two cm-scale layers of charcoal continuous with bedding. Above this, yellowy siltstones grade up into grey-blue coarser siltstone with water escape structures and ripple cross-laminae. The condensed section is taken to end with a 40 cm-thick massive sandstone with some cross-lamination visible towards the base.

The same condensed section crops out a few hundred meters further west, [73389/47195], where it can be reached by climbing down the cliffs towards the sea. A condensed section which correlates with the "Reading Room" band

based on lithostratigraphy, crops out at Kicloher Cliff, on the south coast of Loop Head, just east of Kilbaha Bay and on the western side of Rehy Hill. It also has the same faunal content as the Reading Room band.
This condensed section has been confidently identified in borehole material, specifically in the following boreholes: 10-CE-UCD-03 and 10-CE-UCD-05.

Faunal Composition

Three main fossiliferous intervals could be identified. The lowest contained a particularly large bullion sampled in detail in this study (sample R07): this was 50 cm long (long axis length) and had a rim of black shale around it. It contains abundant ammonoid material, including *Homoceratoides* cf. *prereticulatus, ?Phillipsoceras/Reticuloceras spp.* and *Anthracoceras/Dimorphoceras* sp.*;* bivalves such as *Caneyella* sp. and nautiloids are also present. The second horizon, which is found in the lowest black shale interval, contains only rare 2D ammonoids and spat, as well as small bullions with unidentifiable juvenile ammonoids. The topmost interval, corresponding to the topmost shale interval, contains abundant ammonoids, preserved as 2D moulds and forming a monospecific assemblage (only *Homoceratoides prereticulatus* and *Homoceratoides* cf. *prereticulatus* are present). The same section further west was sampled and seen to contain *?Homoceratoides* sp. and *?Homoceras/Vallites* sp., as well as *Homoceratoides prereticulatus and Homoceratoides* cf. *prereticulatus.*

Overall, if one doesn't consider the bullion at the base, this condensed section is almost entirely monospecific, which is not a trait shared by most of the other highly-condensed sections. This could be related to ecological factors, which produced dominance of this one particular species within ammonoid populations. Lewarne (unpublished notes) similarly found the assemblage to be monospecific with abundant *Ht. prereticulatus* at this locality.

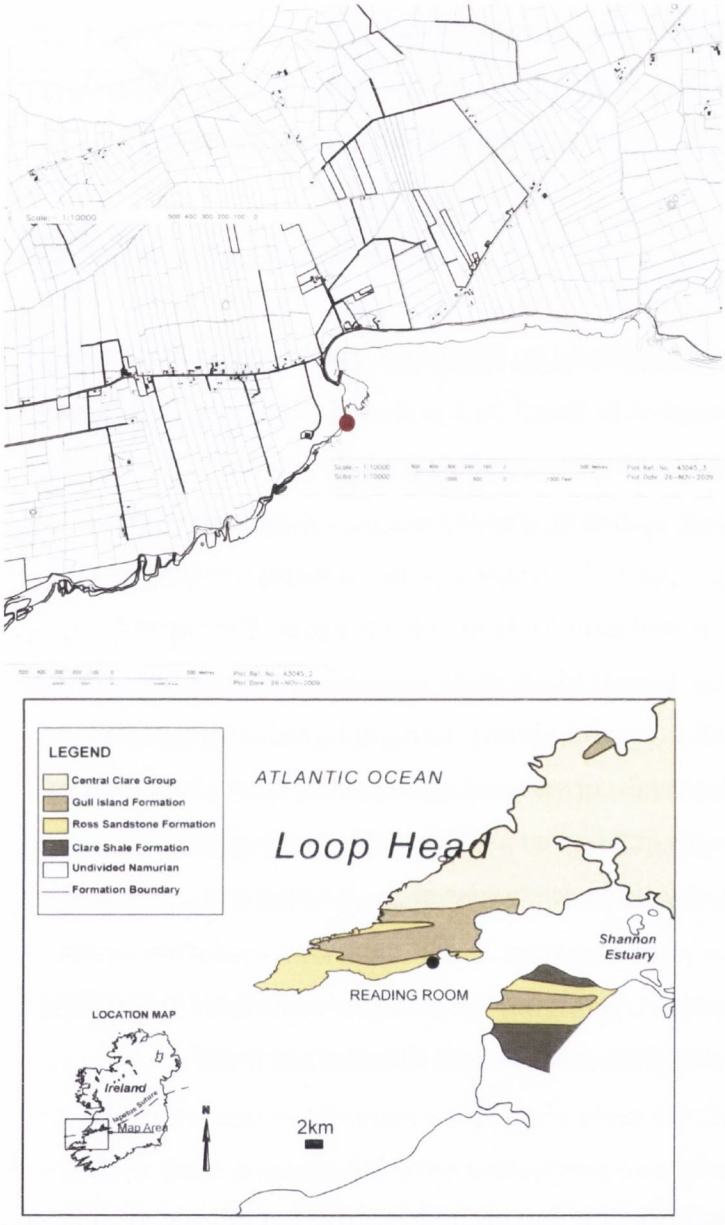

Fig. 2.27. Location map showing Reading Room sampling locality at [73846/47687] and geological map of the Shannon Basin showing the locality and regional geology (OSI rural place maps: http://maps.osi.ie/publicviewer).

Graphic log with lithological descriptions:
Location: Reading Room (Loop Head)
Grid Ref: 73846/47687

Scale: 15mm=30cm
Log prefix=RO

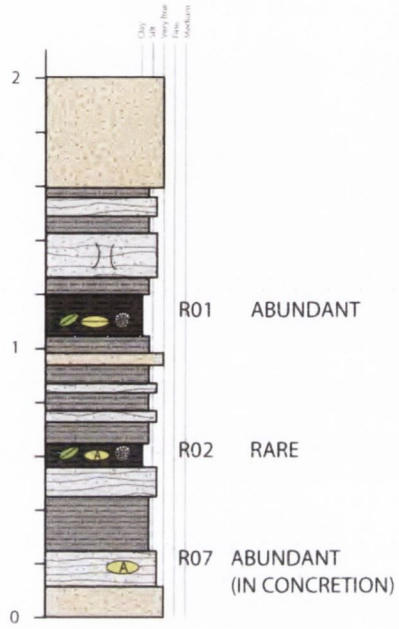

Samples [73846/47687]	Description	Fossil content (taxa in a given horizon are ordered by abundance)
RENO	Ammonoid-bearing bullion material	*A./D.* sp., *Homoceratoides* sp., *Phillipsoceras/ Reticuloceras* spp.?
R07	Ammonoid-bearing bullion material	*Homoceratoides* cf. *prereticulatus*, *Phillipsoceras/ Reticuloceras* spp.?, *Caneyella* sp., *A./D.* sp., Nautiloid
R06	Ammonoid-bearing shale	*Homoceratoides prereticulatus*, *Homoceratoides* cf. *prereticulatus*
R05	Ammonoid-bearing shale	*Homoceratoides prereticulatus*, *Homoceratoides* cf. *prereticulatus*
R04	Ammonoid-bearing shale	*Homoceratoides prereticulatus*, *Homoceratoides* cf. *prereticulatus*
R03	Ammonoid-bearing shale	*Homoceratoides* sp.?, *Homoceras/Vallites* sp.?
R02	Ammonoid-bearing bullion material	Ammonoid material
R01	Ammonoid-bearing shale	*Homoceratoides prereticulatus*, *Homoceratoides* cf. *prereticulatus*

Fig. 2.28. Sedimentary log of "Reading Room" band showing sampled horizons (R03-6 were sampled from the section further west and are not shown here).

Fig. 2.29. Reading Room band exposure, looking towards Kilbaha Bay at [73846/47687].

2.2.2.7 "Dunmore West" Band

This condensed section crops out on the southern coast of Loop Head, [70494/46845], where a lot of minor faults with a dominant strike-slip component create small gullies (Fig. 2.31). It is immediately recognisable as a highly condensed section in the field (Fig. 2.30) due to its dark colour and considerable thickness and consists of 2.8 m of shale, which, when examined close-up, reveals considerable small-scale lithological variation (Fig. 2.32). The section is taken to start at the top of a laterally extensive sandstone bed with sand dykes and disturbed bedding. Although black shale is the dominant lithology, it is accompanied by: frequent interbedded laminated, very fine sandstone beds; frequent siltstone beds with very thin sandstone laminae, which display colour banding; rare décollement brecciated horizons, with disorientated shale and sandstone clasts; rare gouge layers; occasional lenticular, very-fine sand, separated by muddy lenses and with mud drapes. Occasional sand dykes originating from the underlying sandstone beds are present in the black shale horizons above. The ripple cross-laminae and starved ripples in the sandstone beds indicate palaeocurrents from the NE. The condensed section ends with the base of a massive sandstone bed, c.15 cm-thick and laterally traceable. The silts with coarser laminae are interpreted as possible deposits of bottom-current flows (contourites). Elongate ammonoid-bearing bullions are common along bedding in a horizon c.2.25 cm from the base of the condensed section.

The topmost shale section contains folds, which are interpreted as having formed during the Quaternary (when glaciation affected Irish soils and sediments) and probably associated with the soft sediment deformation observed in the sediments below.

Faunal Composition

Even though ammonoids could be found in varying degrees of abundance nearly throughout the condensed section (Fig. 2.32), they are concentrated in

five shale horizons. Bullions were also observed in the uppermost horizons. All of these horizons were sampled in the present study. The bullions contained external moulds of 3D ammonoids as well as ornament fragments.

The lowest horizon (DU1) contains rare ammonoids and bivalve material. The second-lowest contains frequent ammonoids (*Phillipsoceras/Reticuloceras* spp. dominate), mostly in the juvenile growth stage and as spat. Ammonoids are abundant in the third horizon from the base, where they form an extremely diverse assemblage, with *V. henkei* and *V.* cf. *henkei* dominating the assemblage and secondary *Phillipsoceras/Reticuloceras* spp. and *Ht.* cf. *prereticulatus* (for a full list see table below). The fourth horizon sampled contains rare ammonoids, which were mostly juveniles, and some fragments of striae.

Fig. 2.30. "Dunmore West" band at [70494/46845]. Blue pick for scale (c.1 m long).

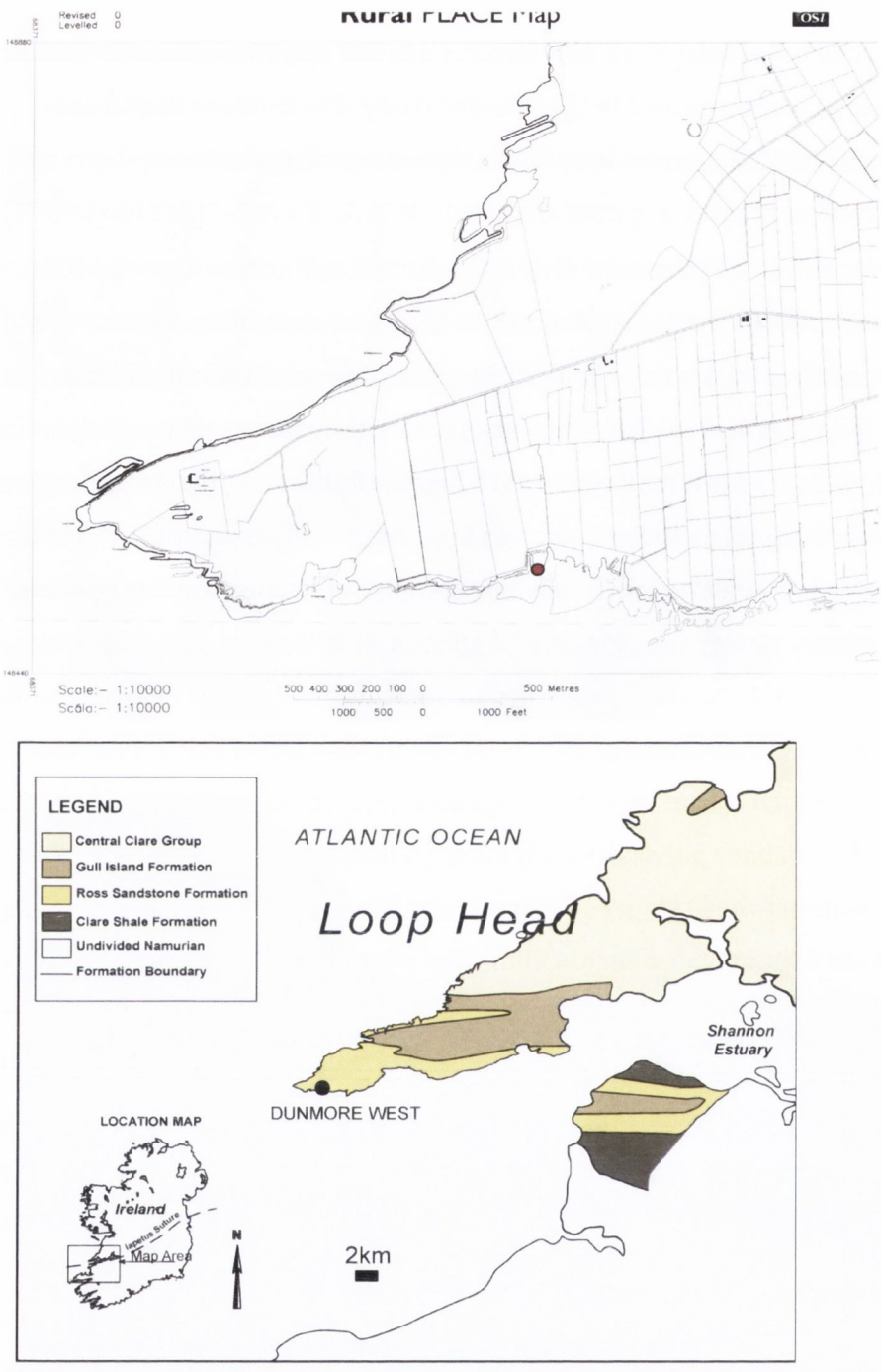

Fig. 2.31. Location map showing Dunmore West sampling locality at [70494/46845] and geological map of the Shannon Basin showing the locality and regional geology (OSI rural place maps: http://maps.osi.ie/publicviewer).

The fifth and topmost horizon, where solid ammonoids in bullions are present, contains a mixed assemblage dominated by *Phillipsoceras/Reticuloceras* spp.; in this case, this assemblage found in the shales is replicated very well in the bullion material. The topmost horizon also contained a trilobite pygidium (see Ch. 3 for palaeoecology discussion). Gillian Lewarne similarly recorded a mixed assemblage with (in order of decreasing abundance): *Ph. circumplicatile* and allied species, *Ph. circumplicatile* late form, *V. henkei* and *Ht. prereticulatus*. Ammonoids were also found west of this outcrop along the coastline towards the lighthouse, on mm-scale shale horizons within low-density turbidite sequences, [70266/46837], below the "Dunmore West" band (see Chapter 4 for details). They are also preserved as external casts at the base of a massive sandstone east of the condensed section in a gully [70662/46893].

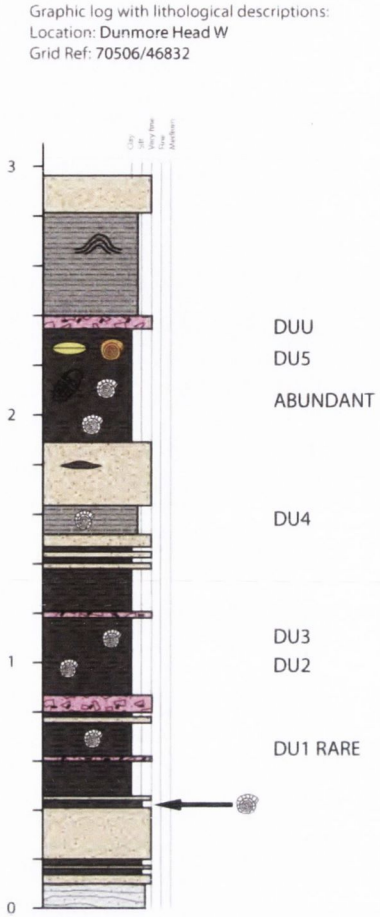

Samples [70494/46845]	Description	Fossil content (taxa in a given horizon are ordered by abundance)
DUU	Ammonoid-bearing bullion material	*V.* cf. *henkei*, *Phillipsoceras/Reticuloceras* spp., *Ht* cf. *varicatus*, *V. henkei*, *Ph. circumplicatile*, *Ph.* cf. *circumplicatile*, *Ht. varicatus*, Family *paucicrenulatum-circumplicatile*, *Ph.* cf. *paucicrenulatum*, *Hod.* cf. *magistrorum*, Bivalve Material
DU5	Ammonoid-bearing shale	*Phillipsoceras/Reticuloceras* spp., *Ph. circumplicatile*, *V. henkei*, *Ph. ? circumplicatile*, *Ph. paucicrenulatum*, Family *paucicrenulatum-circumplicatile*, *Caneyella* sp., *Ht.* cf. *varicatus*, *Ph.* cf. *paucicrenulatum*, *Ph.* cf. *circumplicatile*, *A./D.* sp., Trilobite pygidium
DU4	Ammonoid-bearing shale	Juvenile ammonoids and striae
DU3	Ammonoid-bearing shale	*V. henkei*, *V.* cf. *henkei*, *Phillipsoceras/Reticuloceras* spp., *Ht.* cf. *prereticulatus*, Plant Material, *Hod.* cf. *magistrorum*, *Hod. magistrorum*, *Ht. prereticulatus*, *Ph.* cf. *paucicrenulatum*, *Ht. varicatus*, *Ht.* cf. *varicatus*, *Ph. paucicrenulatum*, *Ph. circumplicatile*, *A./D.* sp., Nautiloid
DU2	Ammonoid-bearing shale	*Phillipsoceras/Reticuloceras* spp., spat and juveniles
DU1	Ammonoid-bearing shale	?*Caneyella* sp. and ammonoid striae

Fig. 2.32. Sedimentary log of "Dunmore West" band showing ammonoid-bearing horizons.

2.2.2.8 "Rehy Hill" Band

On the south coast of Loop Head, on the southern flank of Rehy Hill [80776/48616], there is a condensed section, which was briefly visited but not measured due to its remote location (Fig. 2.33). It comprises at least four fossiliferous shale horizons and bullions.

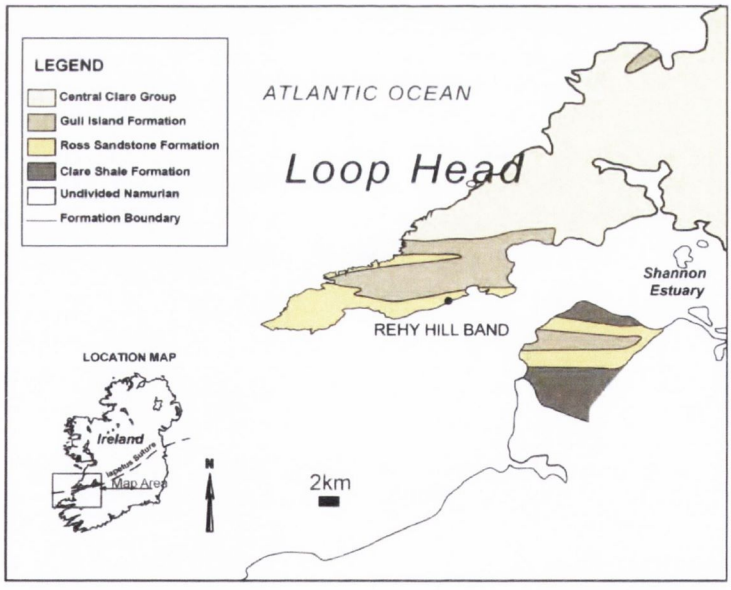

Fig. 2.33. Location map showing Rehy Hill sampling locality at [80776/48616] and geological map of the Shannon Basin showing the locality and regional geology (OSI rural place maps: http://maps.osi.ie/publicviewer).

Faunal Composition

Although bed-by-bed sampling could not be undertaken at this locality, overall the ammonoid assemblages were seen to be very diverse. Two horizons were sampled during this study (see Table 2.9): the lower one contains a mixed assemblage with *Phillipsoceras/Reticuloceras* spp. and *Ht.* cf. *varicatus;* the upper horizon is dominated by the genus *Phillipsoceras/Reticuloceras,* with various species represented, and *V. henkei* and *Ht.* cf. *varicatus* also present; crinoid moulds are abundant, in the shape of disarticulated ossicles. Specimens are often pyritized or preserved as 3D external moulds in bullion material. Outcrop abundance of ammonoids in the two horizons was not described for this band.

Samples [80776/48616]	Description	Fossil content (taxa in a given horizon are ordered by abundance)
REU	Ammonoid-bearing shale and bullion material	*Ph./R.* spp., *Ph. cp., Ph.* cf. *cp., R. cf. pulchellum, V.* cf. *henkei, V. henkei, Ph.* cf. *paucicrenulatum,* Crinoid Material, *Caneyella* sp., *Ht.* cf. *varicatus*
REL	Ammonoid-bearing shale	*Ph./R.* spp., *Ht.* cf. *varicatus,* Plant Material, Pyritized juvenile Ammonoid Material

Table 2.9. "Rehy Hill" band faunal content.

2.2.2.9 "Senan's Beach" Band

On the south coast of Loop Head, just west of Kicloher Cliff, there is a small pebbly beach named Kicloher Bay (Fig. 2.35), or sometimes referred to as Senan's Bay, after Senan's Well, which is just north of the beach. Within this bay, there is a c.2.85 m-thick condensed section, [76725/47707] (see log in Fig. 2.36), which is easily accessed at low tide, but is permanently in part covered by sea drift. This condensed section is taken to start above a sand-rich siltstone c.10 cm-thick, which is underlain by a massive sandstone. The beds here dip steeply and are eroded to near sea level. A small E-W trending fault offsets the condensed section (Fig. 2.34).

Fig. 2.34. Senan's Beach condensed section offset by a small fault, [76725/47707].

The basal part of the section is made up of siltstone with occasional sandy interbeds; overlying this, is a 10 cm-thick black shale bed. A sandstone interbed, which varies laterally in thickness from c.35 to 50 cm, splits locally along strike into two sandstone beds, which then amalgamate along strike.

Above this, is a 30 cm siltstone, which is overlain by a 1 m-thick sequence of sandstone and siltstones. This is overlain by a second shale-dominated sequence c.15 cm-thick. Next, is a sequence of siltstone beds, with occasional thin sandstone interbeds. The condensed section is taken to end above this siltstone sequence, where there is a prominent sandy siltstone bed.

Faunal Composition

There are two fossiliferous beds within this condensed section, corresponding to the two most prominent shale sections: the lower horizon contains frequent to rare ammonoids, with only one identifiable specimen (*V.* cf. *henkei*). The topmost shale had ammonoids concentrated in broadly two horizons. It contained a mixed and abundant assemblage of ammonoids and plant material (non-pyritized), dominated by *Phillipsoceras/Reticuloceras* spp. and *Ph.* cf. *circumplicatile.*

All ammonoids are preserved as 2D moulds of the external shell and some are partially pyritized, so that they can be easily picked out on the exposed surface of the shale, even when partially covered by seawater. In the c.6 m-thick siltstone-dominated, thin-bedded sequence above this condensed section, ammonoid-bearing muddy silts were recorded (for details, see Chapter 4).

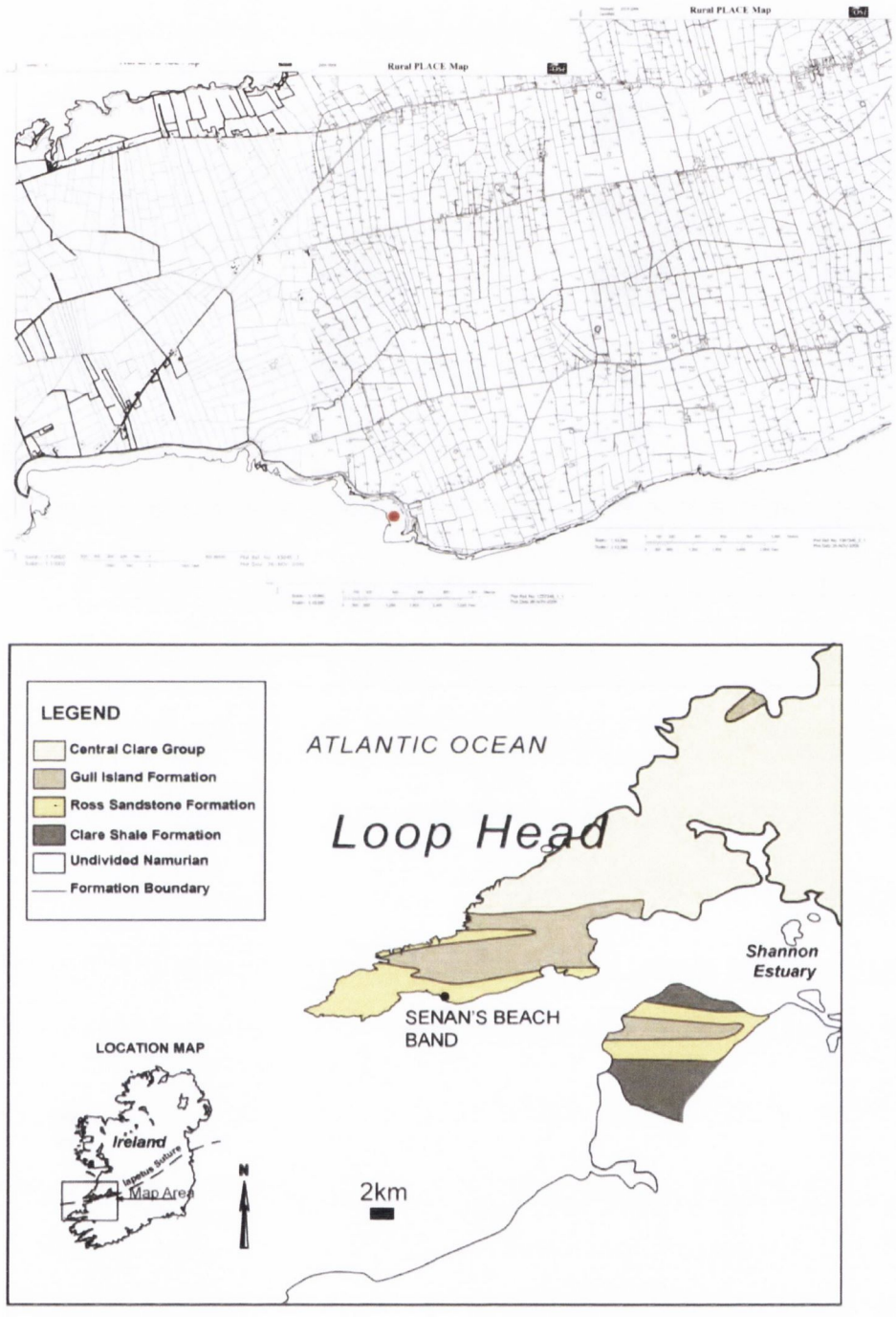

Fig. 2.35. Location map showing Senan's Beach band sampling locality at [76725/47707] and geological map of the Shannon Basin showing the locality and regional geology (OSI rural place maps: http://maps.osi.ie/publicviewer).

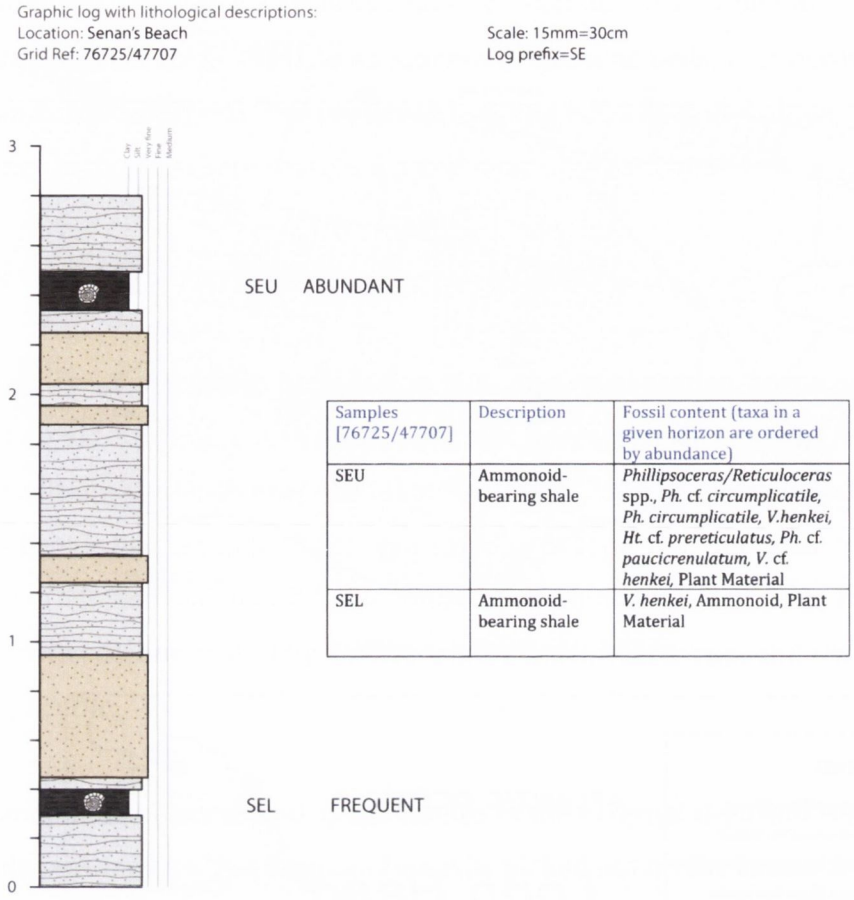

Fig. 2.36 Sedimentary log of "Senan's Beach" band.

2.2.2.10 "West Senan's Beach" Band

Following the coastline west from Senan's Beach, an immediately obvious thinly-bedded, shale-dominated condensed section crops out [76525/47887] and can be traced laterally for c.20-30 m along the coastline (Fig. 2.38). The section starts above a massive sandstone that forms a prominent ledge, and it consists of 1.1 m of siltstone and shale, with occasional laminated sandstone interbeds (Fig. 2.37). There are occasional concretions with pyrite-rich centres and the thickest (c.20 cm-thick) black shale sequence is nested in the centre of the condensed section. The shale beds are sooty and sulphur-leaching gives

them a distinctive yellow staining. The section is taken to end at the base of the first massive sandstone with thickness greater than 90 cm.

Faunal Composition

Ammonoids are rare in this section, and concentrated in resistant, silty shale horizons within the shale sequence (Fig. 2.39). Ammonoids are preserved as 2D moulds on the shales and no ammonoids were found in the bullions. The poor preservation of the specimens does not allow identification beyond the subclass level.

Ammonoids were also found in silt-rich mudstones further west, on the east side of Kilbaha Bay [75394/48264] (see Chapter 4 for details).

Fig. 2.37. West Senan's Beach band at [76525/47887].

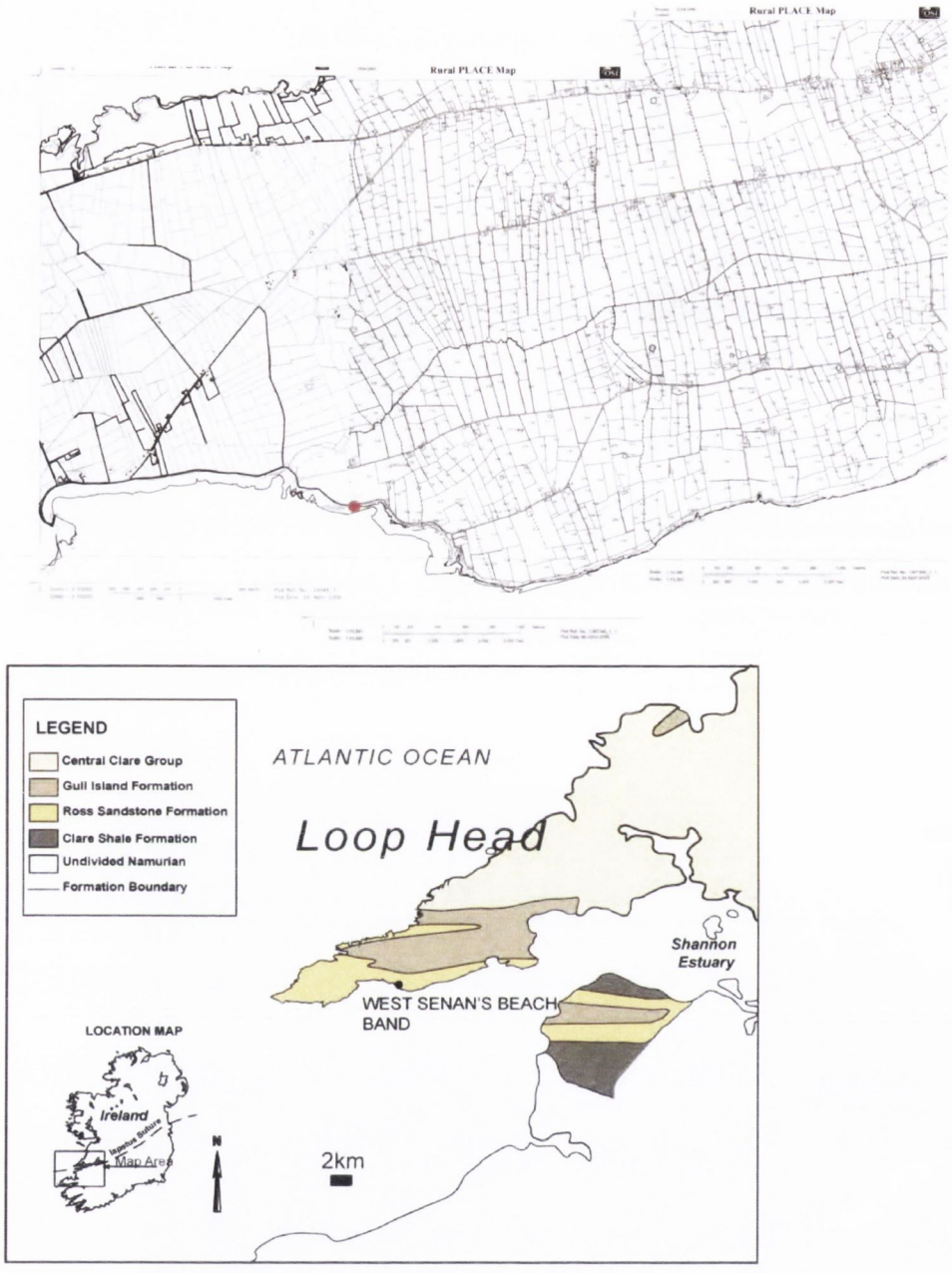

Fig. 2.38. Location map showing West Senan's Beach band sampling locality at [76525/47887] and geological map of the Shannon Basin showing the locality and regional geology (OSI rural place maps: http://maps.osi.ie/publicviewer).

Graphic log with lithological descriptions:
Location: West Senan's Beach Band
Grid Ref: 76525/47887

Log prefix=WSE

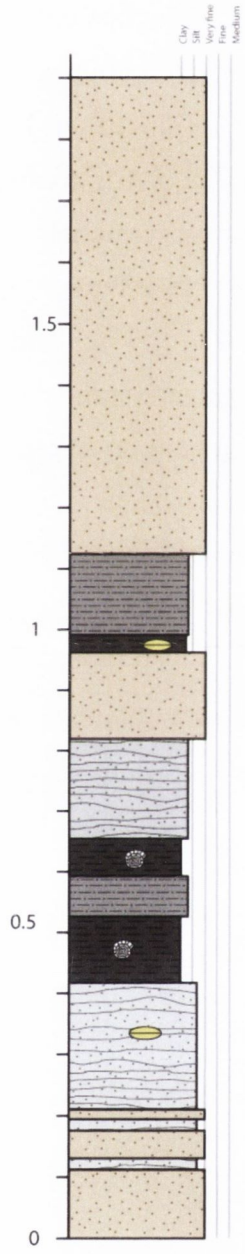

Samples [76525/47887]	Description	Fossil content (taxa in a given horizon are ordered by abundance)
WSE01	Ammonoid-bearing shale	Ammonoids, Plant Material

WSE01 RARE

WSE01 RARE

Fig. 2.39. Sedimentary log of "West Senan's Beach" band showing sampled horizons.

2.2.2.11 "Lighthouse" Band

On the tip of Loop Head, west of the lighthouse and opposite the sea stack locally known as Diarmuid and Grainne's Rock, a condensed section crops out close to the cliff edge [70420/48683] (Fig. 2.40-41). The condensed section is c.2.5 m-thick and its base is taken at the top of the sandstone bed (more than 1 m-thick) below which there is no access due to its location in close proximity to the cliff edge. The section starts off with grey, silt-rich shales with occasional sandstone interbeds less than 2 mm-thick. The main lithology is black shale, which either splits along bedding in thin sheets (paper shale) or is clay rich and difficult to split. This shale is punctuated by two quartz-rich grey sandstone beds (each c.25 cm-thick), and occasional siltstone interbeds. Overall the shale is stained by sulphur-leaching, which gives it a distinctive yellow-orange colour.

The condensed section is taken to end approximately where the black shale is shaped into glacial folds of Quaternary age and there are also rare bullions. Above this, it is covered by grass. It is therefore possible that the section is thicker than the 2.5 m seen here.

Fig. 2.40. Lighthouse band outcrop at tip of Loop Head at [70420/48683].

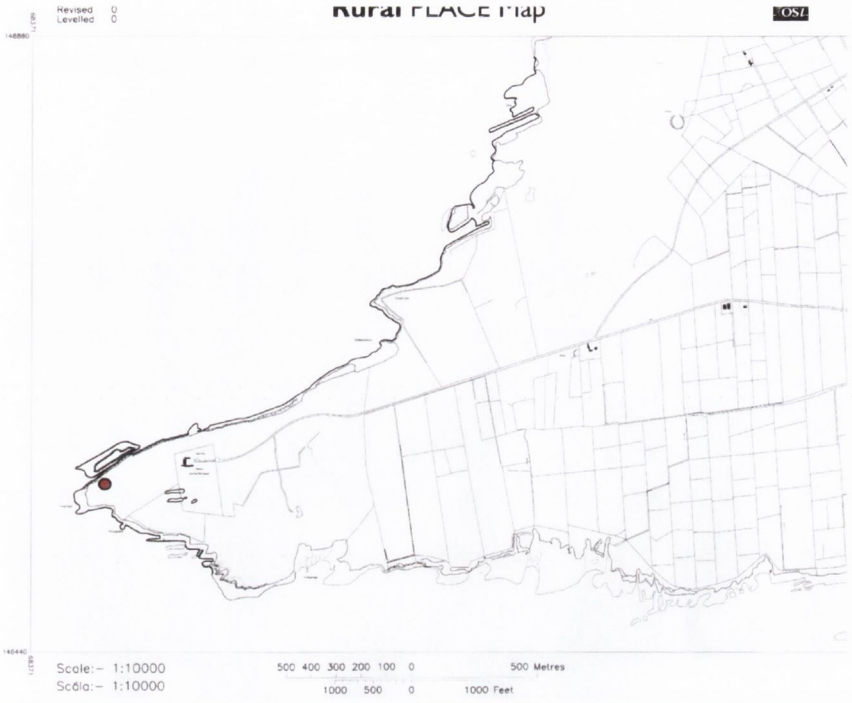

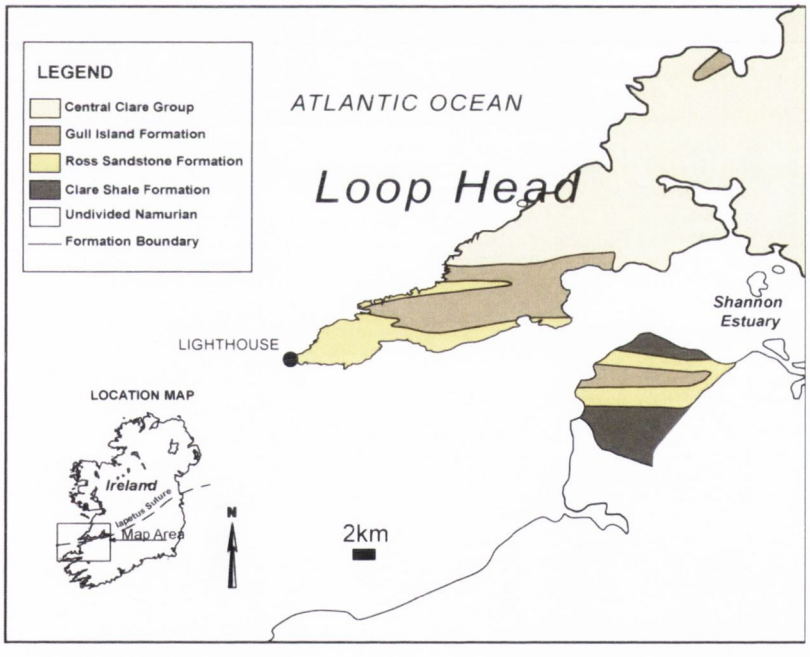

Fig. 2.41. Location map showing Lighthouse sampling locality at [70420/48683] and geological map of the Shannon Basin showing the locality and regional geology (OSI rural place maps: http://maps.osi.ie/publicviewer).

Faunal Composition

A typical assemblage of ammonoids, nautiloids, bivalves and plant material is present.

Ammonoids are found in a range of concentrations within the shale. They are rare in the lowest portion of the condensed section, (from c.75 cm to 1 m; see sedimentary log in Fig. 2.42), but become more abundant from 1.35 to 1.80 m, where they are highly weathered and of poor quality. Ammonoids are also abundant above the topmost sandstone bed, where they are preserved both as 2D moulds (L03) and as solid specimens in bullions found in the topmost shale beds (L03b). Sample L01 encompasses the whole section, whilst sample L02 is taken from a sand-rich siltstone horizon with plant material. The assemblages are varied from bottom to top, *Phillipsoceras/Reticuloceras* spp. (specifically the family *Ph. circumplicatile* to *Ph. paucicrenulatum)* and *V.* cf. *henkei* being the main taxonomical components. Overall, preservation is poor due to weathering, and complete specimens are difficult to sample due to splitting along cleavage in the clay-rich shales. Lewarne (unpublished notes) recorded the presence of the following taxa at this locality, in order of abundance: *V. henkei, Ph. circumplicatile, Ph. circumplicatile* (late form), *Ht. varicatus?.*

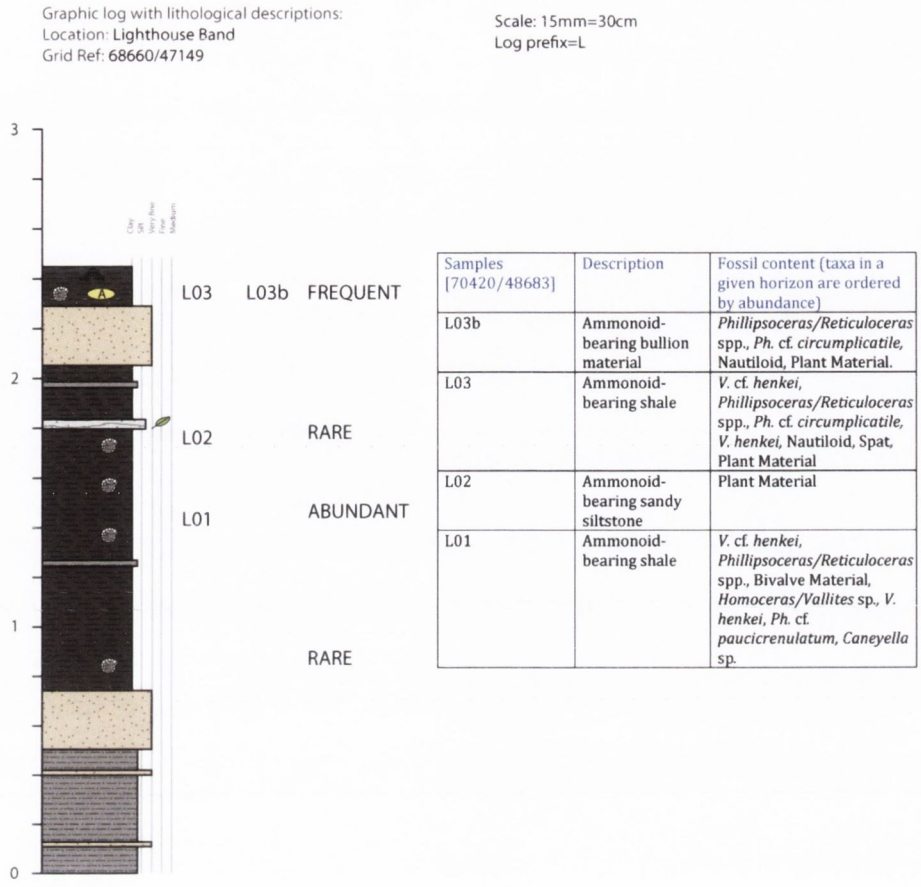

Samples [70420/48683]	Description	Fossil content (taxa in a given horizon are ordered by abundance)
L03b	Ammonoid-bearing bullion material	*Phillipsoceras/Reticuloceras* spp., *Ph.* cf. *circumplicatile*, Nautiloid, Plant Material.
L03	Ammonoid-bearing shale	*V.* cf. *henkei*, *Phillipsoceras/Reticuloceras* spp., *Ph.* cf. *circumplicatile*, *V. henkei*, Nautiloid, Spat, Plant Material
L02	Ammonoid-bearing sandy siltstone	Plant Material
L01	Ammonoid-bearing shale	*V.* cf. *henkei*, *Phillipsoceras/Reticuloceras* spp., Bivalve Material, *Homoceras/Vallites* sp., *V. henkei*, *Ph.* cf. *paucicrenulatum*, *Caneyella* sp.

Fig. 2.42. Sedimentary log of "Lighthouse band", showing sample location.

2.2.2.12 "Toorkeal" Band

On the north coast of Loop Head, about 500 m northeast from Toorkeal Bay, a condensed section crops out in a small exposure near the cliff edge at [76635/51342]. It lies above a double-slumped horizon and, as such, is easily traced laterally in the cliffs from Toorkeal Bay to the examined outcrop to the northeast, which lies close to Quilty (see Fig. 2.44 for location). Above the condensed section, lies a sequence of thick channel sands.

This condensed section is 2.2 m-thick and is dominated by very soft, clay-rich paper shales, which are mostly grey, but also contain some darker horizons where ammonoids are concentrated. The top of the condensed section is taken to be at the base of a grey sandstone bed 40 cm-thick, with mm-scale mud

clasts (Fig. 2.43). The condensed section is very sulphur-rich, with sulphur leaching commonly observed. Occasional very fine sandstone interbeds with cm-scale ripple cross-lamination are observed. In comparison to other condensed sections (for instance, the "Dunmore West" band or the "Reading Room" band), this one is not as thickly developed, nor is the colour as distinctively black.

Faunal Composition

Ammonoids are abundant towards the top of the condensed section (Fig. 2.45), in the 7 cm band below the overlying sandstone and frequent to rare below this level. Ammonoids are solely preserved as 2D moulds of the external shell and the ammonoid assemblage at this condensed section is dominated by *Phillipsoceras/Reticuloceras* spp. and *V.* cf. *henkei*. Bivalves (*Dunbarella* sp.) and plant material are also present.

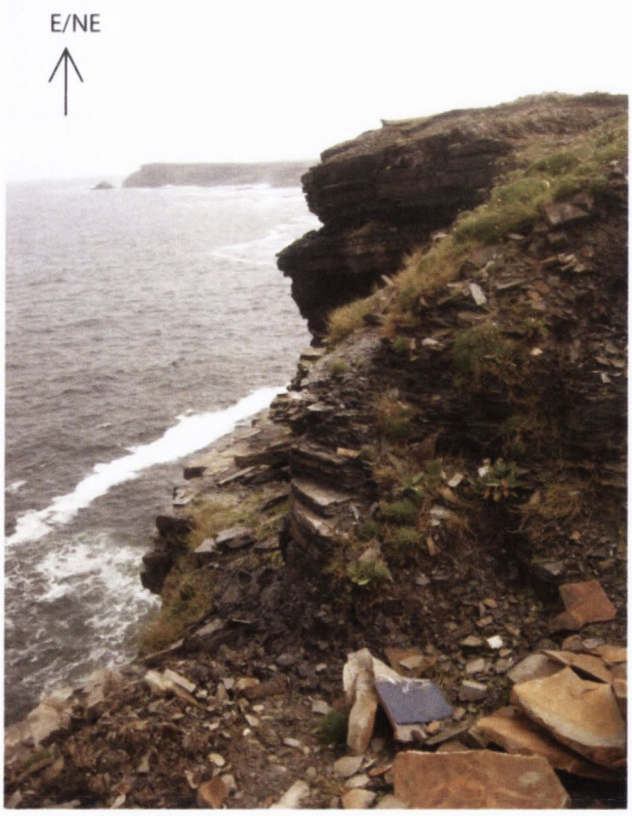

Fig. 2.43. Toorkeal Band, north coast of Loop Head at [76635/51342].

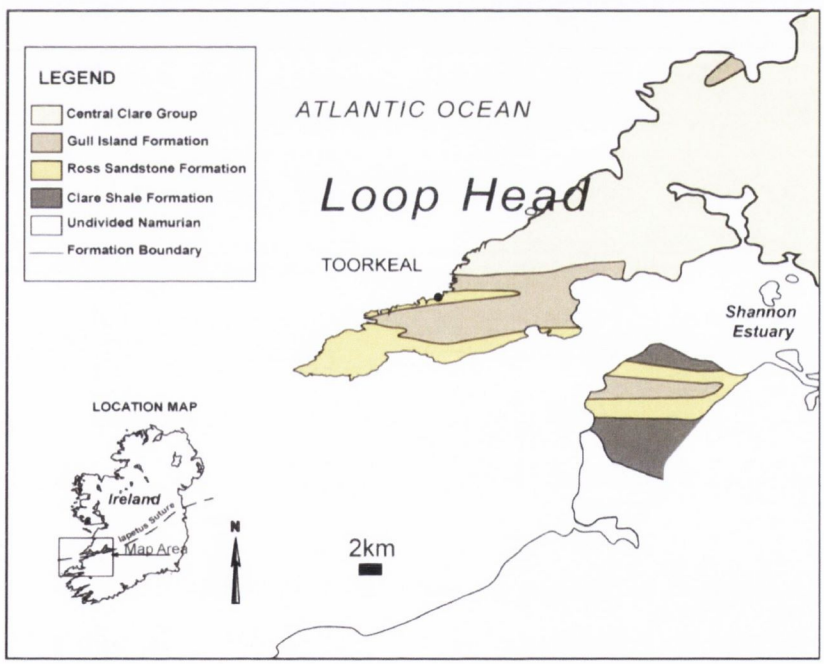

Fig. 2.44. Location map showing Toorkeal sampling locality at [76635/51342] and geological map of the Shannon Basin showing the locality and regional geology (Google Earth map).

Graphic log with lithological descriptions:
Location: Toorkeal
Grid Ref: 76635/51338

Scale: 15mm=30cm
Log prefix=TO

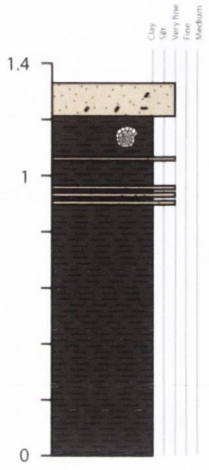

TO ABUNDANT

Samples [76635/51342]	Description	Fossil content (taxa in a given horizon are ordered by abundance)
TO	Ammonoid-bearing shale	*Phillipsoceras/Reticuloceras* spp., *V.* cf. *henkei, V. henkei, Ph.* cf. *circumplicatile, Ph.* cf. *paucicrenulatum, Dunbarella* sp., *Ph. paucicrenulatum, Ph. circumplicatile,* Plant material

Fig. 2.45. Sedimentary log of "Toorkeal band", showing sample location.

2.2.2.13 Rinevella

On the south coast at Rinevella, on the west side of Rinevella Bay, two ammonoid-rich bands were identified and sampled (Table 2.10). The first is located just west of Rinevella Point within a silt-dominated succession at [81692/49008], the second is c.20 m above it, where a small pier is built in a gully created by a mass transport deposit: right above this mass transport deposit, a thin, highly-fossiliferous bed is exposed (Fig. 2.46).

The lowest sampled horizon (RVW) is a dark shale (less than 10 cm in thickness) located within a silt-dominated succession (Fig. 2.47). The upper horizon (RVM), located above the slump at the pier, is a paper-shale only accessible at low tide. Another slump is present among the turbidite beds in the Rinevella Bay succession.

Fig. 2.46. Location map showing Rinevella sampling localities at [81692/49008] and geological map of the Shannon Basin showing the locality and regional geology (OSI rural place maps: http://maps.osi.ie/publicviewer).

Faunal Composition

The lowest horizon contains frequent to rare ammonoids preserved as 2D moulds: the assemblage is dominated by *Phillipsoceras/Reticuloceras* spp., with associated *V.* cf. *henkei* and plant material. The higher horizon contains abundant ammonoids, with dominant *V.* cf. *henkei* and associated *Phillipsoceras/Reticuloceras* spp. and plant material.

Samples	Irish Grid Reference	Description	Fossil content (taxa in a given horizon are ordered by abundance)
RVM	81840/49106	Ammonoid-bearing shale	*V.* cf. *henkei, Ph./R.* spp., Plant Material
RVW	81692/49008	Ammonoid-bearing shale	*Phillipsoceras/Reticuloceras* spp., *V.* cf. *henkei*, Plant Material

Table 2.10. Rinevella faunal content.

Fig. 2.47. Lowest of two sampled horizons (RVW), close to Rinevella Point at [81692/49008]. Hammer for scale.

2.2.2.14 "Holy Well" Band

The Ross Sandstone Formation is well exposed on the south coast of Loop Head (and the northern side of the Shannon Estuary), between the lighthouse at Kilcredaun and Carrigaholt, where a sequence of thin-bedded turbidite deposits with local slumped horizons is present. For details of ammonoid-bearing siltstone horizons found outside of condensed sections, east of the Kilcredaun lighthouse, [84922/49205] (Fig. 2.48), see Chapter 4. On the south coast of Loop Head, there is a holy well close to Kilcredaun Point. Just below it, [85090/49408], on the coastal outcrop, a condensed section (here named after this holy well) forms a gully. This outcrop is easily recognized thanks to a stone cross, and it can be accessed by climbing down a series of man-made steps with a rope attached to them.

The condensed section is c.2.5 m-thick (Fig. 2.49) and it is taken to begin above the prominent sandstone that makes up the base of the gully. Overall, it is dominated by shale, with a siltstone-dominated interval in the middle. At its base is grey, clay–rich shale, with interbedded black shale, which is recessed. This is overlain by siltstone and then a black fossiliferous shale interval (c.10 cm-thick). Then, a sequence of very fine sandstone beds with interbedded siltstones is present. The sandstones have load structures at their base, as well as ripples on their tops. This is succeeded by a c.20 cm-thick fossiliferous black shale. It contains occasional coaly layers and is characterized by yellow sulphur leaching. This is in turn overlain by a siltstone with coarser sandy intercalations and a series of thickening upwards sandstone packages. The condensed section is taken to end with the start of a 1.5 m-thick sequence of thickening upwards sandstone beds that end in a grassy cover.

Faunal Composition

Even though ammonoids are present in varying abundances throughout the section, two main fossiliferous intervals were identified and sampled (Fig. 2.49). They correspond to two black shale packages. It should be noted that the

lowermost black shale package, despite intensive investigation, did not yield any fossils. In the lowest of the two main fossiliferous black shale intervals (sample KILHL) ammonoids were rare: they formed a mixed assemblage dominated by *Phillipsoceras/Reticuloceras* spp., with associated bivalve and plant material. The upper unit (sample KILHU) was rich in ammonoids, with several growth stages represented: the assemblage was very diverse and again dominated by by *Phillipsoceras/Reticuloceras* spp., with associated bivalve and plant material; *V. henkei* (and *V.* cf. *henkei*) also constituted an important element of the assemblage.

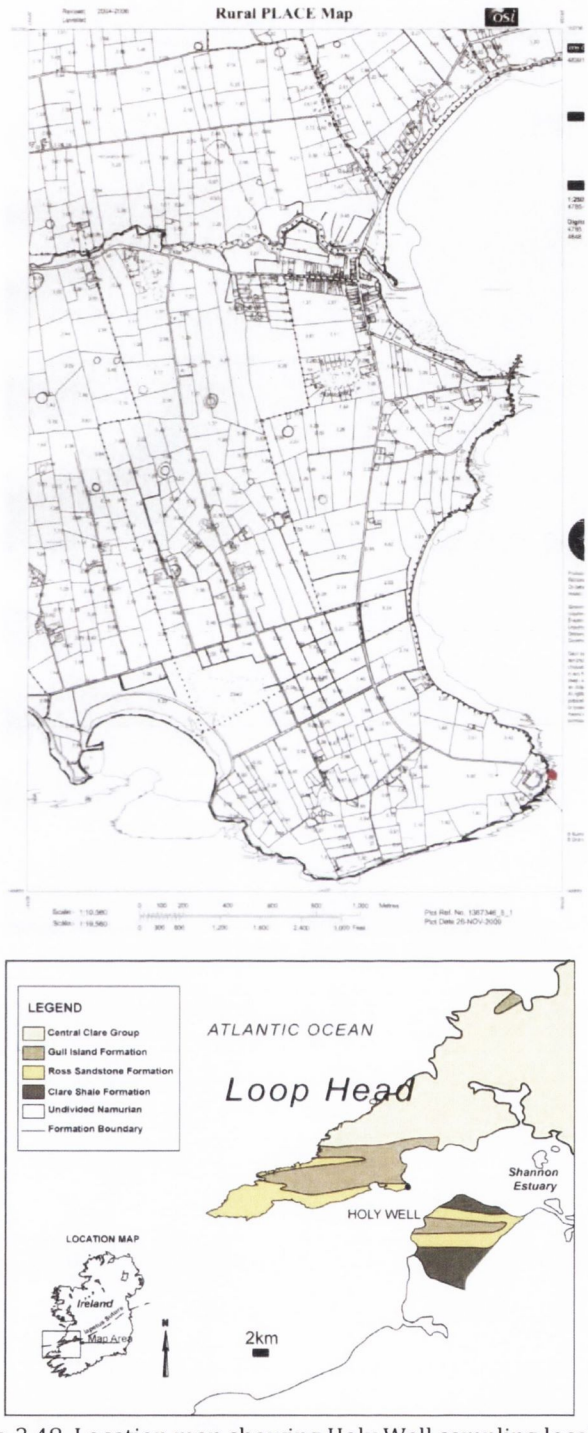

Fig. 2.48. Location map showing Holy Well sampling locality at [84922/49205] and geological map of the Shannon Basin showing the locality and regional geology (OSI rural place maps: http://maps.osi.ie/publicviewer).

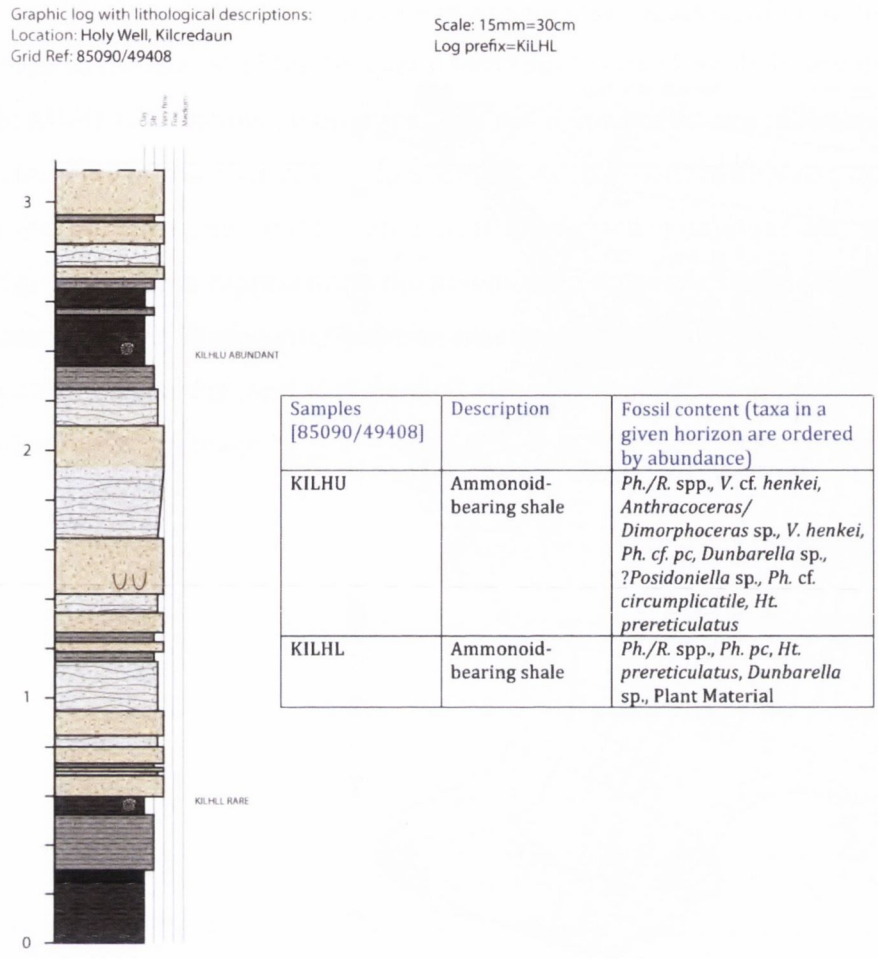

Samples [85090/49408]	Description	Fossil content (taxa in a given horizon are ordered by abundance)
KILHU	Ammonoid-bearing shale	*Ph./R.* spp., *V.* cf. *henkei, Anthracoceras/ Dimorphoceras* sp., *V. henkei, Ph. cf. pc, Dunbarella* sp., *?Posidoniella* sp., *Ph.* cf. *circumplicatile, Ht. prereticulatus*
KILHL	Ammonoid-bearing shale	*Ph./R.* spp., *Ph. pc, Ht. prereticulatus, Dunbarella* sp., Plant Material

Fig. 2.49. Sedimentary log of "Holy Well band", showing sample locations.

2.2.2.15 "Cloonconeen Lower" Band

On the east side of Rinevella Bay, west of Cloonconeen Point, a condensed section crops out at the top of a small gully, [82829/49445] (Fig. 2.51). It is c.2 m-thick and silt-dominated (Fig. 2.50). The start of the section is taken at the base of a sand ledge in the centre of the gully: at the base, there is a 1.35 m-thick sequence of siltstones with occasional sandy intercalations with ripple cross-laminae, punctuated by sandstone interbeds. This is overlain by the first shale sequence c.10 cm-thick, which is composed of a central silty shale separating two fossilifeous shale horizons at either side. Occasional clay-rich siltstone beds pinch in and out along strike. Next, a c.90 cm-thick siltstone

sequence with interbedded rippled sands, which sometimes thin and pinch out laterally, is present. Rare concretions are also present. The section ends with a c.55 cm-thick massive sandstone, which is distinctive since it is the thickest in the visible section. This condensed section is only accessible at low tide.

Faunal Composition

Ammonoids were found concentrated in two horizons within the shale beds (Fig. 2.52).

They are all preserved as 2D moulds of the external shell and form a mixed assemblage dominated by *Phillipsoceras/Reticuloceras* and *Ph.* cf. *circumplicatile* and *V.* cf. *henkei,* with associated *Ph.* cf. *paucicrenulatum.*

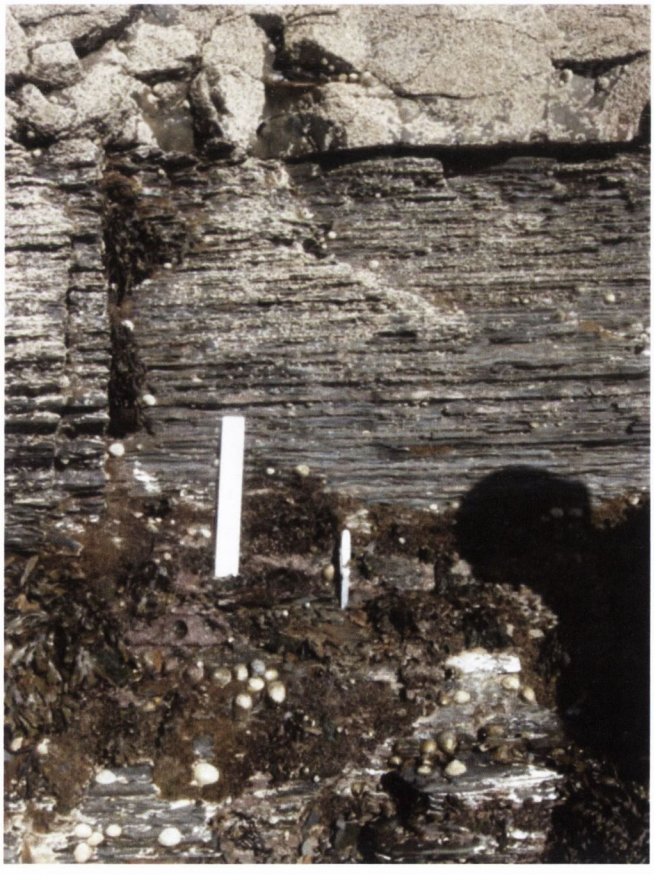

Fig. 2.50. Cloonconeen Lower band, [82829/49445]. Ruler is 30 cm long. Pen also for scale.

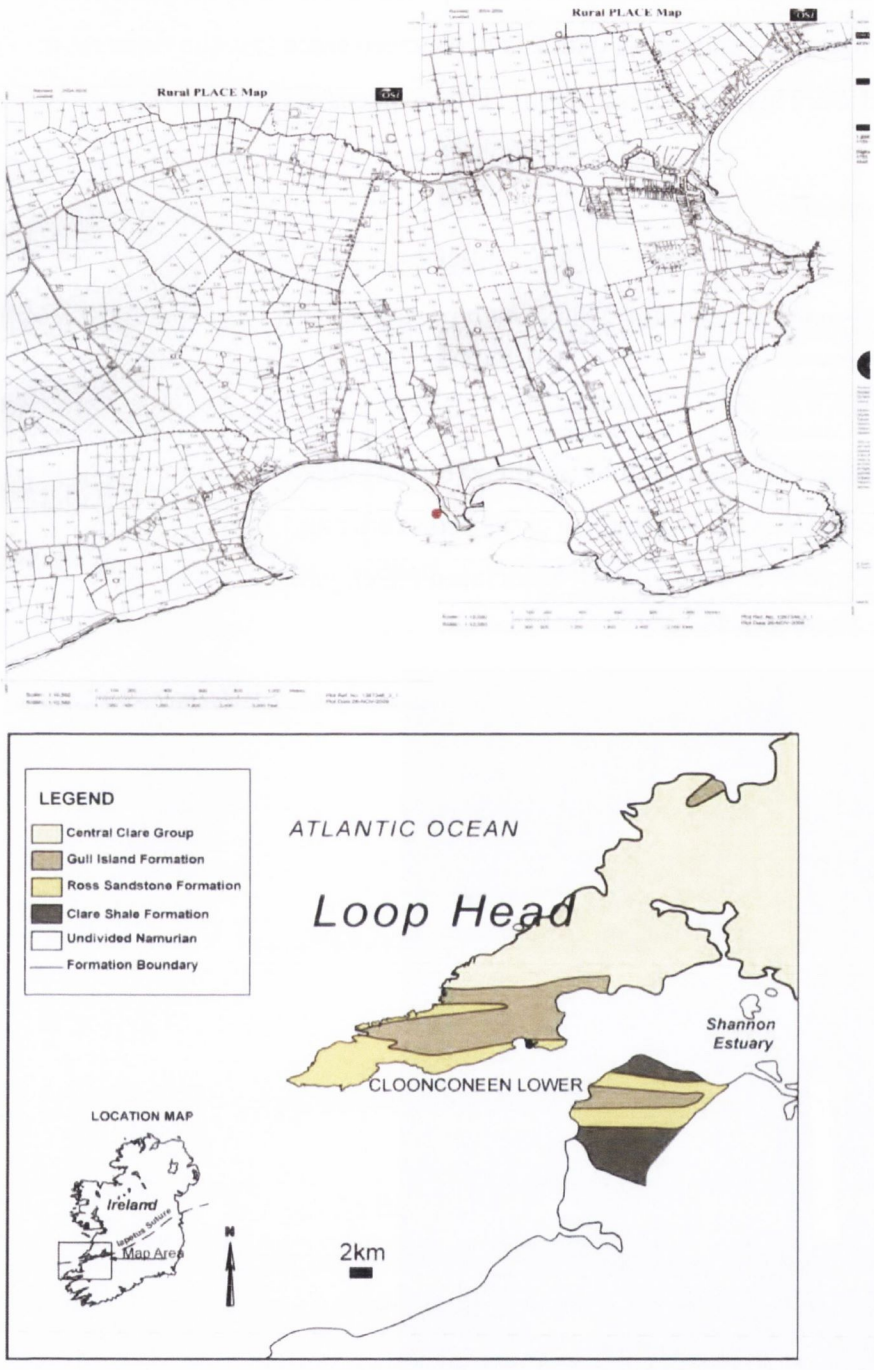

Fig. 2.51. Location map showing Cloonconeen Lower sampling locality at [82829/49445] and geological map of the Shannon Basin showing the locality and regional geology (OSI rural place maps: http://maps.osi.ie/publicviewer).

Graphic log with lithological descriptions:
Location: Cloonconeen Lower
Grid Ref: 82829/49445

Scale: 15mm=30cm
Log prefix=CLOL

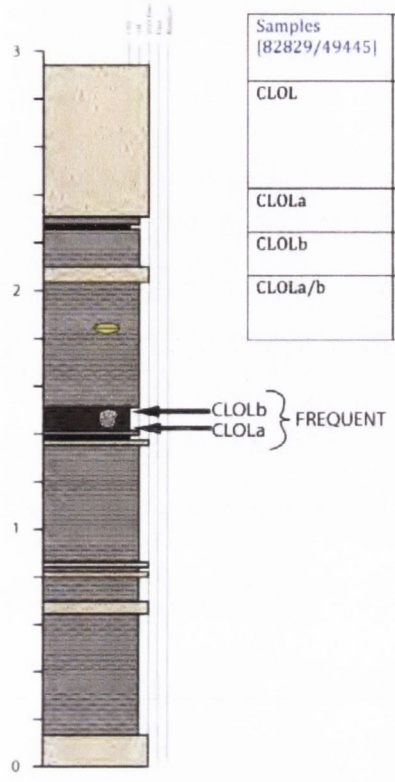

Samples (82829/49445)	Description	Fossil content (taxa in a given horizon are ordered by abundance)
CLOL	Ammonoid-bearing shale	*Ph. cf. circumplicatile, Ph./R.* spp., *V. henkei, Ph.* cf. *paucicrenulatum, V.* cf. *henkei, Dunbarella* sp., Plant Material
CLOLa	Ammonoid-bearing shale	*Phillipsoceras/Reticuloceras* spp., *Ph.* cf. *paucicrenulatum*
CLOLb	Ammonoid-bearing shale	Possible Juveniles
CLOLa/b	Ammonoid-bearing shale	*Phillipsoceras/Reticuloceras* spp., *Ph.* cf. *paucicrenulatum*, Plant Material

Fig. 2.52. Sedimentary log of "Cloonconeen Lower band", showing sampled horizons.

2.2.2.16 "Blackrock West" Band

This section crops out along the north coast at [70419/48692], between Blackrock and Gull Island (Fig. 2.54). It consists of c.1 m of recessed sediments, dominated by siltstone (Fig. 2.53). It starts above a sandstone bed with disturbed surface. This is overlain by a 35 cm-thick series of interbedded clay-rich siltstone, siltstone with sandy intercalations and silty shale. This is then succeeded by a c.10 cm-thick black, sulphur-rich shale, in turn overlain by a 40 cm-thick siltstone with occasional shale interbeds (whose thickness is on a sub-cm scale). Above this, is a c.5 cm-thick black shale horizon, which is overlain by a sequence of siltstone and very thin, mm-scale, sandstone beds thickening upwards to cm-scale. The condensed section is taken to end at the

base of the first bedded sandstone with ripple-cross lamination. Sandstone packages thicken upwards away from the condensed section.

Faunal Composition

Rare ammonoids are concentrated in the topmost dark shale horizon close to the top of the condensed section (no ammonoids were found from the lowest 10 cm-thick shale horizon), where they are all preserved as 2D moulds of the external shell. The ammonoid assemblage is diverse, yet dominated by *Phillipsoceras/Reticuloceras* spp.; plant material was also recovered (Fig. 2.55). This is not a typical highly-condensed section, since it is thinner and dominated by siltstone.

Fig. 2.53. Blackrock West band at [70419/48692]. Ruler is 30 cm long.

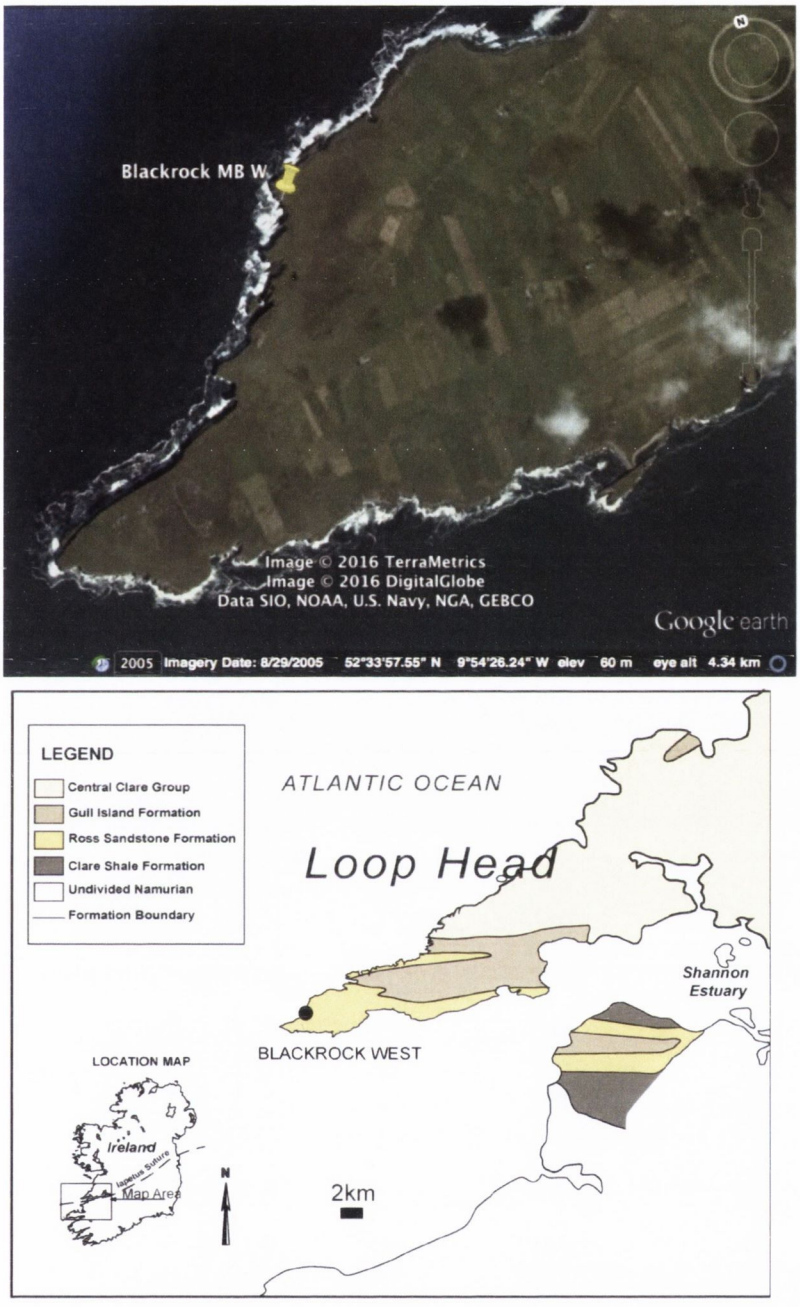

Fig. 2.54. Location map showing Blackrock West sampling locality at [70419/48692] and geological map of the Shannon Basin showing the locality and regional geology (Google Earth map).

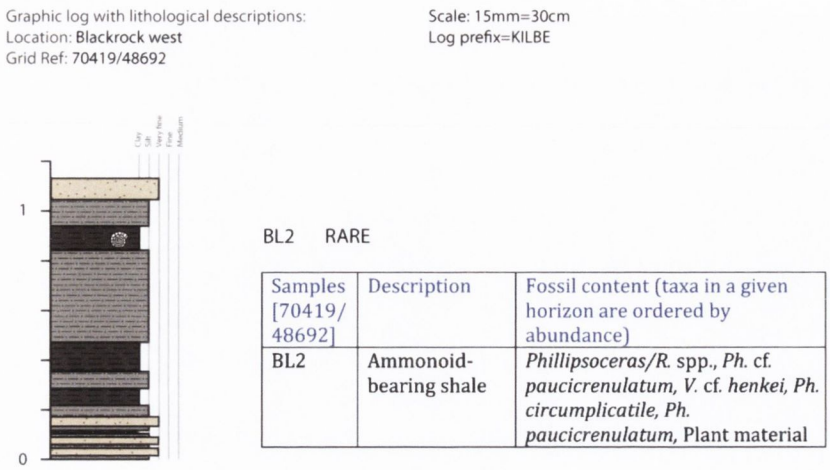

Fig. 2.55. Sedimentary log of "Blackrock west band", showing sample location.

2.2.2.17 Blackrock

Opposite the islet of Blackrock, there is a gully easily recognised by the presence of a parasitic fold and only accessible at low spring tide (Fig. 2.56). Here, among a series of laminated muds and siltstones [70420/48683], a thin, fossiliferous, sulphur-rich, silt-rich shale, grey and not fissile, was sampled (BL1). The laminated mudstones c.3 m below this horizon were also sampled (BL3): these are grey in colour, clay-rich and compacted, and split along cleavage, which has an angular orientation to bedding. The very clay-rich, pale appearance of these beds prompted further investigation in order to test the idea that it might be a bentonite deposit. QEMSCAN analysis of this sample is discussed in Chapter 5. This is not a highly condensed section, but rather, it is considered a siltstone-dominated succession with ammonoid and other faunas concentrated in the most condensed horizons.

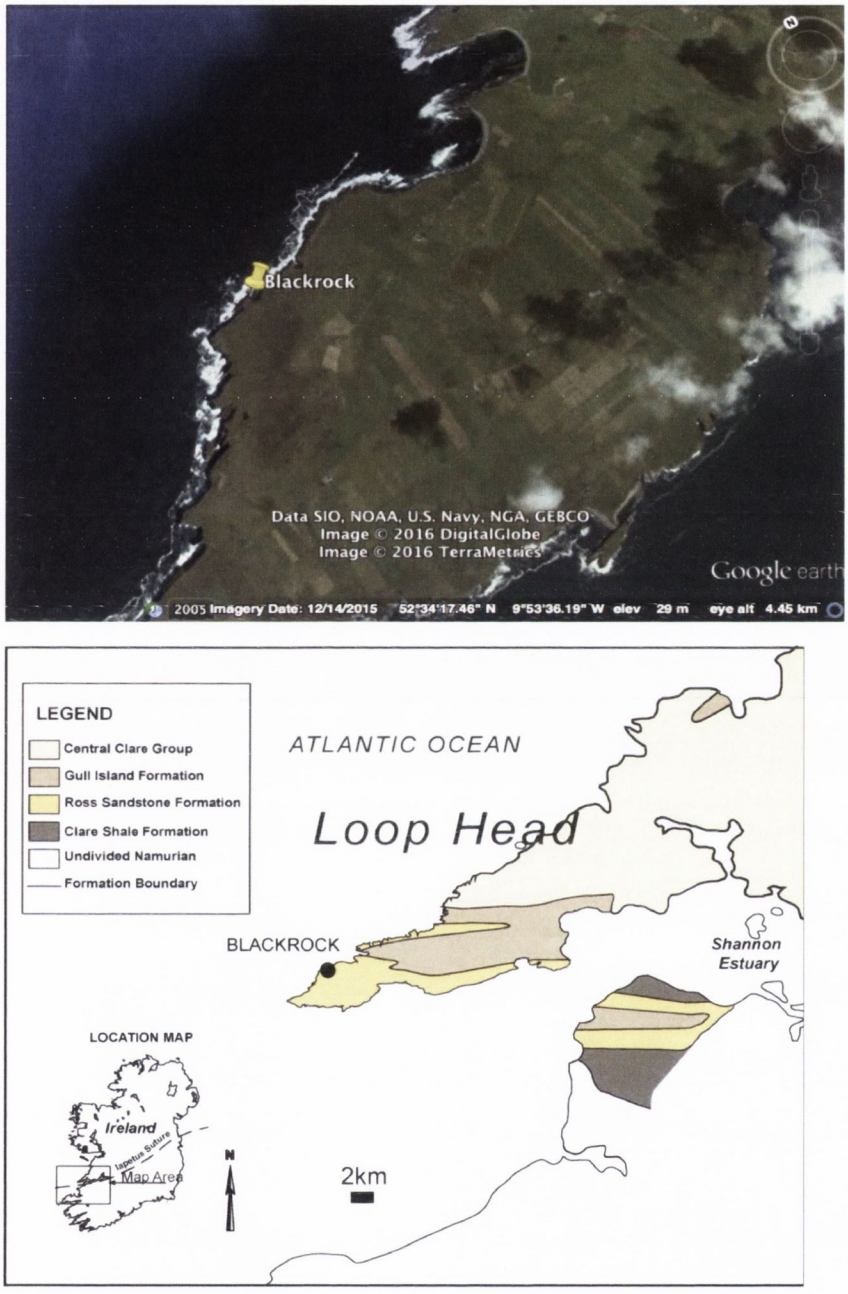

Fig. 2.56. Location map showing Blackrock West sampling locality at [70419/48692] and geological map of the Shannon Basin showing the locality and regional geology (Google Earth map).

Faunal Composition

Of the two horizons (Table 2.11) sampled at this locality, the lowest (BL3), contained abundant fragmentary bivalve material, as well as plant material and ammonoid material. The higher band (BL1) contained plant and ammonoid material (mostly in the juvenile growth stage and all preserved in the form of 2D moulds). If more time had been available at this locality, it is likely that more fossiliferous horizons would have been recognized.

Samples [70420/48683]	Description	Fossil content (taxa in a given horizon are ordered by abundance)
BL1	Ammonoid-bearing silty shale	Plant and Ammonoid Material
BL3	Ammonoid-bearing silty shale	Plant and Ammonoid Material

Table 2.11. Blackrock locality faunal content.

2.2.2.18 "Ross Bay East" Band

On the north side of Loop Head, at [72841/49714], there is a 1.80 m-thick condensed section (Fig. 2.57; 2.59), which starts above a massive sandstone and consists of a basal sequence of siltstone with sandstone and shale interbeds. The siltstone beds thin upwards and give way to c.30 cm of fossiliferous black, paper shale, overlain by a thin-bedded sequence of sandstone and siltstone. The section ends below the first massive sandstone bed. Above it, the sandstone beds thicken stratigraphically upwards.

Faunal Composition

Ammonoids are rare, weathered and of poor quality. They are all preserved as 2D moulds and are not always concentrated in the darkest, clay-rich shale, but

are mostly found in grey, paper shale at this locality. Plant material is abundant and the ammonoid assemblage consists of *Phillipsoceras/Reticuloceras* spp., *Ph. paucicrenulatum* and *V.* cf. *henkei*. Bivalves (*Dunbarella* sp.) and nautiloids are also present, as is typical of Namurian faunal assemblages (Fig. 2.58). Lewarne recorded the presence of *Reticuloceras* sp. at this locality (unpublished notes).

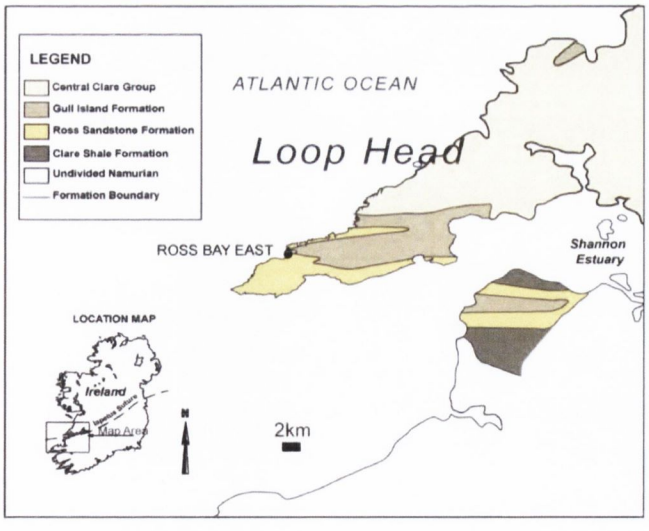

Fig. 2.57. Location map showing Ross Bay east sampling locality at [72841/49714] and geological map of the Shannon Basin showing the locality and regional geology (OSI rural place maps: http://maps.osi.ie/publicviewer).

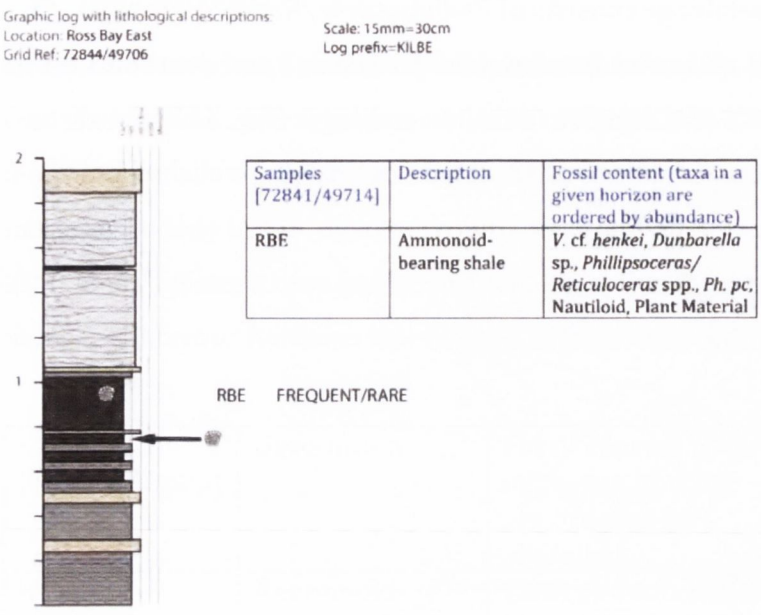

Samples [72841/49714]	Description	Fossil content (taxa in a given horizon are ordered by abundance)
RBE	Ammonoid-bearing shale	*V. cf. henkei*, *Dunbarella* sp., *Phillipsoceras/ Reticuloceras* spp., *Ph. pc*, Nautiloid, Plant Material

Fig. 2.58. Sedimentary log of Ross Bay east band, showing sampled horizons.

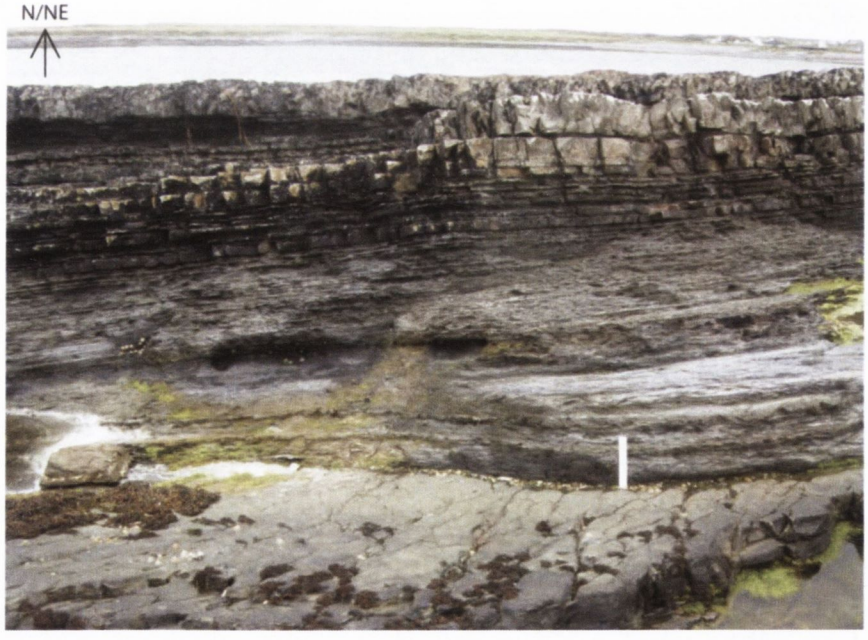

Fig. 2.59. Ross Bay East band at [72841/49714]. Ruler is 30 cm long.

2.2.2.19 "Cloonconeen Top" Band

On the east side of Rinevella Bay, west of Cloonconeen Point, a condensed section forms a prominent gully, [82774/49551], about 50 m above the "Cloonconeen Lower" band and with a prominent slump horizon just below. It is only accessible at low tide (Fig. 2.60). The gully is over 5 m-thick (Fig. 2.62), but the exposed portion of the section is only c.2.5 m-thick. The lowest exposure in the centre of the gully consists of shale. A 1.15 m-thick sequence of pyrite-rich, fossiliferous shales with occasional siltstone (less than 10 cm-thick) interbeds is overlain by a 50 cm-thick sequence of thin-bedded sands with rippled-tops and cross-laminae. Above this, a 60 cm-thick sequence of interbedded muds and thin sandstone beds with abundant bullions are present. The sandstones gradually thicken upwards up to a 40 cm-thick massive sandstone, where the condensed section is taken to end. This condensed section is also thought to be present in core 09-CE-UCD-01.

Faunal Composition

Two main fossil-rich horizons were identified (Fig. 2.61), even though more could be present but are covered by the sea (not in tidal range). Even though the ammonoid assemblage is diverse, the genus *Phillipsoceras* is the most abundant and is dominated by the taxon *Ph. paucicrenulatum,* with associated, minor *Ph. circumplicatile.* Although ammonoids are preserved as 2D moulds, several are partly pyritized. Ammonoids are abundant (as 3D external moulds) in the bullions at the top of the section, but they are unextractable. Ammonoids are abundant in both horizons, with various growth stages represented, but juveniles are preferentially preserved thanks to preferential pyritization of the inner whorls.

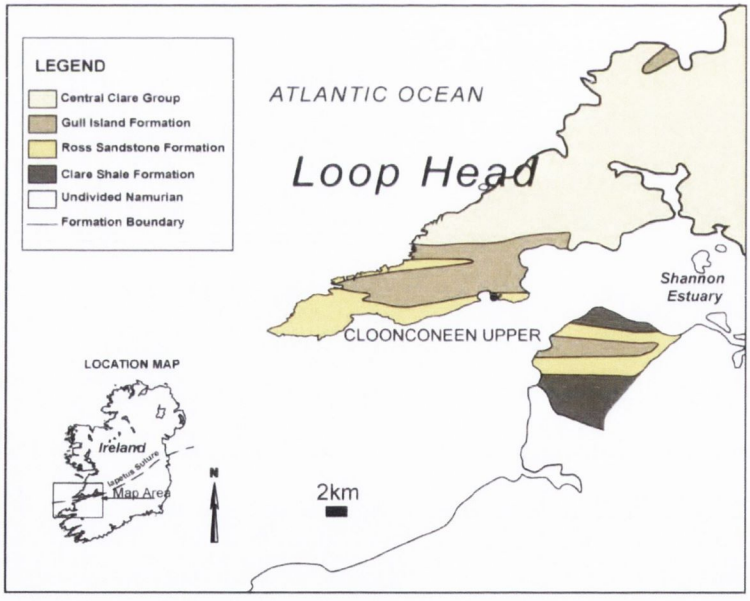

Fig. 2.60. Location map showing Cloonconeen Top sampling locality at [82774/49551] and geological map of the Shannon Basin showing the locality and regional geology (OSI rural place maps: http://maps.osi.ie/publicviewer).

Graphic log with lithological descriptions:
Location: Cloonconeen Top
Grid Ref: 82774/49551

Scale: 15mm=30cm
Log prefix=CLOU

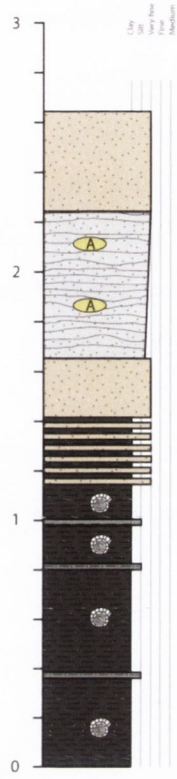

CLOUNO

CLOUa ABUNDANT

CLOUb ABUNDANT

Samples [82774/49551]	Description	Fossil content (taxa in a given horizon are ordered by abundance)
CLOUNO	Ammonoid-bearing bullion material	Ammonoid Material
CLOUa	Ammonoid-bearing shale	*Ph. paucicrenulatum, Phillipsoceras/Reticuloceras* spp., *Ph.* cf. *paucicrenulatum*
CLOUb	Ammonoid-bearing shale	*Phillipsoceras/R.* spp., *Ph.* cf. *paucicrenulatum, Ph. paucicrenulatum Ph.* cf. *circumplicatile, R.* cf. *pulchellum, Ph. circumplicatile*

Fig. 2.61. Sedimentary log of "Cloonconeen Top band".

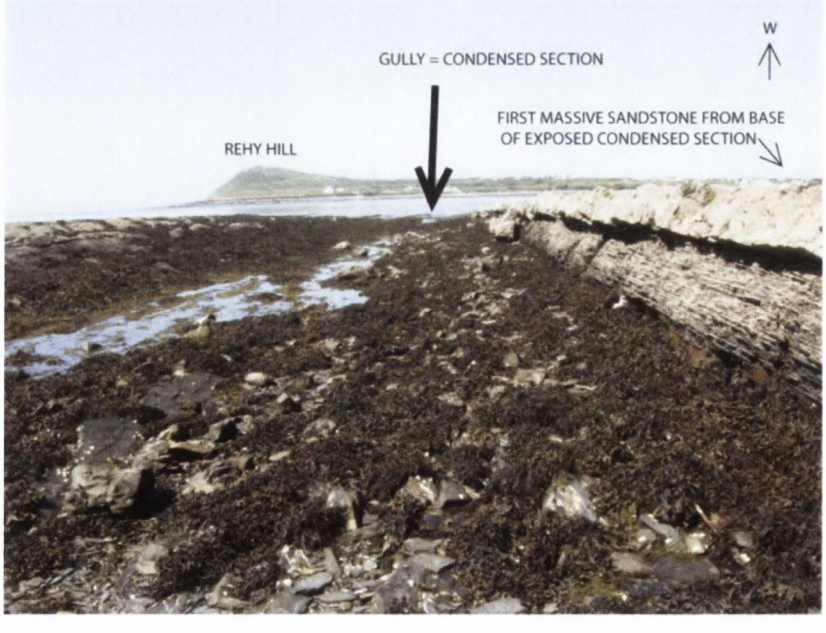

Fig. 2.62. "Cloonconeen Top Band" exposed in gully at [82774/49551].

2.2.2.20 "Kilcredaun Top" Band

On the south coast of Loop Head, a prominent gully is the site of a condensed section which is immediately obvious thanks to its considerable thickness (c.3.50 m) and the very dark colour of the shale, which is the dominant lithology (Fig. 2.64). It lies directly above a slump unit [85029/49504] and is eroded and recessed from its base, starting off with a 20 cm-thick siltstone bed, with sandy intercalations, overlain by silt-rich shale that is not very fissile. This is in turn overlain by c.2 m of shale, which varies between paper shale and clay-rich, resistant shale. Above this, lies a sequence of mud-rich siltstone and siltstone with sandy intercalations, overlain by a thickening upwards sequence of sand packages with ripple cross-lamination. This is overlain by a c.1 m-thick siltstone-dominated sequence, with frequent bullions that can be traced along bedding and sandy siltstone beds with disturbed lamination. The condensed section ends at the base of a 22 cm-thick massive sandstone with cross-lamination. Sandstone packages thicken upwards above this. This condensed section is thought to be present in core 09-CE-UCD-01.

Faunal Composition

Overall, a mixed assemblage of thick-shelled ammonoids, thin-shelled ammonoids, orthoconic nautiloids, plant material and bivalves is present. Ammonoids are found throughout the condensed section, concentrated in seven highly-fossiliferous horizons. Samples were taken from these seven horizons (Fig. 2.63; 2.65), as well as from a broader three-part subdivision of the condensed section (bottom, middle and upper: KILUB, KILMU, KILU).

Ammonoids are preserved as 2D moulds of the external shell, with various growth stages represented, and, in addition, 3D ammonoids are present in bullions in the topmost horizon, but they were unextractable. Broadly speaking, ammonoids from the lower portion of the condensed section form a diverse assemblage dominated by *Phillipsoceras/Reticuloceras* spp., with associated *V.* cf. *henkei, V. henkei* and *Ph.* cf. *paucicrenulatum.* The faunal

content of the middle part is similarly diverse, with *Phillipsoceras/Reticuloceras* spp. being the dominant taxon. The upper part of the condensed section is again dominated by various species of the genera *Phillipsoceras* and *Reticuloceras.* Both the bivalves *Dunbarella* sp. and *Caneyella* sp. are present.

In conclusion, the assemblages are dominated by the species of the genera *Reticuloceras* and *Phillipsoceras*, especially *Ph. circumplicatile* and *Ph. paucicrenulatum.*

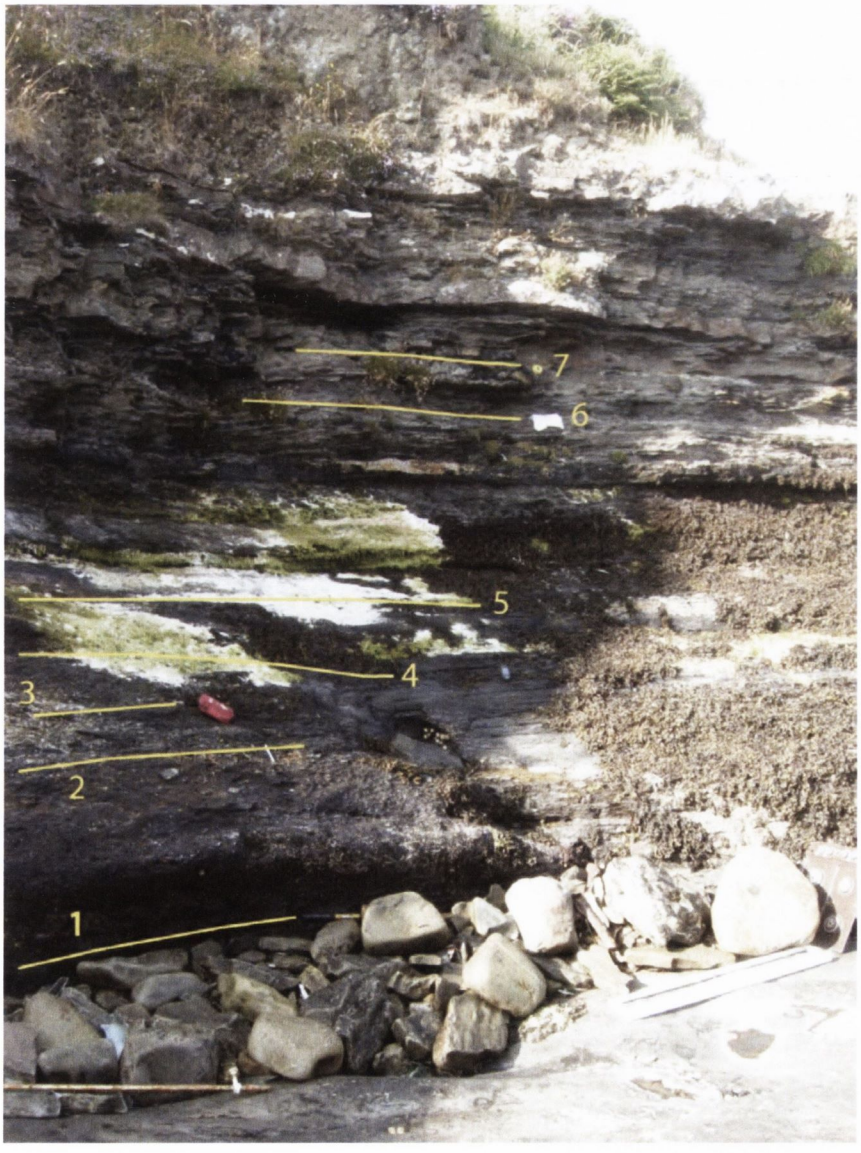

Fig. 2.63. Seven sampled horizons at "Kilcredaun Top band" at [85029/49504].

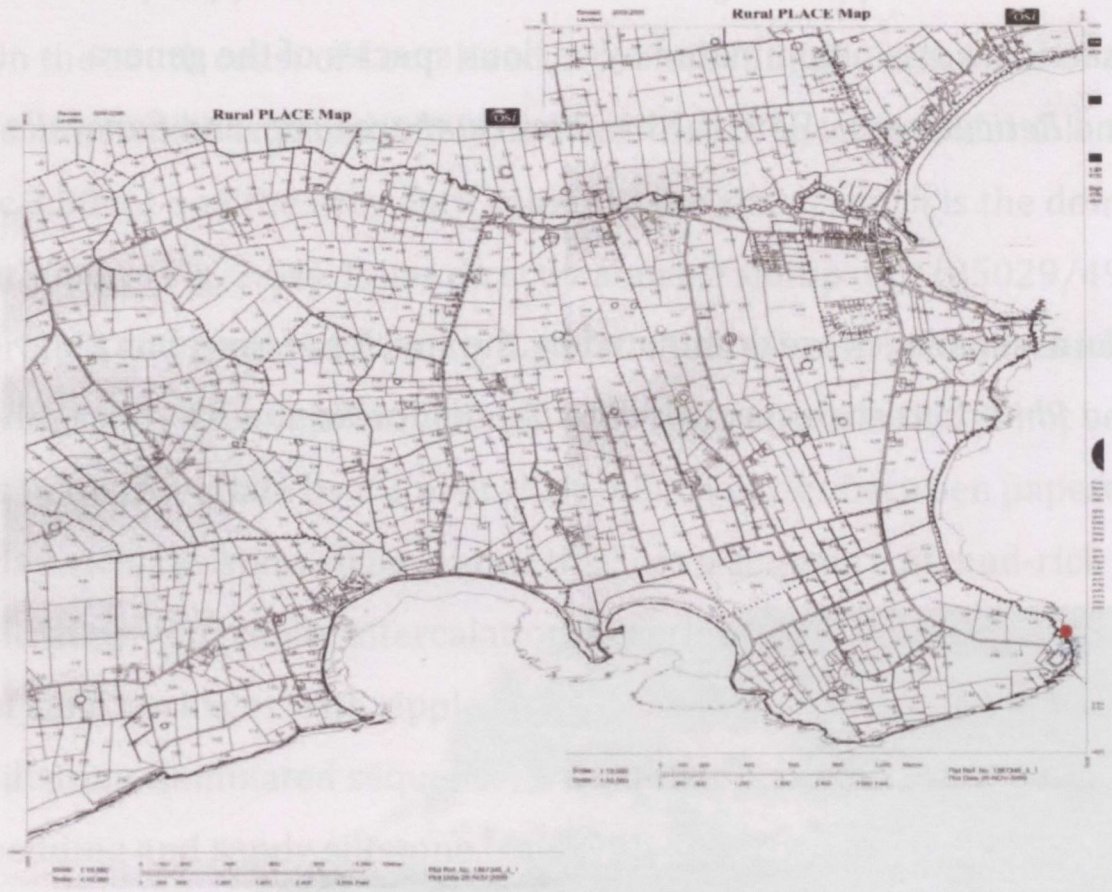

Fig. 2.64. Location map showing Klcredaun Top sampling locality at [85029/49504] and geological map of the Shannon Basin showing the locality and regional geology (OSI rural place maps: http://maps.osi.ie/publicviewer).

Graphic log with lithological descriptions:
Location: Kilcredaun Top
Grid Ref: 850261/49505

Scale: 15mm=30cm
Log prefix=KILT

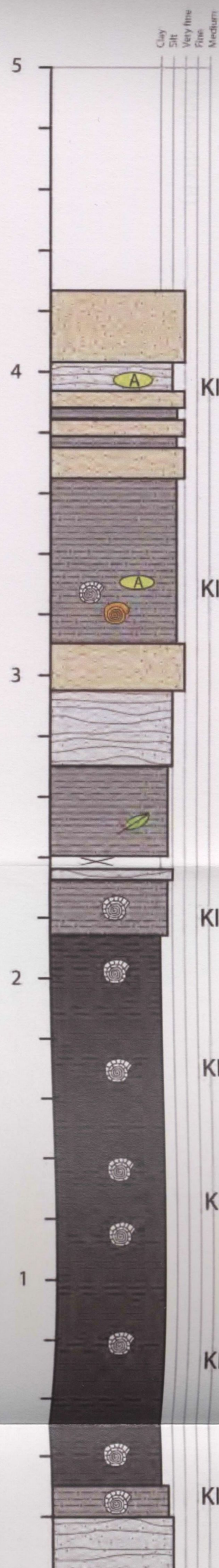

Samples [85029/49504]	Description	Fossil content (taxa in a given horizon are ordered by abundance)
KILU	Ammonoid-bearing shale	*Phillipsoceras/ Reticuloceras* spp., *Ph.* cf. *circumplicatile*, *Ph.* cf. *paucicrenulatum*, Plant Material, *Ph. circumplicatile*
KILMU	Ammonoid-bearing shale	*Phillipsoceras/ Reticuloceras* spp., *Ph.* cf. *circumplicatile*, *Ph.* cf. *paucicrenulatum*, *Ph. circumplicatile*, *Ph. paucicrenulatum*, *Caneyella* sp., Plant Material
KILUB	Ammonoid-bearing shale	*Phillipsoceras/ Reticuloceras* spp., *V.* cf. *henkei*, Plant Material
KILBU	Ammonoid-bearing bullion material	Pyrite-rich bullion
KILT7	Ammonoid-bearing bullion material	*Phillipsoceras/ Reticuloceras* spp., Ammonoids (unidentifiable)
KILT6	Ammonoid-bearing sandy siltstone	Ammonoids (unidentifiable)
KILT5	Ammonoid-bearing shale	*Ph./R.* spp., *Ph.* cf. *paucicrenulatum*, *Ph. paucicrenulatum*, *Ph.* cf. *circumplicatile*, *Dunbarella* sp.
KILT4	Ammonoid-bearing shale	*Phillipsoceras/ Reticuloceras* spp., *Ph.* cf. *paucicrenulatum*, *Ph.* cf. *circumplicatile*, *Ph. circumplicatile*, *R.* cf. *pulchellum*, *Ph. paucicrenulatum*
KILT3	Ammonoid-bearing shale	*Phillipsoceras/ Reticuloceras* spp.
KILT2	Ammonoid-bearing shale	*Ph./Reticuloceras* spp., *V.* cf. *henkei*, *V. henkei*, *Dunbarella* sp.
KILT1	Ammonoid-bearing shale	*Phillipsoceras/ Reticuloceras* spp., *V.* cf. *henkei*, *V. henkei*, *Ph.* cf. *paucicrenulatum*

Fig. 2.65. Sedimentary log of "Kilcredaun Top band", showing sampled horizons.

This locality was sampled by Lewarne (unpublished notes), who recorded the assemblages from four horizons (Table 2.12).

Layer C	*Ph. paucicrenulatum.*
Layer B	*Ph. paucicrenulatum; Ph. circumplicatile.*
Layer A	*Ph. circumplicatile; R.* sp. *(?R. pulchellum); Caneyella* sp.
Layer D	*R.* sp. *(?R. pulchellum); Ph. circumplicatile, Ph. paucicrenulatum.*

Table 2.12. Kilcredaun faunal content in Lewarne (unpublished notes).

2.2.2.21 "Quilty" Band

On the north coast of Loop Head, a 3 m-thick condensed section (see Fig. 2.66) crops out in a gully, [77281/51701]. It lies above a mass transport deposit (with concretions) and is overlain by a sandstone-dominated sequence. The section starts above the siltstones that top the mass transport deposit and consists of 1 m of fossiliferous shale alternating with silt-rich shale. Next, a 1.75 m-thick sequence of black shale, with occasional coaly layers and small bullions, as well as very rare siltstone interbeds is present. Above this, lies 30 cm of grey, resistant siltstones with occasional sandstone interbeds; these are in turn overlain by sandy siltstones with occasional concretions. The condensed section is taken to end with the start of this sequence sandy siltstones (c.1 m-thick). This condensed section can also be identified in core 09-CE-UCD-01 (Appendix B).

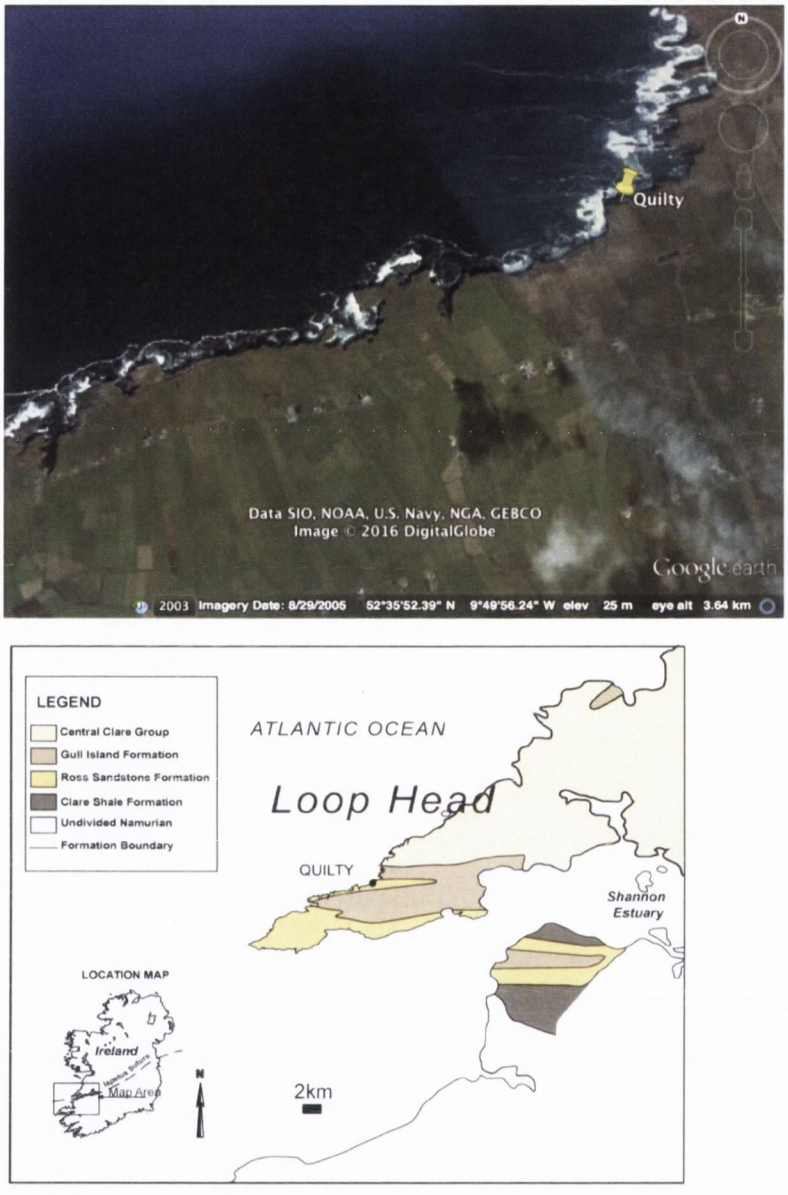

Fig. 2.66. Location map showing Quilty sampling locality at [77281/51701] and geological map of the Shannon Basin showing the locality and regional geology (Google Earth map).

Faunal Composition

Ammonoids are present throughout the condensed section, but are found concentrated in four highly-fossiliferous horizons (Fig. 2.67). They are mostly preserved as 2D moulds, with various growth stages represented, and, even though 3D ammonoids are present in the topmost horizon, these were unextractable.

The lowest horizon has frequent ammonoids that form a mixed assemblage dominated by *Phillipsoceras/Reticuloceras* spp.; the second horizon comprises an abundant and mixed assemblage, with dominant *Ph.* cf. *circumplicatile* and *Ph.* cf. *paucicrenulatum,* and associated *Basch.* cf. *ornatus,* among other taxa. The third horizon contains abundant ammonoids with dominant *Ph.* cf. *circumplicatile;* the uppermost horizon contains abundant specimens, with dominant *Phillipsoceras/Reticuloceras* spp., and associated *Ph. circumplicatile.* Overall, a mixed assemblage of thick-shelled ammonoids, thin-shelled ammonoids, orthoconic nautiloids, plant material and bivalves is present, and the assemblages are completely dominated by the species *Ph. circumplicatile* and *Ph. paucicrenulatum.* Lewarne recorded the presence of *Ph. circumplicatile* and *Caneyella* sp. at this locality (unpublished notes).

Graphic log with lithological descriptions:
Location: Quilty
Grid Ref: 77281/51701

Scale: 15mm=30cm
Log prefix=QUCP

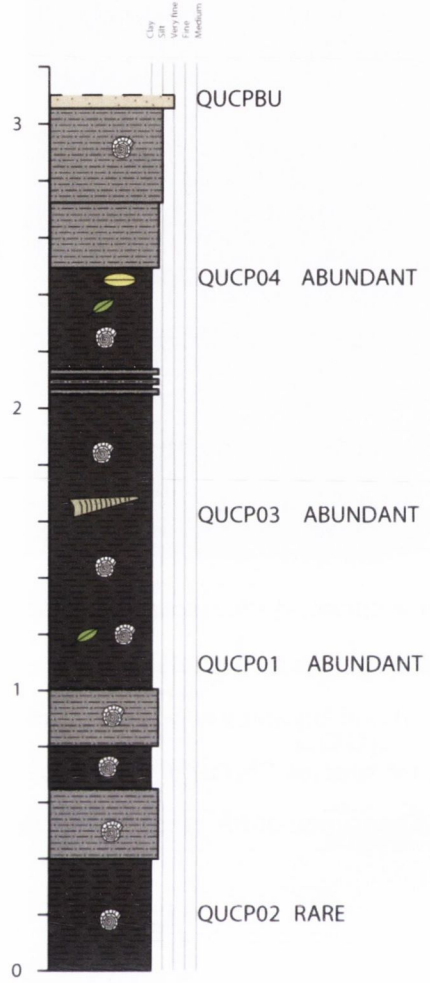

Samples [77281/51701]	Description	Fossil content (taxa in a given horizon are ordered by abundance)
QUCPU	Ammonoid-bearing shale	*Phillipsoceras/Reticuloceras* spp., *Posidonia/Posidoniella* sp., *Basch.* cf. *ornatus*, *Ph. circumplicatile*, *Ph.* cf. *circumplicatile*, *Ph.* cf. *paucicrenulatum*
QUCPBU	Ammonoid-bearing bullion material	Ammonoids (unidentifiable)
QUCP4	Ammonoid-bearing shale and bullion material	*Phillipsoceras/Reticuloceras* spp., *Ph. circumplicatile*
QUCP3	Ammonoid-bearing shale	*Ph.* cf. *circumplicatile*, Nautiloid, Plant Material, *Dunbarella* sp., *Anthracoceras/ Dimorphoceras* sp.
QUCP1 (second layer from base)	Ammonoid-bearing shale	*Phillipsoceras/Reticuloceras* spp., *Ph.* cf. *circumplicatile*, *Ph.* cf. *paucicrenulatum*, *Ph. circumplicatile*, Bivalve Material, *Anthracoceras/ Dimorphoceras* sp., *Basch.* cf. *ornatus*, Plant Material, *R.* cf. *pulchellum*, *R. pulchellum*, Family *circumplicatile-paucicrenulatum*
QUCP2 (lowest layer)	Ammonoid-bearing shale	*Phillipsoceras/Reticuloceras* spp., *Anthracoceras/ Dimorphoceras* sp., *Ph.* cf. *circumplicatile*, *R.* cf. *pulchellum*

Fig. 2.67. Sedimentary log of "Quilty band", showing sampled horizons.

2.2.2.22 "Cloghaunsavaun" Band

Along the north coast [75298/51003] a condensed section crops out on the cliff edge in a quarried exposure (Fig. 2.68). It lies directly above a slumped interval. The condensed section is c.3.5 m-thick (see Fig. 2.69-2.70), and starts off with 1 m of alternating shale and silty shale. Occasional bullions are present and iron oxide staining is common. The overlying 1 m-thick black shale contains several concretions, elongate parallel to bedding. The shale is typically clay rich and resistant, rather than soft and "papery." 30 cm of grey, silt-rich shale follows, which is then overlain by a c.1.50 m-thick sequence of black and grey shales, with occasional 2-3 mm-thick sandy interbeds showing ripple cross-lamination, and laterally continuous (0.5-1 cm-thick) coaly layers. Bullions are also present towards the top of the section, which is taken to end at the base of sandy silts with ammonoids that are in turn overlain by Quaternary drift. This condensed section can be identified in core 09-CE-UCD-01.

Faunal Composition

Ammonoids are present throughout the condensed section, but are found concentrated in four highly-fossiliferous horizons (Table 2.69). Ammonoids are found both as 2D moulds, with various growth stages represented, and as 3D external and internal casts in bullion material.

The lowest horizon contains frequent ammonoids that include *R. pulchellum* and *Basch.* cf. *ornatus* among others; the second horizon comprises an abundant and mixed fauna, with dominant *Phillipsoceras/Reticuloceras* spp., and associated *Ph.* cf. *circumplicatile, R.* cf. *pulchellum* and *Ph. cf. paucicrenulatum*. The third horizon contains abundant ammonoids in an assemblage dominated by *Phillipsoceras/Reticuloceras* spp. and *Ph.* cf. *paucicrenulatum;* the uppermost horizon contains abundant specimens, with *Ph.* cf. *paucicrenulatum* and *Ph.* cf. *circumplicatile* dominating the assemblage.

Fig. 2.68. Location map showing Cloghaunsavaun sampling locality, at [75298/51003], and geological map of the Shannon Basin showing the locality and regional geology (OSI rural place maps: http://maps.osi.ie/publicviewer).

Overall, a mixed assemblage of thick-shelled ammonoids, thin-shelled ammonoids, orthoconic nautiloids, plant material and bivalves is present, and the assemblages are dominated by the species of the genera *Reticuloceras* and *Phillipsoceras*, such as *Ph. circumplicatile* and *Ph. paucicrenulatum.* Lewarne (unpublished notes) recorded the presence of *Ph. circumplicatile* at this locality.

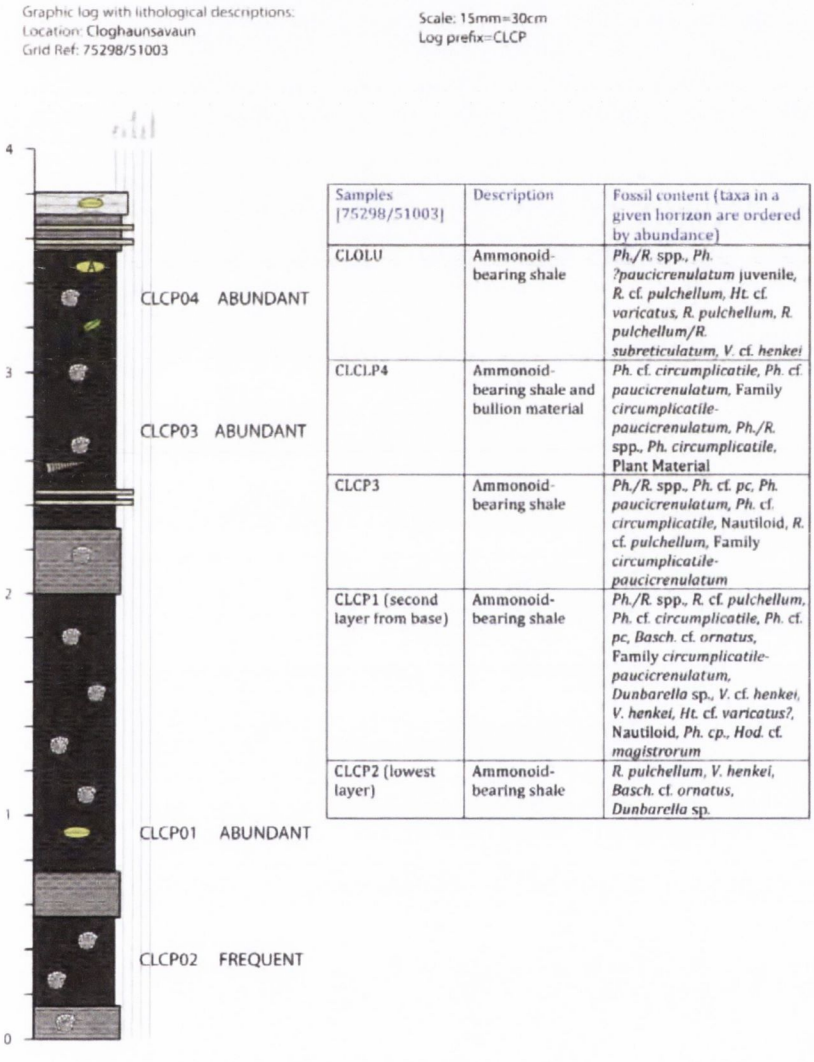

Samples [75298/51003]	Description	Fossil content (taxa in a given horizon are ordered by abundance)
CLOLU	Ammonoid-bearing shale	*Ph./R.* spp., *Ph. ?paucicrenulatum* juvenile, *R.* cf. *pulchellum*, *Ht.* cf. *varicatus*, *R. pulchellum*, *R. pulchellum/R. subreticulatum*, *V.* cf. *henkei*
CLCLP4	Ammonoid-bearing shale and bullion material	*Ph.* cf. *circumplicatile*, *Ph.* cf. *paucicrenulatum*, Family *circumplicatile-paucicrenulatum*, *Ph./R.* spp., *Ph. circumplicatile*, Plant Material
CLCP3	Ammonoid-bearing shale	*Ph./R.* spp., *Ph.* cf. *pc*, *Ph. paucicrenulatum*, *Ph.* cf. *circumplicatile*, Nautiloid, *R.* cf. *pulchellum*, Family *circumplicatile-paucicrenulatum*
CLCP1 (second layer from base)	Ammonoid-bearing shale	*Ph./R.* spp., *R.* cf. *pulchellum*, *Ph.* cf. *circumplicatile*, *Ph.* cf. *pc*, *Basch.* cf. *ornatus*, Family *circumplicatile-paucicrenulatum*, *Dunbarella* sp., *V.* cf. *henkei*, *V. henkei*, *Ht.* cf. *varicatus?*, Nautiloid, *Ph.* cp., *Hod.* cf. *magistrorum*
CLCP2 (lowest layer)	Ammonoid-bearing shale	*R. pulchellum*, *V. henkei*, *Basch.* cf. *ornatus*, *Dunbarella* sp.

Fig. 2.69. Sedimentary log of "Cloghaunsavaun band", showing sampled horizons.

Fig. 2.70. "Cloghaunsavaun band" at [75298/51003].

2.2.2.23 Ross Slump

A prominent mass transport deposit within the Ross Sandstone Formation, known as the "Ross Slump" (Strachan 2002) or "Ross Slide" (Gill 1979), is superbly exposed at Bridges of Ross, and crops out at several localities along the north coast (for instance, close to Fisherman's Point, [74624/50910] in Fig. 2.71, and further east along the coast, [77182/51690]). This particular slump complex was studied in detail by Strachan (2002). Black shale rafted beds are incorporated in the slump and often display tabular geometry despite transport.

Faunal Composition

Ammonoids were sampled from a thin black shale band, which is relatively continuous along bedding, and are here interpreted as a rafted block that moved quite coherently along slope (Table 2.13). It is found c.2.90 m above the base of the slump [74624/50910]. Ammonoids were abundant and the assemblage is dominated by *Phillipsoceras/Reticuloceras* spp., with two

specimens of *Ph.* cf. *paucicrenulatum* and associated plant material. All specimens are preserved as 2D moulds.

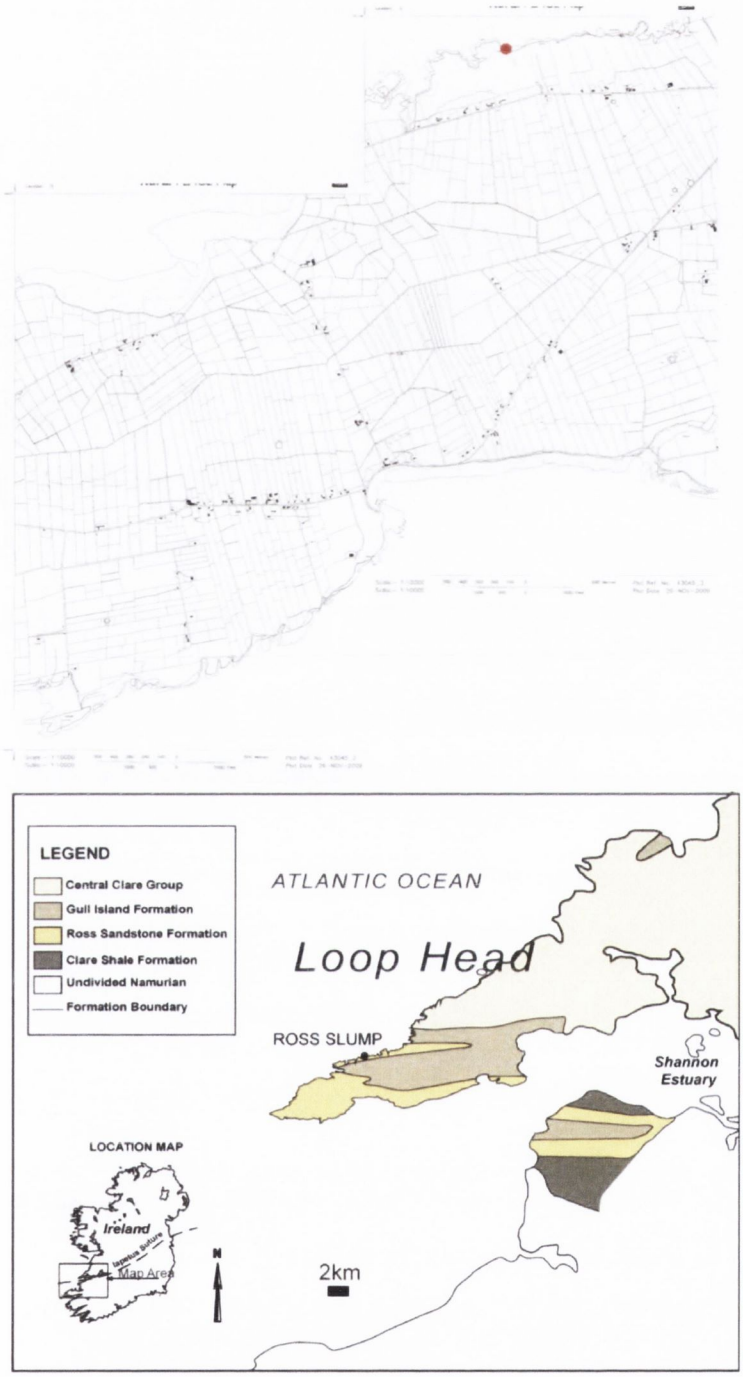

Fig. 2.71. Location map showing Ross Slump sampling locality close to Fishermans's Point, at [74624/50910], and geological map of the Shannon Basin showing the locality and regional geology (OSI rural place maps: http://maps.osi.ie/publicviewer).

Samples [74624/50910]	Description	Fossil content (taxa in a given horizon are ordered by abundance)
SL01	Ammonoid-bearing shale	*Phillipsoceras/Reticuloceras* spp., *Ph.* cf. *paucicrenulatum*, Plant material

Table 2.13. Ross Slump faunal content.

2.2.2.24 "Ross Bay West" Band

This condensed section is located on the west side of Ross Bay in a notch in the cliffs, [70991/49071] (Fig. 2.73). It can be reached by walking along the coast from Ross Bay. It consists of c.1.30 m of sediment (Fig. 2.72) with two prominent shale horizons separated by siltstone packages with intercalated very fine sandstone bands (which give a banded appearance) and occasional bullions. The condensed section lies above a prominent slump package and is therefore taken to begin at the top of this slump. There are a few thin continuous sandstone horizons towards the base of the section, above which a 30 cm-thick siltstone package is found. This is overlain by the first black shale package (c.15 cm-thick), which is separated from the next one by a c.60 cm-thick siltstone package. The top of the condensed section is taken to be at the base of a c.15 cm sandstone bed with underlying load structures and external casts of ammonoids.

Faunal Composition

There are two fossiliferous horizons, corresponding to the two dominant shale beds (none of the concretions sampled yielded ammonoids) (Fig. 2.74). Ammonoids are rare in the upper horizon and abundant in the lower horizon. The assemblage in the lower horizon is very diverse, with many species of *Phillipsoceras/Reticuloceras*, the dominant genus. The thick-shelled ammonoids *Phillipsoceras/Reticuloceras* spp. and thin-shelled ammonoids *Anthracoceras/Dimorphoceras* spp. are present in the upper horizon.

All ammonoids are preserved at 2D moulds in the two dominant horizons, but 3D external casts of ammonoids are present at the base of the overlying sandstone. These are interpreted as having formed from ammonoids that have been dragged up from the condensed section and incorporated into the turbidite sandstone, where they were dragged along the base of the flow. Gillian Lewarne (unpublished notes) recorded *Ph. ? paucicrenulatum* and *Dunbarella* sp. at this locality.

Fig. 2.72. Ross Bay West band at [70991/49071]. Ruler is 30 cm long.

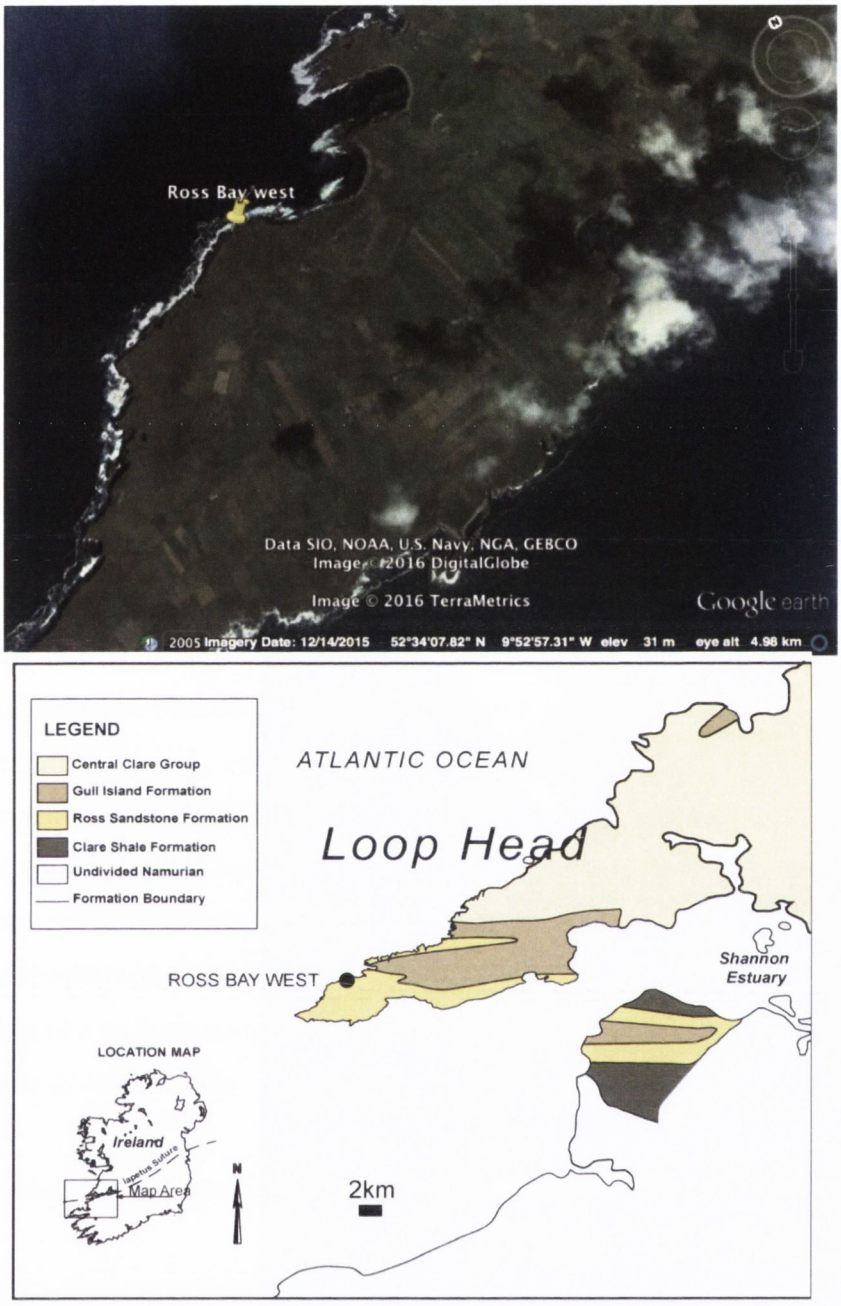

Fig. 2.73. Location map showing Blackrock West sampling locality at [70419/48692] and geological map of the Shannon Basin showing the locality and regional geology (Google Earth map).

Graphic log with lithological descriptions:
Location: Ross Bay west
Grid Ref: 70998/49070

Scale: 15mm=30cm
Log prefix=RBW

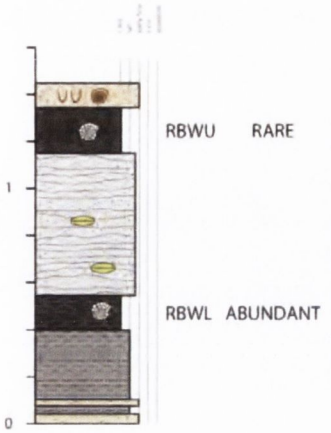

Samples [70991/49071]	Description	Fossil content (taxa in a given horizon are ordered by abundance)
RBWU	Ammonoid-bearing shale	*Phillipsoceras/Reticuloceras* spp., *A./D.* sp., Plant Material
RBWL	Ammonoid-bearing shale	*Phillipsoceras/Reticuloceras* spp., *Ph.* cf. *paucicrenulatum*, *V.* cf. *henkei*, *Ph. paucicrenulatum*, Plant material, *Ph.* cf. *circumplicatile*, Plant Material, *A./D.* sp., *Hod.* cf. *magistrorum*, *Anthracoceras* sp., *Homoceratoides* sp., *Homoceras/Vallites* sp., *Dunbarella* sp., *Caneyella* sp., *V. henkei*, *Hod. magistrorum*

Fig. 2.74. Sedimentary log of "Ross Bay west band", showing sampled horizons.

2.2.2.25 "Bridges of Ross" Band

This condensed section crops out on the north coast of Loop Head, [72732/50231] (Fig. 2.77), east of the characteristic bridge of Ross, a geomorphological feature that attracts many visitors to the area. The section forms an immediately obvious, prominent gully, which can only be accessed at low tide. It is c.8 m-thick and is taken to start above the sandstone bed that also demarcates the start of the gully (Fig. 2.75). The lowest part of the section consists of a sequence of interbedded siltstones and thinning-upward sandstones, with occasional clay-rich resistant siltstone horizons that thicken and thin along strike. Sand-rich siltstones are also present and contain ripple cross-laminae and (up to c.10 cm-thick) sandstone lenses. The first prominent shale package starts c.1.8 m from the base of the section and is c.1 m-thick. It contains occasional sand lenses that pinch out along strike. A 40 cm-thick sandstone interbed is present towards the middle of the section: it thins laterally until it can be seen pinching out towards the sea, to the south. Next, a c.1.80 m-thick sequence of siltstone, often sand-rich, underlies the next shale package, which forms a prominent part of the section (it is c.3 m-thick). This shale is punctuated by occasional thin (less than 10 cm-thick) sandstone beds

and is overlain by a siltstone package with sandy intercalations and occasional concretions. The condensed section is taken to end at the base of the first massive sandstone 20 cm-thick, which has load structures at the base and lamination visible towards the top. The whole section is weathered due to wave action. This condensed section can be identified in core 09-CE-UCD-02 (Appendix B).

Faunal Composition

Two ammonoid-rich horizons were sampled, both from within the topmost shale package: the lower horizon (BRL) contained 3D pyritized ammonoids, mostly in the juvenile growth stage; the upper horizon (BRU) contained both 2D moulds and 3D pyritized specimens (Fig. 2.78). The assemblages in both horizons are dominated by *Ph. paucicrenulatum*, with associated *Dunbarella* sp., as well as thin-shelled ammonoids such as *Dimorphoceras* sp. Although occasional concretions were present towards the top of the section, none of those examined contained ammonoids. Occasional solid, pyritized ammonoids are found incorporated on the surface of the sandstone below the shale, (Fig. 2.76) indicating that sandstone injection occurred after the condensed section was deposited, perhaps injecting into soft sea floor muds.

Fig. 2.75. "Bridges of Ross" band at [72732/50231]. Sandstone injection visible.

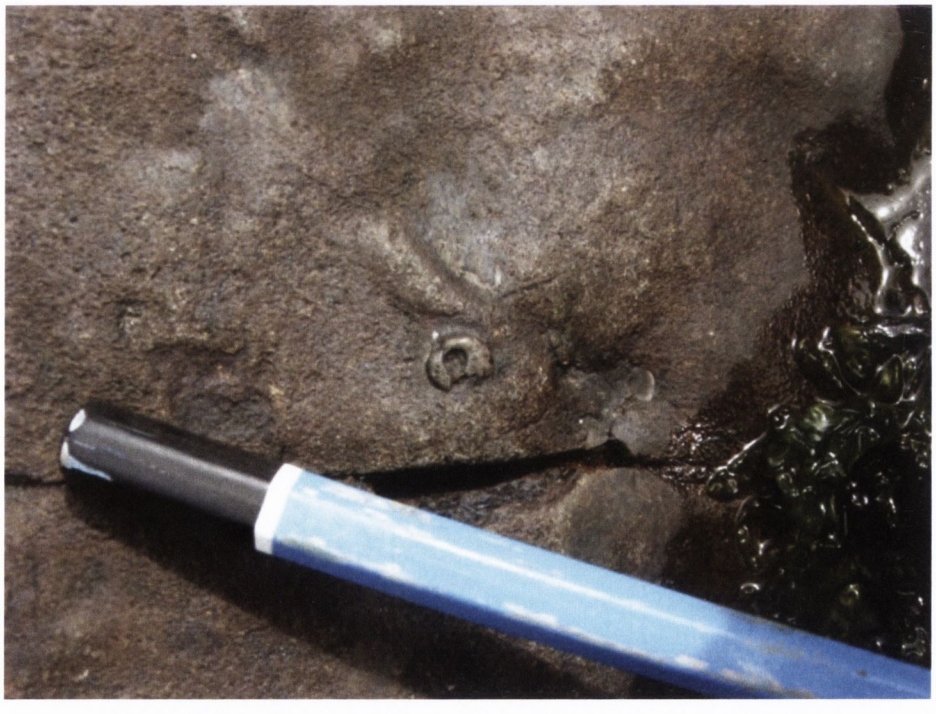

Fig. 2.76. Solid ammonoid in sandstone at "Bridges of Ross" band at [72732/50231].

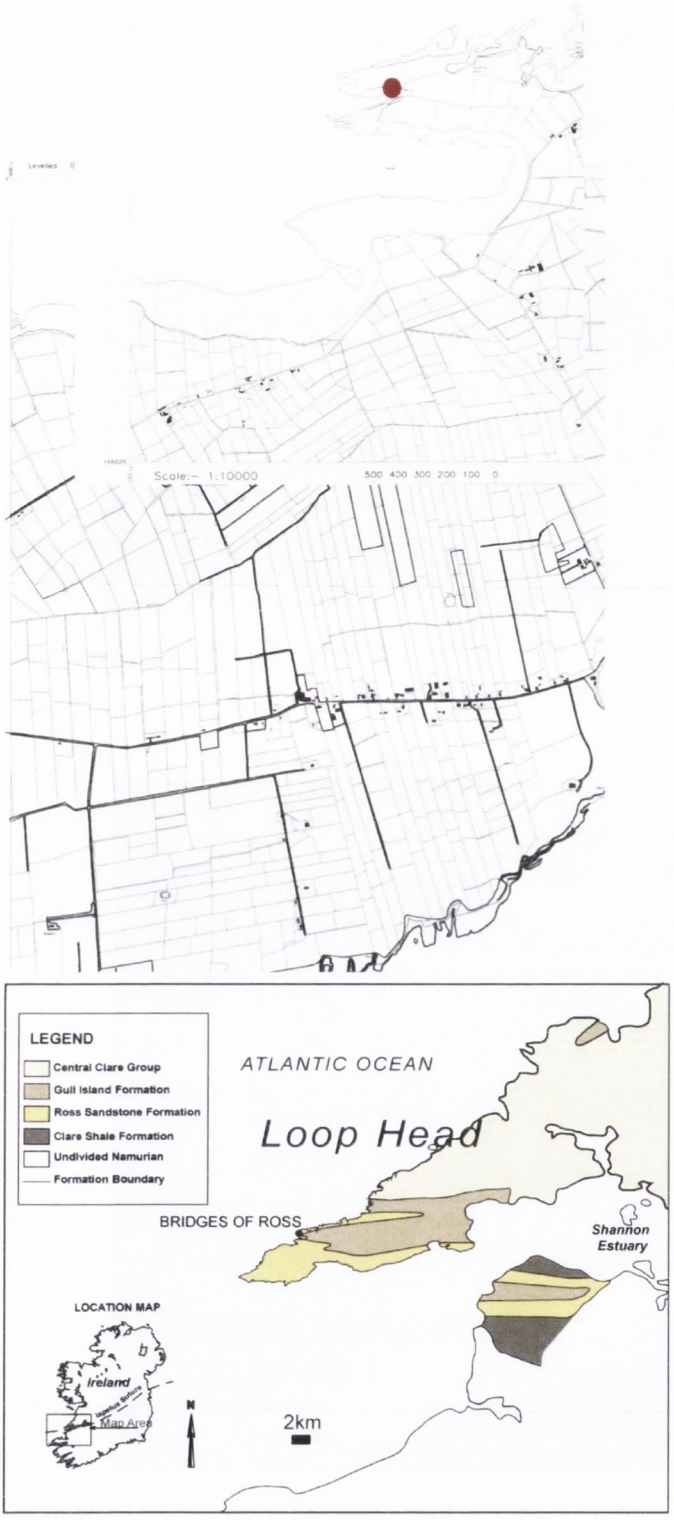

Fig. 2.77. Location map showing Bridges of Ross sampling locality at [72732/50231] and geological map of the Shannon Basin showing the locality and regional geology (OSI rural place maps: http://maps.osi.ie/publicviewer).

Graphic log with lithological descriptions:
Location: Bridges of Ross
Grid Ref: 72732/50231

Scale: 15mm=30cm
Log prefix=BR

Samples [72732/50231]	Description	Fossil content (taxa in a given horizon are ordered by abundance)
BRU	Ammonoid-bearing shale and individual pyritized specimens	*Phillipsoceras/Reticuloceras* spp., *Ph.* cf. *paucicrenulatum*, *Dunbarella* sp.
BRL	Ammonoid-bearing shale and individual pyritized specimens	*Ph. paucicrenulatum*, *Ph.* cf. *paucicrenulatum*, *Phillipsoceras/Reticuloceras* spp., *Dunbarella* sp., *Dimorphoceras* sp., Plant Material

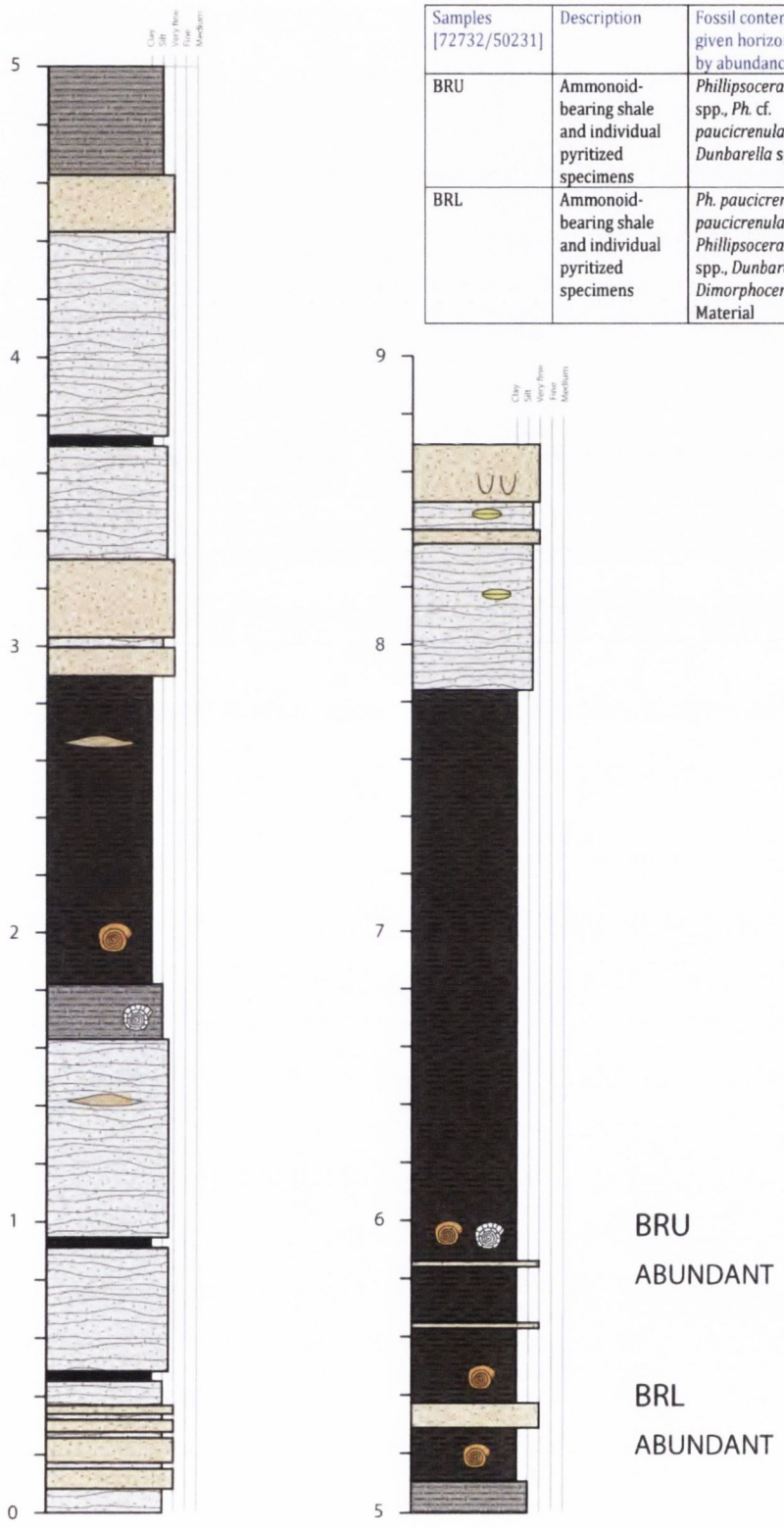

Fig. 2.78. Sedimentary log of Bridges of Ross band showing sampled horizons.

2.2.2.26 "Cross" Band

On the north coast of Loop Head, an obvious gully between Toorkeal Bay and Gull Island, [77499/51786] (Fig. 2.79), contains a 3 m-thick condensed section (Fig. 2.81): this is a well-trodden locality during geology excursions: not only is it relatively easy to access, but it also has abundant easily visible pyritized ammonoids, as well as being the topmost condensed section in the Ross Sandstone Formation. The condensed section is taken to start above a sandstone surface with asymmetrical current ripples. The sequence is dominated by recessive black shale, with associated grey siltstone lenses with sandstone intercalations, and occasional décollement brecciated horizons with disorientated shale and sandstone clasts. Within the shale, which is very pyrite-rich, there are interbedded mm-scale coaly horizons and common sulphur-leaching, which gives it a distinctive yellow-orange colour. The top of the band is clearly demarcated by a 40 cm-thick massive sandstone with groove casts at its base. This condensed section is also evident in core 09-CE-UCD-02 (Appendix B). This locality is also sometimes referred to as Fodry.

Faunal Composition

Ammonoids were sampled throughout the condensed section, where they are concentrated in black shale horizons (Fig. 2.80). Pyritized 3D ammonoid specimens were drilled out of the shale matrix in Trinity College Dublin. The ammonoid assemblage is dominated by *Ph. paucicrenulatum*, with minor associated *Phillipsoceras/Reticuloceras* spp.; the bivalve *Dunbarella* sp. is also abundant in the faunal assemblages. Most ammonoids in this condensed section are 3D pyritized specimens in the juvenile growth stage (this is probably a factor of the preferential pyritization of the inner whorls). The adolescent growth stage is also represented, but is less abundant. 2D moulds of the external shell were also present among the samples. Although occasional bullions were present towards the top of the section, none of those examined contained ammonoids. The presence of *Ph. paucicrenulatum* and *Dunbarella* sp. was already recorded by Lewarne in unpublished notes.

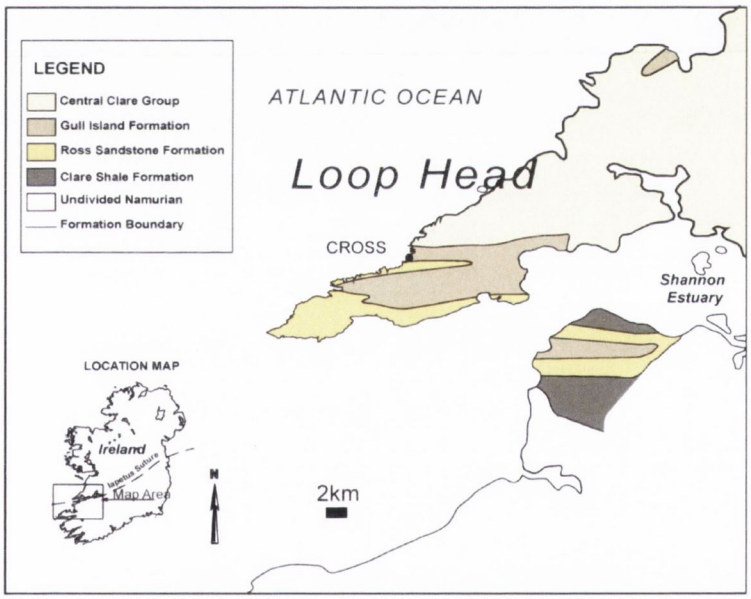

Fig. 2.79. Location map showing Cross sampling locality at [77499/51786] and geological map of the Shannon Basin showing the locality and regional geology (Google Earth map).

Graphic log with lithological descriptions: Cross Gully
Location: North Coast, Loop Head
Grid Ref: 77499/51786

Scale: 15mm=30cm
Log prefix=CRLOG

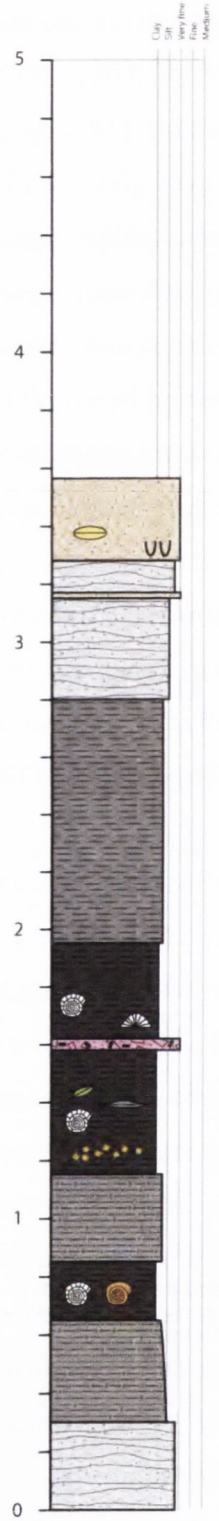

Samples [77499/51786]	Description	Fossil content (taxa in a given horizon are ordered by abundance)
CR	Ammonoid-bearing shale and individual pyritized specimens	*Ph. paucicrenulatum*, *Ph.* cf. *paucicrenulatum*, *Phillipsoceras/Reticuloceras* spp., *Dunbarella* sp., Plant material

CR ABUNDANT

CR ABUNDANT

CR ABUNDANT

Fig. 2.80. Sedimentary log of Cross band, showing location of sampled horizons.

Fig. 2.81. Cross band in gully at [77499/51786].

2.2.3 Other Irish localities

2.2.3.1 Leinster Coalfield: Killeshin Glen and Luggacurren

The stratigraphy of the Leinster Coalfield was described by Nevill (1956) and Higgs (1986), who both provided details of the lithostratigraphy and faunal succession. The area was visited briefly during the course of this study in a one-day sampling trip, with the aim of looking for high-quality 3D ammonoid specimens for taxonomic comparison with Shannon Basin ammonoid material.

Faunal composition

Ammonoids collected from the Luggacurren section are mostly Kinderscoutian in age (R_{1a} biozone), while those collected from the Killeshin Glen section are Marsdenian in age (R_{2a} biozone) (Table 2.14).

Specifically, the Luggacurren material consists of silt-rich shales and bullion material, among which one bullion contains beautiful 3D external moulds of *Ph. circumplicatile* and *Ph. paucicrenulatum*, while the Killeshin Glen material consists of black, paper shale with ammonoid moulds.

Ammonoid material collected by Higgs (1986), which was determined by W.H.C.Ramsbottom and is held in the National Museum of Ireland collections, was examined in order to strengthen the taxonomic diagnoses.

Leinster Coalfield Samples	Irish Grid Reference	Description	Fossil Content (taxa in a given horizon are ordered by abundance)
LUGGA	58608/88298	Ammonoid-bearing shale and bullion	*Homoceratoides* sp., *Ph. paucicrenulatum, Ph. circumplicatile, V. cf. henkei,* Bivalve Material
KILLGL	67324/77827	Ammonoid-bearing shale	*Bilinguites gracilis*

Table 2.14. Leinster Coalfield faunal content.

Chapter 3 Palaeontology

3.1 Typical faunal assemblages

Faunal assemblages in condensed sections or "ammonoid bands" are made up of thin- and thick-shelled ammonoids, bivalves, nautiloids and plant material (Figs. 3.1-3.2). The faunal components can be listed as follows in order of abundance in a given horizon within a condensed section: thick-shelled ammonoids, bivalves/plant material, thin-shelled ammonoids, nautiloids.

Fig. 3.1 Typical faunal assemblage in Shannon Basin condensed sections: an example from Fisherstreet Bay, Doolin, Co. Clare, [Irish Grid 06640/96316], with *Dunbarella* sp. and ammonoid moulds. Scale is 1 cm.

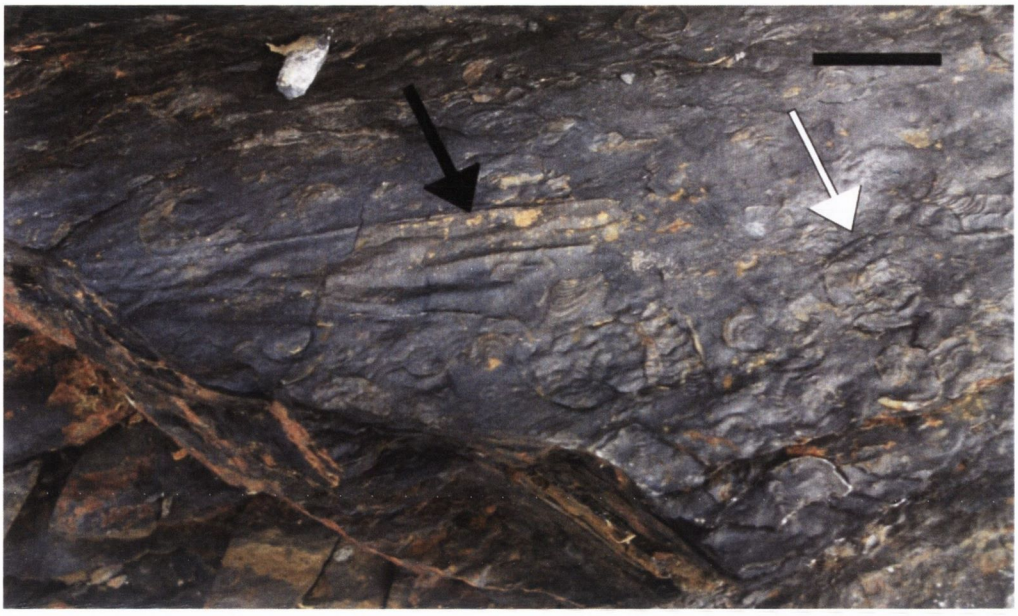

Fig. 3.2. Orthoconic nautiloid (black arrow) and mouldic ammonoids (light arrow), shale bedding surface, "*Phillipsoceras circumplicatile* band", Cloghaunsavaun [75298/51003], north coast Loop Head, Co. Clare. Scale is 1 cm.

In some localities, crinoid debris (disarticulated stem fragments and ossicles) was also a component of the assemblages. In addition, a trilobite pygidium was recorded at a single locality (Dunmore West band; see Ch.2, section 2.2.2.8), and solitary corals were recorded at two localities (see section 3.5.4). Thick-shelled ammonoids are the dominant element of the faunal assemblages and have long been the tool of choice in establishing a biostratigraphic framework for the basin (Hodson 1954a,b; Hodson & Lewarne 1961).

3.2 Ammonoids

3.2.1 Preservation

In the Shannon Basin, ammonoids (both thick- and thin-shelled) display four modes of preservation:

1) 2D moulds (i.e. crushed material) of the external shell (e.g. Figs 3.1-3.2).
2) 3D (unflattened) specimens that either have some external shell preserved or are preserved as internal moulds (e.g. Fig. 3.3). These are usually found within concretions but are also found in mud-rich siltstones, where internal chambers and septa are commonly visible.
3) 3D pyritized specimens found on shale. Usually only juveniles or the inner whorls of adults and adolescents are preserved in this manner (Figs. 3.4-3.5).
4) 3D casts, showing parts of the ornament.

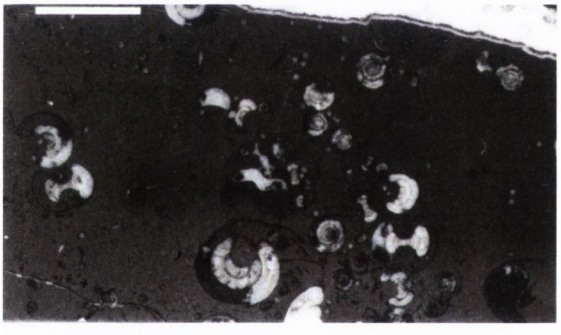

Fig. 3.3. Close-up view of a polished section through a concretion. 3D ammonoids are found in cross sectional view, showing inner whorls, St. Brendan's Well, Lisdoonvarna, Co. Clare, Ireland. Scale is 1 cm.

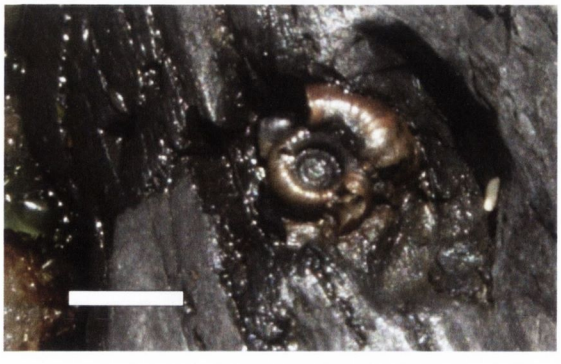

Fig. 3.4. Solid (3D) pyritized ammonoid, "*Ph. paucicrenulatum* band" on shale bedding surface, Bridges of Ross, north coast of Loop Head, Co. Clare. Scale is 1 cm.

Fig. 3.5. Solid (3D) pyritized ammonoids (most are highlighted by circles), "*Ph. paucicrenulatum* band" on shale bedding surface, Bridges of Ross, north coast of Loop Head, Co. Clare. Scale is 1 cm.

3.2.2 Pseudo-ammonoids

Pseudo-ammonoids, which resemble ammonoid conchs in shape but are not biogenic, have been found during the course of this study. They have been found in the Senan's Beach locality, Loop Head, Co. Clare (see Ch. 2). While they are similar in overall shape to ammonoid conchs (see Figs. 3.6, 3.7), on careful inspection they do not possess any ornament, any chamber dividing walls (septa) or other organic indications. In addition, their location on the top of sandstone beds would not be easily explained if they were organic structures. These inorganic structures are instead attributable to water escape (see Gill & Kuenen 1958), upon comparison with small-scale (cm scale) sand volcanoes described in Gill & Kuenen (1958, pl. 35,36). In addition, water escape features are common in the Ross Sandstone Formation, which is famous for its sand volcanoes near Bridges of Ross, north coast, Loop Head (Gill & Kuenen 1958; Gill 1979).

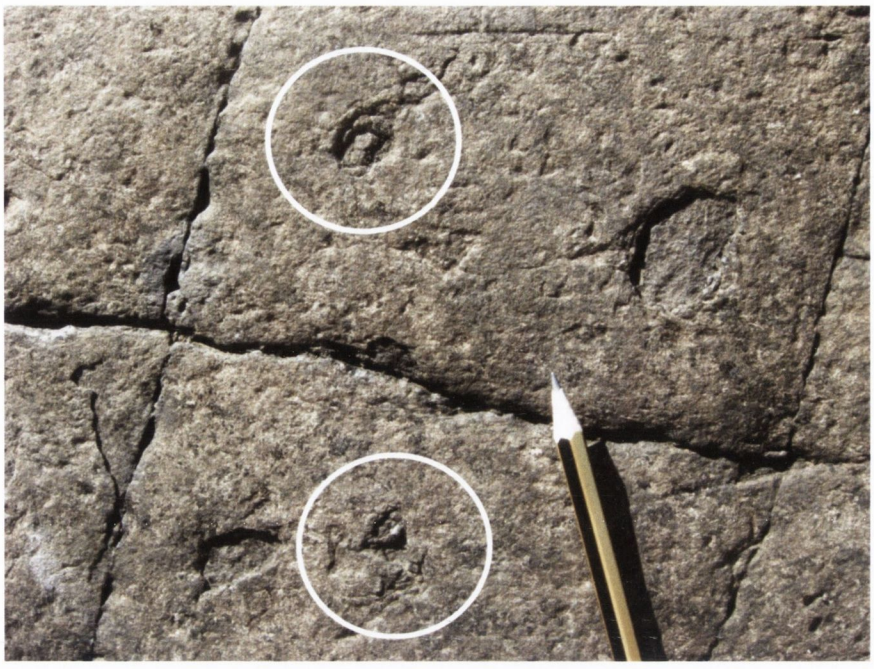

Fig. 3.6. Pseudo-ammonoids on sandstone surface, east of Senan's Beach, [76727/47705].

Fig. 3.7. Pseudo-ammonoids on sandstone surface, east of Senan's Beach, [76727/47705].

Fig. 3.8. Pseudo-ammonoid on sandstone surface, east of Senan's Beach, [76727/47705].

3.2.3 Ammonoid taxonomy

Ammonoid taxonomy is based on knowledge of the morphology of the conch, and generally involves the study of conch shape and size, suture line outline and shell ornament.

While ammonoid generic determinations, described in the *Treatise on Invertebrate Paleontology* (part L, Mollusca), mainly rely on suture line description, ornament is the main tool in specific identification. For instance, Bouckaert (1960; p. 10) noted that the internal mould is of no diagnostic value when dealing with the taxonomy of the genus *Reticuloceras.* The external shell, with its associated ontogenetic changes in ornament, allows the distinction of genera and is also necessary for specific determination.
Most Irish Serpukhovian and Bashkirian ammonoids are preserved as flattened impressions of the shell (2D preservation): in this case, taxonomic information necessarily comes mostly from the ornament. Not only is 2D preservation of external moulds the dominant mode of preservation at outcrop, where concretions with 3D ammonoids are generally rare, but this is also the case for

most borehole material. However, the taxonomy of ammonoids preserved as flattened moulds presents significant challenges.

It is argued here that even where concretions (bullions: Hodson 1954a) are available in the outcrop, flattened ammonoids from surrounding strata record valuable information (in terms of assemblages, biostratigraphy, palaeocommunities, etc.) that ought not to be neglected despite the associated taxonomic problems.

Ammonoid ornament changed through successive developmental stages of the animal, but the changes of ornament with ontogeny have not been studied for many taxa. The systematic study of these changes requires good-quality 3D material with shell preserved (e.g. Saunders & Swan 1984). However, type specimens of many taxa of Serpukhovian and Bashkirian age are preserved as 2D impressions, resulting in incomplete morphological descriptions and diagnoses. Furthermore, whether type specimens are flattened or solid, type descriptions are commonly based on a single growth stage: this is the case for most ammonoid taxa present in the Serpukhovian and Bashkirian strata of Ireland. For instance, within the genus *Reticuloceras*, a thorough ontogenetic study has been published only for *Reticuloceras reticulatum* (Phillips, 1836) (Korn 1997, p. 72).
Changes in ornament through ontogeny have been studied heretofore in the following taxa with associated description (this list refers to taxa that are pertinent to the Shannon Basin):

- *Homoceras undulatum* (Brown, 1841); Bisat 1924, p. 105.
- *Baschkirites/Hudsonoceras ornatus* (Foord & Crick, 1897); Bisat 1924, p. 98.
- *Hudsonoceras proteus* (Brown, 1841); Bisat 1924, p. 110.
- *Homoceratoides prereticulatus* Bisat 1924; Bisat 1924, p. 112.
- *Reticuloceras reticulatum* (Phillips, 1836); Korn 1997, p. 72.
- *Anthracoceras paucilobum* (Phillips, 1836); Gordon 1964, p. 245.
- *Hodsonites magistrorum* (Hodson, 1957); Hodson 1957, p. 21.

Changes in ornament through ontogeny have not been studied in the following taxa (pertinent to the Shannon Basin):

- *Phillipsoceras circumplicatile* (Foord, 1903)
- *Vallites henkei* (Schmidt, 1925)
- *Reticuloceras pulchellum* (Foord, 1903)
- *Reticuloceras subreticulatum* (Foord, 1903)
- *Phillipsoceras paucicrenulatum* (Bisat & Hudson, 1943)
- *Homoceratoides varicatus* Schmidt, 1934
- *Homoceras beyrichianum* (de Koninck, 1843)
- *Isohomoceras subglobosum* (Bisat, 1924)
- *Homoceras smithii* (Brown, 1841)

Clearly, a thorough study of ontogenetic changes of ornament would greatly benefit the taxonomy of Irish Serpukhovian and Bashkirian ammonoids and, in turn, would result in more precise biostratigraphic schemes and information about the structure of palaeocommunities. Until this kind of study is accomplished, identification of 2D material to the species level remains problematic, especially where only fragments are preserved. Here, new data on the changes of ornament through ontogeny of 14 taxa of ammonoids are presented in order to demonstrate the value of this approach.

3.2.4 Issues in the taxonomy of crushed material

Basic conch parameters (Fig. 1.1) such as conch diameter, whorl width and whorl height (Korn 2010) cannot be obtained from 2D material. Improvements in 2D taxonomy can be made only through morphological and ontogenetic analysis of 3D material.

Typically, the minimum requirement to make a diagnosis is a portion of the flank from the umbilicus to the venter (Bouckaert 1961); however, even having

satisfied this prerequisite, the taxonomist can run into a series of pitfalls when dealing with 2D crushed material.

In the case of *Phillipsoceras circumplicatile* (Foord, 1903), it is clear, from study of the type material and from literature descriptions, that the variable ornament of the adult shell makes identification problematic. This problem is exacerbated by the close similarity of *Ph. circumplicatile* to the allied species *Ph. paucicrenulatum* (Bisat and Hudson, 1943). In the case of the syntypes of *Ph. circumplicatile* utilised by Foord (Fig. 3.9), it is impossible to ascertain from museum records whether the specimens all came from the same horizon or from different stratigraphic levels at the same locality (which might result in some morphological change). If one accepts Foord's syntype illustrated in Fig. 3.9c (NMING : F23972), which is very different in ornament (prorsiradiate direction of the ornament, more delicately crenulated growth lines) and in conch shape (more moderate umbilicus and higher whorl section), as *Ph. circumplicatile,* then there is extreme intraspecific variation. It is perhaps more likely that these specimens include more than one species.

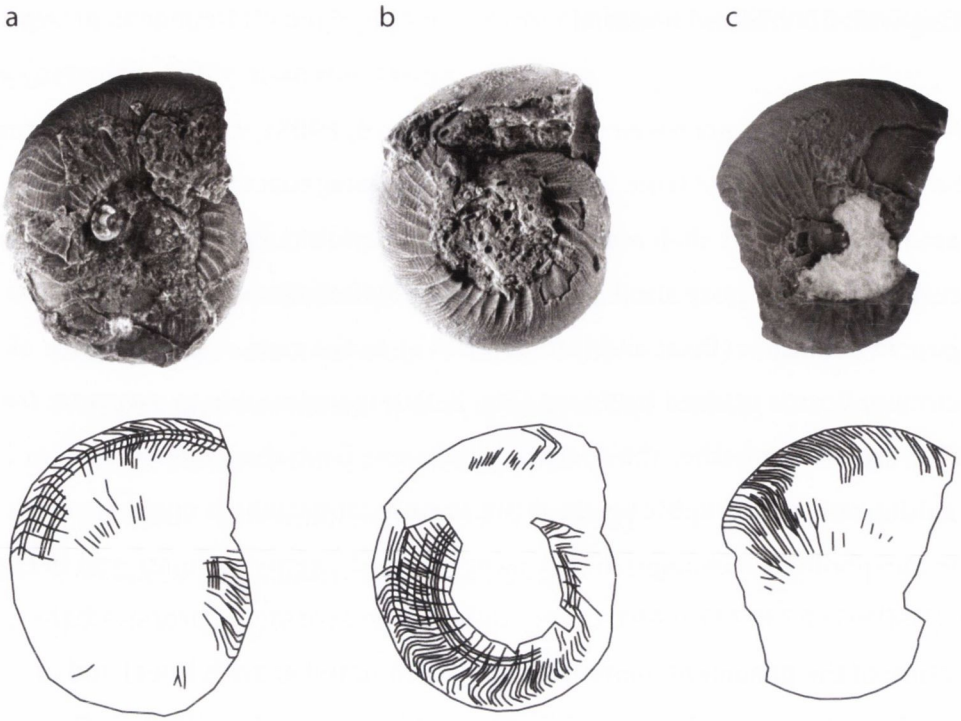

Fig. 3.9. *Phillipsoceras circumplicatile* (Foord, 1903) syntypes and traces of the ornament, (a) Paralectotype (NMING : F23969), (b) Lectotype (NMING : F23968), (c) Syntype (NMING : F23972, *partim*). Note that specimen c is probably not attributable to this species (see text for discussion) but it is included as it is one of the syntypes designated by Foord. Specimens are from Lisdoonvarna, Co. Clare, Ireland. Scale is 10 mm.

3.2.5 Tackling taxonomical issues

3D ammonoids were either extracted from concretions in the Clare Shale Formation, Co. Clare, Ireland, or accessed in museum collections: Geological Museum, Trinity College Dublin (catalogue numbers prefixed TCD); National Museum of Ireland (catalogue numbers prefixed NMING); British Geological Survey, Keyworth, UK (catalogue numbers prefixed GSM); Manchester Museum (catalogue numbers prefixed MANCH); and Geological Sciences Museum of the University of Göttingen (catalogue numbers prefixed GZG.INV).

The systematic palaeontology of 14 ammonoid taxa is presented here. For most of them, prior to this study there was a lack of published information regarding their ontogeny and diagnostic features with which to identify crushed material.

Here, well-preserved specimens were chosen and changes in ornament through ontogeny are described and illustrated diagrammatically. Changes in ornament were also traced above successive growth stages of each ammonoid taxon using Adobe Illustrator. Conch measurements for each species are presented in Tables 1-12, Appendix A.

Once changes of ornament through ontogeny are established using 3D material, this information can then be applied to crushed material in the Shannon Basin (see section 3.3.2), which was previously difficult to determine (also see Lacchia *et al.* 2015).

3.3 Systematic palaeontology

3.3.1 Thick-shelled ammonoids

Note: The following synonymy lists follow the recommendations (including symbols ahead of entries in the lists) in Matthews (1993).

Superfamily Gastrioceratoidea Hyatt, 1884
Family Reticuloceratidae Librovitch, 1957
Subfamily Reticuloceratinae Librovitch, 1957
Genus *Phillipsoceras* Ruzhencev & Bogoslovskaia, 1975, p. 55

Remarks: This genus, which encompasses many species, is described in the *Treatise, Part L, Mollusca*, (Selden 2009, p. 98). It is said to have a wide umbilicus, becoming moderately wide later in ontogeny and frequently narrowly umbilicate in adulthood. Some species have a tendency to form an oxycone venter and the ornament is described as consisting of transverse growth lines crossed by fine spiral lirae, producing strong reticulate ornamentation. Nodes or strong riblets appear near the umbilicus in early whorls. The suture line has an adventitious lobe wider than the ventral lobe (Selden 2009, p. 98).

Ruzhencev & Bogoslovskaia (1975), who created this genus, describe it as having reticulate sculpture, with umbilical nodes or tubercles on young shells, declining with age. They describe clusters of small costae extending from the tubercles to form a ventral sinus that increases in depth with age. The spiral striae are said to be well-developed and the ventral lobe not very wide, with narrow branches, which are basally usually rounded, and median saddle relatively low. It is a very similar genus to *Reticuloceras*, from which it is distinguished by the invariably wider umbilicus, the more strongly developed tubercles and the slightly wider ventral lobe. *Phillipsoceras* and *Reticuloceras* existed in parallel, but the wl/hl (whorl width/whorl height) ratio altered in the course of phylogenetic development from 1.00 to 0.75 in the former, and

from 0.80 to 0.60 in the latter (Ruzhencev & Bogoslovskaia, 1975). See Fig. 3.8 for an illustration of conch parameters.

***Phillipsoceras circumplicatile* (Foord, 1903); Figs. 3.10- 3.12; Table 1, Appendix A.**

?1841 *Goniatites inconstans* Phillips, p. 123, pl. 51, fig. 238a-e.

v*1903 *Gastrioceras circumplicatile* Foord, p. 200, pl. 49, fig. 12a,b, 13.

v1924 *Reticuloceras inconstans* Bisat, p. 118, pl. 3, fig. 6.

1925 *Eumorphoceras inconstans* Schmidt, p. 586, pl. 22, fig. 3, pl. 25, fig. 7-10.

1934 *Reticuloceras inconstans* Phillips; Schmidt, p. 453, fig. 68,69.

1943 *Reticuloceras inconstans* Phillips; Bisat & Hudson, p. 424.

1943 *Reticuloceras circumplicatile* Foord; Bisat & Hudson, p. 425, pl. 24 fig. 1,2, pl. 29 fig. 2a,b.

v1954a *Reticuloceras circumplicatile* Foord; Hodson, p. 157.

v1954b *Reticuloceras circumplicatile* Foord; Hodson, p. 277, pl. 11 fig.4.

v*1957 *Reticuloceras circumplicitale* Foord; Hodson, p. 10, pl. A, pl. B fig. 1,2,4.

Also refer to: Patteisky (1959); Bouckaert (1960); Chalard (1960); Ruzhencev & Bogoslovskaya (1975); and Swan (1984).

Type Locality: Lisdoonvarna (erroneously labelled Cliffs of Moher), Co. Clare (see discussion in Hodson 1954b).

Type Material: Lectotype (NMING : F23968, Fig. 3.10d; Fig. 3.11), Paralectotype (NMING : F23972, Fig. 3.10a), Paralectotype (NMING : F23969, Fig. 3.9a), Paralectotypes (NMING : F23971, NMING : F23973).

Other Material: Adolescent characters, which are missing from the type series, can be ascertained from material identified by Hodson: TCD.60601, GSM 86917 (Figs. 3.10b-c).

Diagnosis: Phillipsoceras with prorsiradiate, strongly-marked plications branching suddenly into "bunches" of usually three or four crenulate growth lines at the same point along the flank.

Description: The juvenile paralectotype (NMING : F23972, Fig. 3.10a), 4 mm in diameter, with 5 whorls preserved, has radial or very slightly prorsiradiate plications, spaced c.6 per mm, regularly branching into growth lines at a similar point along the flank. The ornament is non-crenulate at this stage and occasional intercalations are present in the outer whorls. The number of growth lines to emerge from the plications is normally 3, in some cases 4, with secondary branching present. Growth lines are c.8-10 per mm on the venter and, while no ventral sinus is developed, there is a slight ventrolateral projection and ventral sulcus. Very faint spirals traverse plications at this diameter, but they are much more obvious at later stages of growth. Adolescent characters can be ascertained from material identified by Hodson (TCD.60601, GSM 86917, Figs. 3.10b-c): in these specimens, spirals are strong on the flank, with ventral spirals starting to develop at c.9-10 mm diameter, although these are more clearly marked in certain specimens than others. The ventrolateral projection is pronounced, while the ventral sinus is present but less pronounced. The plications are prorsiradiate and spaced 3 per mm; they thicken on emerging from the umbilical margin and split into three or four growth lines. Secondary branching of the growth lines is common. One or two intercalations are inserted in between the plications on the flank but they do not extend down to the umbilical margin. Growth lines are spaced 10 per mm on the ventrolateral projection. The umbilical margin is rounded with wide umbilical diameter (3.6 mm in NMING : F23968, Fig. 3.10d).

The adult growth lines are coarsely crenulated and, as already noted by Bisat and Hudson (1943), irregularly spaced: for instance, the lectotype (NMING : F23968, Fig. 3.10d; 3.11) has 4-5 growth lines per mm, but a paralectotype (NMING:F23969, Fig. 3.9a) has 1-2 growth lines per mm on the venter. In adult specimens, the plications and the growth lines are prorsiradiate and a ventrolateral projection is present. Interpolated growth lines appear between the primary plications at the branching point along the flank and these vary in number from 2 to about 6. In adult specimens (NMING : F23968, NMING : F23969, Fig. 3.10) described here, the umbilical plications are 2 (in some cases

3) per mm and a ventral sulcus is no longer present. Spirals are strongly marked all over the test, resulting in a strongly reticulate ornament. While the pattern of branching, namely trichotomy and quadrichotomy, is conserved, the number of intercalations grows through ontogeny.

Remarks: A confident diagnosis of this species where preserved flattened can be made where a combination of the following features is present: trichotomy and quadrichotomy; strong spirals between the umbilical plications; forward projection of these plications; obviously reticulate nature of the growth lines. All diagnostic features of the ornament for this species are already present in the early adolescent growth stages and continue into maturity.

Comparisons: In contrast to many other species in the genus, such as *Ph. nodosum* (Bisat & Hudson, 1943), *Ph. stubblefieldi* (Bisat & Hudson, 1943), *Ph. regularum* (Bisat & Hudson, 1943), *Ph. umbilicatum* (Bisat & Hudson, 1943) and *Ph. samlesburyense* (Bisat & Hudson, 1943), dichotomy is not the main mode of branching in the ornament of *Ph. circumplicatile*. The Russian species *Ph. alpharipaeum* (Ruzhencev & Bogoslovskaya, 1975) is closely similar to *Ph. circumplicatile* (see discussion in Ruzhencev & Bogoslovskaya 1975, p. 54) and they are likely to be synonyms, but this merits further investigation. As noted by Bisat (1924) and Swan (1984) there is doubt as to the equivalence of *Ph. circumplicatile* and *Ph. inconstans* (Phillips, 1841): if they are synonyms, then the type of the genus would change in name, becoming *Ph. inconstans*, but Phillips' type specimens first need to be reanalyzed.

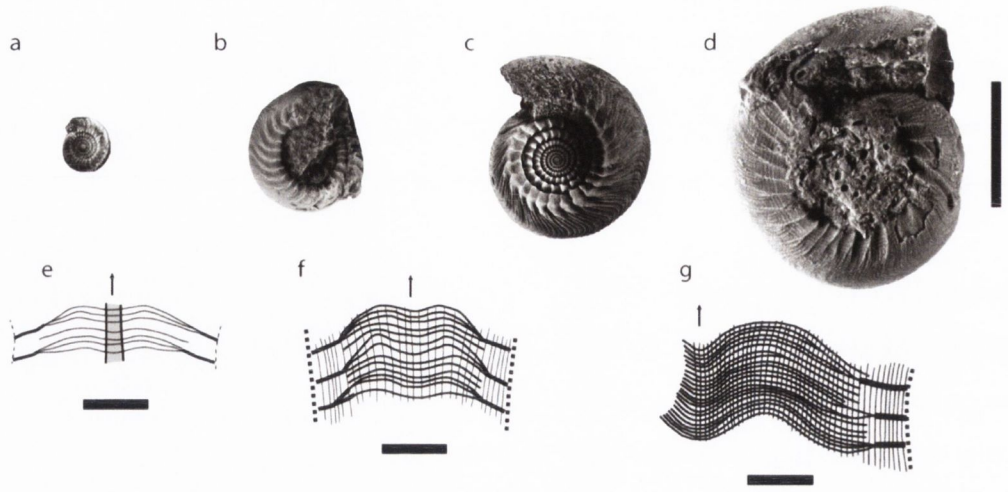

Fig. 3.10. Changes in ornament in *Phillipsoceras circumplicatile* (Foord, 1903) (a) Paralectotype (NMING : F23972 *partim*), Lisdoonvarna, Ireland, (b) TCD.60601, Murphy's Bridge, Ireland, (c) GSM 86917, Neheim, Germany, (d) Lectotype (NMING : F23968), Lisdoonvarna, Ireland. Scale is 10 mm long. (e) Growth lines in paralectotype (NMING : F23972 *partim*) at 4 mm diameter with shaded ventral sulcus, (f) Growth lines in TCD.60601 at 9 mm diameter, (g) Growth lines in lectotype (NMING : F23968). Scale bars are 2 mm long.

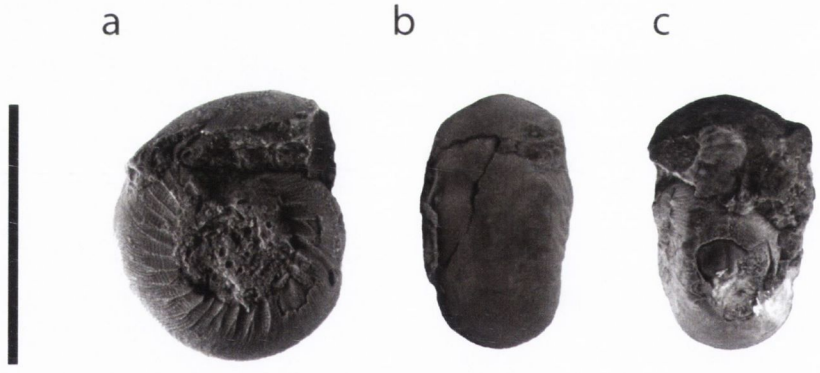

Fig. 3.11. *Phillipsoceras circumplicatile* lectotype (NMING : F23968), Lisdoonvarna area, Co. Clare, (a-b-c) side, dorsal and ventral view. Scale is 20 mm.

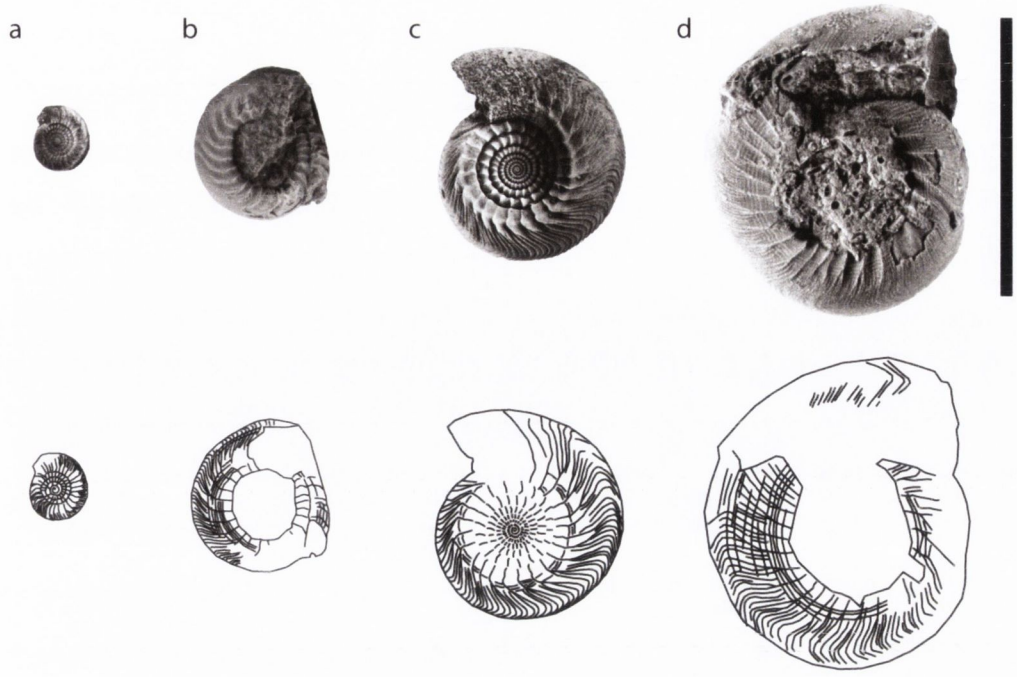

Fig. 3.12. Ontogenetic study of the ornament for *Phillipsoceras circumplicatile* (Foord, 1903) (a) Specimen associated with syntypes (NMING : F23972 *partim*); (b) TCD.60601, Murphy's Bridge, Ireland; (c) GSM 86917, Neheim; (d) Lectotype (NMING : F23968). Scale is 20 mm.

***Phillipsoceras paucicrenulatum* (Bisat & Hudson, 1943); Figs. 3.14-3.16; Table 2, Appendix A.**

v*1943 *Reticuloceras paucicrenulatum* Bisat & Hudson, p. 427.

1960 *Reticuloceras paucicrenulatum* Bisat & Hudson; Bouckaert, p. 65, pl. 2, niv. 10, fig. 1; niv. 11, fig. 2-3; pl. 4, niv.2, fig. 3-5, 7-10,12,14; pl. 4, niv. 4, fig. 4; pl. 5, niv. 1, fig. 1-2; niv. 2; niv. 3, fig. 2-4, 7-8.

v1961 *Reticuloceras paucicrenulatum* Bisat & Hudson; Calver & Ramsbottom, p. 207, pl. 11 fig. 3.

1961 *Reticuloceras paucicrenulatum* Bisat & Hudson; Bouckaert, fig. 3.

1984 *Otleyoceras paucicrenulatum* Bisat & Hudson; Swan, p. 250, pl. 8, fig. 1-2.

Type Locality: Lumbutts Clough, Todmorden, Yorkshire.

Type Specimens: The type specimens are all preserved as partial, 2D shale moulds (Fig. 3.14), mostly in the adolescent growth stage. Some type specimens have umbilical spirals (GSM 71074-5, Fig. 3.14b,e). The holotype is a

mouldic fragment of the external shell (GSM 71074, Fig. 3.14e) with widely spaced umbilical plications (1-3 per mm) traversed by spirals. Therefore it should be noted that spirals are sometimes present until late adolescence, not just "up to the mid-adolescent growth stage," as was thought to be the case by Bisat & Hudson (1943, p. 427). Both ventrolateral projection and ventral sinus are pronounced and growth lines are spaced 3-5 per mm on the ventrolateral projection. Bifurcation is quite irregular, with intercalations, and secondary branching is common. In later parts of the whorl, when adulthood is reached, the growth lines start to extend down to the umbilicus. They are obviously crenulated in the holotype and in the rest of the type series, except in one specimen (GSM 71078, Fig. 3.14c) which is barely crenulate.
The paratypes (GSM 71075-8, Fig. 3.14b,c) consist of various mouldic fragments. One specimen (GSM 71075, Fig. 3.14b) has umbilical spirals crossing well-marked plications and is accompanied by intercalations, with 5 growth lines to the mm on the ventrolateral projection; another paratype (GSM 71076, Fig. 3.14a) with estimated diameter 20 mm has long slender plications branching irregularly into growth lines, and ventrolateral projection pronounced and sharply reflexed back into a ventral sinus. Another paratype (GSM 71078, Fig. 3.14c) has long plications spaced 1-1.5 per mm branching irregularly into barely crenulated growth lines spaced 4 per mm on the ventrolateral projection.

An additional unlabelled specimen (Fig. 3.14d), which may be a detached portion of the holotype, has elongate plications branching irregularly into growth lines spaced 4 per mm on the ventrolateral projection. Here the crenulation is not strong but is obvious. The umbilical plications become more closely set through ontogeny (they are spaced 1-1.5 per mm early on in ontogeny and then 4-5 per mm in later stages). In general, the plications are slightly deflected forward.

Specimens (GSM 71134-6) that were found 7.62 cm below the type horizon are thought to be early forms (Bisat & Hudson 1943, p. 428), with less strongly

marked umbilical plications and a smaller ventrolateral projection on which the growth lines are spaced 3 per mm.

Material: Solid (but partially flattened) *Ph. paucicrenulatum* specimens were sampled from the "*Ph. paucicrenulatum* band" at the top of the Ross Sandstone Formation, Loop Head Peninsula, Co. Clare (see Ch. 5). Previous identification by Gillian Lewarne (unpublished notes) and comparison to museum specimens confirms they are indeed attributable to this taxon.

Description: The highly variable nature of this species was already noted by Bisat. In fact, in an unpublished note in the Manchester Museum (Fig. 3.13), Hudson writes: *"The form is variable as when I sent some solids to Bisat from Roughlee, he immediately divided them into 4 groups and suggested a possible 5th. That was before he had seen any specimen with ventral sulcus. The specimens break badly when one tries to extract them."*

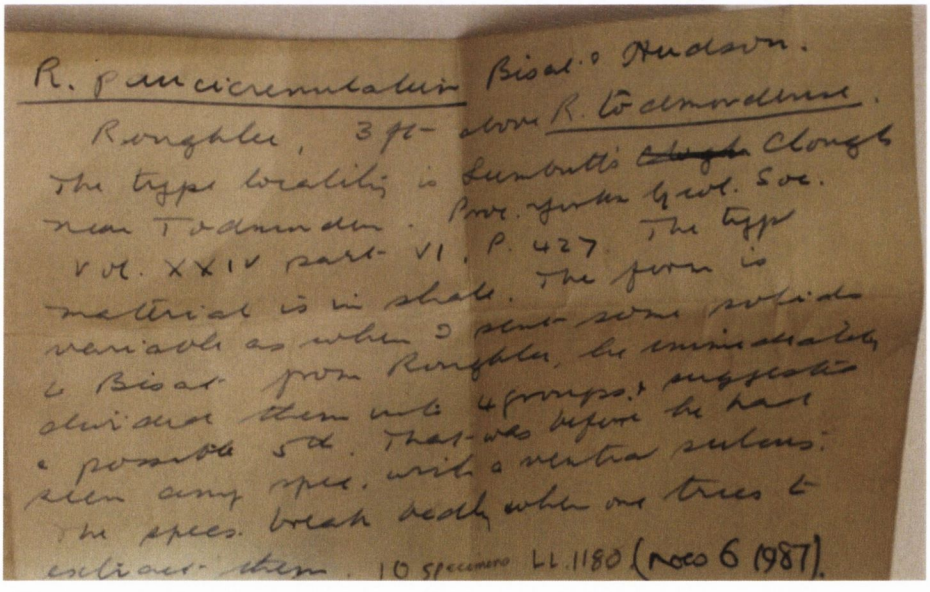
R. paucicrenulatus Bisat & Hudson.
Roughlee, 3 ft- above R. todmordense.
The type locality is Lumbutts Clough
near Todmorden. Proc. Yorks Geol. Soc.
Vol. XXIV part- VI. P. 427. The type
material is in shale. The form is
variable as when I sent some solids
to Bisat from Roughlee, he immediately
divided them into 4 groups & suggested
a possible 5th. That was before he had
seen any spec. with a ventral sulcus.
The spec. break badly when one tries to
extract them. 10 specimens LL.1180 (Nov 6 1987).

Fig. 3.13. Unpublished note in the Manchester Museum written by R.G.S. Hudson mentioning W.S. Bisat (c.1940).

Bisat & Hudson (1943) describe the species as a late form of *Ph. circumplicatile* stock, its ornament showing a further development of the pattern seen in the variety from the *R. todmordenense* band. It is widely umbilicate, with widely

spaced (1 to 1.5 per mm) umbilical plications or subplications in adolescence. These plications are described as branching rather irregularly into strong, barely crenulated, transverse growth lines, which are bent forward on the flank into a pronounced ventrolateral projection on which the growth lines are spaced about 2 per mm (Bisat & Hudson 1943).

Bouckaert (1960) provided a description of *Ph. paucicrenulatum* based on Belgian material and described the juveniles as having a large umbilicus, about 35% of the shell diameter, and plications that in some examples dichotomise along the flank. He observed that secondary branching is common and that intercalations never extend down past the first dichotomizing point. A large ventrolateral projection is present as well as a small ventral sinus. Crenulation is slight and spirals are rare in between the plications. The adolescent form shows more numerous plications surrounding the umbilicus, which is a little reduced in size. Multiple bifurcations are no longer present, with only simple dichotomy observed on the flank. A single striation is intercalated between each pair of dichotomizing growth lines. The ventrolateral projection is sharper and no spirals are observed between the umbilical plications. It should be noted that the regular interpolation of a single striation in between the dichotomizing growth lines described by Bouckaert (1960) was not observed in the type material.

Most information on the ontogeny of this species comes from British Geological Survey (BGS) and Manchester Museum specimens (see Fig. 3.15). Juvenile internal casts from Rough Lee, collected by E.W.J. Moore, with diameters 5-7 mm, have plications spaced c.3 per mm branching irregularly into 4-5 growth lines on the ventrolateral projection. Dichotomy, trichotomy or quadrichotomy are present. One persistent constriction was recorded and spirals are common on the venter. At c.8-9 mm diameter, the plications are quite radial before being projected into a shallow ventrolateral projection. At c.11 mm diameter, umbilical spirals accompany slender plications branching into c.3 growth lines and intercalations are common. Specimens with diameter 14 mm have 3-4 growth lines per mm on flank and 2 umbilical plications per mm. There are

strongly marked spirals on the flank, and dichotomy, trichotomy and secondary branching are common. The ventral sinus is slight. Specimens with diameter c.17 mm have slender plications branching irregularly into growth lines spaced 5 to the mm on the ventrolateral projection. The plications are generally slender and a wide umbilicus is a common feature in all specimens.

Remarks: Inspection of Manchester Museum specimens as well as BGS specimens confirms the highly variable character of the species and helps add to Bisat & Hudson's (1943) original description, which was based solely on fragmented shale impressions. The following characters, which are in addition and sometimes contrast to the type description (cf. Bisat & Hudson 1943), were observed in the solid specimens in both the Manchester Museum and BGS collections (Fig. 3.16):

- The plications are in some cases bent slightly forward and not always radial throughout ontogeny.
- Umbilical spirals are seen until late adolescence (even on the holotype), and thus, cannot be used as a diagnostic feature for *Ph. circumplicatile*.
- There is much overlap in characters between *Ph. paucicrenulatum* and *Ph. circumplicatile*, leading to dubious past identifications.
- Overall, the pattern of branching is more irregular in *Ph. paucicrenulatum* than in *Ph. circumplicatile*.
- Where plications are bent forward, this is taken as a variety closer to *Ph. circumplicatile* than *Ph. paucicrenulatum*. Plications are slender in *Ph. paucicrenulatum* and, when strongly marked and stouter, this is taken as a variety closer to *Ph. circumplicatile*.
- In *Ph. paucicrenulatum*, there are fewer intercalated growth lines between the umbilical plications than in *Ph. circumplicatile*.
- According to Calver and Ramsbottom (1961; p. 192) *Ph. paucicrenulatum* differs from earlier *Ph. circumplicatile* in having a more forwardly directed ventrolateral projection and bifurcating umbilical ridges.

In conclusion, until more good quality, complete and unflattened specimens of *Ph. paucicrenulatum* become available, it will not be possible to fully resolve

the taxonomy of the *Ph. circumplicatile-paucicrenulatum* group and to assess the amount of phenotypic variation that exists both within these species (intraspecific variation) and between them (interspecific variation).

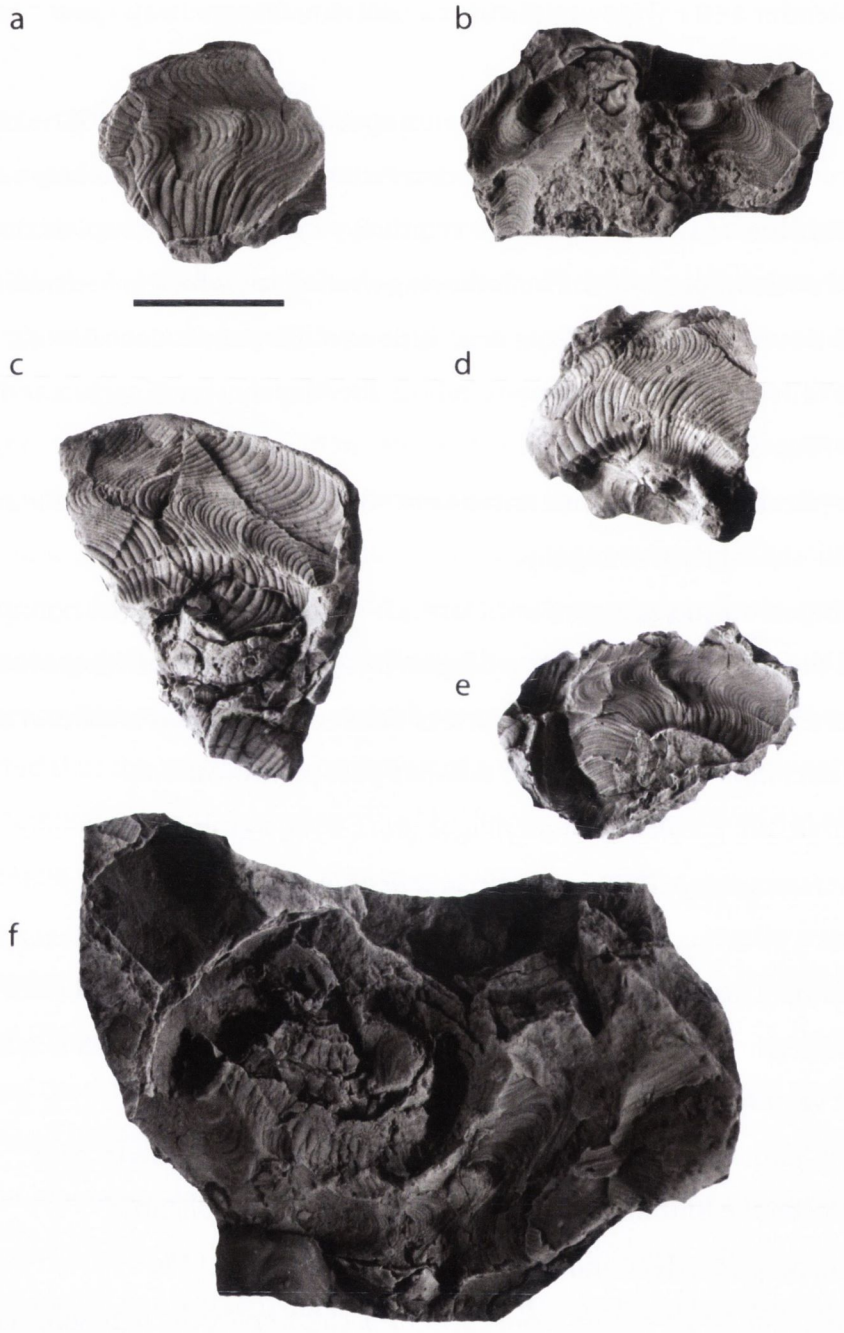

Fig. 3.14. *Phillipsoceras paucicrenulatum* type material. All specimens from Lumbutts Clough, Todmorden, Yorkshire. (a) GSM 71076, paratype, (b) GSM 71075, paratype (c) GSM 71078, paratype, (d) unlabelled specimen associated with type material, (e) GSM 71074, holotype, (f) GSM 71077, paratype. Scale is 10 mm.

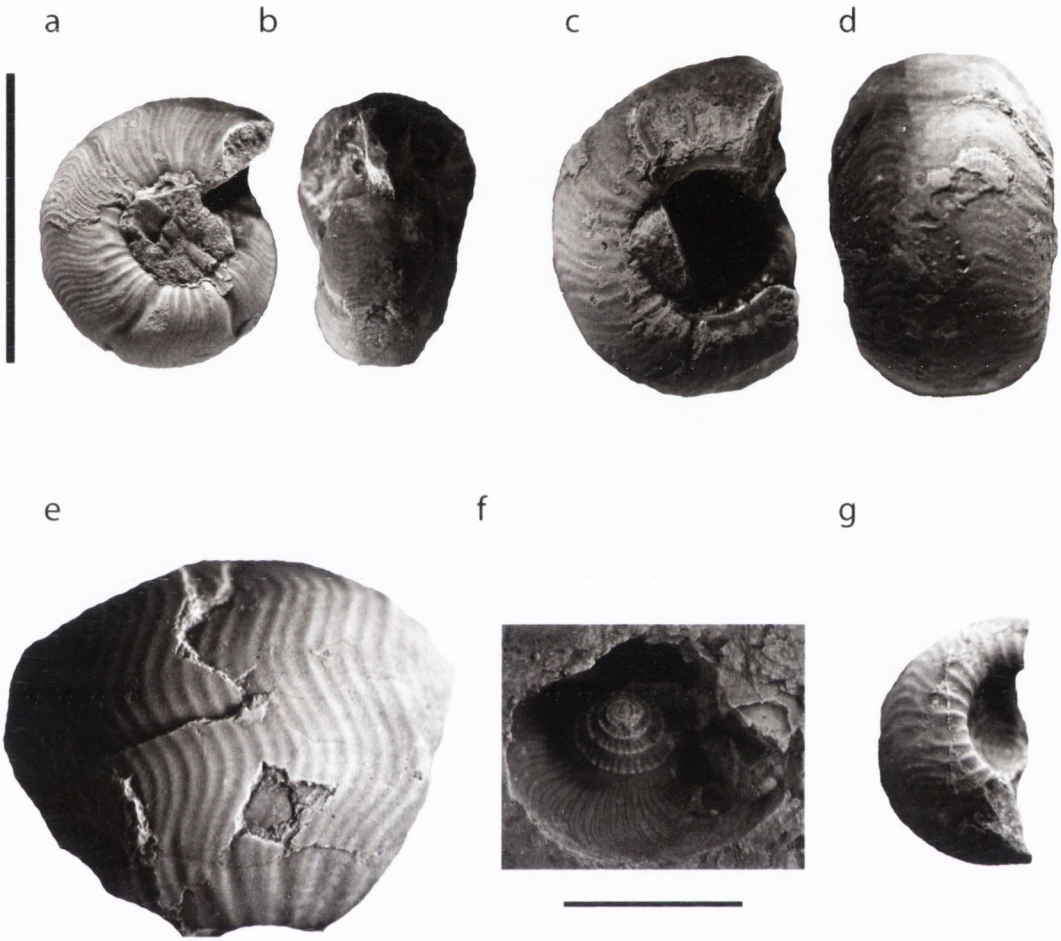

Fig. 3.15. Ammonoids which occur in the Shannon Basin, Ireland. 1 *Phillipsoceras paucicrenulatum* (a-b) zi 7097 (BGS), Fisherstreet Bay, Co. Clare, side and dorsal view; (c-d) zi 7098 (BGS), Fisherstreet Bay, Co. Clare, side and ventral view; (e) zi 7100 (BGS), Fisherstreet Bay, Co. Clare; (f) TCD.61064, Luggacurren section, Co. Laois; (g) zi 7096, Fisherstreet Bay, Co. Clare, side view. Scale is 10 mm.

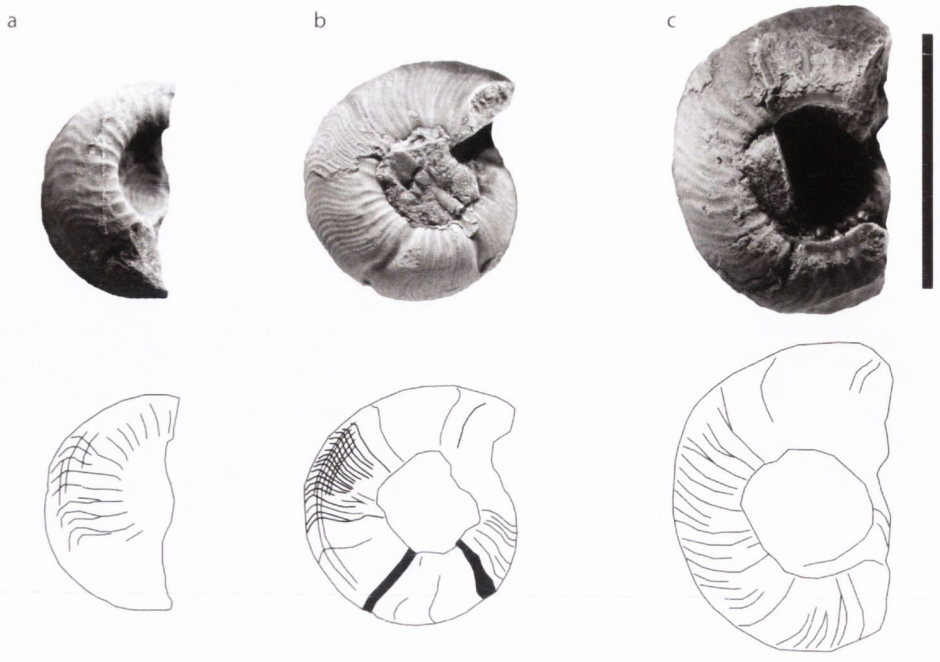

Fig. 3.16. Ontogenetic study of the ornament for *Phillipsoceras paucicrenulatum* (Bisat & Hudson, 1943) (a) zi 7095 (BGS), Fisherstreet Bay, Co. Clare, (b) zi 7097 (BGS), Fisherstreet Bay, Co. Clare, (c) zi 7096 (BGS), Fisherstreet Bay, Co. Clare, scale is 10 mm.

Genus *Reticuloceras* Bisat, 1924, p. 114

Remarks: This genus, which is closely related to and transitional to *Phillipsoceras*, is described in the Treatise on Invertebrate Palaeontology (Selden 2009, p. 95) as being characterized by an involute conch, with wie or narrow umbilicus. It is said to have ornamentation that is, in general, weakly developed. The ornament consists of transverse growth lines, sometimes crenulated, with vetrolateral projection and ventral sinus, usually crossed by fine spiral lirae, producing reticulate ornamentation. At early whorls, small riblets near umbilicus and faint umbilical nodes are common.

***Reticuloceras pulchellum* (Foord, 1903); Fig. 3.17.**

v*1903 *Glyphioceras (Beyrichoceras) pulchellum* Foord, p. 190, pl. 49, fig. 5.
?1924 *Glyphioceras (Beyrichioceras) reticulatum* Foord; Bisat, p. 115.
v*1943 *Reticuloceras pulchellum* Foord; Bisat & Hudson, p. 422, pl. 28, fig. 8.
1984 *Reticuloceras pulchellum* Foord; Swan, p. 254, pl. 8, fig. 5-6, pl. 9, fig. 3-4.

Type Locality: Rathcahill, Co. Limerick.

Remarks: Hodson (1954b, p. 157) stated that he had not been able to find the type locality.

Interim Diagnosis: The late appearance of a ventrolateral projection, the cone-shaped umbilicus, the narrow dichotomy and closely-set nature of the weakly crenulated growth lines are features that, when combined, help identify the species. Until juvenile and adolescent specimens are described, it is not possible to provide a full diagnosis, nor a systematic description of the ontogeny of this species.

Description: This Irish species is in need of some revision. Foord (1903) does not provide an ontogenetic description, limiting his description to a single growth stage. The holotype consists of an adult specimen with external shell showing ornament (Fig. 3.17). Only one-half of the shell is preserved.

Inspection of the specimen shows that Foord's (1903) description is accurate: *"Test ornamented with very fine but perfectly distinct thread-like lines, apparently with crenulations; proceeding from the umbilicus they pursue at first a nearly straight course, but soon make a slight curve backwards, then curving boldly forward they pass over the periphery in a strong backwardly directed curve, thus forming a deep sinus in that region. Towards the aperture the anteriorly directed curve becomes narrower and more tongue-like in form and the lines have here a tendency to form little bundles, which cause them to stand out more prominently. Two narrow and shallow constrictions, which conform in direction to the lines of the ornamentation, are developed upon the test. Very faint spiral lines are seen covering the test all over."* The growth lines are very closely set, spaced about 10-12 per mm on the flank, and very narrow dichotomy is present. Bisat & Hudson (1943) also figure young and adolescent UK specimens, but it must be noted that these are diagnosed as *R.* aff. *pulchellum*, so their use in inferring ontogenetic changes of ornament with ontogeny is limited. The young specimens are described as *"all rather broad on the venter. In adolescence the umbilical plications fork into strong growth lines, which are spaced about four to the mm at the centre of the venter at all the diameters seen. The bifurcations are sometimes irregular. There is a tendency in late adolescence to regular narrow dichotomy. Occasional specimens occur with a larger umbilicus and coarser ornament spaced two to three growth lines to the mm on the venter, and there is also a variant more closely and delicately ornamented, with growth lines 6 to the mm and a smaller umbilicus."*

Thus the strength of the growth lines appears to decrease through ontogeny, becoming delicate in adulthood. Dichotomy is a recurring feature and the dichotomizing point seems to distance itself further from the umbilicus towards the venter with age. Even though dichotomy is the main mode of branching, trichotomy cannot be excluded at present.

Comparisons: See *R. subreticulatum* for comparison with this species.

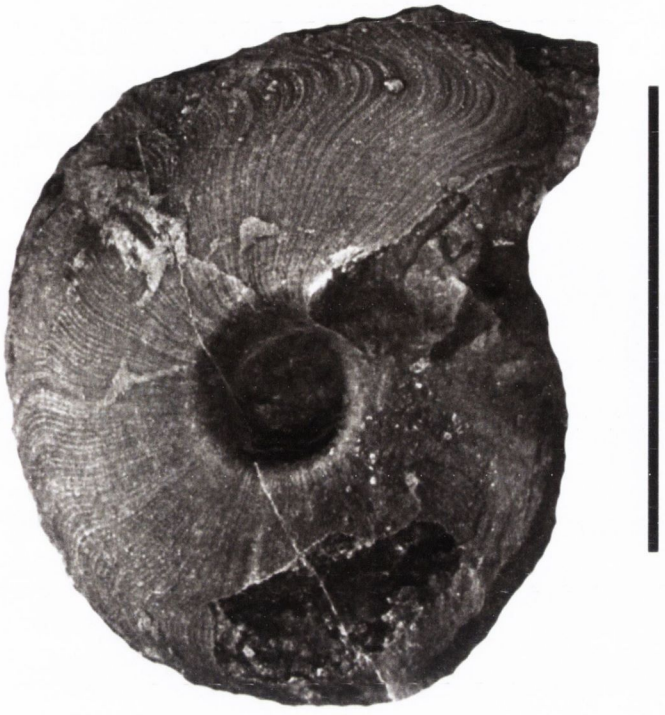

Fig. 3.17. *Reticuloceras pulchellum* holotype (NMING specimen, unlabelled). Scale is 20 mm.

***Reticuloceras subreticulatum* (Foord, 1903); Figs. 3.18-3.21; Table 3, Appendix A.**

v*1903 *Glyphioceras (Beyrichoceras) subreticulatum* Foord, p. 184, pl. 49 fig. 6a-b, 7 a-d.

1925 *Eumorphoceras subreticulatum* Foord; Schmidt, p. 585, pl. 22 fig. 1, pl. 25, fig. 4-6.

v1943 *Reticuloceras subreticulatum* Foord; Bisat & Hudson, p. 423, pl. 26, fig. 3.

Also refer to: Bouckaert (1960, 1961); Hodson (1954a-b); Patteisky (1959); Calver & Ramsbottom (1961); Swan (1984).

Type Locality: Foynes Island, Co. Limerick, Ireland.

Type Material: Lectotype (NMING : F23964, Fig. 3.18d; Fig. 3.20), and associated paralectotypes (NMING : F23965, NMING : F23966, NMING :

F23967) with greater diameter than the lectotype, showing features of the ornament and internal cast.

Other Material: Irish specimens collected by Hodson from Blake's Bridge and Fisherstreet Bay, Co. Clare, and reposited in the collections of Trinity College Dublin (TCD.60602, TCD.60603, TCD.60604, TCD.60605, Fig. 3.18a-c, e; Fig. 3.19).

Diagnosis: Ellipsocone shell with narrowly rounded umbilical edge and closely set, clearly crenulated growth lines, which dichotomize narrowly in a regular fashion one-third of the way up the flank. The spirals are less pronounced than the growth lines but still clearly visible. Trichotomy and quadrichotomy are absent and there is early development of a ventrolateral projection, which is not pronounced. In adult specimens, growth lines are slightly rursiradiate at the dichotomizing point, which is about one third of the distance from umbilicus to venter, before bending in a prorsiradiate direction.

Description: The inner whorls are ribbed (except in the first whorl). Juvenile specimens (TCD.60602, Fig. 3.18a, and other specimens from Hodson's collection) at c.8 mm diameter have ribs spaced c.10 per mm and projected slightly forward into a ventrolateral projection. Three well-marked constrictions are present on the internal cast (Fig. 3.18a). At 9 mm diameter, umbilical plications dichotomise into growth lines, which are accompanied by intercalated growth lines (Fig. 3.18a,f). As adolescence is reached, the plications degenerate into growth lines which bifurcate along the flank. A ventrolateral projection is present, becoming gradually more pronounced through ontogeny. At 15 mm diameter (TCD.60603, Fig. 3.18b), the growth lines are spaced 8-10 per mm on the ventrolateral projection; the same is true for a specimen at 19.5 mm diameter (TCD.60604, Fig. 3.18c). Dichotomy is always narrow and in rare cases intercalations are present. Spiral growth lines cross the shell in the ventral area and around the ventrolateral projection. In the lectotype (NMING : F23964, Fig. 3.18d,g; Fig. 3.20), at 23 mm diameter, growth lines bifurcate at the point where they start to become slightly

rursiradiate on the flank, about one third of the distance from umbilicus to venter, before bending in a prorsiradiate direction. Dichotomy is narrow and growth lines are closely spaced, averaging 16 per mm on the umbilical margin and 10 per mm on the ventrolateral projection. No ventral sulci are observed on the type material. Spiral growth lines decorate several areas of the flank. Constrictions (three to the whorl) remain well marked through ontogeny. As observed in the adult paralectotypes (NMING : F23965, NMING : F23966, NMING : F23967), the growth lines tend to form bundles on the ventrolateral projection in more mature specimens and these bundles form indentations or grooves on the internal cast. The small ridges on the test produced by slightly raised growth lines mentioned by Foord (1903) are visible on the lectotype (NMING : F23964, Fig. 3.18d,g; Fig. 3.20) and are also present in adult specimens from Blake's Bridge, Co. Clare, Ireland (Fig. 3.18e). Umbilical walls shallow in gradient and suture line with parallel sided external lobe (Fig. 3.21), typical of *Reticuloceras* (see Ruzhencev & Bogoslovskaya 1978).

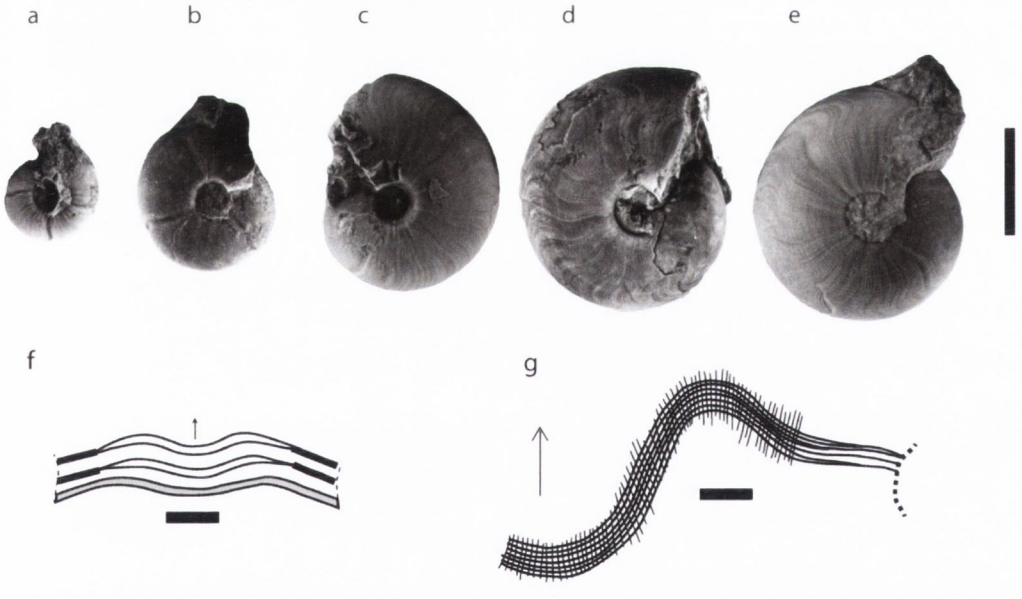

Fig. 3.18. Changes in ornament in *Reticuloceras subreticulatum* (Foord, 1903) (a) TCD.60602, Blake's Bridge, (b) TCD.60603, Blake's Bridge, (c) TCD.60604, Blake's Bridge, (d) Lectotype (NMING : F23964), Foynes Island, Co. Limerick, Ireland, (e) TCD.60605, Blake's Bridge. Scale bar is 10 mm long. (f) Growth lines of TCD.60602, Blake's Bridge, and shaded constriction, (g) Growth lines in lectotype (NMING : F23964), Foynes Island, Co. Limerick, Ireland. Scale bars are 2 mm long.

Comparisons: This species shares many features of the ornament with *Reticuloceras pulchellum* (Foord, 1903), but the cone shaped umbilicus of the latter, with nearly vertical umbilical walls, is a distinguishing feature since *R. subreticulatum* has a narrowly-rounded umbilical edge. Furthermore the rursiradial projection of growth lines is far slighter in *R. pulchellum,* if present at all. Both species possess a ventrolateral projection, but in *R. pulchellum* the overall course of the growth lines appears to be more radial. As mentioned by Bisat & Hudson (1943, p. 424), in *R. subreticulatum* the ventral sinus is not very pronounced, in contrast to species such as *Ph. paucicrenulatum. Reticuloceras melanum* (Korn, 1997) has more delicate growth lines and less obvious spirals. Compared to *Reticuloceras bisorsale* (Phillips, 1836), the ornament is more subdued in *R. subreticulatum.*

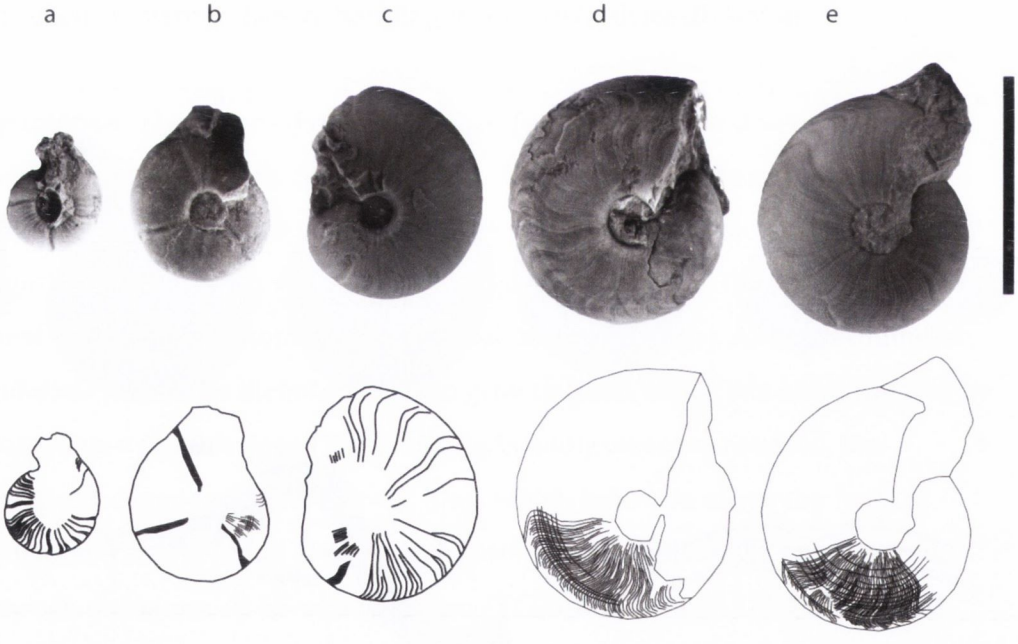

Fig. 3.19. Ontogenetic study of the ornament for *Reticuloceras subreticulatum* (Foord, 1903) (a) TCD.60602, Blake's Bridge; (b) TCD.60603, Blake's Bridge; (c) TCD.60604, Blake's Bridge; (d) Lectotype (NMING : F23964); (e) TCD.60605, Blake's Bridge. Scale is 20 mm.

Fig. 3.20. *Reticuloceras subreticulatum* lectotype (NMING : F23964), Foynes Island, Co. Clare, (a-b) side and ventral view. Scale on top left is 20 mm.

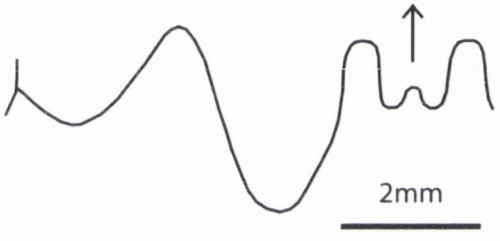

Fig. 3.21. Suture line, *R. subreticulatum* Foord lectotype (NMING : F23964), at 11 mm diameter.

Superfamily Gastrioceratoidea Hyatt, 1884

Family Homoceratidae Spath, 1934

Subfamily Homoceratinae Spath, 1934

Genus *Homoceras* Hyatt, 1884

Genotype: Homoceras (Goniatites) smithi, Brown 1841 (see discussion in Titus & Manger 2001, p. 22).

Remarks: This genus can be distinguished from *Reticuloceras* by the absence of ribs in the young (serpenticone stage), by the general absence of spiral growth lines, or the width of the ventral lobe. However, adult *Homoceras* shells are probably indistinguishable from adult *Isohomoceras* shells (Bisat 1924; Ruzhencev & Bogoslovskaya 1971).

***Homoceras beyrichianum* (de Koninck, 1843); Figs. 3.22-3.23; Table 4, Appendix A.**

1833 *Ammonites listeri* de Koninck; Davreux, pl. 5, fig. 6, pl. 8, fig. 4c.

1837 *Ammonites listeri* Beyrich, p. 39, pl. 7, fig. 1.

p.1897 *Glyphioceras diadema* Foord & Crick, p. 202.

p.1897 *Glyphioceras (Beyrichoceras) diadema*? Beyrich; Foord, p. 179.

1898 *Glyphioceras beyrichianum* Haug, p. 95, pl. 1, fig. 1-21, 23.

1921 *Homoceras diadema* Schmidt, p. 302.

1925 *Glyphioceras leodicense* Schmidt, p. 574, pl. 21, fig. 15, pl. 24, fig. 8,9,29.

1925 *Homoceras beyrichianum* Schmidt, p. 579, pl. 21, fig. 21, pl. 24, fig. 28, pl. 25 fig. 1.

1925 *Homoceras beyrichianum* Schmidt, p. 70, pl. 14, fig. 1,2.

1928 *Homoceras beyrichianum* Bisat, p. 130.

1929 *Homoceras beyrichianum* Schmidt, p. 70, pl. 29, fig. 1,2.

1933 *Homoceras beyrichianum* Bisat, p. 257.

1934 *Homoceras beyrichianum* Schmidt, p. 451, p. 452, fig. 56-58.

1934 *Homoceras beyrichianum* Schmidt, p. 443, fig. 57-59.

1957 *Homoceras beyrichianum* de Koninck; Patteisky, p. 515, pl. 1, fig. 2.

1959 *Homoceras beyrichianum* de Koninck; Patteisky, p. 15, pl. 2, fig. 2a-18, pl. 3, fig. 1-4.

1960 *Homoceras beyrichianum* de Koninck; Butcher & Hodson, p. 78, pl. 19, fig. 3.

1961 *Homoceras beyrichianum* de Koninck; Bouckaert, fig. 1.

1985 *Homoceras beyrichianum* Haug; House, p. 130, pl. 6,7,39.

2001 *Homoceras diadema* Beyrich; Titus & Manger, fig. 14.17, 14.22, 20.2.

Also refer to: Hind (1905, 1918); Demanet (1941); Leggewie & Schonefeld (1957); and Korejwo (1986).

Diagnosis: Overall, the open cadicone shell and the very pronounced, 'armour-like' ornament, where the ribs cover the test all over, make this an easily identifiable species. The ribs are stronger than those in *Ho. smithii* or *Ht. prereticulatus*

Description: A well-preserved specimen (TCD.61011) from the Phosphate Mine, Roadford, Co. Clare, which was collected by Hodson, allows the early whorls to be described: ribs first appear on the fourth whorl and they are spaced c.6 per mm. The ventrolateral projection is already present at this diameter and it forms a ventral sinus (which can be referred to as ventral bow); the costae on the sinus are more widely spaced, averaging 3 per mm. It is also typified by a pronounced ventrolateral projection and an umbilical rim. At 9 mm diameter (in TCD.61003; Fig. 3.22a), the costae are spaced 3 per mm on the venter. At 12 mm diameter (in TCD.61004; Fig. 3.22b), the growth lines are spaced 3-4 per mm on the umbilical margin. At 17.5 mm diameter (in TCD. 61000; Fig. 3.22c), four constrictions intersecting in the umbilicus at 90° angles are visible. At these diameters, specimens have a raised umbilical wall and sharp umbilical rim which are typical of the open cadicone shell shape. Between 18 and 23 mm, costae are spaced 2 per mm and the umbilical rim becomes more obvious.

Dichotomy is very rarely observed, in varieties with less pronounced ornament, perhaps closer in affinity to *Ho. smithii*. Both ventrolateral projection and ventral sinus persist and remain constant in strength through ontogeny. The venter is broad through ontogeny, while the umbilical diameter generally decreases in proportion to the overall diameter: at 8 mm diameter, it is 3.7 mm (measured from side to side of the pronounced umbilical rim surrounding the barrel shape umbilicus); at 11 mm it is c.3 mm and at 16 mm it is 4.8 mm.

Material: Specimens from the National Museum of Ireland collections from Roadford or Spectacle Bridge, Co. Clare, Ireland, conform to the above description.

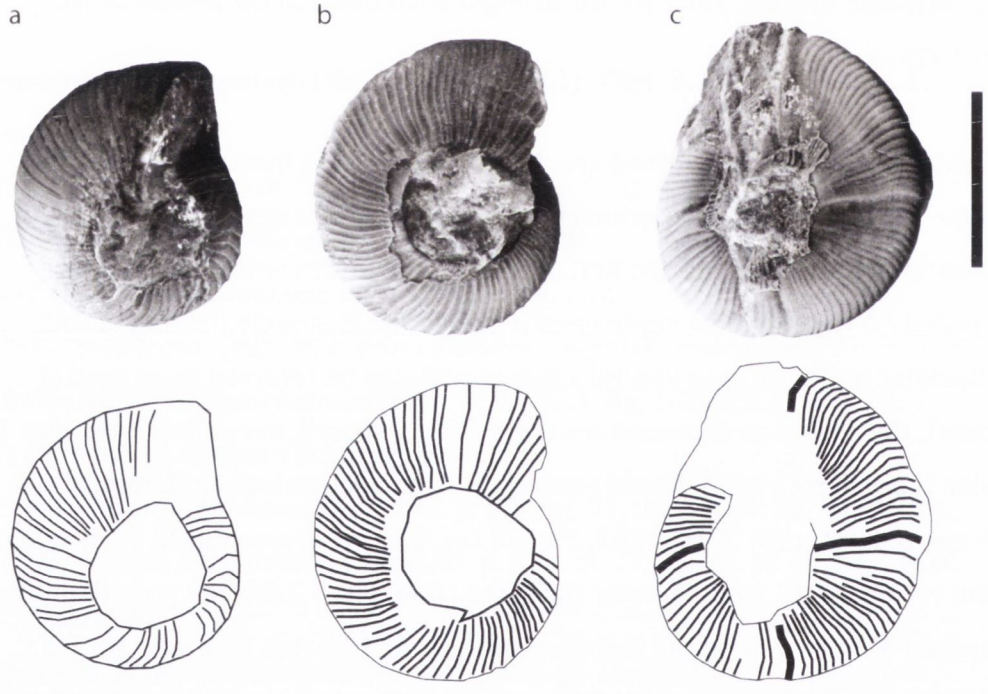

Fig. 3.22. Changes in ornament in *Homoceras beyrichianum* (de Koninck, 1843) (a) TCD.61003, Lisdoonvarna district, Co. Clare (b) TCD.61004, Lisdoonvarna district, Co. Clare, (c) TCD. 61000, Coolagh River, Co. Clare, scale is 10 mm.

Remarks: This is Bisat's (1924) and Schmidt's (1921) *Homoceras diadema*. As mentioned by Bisat (1924), this is a very variable species. He describes *Ho. undulatum* and *Ho. smithii* are two varieties of *Ho. beyrichianum* (*diadema*).

These closely allied species can be distinguished by the features summarized in Table. 3.1.

***Ho. beyrichianum* (de Koninck, 1843)**	***Ho. smithii* (Brown, 1841)**	***Ho. undulatum* (Brown, 1841)**
Strong ribs projected into ventral bow	Little to no ventrolateral projection, open cadicone shape	Dichotomy and ventrolateral projection

Table 3.1. Diagnostic features in *Ho. beyrichianum*, *Ho. smithii* and *Ho. undulatum*.

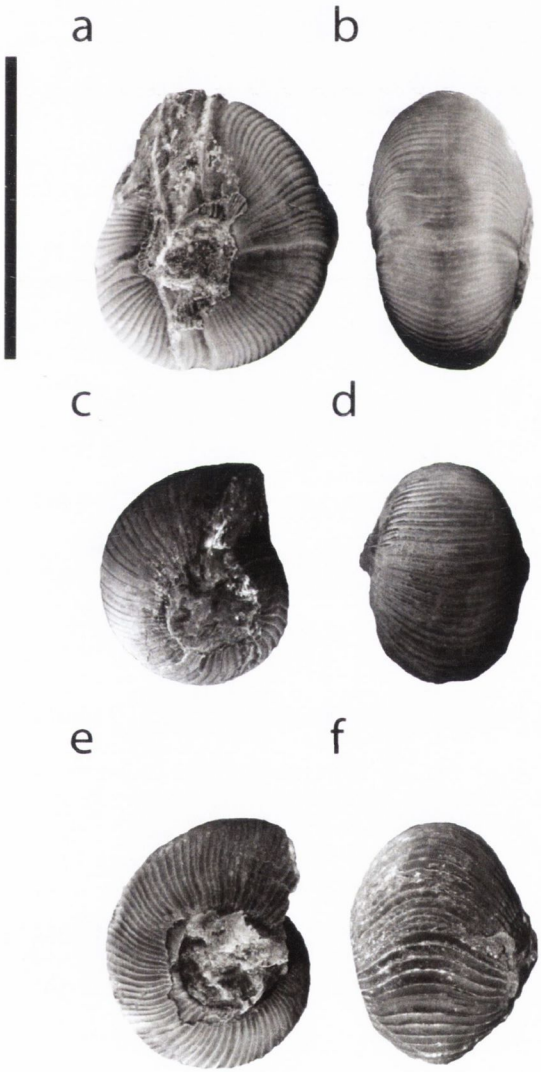

Fig. 3.23 *Homoceras beyrichianum* (a-b) TCD.61000, Coolagh River, Co. Clare, side and ventral view; (c-d) TCD.61003, Lisdoonvarna district, Co. Clare, side and ventral view; (e-f) TCD.61004, Lisdoonvarna district, Co. Clare, side and ventral view. Scale on top left is 20 mm.

***Homoceras smithii* (Brown, 1841); Figs. 3.24-3.25; Table 5, Appendix A.**

v*1841 *Goniatites smithii* Brown, p. 218, pl.7 ,fig.34,35.

v*1924 *Homoceras diadema var. smithi* Brown; Bisat, p. 104, pl.4, fig.3-5.

1957 *Homoceras smithi* Patteisky, p. 515, pl.1, fig.3a.

1957 *Homoceras diadema* Leggewie & Schonefeld, p. 233, pl.17, fig.1.

1957 *Homoceras smithi* Brown; Hodson, p. 8, fig.2-4, pl.B, fig.6.

1958 *Homoceras smithi* Brown; Hodson & Van Leckwijck, p. 8, pl.A, fig.2-4, pl.B, fig.6.

1959 *Homoceras smithi* Brown; Patteisky, p. 17, pl.3, fig.8,9,10.

1961 *Homoceras smithi* Brown; Bouckaert, fig.2.

1971 *Homoceras smithii* Brown; Ramsbottom, p.162.

1984 *Homoceras smithii* Brown; Swan, p. 216, pl. 2, fig. 5-6.

Type Locality: Todmorden, UK.

Type Material: The type material, housed in the Manchester Museum, consists of two specimens (MANCH L.10244a,b): one is figured in Brown (1841) (MANCH L.10244a), the other he used for suture line description (MANCH L.10244b). Unfortunately the weathering away of the umbilical rim does not allow dichotomy to be recognised in the type material (MANCH L.10244a), as already noted by Bisat (1924), making it unclear whether dichotomy is an important feature.

Other Material: Irish specimens collected by Hodson and housed in Trinity College Dublin allow an ontogenetic description for this species to be made for the first time, as well as a comparison to Bisat's (1924) description.

Diagnosis: *Homoceras* with umbilical rim up to c.16 mm diameter and costae that remain quite radial through ontogeny. The open cadicone shell shape transitions first to sphaerocone (at c.9 mm diameter), and eventually to ellipsocone (at 21 mm diameter).

Description: At 7.7 mm diameter, the shell is open cadicone with 4 radial costae per mm. A rim is already present. The umbilicus is very large, with diameter 4.4 mm, and it remains large in proportion to conch size throughout ontogeny. The umbilical rim remains prominent until about 16 mm diameter, becoming much fainter at c.20 mm diameter. The costae are mostly radial or very rarely bent forward into a slight ventrolateral projection. This was observed at 11 mm (in TCD.61002; Fig. 3.24a; Fig. 3.25a-b) diameter and at 21 mm (in TCD.61005; Fig. 3.24b; Fig. 3.25c-d) diameter. Dichotomy is very rare but it can occur irregularly and was observed at 21 mm diameter. An internal cast at 21 mm diameter (TCD.61005; Fig. 3.24b; Fig. 3.25c-d) shows four constrictions spaced at 90° angles (these were also observed on other specimens). Spacing of costae is quite conserved throughout ontogeny, ranging from 4 to 6 costae per mm.

Remarks: The species is most easily diagnosed early in ontogeny, when shell shape and ornament are most distinct from other allied species.

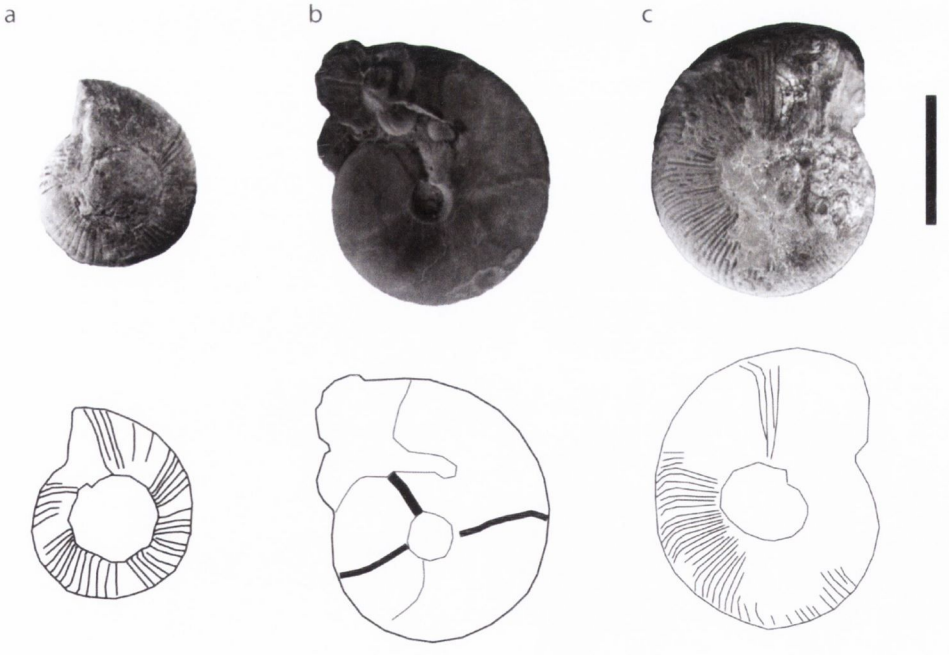

Fig. 3.24. Changes in ornament in *Homoceras smithii* (Brown, 1841) (a) TCD.61002, Lisdoonvarna, Co. Clare, (b) TCD.61005, Lisdoonvarna, Co. Clare, (c) TCD.61006, Lisdoonvarna, Co. Clare, scale is 10 mm.

Comparisons: The umbilical rim could lead this species to be confused with certain *Vallites henkei* specimens with accentuation of growth lines on the rim. However, this is easily avoided when one considers that in *V. henkei* the growth lines are much more delicate and rim has very small nodes ("beading"), which are lacking in *Ho. smithii*. This species is very closely allied to *Ho. undulatum*: in fact, Bisat grouped them together under the name *Ho. diadema*, while recognizing the two variants. The most important feature that allows this species to be distinguished from *Ho. undulatum* is the open, barrel-shaped shell. In addition, dichotomy is far more common in *Ho. undulatum*. The main difference between *Ho. beyrichianum* and *Ho. smithii* is the lesser strength of the costae in *Ho. smithii*, but there are other differentiating features, such as the less pronounced ventrolateral projection (if at all present) in *Ho. smithii*.

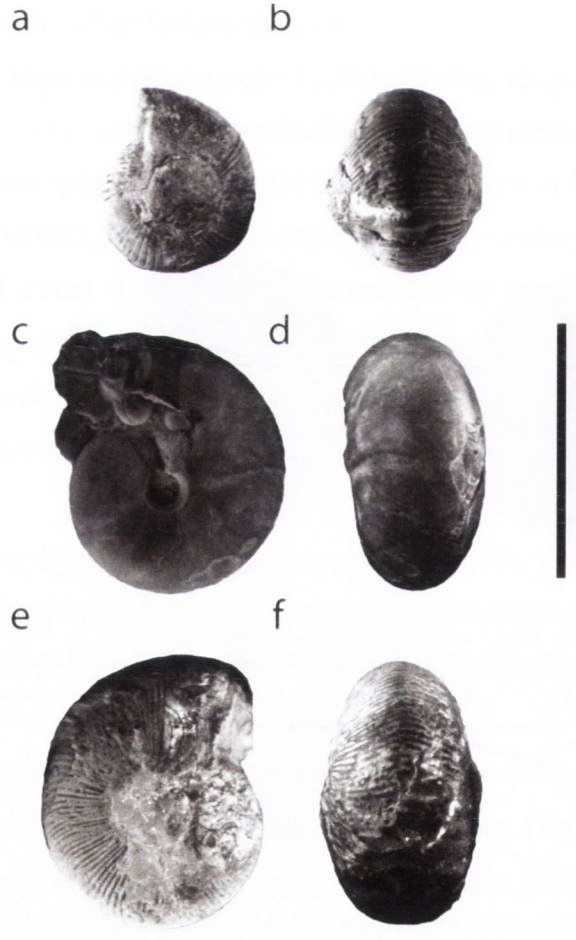

Fig. 3.25. *Homoceras smithii* (a-b) TCD.61002, Lisdoonvarna, Co. Clare, side and ventral view; (c-d) TCD.61005, Lisdoonvarna, Co. Clare, side and ventral view; (e-f) TCD.61006, Lisdoonvarna, Co. Clare, side and ventral view. Scale on top left is 20 mm.

***Homoceras undulatum* (Brown, 1841); Fig. 3.26.**

v*1841 *Goniatites undulatus* Brown, p. 213, pl. 7, figs. 1, 2, 3, 4, 5.

v*1905 *Homoceras undulatum* Brown; Hind, pl. 6, fig. 15.

1924 *Homoceras diadema var. undulatum* Brown; Bisat, p. 105.

v*1943 *Homoceras undulatum* Brown; Bisat & Hudson, p. 408, pl. 26, fig. 1a,1b,2.

1960 *Homoceras undulatum* Brown; Butcher & Hodson, p. 78, pl. 19, fig. 2.

1960 *Homoceras undulatum* Brown; Chalard, pl. B, fig. 1-2.

1984 *Homoceras undulatum* Brown; Swan, pl. 4, figs. 2-3.

1985 *Homoceras undulatum* Brown; Manger, Weyant & Pareyn, p. 192, pl. 1, fig. D, L.

1985 *Homoceras undulatum* Brown; Lemosquet, Conrad & Manger: p. 421, pl. 8 fig. 12.

Type Locality: Cross Hills, Skipton, UK.

Type Specimens: The type series is currently housed in the Manchester Museum and consists of two solid specimens: an adult lectotype (MANCH L.10241a) and an adolescent paralectotype (MANCH L.10241b).

Material: Solid specimens at different growth stages from Roadford, Co. Clare, housed at the National Museum of Ireland, together with the type series, specimens from a loose bullion found in the Lisdoonvarna area, and specimens from the Kilmoon River, Lisdoonvarna, housed in the BGS and collected by Hodson provide ontogenetic information available for comparison with published data.

Diagnosis: The species is typified by a broad transition (around 14-19 mm diameter) from specimens with an umbilical rim, constrictions and strong ribs to specimens lacking a rim, and with a slight ventral sinus and slightly more delicate ornament. Constrictions (about three per whorl) persist until about 15 mm diameter.

Description: A juvenile specimen (NMING : F24480/1) at 3.5 mm diameter with a serpenticone (slowly expanding, open coiling) shell has no growth lines or ribs in the inner whorls, thus confirming it belongs to the genus *Homoceras* and not *Homoceratoides*. Growth lines develop in the outer whorls at this diameter and they are spaced 20 per mm. At 5 mm diameter, the ornament is still subdued, with delicate radial growth lines present. At least two constrictions are visible. One sphaerocone specimen (NMING : F24480/2) at c.6 mm diameter has radial growth lines (9 per mm) and three constrictions on the internal cast.

At 7.8 mm diameter (NMING : F24480/3, Fig. 3.26c-d) the growth lines become stronger and are better called ribs or costae, and an umbilical rim is present. At 9.9 mm diameter, the costae are mostly still radial: they start to become deflected forward into a slight ventrolateral projection at about 15.6 mm diameter. At 19.3 mm (NMING : F24480/6, Fig. 3.26e), the ventrolateral projection is still slight and no constrictions are present. A slight ventral sinus develops in parallel to the ventrolateral projection, but is a little more pronounced than it. Dichotomy, first seen at 9.9 mm diameter, persists through ontogeny. It occurs half way up the flank at c.25 mm diameter and closer to the umbilical rim in earlier growth stages. The adolescent paralectotype (MANCH L.10241b, diameter 14.2 mm) has narrowly dichotomizing ribs, with radial course along the flank, an umbilical rim and three constrictions. The ribs are 5 per mm halfway along the flank and dichotomy occurs close to the umbilicus. The adult lectotype (MANCH L.10241a, diameter 19.2 mm) has slightly more delicate ornament compared to the adolescent and ribs that average 6 per mm halfway up the flank. There are no constrictions and no umbilical rim, and the umbilical walls are rounded. Dichotomy occurs somewhere between the halfway point along the flank and the umbilicus. There is a slight ventral sinus and an even slighter ventrolateral projection. The rim remains a conspicuous feature of this species until about 11 mm diameter, when it starts to die away gradually. However, the loss of the umbilical rim occurs at different stages in different specimens. Specimens from the loose bullion (TCD.61012-TCD.61020) have a rim up to 15 mm diameter, while in those from the Kilmoon

River, a rim is first seen at 7.8 mm diameter, and is still present at 16.4 mm diameter. It starts to disappear at 16.6 mm. An excellent adult solid specimen with diameter 38 mm has no umbilical rim. A steep umbilical wall is recorded at c.20 mm diameter, and it becomes shallower at 25 mm diameter in the Kilmoon River specimens. The ribs are spaced about 4-5 per mm on the ventrolateral projection in adolescence, and this was also observed in the type material. The shell takes on ellipsocone shape from c.9 mm diameter onwards. These observations are in accordance with the characters observed in the type material and conform well to the taxonomic descriptions in Bisat (1924), Brown (1841) and Bisat & Hudson (1943). Therefore no further taxonomic revision is deemed necessary.

Comparisons: This species is closely allied to *Homoceras smithii*, and was described as a variant of the species *Homoceras diadema* (Beyrich, 1837) by Bisat (1924). While *Ho. smithii* is typified by its open cadicone shell and barrel-shaped umbilicus, *Ho. undulatum* typically has ellipsocone shell shape with more or less strong, dichotomizing growth lines (Bisat 1924). Some juveniles (at c.7 mm diameter) do have an open cadicone shape, which allows them to be mistaken for *Ho. smithii*. However, where ornament is present, it is slightly stronger in *Ho. undulatum* than in *Ho. smithii* at similar diameters.

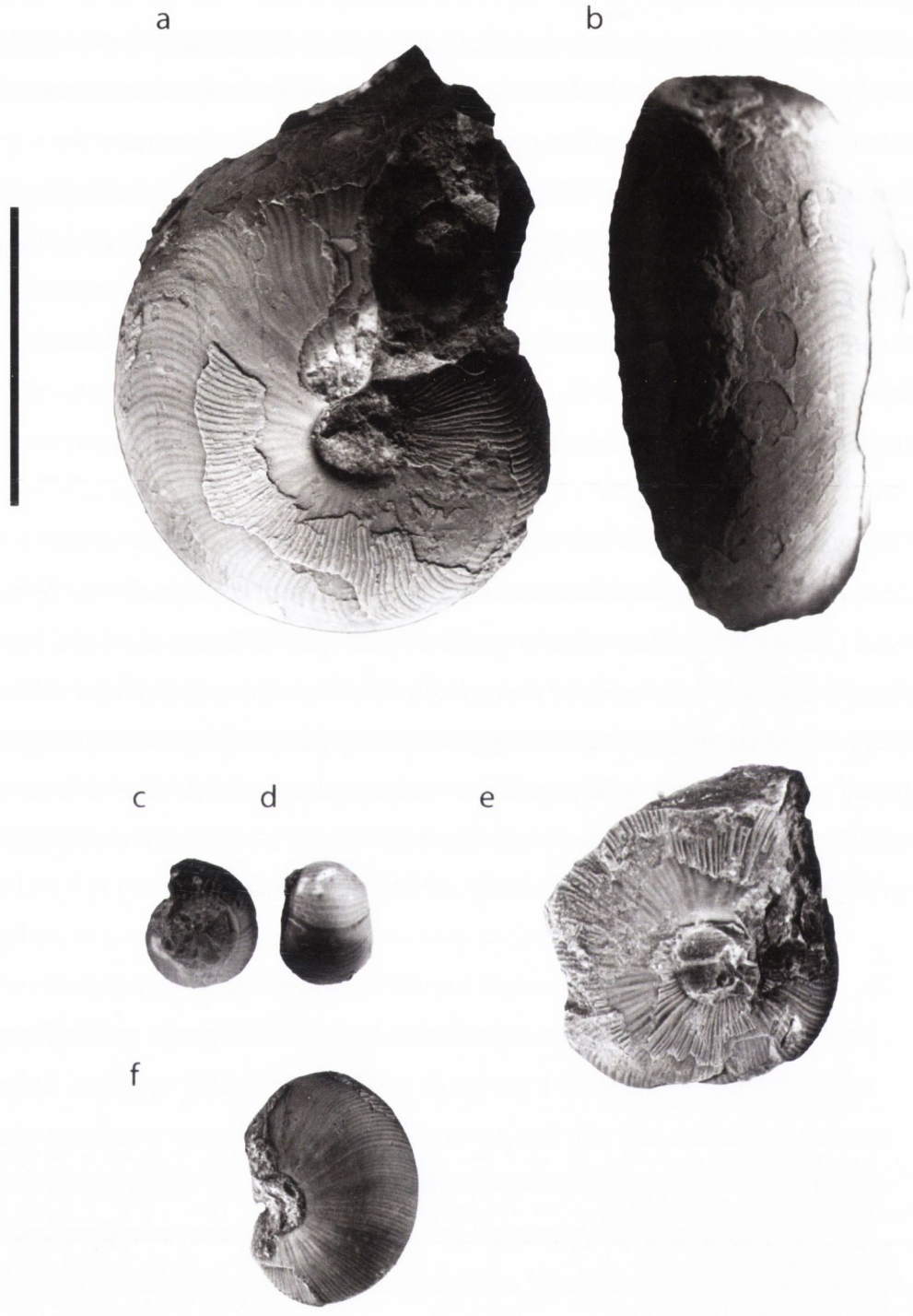

Fig. 3.26. *Homoceras undulatum* (a-b) zi 4534 (BGS), Kilmoon Stream, Lisdoonvarna, Co. Clare, side and ventral view; (c-d) F24480/3, Roadford, Co. Clare, side and ventral view; (e) F24480/6, Roadford, Co. Clare, side view; (f) F24480/5, Roadford, Co. Clare, side view. Scale is 20 mm.

Genus *Isohomoceras* Ruzhencev & Bogoslovskaia, 1971

Genotype: Glyphyioceras inostranzewi, Karpinskii 1889, p. 60.

***Isohomoceras subglobosum* (Bisat, 1924); Fig. 3.27a-c; Table 7, Appendix A.**

.1924 *Homoceras striolatum var. subglobosa* Bisat, p. 110.

1928 *Homoceras subglobosum* Bisat; Bisat, p. 130, pl. 6.

1933 *Homoceras subglobosum* Bisat, p. 258, pl. 30.

1957 *Homoceras subglobosum* Dolle'; Patteisky, p. 515, pl. 1, fig. 1a,1b.

1959 *Homoceras subglobosum* Dolle'; Patteisky, p. 15, pl. 2, fig. 1a-1g.

1961 *Homoceras subglobosum* Bisat; Calver & Ramsbottom, p. 207, pl. 11, fig. 13.

1961 *Homoceras subglobosum* Dolle'; Bouckaert, fig. 2.

1984 *Homoceras subglobosum* Bisat; Swan p. 213, pl. 1, fig. 3-4.

1987 *Isohomoceras subglobosum* Bisat; Riley, p. 30, text-fig. 5, 6E, pl. 2, fig. 3,4,7,18,20,21.

1994 *Homoceras subglobosum* Tanabe, Landman & Mapes, p. 392, fig. 5 1a-b.

2001 *Isohomoceras subglobosum* Bisat; Titus & Manger, p. 20, figs. 14.6-14.11, 17.

Also refer to: Moore (1930); Demanet (1941); and Titus, Webster & Manger (1997).

Type Locality: Stonehead Beck, UK.

Type Material: The type material is housed in the British Geological Survey and was not examined in this study. It is described and figured by Riley (1987).

Diagnosis: Weakly ornamented *Isohomoceras* with short juvenile serpenticonic stages and a subparallel-sided ventral lobe in the suture (Riley 1987; Titus & Manger 2001). No dichotomy or ventral sinus present.

Material and Description: As noted by Bisat (1924), the growth lines are slightly deflected backwards between 4 and 8 mm diameter, but are otherwise radial. Specimens from an *in-situ* bullion at Inishcorker, Co. Clare, have been identified as *I. subglobosum* in this study based on ornament and shell shape. Specimens collected by Hodson from the Aille River and Inishcorker, Co. Clare, have also been examined. At 4.4 mm (TCD.61021, Fig. 3.27a), the shell is sphaerocone in shape and delicate growth lines spaced c.10 per mm are radial. One very faint constriction is present. At 11 mm diameter (TCD.61022, Fig. 3.27b,c), growth lines are spaced c.7 per mm on the venter, becoming more closely set towards the umbilical margin.

A specimen from the Aille River (from Hodson's Southampton collection housed at Trinity College Dublin), at 12.6 mm diameter, has four constrictions and growth lines spaced 6 per mm on the venter. No dichotomy was recorded. The growth lines are still very slightly deflected backwards close to the umbilicus at this diameter, before following a radial course along the test. The constrictions follow the course of the ornament. The shell shape is sphaeroconic.

Comparisons: There is no umbilical rim, which allows easy distinction between this species and *Ho. smithii*. The course of the ornament is far more radial than *Ho. undulatum*.

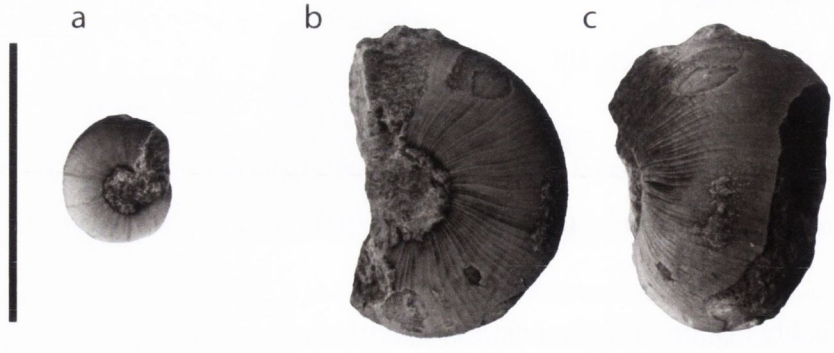

Fig. 3.27. *Isohomoceras subglobosum* (a) TCD.61021, Inishcorker, Co. Clare, side view; (b-c) TCD.61022, Inishcorker, Co. Clare, side and ventral view. Scale is 10 mm.

Genus *Vallites* Ruzhencev & Bogoslovskaya, 1971

Genotype: Homoceras henkei (Schmidt, 1925), p. 453.

***Vallites henkei* (Schmidt, 1925); Figs. 3.28-3.30; Table 10, Appendix A.**

1925 *Eumorphoceras subreticulatum* Foord; Schmidt, p. 585, pl. 22, fig. 1, pl. 25, fig. 4-6.

v*1934 *Homoceras henkei* Schmidt; p. 456, p. 453, fig. 70-72.

1943 *Homoceras henkei* Schmidt; Bisat & Hudson, p. 406, pl. 25, fig. 4-7, pl. 30, fig. 2.

v*1957 *Homoceras henkei* Schmidt; Hodson, pl. C fig. 2, pl. E, fig. 4-6.

Also refer to: Patteisky (1959), Bouckaert (1960, 1961), Chalard (1960), Ruzhencev & Bogoslovskaya (1971, 1978); Swan (1984); Manger, Weyant and Pareyn (1985); Lemosquet, Conrad and Manger (1985); and Korejwo (1986).

Type Locality: Neheim, Germany (former Emde brickworks quarry).

Type Material: Syntypes GZG.INV.48185, GZG.INV.48186, GZG.INV.48184 (Fig. 3.28a-c; Fig. 3.29a-c).

Other Material: Specimens of *V. henkei* from the Aille River, Co. Clare, associated with *Hod. magistrorum* (Hodson, 1957), allow juvenile growth stages to be studied. Late adolescent and adult growth stage features were seen in beautifully preserved Irish specimens collected by F. Hodson.

Diagnosis: *Vallites* with nodes, also called "beading", ornamenting the umbilical margin. The umbilical margin forms a pronounced rim and the growth lines do not dichotomize. The ribs gradually decrease in strength through ontogeny until they give way to the elegant, biconvex growth lines.

Description: In all juvenile specimens (NMING : F23971 and the Hodson material from the river Aille; Fig. 3.30f), growth lines are delicate, radial and

occur c.6 per mm. The umbilical edge is raised, with gently sloping walls; at 8-9 mm diameter (in the Hodson material from the River Aille) growth lines occur c.7 per mm and the elevated umbilical rim is still raised (Figs. 3.28d-e). The growth lines thicken as they cross the rim, but umbilical nodes are absent. A syntype (GZG.INV.48185, Figs. 3.28a,d) at 7.1 mm diameter has strong, radial growth lines. It has very faint umbilical nodes at this early developmental stage. A specimen from Slieve Elva from Hodson's Irish collection (TCD.60610) at 18.5 mm diameter illustrates the biconvex growth lines well, which are slightly bent forward immediately after exiting the umbilicus past the nodes, and then turn back slightly, before pushing forward again on the ventrolateral projection (Fig. 3.28f). The ventral sinus is extremely faint. Growth lines are spaced 5 per mm on the ventrolateral projection. A syntype (GZG.INV.48186, Fig. 3.28b) is an adult specimen with diameter 21.9 mm, showing beading of growth lines (i.e. nodes) on the umbilical margin, and both ventrolateral projection (with 5 growth lines per mm) and ventral sinus (which is more developed in other specimens). The nodes, which give the appearance of several closely set, pseudo-spiral lines that are formed where the transverse growth lines become slightly crenulated, appear in adolescence. An internal cast (GZG.INV.48184, Fig. 3.28c) with a diameter of 30.7 mm with faint impressions of the ornament shows both ventrolateral projection and ventral sinus. A specimen with a diameter of 41 mm (from Hodson's Irish collection reposited in the Geological Museum of Trinity College Dublin) has growth lines spaced 2 per mm and both ventrolateral projection and ventral sinus pronounced. The umbilical edge is broad and rounded, and the walls are shallowly sloping. There are no nodes, as is the case in other very mature specimens.

Comparisons: The umbilical rim is more pronounced and the shell is narrower in *V. henkei* than in *V. schmidti* (Ruzhencev & Bogoslovskaya, 1971). The umbilical rim is more pronounced in *V. henkei* than in *V. kullmanni* (Korn, 1997). Growth lines in *V. henkei* are coarser than in *V. striolatus* (Phillips, 1836). Lack of dichotomy in the growth lines of *V. henkei* distinguishes this species from *Ht. varicatus* and *Hod. magistrorum.*

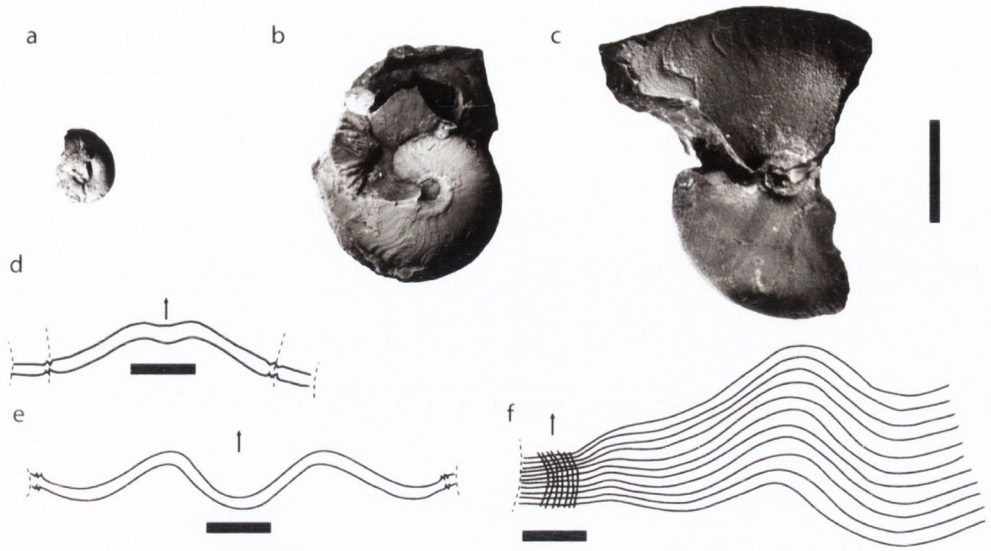

Fig. 3.28. Changes in ornament in *Vallites henkei* (Schmidt, 1925) (a) Syntype GZG.INV.48185, (b) Syntype GZG.INV.48186, (c) Syntype GZG.I NV.48184. Specimens are from Neheim, Germany. Scale bar is 10 mm long. (d) Growth lines (NMING : F23971) at 7 mm with dashed lines at edges of umbilical wall, (e) Growth lines of TCD.60608 at 10 mm diameter, (f) Growth lines of TCD.60608 at 15 mm diameter. Specimens are from Lisdoonvarna, Ireland. Scale bars are 2 mm long.

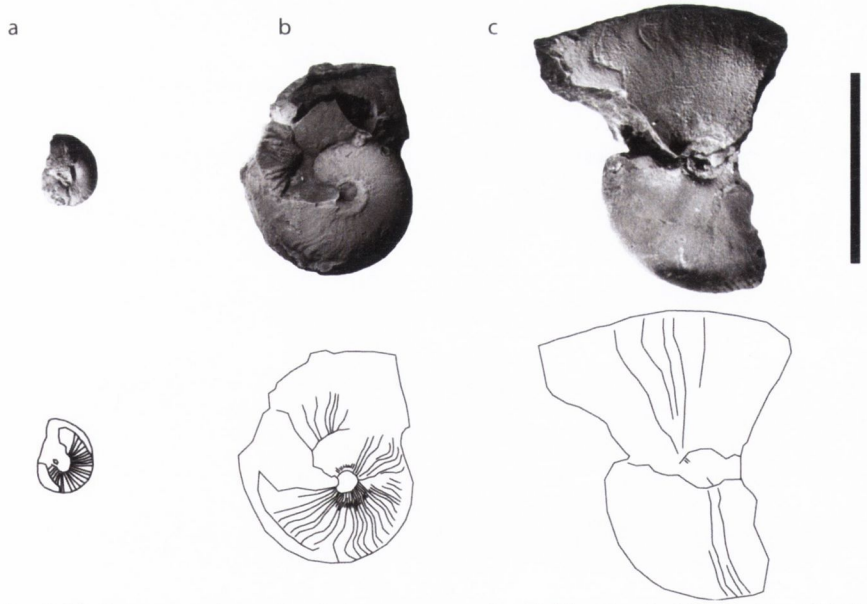

Fig. 3.29. Ontogenetic study of the ornament for *Vallites henkei* (Schmidt, 1934) (a) GZG.INV.48185; (b) GZG.INV.48186; (c) GZG.INV.48184. Specimens are from Neheim, Germany. Scale is 20 mm.

Fig. 3.30. *Vallites henkei* (a-b) NMING : F13974, Lisdoonvarna area, Co. Clare, side and dorsal view; (c) TCD.61030, Aille River, Co. Clare; (d-e) TCD.60608, Lisdoonvarna, Co. Clare, side and ventral view; (f) NMING : F23971, Lisdoonvarna area, Co. Clare, side view. (g) Corofin, Co. Clare, enlarged x 5, after Lewarne (1959). Scale bar on top left is 20 mm.

Superfamily Neodimorphoceratoidea Furnish & Knapp, 1966

Family Ramositidae Ruzhencev & Bogoslovskaia, 1969

Genus *Homoceratoides* Bisat, 1924

Genotype: *Homoceratoides prereticulatus* Bisat, 1924, p. 112.

Remarks: The genus *Homoceratoides* was first coined by Bisat (1924), who described it as closely related to both *Homoceras* and *Reticuloceras*. Bisat based his descriptions on specimens from Rough Lee, Pendle, Holden Gill, Silsden, and Mam Tor, Derbyshire, UK.

***Homoceratoides prereticulatus* Bisat, 1924; Fig. 3.31; Table 8, Appendix A.**

v*1924 *Homoceratoides prereticulatum* Bisat, p. 112, pl. 1, fig. 3.

v*1943 *Homoceratoides prereticulatum* Bisat; Bisat & Hudson, p. 410, pl. 24, fig. 3.

1960 *Homoceratoides prereticulatus* Bisat; Bouckaert, p. 55, pl. 4, niv. 5, pl. 5, niv. 6, fig. 1,2.

1960 *Homoceratoides prereticulatus* Bisat; Chalard, pl. C, fig. 1-10.

1961 *Homoceratoides prereticulatus* Bisat; Bouckaert, fig. 1.

1984 *Homoceratoides prereticulatus* Bisat; Swan, pl. 4, fig. 1,3,4.

Type Locality: Holden Beck, Silsden, Yorkshire, UK.

Type Material: The lectotype is a solid specimen housed in the Natural History Museum, London (C25749). Paratypes extracted from a bullion (not *in situ*) are housed in the BGS collections (GSLM 71107-10); they are preserved as fragmented solid specimens, showing features of the ornament.

Other Material: Solid specimens were recovered from bullion material from the Phosphate Mine, Roadford, Co. Clare, and from a layer of bullions at Fisherstreet Bay, Co. Clare (TCD.61023-60127). These specimens, coupled with the lectotype, Irish specimens housed at the British Geological Survey (BGS)

and specimens from Hodson's Irish collection at Trinity College Dublin, allow a detailed study of the species and its diagnostic features.

Diagnosis: Evolute and ribbed larval stage. Strong, irregularly spaced costae dichotomise, trichotomise and quadrichotomise at a point which recedes progressively from the umbilicus through ontogeny.

Description: Bisat (1924) describes the ornament as composed of many costae, di-, tri- and even quadrichotomising somewhat irregularly at the umbilical edge. The costae are said to swing very slightly for and aft and to be forwardly inclined on the umbilical area. Bisat (1924) remarks that, with increasing age, the dichotomising point recedes from the umbilicus up the lateral area and the direction of costae always tends to be forwardly inclined on lateral area. The larval stage is evolute and ribbed, except for the first whorl, which is smooth and closely coiled. This was observed in a specimen from Blake's Bridge (TCD.61028, Fig. 3.31a), from Hodson's collection, which showed inner whorls. As Bisat mentions, strong, obtuse growth lines appear at 1.5 mm diameter and they are either radial or bent into a slight ventral sinus. At 5 mm diameter, costae are quite closely set (c.12 per mm) on the flank and they are very slightly prorsiradiate. One faint constriction was observed and intercalations are common amid trichotomising and dichotomizing costae.
At 5.8 mm diameter, costae are c.8-10 per mm on the venter. The open cadicone shape of the shell at c.6-7 mm diameter, which was already observed in Bisat's specimens (1924), is confirmed in specimens from Fisherstreet Bay. In effect, many of the diagnostic features of this species (the branching of the costae and the open cadicone shell) are already present at this diameter. A specimen from Roadford (NMING : F24477/6) with diameter 7.7 mm shows 5 costae per mm and one constriction. This is in agreement with Bisat's description of constrictions at this diameter. The ventrolateral projection and ventral sinus are slight at this diameter and the venter is subacute. At c.8 mm diameter the costae are c.6 per mm on the ventrolateral projection and both dichotomy and trichotomy are present. At c.11 mm diameter (NMING : F24477/6), both ventrolateral projection and ventral sinus are present, as well

as one constriction. Costae are spaced 4-5 to the mm on the ventrolateral projection. Quadrichotomy and trichotomy are present, as well as intercalations. As also described by Bisat (1924), at 14 mm diameter the ventrolateral projection is slight. The umbilical edge is subacute at this diameter, with vertical umbilical slopes. At 16-18 mm diameter, the costae show similar pattern of branching as before, but the ventrolateral projection is a little more pronounced.

In general, costae are irregularly spaced through ontogeny: at 13-18 mm diameter, they occur c.3-4 per mm, but also 10 per mm on other specimens. They are usually spaced c.5-7 per mm at 7-8 mm diameter, but can also be more closely set in certain specimens (9 per mm at 7-8 mm diameter), in which case they tend to become more widely spaced with ontogeny. The dichotomizing point progressively recedes from the umbilicus through ontogeny, but it rarely exceeds a distance of 1.5 mm from the umbilicus. The specimens from Roadford and from Fisherstreet Bay are mostly ellipsocone in conch shape. Specimens from a loose bullion found at the Phosphate Mine, R. Aille, Doolin, and collected by E.W.J Moore (LZ3034, BGS collection), were measured in order to obtain conch parameters and were seen to conform to the above description.

Remarks: Diagnostic features are already present at 6-7 mm diameter.

Comparisons: As Bisat mentions, it may be possible to mistake *Ht. prereticulatus* for *Ho. smithii* or *Ho. undulatum* (varieties of Bisat's no longer valid *Homoceras diadema*), but the ribs at the serpenticone stage, the lack of umbilical rim and the trichotomy and quadrichotomy of costae are all features that distinguish it. Therefore no confusion should arise provided that a portion of the test starting from the umbilical margin and extending to the venter is available. Amongst Hodson's collection, an isolated adult fragment found in a loose bullion from the Phosphate Mine has spirals on the umbilical margin. The fragment is accompanied by a hand-written note noting this feature, which was

not recorded in any other specimen. However, it is consistent with the close association of the genus *Homoceratoides* with *Reticuloceras*.

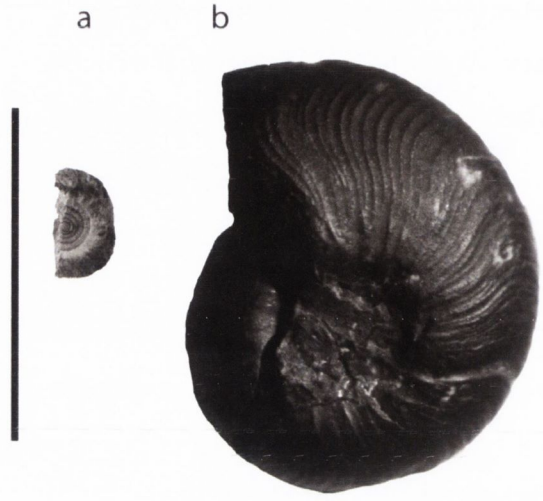

Fig. 3.31. *Homoceratoides prereticulatus* (a) TCD.61028, below Blakes Bridge, Co. Clare; (b) C25749, Lectotype, Holden Beck, Silsden, Yorkshire, UK; Scale is 20 mm.

***Homoceratoides varicatus* Schmidt, 1934; Fig. 3.32; Table 9, Appendix A.**

v*1934 *Homoceratoides varicatum* Schmidt, p. 457, fig. 73,74.

1943 *Homoceratoides varicatum* Schmidt; Bisat & Hudson, p. 409, pl. 25, fig. 1.

1957 *Homoceratoides varicatus* Schmidt; Hodson, p. 12, pl. E, fig. 1,2,3.

1959 *Homoceratoides varicatus* Schmidt; Patteisky, p. 18, pl. 1, fig. 28,27.

1960 *Homoceratoides varicatus* Schmidt; Bouckaert, p. 56, pl. 2, niv. 13, fig. 1,3; pl. 2, niv. 15, fig. 3-5; pl. 3, niv. 796, fig. 1,2,5,6; pl. 3, niv. 3, fig. 2.

1960 *Homoceratoides varicatus* Schmidt; Chalard, pl. F, fig. 2-8.

1961 *Homoceratoides varicatus* Schmidt; Bouckaert, fig. 2.

1984 *Homoceratoides varicatum* Schmidt; Swan, p. 231, pl. 5, fig. 5,8.

Type Locality: Neheim, Germany.

Material: The type series (paratype GZG.INV.48188 and holotype GZG.INV.48187; Fig. 3.32a,d) together with specimens from Hodson's Irish collection (from Kilfenora and the Kilmoon River, Co. Clare), allow a

description of ontogeny to be made. Specimens from Brendan's Well, Co. Clare, Ireland, were also identified as *Ht. varicatus*.

Diagnosis: Homoceratoides with persistent, narrow dichotomy. Long plications accentuated on the umbilical rim and dichotomizing half way up the flank. Ventrolateral projection late and slight.

Description: Ribs first appear on the second whorl. At 6.5 mm diameter, plications spaced 6 per mm branch into radial growth lines spaced c.10 per mm. A constriction is also visible. The same pattern of branching is conserved throughout ontogeny. The smaller paratype (GZG.INV.48188, Fig. 3.32a), with diameter 9.2 mm and whorl width 5.3 mm, is an internal cast with fragments of the external shell. It has four well-marked constrictions and delicate radial growth lines with no ventrolateral projection and little to no ventral sinus. The plications are accentuated near the rim and are seen to dichotomize and degenerate into growth lines about half way up the flank. Dichotomy is narrow. The same pattern of branching is conserved throughout ontogeny. Growth lines are seen to dichotomize about halfway up the flank at c.9 mm diameter, in accordance with the description in Bisat & Hudson (1943) and with the type material. Constrictions are well marked and accentuation of growth lines on the rim is observed. The course of the growth lines is radial, with no ventrolateral projection or ventral sinus. At 10 mm diameter (in TCD. 61007, Fig. 3.32b), the umbilical walls are steeply sloping and growth lines are again spaced 10 to the mm. At 13 mm diameter (TCD.61008, Fig. 3.32c), the growth lines are spaced c.6 per mm and still radial. At 17.5 mm, the constrictions on the internal cast are well marked and the usual narrow dichotomy is still present. There are intercalated growth lines throughout ontogeny. It should be noted that certain adult specimens do have a ventrolateral projection developed, and this is the same width as the ventral sinus. The holotype (GZG.INV.48187, Fig. 3.32d) is an internal cast with no ornament: it has diameter c.28 mm and whorl width 11.9 mm. It shows suture lines, three faint constrictions and steep-sloping umbilical walls. The constrictions are bent into

a slight ventral sinus. The plications become slightly less pronounced in late adolescence and adulthood.

Remarks: This species shares features with *Vallites henkei* and *Homoceras magistrorum*. The main differences are summarized in Table 3.2.

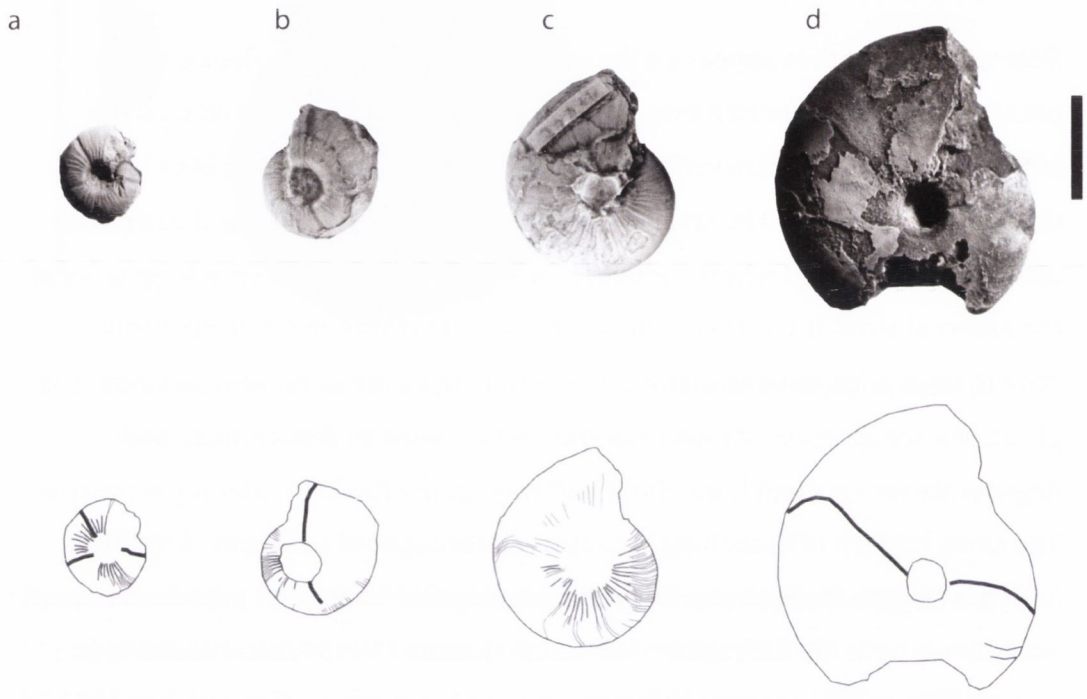

Fig. 3.32. Ontogenetic study of the ornament for *Homoceratoides varicatus* Schmidt, 1934 (a) GZG.INV.48188, paratypoid, Neheim, (b) TCD. 61007, Loose bullion, Kilmoon River, (c) TCD.61008, Loose bullion, Kilmoon River, (d) GZG.INV.48187, holotype, Neheim. Scale is 10 mm.

Character /Species	Dichotomy	Ribs in juveniles	Presence of ventrolateral projection/sinus	Umbilical margin in adolescence	Best diagnosed during:
Homoceratoides varicatus	Present through ontogeny	As in adolescence. Plications dichotomizing. Ribs on inner whorls	Ventrolateral projection late in adulthood and slight, sinus late but more pronounced	Plications, quite long, dichotomizing halfway up the flank	Early adolescence
Vallites henkei	None	Well-marked, radial, not branching; umbilical margin raised	Present and becoming more pronounced through ontogeny	"Beading" (nodes) around the umbilicus	Adolescence
Hodsonites magistrorum	Trichotomy common as well as dichotomy	At 6 mm diameter, the growth lines are widely spaced and there is a steep sloping umbilical wall	Late in adolescence and slight	Short plications bent forward	Adolescence (10-18 mm)

Table. 3.2. Summary of differences in diagnostic characters between *Hod. magistrorum*, *Ht. varicatus* and *V. henkei*.

Genus *Hodsonites* Ramsbottom, 1977

Genotype: Hodsonites magistrorum (Hodson, 1957), p. 21.

***Hodsonites magistrorum* (Hodson, 1957); Fig. 3.33; Table 12, Appendix A.**

v*1943 *Homoceras* sp. nov. *A.* Bisat & Hudson, p. 404.

1954 *Homoceras* sp. nov. *A.* Hodson, p. 265.

v*1957 *Homoceras magistrorum* Hodson, p. 21, pl. C, fig. 1, pl. D, fig. 1-6, textfig. 3a-e.

1959 *Homoceras magistrorum* Hodson; Patteisky, p. 17, pl. 5, fig. 1a,1b.

1960 *Homoceras magistrorum* Hodson; Butcher & Hodson, p. 78, pl. 19, fig. 1.

1960 *Homoceras magistrorum* Hodson; Chalard, pl. D, fig. 1-2.

1961 *Homoceras magistrorum* Hodson; Bouckaert, fig. 1.

.1977 *Hodsonites magistrorum* Hodson; Ramsbottom, p. 288.

1984 *Vallites magistrorum* Hodson; Swan, p. 227, pl. 5, fig. 2-3.

1986 *Homoceras magistrorum* Korejwo, pl. 23, fig. 1-3.

Type Locality: River Aille, Lisdoonvarna, Co. Clare, Ireland.

Material: The type material, which is housed in the British Geological Survey, as well as specimens from the Phosphate Mine, Roadford, and from a bullion loose in the River Aille, have been investigated and were found to conform well to Hodson's (1957) description. Juveniles from St. Brendan's Well, Co. Clare, which are found accompanying *Ht. varicatus*, have inner whorls with no ribs, which implies they do not belong to the genus *Homoceratoides*. They have a raised umbilical margin with widely spaced growth lines (6-7 per mm at 6 mm diameter) and have been identified as *Hod.* cf. *magistrorum*.

Diagnosis: *Hodsonites* with forwardly deflected, short plications at the umbilical edge bifurcating or trifurcating into growth lines; persistent constrictions present on the internal mould and suture with wide ventral lobe and low median saddle (Hodson 1957, p. 21; Ramsbottom 1977, p. 288). Ventrolateral projection late in adolescence and slight.

Description: The smallest of the Roadford specimens with 3.8 mm diameter is openly coiled and has faint transverse growth lines. Two constrictions are present. These are also seen in other 4 mm diameter juveniles from the Phosphate Mine, Co. Clare. At 6 mm diameter, the growth lines are widely spaced (6 per mm). The specimens from the River Aille illustrate very well the distinctive umbilical margin of *Hod. magistrorum.* At 6-7 mm diameter (NMING : F2028; Fig. 3.33a), the fulcate plications are already developed and the growth lines are spaced c.20 per mm. At 6.7 mm diameter, in the Roadford specimens, plications are prorsiradiate and growth lines are strongly marked. The umbilical edge is rounded with steeply sloping walls. In contrast, in the type material growth lines are quite radial, with only a hint of ventrolateral projection and ventral sinus. At 12 mm diameter, the average spacing of the growth lines is 3.5 per mm.

As the ammonoid transitions into adulthood (shell diameter greater than 18 mm), the plications become weaker until the umbilical edge becomes plain and, at the same time, the ventrolateral projection and ventral sinus become more pronounced. At 12 mm diameter the umbilical rim is elevated and quite angular. Typical features, such as the short fulcate umbilical plications, are all present at 10 mm diameter. As is the case for the ornamentation of most ammonoids, the most diagnostic features appear in adolescence, when short, forwardly directed umbilical plications degenerate into growth lines as they are traced along the flank (GSM.86913; Fig. 3.33b-c). Trichotomy is the typical mode of branching.

Overall, dichotomy and trichotomy are both observed but they do not always co-occur: in fact, in one specimen from Roadford with 27 mm diameter dichotomy is the only mode of branching. At 21.3 mm diameter, ventrolateral projection and ventral sinus are present and a little more pronounced than at earlier diameters. In adulthood, the umbilical plications become significantly reduced in strength. As described by Hodson (1957), the shell is relatively involute, with flattish flanks converging to a well-rounded venter. More globose forms have also been found in the Shannon Basin.

Remarks: Ramsbottom (1977) assigned this species to the genus *Hodsonites* based on the presence of bifurcation and intercalation of growth lines. Swan (1984, p. 227) did not consider these important criteria based on his cluster analysis, which emphasized instead the wide spacing of plications at the umbilical edge in young specimens. In this study, they are spaced 3 per mm in specimens at 6-7 mm diameter (NMING : F2028; Fig. 3.33a), but they are spaced 9 per mm in another specimen at 6.6 mm diameter (NMING : F24476/1). This species is best diagnosed during adolescence.

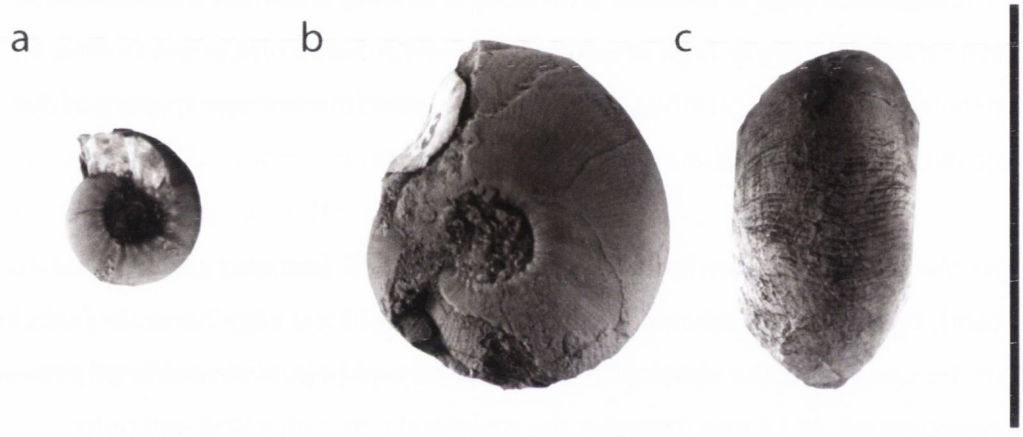

Fig. 3.33. *Hodsonites magistrorum* (a) NMING : F2028, River Aille, Phosphate Mine, Roadford, Co. Clare; (b-c) GSM.86913, River Aille, Phosphate Mine, Roadford, Co. Clare, side and ventral view. Scale is 20 mm.

Family Girtyoceratidae Wedekind, 1918

Subfamily Girtyoceratinae Wedekind, 1918

Genus *Hudsonoceras* Moore, 1946

Genotype: Hudsonoceras proteus (Brown, 1841), p. 217.

***Hudsonoceras proteus* (Brown, 1841); Fig. 3.34; Table 11, Appendix A.**

v*1841 *Goniatites proteus* Brown, p. 217, pl. 7, fig. 27,28.

1849 *Goniatites proteus* Brown, p. 248, pl. 21, fig. 27,28.

1918 *Glyphioceras spirale* Phillips; Hind, p. 443.

v*1924 *Homoceras proteum* Brown; Bisat, p. 110, pl. 4, fig. 7, pl. 10, fig. 4,5.

v1946 *Hudsonoceras proteum* Brown; Moore, p. 434, pl. 27, fig. 5-7, textfig. 31.

1954a *Hudsonoceras proteum* Brown; Hodson, p. 226, fig. 6, p. 275, fig. 7, p. 276, pl. 11, fig. 5.

1957 *Homoceras proteum* Brown; Patteisky, p. 517, fig. 6b.

1957 *Hudsonoceras proteum* Brown; Hodson, p. 8.

1958 *Hudsonoceras proteum* Brown; Hodson & Leckwijck, pl. A, fig. 1, pl. B, fig. 1-3, 5.

1958 *Hudsonoceras proteum* Brown; Chalard, p. 2635.

1958 *Hudsonoceras proteum* Brown; Chalard, pl. 5, figs. 1-3,1a,3a.

1959 *Hudsonoceras proteum* Brown; Patteisky, p. 11, pl. 3, fig. 8-10.

1960 *Hudsonoceras proteum* Brown; Chalard, pl. A, fig. 1-4.

1961 *Hudsonoceras proteum* Brown; Bouckaert, fig. 1.

1968 *Hudsonoceras proteum* Brown; Quinn & Saunders, p. 398, pl. 57, fig. 14,15.

1985 *Hudsonoceras proteus* Brown; House, p. 127, pl. 6.7.30.

1993 *Hudsonoceras proteum* Brown; Saunders & Ramsbottom, p. 996, fig. 1,8.

Also refer to: Ruzhencev & Bogoslovskaya (1978).

Type Locality: Todmorden, UK.

Type Material: The type material is currently housed in the Manchester Museum and consists of six specimens (MANCH L.11797a-f). Diameters start at 5.8 mm and reach 11.6 mm. Thus adult growth stages are lacking. In addition,

the specimens are fragmentary and do not show as much detail of the ornament as the Irish samples from Roadford, Co. Clare, described herein, but they do illustrate the main features of the species. At 5.8 mm diameter, there are three constrictions, spiral and radial growth lines, and the presence of ventrolateral projection at this early stage is also noted. At c.8 mm diameter, an umbilical rim is present and the umbilicus is large and funnel-shaped. At this stage, radial growth lines are more widely spaced (7-8 per mm) than spiral growth lines (more than 10 to the mm on the venter). At c.11 mm diameter, the spiral growth lines appear slightly granulated.

Other Material: 3D specimens from the Phosphate Mine at Roadford, Co. Clare, were extracted from concretions. Their ontogeny conforms very well to that described in Bisat (1924) for UK material (from Rough Lee, Lancashire and Congleton Edge, Cheshire).

Diagnosis: *Hudsonoceras* with granulated appearance due to the strongly marked spirals and transverse growth lines intersecting all over the test. Pronounced ventrolateral projection present from late juvenile growth stages through adulthood; umbilical rim present in later growth stages and number of spirals increasing with age. Shell strikingly oxyconic, generally through ontogeny. In some cases, a very shallow groove appears on the ventral margin.

Description: Brown (1841) describes the species as being discoidal, compressed and lenticular, with deep, funnel-shaped umbilicus. The umbilical margin is described as having an elevated ridge and the sides of the umbilicus to be spirally striated and crossed by numerous, nearly obsolete growth lines. Brown (1841) goes on to note that the suture line has all lobes and sinuses rounded. Young shells are considerably compressed, and the constrictions are distinct, broad and deep; they fill up as the shell advances in growth.

At 2.6 mm diameter, the shell is serpenticone (open-coiled) in shape and the ornament is in the form of faint, transverse growth lines, with no ventrolateral projection. In one specimen from Roadford (NMING : F24477), growth lines are

spaced 15 per mm on the flank and constrictions are already present. At 3.8 mm (NMING : F24477), three well-marked constrictions are clearly visible on the internal cast. At 5.7 mm diameter, the transverse growth lines are slightly crowded together to form faint bundles, but it should be noted that this was observed in only one specimen. The spirals are more pronounced on the ventrolateral projection and ventral sinus than on the rest of the test. At 6.6 mm diameter, the umbilicus is barrel or crater-shaped and the transverse growth lines are c.20 to the mm on the ventrolateral projection. At 7.3 mm diameter, strong spirals have already developed and there is a pronounced ventrolateral projection. As described in Korn (1997, p. 43), the number of delicate granulated spirals increases with age. At 14.7 mm diameter (NMING : F24478), the spirals are strong on the ventral area and around the umbilicus, and the ventrolateral projection is pronounced. A specimen (TCD.61050; Fig. 3.34a-b) at 18.5 mm diameter from the Coolagh River, Co. Clare, collected by Hodson, shows a pronounced ventrolateral projection and an umbilical rim. Spirals are more widely spaced closer to the umbilicus (12 per mm) than on the ventrolateral projection (about 24 per mm). Another specimen from the same locality (TCD.61051; Fig. 3.34c-d), at 26 mm diameter, has very strongly granulated ornament. In addition, the radial component of the ornament is well marked and the umbilical rim is present.

Remarks: This species is sometimes assigned to the genus *Baschkirites* (Librovitch, 1957). Korn (1997, p. 43) describes the main features of this genus, which conform with the description of *Hudsonoceras proteus*. This was not deemed reason enough to abandon the genus *Hudsonoceras* in favour of *Baschkirites*, so both are considered valid for the purposes of this study.

Fig. 3.34. *Hudsonoceras proteus* (a-b) TCD.61050, Coolagh River, Co. Clare, side and ventral; (c-d) TCD.61051, Coolagh River, Co. Clare, side and ventral; Scale is 20 mm.

***Hudsonoceras (Baschkirites) ornatus* (Foord & Crick, 1897); Fig. 3.35.**

1897 *Nomismoceras ornatum* Foord & Crick, p. 218, fig. 104.

1905 *Glyphioceras (Beyrichoceras) spirale* Phillips; Hind, p. 114, pl. 6, fig. 8.

?1918 *Nomismoceras ornatum* Hind, p. 444.

1924 *Eumorphoceras ornatum* Foord & Crick; Bisat, p. 98.

1925 *Eumorphoceras ornatum* Foord & Crick; Schmidt, p. 585, pl. 22, fig. 6, pl. 25, fig. 11-13.

1946 *Nomisnoceras ornatum* Foord & Crick; Moore, p. 438.

1958 *Hudsonoceras ornatum* Foord & Crick; Hodson & Leckwijck, pl. B, fig. 4.

1959 *Hudsonoceras ornatum* Foord & Crick; Patteisky, p. 11, pl. 1, fig. 34,35, pl. 6, fig.23.

1960 *Hudsonoceras ornatum* Foord & Crick; Bouckaert, p. 68, pl. 2, niv. 1, fig. 1; pl. 3, gis. 809, fig. 2.

1961 *Hudsonoceras ornatum* Foord & Crick; Bouckaert, fig. 2-3.

1978 *Baschkirites ornatus* Ruzhencev & Bogoslovskaia, p. 136.

1993 *Hudsonoceras ornatum* Foord & Crick; Saunders & Ramsbottom, p. 996, fig. 1,9; 1,10; 3,1.

1997 *Baschkirites ornatus* Foord & Crick; Korn, p. 43, pl. 2, fig. 12.

Type Locality: Halifax, Yorkshire, UK.

Type Specimen: C5279, Natural History Museum, London (Fig. 3.35a).

Material: No solid specimens could be found either in the field area of the Shannon Basin and from museum collections in order to study the ontogeny of this species. Only crushed specimens have been recovered from ammonoid bands in the Shannon Basin.

Description: The involute nature of the species was noted by Bouckaert (1960). Delicate spiral lines are present: they intersect even more delicate radial growth lines to give a granulated texture. The pronounced ventrolateral spiral groove is a useful diagnostic feature.

Comparisons: In contrast to the closely related *Hud. proteus*, the spirals are irregularly spaced and the shell is more involute (Bouckaert 1960).

Remarks: This species is sometimes assigned to the genus *Baschkirites* (e.g. Korn 1997).

Fig 3.35. *Hudsonoceras ornatus/Baschkirites ornatus* type material. British Museum of Natural History, London. (a) c5279, syntype, Halifax, Yorkshire, side, ventral and dorsal views; (b) c70994, syntype, Halifax, Yorkshire, side, ventral and dorsal views; (c) c70995, syntype, Halifax, Yorkshire, side, ventral and dorsal views. Photographs were taken by Svetlana V. Nikolaeva.

3.3.2 Discussion

For most of the taxa above (namely *V. henkei, Ph. circumplicatile* and *R. subreticulatum, Ph. paucicrenulatum, Ht. varicatus, Ho. beyrichianum, Iso. subglobosum* and *Ho. smithii*) changes in ornament are described systematically here for the first time.

This kind of detailed description leads to more confident identifications and acts as an aid to taxonomists working on crushed material, who can refer to the ornament description for a given growth stage. For instance, *V. henkei* is usually diagnosed by features at or close to the umbilical edge (such as presence of "beading" and an umbilical ridge). However, when these features are absent due to incomplete preservation, information such as the spacing (5 per mm in Fig. 3.36b) and strength of the growth lines can be used to make a determination (Fig. 3.36b). Similarly, *Ph. circumplicatile* shares many features of the ornament with *Ph. paucicrenulatum*, which leads to uncertainty in identifications. However, even incomplete 2D specimens can be identified where diagnostic features of the ornament are combined: for example, a crushed specimen from Co. Clare (TCD.60606, Fig. 3.36a) was identified as *Ph. circumplicatile* because of the presence of trichotomy and quadrichotomy as primary mode of branching, spirals along the flank and spacing of the growth lines (5 per mm).

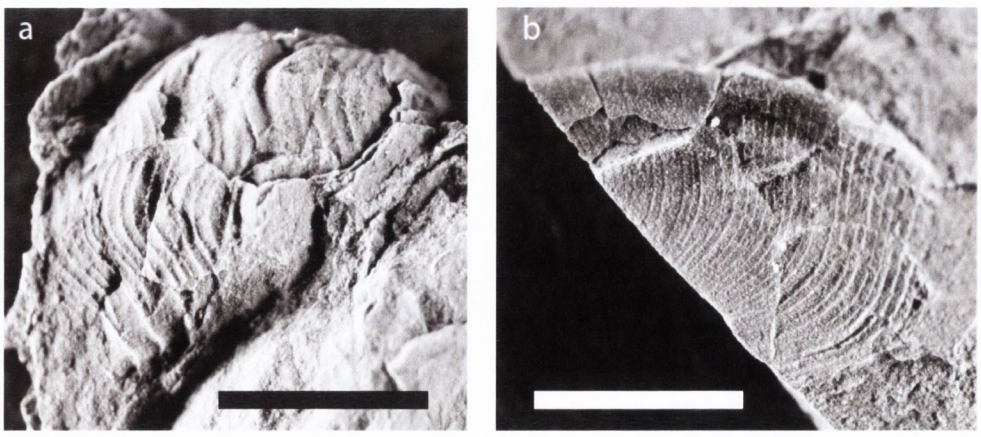

Fig. 3.36. Irish ammonoids preserved in 2D. (a) *Ph. circumplicatile* (TCD.60606) (b) *V. henkei* (TCD.60607). Specimens are from Loop Head, Co. Clare, Ireland. Scale bars are 5 mm long.

Changes in ornament with ontogeny can be examined by plotting changes in the number of growth lines with increasing diameter of a given species using several specimens at different stages of ontogeny (Figs. 3.37-3.39). As ammonoids grew, the number of growth lines on the flank of the organism (taken here to broadly be placed between the umbilicus and the venter) varied. These changes are plotted below.

When number of growth lines is plotted against diameter, the species *R. subreticulatum*, *Ph. circumplicatile* and *Ph. paucicrenulatum* (Fig. 3. 37) follow distinct trends. The same is true for *Ho. beyrichianum*, *Iso. subglobosum*, *Ho. smithii*, *V. henkei*, *Ho. undulatum* and *Hod. magistrorum* (Fig. 3.38), and for *Ht. prereticulatus* and *Ht. varicatus* (Fig. 3.39). These plots show that the number of growth lines does not simply increase with age of the ammonoid, but follows a more complex pattern. In general, it is possible to infer that, in most species, the number of growth lines tends to increase and then decrease as adulthood is reached. However, in some cases such as with *Ho. smithii* (for which only two data points are available), too few measurements were made to be able to draw valid conclusions about ontogeny. In the case of *R. pulchellum*, *Hud. proteus* and *Hud. ornatus* no data was available. In species where plications branch into growth lines, the number of growth lines was counted rather than number of plications.

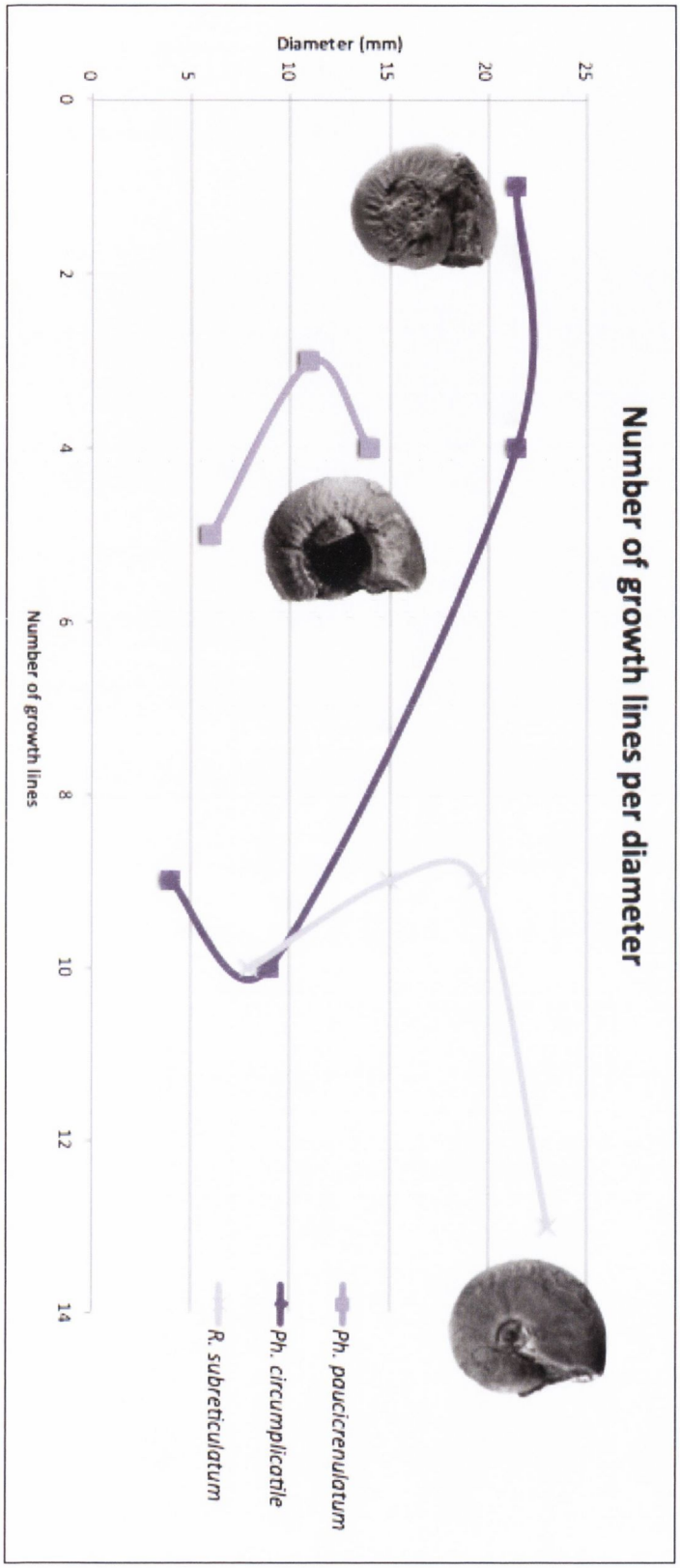

Fig. 3.37. Number of growth lines per diameter (mm) in the species *R. subreticulatum, Ph. circumplicatile* and *Ph. paucicrenulatum.* A representative solid specimen is shown next to each trend line.

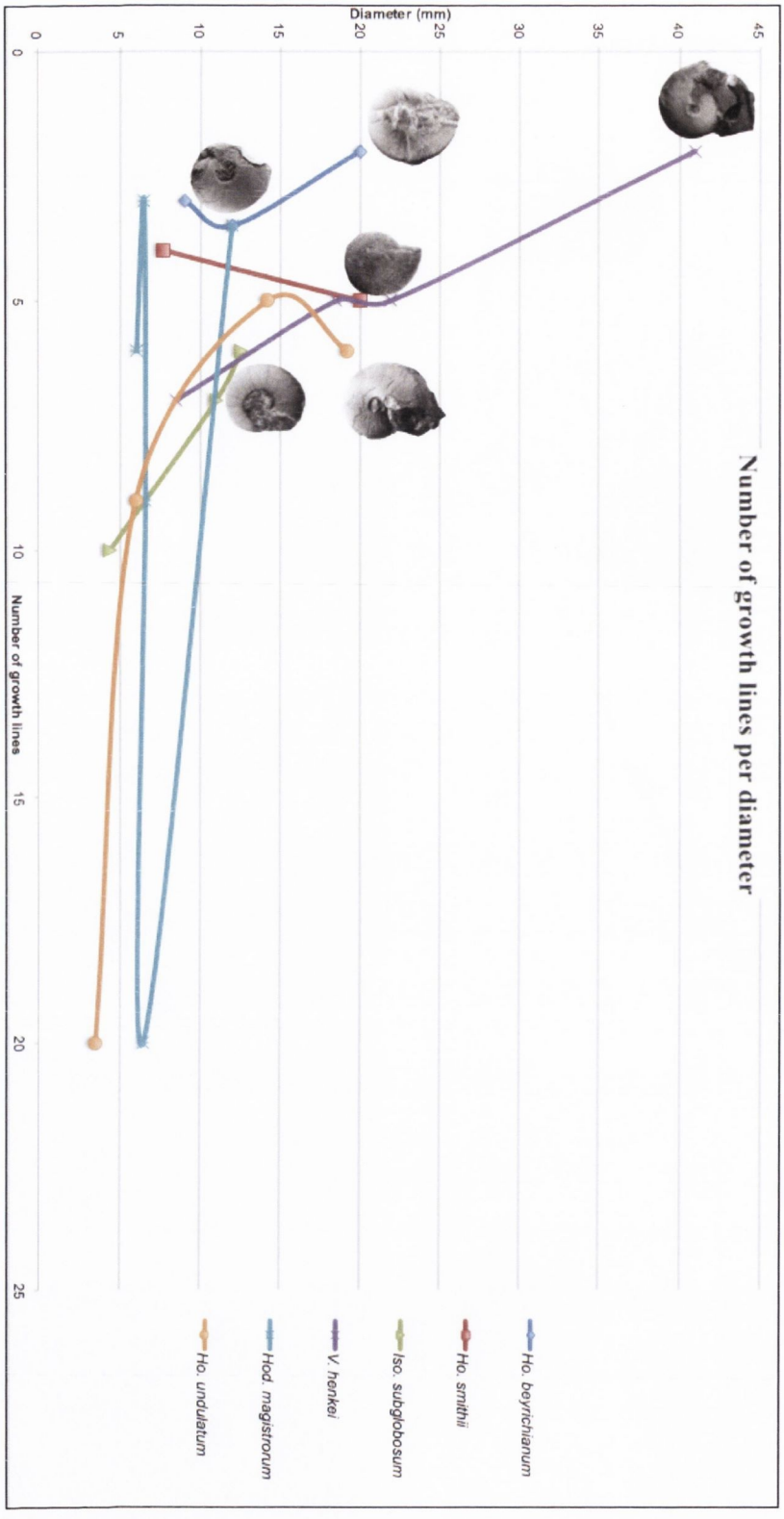

Fig. 3.38. Number of growth lines per diameter in *Ho. beyrichianum*, *Iso. subglobosum*, *Ho. smithii*, *V. henkei*, *Ho. undulatum* and *Hod. magistrorum*. A representative solid specimen is shown next to each trend line.

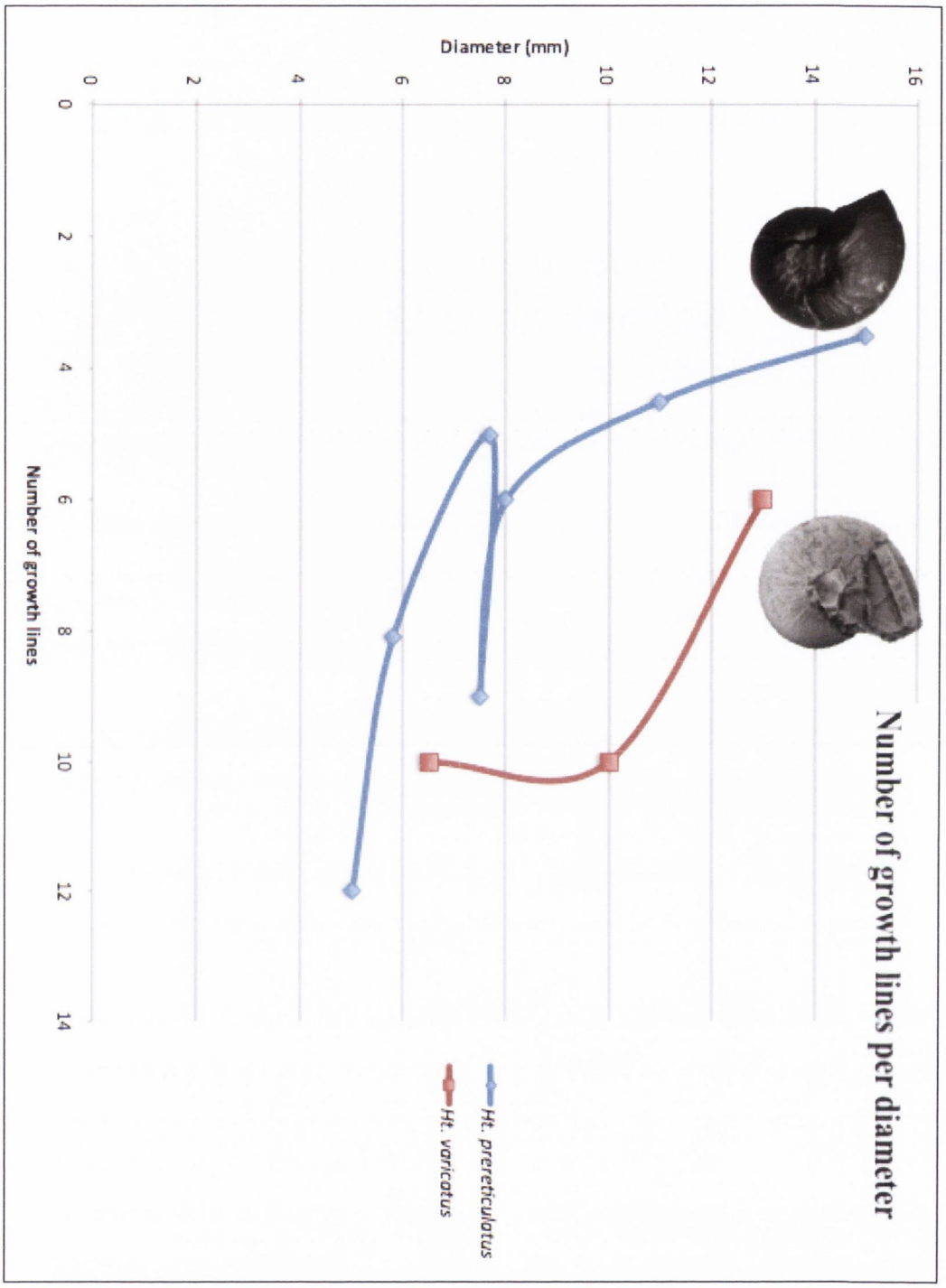

Fig 3.39. Number of growth lines per diameter plotted for *Ht. prereticulatus* and *Ht. varicatus.* A representative solid specimen is shown next to each trend line.

3.3.3 Thin-shelled ammonoids

3.3.3.1 Notes on systematics

Thin-shelled ammonoids in the Shannon Basin are represented by the two genera *Anthracoceras* and *Dimorphoceras* (see Table 3.3).

Suborder Goniatitina Hyatt, 1884	Suborder Goniatitina Hyatt, 1884
Superfamily Dimorphoceratacae Hyatt, 1884	Superfamily Dimorphoceratacae Hyatt, 1884
Family Dimorphoceratidae Hyatt, 1884	Family Anthracoceratidae Plummer
Subfamily Dimorphoceratinae Hyatt, 1884	& Scott, 1937
Genus *Dimorphoceras* Hyatt, 1884	**Genus *Anthracoceras* Frech, 1899**
Type species: *Goniatites gilbertsoni* Phillips,	Type species: *Nomismoceras*
1836, pl.20.	*(Anthracoceras) discus* Frech, 1899, p. 337.

Table 3.3. Systematics of thin-shelled ammonoid genera *Anthracoceras* and *Dimorphoceras*.

Bisat (1933) describes *Dimorphoceras* as *"a genus of highly compressed species, with small subsidiary saddles in the suture lines, and with a markedly sinuous feeble transverse test ornament."* The very similar genus *Anthracoceras* is often indistinguishable from *Dimorphoceras*, due to similar shell shape and ornament (Moore 1939; Ramsbottom 1962). Indeed they are both small, compressed forms with a small or closed umbilicus and weak ornamentation. The principal difference between these two genera lies in the suture line: *Anthracoceras* lacks the subsidiary saddles present in *Dimorphoceras* (Bisat 1924, Bisat 1933, Moore 1939). However, as has been pointed out by some authors (Moore 1936), subtle differences in ornament can also sometimes be used to distinguish these two genera: Moore (1939) describes the ornament of *Dimorphoceras* as consisting of *"delicate, transverse growth lines, which generally bow forward markedly on leaving the umbilicus, and then backwards on the lateral area, go forward again at the latero-venter, and bend backwards again somewhat sharply to form a deep ventral sinus. Faint spirals may appear at the latero-venter, but spiral ornament is never pronounced."* As noted by Bisat (1924), the development of subsidiary waves on the lateral area near the umbilicus in *Dimorphoceras*, *"takes place in the same genus as that characterized by the development of small subsidiary saddles in the sutures."* In contrast to this, *Anthracoceras* lacks the

prominent bowing of the growth lines on the flank (i.e. has a moderate ventral sinus), even though the ventrolateral projection is pronounced (Moore 1936). These two genera are linked by certain species such as those described by Moore from the Bowland Shales (1936).

Material: Two solid specimens (NMING : F24477/1,2) from the Roadford Phosphate Mine, Co. Clare, are small, compressed with a very small umbilicus (5.9 and 4.7 mm in diameter). One of these (NMING : F24477/2) has visible suture line with considerable complexity, including subsidiary saddles. Therefore the specimen can be placed with confidence within the genus *Dimorphoceras*, and is diagnosed as *D.* cf. *moorei* based on Hodson's (1954c) description of the suture line. The ornament is extremely subdued in both specimens. The other specimen (NMING : F24477/1) can be identified to the genus level as *Anthracoceras/Dimorphoceras* sp..

Remarks: Juvenile specimens from the "*Ph. paucicrenulatum* band" at Bridges of Ross (see Ch. 2, section 2.2.2.26) have a ventral sulcus.

3.3.3.2 Occurrence

Thin-shelled ammonoids are usually found as a minor component of faunas in condensed horizons in the Shannon Basin, where they accompany the more abundant thick-shelled ammonoids (see section 3.1).
They were found in all highly condensed sections in the Ross Sandstone Formation. In general, they are a minor component of the faunas and are not useful in correlation.

3.4 Bivalves

3.4.1 Notes on systematics

The following bivalve genera are the main ones recorded in this study and in previous studies (Lewarne 1959) from the Shannon Basin:

- *Caneyella* Girty, 1909
- *Dunbarella* Newell, 1938
- *Posidonia* Bronn, 1828
- *Posidoniella* de Koninck, 1885

In 1999, Amler reviewed the Carboniferous bivalve groups of the Central European Culm facies, and in doing so reviewed all of the genera listed above, revising their taxonomy, where necessary.

These bivalves are also often informally referred to as "*paper pectens*" (Wignall 1994, p. 34), a term which encompasses thin-shelled, flat-valved bivalve morphologies. Three broad morphologies can be recognized: mytiliform, dunbarelliform and posidoniform bivalves (Fig. 3.40). Even though groupings such as paper pectens are informal rather than a strict taxonomic grouping, they are useful locally, for instance in the Shannon Basin. Therefore these terms are maintained for the purposes of this study.

	Description	Examples
Dunbarelliform	Hinge line around maximum width with centrally placed umbone. Fine radial ribs are the dominant ornament. Circular outline. Some varieties, such as *Dunbarella*, are inequivalved	*Dunbarella, Pterinopectedn, Claraia, Daonella, Halobia, Aulacomyella*
Posidoniform	Hinge line shorter than maximum width, umbone centrally placed. Concentric ornament. Circular to elongate outline. Equivalved.	*Posidonia, Bositra, Steinmannia, Inoceramya*
Mytiliform	Medium length hinge with umbone at anterior end. Weak ornament. Trigonal to quadrate outline.	*Posidoniella, Selenimyalina, Caneyella, Plaglostoma, Parainoceramus, Pterochaenia, Pseudomytiloides, Annigella, Semuridia*

Fig. 3.40. Paper pecten morphotypes (after Wignall 1994, p. 35).

3.4.2 Occurrence

The presence of two main bivalve groups, *Dunbarella* and *Caneyella*, in the Shannon Basin was already recognized by Lewarne (1959), who describes *"an early Caneyella population associated with Phillipsoceras (Reticuloceras) circumplicatile and a later Dunbarella fauna associated with Ph. (Reticuloceras) paucicrenulatum"* (Lewarne unpublished notes).

While the present study confirmed this as a broad trend, there are also many localities where *Caneyella* sp. and *Dunbarella* sp. co-occur (Fig. 3.41). Their first occurrences and ranges through the Ross Sandstone Formation are shown in Fig. 3.41, as well as the numbers of taxa in each locality. While *Caneyella* first appears in the lowermost condensed section in the Ross Sandstone Formation (the "*Hud. proteus- Ho. smithii* band"), *Dunbarella* first appears in the mid-upper Ross Sandstone Formation. *Dunbarella* sp. becomes more abundant towards the top of the Ross Sandstone Formation. Occurrence of thin-shelled ammonoids is also shown in Fig, 3.41: there are no distinctive trends when one examines the numbers of thin-shelled ammonoids at each locality through the Ross Sandstone Formation.

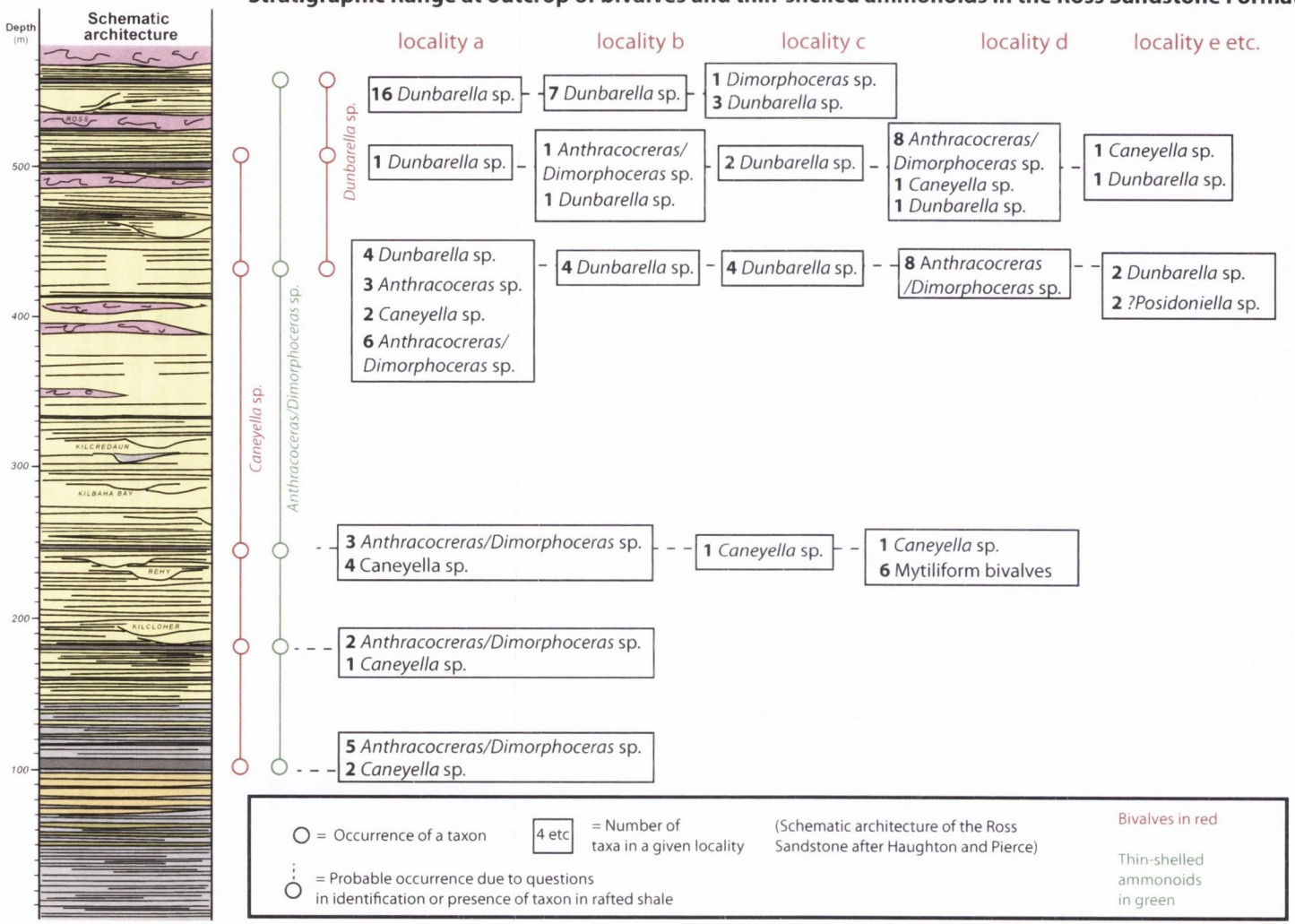

Fig 3.41. First occurrences of taxa and stratigraphic ranges through the Ross Sandstone Formation. Number of specimens in each locality is shown. Ranges of bivalves are highlighted in red. Ranges of thin-shelled ammonoids are highlighted in green.

In a few isolated localities in the Shannon Basin, bivalves are the dominant element of the fauna in a given horizon or section: this is the case in the upper 2 m of the Fisherstreet Bay section, Doolin, north Clare, where *Dunbarella* sp. is very abundant, whilst ammonoids are rare (see Ch. 2, Fig. 2.4). Similarly, a less than 30 cm-thick bed at Foynes Island is dominated exclusively by posidoniform bivalves (see Ch. 2, Table 2.3).

3.5 Palaeoecology

3.5.1 Ammonoid basinal communities

The basinal community of the British Serpukhovian and Bashkirian has been portrayed by Ramsbottom (1978) as relatively deep water, dominated by free-swimming forms including ammonoids and pterioid bivalves (Fig. 3.42). This model is consistent with faunal assemblages presented here and is therefore taken to be valid for the Shannon Basin. Thick-shelled ammonoids are thought to have had a nekto-benthic lifestyle (Westermann 1996). Benthic communities are commonly reported as absent or limited to a few brachiopods, crinoids, and trilobites (Saunders & Swan 1984; Ramsbottom 1978).

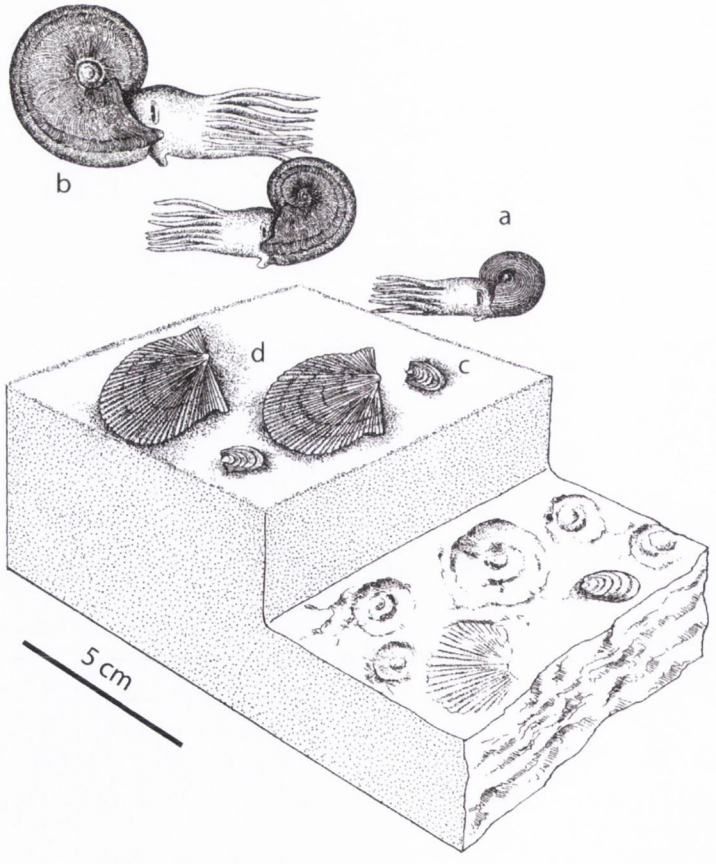

Fig. 3.42. Serpukhovian-Bashkirian ammonoid community (after Ramsbottom 1978). (a) *Hudsonoceras* (ammonoid), (b) *Reticuloceras* (ammonoid), (c) *Posidonia* (bivalve), (d) *Dunbarella* (bivalve).

Fig. 3.43. Trilobite pygidium from "Dunmore Head west band" sample (Chapter 2, section 2.2.2.8). Pencil for scale.

3.5.2 Thin-shelled ammonoids

The two genera *Anthracoceras* and *Dimorphoceras* are sometimes thought to occur together in conditions that are not favourable to other groups of ammonoids (Bisat 1933). Indeed, thin-shelled goniatites are generally thought to be able tolerate lower salinities compared to thick shelled goniatites, which are thought to have lived in environments with normal salinity (Sevastopulo 2009). However, in the Shannon Basin they are a minor component of the faunas in all highly condensed sections, which are dominated by thick-shelled ammonoids (Fig. 3.41 shows the stratigraphic ranges of *Anthracoceras* and *Dimorphoceras* through the Ross Sandstone Formation). For further discussion on palaeosalinities in the Shannon Basin, see Chapter 4.

3.5.3 Bivalves

The palaeoecology of Palaeozoic bivalves is still largely unknown: proposed modes of life range from pseuplankton, to planktonic larvae, to epibyssate

(Wignall 1994). It has been suggested that they were either free swimming or attached to plants (Ramsbottom 1978).

The presence of a byssal notch would represent strong evidence for the bivalves to have been epybissate in life (through pseudoplanktonic attachment), perhaps attaching to plant debris or other substrate, but no such notch has been seen on any bivalve specimen from the Shannon Basin. The asymmetry of the hinge line (with respect to the umbone) that typifies most *Dunbarella* specimens examined suggests that, if these organisms were free-swimming, they most likely would not have swum in a straight line. One could therefore speculate that perhaps they were pseudo-nektonic animals, swimming only occasionally and for brief intervals. They may have been suspension feeders. In addition, *Dunbarella* specimens are often associated with disoxyc conditions (Wignall 1994).

Recently, the Latest Visean bivalve *Ptychopteria (Actinopteria) lepida* has been interpreted as pseudoplanktonic in lifestyle based on palaeobiological constraints at the sea floor (Nyhuis *et al.* 2015).

3.5.4 Benthic fauna (crinoids, corals and trilobites)

Occurrence

A zaphrentid-type solitary coral specimen (3D external mould with details of the ornament) was found in Foynes Island, in the uppermost part of the section, at the type locality for *R. subreticulatum* (FOY14: Chapter 2, Table 2.3). The same horizon contains abundant crinoid ossicle- and stem moulds, as well as ammonoids, plant and bivalve material.
Two additional coral specimens, with accompanying crinoid and ammonoid material, were found in a loose block at Fisherstreet Bay, Doolin (see Chapter 2, section 2.2.1.4, for a discussion on the correlation of this block).

Discussion

The presence of crinoids, corals and trilobites in the Shannon Basin is surprising given that Serpukhovian-Bashkirian basinal areas are believed to represent a nektic or planktonic palaeocommunity, with no benthic forms due to anoxic sea floor conditions (Ramsbottom 1978). The fragmented and disarticulated nature of the crinoids suggests they were subjected to post-mortem transport. Similarly, the corals may have been transported, since there is no evidence to suggest they are *in situ*. However, the lack of any coarser debris and other detritus, and the lack of indication of significant currents argue against the idea of transportation from shallower water. If indeed allochthonous, they must have been living elsewhere in the basinal area, indicating at the very least that oxic/dysoxic bottom conditions prevailed at least in some parts of the basin.

Furthermore, the presence of "deep water" crinoids at Fisherstreet Bay (see Chapter 2, section 2.2.1.1) indicates disarticulation could have occurred *in situ*, without need for transport. Consistently with this, evidence for bioturbation in the Clare Shale succession in the shape of pyrite burrows both at Foynes and Inishcorker, suggests that the Clare Shale Formation was not deposited under anoxic conditions and adds support to the theory of an oxic/dysoxic ocean floor (see Braithwaite 1993 for discussion). It is also possible that temporary oxygen-rich bottom currents allowed periodical colonization of the sea floor in Serpukhovian-Bashkirian times (Ramsbottom 1978).

The finding of a single trilobite pygidium (Fig. 3.43) at Dunmore Head west (Chapter 2, section 2.2.2.8) is consistent with this, even though it was probably transported from elsewhere in the basin and may be the result of moulting. A trilobite specimen was also recovered from the Clare Shale Formation in Ballybunnion (Fallon pers. comm. 2015).

Chapter 4 Ammonoid Distribution and Salinity Implications

4.1 Introduction

Thick- and thin-shelled ammonoids and thin-shelled bivalves have long been known from widespread, black, carbonaceous shale units known as "marine bands" (Bisat & Hudson 1943; Ramsbottom 1979) in Late Mississippian to Pennsylvanian basins of northwest Europe. Indeed, the assemblages of thick-shelled ammonoids are used extensively in biostratigraphic zonation for rocks of this age (Bisat 1924; Riley *et al.* 1995). Ammonoids, on the basis of comparisons with living *Nautilus*, are generally thought to have lived in environments of normal marine salinity (Ramsbottom 1969). Suggestions that some may have been able to live in hypohaline and hyperhaline waters have also been put forward (Westermann 1996). However, while this may be the case for thin-shelled ammonoids such as *Anthracoceras* and *Dimorphoceras* (Hudson & Cotton 1943, p. 151), it has not been suggested for thick-shelled ammonoids. Therefore the latter serve as useful palaeoenvironmental indicators that can help settle debates on salinity. This is investigated here. The salinity of these late Mississippian-Pennsylvanian basins have been the subject of much debate with lower salinity values suggested for parts of the succession (Holdsorth & Collinson 1988; Pyles 2009). Higgs (2009) presented an extreme view that the succession in County Clare was deposited in a freshwater lake with brief marine incursions. Here the presence of several new ammonoid-bearing horizons in the siliciclastic fill of the Shannon Basin, western Ireland, is recorded and the evidence for salinity throughout deposition is discussed.

4.2 Highstand-lowstand model

Within the Ross Sandstone Formation of the Shannon Basin, ammonoids are concentrated in laterally extensive black shale intervals, which are interpreted as condensed sections produced during intervals of sediment starvation. These have commonly been referred to as "marine bands" (e.g. Hudson & Cotton 1943; Hampson *et al.* 1997), implying that the intervening strata may not have been fully marine.

It has been argued that ammonoids are restricted to the condensed sections and the bounding strata were barren (e.g. Bisat & Hudson 1943; Ramsbottom 1969, 1977; Collinson 1988). The idea that, during the Serpukhovian and Bashkirian, sediments show cyclical patterns (Collinson 1988) was already well known when Holdsworth & Collinson (1988) established the concept of faunal and salinity cycles in the Serpukhovian and Bashkirian of Britain, building upon work by Ramsbottom (1962) on four boreholes in the Ashover area of Derbyshire. Each cycle was interpreted as recording changing salinity, from an intra-basinal peak at the lowest level to lower salinity in the upper part (Fig. 4.1). This model, which can be referred to as the "highstand-lowstand" model, envisages highstands of sea level affecting small, intracratonic basins, otherwise cut off from the open ocean (Fig. 4.2). This series of basins in northwestern Europe are thought to have developed as a result of crustal extension in the latest Devonian and Mississippian time (Leeder 1976; Leeder & McMahon 1988). The presence of eustatic sea level fluctuations related to the Gondwanan ice sheet is now well established (Davies 2008; Holdsworth & Collinson 1988; Maynard & Leeder 1992; Waters & Condon 2012). Flooding of these basins linked to high-frequency, eustatic changes in sea level (Davies *et al.* 1999) controlled by fluctuations in ice-sheet extent in Gondwana is thought to have resulted in normal marine fauna populating the basin waters (Fig. 4.2a) and salinity reaching typical marine values (Ramsbottom 1977; Maynard & Leeder 1992). Conversely, at lowstands of sea level, when basin connections to the open ocean were more restricted, it has been proposed that salinity was reduced due to substantial influx of fresh

water from large adjacent river systems (Fig. 4.2b). Moreover, successive salinity peaks were suggested to be associated with distinctive ammonoid assemblages (Ramsbottom 1969). However, the mechanisms behind this are not clear and more recent work suggests that the pattern is not as simple as originally envisaged. Thus the question is whether the basins were so isolated from the oceans that it was possible to develop hyposaline conditions thoughout individual basins.

This model was subsequently discussed in several studies such as that by Martinsen *et al.* (1995), where the relationship of ammonoid-bearing bands to sea level was examined, and that by Waters *et al.* (2008) who discussed the fluvio-deltaic succession in the Pennsylvanian of the Central Pennine Basin (UK) and related two ($R_{2c}1$ and $R_{2c}2$ sub-biozones) ammonoid bands to fourth-order marine highstands.

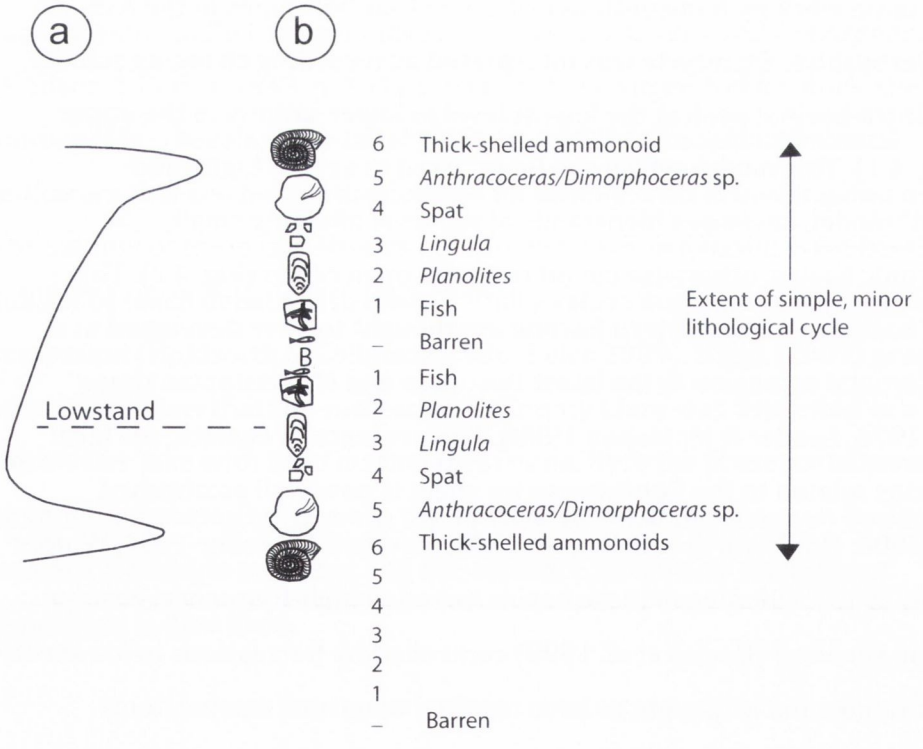

Fig. 4.1. Ideal faunal and salinity cycles in the Serpukhovian and Bashkirian of Britain, after Ramsbottom (1962), Holdsworth & Collinson (1988) and Martinsen *et al.* (1995). (a) Eustatic sea level curve varying from highstand to lowstand and its probable relation to the faunal changes through the cycle in (b).

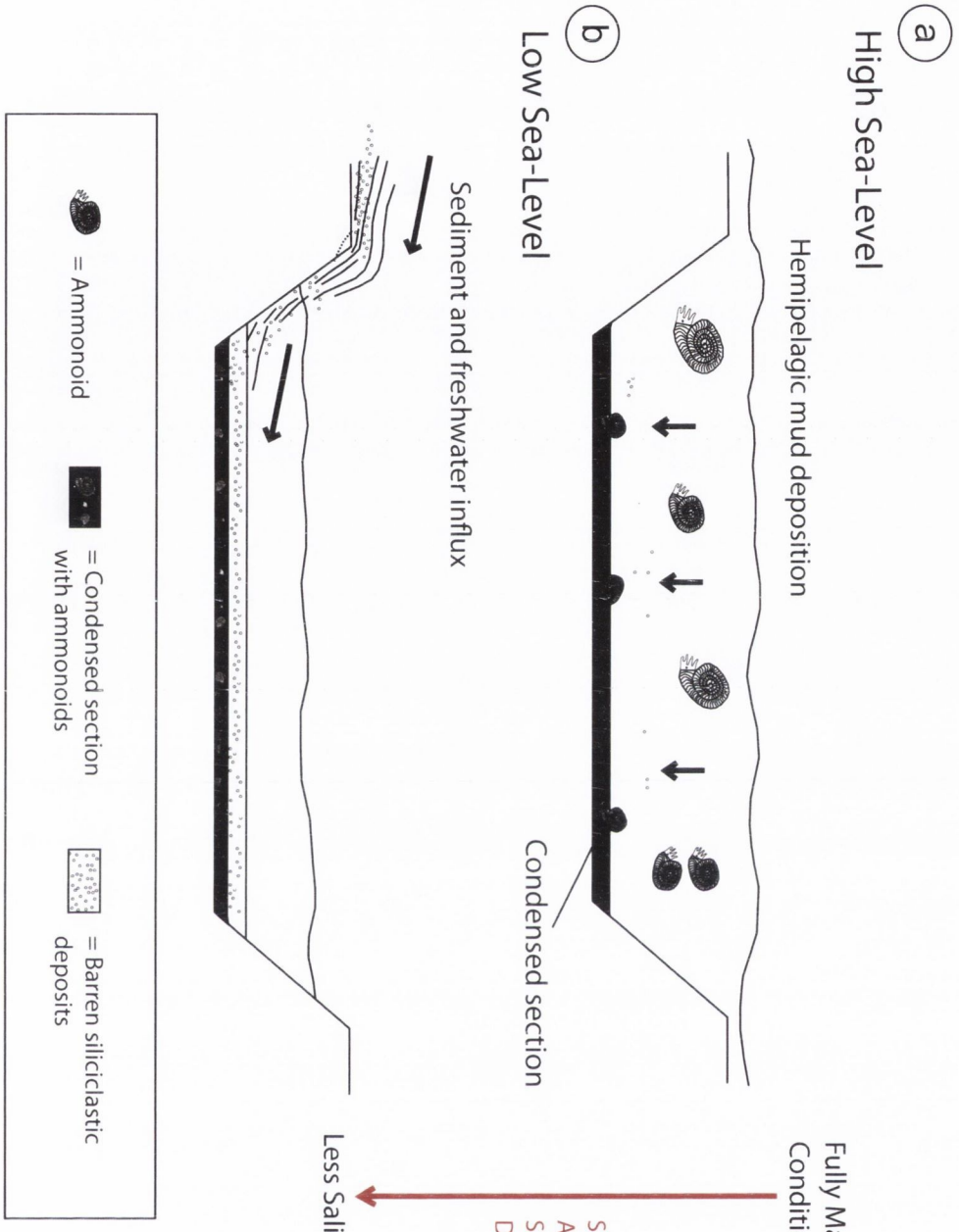

Fig. 4.2. Schematic representation of the "highstand-lowstand" model for sedimentation in Late Mississippian and Pennsylvanian basins in north-west Europe (based on Holdsworth & Collinson 1988). (a) At times of sea level highstand fully marine conditions are established (b) At times of lower sea level, basins become restricted and there is fresh water influx, resulting in salinity decrease.

4.3 Ammonoid distribution in the Shannon Basin

The cyclothemic deposits (the Central Clare Group; R_{1b}-R_{2c}; Fig. 1.8), each contain a unit of ammonoid-bearing black shale interpreted as a maximum flooding surface with normal marine salinity, overlain by complexes of deltaic siltstones and sandstones barren of ammonoids and interpreted as having been for the most part hyposaline. Ammonoids have not been found in the slumped slope deposits of the Gull Island Formation (Fig. 1.8). The underlying Ross Sandstone Formation (H_{2a}-R_{1a}) and Clare Shale Formations (P_2 -H_{2a}) are, however, the focus of this chapter.

New evidence from the Ross Sandstone Formation (Figs. 4.3-4.6) shows that waters were not devoid of normal marine fauna during times of higher sedimentation rates in between the condensed sections.

Ammonoids in the Ross Sandstone Formation are concentrated in the highly-condensed sections, but have also now been recovered in smaller numbers in shale horizons within low-density turbidite sequences, in silt-rich mudstones, and as casts of the shells at the base of turbidite sandstones. Locality details are presented in Fig. 1.8 and in Chapter 2. Details of the different lithological settings in which the ammonoids have been found in the Ross Sandstone Formation (see Fig. 4.3) are shown in Figs. 4.3-4.6.

Highly-condensed sections

Five principal highly-condensed sections (see Ch. 5) have been identified within the Ross Sandstone Formation, and several others have been examined from the Clare Shale Formation during the course of this study (Fisherstreet Bay, Foynes Island and Inishcorker localities in Chapter 2) in order to gather evidence representative of the entire basin fill. Pulham *et al.* (2014) interpreted the condensed sections as corresponding to highstands coincident with interglacials and the intervening strata as corresponding to glacial episodes in Gondwana.

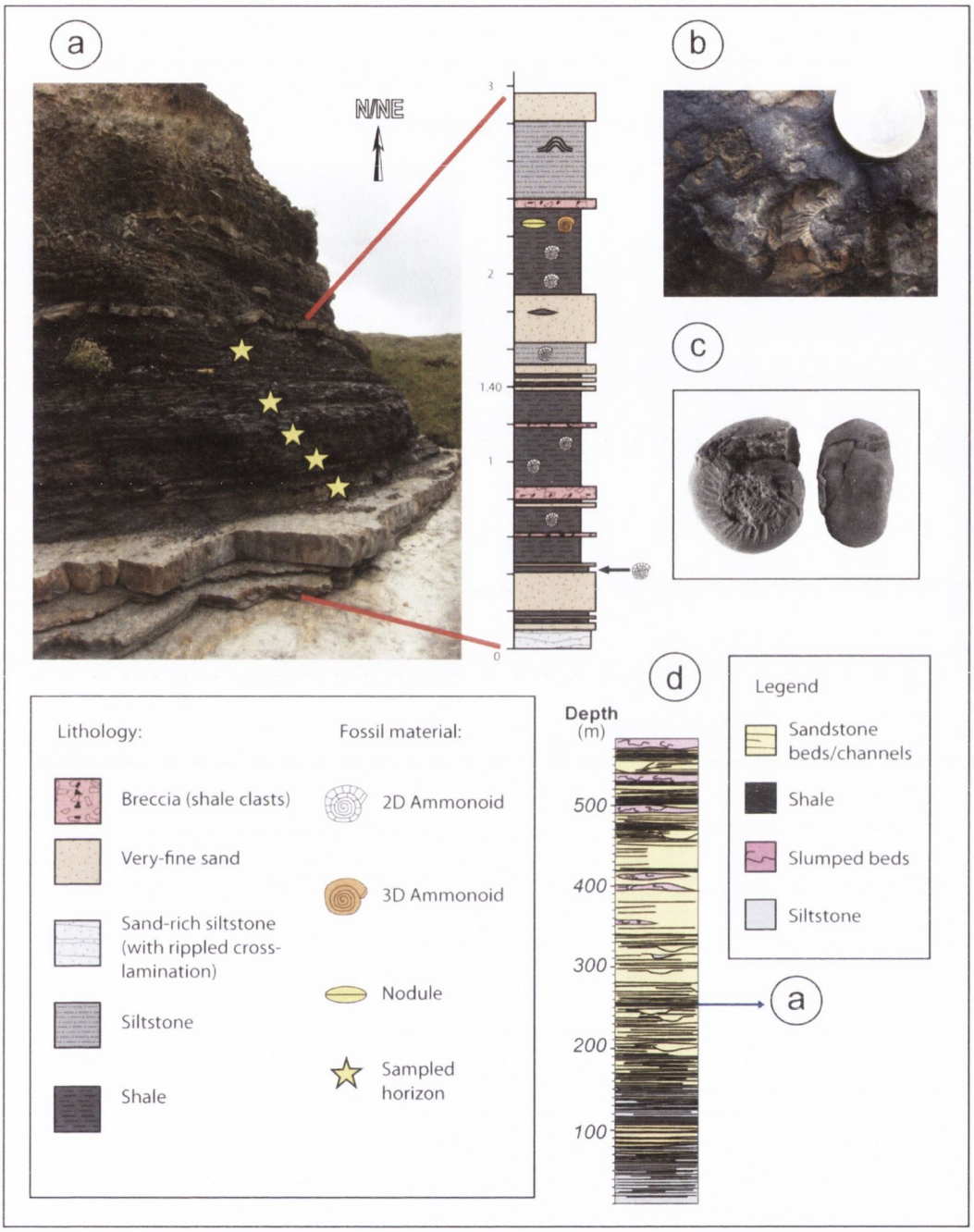

Fig. 4.3. (a) Field photo and sedimentary log through a highly-condensed section in the Shannon Basin, located west of Dunmore Head, Loop Head, Ireland, Irish Grid coordinates [70494/46845], showing both (b) mouldic (2D) preservation and (c) solid (3D) preservation of ammonoids. (d) Summary stratigraphic log of the Ross Sandstone Formation, showing the stratigraphic position of the consensed section shown in (a).

Shale horizons within low-density turbidite sequences

Ammonoids have also been recovered from thin (c.2-3 mm thick) hemipelagic shale veneers within low-density turbidite sequences in the Ross Sandstone Formation, both from outcrop and behind-outcrop core material. In this lithological setting, ammonoids have been found preserved as flattened moulds of the external shell (2D preservation) and they have been recorded at four outcrop localities and at least 94 intervals within the borehole material.

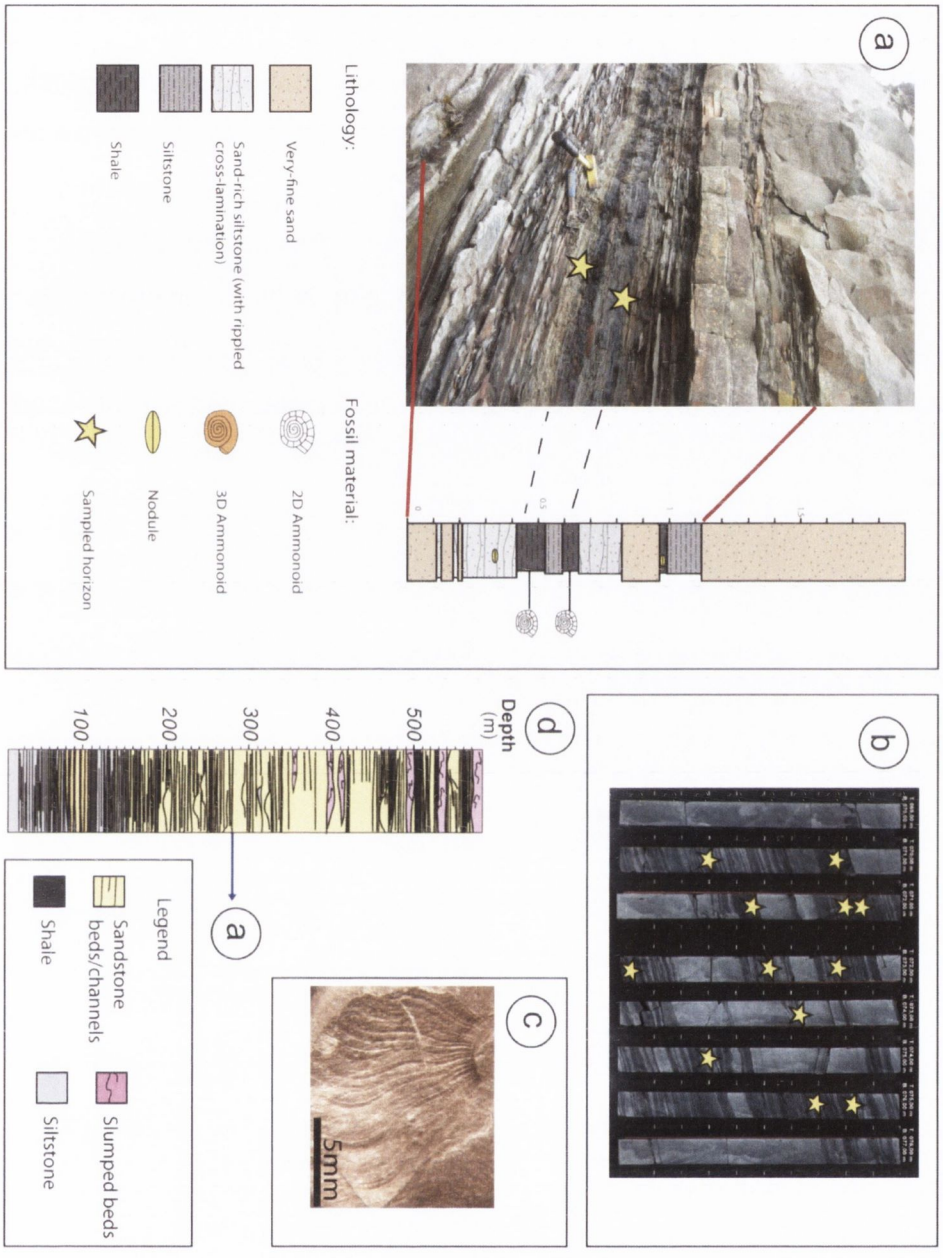

Fig. 4.4. (a) Field photo and stratigraphic log of low-density turbidite sequence in northern Senan's Bay, south coast of Loop Head (Irish Grid Coordinates [76525/47887]) from which ammonoids have been recovered. (b) Location of ammonoids found in shale veneers in borehole 10-CE-UCD-04 (1 m-long core intervals from borehole 10-CE-UCD-04 were chosen as a representative example). (c) *Vallites henkei* (Schmidt, 1925), an ammonoid preserved in borehole material. (d) Summary stratigraphic log of the Ross Sandstone Formation, showing the stratigraphic position of the section shown in (a).

Silt-rich mudstones

Ammonoids have also been found preserved as 3D external casts of the shell within silt-rich, fine-grained, resistant layers that vary in thickness from a few mm to c.5 cm. These layers form rounded, nodule-like ribs along bedding, within which the ammonoids are found. The layers can be traced along bedding for tens of metres (for c.90 m in the Kilbaha Bay East locality in Fig. 4.5) and are part of hybrid bed successions (Haughton *et al.* 2009a) in the Ross Sandstone Formation. Here, shell features such as chamber walls (septa) and coiled shell shape are preserved in the external moulds.

Fig. 4.5. (a) Field photo and sedimentary log of Kilbaha Bay locality (Irish Grid Reference [75394/48264]) showing position of ammonoid-bearing siltstone shown in (b). (c) Ammonoids found in silt-rich mudstones, showing internal chambers in the shell. (d) Summary stratigraphic log of Ross Sandstone Formation, showing the stratigraphic position of the locality shown in (a).

Massive sandstones

Casts of ammonoids (Fig. 4.6) were first recorded by Goodhue (1996) on the underside of a massive sandstone west of Dunmore Head, [70662/46893], on the south coast of Loop Head, Co. Clare, Ireland. These casts are postulated to have formed as the ammonoids were dragged along the substrate, subsequently deposited and covered by the overlying turbidite flow. It is possible to see the drag marks created by the ammonoids, which may indicate a palaeocurrent flow to the south. However, the irregular shape of these marks suggests that is it is also possible that they are sole markings indicating palaeocurrent to the north.

The casts show features of the ornament such as constrictions, which are grooves on the interior of the shell. Most specimens show three constrictions suggesting the assemblage was dominated by a single ammonoid species, which is not identifiable to the genus or species level.

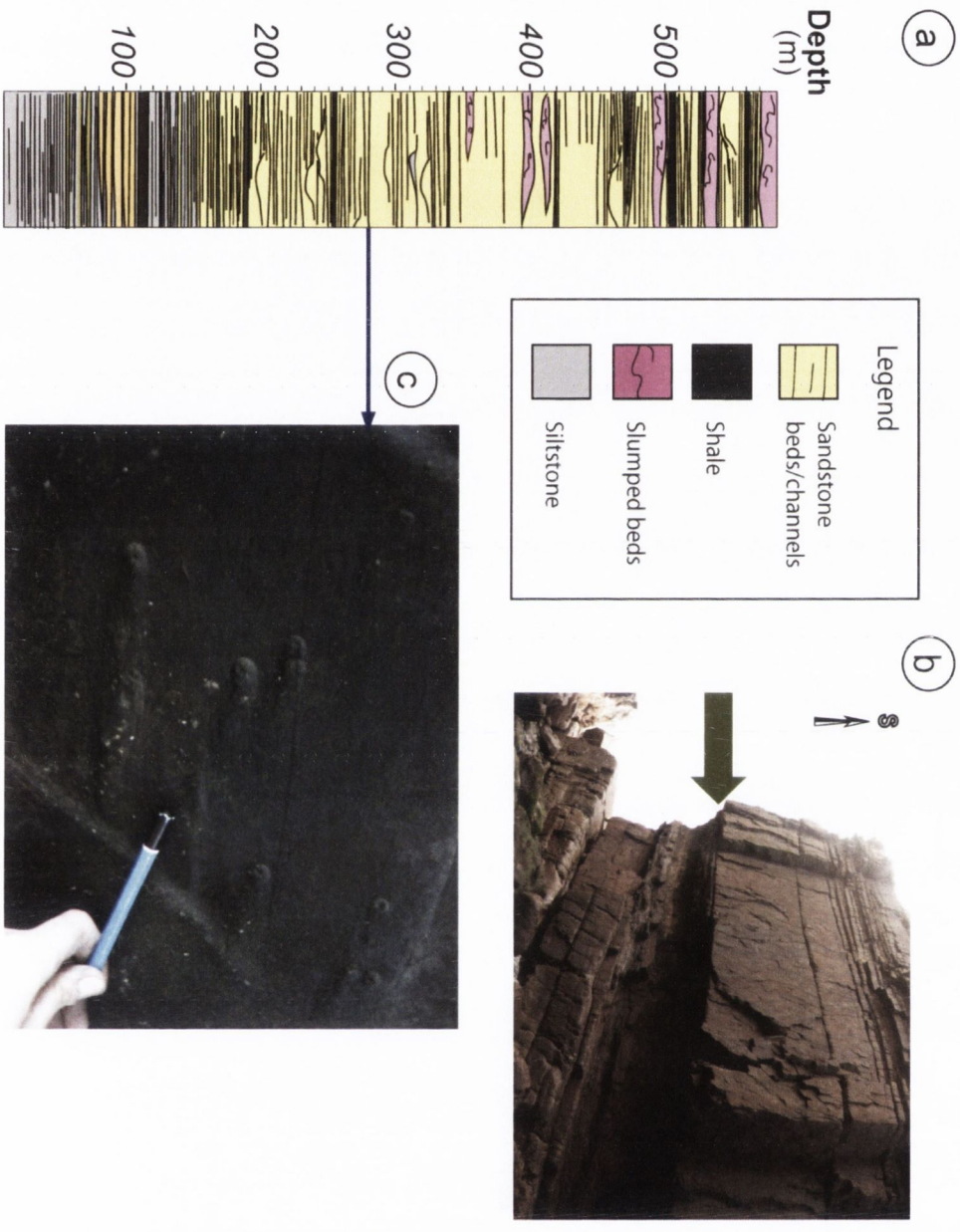

Fig. 4.6. (a) Stratigraphic position within the Ross Sandstone Formation of massive sandstone on the south coast of Loop Head, west of Dunmore Head, Irish Grid Coordinates [70662/46893]). Here, ammonoid casts shown in (c) are preserved on the underside of the sandstone bed indicated by the arrow in (b).

Ammonoid distribution within the Clare Shale Formation

The Clare Shale Formation, in its lower part, is characterized by black shale and, in its upper part, by grey shale, with darker horizons containing ammonoid-bearing concretions (Sevastopulo 2009). In all localities examined, it was evident that throughout the Clare Shale succession ammonoid-bearing horizons are common in the shale between the highly-condensed sections. This is particularly well seen at Fisherstreet Bay.

4.4 Discussion

During the late Mississippian and Pennsylvanian, sea level fluctuations are estimated to have been of the magnitude of 40-100 m (Rygel *et al.* 2008) and are generally thought to have reached peak development during the Serpukhovian and Bashkirian Stages, attaining a scale comparable to that of the Pleistocene glaciation (Frank *et al.* 2008; Fielding *et al.* 2008). Even though the Shannon Basin has been considered to be part of a shallow epicontintental seaway (Davies 2008), the new data discussed above and summarised in Figs. 4.7-4.8 suggest that sea level could not have dropped enough to cut off the supply of marine waters to the Shannon Basin until the onset of the shallow water deltaic environments of the Central Clare Group. During deposition of the Ross Sandstone Formation, marine faunas populated the basin waters throughout deposition, including during those times which have been interpreted as representing low stands. Fig. 4.7 shows the stratigraphic position of ammonoid-bearing horizons in and between the main highly-condensed sections.

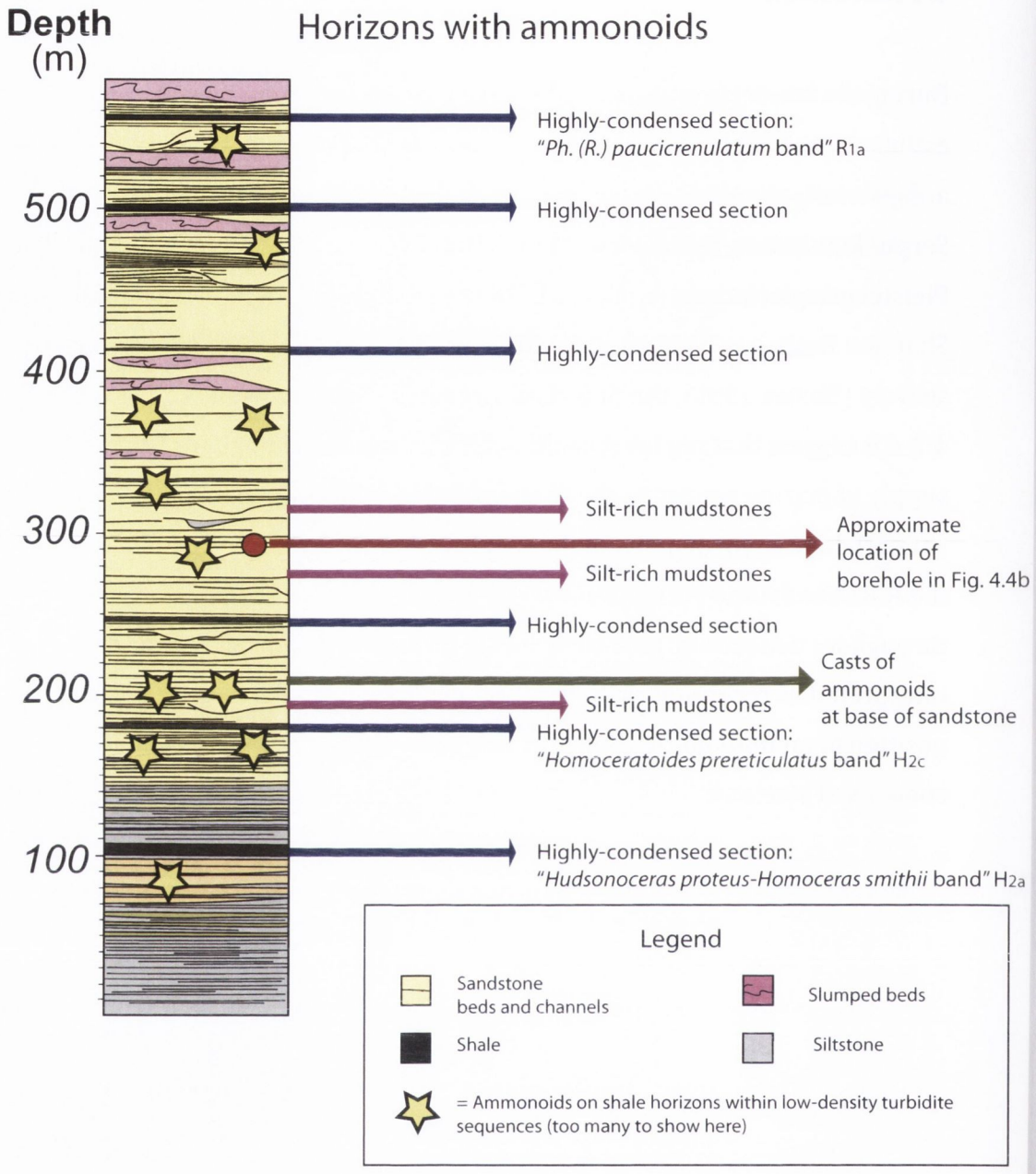

Fig. 4.7. Summary log of the Ross Sandstone Formation, Shannon Basin, with the stratigraphic position of ammonoid-bearing horizons (indicated by arrows) in and between the main highly-condensed sections. Stars show approximate (within 10 m of stratigraphic thickness) positions of ammonoids on selected shale horizons within low-density turbidite sequences, which are too many to show on this scale.

Based on these data, the emerging model of sedimentation in the Shannon Basin (Fig. 4.8) envisages that at times of high seal level, ammonoids populated the basin, whereas at times of low sea-level, despite an influx of sediment and freshwater, a connection to marine waters was maintained, allowing ammonoids to still populate the basin waters. Freshwater influx into the basin would have led to stratification of the water column, with denser saltwater forming a wedge below overlying freshwater. This would then lead to development of a pycnocline, which may have affected the ecological niches ammonoids were able to occupy. It is likely that in such a restricted, stratified basin the ammonoids restricted their vertical range to the deeper waters. Such statification is then likely to have broken down at times of high sea level, when full marine conditions were established (cf. Braithwaite 1995, p. 202).

In such a model, the basin is envisaged as asymmetrical, with one side higher than the other, allowing for sediment input from one side and continued connection to marine waters on other side.

The presence of marine organisms such as coral, trilobite and crinoids (see Chapter 3 for palaeoecology discussion) throughout the basin fill succession (both in the Clare Shale Formation and Ross Sandstone Formation) is entirely consistent with and adds evidence for this new model.

Fig. 4.8. (a) Schematic representation of emerging model for sedimentation in the Shannon Basin, western Ireland. (b) Concentration of ammonoids in the Shannon Basin visualized in an idealized log through the basin fill, showing greater numbers of ammonoids corresponding to times of lower sedimentation rate and fewer at times of higher sedimentation rate.

Braithwaite (1993; 1995)'s inspection of a Clare Shale Formation section at Inishcorker is consistent with the data presented here in that she did also not observe classical faunal salinity cycles. In addition, the geochemical analyses described in Braithwaite (1995) (using sulphur in pyrite, organic carbon and uranium) suggest most (at least 60%) of the Clare Shale Formation succession was deposited under marine conditions (Braithwaite 1995, p. 167).

In light of the data presented here for the Shannon Basin, it is clear that other basinal successions merit re-investigation. It is likely that previous workers have targeted highly-condensed sections rather than the sections in between, when looking for marine fossils. In addition to the evidence available from ammonoids presented here, conodonts, which are exclusively marine fossils, have been recovered from bullions (outside of condensed sections) in the Clare Shale Formation by Fallon (Fallon & Murray 2015). Conodonts have also been recovered from various intervals outside traditional "marine bands" in Stonehead Beck, north Yorkshire, UK by Varker *et al.* (1990) and Varker (1994).

4.5 Conclusions

The presence of ammonoids at various intervals outside the condensed sections is good evidence is for normal marine salinity in the Ross Sandstone Formation and Clare Shale Formations of the Shannon Basin. It suggests that the concentration of ammonoids in black shale intervals rather than in silt and sand sequences is not controlled by salinity fluctuations. Rather, their distribution is dictated by different sedimentation rates, which in turn may be a consequence of sea level change, with higher concentrations at times of sediment starvation and fewer at times of higher sediment input, when they are "occluded" (*sensu* Holdsworth & Collinson 1988) by sediment supply. There may also have been different taphonomic outcomes in these two regimes.

The salinity cycles (Fig. 4.1) described in Holdsworth & Collinson (1988) for the Pennine Basin, UK, have not been found during fieldwork and borehole analysis in the Shannon Basin. This may be due to differing basin topographies, as clearly more marginal areas would be expected to show salinity variation during times of sea level variation. It may be that the Shannon Basin was deeper and less susceptible to these fluctuations.

What is clear from the data presented here is that the simple notion of "marine bands" as the only levels with marine fauna and "barren intervals" is no longer tenable. These data are incompatible with the suggestion that the Ross Sandstone Formation presents evidence for less than marine salinity put forward by Higgs (2009) (also see Pyles 2009). Furthermore, given that marine conditions persisted throughout deposition, the term "marine band" is better replaced by the term "condensed section".

Chapter 5 Correlations within the Ross Sandstone Formation

5.1 Introduction

The Pennsylvanian Ross Sandstone Formation in the west of Ireland provides an important analogue for deep-water reservoirs elsewhere (see Chapter 1). One of the major aims of this research was to investigate the biostratigraphy of the Ross Sandstone Formation. A parallel doctoral study by Colm Pierce at University College Dublin (UCD) used both outcrop data and behind-outcrop drilling results to establish detailed sedimentological, lithostratigraphical and event correlations within this unit (Pierce 2015). The aim of the combined studies was to provide an integrated high-resolution subdivision of the Ross Sandstone Formation that will underpin a better understanding of lateral facies changes, vertical changes in bed and element types, the expression of high-frequency external forcing and the wider evolution of the system. Another aim of the present biostratigraphic study was to help correlate the behind-outcrop cores with the adjacent outcrops. Where there is detailed and reliable physical correlation, this provides an important cross check from what would be deduced from biostratigraphy alone. If the biostratigraphic correlation proved to be of similar high resolution, this would strengthen its efficacy in cases where the physical correlation is more equivocal. Assessing the reliability of different approaches is important when dealing with more incomplete datasets such as those encountered during hydrocarbon exploration. In addition, together with the borehole datasets, a better biostratigraphic framework will further enhance the training potential of the wider Shannon Basin and underpin applied research of direct relevance to subsurface reservoir description.

The data from intensive faunal sampling and identification of ammonoid taxa from several condensed sections in the Ross Sandstone Formation have been outlined in Chapter 2. Here, previous biostratigraphic efforts are summarized (section 5.2) and stratigraphic ranges of ammonoids within the Ross Sandstone Formation are re-evaluated in light of the present study (sections 5.3 and 5.4).

5.2 Ammonoid biostratigraphy in context

Alongside the key role of conodonts as biostratigraphic tools for identifying the Mid-Carboniferous boundary (Richards *et al.* 2011; Sevastopulo & Barham 2014; Barham *et al.* 2015; Fallon & Murray 2015), thick-shelled ammonoids, plant spores and thin-shelled bivalves (Sevastopulo 2009) have been used to subdivide and zone rocks of Carboniferous age. In particular, the usefulness of ammonoids in biostratigraphy has long been recognized. Ramsbottom and Saunders (1985) summarized the main reasons why ammonoids are commonly the preferred organisms for zoning the Carboniferous: they changed form rapidly through various successive evolutionary radiations and faunal turnovers (also see Becker & Kullmann 1996), and they had a nektonic mode of life, resulting in good potential for cosmopolitan post-mortem distribution. Indeed, after a drastic decline in ammonoid genera and species (from more than 100 genera to about 20) at the end of the Early Carboniferous, the Serpukhovian-Bashkirian stages saw a proliferation of ammonoids, with an increase to 47 genera and more than 200 species (Becker & Kullmann 1996). This rapid evolution has been linked to high-frequency eustatic sea level variation (Ramsbottom 1977; 1979). As reported by Korn *et al.* (2005; 2012), ammonoid faunas in the Tournaisian and early Late Visean are globally similar in their tropical occurrences, with the genera *Goniatites* and *Entogonites* having wide palaeogeographical distribution, indicating cosmopolitism at the genus level. Faunas became more provincial in the middle Late Visean and dissimilarities become pronounced in the latest Visean, Pendleian, and Arnsbergian (Korn *et al.* 2011; 2012). Even when provincial, ammonoids can be extremely useful in more local studies (Lacchia 2012).

In northwestern Europe, Serpukhovian and Bashkirian ammonoid biostratigraphy was first established by Bisat (1924; 1928) and Bisat & Hudson (1943), and later developed by Ramsbottom (1969; 1971), largely resulting from work in the Central Pennine Basin of northern England (see Waters *et al.* 2011).

Thick-shelled ammonoids in the Shannon Basin span the E_1 to R_2 biozonal indices (Serpukhovian-Bashkirian Stages) (Hodson & Lewarne 1961; Lacchia *et al.* 2015). Most species in the *Homoceras* zone continued into the *Reticuloceras* zone and gave rise to a huge variety of forms (Becker & Kullmann 1996).

Taxon/ Localities	Reading Room (Kilbaha)	Dunmore Head west, (Lisdoondal-hen)	Light-house	Quilty	Cloghaun-savaun	Kilcredaun Top band, Kildredaun	Cross (Oughter-ard)	Bridges of Ross (Ross)	Ross Bay E (Moreen)	Ross Bay W (Endry)
Ph. (R.) paucicrenulatus										✓
R./Ph. sp.									✓	
?R. pulchellum						✓✓✓✓				
Ph. (R.) paucicrenulatus						✓✓✓✓	✓✓✓✓	✓✓✓✓		
Ht. varicatus?			✓							
V (H). henkei		✓✓	✓✓✓✓							
Ph. (R.) circumplicatile late form		✓✓	✓✓							
Ph. (R.) circumplicatile		✓✓✓✓	✓✓✓	✓✓✓	✓✓✓	✓✓✓✓				
Ht. prereticulatus	✓✓✓✓	✓								

Fig. 5.1. A compilation of ammonoid taxa recoded by Gillian Lewarne for localities in stratigraphic order within the Ross Sandstone Formation (from unpublished notes). Locality names have been updated to reflect locality names in Chapter 3. Ticks indicated presence of a given taxon in a locality. Number of ticks indicate abundance, as recorded by Lewarne: ✓= rare to very rare, ✓✓= frequent to rare, ✓✓✓= frequent, ✓✓✓✓= abundant. Where this occurrence has been confirmed in the present study (not necessarily in the same abundance), the box is shaded. Boxes were shaded whether or not specimens were identified confidently or were prefixed with cf (confer).

While the majority of occurrences recorded by Lewarne were also confirmed in the present study (confirmed occurrences are represented by shaded boxes in Fig. 5.1), several taxa new to a given locality and taxa which had not previously been recorded in the Clare Shale Formation and the Ross Sandstone Formation have been found in the present study; these are presented with respective localities in Chapter 2. The first occurrence of these taxa is also discussed.

5.3 Lithostratigraphic correlations

The present study is the first to present details of abundance and proportion of ammonoid taxa (beyond recording the presence of a given ammonoid band name) at localities within the Ross Sandstone Formation since the work of Hodson (1954a,b) and Hodson & Lewarne (1961).

5.3.1 Results of current study

During the course of the present study and in conjunction with research by Colm Pierce (Pierce 2015), at least ten ammonoid-rich shale intervals outside of condensed sections, as well as eight condensed sections, have been identified within the Ross Sandstone Formation. Amongst the condensed sections, five are classified as highly-condensed sections because of their distinctive lithology, thickness and fossil content (see Ch. 1) and three are classified simply as condensed sections, due to their thinner and less fossiliferous nature, and less consistent expression (namely the Toorkeal band and the two ammonoid bands at Rinevella; see Ch. 2 for locality details).

This work allowed for a revised intra- Ross Sandstone Formation stratigraphic subdivision (with stratigraphic cycles/units R5 to R90 from base to top) to be made (presented in Pierce 2015). This "R subdivision" (Table 5.1) is used to provide a new stratigraphic framework in order to tie the Loop Head subsurface data to the outcrops and to reassess the stratigraphic position of some of the outcrops that were not as well constrained prior to this combined study (Pierce 2015). In the subdivision, eight condensed sections (including one fossiliferous interval identified in the borehole material outside the main condensed sections) are used as the upper surfaces of the R units (except in R70, which is topped by the base of the Ross Slump, and the topmost unit, R90, which is topped by a lithostratigraphic boundary with the Gull Island Formation above).

The associated correlation panel is shown in Fig. 5.2, with condensed sections helping to link outcrops and borehole sections. The relative ammonoid taxa identified in this study are shown in Fig. 5.2 and relevant localities are shown in Fig. 5.3.

Unit name (R subdivision)	Unit-bounding condensed section/slump (at top of unit)	Main outcrop/core localities where unit-bounding surface is expressed
R90	Lithostratigraphic boundary: Ross Sandstone Formation/Gull Island Formation	Cross
R80	*Ph. paucicrenulatum* band	Cross
R70	Ross Slump with fossiliferous shale rafts	Quilty, Kilcredaun, Bridges of Ross
R60	*Ph. circumplicatile* band	Quilty, Cloghaunsavaun, Cloonconeen, Kilcredaun, Blackrock west, Blackrock east and Moneen Point
R50	Toorkeal band	Toorkeal, Cloonconeen, Fodry, -01 borehole, Kilcredaun (Holy Well)
R40	Rinevella band	Rinevella, St. Senan's Bay
R30	Dunmore West band	Rehy Hill, Dunmore West, Lighthouse, St. Senan's Bay
R20	*Ht. prereticulatus* band	Reading Room, Ballybunion -03 and -05 boreholes
R10	*Hud. proteus/Ho. smithii* band	Ballybunion, -03 and -05 boreholes
R5	Fossiliferous shale	-03 and -05 boreholes

Table. 5.1. Summary of high-resolution stratigraphic subdivision of the Ross Sandstone Formation with unit-bounding condensed sections/slump horizons/fossiliferous intervals and main core and outcrop localities (after Pierce 2015).

Importantly, not all of the condensed sections used in the subdivision contain distinctive assemblages. The faunal assemblages identified in this study acted as a cross-check for the lithostratigraphic correlations, either supporting them where the assemblages were very similar from locality to locality, or neither opposing or supporting them where the number of identifiable specimens was insufficient to provide reliable information.

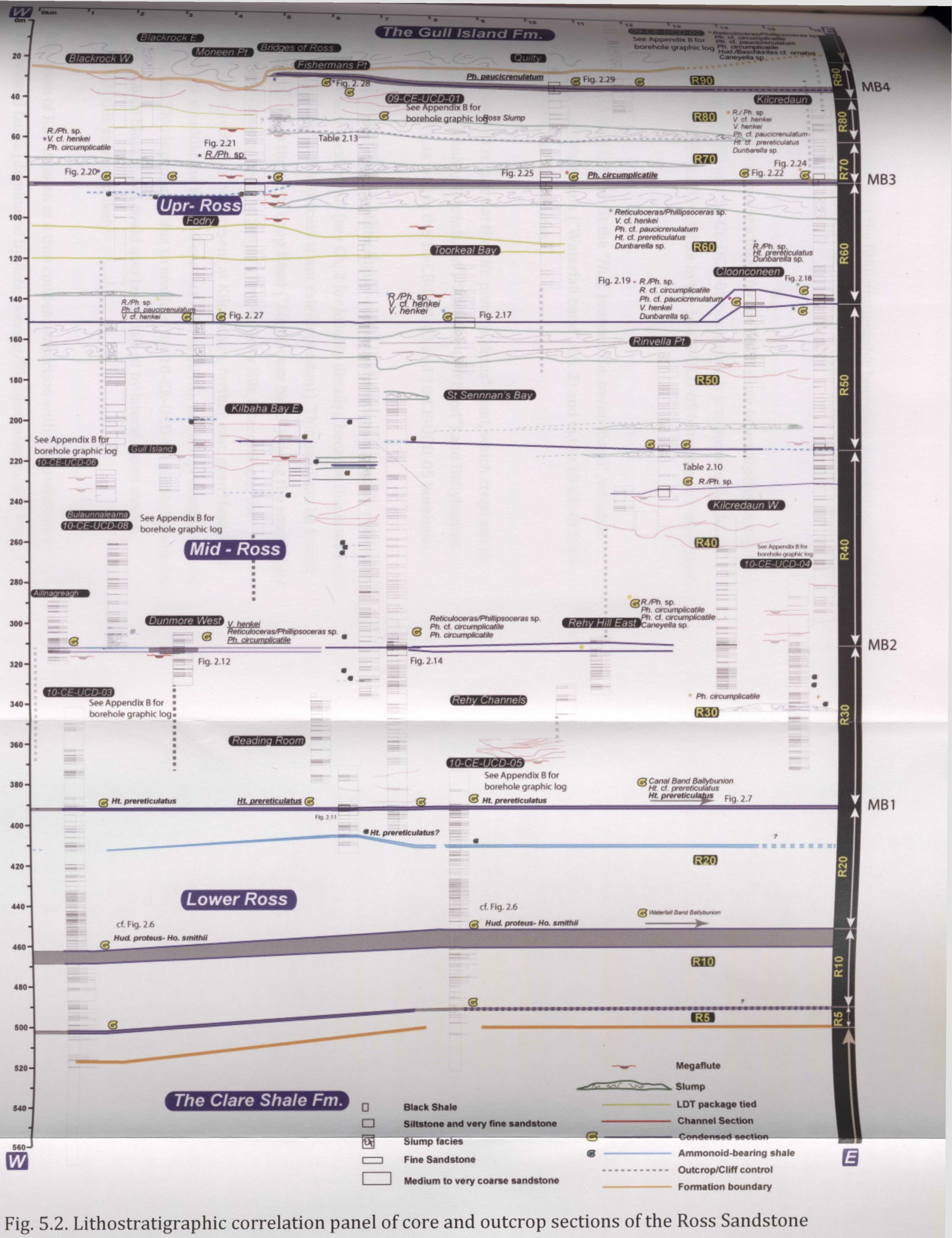

Fig. 5.2. Lithostratigraphic correlation panel of core and outcrop sections of the Ross Sandstone Formation (modified after Pierce 2015). Taxa that were also identified by Gillian Lewarne are underlined (cf Fig. 5.1). Logs that are measured by Pierce (2015) are grey, while sections measured in this work (mostly around the condensed sections) are black. For detailed logs, see relevant Figs. in Chapter 2 and Appendix B.

The base of R5 is taken at the lithostratigraphic boundary between the Clare Shale Formation and the Ross Sandstone Formation, which is seen in outcrop at Ballybunion.

The base of R10 is taken at a fossiliferous black shale interval observed in both the 10-CE-UCD-03 and 10-CE-UCD-05 boreholes. It is thinner in the 10-CE-UCD-03 borehole (c.20 cm) than in the 10-CE-UCD-05 borehole (c.1 m) (Pierce 2015).

The base of R20 is taken at the "*Hud. proteus/Ho. smithii* band", which is expressed in Ballybunion ("Waterfall band", Ch. 2) and in the 10-CE-UCD-03 and 10-CE-UCD-05 boreholes.

The base of R30 is taken at the "*Ht. prereticulatus*" band, which crops out in Loop Head ("Reading Room band", "Kicloher Cliff band") and Ballybunion ("Canal band"), as well in the 10-CE-UCD-03 and 10-CE-UCD-05 boreholes.

The base of R40 is taken at the highly-condensed section commonly referred to as "Dunmore West band" (see Ch. 2 for locality details), because this is where it is most easily studied (access is not tide-dependent). This band can be traced physically from the tip of Loop Head ("Lighthouse band") along the south coast west of Dunmore Head, to Senan's Bay, to Rehy Hill. Interestingly, the condensed section is not present at Kilcredaun, further east, even though the localities straddle the R30/40 contact (Pierce 2015), nor is it present in the -04 borehole. This is probably due to erosion (the 10-CE-UCD-04 borehole contains rafted shale blocks), but could also be explained by lateral facies change, although this seems unlikely.

The base of R50 is taken at a thin condensed section with a non-distinctive ammonoid fauna (dominated by *Reticuloceras/Phillipsoceras* sp. and *V.* cf. *henkei)* which crops out at Rinevella Bay (60 cm black shale above a slump at Rinevella point), St. Senan's Bay and Kilcredaun.

The base of R60 is taken at the "Toorkeal band" (see Ch. 2), which is also expressed at various outcrop sections (Fodry; Holy Well; Cloonconeen) and in the 09-CE-UCD-01 borehole. The faunal assemblage is rich, but not diagnostic, with dominance by *Reticuloceras/Phillipsoceras* spp.

The base of R70 is taken at the "*Ph. circumplicatile* band", which is a highly-condensed section expressed at Quilty, Cloghaunsavaun, Cloonconeen, Kilcredaun, Blackrock west, Blackrock and Moneen Point. Interestingly, the section is much thinner (a change from c.3 m to c.40 cm: Pierce 2015) and less prolific at Blackrock and Moneen Point, implying a significant lateral change in expression westwards for this band.

The base of R80 is placed at the base of the Ross Slump (Gill 1979; Strachan 2002) where rafted beds of black shale are present (*Phillipsoceras/Reticuloceras* spp. and *Ph.* cf. *paucicrenulatum* were sampled on the north coast of Loop Head, [74624/50910].

The base of R90 is placed at the "*Ph. paucicrenulatum* band", which is a highly condensed section that crops out at Cross, Bridges of Ross and Ballybunion, as well as in the 09-CE-UCD-02 borehole. The top of R90 is at the lithostratigraphic boundary between the Ross Sandstone Formation and the Gull Island Formation.

Interestingly, no "*R. dubium* band" was identified in the course of this study at Ballybunion or at Loop Head, despite several mentions of such a band as the biostratigraphical top of the Ross Sandstone Formation in the literature (Collinson *et al.* 1991; Lien *et al.* 2003). While the taxon *R. dubium* Bisat & Hudson, 1943 was recorded at Ballybunion as a minor component of the "*Ph. paucicrenulatum* band", it was not found at all on Loop Head.

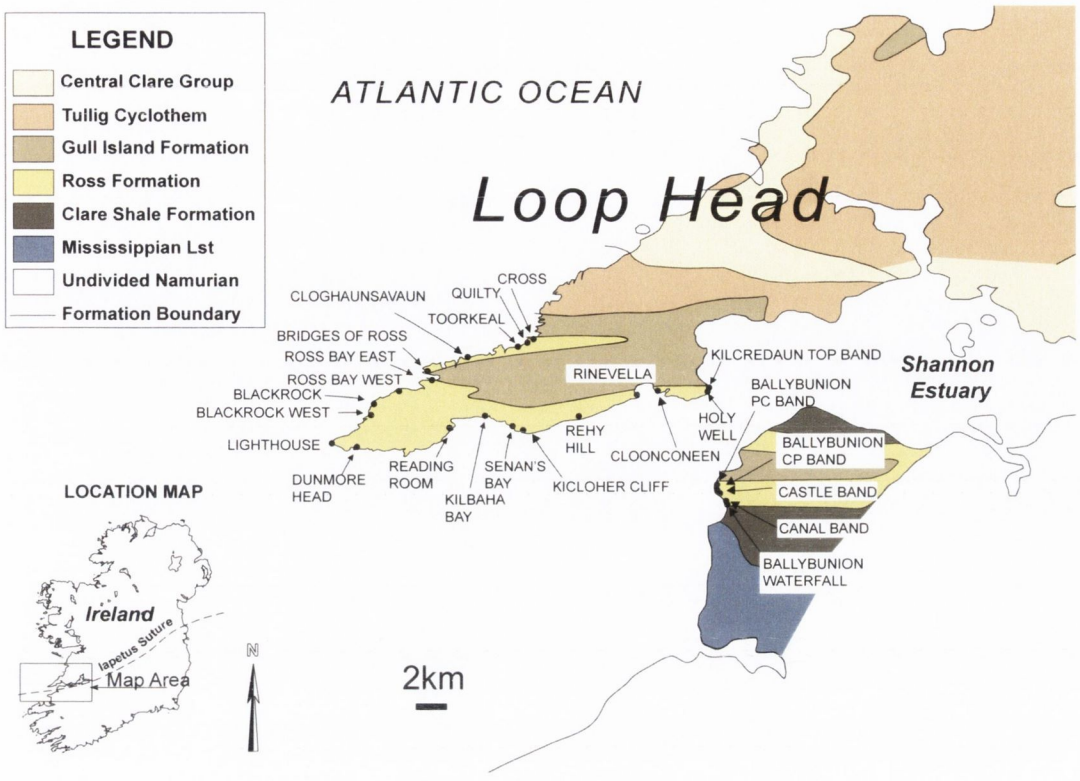

Fig. 5.3. Geological map of the Shannon Basin, showing localities mentioned in the text.

5.3.2 Discussion

The main five highly-condensed sections that have been recognized in the Ross Sandstone Formation in the present study are employed as unit-bounding surfaces in the R subdivision (Table 5.1). In addition, lesser-condensed sections are also included (top R5, R40, R50), as well as slump horizons (top R70) and lithostratigraphic boundaries (top R90). Whilst lithostratigraphic correlations in the lower Ross Sandstone Formation are well constrained, the mid- to upper Ross Sandstone Formation sections proved to be the most difficult to correlate. This is mostly because the condensed sections are thinner and less distinctive in terms of lithology and faunal assemblages.

Certain condensed sections appear to be laterally discontinuous (e.g. Dunmore Head west band eastwards to Kilcredaun) and others are split by event beds such as thick (c.30 cm) interbedded sandstone beds (e.g. Bridges of Ross or Senan's Bay). This suggests sand supply punctuated times of sediment starvation. Overall, condensed sections appear to be better expressed to the

west and thin and split as they are traced eastwards (e.g. Dunmore West band), which is surprising given the dominant sediment supply direction to the NE (Lien *et al.* 2003). It might be expected that intervening sediment packages would split the condensed sections westwards rather than eastwards. This may suggest that sediment supply direction at the time of deposition of the condensed sections was somewhat different than the dominant palaeoflow (to the NE) at times of major sediment input.

5.4 Ammonoid biostratigraphy

5.4.1 Material

More than 3000 specimens from Loop Head, Ballybunion and north Clare were investigated during the course of this study. Specimens from the Leinster Coalfield, Ireland, and museum collections (National Museum of Ireland, Manchester Museum, British Geological Survey, Keyworth, UK, and Geological Sciences Museum of the University of Göttingen) were also examined in order to strengthen identifications. While many of the specimens from the Ross Sandstone Formation could not be identified to the species level due to poor preservation and lack of diagnostic features of the ornament (see Chapter 3), detailed sampling and identification through much of the basin fill provide new data on ammonoid occurrence and biostratigraphy in the Shannon Basin. Having described the taxa systematically in Chapter 3, assemblages and first occurrence data are presented and analysed here (Fig. 5.4).

5.4.2 Rationale and methods

First appearance defines the ammonoid biozones used in correlation (e.g. Ramsbottom *et al.* 1978; Holdsworth & Collinson 1988; Davies *et al.* 2008; Waters & Condon 2012), with the bases of biozones coinciding with the base of specific ammonoid bands (also see Ch.1). A first appearance diagram with ammonoid occurrences and ranges in the Ross Sandstone Formation is presented in Fig. 5.4. Assemblage data for the five main highly-condensed sections in the Ross Sandstone Formation are presented in Figs. 5.5 to 5.11 (for details of taxa at a given locality, see Ch. 2).

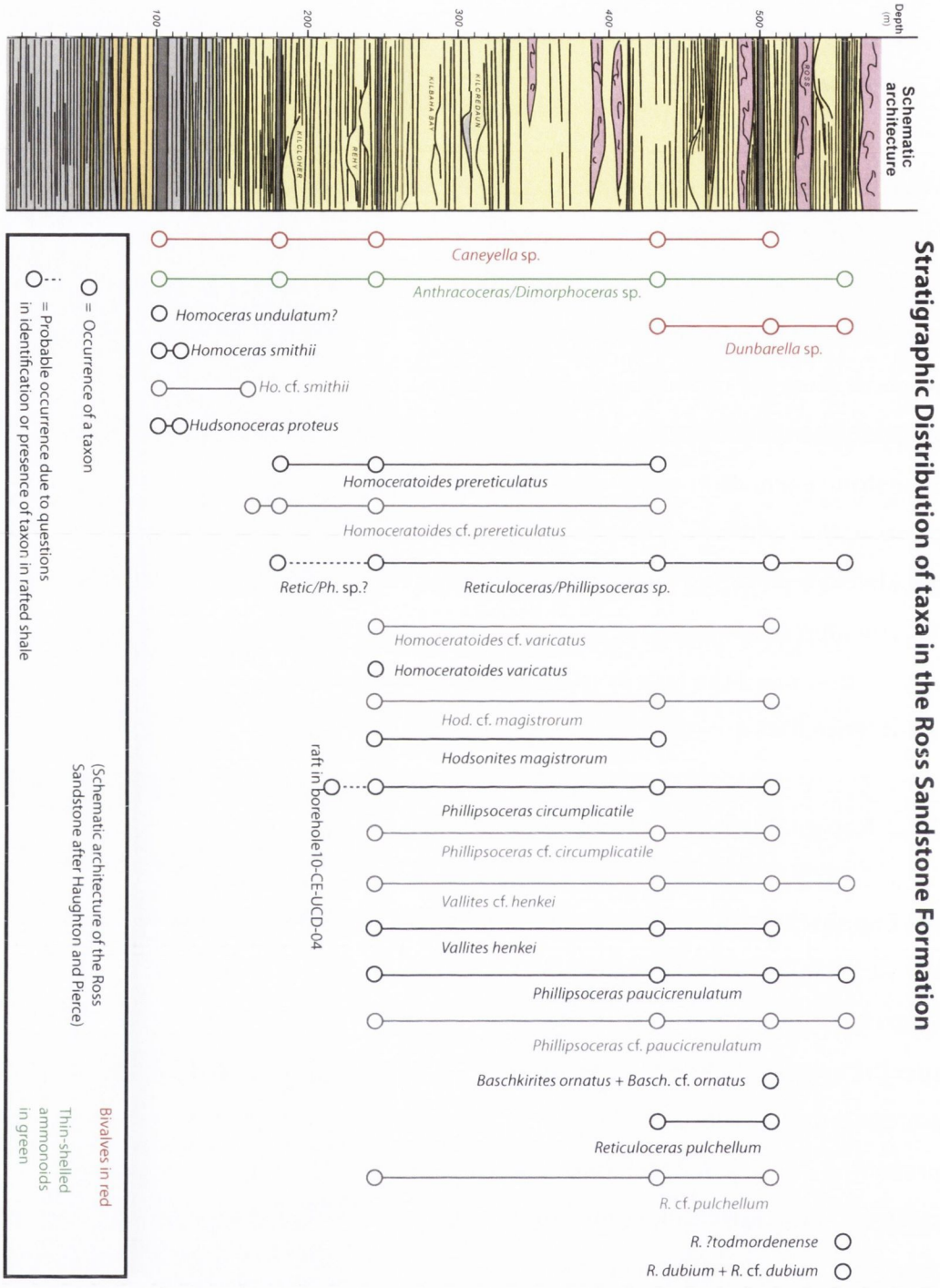

Fig. 5.4. Range chart for ammonoids and thin-shelled bivalves in the Ross Sandstone Formation, western Ireland.

Following sample examination and identification, the Chi-square test of independence was performed using Palaeontological Statistics software (PAST version 3.04) in order to test the association between the frequency of

assemblages and the locality, i.e. whether the differences in assemblages from locality to locality are statistically significant. The question the test seeks to answer is: are there statistical differences between the distribution of the assemblages? The test compares observed data (observed frequencies) with what you would expect to find by chance alone (expected frequencies) and determines whether the observed frequencies are statistically different from the expected frequencies (Urdan 2005). This test is used when dealing with qualitative (categorical) variables: in the case of assemblages of ammonoids, the categorical variable (factor) is the location. Variables to be analysed are entered into so-called contingency tables, where the cells contain observed and expected frequencies.

The null hypothesis states that taxon numbers for individual localities are the result of chance on selection from a common pool. That is, if one rejects the null hypothesis, the two populations have not been drawn from a common population and therefore are different. Once the observed Chi-square value is computed (using PAST in this case), widely-available tables (e.g. p. 178, Urdan 2005) can be used to obtain a critical value of certainty, using the degrees of freedom (df), where df = (R-1)(C-1) and R is the number of rows and C is the number of columns in a contingency table.

Using this test, assemblages in the five main highly-condensed sections were compared from locality to locality, where localities had been correlated by physical means to test whether there were statistical differences between the assemblages and results are presented in Tables 5.2 to 5.9.

5.4.3 Results

The first appearance of *Hud. proteus* and *Ho. smithii* can be used to distinguish the lowermost highly condensed section. In fact, it has a distinctive assemblage (Fig. 5.5) dominated by *Hud. proteus* and *Ho. smithii* both in Ballybunion and in boreholes 10-CE-UCD-03 and 10-CE-UCD-05. This corresponds to the H_{2a}(i) of Holdsworth and Collinson (1988).

Ammonoid assemblages in the "*Hud. proteus- Ho. smithii*" band (Chapter 2, Section 2.2.2.1) were compared from locality to locality using the Chi-square test. In the contingency tables, species preceded by cf. (confer) are treated as the same as those not preceded by cf. (since the difference is mainly thought to be due to preservation). Since the critical value is greater than the observed Chi-square value, the null hypothesis that the assemblages arose by chance from a common pool is accepted with an alpha level of 0.05 (Table 5.2). In other words, the results are statistically insignificant.

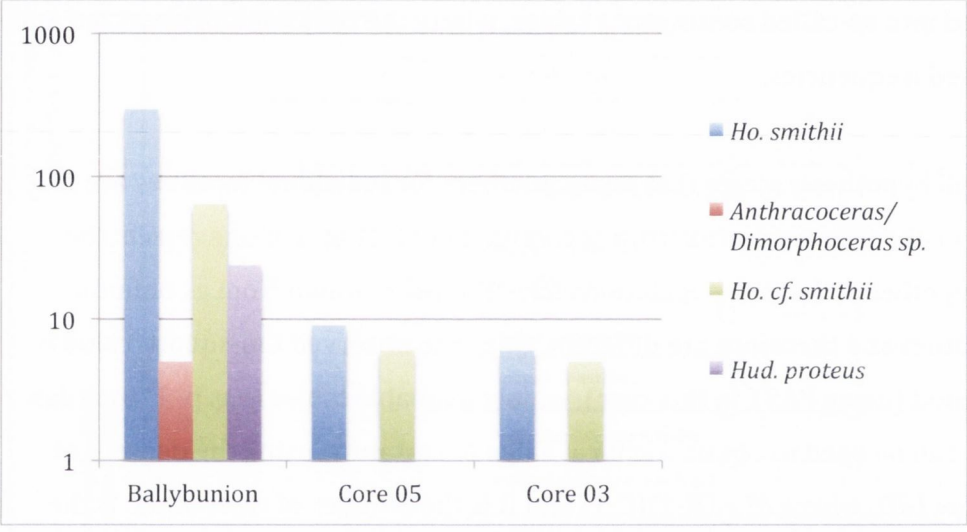

Fig. 5.5. Comparison of ammonoid assemblages in the "*Hud. proteus-Ho.smithii* band" at different localities. The vertical axis shows the number of specimens on a log scale.

Taxa	Core 05	Core 03	Ballybunion Waterfall band
Ho. smithii	15	11	360
Ho. undulatum ?	0	0	1
Hud. proteus	1	1	24
OUTPUT			
Rows, columns:	3, 3	Degrees freedom:	4
Chi2:	**0.15863**	p (no assoc.):	0.99702
Monte Carlo p:	1		
The null hypothesis is accepted, using 5% alpha			

Table 5.2. Contingency table and Chi-square test results for the "*Hud. proteus- Ho. smithii*" band using PAST software.

The first appearance of *Ht. prereticulatus* can be used to distinguish the second lowermost highly condensed section. In addition, this band is again distinctive and easily recognized by its assemblage, which is almost entirely monospecific and dominated by *Ht. prereticulatus* (and *Ht.* cf. *prereticulatus*) in outcrop localities at Ballybunion and Loop Head, and in boreholes 10-CE-UCD-03 and 10-CE-UCD-05 (Fig. 5.6). This corresponds to the H_{2c}(ii) of Holdsworth and Collinson (1988).

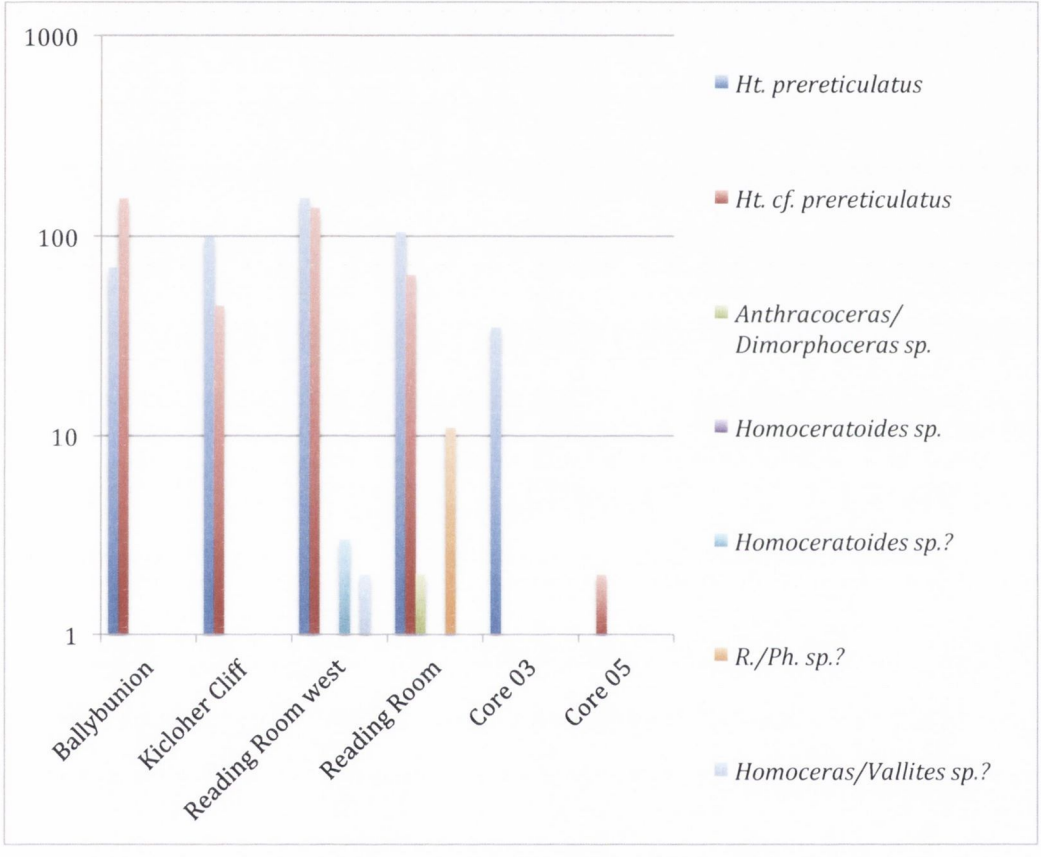

Fig. 5.6. Comparison of ammonoid assemblages in the "*Ht. prereticulatus* band" at different localities. The vertical axis shows the number of specimens on a log scale.

When one compares assemblages from locality to locality using the Chi-square test for the "*Ht. prereticulatus*" band (Table 5.3), the null hypothesis was accepted and the assemblages tested as arising from a common pool (i.e. the results were statistically insignificant).

	Reading Room	Reading Room west	Kicloher Cliff	Ballybunion
Ht. prereticulatus	166	294	144	225
Homoceratoides sp.	1	3	0	0
OUTPUT				
Rows, columns:	2, 4	Degrees freedom:	3	
Chi2:	**3.5748**	p (no assoc.):	0.31119	
Monte Carlo p:	0.3267			
The null hypothesis is accepted, using 5% alpha				

Table 5.3. Observed frequencies for the "*Ht. prereticulatus*" band and results from the Chi-square test using PAST software.

The genera *Reticuloceras/Phillipsoceras* first appear (without uncertainty denoted by confer or question marks) at the third highly-condensed section: the "Dunmore Head west band". The presence of *Reticuloceras/Phillipsoceras* spp. in the 10-CE-UCD-04 borehole, which is placed slightly below the "Dunmore Head west band" (Fig. 5.4) is not taken into account because they are preserved on rafted shale debris.

The "Dunmore Head west band" has a diverse and rich ammonoid assemblage (Fig. 5.7), which is not distinctive and thus cannot be confidently linked to a given ammonoid band in the western European framework. However, the diversity of the assemblage and the presence of *Reticuloceras/Phillipsoceras* spp. help constrain its level in the Ross Sandstone Formation, which is shown in Fig. 5.4.

Whilst the assemblage is diverse, the proportion of *Reticuloceras/Phillipsoceras* spp. compared to all other taxa is very high, as shown in Fig. 5.8.

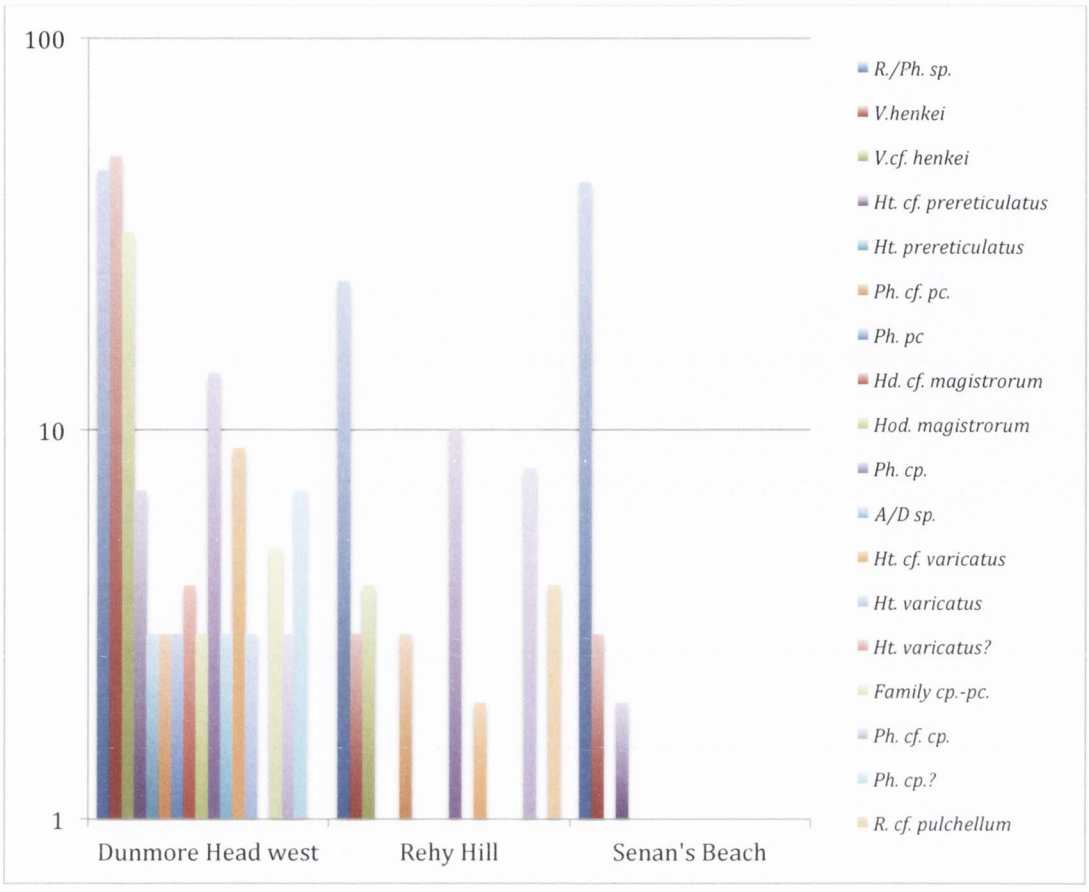

Fig. 5.7. Comparison of ammonoid assemblages in the "Dunmore Head west band" at different localities. The vertical axis shows the number of specimens on a log scale.

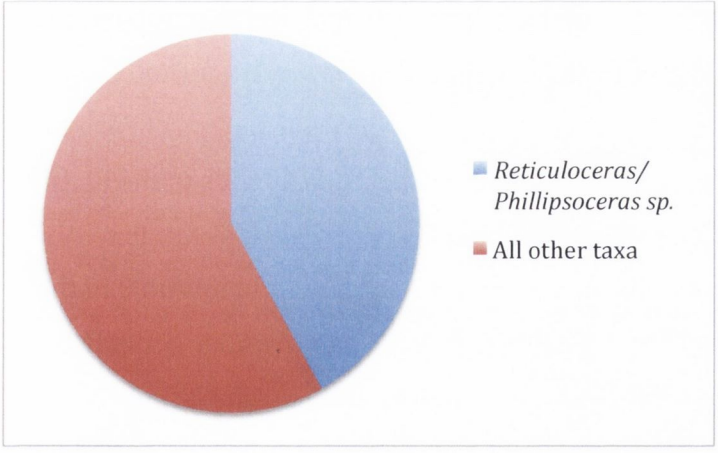

Fig. 5.8. Proportion of *Reticuloceras/Phillipsoceras* spp. compared to all other taxa at the Dunmore Head west locality, where the "Dunmore Head west band" crops out.

In the case of the "Dunmore Head west band", there is a statistically significant relationship between locality and assemblage (Table 5.4). In fact, the results are very statistically significant with Chi-square of 114.99 and p of 0.0001.

Therefore the two populations have not been drawn from a common population and are statistically different.

	Dunmore Head W Band	Rehy Hill Band	Senan's Beach Band
R./Ph. sp.	46	24	43
V.henkei	82	7	4
Ht. prereticulatus	10	0	2
Ph. paucicrenulatum	6	3	1
Hod. magistrorum	7	0	0
Ph. circumplicatile	17	18	0
Ht. varicatus	12	2	0
R. cf. *pulchellum*	0	4	0
OUTPUT			
Rows, columns:	8, 3	Degrees freedom:	14
Chi2:	114.99	p (no assoc.):	6.01E-18
Monte Carlo p:	0.0001		
Reject the null hypothesis, using 5% alpha			

Table 5.4. Observed frequencies for the "Dunmore Head West" highly-condensed section and results from the Chi-square test using PAST software.

In the case of the next highly-condensed section, the "*Ph. circumplicatile* band", no first appearance can be used to distinguish it in the Ross Sandstone Formation and its assemblage is diverse (Fig. 5.9). In fact, the first appearance of *R. pulchellum*, which appears at this level in the stratigraphy at Quilty and Cloghaunsavaun (see Ch. 2 for locality details), is not confirmed at all localities where "the *Ph. circumplicatile* band" crops out. This corresponds to the R_{1a}(ii) of Holdsworth and Collinson (1988). This band can be recognised in the Shannon Basin on the basis of the last appearance of *Ph. circumplicatile* in the Ross Sandstone Formation (Fig. 5.4), although its last appearance globally is placed at a higher level, specifically at the $R1_{a3}$-$R1_{a4}$ indices (the last appearance datum was sourced from the database Goniat.org) corresponding to the *R. subreticulatum* and *R. todmordenense* ammonoid bands in the western European framework.

The proportion of *Reticuloceras/Phillipsoceras* spp. compared to all other taxa is again very high, as shown in Fig. 5.10.

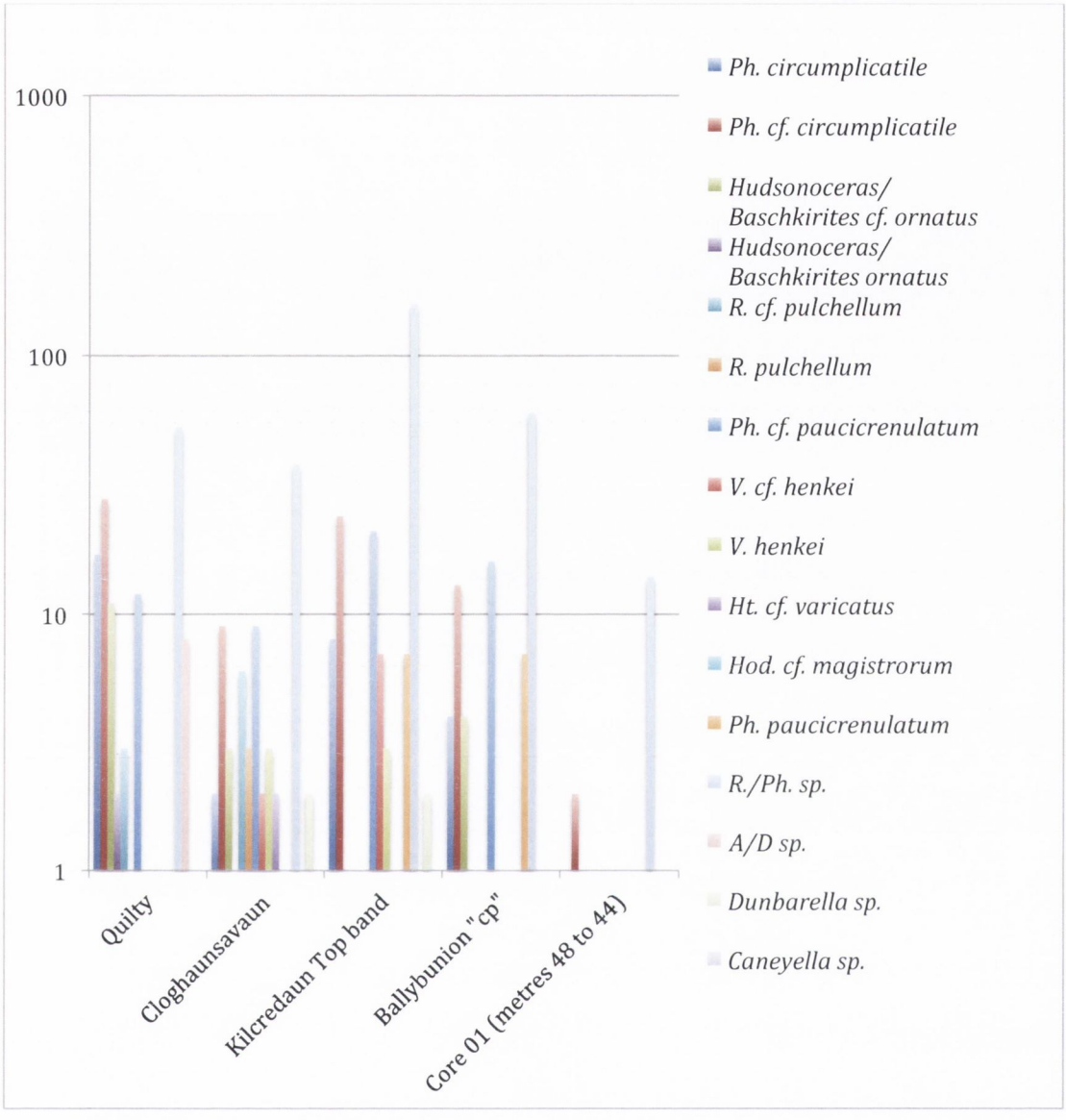

Fig. 5.9. Comparison of ammonoid assemblages in the "*Ph. circumplicatile* band" at different localities. The vertical axis shows the number of specimens on a log scale.

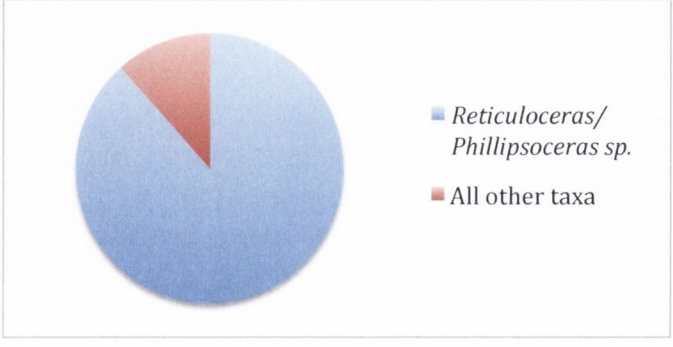

Fig. 5.10. Proportion of *Reticuloceras/Phillipsoceras* spp. compared to all other taxa at the Quilty locality where the "*Ph. circumplicatile* band" crops out.

In the case of the fourth highly-condensed section, i.e. "*Ph. circumplicatile* band", there is a statistically significant relationship between locality and assemblage (Table 5.5). Therefore the two populations have not been drawn from a common population and are different.

	Quilty	Cloghaunsavaun	Kilcredaun Top Band	Ballybunion cp
Ph. circumplicatile	45	11	32	17
Hudsonoceras ornatum/Baschkirites ornatus	13	3	0	4
Reticuloceras pulchellum	4	9	1	0
V. henkei	2	5	10	1
Ht. cf. *varicatus*	0	2	0	0
Hod. cf. *magistrorum*	0	1	0	0
Ph. paucicrenulatum	12	10	28	23
OUTPUT				
Rows, columns:	7, 4	Degrees freedom:	18	
Chi2:	78.894	p (no assoc.):	1.34E-09	
Monte Carlo p:	0.0001			
Null hypothesis rejected, using 5% alpha				

Table 5.5. Observed frequencies for the "*Ph. circumplicatile*" highly-condensed section and results from the Chi-square test using PAST software.

The topmost highly-condensed section in the Ross Sandstone Formation, the "*Ph. paucicrenulatum* band" cannot be defined by first appearance of any taxon. However, this band is characterized by dominance of *Ph. paucicrenulatum*, which makes it a distinctive band, useful in local correlation (Fig. 5.11). However, although probably corresponding to the "*R. todmordenense* band", the "*Ph. paucicrenulatum* band" is not recognized in the western European framework of ammonoid bands. The occurrence of *R. dubium* in this band is restricted to the Ballybunion locality, thus it is not diagnostic.

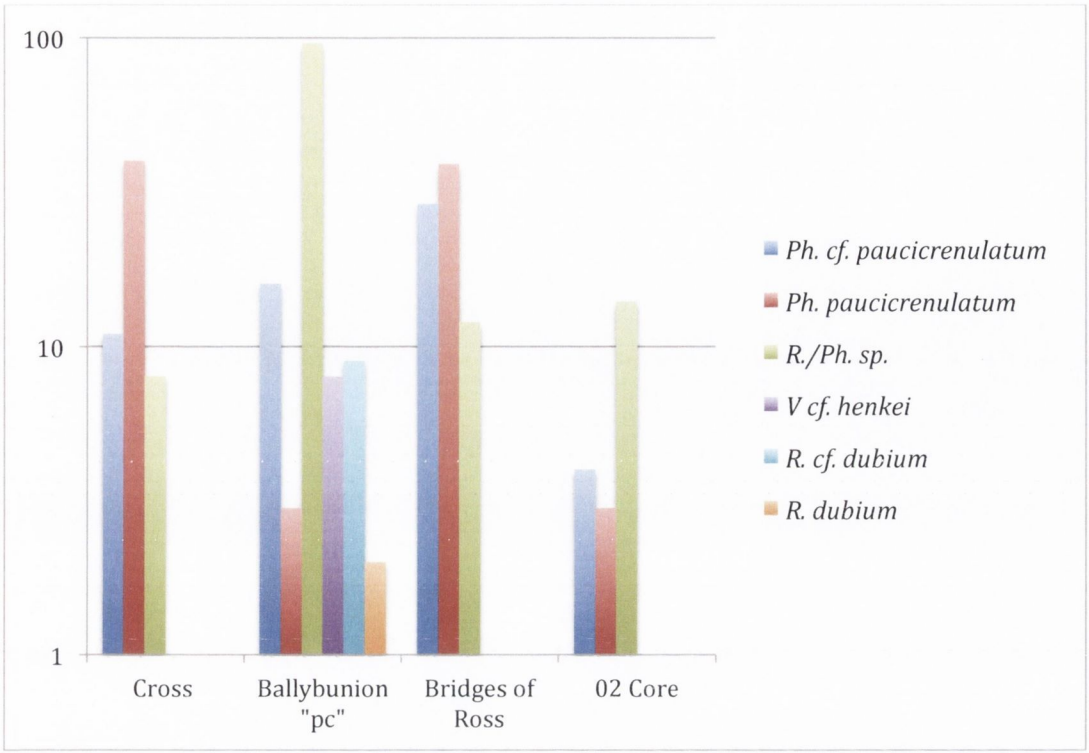

Fig. 5.11. Comparison of ammonoid assemblages in the "*Ph. paucicrenulatum* band" at different localities. The vertical axis shows the number of specimens on a log scale.

As in the case of the "*Ph. circumplicatile* band" below, the topmost highly-condensed section displays a statistically significant association between locality and distribution of assemblage (Table 5.6).

	Cross	Ballybunion pc	Bridges of Ross	02 Core
Ph. paucicrenulatum	51	19	68	7
R./Ph. sp.	8	96	12	14
V cf. *henkei*	0	8	0	0
R. dubium	0	11	0	0
OUTPUT				
Chi-squared				
Rows, columns:	4, 4	Degrees freedom:	9	
Chi2:	**147.63**	p (no assoc.):	2.73E-27	
Monte Carlo p :	0.0001			
Reject null hypothesis, using 5% alpha				

Table 5.6. Observed frequencies for the "*Ph. paucicrenulatum*" highly-condensed section and results from the Chi-square test using PAST software.

The Chi-square test was also performed on another condensed section, in addition to the five highly condensed sections: the condensed section that crops out at Toorkeal (Chapter 2, section 2.2.2.13) and is correlated with Cloonconeen (Chapter 2, section 2.2.2.16), Holy Well (Chapter 2, section 2.2.2.15) and Fodry/R. Bay West (Chapter 2, section 2.2.2.25). In this case, there is a statistically significant association between locality and distribution of assemblage. The null hypothesis is rejected and the assemblages are statistically different (Table 5.7).

	Holy Well	Toorkeal	Cloonconeen	Fodry
R./Ph. sp.	36	43	54	52
Ht. prereticulatus	3	0	0	0
Ph. paucicrenulatum	4	3	41	24
V. henkei	15	45	11	11
R. pulchellum	0	5	0	0
Ph. cf. *circumplicatile*	0	0	18	5
Hod. magistrorum	0	0	0	5
OUTPUT				
Rows, columns:	7, 4	Degrees freedom:	18	
Chi2:	**146.4**	p (no assoc.):	3.71E-22	
Monte Carlo p:	0.0001			
Reject null hypothesis, using 5% alpha				

Table 5.7. Observed frequencies for the Toorkeal condensed section and results from the Chi-square test using PAST software.

Next, comparisons were made between assemblages in different condensed sections to test whether they were statistically independent. This was not the case for the "*Ph. circumplicatile*" assemblage at Quilty, compared to the "*Ph. paucicrenulatum*" assemblage at Cross (Table 5.8). In this case, there is a statistically significant association between locality and distribution of assemblage. The null hypothesis is rejected (the assemblages are statistically different). This same result was obtained when comparing the Dunmore Head W assemblage (third highly-condensed section from the base of the Ross

Sandstone Formation) with the Quilty assemblage ("*Ph. circumplicatile*" band; Table 5.9).

	Cross	Quilty
Ph. paucicrenulatum	51	13
R./Ph. sp.	8	53
V cf. *henkei*	0	2
Ph. circumplicatile	0	44
Reticuloceras pulchellum	0	4
Hudsonoceras ornatum/Baschkirites ornatus	0	13
OUTPUT		
Rows, columns:	6, 2	Degrees freedom: 5
Chi2:	**107.61**	p (no assoc.): 1.31E-21
Monte Carlo p:	0.0001	
Reject null hypothesis, using 5% alpha		

Table 5.8. Chi-square test for ammonoid assemblage at Quilty and Cross, Loop Head.

	Quilty	Dunmore W
Ph. circumplicatile	28	22
Ph. paucicrenulatum	12	6
V. henkei	1	65
Hudsonoceras ornatum/Baschkirites ornatus	13	0
R. pulchellum	4	0
Ht. prereticulatus	0	9
Hod. magistrorum	0	6
OUTPUT		
Rows, columns:	7, 2	Degrees freedom: 6
Chi2:	**89.874**	p (no assoc.): 3.22E-17
Monte Carlo p:	0.0001	
USING 5% ALPHA		
Reject null hypothesis, using 5% alpha		

Table 5.9. Chi-square test for ammonoid assemblage at Quilty and Dunmore W, Loop Head.

5.4.4 Summary of results

Firstly, while some assemblages are globally distinctive (namely those indicative of the "*Hud. proteus-Ho.smithii* band" and the "*Ht. prereticulatus* band"), most are not, and some are only locally distinctive (such as that of the "*Ph. paucicrenulatum* band"); therefore most bands in the Ross Sandstone Formation cannot be confidently linked to a given ammonoid band in the Western European framework (see Ch. 1, Fig. 1.17).

While first appearances can be used to correlate in the lower Ross Sandstone Formation, in the mid- to upper Ross Sandstone Formation it is not possible to distinguish ammonoid bands on the basis of first appearance. Similarly, assemblages become more diverse in the mid- to upper Ross Sandstone Formation, starting from the third highly-condensed section upwards. There is a lack of distinctive ammonoid bands up until the top band, the "*Ph. paucicrenulatum* band", which has a distinctive assemblage dominated by *Ph. paucicrenulatum*.

In some cases (lowermost two highly-condensed sections) the Chi-square test results suggest that assemblages from the same condensed section have arisen by chance from a common pool (i.e. are the same), which is a result in accordance with lithostratigraphical correlations. In other cases, assemblages that are known, by lithostratigraphical means, to correlate, test as statistically different (i.e. they have not arisen from a common pool). Assemblages from bands that are known (by physical means) not to correlate, also test as being different, which is in accordance with correlations. So while this test is in accordance with correlations in some cases (the lower most two highly-condensed sections), it does not always do so (the next three highly-condensed section in the Ross Sandstone Formation).

It must be cautioned that this test is of limited use when drawing inferences on the validity of the correlations when specimens in the contingency table are less than five in number (no more than 20% of the cells should have a value

less than 5). It is likely that other factors are influencing the make up of the assemblages: these could range from reworking to selective preservation to insufficient sampling/sampling bias, to ecological exclusion. Sampling bias is considered the most likely of these factors.

5.4.5 Discussion

A three-part subdivision is apparent from these data, whereby the lower Ross Sandstone Formation can be easily correlated using ammonoid bands. Conversely, in the mid- to upper Ross Sandstone Formation, ammonoid bands are thinner and sometimes split, as well as not having diagnostic assemblages. In the upper Ross Sandstone Formation, there is a return to bands that are easily correlated accompanied by a more distinctive assemblage in the topmost ammonoid band, the "*Ph. paucicrenulatum*" band.

Interestingly, this three-part subdivision is mirrored in a lithological change: from the lower Ross Sandstone Formation dominated by fine grained lithologies (shale and silt) there is a switch to a sand-rich mid- Ross Sandstone Formation, until the system reverts to a siltstone and slump-rich upper Ross Sandstone Formation. The significance of this subdivision perhaps may be related to far field, sedimentary response to glaciation in the southern hemisphere.

If the Shannon Basin succession is placed alongside the compilation of glacial-interglacial cycles in Waters & Condon (2012, Fig. 8) it appears that the Ross Sandstone Formation could straddle a glacial to interglacial boundary (Fig. 5.12), despite the large uncertainty in the diagram. The sandy central part could then reflect a lowstand sequence set with poor definition of condensed sections (Haughton pers. comm., 12 May 2015). The glacial to interglacial boundary is placed right at R_{1a1}, when the condensed sections become poorly defined and *Reticuloceras/Phillipsoceras* begins to dominate the assemblages. Waters & Condon (2012) already noted that interglacial intervals are associated with turnover of ammonoid genera. Perhaps temperature

fluctuations in the ocean, closing of seaways (e.g. Palaeothethys) related to the Variscan Orogeny or changing ocean currents related to glaciation influenced ammonoid evolution. However, it must be pointed out that the glacial cycles in Fig. 5.12 are quite broad and may fit many smaller, interglacial cycles. It is also likely that the condensed sections reflect lower order, higher frequency cycles.

The Ross Sandstone Formation is thought to have been deposited over about 1.5 Ma, with an error of +/- 1.1 to 1.6 Ma (Pulham *et al.* 2014), based on age estimates in Gradstein *et al.* 2004 (cf Gradstein *et al.* 2012). Given that at least eight condensed sections are present within the Ross Sandstone Formation, the resulting duration is c.200 ka for each. This is consistent with Ramsbottom's (1969) suggestion that Serpukhovian-Bashkirian ammonoid faunas renewed every 200 ka (also see Maynard & Leeder 1992), but is not fully consistent with the estimated periodicity of ammonoid bands in Waters and Condon (2012) and Pointon *et al.* (2012b), which is thought to approximate a c.100 ka short eccentricity cycle (see discussion in Bailey 2013). It may also be possible that Milankovitch cycles were not the same in duration during the Carboniferous, since the earth rotated faster at this time (Lambeck 2005).

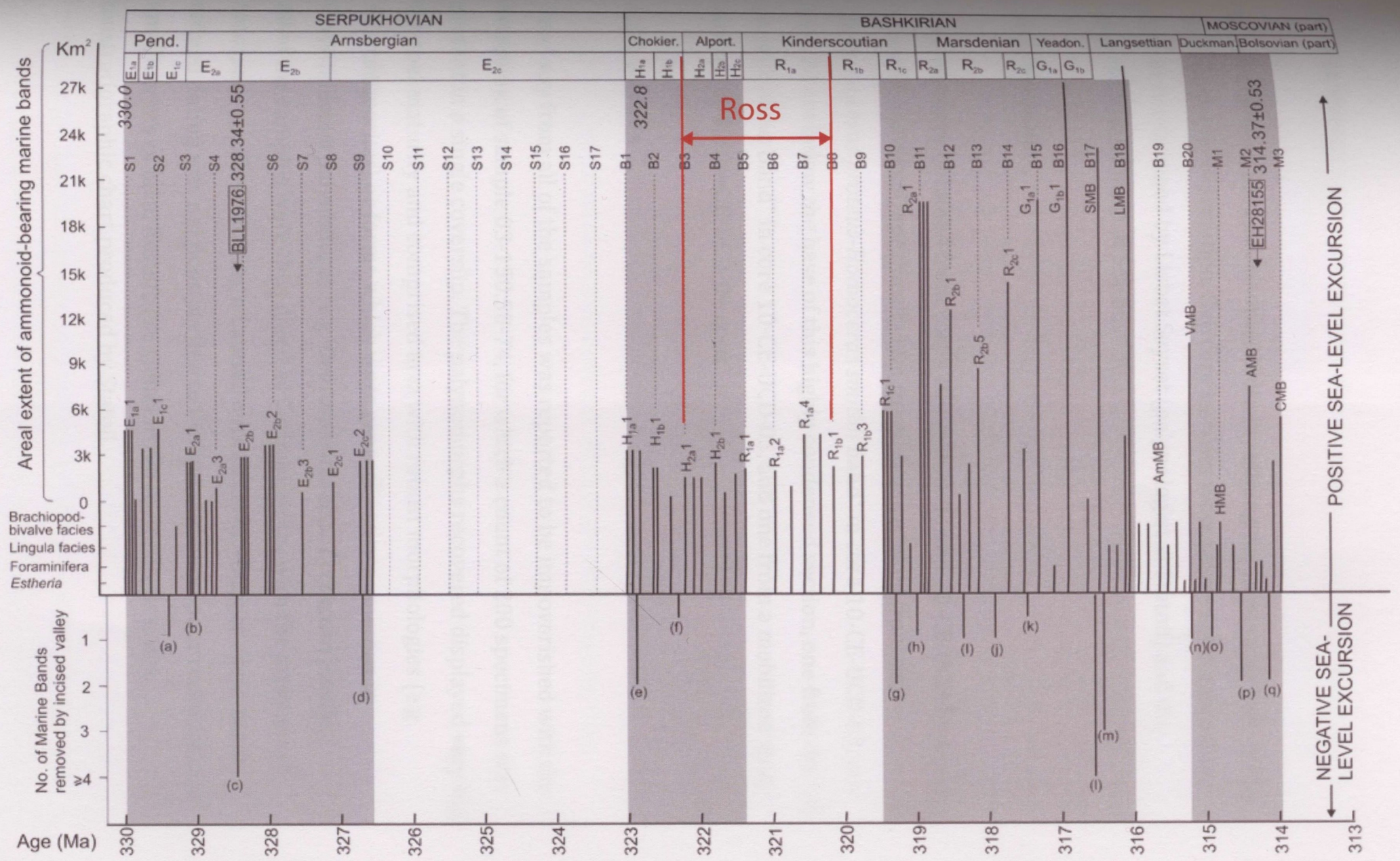

Fig. 5.12. Magnitude and duration of sea-level oscillations (after Waters & Condon 2012: Fig. 8). Sea-level maxima are estimated through the determination of maximum areal extent of acme ammonoid facies. For marine bands lacking ammonoid fauna the magnitude of sea level is determined through the acme marine fauna, ranging from *Estheria* to brachiopod–bivalve facies. Sea-level minima are determined through the presence of incised valleys, with the magnitude recorded by the number of underlying marine bands removed beneath the sequence boundary. The proposed four main glaciations are highlighted as grey bands. The Ross Sandstone Formation is shown straddling a glacial-interglacial boundary.

5.5 Palynology

In order to test the value of other biota in refining the biostratigraphy of the Ross Sandstone Formation, five core samples were selected for palynology: they were examined by Lisbet Søyset (palynologist at Statoil) and the biostratigraphy team at Statoil.

5.5.1 Methods

Samples were obtained from cores 10-CE-UCD-03 and 10-CE-UCD-04 using a hammer and chisel: specifically two samples were taken from the "*Hudsonoceras proteus-Homoceras smithii* band" in core 10-CE-UCD-03, one from 20 cm below the base of this highly condensed section, one from the "*Ht. prereticulatus* band" in core 10-CE-UCD-03, and one from a mobilized shale interval in the 10-CE-UCD-04 core.

5.5.2 Results

Recovery from all of the samples was reported to be impoverished with the exception of sample 03-150.50-74, for which a count of 200 specimens was present in a single coverslip. The palynomorphs recovered displayed very high thermal maturity and comprised taxa with robust morphologies (e.g. *Punctatisporites*) or forms which were generally very numerous in Carboniferous palynofloras (e.g. *Densosporites* spp., *Lycospora pusilla*).
All of the samples were thus dated as Carboniferous, with the presence of *Lycospora pusilla* indicating a Latest Tournaisian or younger age; a more refined dating was not possible due to the low numbers (poor recovery) and low diversity of taxa. Results are summarized in Appendix C in a biostratigraphic chart produced by Statoil.

5.5.3 Discussion

As expected, the potential for correlating within the Ross Sandstone Formation using palynology is poor. High maturation levels had already been reported in Goodhue and Clayton (1999), who obtained vitrinite reflectance data from borehole and outcrop material.

5.6 Biostratigraphy: summary and discussion

These new biostratigraphic data, coupled with the lithostratigraphical (i.e. physical) correlations, provide the most detailed dataset for the Ross Sandstone Formation to date. This allows biostratigraphy to be cross-checked against lithostratigraphical correlations and some general conclusions to be drawn.

Firstly, biostratigraphy does not work with as high a resolution as one might have hoped in that statistical analysis of the faunal assemblages does not always confirm that bands which are known to correlate by physical means are indeed indistinguishable. In other words, there are some cases, where there are statistical differences between assemblages in bands that are known to correlate by physical means. This suggests that even where there is a strong database, biostratigraphic correlation may not be statistically possible.

Secondly, while first appearances can be used to correlate the lower most two highly condensed sections, this does not work in the mid- to upper Ross Sandstone Formation, where ammonoid assemblages become more diverse. The appearance of the genera *Reticuloceras/Phillipsoceras* at the third highly-condensed section (mid- to lower Ross Sandstone Formation) can be used in correlation, but is put into question by the appearance of *?Reticuloceras/Phillipsoceras* spp. (11 occurrences) in the "*Ht. prereticulatus* band" below (Fig. 5.4).

Davies *et al.* (1999) envisaged a hierarchy of bands based on the taxonomic level to which ammonoids can be identified: firstly, index ammonoid bands (e.g. $R_{1b}1$); secondly, those that can be identified to the zone level (e.g. R_{1b}); thirdly, bands that can be classified to the stage level (e.g. R_1). Using this hierarchy for the eight condensed sections in Ross Sandstone Formation: all ammonoid bands can be classified to the stage level (either H_2 or R_1); all bands can be classified to the zone level (H_{2a}, H_{2c}, R_{1a}); and only three bands can be

classified as index ammonoid bands: $H_{2a}1$, $H_{2c}2$, $R_{1a}2$ (referring to the ammonoid scheme in Ch.1, Fig. 1.17).

Interestingly, the H_{2b} biozone was not identified in the Ross Sandstone Formation and the $H_{2c}1$, $R_{1a}1$, $R_{1a}3$, $R_{1a}4$, $R_{1a}5$ ammonoid bands also appear to be missing (cf Pyles 2008, p. 563). However, the presence of most diagnostic ammonoids and associated ammonoids (all except *V. eostriolatus, R. compressum* and *R. adpressum)* has been confirmed in the bands within the Shannon Basin (Ross Sandstone Formation and Clare Shale Formation bands which are coeval with the Ross Sandstone Formation), but the assemblages are more diverse than this scheme suggests and, for most of the bands in the R_{1a} stage, lack of a diagnostic ammonoid or first appearance taxon renders the assemblages non-diagnostic of a particular band in this scheme (see Fig. 5.13). This suggests that the western European ammonoid band framework mainly developed from Pennine Basin faunas is not entirely applicable to the Shannon Basin and thus possibly, by implication, elsewhere.

Indeed, when one compares the ammonoid assemblages in the highly condensed sections in the Shannon Basin with the assemblages in the Western European ammonoid band scheme developed largely from data from the Pennine Basin (Fig. 1.17), they rarely match up. Only the lowermost two highly condensed sections can be correlated with confidence to this scheme (Fig. 5.13).

Not only are these two bands the most distinctive in the Ross Sandstone Formation, but they are widespread outside the Shannon Basin, making them useful in basinal and extra-basinal correlation. The "*Hud. proteus-Ho.smithii* band" is known in Britain, Belgium, France, Germany, the south Urals and as far as central Asia. The "*Ht. prereticulatus* band" is known in Britain, Belgium and France (Chalard 1960; Hodson 1957; Hodson & Leckwijck 1958; Nikolaeva & Kullmann 1998).

This indicates that these highly condensed sections represent widespread, global sea level rise, in contrast to other minor condensed sections, which may represent more local events.

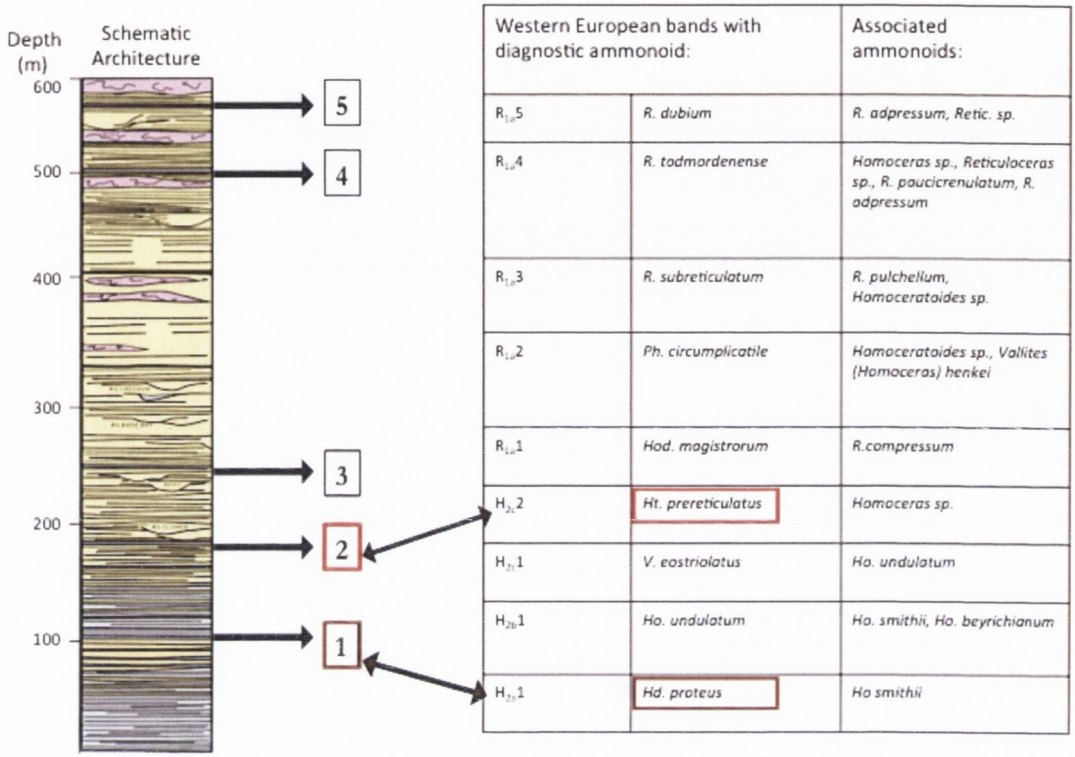

Western European bands with diagnostic ammonoid:		Associated ammonoids:
$R_{1a}5$	*R. dubium*	*R. adpressum, Retic. sp.*
$R_{1a}4$	*R. todmordenense*	*Homoceras sp., Reticuloceras sp., R. paucicrenulatum, R. adpressum*
$R_{1a}3$	*R. subreticulatum*	*R. pulchellum, Homoceratoides sp.*
$R_{1a}2$	*Ph. circumplicatile*	*Homoceratoides sp., Vallites (Homoceras) henkei*
$R_{1a}1$	*Hod. magistrorum*	*R.compressum*
$H_{2c}2$	*Ht. prereticulatus*	*Homoceras sp.*
$H_{2c}1$	*V. eostriolatus*	*Ho. undulatum*
$H_{2b}1$	*Ho. undulatum*	*Ho. smithii, Ho. beyrichianum*
$H_{2a}1$	*Hd. proteus*	*Ho smithii*

Fig. 5.13. Comparison of Shannon Basin ammonoid bands (the five main highly-condensed sections are shown in the Ross Sandstone Formation schematic architecture) with Pennine Basin ammonoid bands (modified after Waters & Condon 2012).

5.7 Analytical techniques

5.7.1 QEMSCAN analysis

Methodology and aims

QEMSCAN (Quantitative Evaluation of Materials by Scanning Electron Microscopy) is a microanalysis system that images rocks and provides information on which minerals are present in a sample (mineralogy) and how they occur spatially (microtexture). It uses both scanning electron microscopy (SEM) and energy-dispersive X-ray spectrometry (EDS) in order to generate mineral maps and images. X-ray emission spectra are used to classify mineralogy and mineral identities are assigned to each measurement point (pixel by pixel) by comparing the signals against a database (Ayling *et al.* 2012; Gottlieb *et al.* 2000). Analyses were carried out by Rannveig Litlabø and Ørjan Bjorøy at QEMSCAN facilities at Statoil Lab, Bergen, Norway. Results were interpreted in collaboration with Simon Barker, Statoil.
For each of the three phases of study described below, samples were prepared as epoxy stubs, polished and analyzed. The QEMSCAN analyses were performed using a Quanta FEG 650F scanning electron microscope (SEM) equipped with two Bruker XFlash 5030 EDS detectors.

The overall aim of QEMSCAN analysis in the present study was to test its use as an aid to biostratigraphic and lithostratigraphic correlation within the Ross Sandstone Formation. Three phases of study were completed and details of each are presented below.

QEMSCAN Phase 1

Phase 1 analysed four samples (Table 5.10) from Shannon Basin borehole material held at the Statoil core store, Bergen, Norway. The aim of Phase 1 was to perform an initial test that would check for mineralogical differences and any general trends from a selection of samples from the main highly-

condensed sections (with a maximum of one sample per condensed section). Shale rather than silt was preferentially sampled in order to maintain lithological consistency.

Core number-depth in m	Sample name	Sample from: Core/Outcrop	Description
Q05RE-20.20	Sample 1	Core	Reading Room band
Q01-47.73	Sample 2	Core	*Ph. circumplicatile* band
Q02-73.92	Sample 3	Core	*Ph. paucicrenulatum* band
Q05PROT-82.70	Sample 4	Core	*Hud. proteus-Ho. smithii* band

Table 5.10. QEMSCAN Phase 1 samples with associated borehole depths and descriptions.

Results

Phase 1 results (Figs. 5.14-5.15) show minor mineralogical differences between the four samples, mainly in mica and quartz. However, given that pyrite is a diagenetic mineral that may be masking the variations among the other detrital minerals, it was deemed necessary to normalize results with respect to pyrite. Indeed, once results are normalized, the differences in mineralogy are minimal (Figs. 5.16-5.20 show details of normalized results).

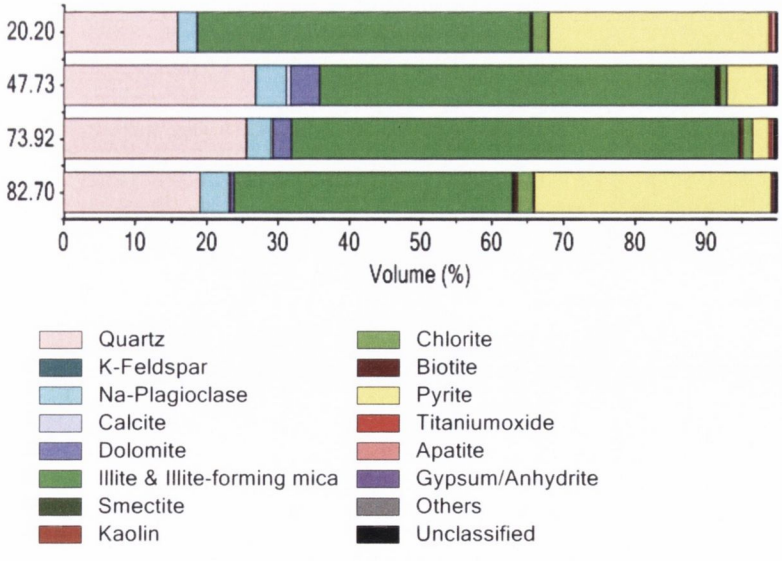

Fig. 5.14. Mineralogical composition of Phase 1 samples (volume %) with relative core depth of each sample (Samples 1 to 4).

Depth (m)	Sample 1 20.20	Sample 2 47.73	Sample 3 73.92	Sample 4 82.70
Quartz	15,8	26,8	25,6	19,0
K-Feldspar	0,0	0,0	0,0	0,0
Na-Plagioclase	2,7	4,3	3,4	4,1
Calcite	0,0	0,6	0,3	0,2
Dolomite	0,1	4,1	2,6	0,5
Illite & Illite-forming mica	46,7	55,5	62,7	39,1
Smectite	0,1	0,3	0,2	0,3
Kaolin	0,2	0,3	0,3	0,4
Chlorite	2,1	0,9	1,3	2,2
Biotite	0,2	0,1	0,0	0,2
Pyrite	30,8	5,8	2,3	33,2
Titaniumoxide	0,3	0,3	0,4	0,3
Apatite	0,6	0,3	0,3	0,2
Gypsum/Anhydrite	0,1	0,3	0,1	0,2
Others	0,0	0,0	0,0	0,0
Unclassified	0,2	0,3	0,4	0,2

Fig. 5.15. Volume % mineralogy for Phase 1 samples.

	Sample 1 20.20	Sample 2 47.73	Sample 3 73.92	Sample 4 82.7
Quartz	0.228654124	0.284803401	0.262295082	0.284005979
K-Feldspar	0	0	0	0
Na-Plagioclase	0.039073806	0.045696068	0.034836066	0.061285501
Calcite	0	0.006376196	0.00307377	0.002989537
Dolomite	0.001447178	0.04357067	0.026639344	0.007473842
Illite & Illite-forming mica	0.675832127	0.589798087	0.642418033	0.58445441
Smectite	0.001447178	0.003188098	0.00204918	0.004484305
Kaolin	0.002894356	0.003188098	0.00307377	0.005979073
Chlorite	0.030390738	0.009564293	0.013319672	0.032884903
Biotite	0.002894356	0.001062699	0	0.002989537
Titaniumoxide	0.004341534	0.003188098	0.004098361	0.004484305
Apatite	0.008683068	0.003188098	0.00307377	0.002989537
Gypsum/Anhydrite	0.001447178	0.003188098	0.00102459	0.002989537
Others	0	0	0	0
Unclassified	0.002894356	0.003188098	0.004098361	0.002989537

Fig. 5.16. Normalized values of volume % mineralogy for Phase 1 samples.

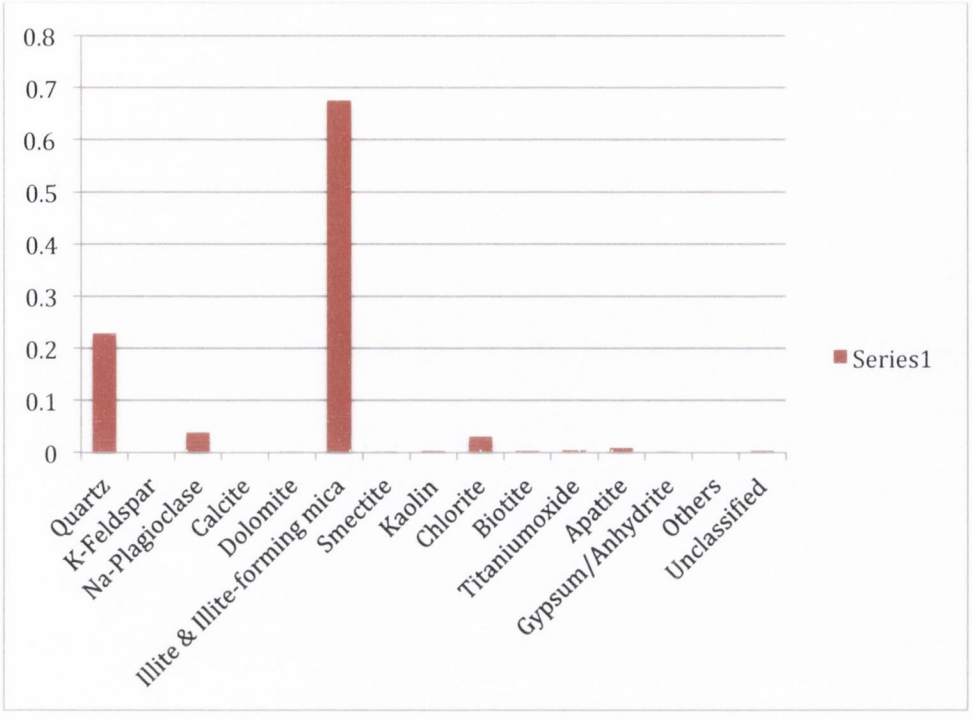

Fig. 5.17. Sample 1 normalized mineralogy (20.20 m depth in borehole 10-CE-UCD-05, sampled from the "Reading Room band").

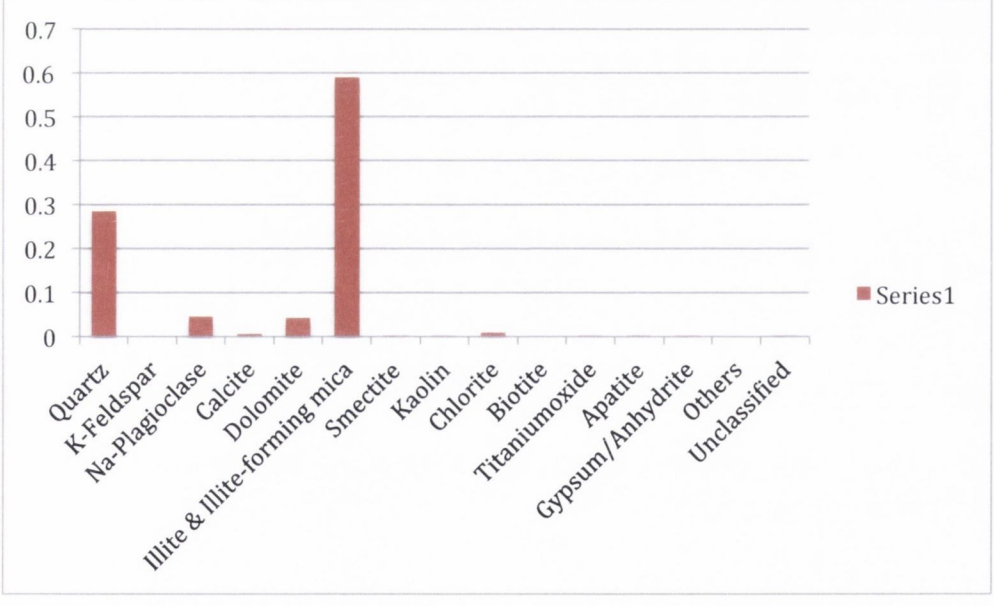

Fig. 5.18. Sample 2 normalized mineralogy (47.73 m depth in borehole 09-CE-UCD-01, from the *"Ph. circumplicatile* band".

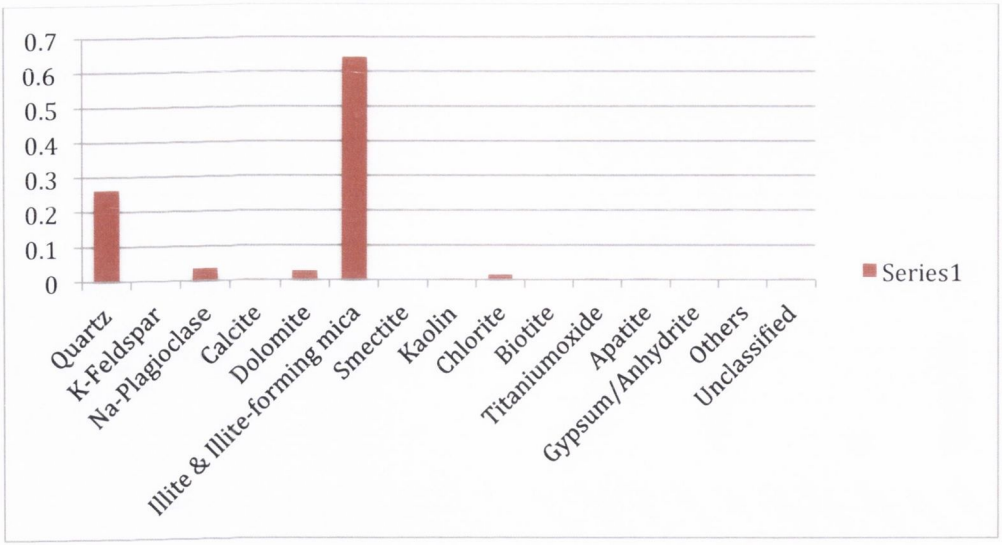

Fig. 5.19. Sample 3 normalized mineralogy (73.92 m depth in borehole 09-CE-UCD-02, from the "*Ph. paucicrenulatum* band".

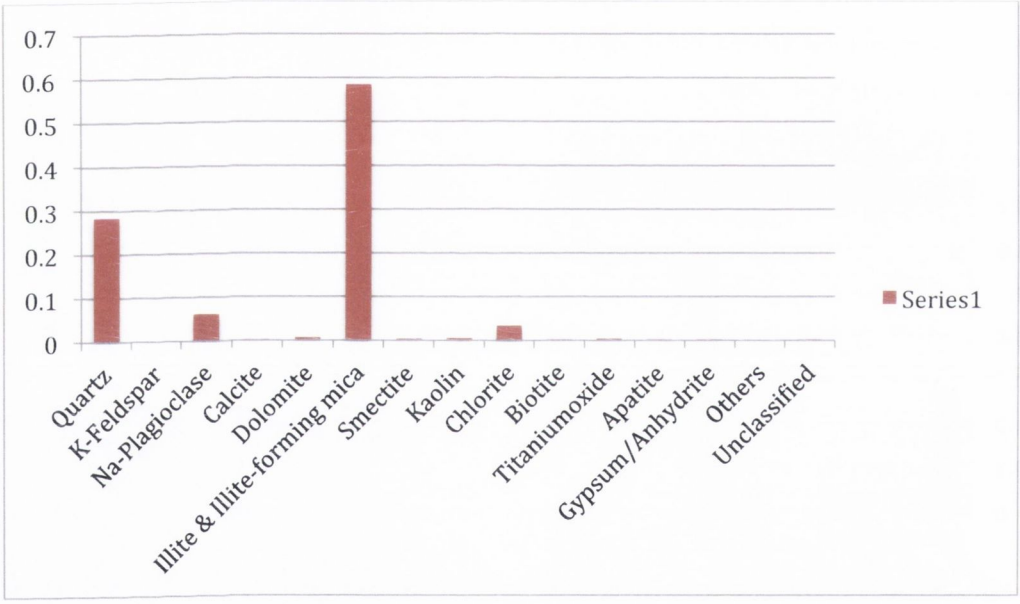

Fig. 5.20. Sample 4 normalized mineralogy (82.7 m depth from borehole 10-CE-UCD-05 part of the "*Hud. proteus-Ho. smithii* band".

QEMSCAN Phase 2

In Phase 2, samples from one condensed section were analysed in order to determine whether mineralogy varies within a single condensed section across two boreholes. Phase 2 tested for mineralogical variation within the 10 m-thick "*Hud. proteus-Ho. smithii* band", which is found in the lower Ross Sandstone

Formation stratigraphy. This band was sampled from boreholes 10-CE-UCD-05 and 10-CE-UCD-03 at the Statoil core store, Bergen, Norway (Fig. 5.21).

03 core samples (with depth in m)	05 core samples (with depth in m)
Q03-125.94	Q05-79.85
Q03-126.92	Q05-80.60
Q03-126.47	Q05-81.83
Q03-127.64	Q05-82.57
Q03-127.12	Q05-83.52
Q03-128.90	Q05-83.71
Q03-128.35	Q05-84.58
Q03-129.74	Q05-85.25
Q03-129.27	Q05-85.56
Q03-130.70	Q05-86.20
Q03-130.11	Q05-86.70
Q03-131.49	Q05-87.86
Q03-131.12	Q05-88.60
Q03-132.34	Q05-89.57

Fig. 5.21. Phase 2 samples from "*Hud. proteus-Ho. smithii* band" in boreholes 10-CD-UCD-03 and 10-CE-UCD-05.

Results

Results showed samples were dominated by illite-forming mica and quartz, with some minor mineralogical variation (Fig. 5.22). However, once again, once values were normalized with respect to pyrite (Figs. 5.23-5.24), no significant variation in mineralogy was observed within the "*Hud. proteus-Ho. smithii*" highly-condensed section. Similarly, there were no significant differences across the two boreholes where it is found.

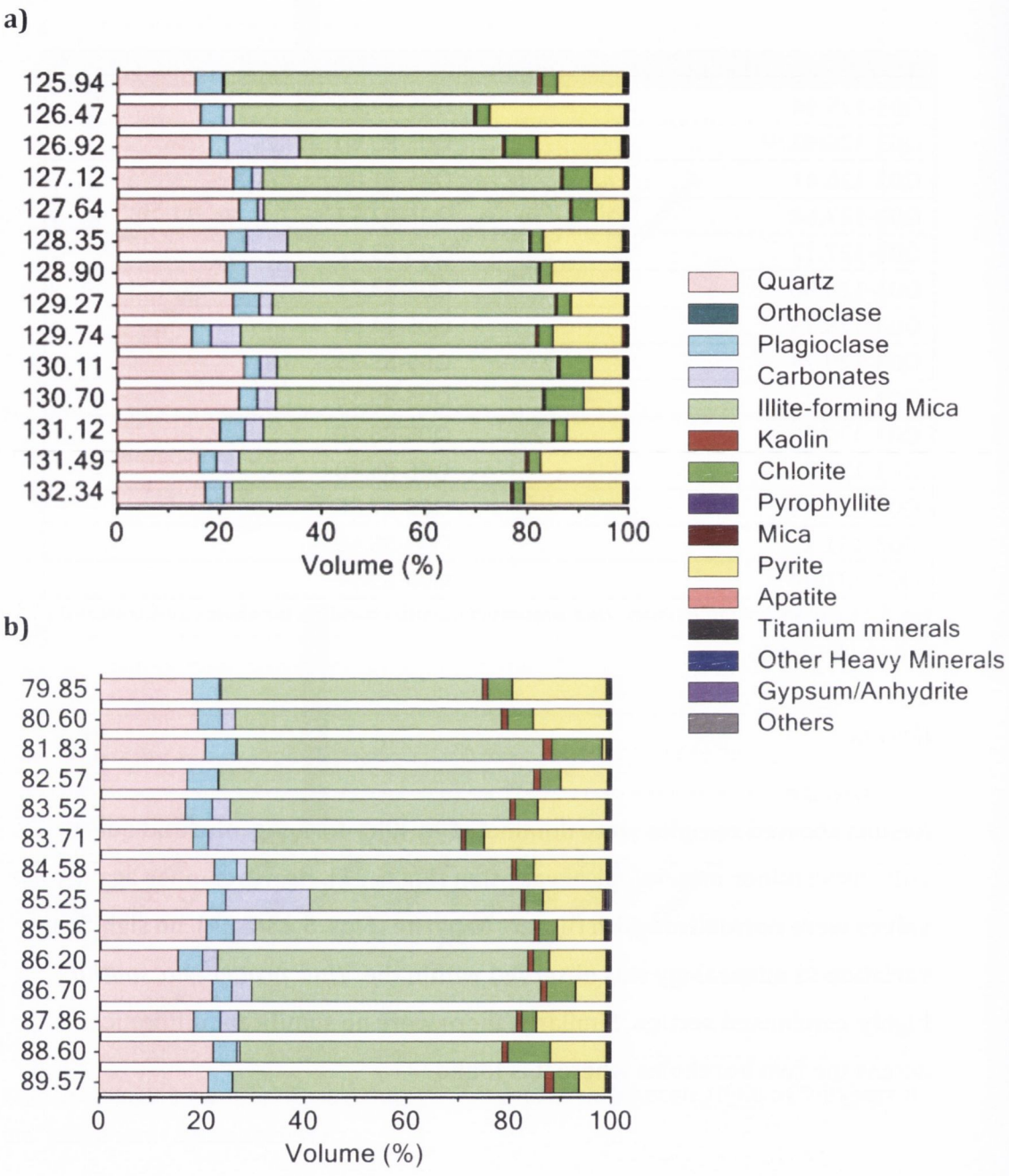

Fig. 5.22 (a) Mineralogy of samples taken from borehole 10-CD-UCD-03; (b) Mineralogy of samples taken from borehole 10-CD-UCD-05.

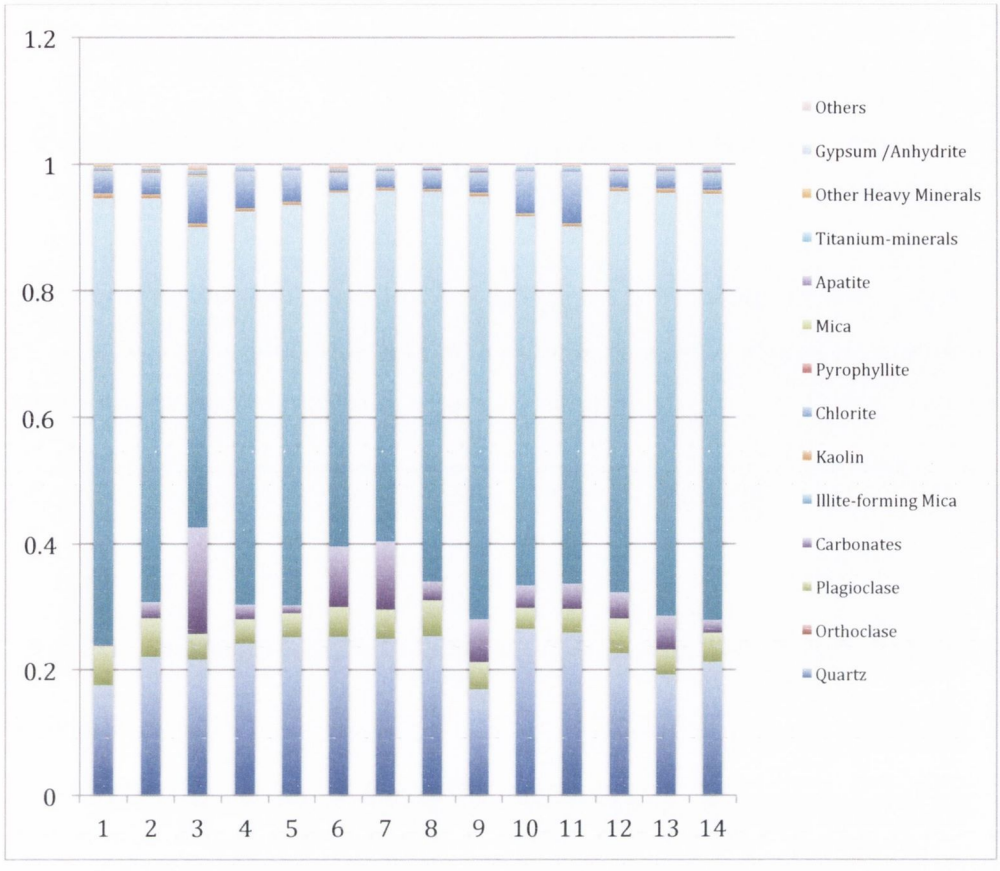

Fig. 5.23. Normalized results of Phase 2 samples from borehole 10-CE-UCD-03.

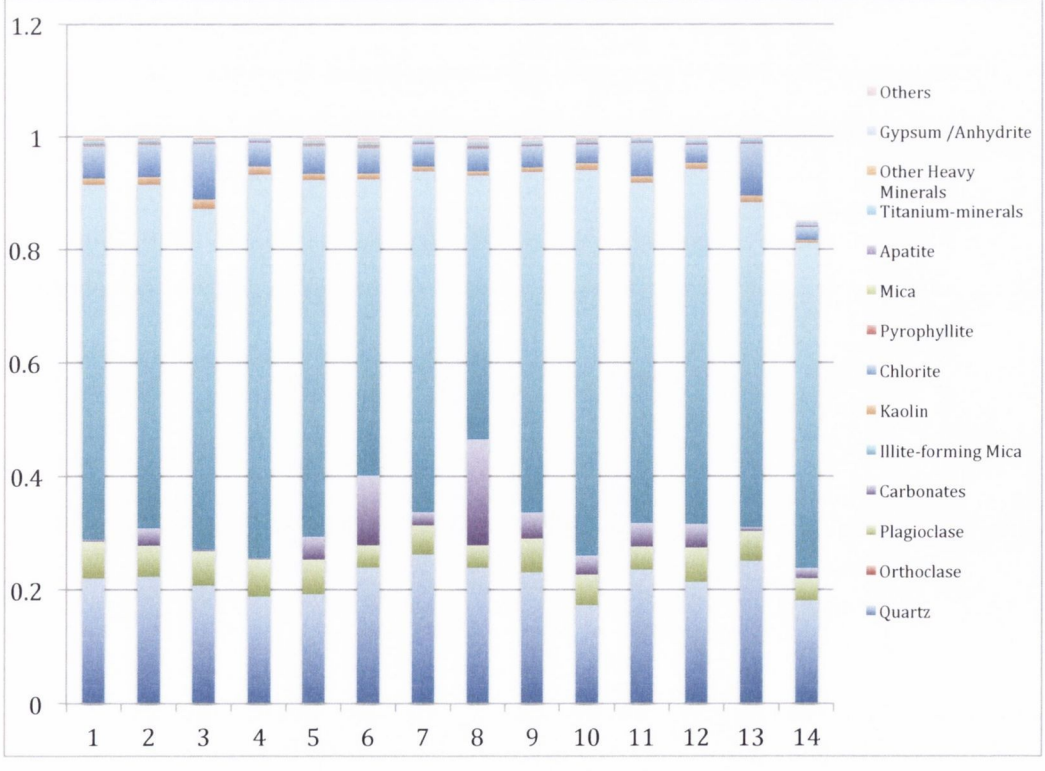

Fig. 5.24. Normalized results of Phase 2 samples from borehole 10-CD-UCD-05.

QEMSCAN Phase 3

Fourteen samples (both from borehole and outcrop material) were selected in Phase 3 of QEMSCAN analysis (Fig. 5.25). The aim of this phase was to cross-check the results of Phase 2 (which included a single condensed section) with results from other condensed sections and, in doing so, to test more completely the usefulness of the QEMSCAN method as a tool for correlation.
The samples were taken at regular intervals within the condensed section, with shale preferentially chosen over other coarser lithologies in the condensed sections.

Details of samples are as follows:

- Samples from the "*Ht. prereticulatus*" band were taken from boreholes 10-CE-UCD-03 and 10-CE-UCD-05 (three samples taken from each borehole at similar levels within the condensed sections). One sample from the outcrop section (Reading Room, R01 horizon, see Ch. 2) of the "*Ht. prereticulatus*" band was also included for comparison.
- Three samples from the "*Ph. circumplicatile*" band were taken from borehole 09-CE-UCD-01 as well as three samples from the "*Ph. paucicrenulatum*" band from borehole 09-CE-UCD-02.
- One sample from the Blackrock outcrop locality (Ch. 2: BL3 horizon) was also included due to its very pale, fine-grained lithology in hand sample, which had not been observed in any other locality or borehole sample.

Sample	Description	Core/Outcrop
Q03-55.46	*Ht. prereticulatus* band	Core
Q03-55.57	*Ht. prereticulatus* band	Core
Q03-55.96	*Ht. prereticulatus* band	Core
Q05-20.20	*Ht. prereticulatus* band	Core
Q05-20.64	*Ht. prereticulatus* band	Core
Q05-20.93	*Ht. prereticulatus* band	Core
Q-READING	*Ht. prereticulatus* band, from R01 outcrop sample	Outcrop
Q01-46.88	*Ph. circumplicatile* band	Core
Q01-47.15	*Ph. circumplicatile* band	Core
Q01-47.51	*Ph. circumplicatile* band	Core
Q02-73.99	*Ph. paucicrenulatum* band	Core
Q02-74.12	*Ph. paucicrenulatum* band	Core
Q02-74.48	*Ph. paucicrenulatum* band	Core
Q-BLACKROCK	Blackrock BL3 locality clay-rich shale	Outcrop

Fig. 5.25. Samples included in Phase 3, with sample name (including core number and depth), description and source (core or outcrop).

Results

The samples are dominated by illite and illite-forming mica (muscovite) (Figs. 5.26-5.27), with no significant differences in mineralogy between the samples. The only observed differences are minor, especially in the relative amounts of carbonate, sphalerite and apatite (Figs. 5.28-5.31).

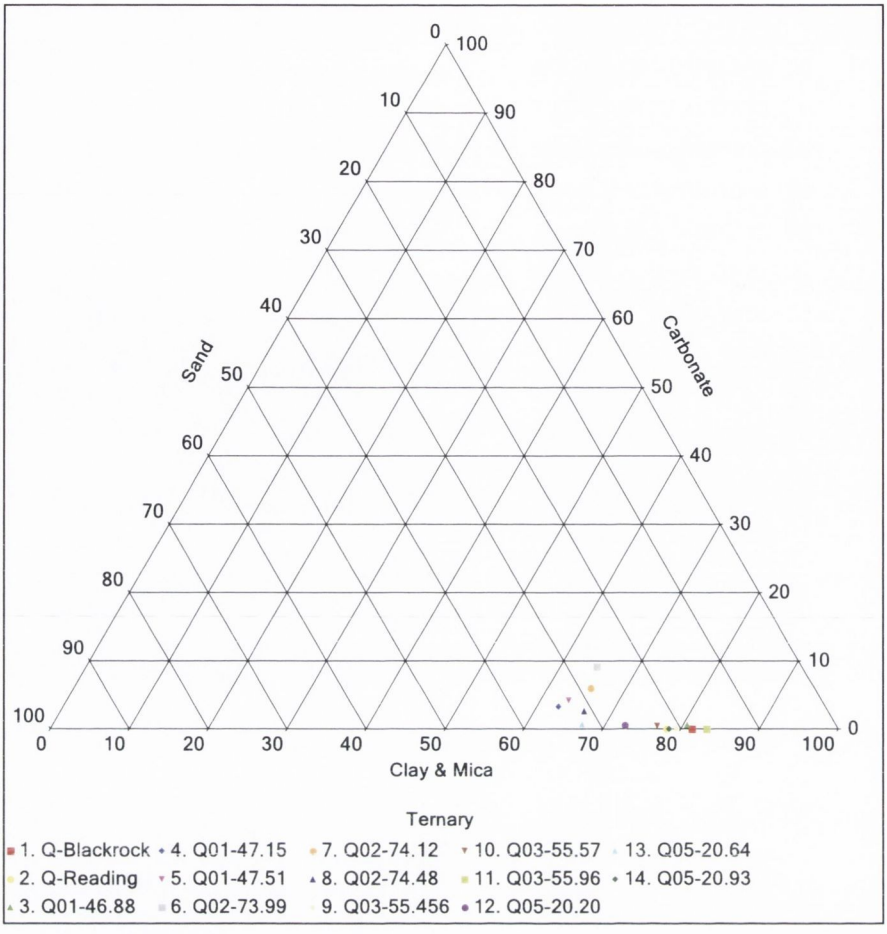

Fig. 5.26. QEMSCAN Phase 3 mineralogy results visualised in a ternary diagram with the three axes showing carbonate, sand and clay/mica. Results are normalized with respect to pyrite.

As in previous QEMSCAN phases, results were normalized with respect to pyrite. Figs. 5.26 shows results already normalized, and results before and after normalization are shown in Fig. 5.27.

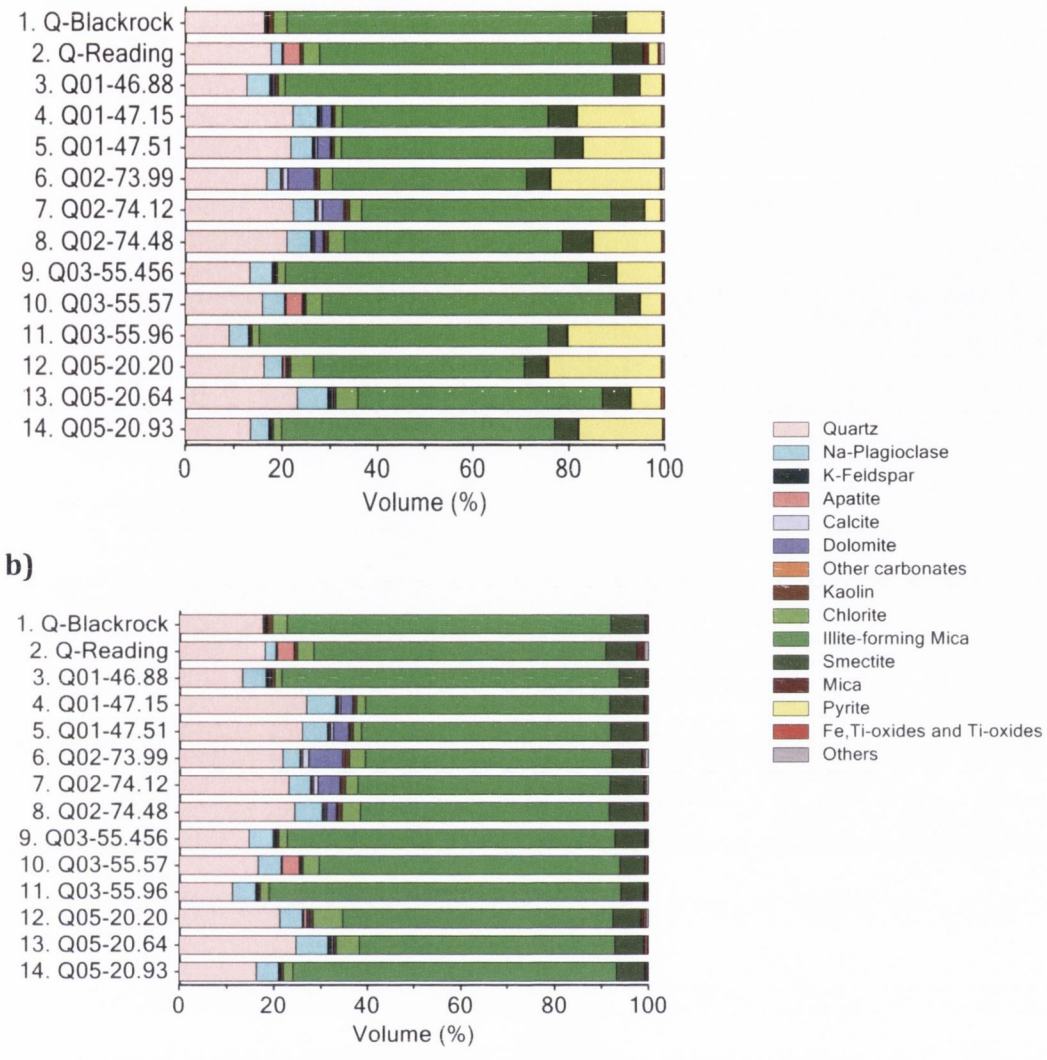

Fig. 5.27. (a) QEMSCAN Phase 3 results; (b) Results once normalized with respect to pyrite.

Carbonate (volume %) levels are greater in boreholes 09-CE-UCD-01 and 09-CE-UCD-02 than in other samples (Fig. 5.28). This may be related to porosity and is not taken as a useful result in correlation.

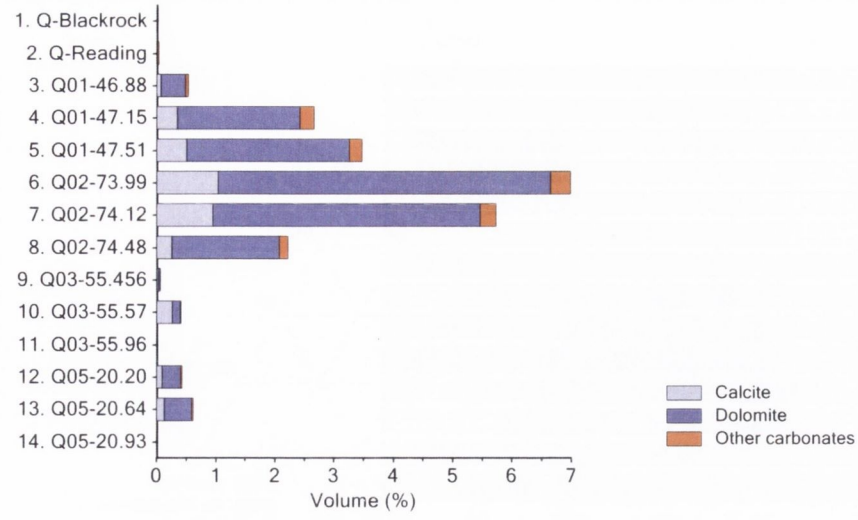

Fig. 5.28. Carbonate (dolomite, calcite and others) content (volume %) across Phase 3 samples.

Interestingly, the Reading Room band (i.e. "*Ht. prereticulatus* band"), both in outcrop (Q-Reading sample) and certain borehole intervals (Q03-55.57, Q05-20.20), has a high concentration (volume %) of apatite (Fig. 5.29). This result is also supported by the relatively high concentration of apatite in Sample 1 (20.20 m depth in borehole 10-CE-UCD-05) from Phase 1, which was also taken from the Reading Room band. This suggests apatite could have potential as a marker that may be used in correlation. It is currently unclear whether the apatite in the samples is detrital or diagenetic (conodont or fish material may be the source of apatite but this is thought to be unlikely). If it is diagenetic, it may be useful in correlation and also in dating (fission track dating).

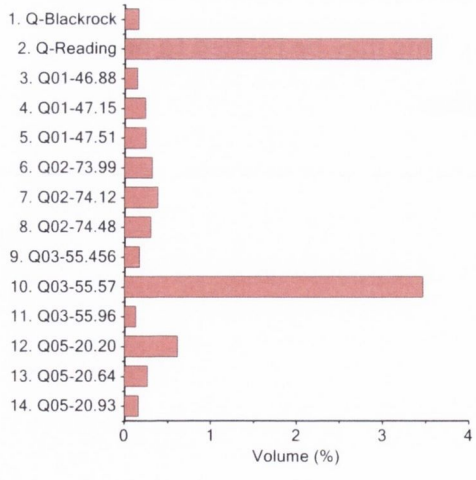

Fig. 5.29. Apatite content (volume %) across Phase 3 samples.

Sphalerite -(Zn,Fe)S- shows variation (volume %) across the samples included in Phase 3 (Fig. 5.30). In particular, sphalerite shows a distinctive trend in the "*Hd. proteus-Ho. smithii* band", with initial higher values, followed by lower values from top to base of the condensed section sampled in borehole 10-CE-UCD-03 and borehole 10-CE-UCD-05 (Fig. 5.31). Since sphalerite is not a detrital mineral, this variation is taken to reflect some local factor such as the chemistry of pore waters, or it may be related to hydrothermal activity or fractures.

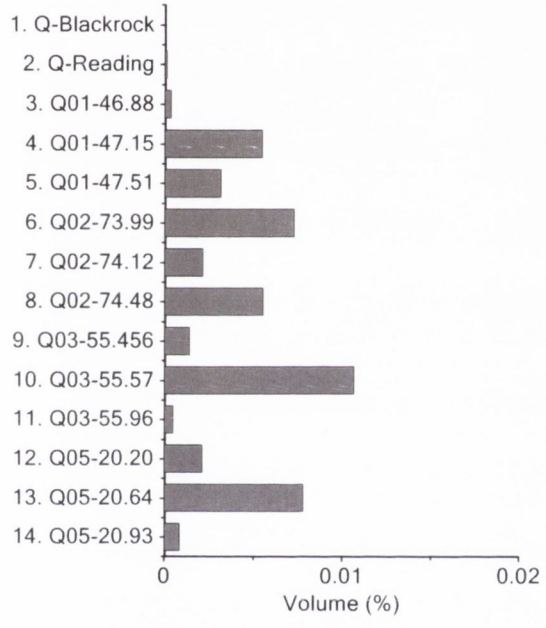

Fig. 5.30. Sphalerite concentration (volume %) across Phase 3 samples.

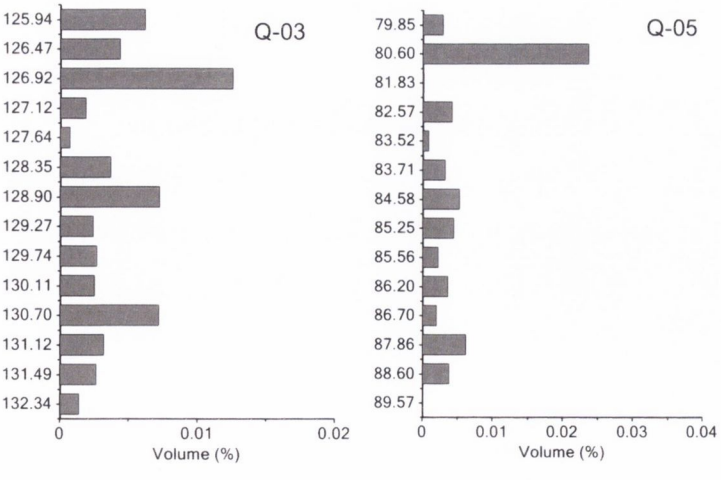

Fig. 5.31. Sphalerite concentration (volume %) across QEMSCAN Phase 2 samples from boreholes 10-CE-UCD-03 and 10-CE-UCD-05.

Summary and discussion

Phase 1 included samples from four different condensed sections. QEMSCAN results show that variations in mineralogy between the samples are probably related to variation in diagenetic minerals such as pyrite, since, when normalised with respect to these diagenetic minerals, variations become very slight. However, it is noted that information on pyrite variation may be significant and useful in local correlation studies.

Phase 2 included samples from a single condensed section, sampled in two boreholes (10-CE-UCD-03 and 10-CE-UCD-05). No significant mineralogical variations were present within this single band, and this was tested in both borehole 10-CE-UCD-03 and 10-CE-UCD-05.
While the lack of mineralogical variations within a single band is potentially useful in terms of correlations, the fact that the same was found across several condensed sections (Phase 1 results) casts doubt on the usefulness of this method in aiding correlation.

Phase 3 was undertaken to test whether the same was true in other condensed sections, when several samples were taken from each. Phase 3 included samples from both outcrop and core taken from several condensed sections, with a focus on the "*Ht. prereticulatus* band", the "*Ph. circumplicatile* band" and the "*Ph. paucicrenulatum* band".

Overall, no significant variation in mineralogy was observed in the different condensed sections, suggesting the QEMSCAN method is not useful in distinguishing different condensed sections in a deep-water fan system such as the Ross Sandstone Formation. Nevertheless, Phase 3 results have shown that apatite has potential to be a useful correlation marker in the Ross Sandstone Formation system.

5.7.1.1 Further work

While QEMSCAN results did not provide a means of distinguishing the condensed sections within the Ross Sandstone Formation, it is hoped that the results presented here will inform future studies. It is proposed that future research could follow two directions:

- The results presented above have shown that apatite has potential in aiding correlation in deep-water fan systems such as the Ross Sandstone Formation. It would be interesting to test this further both by investigating the presence of apatite across the condensed sections in the Shannon Basin and in other deep-water systems. It would also be interesting to attempt to date the apatite in order to obtain an absolute age for the sample.
- It would be interesting to replicate these analyses in other coeval basins such as the Pennine Basin, UK. For instance, sampling from another basin and analysing the "*Hud. proteus-Ho. smithii* band", which is a widespread highly-condensed section known across Britain, Ireland, France, Germany, Belgium, the south Urals and central Asia (Hodson 1957; Hodson & Leckwijck 1958), would allow to test whether mineralogy is conserved over wide lateral distances.

5.7.2 XRD analysis

Introduction and methodology

X-ray powder diffraction (XRD) analysis of samples from different condensed sections was undertaken at Trinity College Dublin laboratory facilities using a Bruker D5000 in TCD Geochemistry[1].

XRD is a non-destructive analytical technique that is used for phase identification in crystalline material. It provides information on which phases are present in a homogenized powder (Bish & Reynolds 1989).

Firstly, samples were chosen from a selection of condensed sections from core and outcrop. These were powdered in an agate pestle and mortar. Next, 0.6 – 1.0 g of each sample was placed in a bulk cavity mount and loaded into the sample changer. The x-ray source and detector were rotated by the goniometer and the intensity of the diffracted X-ray beam was recorded. Peaks in intensity are recorded when constructive interference occurs as the Bragg Equation ($n\lambda=2d\sin\theta$) is satisfied, (Bish & Reynolds 1989). Then the XRD trace was processed with dedicated software[2]. The traces were interpreted and phases were matched using a database[3].

13 samples (Table 5.11), from both outcrop and core, were analysed in order to assess their mineralogy and compare results from different condensed sections (at least one powdered sample from each condensed section was analysed).

---

[1] The Bruker D5000 has a 2.2 kW Cu long fine focus (0.4 x 12mm filament), with the following optical configuration: 2.5° primary soller, 1 mm aperture diaphragm, 1 mm scattered radiation diaphragm, no secondary soller, 0.2 mm detector diaphragm and a secondary curved graphite monochromator ahead of the scintillation counter. A scan of sample was made from 5 to 70 °2θ at a speed of 2 seconds / 0.02° step at 40 kV and 40 mA. Sample rotation was used.

[2] Bruker AXS, Diffrac.EVA software, 2012 Release, Version 3.0.

[3] International Centre for Diffraction Data, Pennsylvania, PDF-4 3+

Sample Number	XRD log book name	Sample name	Sample from: Core/ Outcrop	Description
1)	TD14_0130	X01-47.76	Core	*Ph. circumplicatile* band
2)	TD14_0132	X02-74.63	Core	*Ph. paucicrenulatum* band
3)	TD14_0124	X05RE-20.87	Core	Reading Room band
4)	TD14_0127	X05PROT-89.84	Core	*Hud. proteus-Ho. smithii* band
5)	TD14_0123	X08-55.97	Core	Dunmore west band
6)	TD14_0131	X01RETO-116.23	Core	Probable Torkeal band
7)	TD14_0121	X01RERV-187.38	Core	Probable Rinevella band
8)	TD14_0128	X05MB-1-38.60	Core	Band below Reading Room
9)	TD14_0126	XQUILTYCP	Outcrop	*Ph. circumplicatile* band
10)	TD14_0133	XCROSSPC	Outcrop	*Ph. paucicrenulatum* band
11)	TD14_0122	XKILT4	Outcrop	Kilcredaun Top band
12)	TD14_0129	XTORQUEAL	Outcrop	Torqueal band
13)	TD14_0125	XCLOONUP (CLOUB2)	Outcrop	Cloonconeen Upper band

Table 5.11. Samples analysed by XRD and description of sample location.

Results

XRD results suggest that the main mineral phases present in the samples are muscovite, quartz, pyrite and plagioclase feldspar (Table 5.12, Fig. 5.32). The peaks for sample X05PROT-89.84 (shown in Fig. 5.32) are similar to those of the other samples and are thus deemed representative (see Appendix D for full set of XRD results). Sample peaks were compared visually, in the knowledge that one of the limitations of the method is the effect of preferred crystal orientation and sample packing; in fact, when crystals take on a preferred orientation or there is a non-random pattern of crystal faces resulting from sample packing, the peak heights (especially the smaller ones) can be affected.

The main observed mineralogical variation was in pyrite and chlorite, which

was also seen in QEMSCAN results (see previous section). Since pyrite is diagenetic, it is not revealing true mineralogical variation (of detrital minerals); however, recording pyrite variation (any trends) may still be useful in order to see if it can be used for correlation in core and outcrop. Interestingly, very little pyrite is present in sample XCROSSPC, taken from the Cross "*Ph. paucicrenulatum* band" (outcrop sample), despite this band being known for its pyritized ammonoids both at this locality and further west, at Bridges of Ross, and in the core (borehole 09-CE-UCD-02). Similarly, sample X02-74.63, taken from the "*Ph. paucicrenulatum* band" in borehole 09-CE-UCD-02, contains little pyrite relative to other minerals to other samples examined in this study (see Appendix D). This suggests pyrite is concentrated in the ammonoid shells (which were not targeted during XRD study) at these localities.

Sample Number	XRD log book name	Sample name	Minerals present
1)	TD14_0130	X01-47.76	Quartz, Dolomite, Muscovite, Chlorite, Pyrite, Albite
2)	TD14_0132	X02-74.63	Quartz, Pyrite, Muscovite, Chlorite, Albite
3)	TD14_0124	X05RE-20.87	Quartz, Pyrite, Muscovite, Chlorite, Albite
4)	TD14_0127	X05PROT-89.84	Quartz, Pyrite, Muscovite, Chlorite, Albite
5)	TD14_0123	X08-55.97	Quartz, Muscovite, Chlorite, Albite, Ankerite, Pyrite
6)	TD14_0131	X01RETO-116.23	Quartz, Chlorite, Muscovite, Pyrite, Albite
7)	TD14_0121	X01RERV-187.38	Quartz, Pyrite, Chlorite, Albite, Muscovite
8)	TD14_0128	X05MB-1-38.60	Quartz, Pyrite, Chlorite, Muscovite, Albite
9)	TD14_0126	XQUILTYCP	Quartz, Muscovite, Albite, Pyrite, Dolomite, Gypsum, Chlorite
10)	TD14_0133	XCROSSPC	Quartz, Pyrite, Chlorite, Albite, Illite, Muscovite
11)	TD14_0122	XKILT4	Quartz, Muscovite, Pyrite
12)	TD14_0129	XTORQUEAL	Quartz, Muscovite, Chlorite, Albite
13)	TD14_0125	XCLOONUP (CLOUB2)	Quartz, Albite, Pyrite, Muscovite

Table 5.12. Summary table of sample and mineral presence based on XRD analysis.

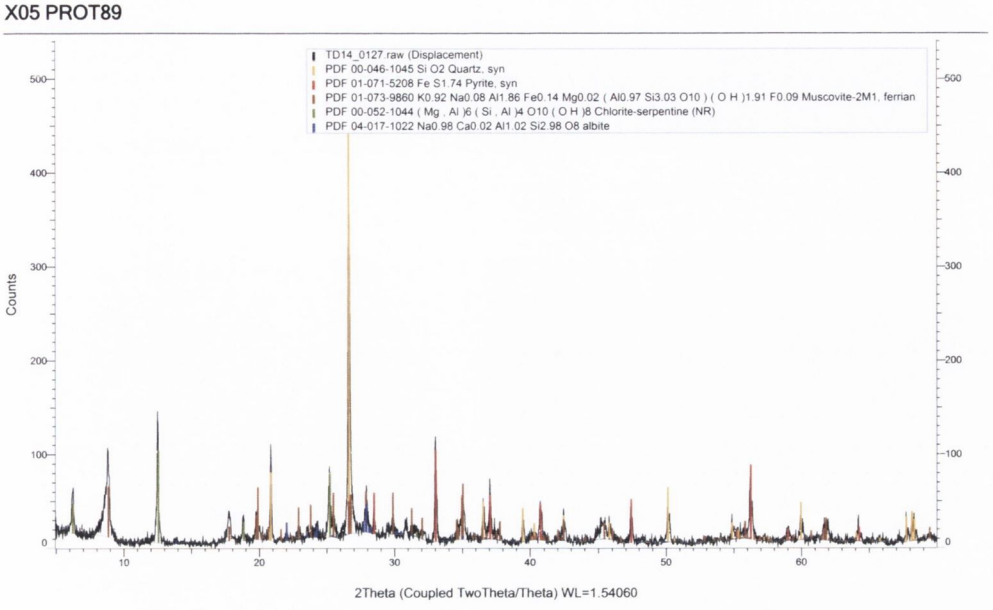

Fig. 5.32. Plot of angle (°2Θ) versus Intensity (Counts) for sample X05PROT-89.84, from the "*Hud. proteus-Ho. smithii* band" after XRD analysis. Peak positions and intensities are matched to lines from the ICDD database.

Discussion

When compared with QEMSCAN results, XRD results show similar mineralogical trends. Any differences can be attributed to orientation and packing effects. While in the QEMSCAN study data were normalised with respect to pyrite, this was not done for XRD results, in which pyrite concentration was deemed interesting (see *Results* above).

5.7.3 Further work: trace element analysis

Given the limitations of the QEMSCAN method in aiding detailed correlations within the Ross Sandstone Formation, a detailed trace element analysis of samples from core and outcrop has potential to be more useful in acting as a correlation tool. It could also provide information on palaeoenvironment including palaeoredox conditions on the seafloor. This type of analysis has yielded useful information in other basins (see e.g. Caswell & Coe 2013; Fu *et al.* 2014). It is therefore proposed that further geochemical work should be focused in this direction and results interpreted in conjunction with QEMSCAN data.

Chapter 6 Conclusions and Further Work

6.1 Taxonomy of crushed ammonoids

6.1.1 Main findings

- Most Irish Serpukhovian and Bashkirian ammonoids (E_1 to R_2 biozonal indices) are preserved as flattened moulds of the shell (2D preservation): in this case, taxonomic information necessarily comes mostly from the ornament. Once changes of ornament through ontogeny are established using 3D material, this information can then be applied to crushed material in the Shannon Basin (Ch. 3, section 3.3.2), which was previously difficult to determine.

- New systematic data on 14 Serpukhovian-Bashkirian ammonoids for which ontogenetic information was previously incomplete or lacking are presented herein (Ch. 3; also see Lacchia *et al.* 2015). This information not only furthers knowledge of the ontogeny of these ammonoids in general, but leads to more confident specific identification of ammonoids preserved as flattened external moulds.

- For the first time, ontogenetic changes in ornament are described systematically for the ammonoid taxa *V. henkei* (Schmidt, 1925), *Phillipsoceras circumplicatile* (Foord, 1903), *R. subreticulatum* (Foord, 1903), *Ph. paucicrenulatum* (Bisat & Hudson, 1943), *Homoceratoides varicatus* Schmidt, 1934, *Homoceras beyrichianum* (de Koninck, 1844), *Isohomoceras subglobosum* (Bisat, 1924) and *Homoceras smithii* (Brown, 1841).

- For the remaining six taxa, *Hodsonites magistrorum* (Hodson, 1957), *Hudsonoceras (Baschkirites) ornatus* (Foord & Crick, 1897),

Hudsonoceras proteus (Brown, 1841), *Homoceratoides prereticulatus* Bisat, 1924, *Homoceras undulatum* (Brown, 1841) and *Reticuloceras pulchellum* (Foord, 1903), diagnostic features are revised and new information for various growth stages is presented where available.

- These new data lead to more confident identifications and act as an aid to taxonomists working on crushed material, who can refer to the ornament description for a given growth stage. It is argued here that even where concretions (bullions: Hodson 1954a) are available in the outcrop, flattened ammonoids from surrounding strata record valuable information (in terms of assemblages, biostratigraphy, palaeocommunities, etc.) that ought not to be neglected despite the associated taxonomic challenges.

- This work represents a first step in advancing 2D ammonoid taxonomy, which will improve biostratigraphic resolution, with implications for large-scale ammonoid diversity and evolutionary studies.

6.1.2 Further work

- Within the R1 biozonal ammonoid indices, outstanding issues include the degree of variation within the group *Ph. circumplicatile-Ph. paucicrenulatum.*

- Further research on the taxonomy of 2D ammonoids should focus on updating existing descriptions (often limited to a single growth stage) and diagnoses. In order to achieve this, good quality 3D material needs to be available.

- In order to make large-scale advances in 2D ammonoid taxonomy, it is necessary that future ontogenetic studies based on 3D shells should encompass details of changes of ornament as well as basic conch parameters.

- Assembling a digital atlas and reference set of fossil material will aid future biostratigraphic work and preserve expertise that may otherwise be lost.

6.2 Palaeosalinity in the Shannon Basin

6.2.1 Main findings

- It has been argued that, in the Late Mississippian and Pennsylvanian basins of northwest Europe, ammonoids are restricted to the condensed sections and the bounding strata are barren due to salinity fluctuations between fully marine and less saline water.

- The cycles described in Holdsworth & Collinson (1988) for the Pennine Basin, UK, which were interpreted as recording changing salinity, from an intra-basinal peak at the lowest level to lower salinity in the upper part, have not been found during fieldwork and borehole analysis in the Shannon Basin. This may be due to differing basin topographies, as clearly more marginal areas would be expected to show salinity variation during times of sea level variation. It may be that the Shannon Basin was deeper and less susceptible to these fluctuations. Alternatively it may be due to an incorrect interpretation of the Pennine succession.

- Several new ammonoid-bearing horizons have been found in between the "marine bands" in the Shannon Basin, implying normal marine fauna during times of higher sedimentation rates between the ammonoid-rich layers.

- The presence of ammonoids at various intervals outside the condensed sections is good evidence for normal marine salinity in the Clare Shale and Ross Sandstone formations of the Shannon Basin. It suggests that the concentration of ammonoids in black shale intervals rather than in silt and sand sequences is not controlled by salinity fluctuations. Rather, their distribution is dictated by different sedimentation rates, which in turn may be a consequence of sea level change, with higher

concentrations at times of sediment starvation and fewer at times of higher sediment input.

- The new ammonoid-bearing horizons suggest that sea level could not have dropped enough to cut off the supply of marine waters to the Shannon Basin until the onset of the shallow water deltaic environments of the Central Clare Group. During deposition of the Ross Sandstone Formation, marine faunas populated the basin waters throughout deposition, including during those times that have been interpreted as representing low stands.

- What is clear from the data presented here is that the simple notion of "marine bands" as the only levels with marine fauna and "barren intervals" is no longer tenable. Furthermore, given that marine conditions persisted throughout deposition, the term "marine band" is better replaced by the term "condensed section".

- Oxygen levels in the basin are also an important consideration and are linked to salinity levels. Organic-rich, black shales, such as those in the Shannon Basin, build up when not enough organic matter is consumed via respiration (as oxygen is broken up in the decay process) (see Wignall 1994, p. 56, for a discussion on the models that can explain the co-existence of anoxia and organic matter preservation). The finding of coral, crinoid and trilobite specimens — i.e. benthic organisms — points to fluctuating oxygen levels in the basin, and suggests that the shales of the Clare Shale Formation and those of the Ross Sandstone Formation were not deposited under anoxic conditions. This adds support to the theory of an oxic/dysoxic ocean floor (also see Braithwaite 1993 for discussion).

- It is also possible that temporary oxygen-rich bottom currents allowed periodical colonization of the sea floor in Serpukhovian-Bashkirian times and that the development of a stratified water column and a

pycnocline (which would occur at times of low sea level in the emerging model of differential sedimentation described in Ch. 4) may have also been accompanied by that of a fluctuating oxycline (i.e. a changing interface between oxic and anoxic water bodies).

6.2.2 Further work

- The presence of normal marine faunas outside the condensed sections suggests that salinity values of the Shannon Basin and, by implication, other deep-water basins may well have been normal between periods of sediment starvation. The next step is to test this hypothesis by investigating other coeval successions, where it may well be the case that previous sampling efforts have focused on the condensed sections, without targeting the sedimentary successions in between.

- The salinity cycles described in Holdsworth & Collinson (1988) for the Pennine Basin, UK, build upon work by Ramsbottom (1962) on four boreholes in the Ashover area of Derbyshire. These boreholes could be reinvestigated in light of this work.

- Trace element analysis could provide further information on palaeoenvironment, including palaeoredox conditions on the seafloor.

6.3 Biostratigraphy

6.3.1 Main findings

- The present study is the first to present details of abundance and proportion of ammonoid taxa (beyond recording the presence of a given ammonoid band) at localities within the Clare Shale Formation and Ross Sandstone Formation since the work of Hodson and Lewarne (1954a,b; 1961). More than 3000 specimens from Loop Head, Ballybunion and north Clare were investigated during the course of this study and faunal assemblages from the five main highly-condensed sections in the Ross Sandstone Formation are described in detail here (Ch. 5).

- Recognition of ten ammonoid-rich horizons (including eight condensed sections) in the Ross Sandstone Formation allowed for a revised intra-Ross Sandstone Formation stratigraphic subdivision (with stratigraphic cycles/units R5 to R90 from base to top), where the condensed sections are employed as unit-bounding surfaces. The "R subdivision" (Ch. 5, Fig. 4) is used to provide a new stratigraphic framework in order to tie the Loop subsurface data to the outcrops and to reassess the stratigraphic position of some of the outcrops that were not as well constrained prior to this combined study.

- The new biostratigraphic data, coupled with the lithostratigraphical (i.e. physical) correlations resulting from parallel work at University College Dublin (UCD; see Pierce 2015), provide the most detailed dataset for the Ross Sandstone Formation to date. This allows biostratigraphy to be cross-checked against lithostratigraphical correlations and some general conclusions to be drawn.

- The resulting biostratigraphic dataset was more complex than expected at the start of the project.

- While some assemblages in condensed sections are globally distinctive (namely those indicative of the "*Hud. proteus-Ho.smithii* band" and the "*Ht. prereticulatus* band"), most are not, and some are only locally distinctive (that of the "*Ph. paucicrenulatum* band"); therefore most bands in the Ross Sandstone Formation cannot be confidently linked to a given ammonoid band in the Western European framework. In other words, this work shows that, while some bands are distinctive and useful in correlation, others are not dominated by a diagnostic ammonoid species, nor are they characterised by a diagnostic assemblage.

- This indicates that some highly condensed sections (namely the "*Hud. proteus-Ho.smithii* band" and the "*Ht. prereticulatus* band") represent widespread, global sea level rise, while others (though not different in lithology and containing faunas as abundant as those in the more distinctive condensed sections), may represent more local sea level rise.

- Overall, ammonoid biostratigraphy for the Ross Sandstone Formation was not as high-resolution as one might have hoped, in the sense that statistical analysis of the faunal assemblages does not always confirm that bands which are known to correlate by physical means are indeed indistinguishable. In other words, there are some cases, where there are statistical differences between assemblages in bands that are known to correlate by physical means. This suggests that even where there is a strong database, biostratigraphic correlation may not be statistically sound.

- While first appearances can be used to correlate in the lower Ross Sandstone Formation, in the mid to upper Ross Sandstone Formation it is not possible to distinguish ammonoid bands on the basis of first appearance of taxa. Similarly, assemblages become more diverse in the mid to upper Ross Sandstone Formation, starting from the third highly-condensed section upwards. There is a lack of distinctive ammonoid

bands up until the top band, the "*Ph. paucicrenulatum* band", which has a distinctive assemblage dominated by *Ph. paucicrenulatum*.

- A three-part subdivision is apparent from these data, whereby the lower Ross Sandstone Formation can be easily correlated using ammonoid bands. Conversely, in the mid- to upper Ross Sandstone Formation, ammonoid bands are thinner and sometimes split, as well as not having diagnostic assemblages. In the upper Ross Sandstone Formation, there is a return to bands that are easily correlated accompanied by a more distinctive assemblage in the topmost ammonoid band, the "*Ph. paucicrenulatum*" band. Interestingly, this three-part subdivision is mirrored in a lithological change: from a lower Ross Sandstone Formation dominated by fine grained lithologies (shale and silt) there is a switch to a sand-rich mid Ross Sandstone Formation, until the system reverts to a siltstone and slump-rich upper Ross Sandstone Formation.

- This work puts into question the validity of both intrabasinal and extrabasinal correlation using ammonoid-bearing condensed sections.

6.3.2 Further work

- The next step in furthering this work is to reinvestigate coeval ammonoid assemblages in the Pennine Basin (UK). It is expected, from this work, that assemblages in condensed sections in other basins, once re-examined, may turn out to be more complex and diverse that previously thought. Since museum records rarely record species abundance in a given locality, intensive fieldwork would be the best way to test this hypothesis.

- It would also be interesting to compare and cross check the existing biostratigraphic data set, which is reliant on crushed (2D) material, with a coeval succession with available 3D ammonoids. Given the complexity

of the ammonoid assemblages in most condensed sections in the Shannon Basin, one might expect that the ammonoid assemblages in a coeval succession may be more complex than one would have thought prior to this study.

Reference List

Amler, M.R.W. 1999. Early Carboniferous Bivalves from the central European Culm Facies. *In:* Johnston, P.A. & Haggart, J.W. (*eds.*), *Bivalves: an eon of evolution*, University of Calgary Press, Calgary, 51-67.

Arkell, W.J. 1957. Introduction to Mesozoic Ammonoidea. *In:* Moore, R.C. (*ed.*) *Treatise on Invertebrate Paleontology*. Part L, Mollusca 4, Cephalopoda-Ammonoidea. GSA and University of Kansas Press, L80–L100.

Ayling, B., Rose, P., Petty, S., Zemach, E. & Drakos, P. 2012. QEMSCAN (Quantitative Evaluation of Minerals by Scanning Electron Microscopy): capability and application to fracture characterization in geothermal systems. *Proceedings, 37th Workshop on Geothermal Reservoir Engineering, Stanford University, Stanford, California, January 30- February 1, 2012.*

Barham, M., Murray, J., Sevastopulo, G.D. & Williams, D.M. 2015. Conodonts of the genus *Lochriea* in Ireland and the recognition of the Viséan–Serpukhovian (Carboniferous) boundary. *Lethaia* **48(2),** 151–71.

Bailey, R.J. 2013. Discussion on "Nature and timing of Late Mississippian to Mid-Pennsylvanian glacio-eustatic sea-level changes of the Pennine Basin, UK". *Journal of the Geological Society*, **170**, 849.

Becker, R.T. & Kullmann, J. 1996. Paleozoic ammonoids in time and space. *In:* Landman, N.H., Tanabe, K., & Davis, R.A. (*eds.*) *Ammonoid Paleobiology.* Plenum Press, New York, 711-753.

Beyrich, E. 1837. Beiträge zur Kenntnis der Versteinerungen des Rheinischen Uebergangsgebirges. *Abhandlungen der Akademie der Wissenschaften*, 1-44.

Bisat, W.S. 1924. The Carboniferous goniatites of the North of England and their zones. *Proceedings of the Yorkshire Geological Society,* **20**, 40-124.

Bisat, W.S. 1928. The Carboniferous goniatite zones of England and their continental equivalents. *Compte Rendue Congrès International de Stratigraphie et de Géologie du Carbonifère (Heerlen 1927)*, 117–133.

Bisat, W.S. 1933. The phylogeny of the north of England goniatites. Proceedings of the Geologists' Association, **44(3)**, 255-260.

Bisat, W.S. & Hudson, R.G.S. 1943. The lower *Reticuloceras* (R_1) goniatite succession in the Namurian of the north of England. *Proceedings of the Yorkshire Geological Society,* **24**, 383-440.

Bish, D.L. & Reynolds, R.C. 1989. Sample preparation for X-ray diffraction. *Reviews in Mineralogy,* **20**, 73-99.

Butcher, N.E. & Hodson, F. 1960. A Review of the Carboniferous Goniatite Zones in Devon and Cornwall. *Palaeontology*, **3(1)**, 75-81.

Bouckaert, J. 1960. Stratigraphie et paleóntologie de la super-zone R1 dans les vallées de la Berwinne et de la Geule. *Mémoires de l'Institut Géologique de l'Université de Louvain*, **21**, 3-94, Louvain.

Bouckaert, J. 1961. Les goniatites du Carbonifère belge. *Documents pour l'Étude Paléontologie du Terrain Houiller*, 1-9, Bruxelles.

Braithwaite, K. 1993. Stratigraphy of a mid-Carboniferous section at Inishcorker, Ireland. *Annales de la Société Géologique de Belgique.* **116(2)**, 209-219.

Braithwaite, K. 1995. Stratigraphy of the mid-Carboniferous boundary. *Unpublished PhD Thesis*, University of Leeds, Department of Earth Sciences. 351pp.

Bronn, H. G., 1828, Posidonia becheri eine neue fossile Muschel der Uebergangs-Periode: Leonhard Taschenbuch fur die gesammte Mineralogie, Zeitschrift fur Mineralogie, **1(4)**, 262-269.

Brown, T. 1841. Description of some new species of fossil shells, found chiefly in the Vale of Todmorden, Yorkshire. *Transactions of the Manchester Geological Society*, **1**, 211-232, London.

Brown, T. 1849. *Illustrations of the Fossil Conchology of Great Britain and Ireland with descriptions and localities of all the species. Genus V. Goniatites.* Smith, Elder and Co. London, 28-31.

Bucher, H., Landman, N.H., Klofak, S.M. & Guex, J. 1996. Mode and rate of growth in ammonoids. *In:* Landman, N.H., Tanabe, K., & Davis, R.A. (*eds.*) *Ammonoid Paleobiology.* Plenum Press, New York, 407-461.

Calver, M.A. & Ramsbottom, W.H.C. 1961. Stratigraphical Palaeontology. *In:* Earp, J.R. *et al.* (*eds.*), *Geology of the Country around Clitheroe an Nelson. Memoir of the Geological Survey of Great Britain, Expl. one-inch Geol. Sheet 68, New Series*, 174-207, London.

Caswell, B.A. & Coe, A.L. 2013. Primary productivity controls on opportunistic bivalves during Early Jurassic oceanic deoxygenation. *Geology*, **41(11)**, 1163-1166.

Chalard, J. 1958. Découverte d'un banc à Hudsonoceras proteum Brown dans le Namurien de la région de Valenciennes. *Compte Rendu Academie Sciences Paris*, **246**, 2635-2636, Paris.

Chalard, J. 1960. Les Horizons à Goniatites du Namurien du Nord de la France. *Compte Rendu du 4e Congrès Stratigraphie et de Géologie du Carbonifère Heerlen 1958*, 87-92, Maestricht.

Chapin, M.A., Davies, P., Gibson, J.L. & Pettingill, H.S. 1994. Reservoir architecture of turbidite sheet sandstones in laterally extensive outcrops, Ross Formation, Western Ireland. *GCSSEPM Foundation 15th Annual Research Conference, Submarine Fans and Turbidite Systems*, December 4-7, 1994.

Clayton, G., Haughey, N., Sevastopulo, G.D. & Burnett, R. 1989. *Thermal maturation levels in the Devonian and Carboniferous rocks in Ireland.* Geological Survey of Ireland, 36pp.

Clayton, G. & Baily, H. 1999. Organic maturation levels of pre-Westphalian Carboniferous rocks in Ireland and in the Irish offshore. *Neues Jarbuch für Geologie und Paläontologie*, **107**, 25-41.

Collinson, J.D. 1988. Controls on Namurian sedimentation in the Central Province Basins of northern England. *In*: Besly, B.M. & Kelling, G. (*eds.*) *Sedimentation in a synorogenic basin complex: the Upper Carboniferous of northwest Europe.* Blackie, Glasgow, 85–101.

Collinson, J.D., Martinsen, O. Bakken, B. & Kloster, A. 1991. Early fill of the western Irish Namurian Basin: a complex relationship between turbidites and deltas. *Basin Research*, **3**, 223-242.

Davies, S., Hampson, G., Flint, S. & Elliott, T. 1999. Continental-scale sequence stratigraphy of the Namurian, Upper Carboniferous and its applications to reservoir prediction. *In*: Fleet, A.J. & Boldy, S.A.R. (*eds.*) *Petroleum Geology of Northwest Europe: Proceedings of the 5th Conference,* 757-770.

Davies, S.J. 2008. The record of Carboniferous sea-level change in low-latitude sedimentary successions from Britain and Ireland during the onset of the late

Paleozoic ice age. *In:* Fielding, C.R., Frank, T.D., & Isbell, J.L. (*eds.*) *Resolving the Late Paleozoic ice age in time and space.* Geological Society of America Special Paper, **441**, 187-204.

Davies, S.J., Guion, P.D. & Gutteridge, P. 2012. Carboniferous sedimentation and volcanism on the Laurussian Margin. *In:* Woodcock, N.H. & Strachan, R. (*eds.*) *Geological History of Britain and Ireland, Second Edition.* Chichester: Wiley-Blackwell, 73-231.

Davreux, C.J., 1833. Essai sur la composition géognostique de la province de Liège. *Mémoires couronnés de l'Académie royale des Sciences et BellesLettres de Bruxelles*, **9**, 1-297.

Demanet, F. 1941. Faune et Stratigraphie de l'Étage Namurien de la Belgique. *Mémoires du Musée Royal d`Histoire Naturelle de Belgique*, **97**, 1-327

Dzik, J. 1997. Emergence and succession of Carboniferous conodont and ammonoid communities in the Polish part of the Variscan sea. *Acta Palaeontologica Polonica*, **42(1)**, 57-170.

Engeser, T. 1996. The Position of the Ammonoidea within the Cephalopoda. *In:* Landman, N.H., Tanabe, K., & Davis, R.A. (*eds.*) *Ammonoid Paleobiology.* Plenum Press, New York, 3-19.

Elliott, T. 2000a. Depositional architecture of a sand-rich, channelized turbidite system: the Upper Carboniferous Ross Sandstone Formation, western Ireland. *In:* Weimer, P. *et al. (eds.), Deep-Water Reservoirs of the World, Gulf Coast Section SEPM Foundation, 20th Annual Research Conference,* 342-373.

Elliott, T. 2000b. Megaflute erosion surfaces and the initiation of turbidite channels. *Geology*, **28**, 119-122.

Fallon, P. & Murray, J. 2015. Conodont biostratigraphy of the mid-Carboniferous boundary in Western Ireland. *Geological Magazine*, available on CJO2015. doi:10.1017/S0016756815000072.

Fielding, C.R., Frank, T.D., Birgenheier, L.P, Rygel, M.C., Jones, A.T., & Roberts, J. 2008. Stratigraphic imprint of the Late Palaeozoic ice age in eastern Australia: a record of alternating glacial and nonglacial climate regime. *Journal of the Geological Society, London,* **165**, 129-140.

Fitzgerald, E., Feely, M., Johnston, J.D., Clayton, Fitzgerald, L.J. & Sevastopulo, G.D. 1994. The Variscan thermal history of west Clare, Ireland. *Geological Magazine,* **131**, 545-558.

Foord, A.H. 1903. Monograph of the Carboniferous Cephalopoda of Ireland, Part V, Containing the families Glyphioceratidae (concluded) and Prolecanitidae. *Palaeontographical Society*, **57**, 147-234, London.

Foord, A.H. & Crick, G.C. 1897. *Catalogue of the fossil Cephalopoda in the British Museum (Natural History). Part III, containing the Bactritidae and part of the Suborder Ammonoidea.* 1-303. London.

Frank, T.D., Birgenheier, L.P, Montañez, I.P., Fielding, C.R., Rygel, M.C. 2008. Late Paleozoic climate dynamics revealed by comparison of ice-proximal stratigraphic and ice-distal isotopic records. *In:* Fielding, C.R., Frank, T.D., and Isbell, J.L. (*eds.*) *Resolving the Late Paleozoic ice age in time and space.* Geological Society of America Special Paper, **441**, 331-342.

Frech, F. 1899. *Lethaea geognostica, Teil 1: Lethaea palaeozica, Band 2, Lieferung 2: Die Steinkohlenformation.*Stuttgart (Schweizerbart), 257-452.

Fu, X., Tan, F., Feng, X., Wang, D., Chen, W., Song, C. & Zeng, S. 2014. Early Jurassic anoxic conditions and organic accumulation in the eastern Tethys. *International Geology Review*, **56(12)**, 1450-1465.

Furnish, W.M. & Knapp, W.D. 1966. Lower Pennsylvanian fauna from Eastern Kentucky; Part 1, Ammonoids. *Journal of Paleontology*, **40**, 296-308.

Gill, W.D. 1979. Syndepositional sliding and slumping in the West Clare Namurian Basin, Ireland. *Geological Survey of Ireland Special Paper*, **4**, 1-31.

Gill, W.D. & Kuenen, P.H. 1958. Sand volcanoes on slumps in the Carboniferous of County Clare. *Quarterly Journal of the Geological Society of London*, **133**, 441-460.

Girty, G.H. 1909. The fauna of the Caney Shale of Oklahoma, *Bulletin, U.S. Geological Survey*, **377**, 1-106.

Gordon, M.J. 1964. Carboniferous Cephalopods of Arkansas. *Professional Papers, U.S. Geological Survey*, **460**, 1-322, Washington.

Gottlieb, P., Wilkie, G., Sutherland, D., Ho-Tun, E., Suthers, S., Perera, K., Jenkins, B., Spencer, S., Butcher, A., & Rayner, J. 2000. Using Quantitative Electron Microscopy for Process Mineralogy Applications. *Journal of the Minerals, Metals and Materials Society*, **52(4)**, 24-25.

Goodhue, R. 1996. A palynofacies, geochemical and maturation history of the Namurian rocks of County Clare. *Unpublished PhD thesis*, Trinity College Dublin, 168pp.

Goodhue, R. and Clayton, G. 1999. Organic maturation levels, thermal history and hydrocarbon source rock potential of the Namurian rocks of the Clare Basin, Ireland. *Marine and Petroleum Geology*, **16**, 667-675.

Gradstein, F.M., Ogg, J.G. & Smith, A.G. (*eds.*) 2004. *A geologic timescale.* Cambridge University Press, 589pp.

Gradstein, F.M., Ogg, J.G., Smith, A.G. & Ogg, G. (*eds.*) 2012. *The geologic timescale 2012*. Elsevier, 1176pp.

Graham, J.R. 2009. Variscan deformation and metamorphism. *In*: Holland, C.H. and Sanders, I.S. (*eds.*) *The Geology of Ireland*. Dunedin Academic Press, 295-310.

Graham, J.R. 2015. The Shannon Basin: structural setting and evolution. *In:* Best, J.H. & Wignall, P.B. (*eds.*) A field guide to the Carboniferous sediments of the Shannon Basin, western Ireland. Wiley on behalf of IAS, *in press.*

Hampson, G.H., Elliott, T. & Davies, S.J. 1997. Application of sequence stratigraphy to Upper Carboniferous fluvio-deltaic strata of the onshore UK and Ireland: implications for the southern North Sea. *Journal of the Geological Society, London,* **154**, 719-733.

Haug, E. 1898. Études sur les goniatites. *Mémoires de la Societé Géologique de France*, **18**, 1-112.

Haughton, P. 2009. The Ross Formation on Loop Head, SW County Clare, Ireland. *Super Sedimentological Exposures, International Association of Sedimentologists,* Newsletter **224**.

Haughton, P., Davis, C., Mccaffrey, W. & Barker, S. 2009. Hybrid sediment gravity flow deposits- classification, origin and significance. *Marine and Petroleum Geology*, **26(10)**, 1900-1918.

Hind, W. 1905. Notes on the homotaxial equivalents of the beds which immediately succeed the Carboniferous Limestone in the west of Ireland. *Proceedings of the Royal Irish Academy*, **25** (sect. B), 93-116.

Hind, W. 1918. On the distribution of the British Carboniferous Goniatites, with a description of one new genus and some new species. *Geological Magazine*, **5(10)**, 434-450.

Higgs, K. 1986. The Stratigraphy of the Namurian Rocks of the Leinster Coalfield. *Geological Survey of Ireland Bulletin*, **3,** 257-276.

Higgs, R. 2009. Multiscale stratigraphic analysis of a structurally confined submarine fan: Carboniferous Ross Sandstone, Ireland: Discussion. *AAPG Bulletin*, **93(12)**, 1705-1709.

Hodson, F. 1954a. The beds above the Carboniferous Limestone in North-West County Clare, Eire. *Quarterly Journal of the Geological Society of London*, **109**, 259-283.

Hodson, F. 1954b. The Carboniferous rocks of Foynes Island, County Limerick. *Geological Magazine*, **91(2),** 153-160.

Hodson, F. 1954c. A new species of *Dimorphoceras* from the *Homoceras* Zone of the Irish Millstone Grit. *Annals and Magazine of Natural History*, **12(7)**, p. 362.

Hodson, F. 1957. Marker horizons in the Namurian of Britain, Ireland, Belgium and Western Germany. *Association pour l'Etude de Paléontologie et de la Stratigraphie Houillères*, **24**, 26pp.

Hodson, F. & Leckwijck, F. 1958. A Namurian marker horizon at Büsbach near Aachen, western Germany. *Association pour l'Etude de Paléontologie et de la Stratigraphie Houillères,* **35**, 13pp.

Hodson, F. & Lewarne, G.C. 1961. A mid-Carboniferous (Namurian) basin in parts of the counties of Limerick and Clare, Ireland. *Quarterly Journal of the Geological Society of London*, **117**, 307-333.

Holdsworth, B.K. & Collinson, J.D. 1988. Millstone Grit cyclicity revisited. *In:* Besly, B.M. & Kellig, G. (*eds.*) *Sedimentation in a Synorogenic Basin Complex- the Upper Carboniferous of Northwest Europe*, 132-152.

House, M.R. 1985. Class Cephalopoda. *In*: Murray, J.W. (*ed.*), *Atlas of invertebrate macrofossils*, 114-152.

Hudson, R.G.S. & Cotton, G. 1943. The Lower Carboniferous in a boring at Alport, Derbyshire. *Proceedings of the Yorkshire Geological Society*, **25**, 254-311.

Hyatt, A. 1884. Genera of fossil cephalopods. *Boston Society of Natural History, Proceedings*, **22**, 253-338, Boston, Massachussetts.

Jacobs, D.K. 1992. Shape, drag, and power in ammonoid swimming. *Paleobiology*, **18(2)**, 203-220.

Karpinskii, A.P. 1889. Über die Ammoneen der Artinsk-Stufe und einige mit denselben verwandte carbonische Formen. *Mémoires de l'Académie Impériale des Sciences de St.-Pétersbourg, VIIe Série,* **37 (2)**, 1-104.

Kelk, B. 1960. Studies in the Carboniferous Stratigraphy of Western Eire. *Unpublished PhD thesis*, University of Reading. Part 1: 43pp., Part 2: 73pp.

Klug, C. & Korn, D. 2004. The origin of ammonoid locomotion. *Acta Palaeontologica Polonica,* **49(2)**, 235–242.

Klug, C., Korn, D., Landman, N. H., Tanabe, K., De Baets, K., and Naglik, C. Describing Ammonoid Conchs. 2015. *In:* Klug, C. et al. (eds.) Ammonoid Paleobiology: From Anatomy to Ecology, Topics in Geobiology 43, DOI 10.1007/978-94-017-9630-9_1.

Koninck, L. G. de 1843. *Description des animaux fossiles qui se trouvent dans le*

terrain carbonifère de la Belgique. 1-650, Liège.

Koninck, L. G. de 1885. Faune du calcaire Carbonifere de la Belgique. Lamellibranches. *Annales Mus. Hist. Nat. Belgique*, **11**, 285pp.

Korejwo, K. 1986. Biostratigraphy of the Carboniferous deposits of the Swidnik blocks (Lublin Coal Basin). *Acta Geologica Polonica*, **36(4),** 337-346, Warszawa.

Korn, D. 1997. The Palaeozoic ammonoids of the South Portuguese Zone. *Memórias do Instituto Geologico e Mineiro*, Lisboa, **33**, 1-131.

Korn, D., Klug, C. & Mapes, R.H. 2005. The Lazarus Ammonoid Family Goniatitidae, the Tetrangularly Coiled Entogonitidae, and Mississippian Biogeography. *Journal of Paleontology*, **79(2)**, 356-365.

Korn, D. 2010. A key for the description of Palaeozoic ammonoids. *Fossil Record*, **13(1),** 5-12.

Korn, D., Kulagina, E., Lane, R., Mamet, B., Nemyrovska, T., Nikolaeva, S.V., Pazukhin, V., Qi, Y.P., Sanz-López, J., Saltzman, M. R., Titus, A., Utting, J. & Wang, X. 2011. Report of the Task Group to establish a GSSP close to the existing Viséan–Serpukhovian boundary. *Newsletter on Carboniferous Stratigraphy,* **29**, 26–30.

Korn, D., Titus, A.L., Ebbighausen, V., Mapes, R.H. & Sudar, M.N. 2012. Early Carboniferous (Mississippian) ammonoid biogeography. *Geobios*, **45**, 67-77.

Kulicki, C. 1996. Ammonoid shell microstructure. *In:* Landman, N.H., Tanabe, K., & Davis, R.A. (*eds.*) *Ammonoid Paleobiology.* Plenum Press, New York, 65-101.

Kullmann, J. 1980. Carboniferous goniatites. *In*: House, M.R. & Senior, J.R. The Ammonoidea, *Systematics Association Special Volume*, **18**, 37-48, Academic Press, London and New York.

Lambeck, K. 2005. The Earth's variable rotation: geophysical causes and consequences. *Cambridge University Press*, 453pp.

Lacchia, A.R. 2012. Goniatites Explained. *Geology Today*, **28(5)**, 192-196.

Lacchia, A.R., Sevastopulo, G.D.S., & Graham, J.R. 2015. Mid Carboniferous Ammonoids from the Shannon Basin, Western Ireland: identification of crushed material. *Swiss Journal of Palaeontology.* Available online at: *http://link.springer.com/article/10.1007/s13358-015-0090-1*, DOI: 10.1007/s13358-015-0090-1.

Landman, N.H., Tanabe, K., & Davis, R.A. 1996. *Ammonoid Paleobiology.* Plenum Press, New York, 857pp.

Leeder, M.R. 1976. Sedimentary facies and the origins of basin subsidence along the northern margin of the supposed Hercynian Ocean. *Tectonophysics*, **36**, 167-179.

Leeder, M.R. 1982. Upper Palaeozoic basins of the British Isles: Caledonide inheritance versus Hercynian plate margin processes. *Journal of the Geological Society of London*, **139**, 479-491.

Leeder, M.R. & Mc Mahon, A.H. 1988. Upper Carboniferous (Silesian) basin subsidence in northern Britain. *In:* Besly, B.M. and Kelling, G. (*eds.*) Sedimentation in a synorogenic basin complex: the Upper Carboniferous of Northwest Europe. Blackie, Glasgow, 43-52.

Leggewie, W. & Schonefeld, W. 1957. Fauna und Flora aus dem Ziegeleisteinbruch Uhlenbruch in Wuppertal-Nächstebreck. *Neues Jahrbuch für Mineralogie, Geologie und Paläontologie, Abhandlungen*, **105**, 231-238.

Lehmann, U. 1981. *The ammonites: their life and their world.* Cambridge University Press. 246pp.

Lemosquet, Y., Conrad, J. & Manger, W.L. 1985. Ammononoids. In Diaz, M. et al. (Eds.), *The Carboniferous of the World, 2. International Union of Geological Sciences Publication*, **20**, 367-372, Madrid.

Lewarne, G.C. 1959. The junction of the Upper and Lower Carboniferous in County Clare and County Limerick, Eire. *Unpublished PhD Thesis.* University of Reading. 172pp.

Librovitch, L.S. 1957. O nekotorykh novykh gruppakh goniatitov iz kamennougol'nykh otlozhenii SSSR. *Ezhegodnik vesuyuznogo paleontologicheskogo obshchestva*, **16**, 246-273, Moskva.

Lien T., Walker, R. G., & Martinsen, O. J. 2003. Turbidites in the Upper Carboniferous Ross Formation, Western Ireland - reconstruction of a sinuous channel and sandy spillover system, *Sedimentology*, **50**, 113-148.

Manger, W.L., Weyant, M., & Pareyn, C. 1985. Mid-Carboniferous ammonoid biostratigraphy, Bechar Region, Algeria. *Courier Forschungsinstitut Senckenberg*, **74**, 181-196, Frankfurt am Main.

Martinsen, O.J. 1989. Styles of soft sediment deformation on a Namurian (Carboniferous) delta slope, western Ireland Namurian Basin, Ireland. In: Whatley, M.K.G. & Pickering, K.T. (*eds.*), *Deltas: sites and traps for fossil fuels* (pp. 167-177). Geological Society Special Publication, **41.**

Martinsen, O.J. & Bakken, B. 1990. Extensional and compressional zones in slumps and slides in the Namurian of County Clare, Ireland. *Journal of the Geological Society of London*, **147**, 153-164.

Martinsen, O.J., Collinson, J.D. & Holdsworth, B.K. 1995. Millstone Grit cyclicity revisited, II: sequence stratigraphy and sedimentary responses to changes of relative sea-level. *In*: Plint, A.G. (ed.) *Sedimentary Facies Analysis*. International Association of Sedimentologists, Special Publication, **22**, 305–327.

Martinsen, O.J. & Collinson, J.D. 2002. The Western Irish Namurian Basin reassessed- a discussion. *Basin Research*, **14**, 523-542.

Matthews, S.C. 1993 Notes on open nomenclature and on synonymy lists. *Palaeontology*, **16(4)**, 713-719.

Maynard, J.R. & Leeder, M.R. 1992. On the periodicity and magnitude of Late Carboniferous glacio-eustatic sea-level changes. *Journal of the Geological Society, London*, **149**, 303–311.

Mii, H.S., Grossman, E. L. & Yancey, T. E. 1999. Carboniferous isotope stratigraphies of North America: Implications for Carboniferous paleoceanography and Mississippian glaciation. *Geological Society of America Bulletin*, **111(7)**, 960–73.

Moore, E.W.J. 1930. Species of the Genus *Dimorphoceras* in the Bowland Shales. *Geological Magazine*, **67**, 162-168.

Moore, E.W.J. 1936. The Bowland Shales from Pendle to Dinckley. *Journal of the Manchester Geology Association*, **1**, 167-192.

Moore, E.W.J. 1939. The goniatite genus *Dimorphoceras* and its development in the British Carboniferous. *Proceedings of the Yorkshire Geological Society*, **24(2)**, 103-128.

Moore, E.W.J. 1946. The Carboniferous goniatite genera *Girtyoceras* and *Eumorphoceras*. *Proceedings of the Yorkshire Geological Society*, **25**, 387-445.

Nevill, W.E. 1956. The Millstone Grit and Lower Coal Measures of the Leinster Coalfield. *Proceedings of the Royal Irish Academy*, **58B**, 1-16.

Newell, N.D. 1938. Late Paleozoic pelecypods: Pectinacea. *University of Kansas Publications, State Geological Survey of Kansas,* **10(1)**, 1-123.

Nihuis, C.J., Amler, M.R.W. & Herbig, H-G. 2015. Facies and palaeoecology of the late Visean *Actinopteria* black shale event in the Rhenish Mountains (Germany, Mississippian). Z. Dt. Ges. Geowiss. (German J. Geosci.), **166(1)**, 55-69.

Nikolaeva, S.V. & Kullmann, J. 1998. A review of Middle Namurian ammonoid biostratigraphy. *Newsletters on Stratigraphy*, **36(2/3)**, 117-144.

Patteisky, K. 1957. Die stratigraphische stellung der Sprockhoveler Schichten und des Flozleeren nach ihren goniatiten-horizonten. Bergfreiheit, **22**, Essen, 515-518.

Patteisky, K. 1959. Die Goniatiten im Namur des Niederrheinisch-Westfälischen Karbongebietes. *Mitteilungen der Westfälischen Berggewerkschaftskasse*, **14**, 1-66, Herne (Kartenberg).

Philcox, M.E. 2007. Namurian Exposures above the Clare Shales on Inishcorker, Co. Clare. *In:* Holdstock, M. Farrelly, I. Loske, B. Neele, F. *Assessment of the Potential for Geological Storage of CO2 in Hypothetical Deep Saline Aquifers in the vicinity of Moneypoint, Co. Clare.* Environmental Protection Agency Ireland, Appendix 7-1, 1-5. Available online at: http://erc.epa.ie/safer/resource?id=bf4fa1b4-b564-102d-af1a-60cde515b757

Phillips, J. 1836. Illustrations of the geology of Yorkshire, part II. The Mountain Limestone Districht. I-XX, 1-259, pl.1-25; London.

Phillips, J. 1841. *Figures and descriptions of the Palaeozoic fossils of Cornwall, Devon, and West Somerset.* I-XII, 1-231, London.

Pierce, C., Haughton, P., Shannon, P.M., Martinsen, O.J., Pulham, A. & Elliott, T. 2014. First results from behind-outcrop boreholes in Clare Basin turbidites, Western Ireland, *AAPG Annual Convention and Exhibition*, 11-14 April, New Orleans, Abstract Volume, #728613.

Pierce, C. 2015. Development, distribution and evolution of gravity flow processes in the Pennsylvanian Ross Formation, western Ireland. *Unpublished PhD thesis*. University College Dublin.

Plummer, F.B., & Scott, G. 1937. Upper Paleozoic ammonites in Texas. *Bulletin of Texas University*, **3701**, 1-516.

Pointon, M. A., Cliff, R. A. & Chew, D. M. 2012a. The provenance of Western Irish Namurian Basin sedimentary strata inferred using detrital zircon U–Pb LA-ICPMS geochronology. *Geological Journal* **47**(1), 77–98.

Pointon, M.A., Chew, D.M., Ovtcharova, M., Sevastopulo, G.D. & Crowley, Q.G., 2012b. New high-precision U–Pb dates from western European Carboniferous tuffs; implications for time scale calibration, the periodicity of late Carboniferous cycles and stratigraphical correlation. *Journal of the Geological Society*, **169**, 713-721.

Pointon, M.A., Chew, D.M., Ovtcharova, M., Sevastopulo, G.D. & Delcambre, B. 2014. High-precision U-Pb zircon CA-ID-TIMS dates from western European late Visean bentonites. *Journal of the Geological Society*, **171**, 649-658.

Pulham, A.J. 1989. Controls on internal structure and architecture of sandstone bodies within Upper Carboniferous deltas, Co. Clare, western Ireland. *In:* Whately, M.K.G. and Pickering, K.T. (*eds.*) *Deltas: sites and traps for fossil fuels.* Geological Society of London Special Publications, **41**, 179-203.

Pulham, A.J., Haughton, P., Shannon, P.M., Pierce, C., Martinsen, O. J, Handler-Jacobsen, F. & Barker, S. 2014. The Late Carboniferous Ross Sandstone of Western Ireland: deepwater insights from behind outcrop drilling. *4th Atlantic Conjungate Margins Conference*, St. John's NL, Canada. 1-4.

Pyles, D.R. 2008. Multiscale stratigraphic analysis of a structurally confined submarine fan: Carboniferous Ross Sandstone, Ireland. *AAPG Bulletin*, **92(5)**, 557-587.

Pyles, D.R. 2009. Multiscale stratigraphic analysis of a structurally confined submarine fan: Carboniferous Ross Sandstone, Ireland: Reply. *AAPG Bulletin*, **93(12)**, 1710-1721.

Pyles, D.R. & Jennette, D. 2009. Geometry and architectural associations of co-genetic debrite-turbidite beds in basin-margin strata, Carboniferous Ross Sandstone (Ireland): Applications to reservoirs located on the margins of structurally confined submarine fans. *Marine and Petroleum Geology*, **26(10)**, 1974-1996.

Quinn, J.H. & Saunders, W.B. The ammonoids Hudsonoceras and Baschkirites in the Morrowan series of Arkansas. *Journal of Paleontology*, **42**, 397-402.

Ramsbottom, W.H.C. 1962. Boreholes in the Carboniferous rocks of the Ashover District, Derbyshire. *Bulletin of the Geological Survey of Great Britain*, **19**, 75-168.

Ramsbottom, W.H.C. 1969. The Namurian of Britain. *Compte Rendue 6ième Congrès International de Stratigraphie et de Géologie Carbonifère (Sheffield 1967)*, **1**, 219-232.

Ramsbottom, W.H.C. 1971. Palaeogeography and goniatite distribution in the Namurian and early Westphalian. *Compte Rendu Congres International de Stratigraphie et de Géologie Carbonifère*, **4**, 1395-1400.

Ramsbottom, W.H.C. 1977. Major cycles of transgression and regression (mesothems) in the Namurian. *Proceedings of the Yorkshire Geological Society*, vol. **41(3)**, no. 24, 261-291.

Ramsbottom, W. H. C. 1978. Carboniferous. *In*: McKerrow, W. S., (ed.) *The Ecology of Fossils.* MIT Press, Cambridge, Massachussetts, 146-183.

Ramsbottom, W.H.C. 1979. Rates of transgression and regression in the Carboniferous of NW Europe. Journal Geological Society of London, **136**, 147-153.

Ramsbottom, W.H.C. & Saunders, W.B. 1985. Evolution and evolutionary biostratigraphy of Carboniferous ammonoids. *Journal of Palaeontology*, **59(1)**, 123-139.

Richards, B.C., Aretz, M., Barnett, A., Barskov, I., Blanco-Ferrera, S., Brenckle, P.L., Clayton, G., Dean, M., Ellwood, B., Gibshman, N., Hecker, M., Konovalova, V.A., Korn, D., Kulagina, E., Lane, R., Mamet, B., Nemyrovska, T., Nikolaeva, S. V., Pazukhin, V.,Qi, Y.-P., Sanz-López, J., Saltzman, M.R., Titus, A., Utting, J. & Wang, X. 2011. Report of the Task Group to establish a GSSP close to the existing Viséan–Serpukhovian boundary. *Newsletter on Carboniferous Stratigraphy*, **29**, 26–30.

Rider, M.H. 1974. The Namurian of West County Clare. *Proceedings of the Royal Irish Academy*, **74B**, 125-142.

Riley, N.J. 1987. Type ammonoids from the Mid-Carboniferous boundary interval in Britain. *Courier Forschungsinstitut Senckenberg*, **98**, 25-37.

Riley N.J. 1993. Dinantian (LowerCarboniferous) biostratigraphy and chronostratigraphy in the British Isles. *Journal of the Geological Society* **150(3)**, 427–46.

Riley, N.J., Claoué-Long, J.C., Higgins, A.C., Owens, B., Spears, A., Taylor, L. & Varker, W.J. 1995. Geochronometry and geochemistry of the European mid-Carboniferous boundary global stratotype proposal, Stonehead Beck, North Yorkshire, UK. *Annales de la Société Géologique de Belgique*, **116**, 275–289.

Ritterbush, K. A. & Bottjer, D.J. 2012. Westermann Morphospace displays ammonoid shell shape and hypothetical paleoecology. *Paleobiology*, **38(3)**, 424-446.

Ruzhencev, V.E. & Bogoslovskaya, M.F. 1969. Reviziya semeystva Dimorphoceratidae. Paleontologicheskiy Zhurnal, **1**, 51-66, Moscow.

Ruzhencev, V.E. & Bogoslovskaya, M.F. 1971. O semeistve Homoceratidae. *Paleontologicheskiy Zhurnal*, **4**, 17-34, Moskva.

Ruzhencev, V.E. & Bogoslovskaya, M.F. 1975. O semeistve Reticuloceratidae i smezhnykh taksonakh. *Paleontologicheskii Zhurnal*, **1**, 46-61, Moskva.

Ruzhencev, V.E. & Bogoslovskaya, M.F. 1978. Namyurskiy etap v evolyutsii ammonodey. Pozdnenamyurskiye ammonoidei. Trudy Paleontologicheskogo Instituta Akademiya Nauk SSSR, **167**, 1-336. Moskva.

Rygel, M.C., Fielding, C.R., Frank, T.D. & Birgenheier, L.P. 2008. The magnitude of Late Palaeozoic glacioeustatic fluctuations: a synthesis. *Journal of Sedimentary Research*, **78**, 500-511.

Saunders, W.B. & Ramsbottom, W.H.C 1993. Re-evaluation of two Early Pennsylvanian (Middle Namurian) ammonoids and their bearing on mid-Carboniferous correlations. *Journal of Paleontology*, **67**, 993-999.

Saunders, W.B. & Swan, A.R.H. 1984. Morphology and morphologic diversity of mid-Carbonifeorus (Namurian) ammonoids in time and space. *Paleobiology*, **10(2)**, 195-228.

Schmidt, H. 1921. Über Goniatiten - eine Revision ihrer Systematik mit Beifügung neuer Beobachtungen. *Centralblatt für Mineralogie, Geologie und Paläontologie*, 538-544.

Schmidt, H. 1925. Die carbonischen Goniatiten Deutschlands. *Jahrbuch der Preußischen Geologischen Landesanstalt*, **45**, 489-609.

Schmidt, H. 1929. *Tierische Leitfossilien des Karbon. Gürich,G.: Leitfossilien*, 1-107, Berlin (Borntraeger).

Schmidt, H. 1934. Cephalopodenfaunen des älteren Namur aus der Umgegend von Arnsberg in Westfalen. *Jahrbuch der Preußischen Geologischen Landesanstalt*, **54** (for 1933), 440-461, Berlin.

Scotese, C.R. & McKerrow, W.S. 1990. Revised world maps and introduction. *In:* McKerrow, W.S. & and Scotese, C.R. (*eds.*) Palaeozoic Palaeogeography and Biogeography, *Geological Society of London Memoir*, **12**, 1-21.

Sevastopulo, G.D. 2009. Carboniferous: Mississippian (Serpukhovian) and Pennsylvanian. *In:* Holland C.H. & Sanders, I.S. (*eds.*) The Geology of Ireland, Dunedin Academic Press, 269-294.

Sevastopulo, G. D. & Barham, M. 2014. Correlation of the base of the Serpukhovian Stage (Mississippian) in NW Europe. *Geological Magazine*, **151(2)**, 244–53.

Selden, P.A. 2009. (ed.) *Treatise on Invertebrate Paleontology, Part L, revised, Mollusca 4, Volume 2.* The University of Kansas Paleontological Institute. Lawrence, Kansas, 258pp.

Spath, L.F. 1934. *Catalogue of the fossil Cephalopoda in the British Museum (Natural History).* Part IV. The Ammonoidea of the Trias. 1-521, London.

Strachan, L.J. 2002. Slump-initiated and controlled syndepositional sandstone remobilization: an example from the Namurian of County Clare, Ireland. *Sedimentology*, **49**, 25-41.

Swan, A.R.H. 1984. A revision of some Silesian goniatites using cluster analysis. *Unpublished PhD Thesis, Department of Earth Sciences, University of Leeds,* 341pp.

Swan, AR.H. & Saunders, W.B. 1987. Function and shape in late Paleozoic (mid-Carboniferous) ammonoids. *Paleobiology*, **13(3)**, 297-311.

Tanabe, K. Landman, N.H. & Mapes, R.H. 1994. Early shell features of some late Paleozoic ammonoids and their systematic implications. *Transactions and Proceedings of the Palaeontological Society of Japan*, **173**, 384-400.

Taylor, P. & Lewis, D.N. 2005. *Fossil Invertebrates.* Harvard University Press, Cambridge, Massachussetts, 208pp.

Teichert, C. 1964. Morphology of Hard Parts. *In:* Moore, R.C. (*ed.*) *Treatise on Invertebrate Paleontology, Part K, Mollusca 3, Cephalopoda-General Features-Endoceratoidea-Actinoceratoidea-Nautiloidea-Bactritoidea.* Geological Society of America and University of Kansas Press, K13-K59.

Titus, A.L., Webster, G.D. & Manger, W.L. 1997. Biostratigraphic analysis of the Mid-Carboniferous boundary at the South Syncline Ridge section, Nevada Test Side, Nevada, United States. *Proceedings of the 13th International Congress on the Carboniferous and Permian,* **157**, 207-212.

Titus, A.L. & Manger, W.L. 2001. Mid-Carboniferous ammonoid biostratigraphy, Southern Nye County, Nevada: Implications of the first North American *Homoceras*. *Journal of Paleontology*, **75** (4, Supplement, Memoir 55), 1-31.

Urdan, T.C. 2005. *Statistics in Plain English*. Lawrence Erlbaum Associates, Publishers, New Yersey. 184pp.

Varker, W.J., Owens, B. & Riley N.J. 1990. Integrated biostratigraphy for the proposed Mid-Carboniferous boundary stratotype, Stonehead Beck, Cowling, north Yorkshire, England. *Courier Forsch.-Inst. Senckenberg*, **130**, 221-235.

Varker, W.J. 1994. Multielement conodont faunas from the proposed Mid-Carboniferous boundary stratotype locality at Stonehead Beck, Cowling, north Yorkshire, England. *Annales de la Société Géologique de Belgique,* **116**, 301-321.

Waters, C.N., Chisholm, J.I., Benfield, A.C. & O'beirne, A.M. 2008. Regional evolution of a fluviodeltaic cyclic succession in the Marsdenian (Late Namurian Stage, Pennsylvanian) of the Central Pennine Basin, UK. *Proceedings of the Yorkshire Geological Society*, **57**, 1–28.

Waters, C.N., Somerville, I.D., Stephenson, M.H., Cleal, C.J. & Long, S.L. 2011. Biostratigraphy. *In*: C.N. Waters (Ed.), *A revised correlation of Carboniferous rocks in the British Isles*. Geological Society of London, 11-22.

Waters, C.N. & Condon, D.J. 2012. Nature and timing of Late Mississippian to Mid-Pennsylvanian glacio-eustatic sea-level changes of the Pennine Basin, UK. *Journal of the Geological Society, London*, **169**, 37-51.

Wedekind, R. 1918. Die Genera der Palaeoammonoidea (Goniatiten). *Palaeontographica*, **62**, 85-184, Stuttgart.

Westermann, G.E.G. 1996. Ammonoid life and habitat. *In:* Landman, N.H., Tanabe, K., & Davis, R.A. (eds.) *Ammonoid Paleobiology.* Plenum Press, New York, 608-707.

Wignall, P.B. 1994. *Black Shales.* Oxford Science Publications. 127pp.

Wignall, P.B. & Best, J.L. 2000. The western Irish Namurian Basin reassessed. *Basin Research*, **12**, 59-78.

Appendix A:

Tables (1-12)

Species	Specimen Number	D (mm)	WW (mm)	WW/D
***Phillipsoceras circumplicatile* (Foord, 1903)**	NMING : F23972	4	2	0.5
	TCD.60601	9.6	5.5	0.572916667
	GSM.95233	11.8	7.7	0.652542373
	GSM.95234	12.5	6.2	0.496
	GSM.86939	13.6	8.6	0.632352941
	GSM.86917	14.5	7.3	0.503448276
	GSM.95231	14.8	8	0.540540541
	GSM.85388	14.9	7.9	0.530201342
	GSM.95236	16	9.6	0.6
	GSM.95232	16.3	8.6	0.527607362
	NMING : F23968	21	12.5	0.5952381
	NMING: F23969	21.6	12.8	0.59259259

Table 1. Conch measurements for *Phillipsoceras circumplicatile* (Foord, 1903). Measurements include: diameter (D), whorl width (WW) and (WW/D). Specimens were either collected from the Clare Shale Formation, Co. Clare, Ireland, or accessed in museum collections. Measurements of diameter (D) and whorl width (WW) are in mm.

Species	Specimen Number	D	WW	WW/D
***Phillipsoceras paucicrenulatum* (Bisat & Hudson, 1943)**	LZ1868	4.3	2.5	0.581395349
	LZ1918	4.5	3.1	0.688888889
	LZ1881	4.9	3.1	0.632653061
	LZ1929	5.3	3.4	0.641509434
	LZ1873	5.7	4	0.701754386
	LZ1876	5.7	3.9	0.684210526
	LZ1927	5.7	3.5	0.614035088
	LZ1922	5.7	3.3	0.578947368
	LZ1925	5.7	3.5	0.614035088
	LZ1917	5.9	3.8	0.644067797
	LZ1872	6	4.3	0.716666667
	LZ1915	6.1	3.8	0.62295082
	LZ1930	6.3	3.8	0.603174603
	LZ1965	6.5	4.3	0.661538462
	LZ1954d	6.5	4	0.615384615
	LZ1914	6.7	4.2	0.626865672
	LZ1963	6.7	4.4	0.656716418
	LZ1937	6.8	4.2	0.617647059
	LZ1910	6.9	4.2	0.608695652
	LZ1967	7	4.9	0.7
	LZ1947	7.1	4.9	0.690140845
	LZ1951	7.1	4.4	0.61971831
	LZ1871	7.2	4.2	0.583333333
	LZ1980	7.2	5.7	0.791666667
	LZ1905	7.5	5.3	0.706666667
	LZ1882	7.5	4.3	0.573333333
	LZ1906	7.7	5.8	0.753246753
	LZ1888	7.8	6	0.769230769
	LZ1940	7.9	5.4	0.683544304
	LZ1912	8	5.2	0.65
	LZ1911	8.2	5.5	0.670731707
	LZ1948	8.3	5.2	0.626506024
	LZ1962	8.4	4.5	0.535714286
	LZ1954c	8.5	6.3	0.741176471
	LZ1909	8.6	4.4	0.511627907
	LZ1955	8.7	5.6	0.643678161
	LZ1908	8.8	5.9	0.670454545
	LZ1936	8.8	6.4	0.727272727
	Zi7338	8.8	4.6	0.522727273
	Zi7095	8.8	5.1	0.579545455
	LZ1933	9	6	0.666666667
	LZ1887	9.3	6.2	0.666666667
	Zi7097	9.3	5.9	0.634408602
	LZ1942	9.4	6.4	0.680851064
	LZ1883	9.8	6.6	0.673469388
	LZ1932	9.9	6.1	0.616161616
	LZ1954b	10.2	6.6	0.647058824
	LZ1884	10.4	6.5	0.625
	LZ1934	11.4	7.5	0.657894737
	LZ1895	11.9	7.5	0.630252101
	Zi7096	11.9	8.5	0.714285714
	Zi7339	12.3	5.2	0.422764228

	LZ1897	12.6	6.7	0.531746032
	GSM.95252	13.2	7.8	0.590909091
	LZ1958	13.3	7.1	0.533834586
	LZ1893	14.1	9.6	0.680851064
	LZ1954a	14.7	7.8	0.530612245
	GSM.95249	15	10.4	0.693333333
	Zi7103	16.5	9.7	0.587878788
	GSM.95251	16.9	9.6	0.568047337
	EWJ3151	17.6	8.7	0.494318182
	GSM.1866	17.7	11	0.621468927
	GSM.95250	18.7	11	0.588235294
	GSM.82814	18.8	10.9	0.579787234

Table 2. Conch measurements for *Phillipsoceras paucicrenulatum* (Bisat & Hudson, 1943). Measurements include: diameter (D), whorl width (WW) and (WW/D). Specimens were either collected from the Clare Shale Formation, Co. Clare, Ireland, or accessed in museum collections. Measurements of diameter (D) and whorl width (WW) are in mm.

Species	Specimen Number	D (mm)	WW (mm)	WW/D
***Reticuloceras subreticulatum* (Foord, 1903)**	Zi7113	6.7	4.2	0.626865672
	Zi7112	7.3	4	0.547945205
	Zi7115	8.2	4.6	0.56097561
	Zi7118	8.8	6.2	0.704545455
	Zi7116	11.9	6.3	0.529411765
	LZ1988	13.7	8.3	0.605839416
	Zi7114	15.5	9.2	0.593548387
	Zi7117	15.7	8.2	0.522292994
	Zi7123	16.8	9.8	0.583333333
	Zi7119	18.5	8.9	0.481081081
	TCD.60604	19.6	10.1	0.515306122
	NMING : F23964	22.9	12	0.524017467

Table 3. Conch measurements for *Reticuloceras subreticulatum* (Foord, 1903). Measurements include: diameter (D), whorl width (WW) and (WW/D). Specimens were either collected from the Clare Shale Formation, Co. Clare, Ireland, or accessed in museum collections. Measurements of diameter (D) and whorl width (WW) are in mm.

Species	Specimen number	D	WW	WW/D
***Homoceras beyrichianum* (de Koninck, 1843)**		4	2.8	0.7
		4	2.2	0.55
	L.12242h	4	2.4	0.6
	L.12242b	4.6	2.7	0.586956522
		5.2	4.3	0.826923077
		5.9	3.3	0.559322034
		6.4	5.2	0.8125
	TCD.61011	7	4.1	0.585714286
		7.1	4.6	0.647887324
	L12242i	7.5	5.7	0.76
		7.9	4.7	0.594936709
		8	5.3	0.6625
	TCD.61003	9	7.5	0.833333333
		9.2	6.9	0.75
		9.3	7.8	0.838709677
		9.3	7.1	0.76344086
		9.5	6	0.631578947
		10.3	8	0.776699029
		10.5	7.7	0.733333333
		10.7	8.2	0.76635514
		11.2	9	0.803571429
		11.3	8	0.707964602
	STR0600a	11.8	9.7	0.822033898
	TCD.61004	12.2	11.3	0.926229508
		12.6	9.6	0.761904762
		12.8	9.4	0.734375
		13	8.8	0.676923077
		13	10.3	0.792307692
		14	12.1	0.864285714
		14.4	11.3	0.784722222
		15	11.3	0.753333333
		15.2	10.6	0.697368421
		16.8	12.7	0.755952381
		17	11.2	0.658823529
	TCD.61000	17.5	10.5	0.6
		17.8	12.3	0.691011236
		18.7	11.6	0.620320856
		18	9.7	0.538888889
		18.2	13.5	0.741758242
		18.8	11.8	0.627659574
		19.2	12.5	0.651041667
	STR0600b	19.5	11.7	0.6
	STR0600c	28.6	17.1	0.597902098

Table 4. Conch measurements for *Homoceras beyrichianum* (de Koninck, 1843). Measurements include: diameter (D), whorl width (WW) and (WW/D). Specimens were either collected from the Clare Shale Formation, Co. Clare, Ireland, or accessed in museum collections. Measurements of diameter (D) and whorl width (WW) are in mm. Where specimens don't have a specimen number, they are from Hodson's Southampton collection housed in Trinity College Dublin.

Species	Specimen Number	D	WW	WW/D
***Homoceras smithii* (Brown, 1841)**	TCD.61010	6.7	4.8	0.71641791
		7.7	5.5	0.714285714
		8.4	6.5	0.773809524
		8.6	6.4	0.744186047
		9	7.8	0.866666667
		9	7.1	0.788888889
		10.6	8.1	0.764150943
		10.7	8.2	0.76635514
		10.8	8.2	0.759259259
		10.8	7.8	0.722222222
	L.10244	11	7.5	0.681818182
	TCD.61002	11.2	9.1	0.8125
		11.4	9.3	0.815789474
		12	8.8	0.733333333
		12.1	8.9	0.73553719
		12.8	9.6	0.75
		12.8	7	0.546875
		13.4	7.9	0.589552239
		13.5	9.2	0.681481481
		13.7	7	0.510948905
		13.7	9.6	0.700729927
		13.8	8.7	0.630434783
		14	9.3	0.664285714
		14	9.7	0.692857143
		14.4	8	0.555555556
		14.9	9.8	0.657718121
		16	10.2	0.6375
	TCD.61009	17	10.3	0.605882353
	TCD.61005	21	11.5	0.547619048
	TCD.61006	21	12.5	0.595238095

Table 5. Conch measurements for *Homoceras smithii* (Brown, 1841). Measurements include: diameter (D), whorl width (WW) and (WW/D). Specimens were either collected from the Clare Shale Formation, Co. Clare, Ireland, or accessed in museum collections. Measurements of diameter (D) and whorl width (WW) are in mm. Where specimens don't have a specimen number, they are from Hodson's Southampton collection housed in Trinity College Dublin.

Species	Specimen Number	D	WW	WW/D
***Homoceras undulatum* (Brown, 1841)**	NMING : F24480	3.5	1.9	0.542857143
		5.3	3.3	0.622641509
	NMING : F24480	6.2	5	0.806451613
		7.4	5.1	0.689189189
	Zi4546	7.6	5.9	0.776315789
	NMING : F24480	7.8	5.5	0.705128205
	Zi4547	7.8	6	0.769230769
		8.1	5.6	0.691358025
	Zi4548	8.6	4.9	0.569767442
		9.2	5.8	0.630434783
	Zi4545	9.2	6.2	0.673913043
	TCD.61018	9.2	5.9	0.641304348
	Zi4541	9.3	6.8	0.731182796
	Zi4542	9.4	6.4	0.680851064
	NMING : F24480	9.5	5.8	0.610526316
		9.6	6.1	0.635416667
		9.7	7.3	0.75257732
		9.7	6.1	0.628865979
		9.8	6.6	0.673469388
	TCD.61014	9.8	7	0.714285714
	NMING : F24480	9.9	6.3	0.636363636
	TCD.61016	10	7	0.7
	NMING : F24480	11.1	7.5	0.675675676
	Zi4548	11.2	7.4	0.660714286
		11.4	8	0.701754386
	Zi4548	11.5	7.6	0.660869565
	TCD.61019	11.7	9.1	0.777777778
		11.7	6.8	0.581196581
		12	8.5	0.708333333
		12.1	7.5	0.619834711
	Zi4548	12.3	7.6	0.617886179
		12.3	8.2	0.666666667
	L.12343	12.3	8.6	0.699186992
		12.4	8	0.64516129
	Zi4548	12.5	9.4	0.752
	Zi4548	12.7	8.6	0.677165354
		12.6	8.8	0.698412698
		12.6	7.8	0.619047619
	TCD.61013	12.8	8.7	0.6796875
		12.9	8.4	0.651162791
		12.9	8.7	0.674418605
	Zi4548	13.2	8.1	0.613636364
		13.2	8.4	0.636363636
	Zi4548	13.3	9.3	0.69924812
	TCD.61017	13.5	8.2	0.607407407
		13.6	8.9	0.654411765
		13.6	9.2	0.676470588
		13.6	7.7	0.566176471
		13.9	7.3	0.525179856
		14.1	8.3	0.588652482
	L.10241b	14.2	10	0.704225352
	Zi4540	14.6	8	0.547945205
		14.6	8.1	0.554794521
		14.7	9.1	0.619047619
		15	9.2	0.613333333
	Zi4548	15	7.4	0.493333333
		15.2	10	0.657894737
	TCD.61020	15.3	8.8	0.575163399

	TCD.61015	15.4	9	0.584415584
	NMING : F24480	15.6	9.2	0.58974359
	Zi4548	15.7	9.7	0.617834395
	Zi4548	15.8	9.5	0.601265823
		16	9.9	0.61875
		16	9.2	0.575
		16	9.3	0.58125
		16.1	8.4	0.52173913
	Zi4548	16.2	9.2	0.567901235
	Zi4548	16.4	8.2	0.5
		16.5	9.6	0.581818182
		16.5	9.1	0.551515152
	Zi4548	16.6	9.9	0.596385542
		16.8	9.6	0.571428571
		17	8.9	0.523529412
		17.1	9	0.526315789
	Zi4539	17.4	9.7	0.557471264
		17.6	10.2	0.579545455
	Zi4548	17.7	9.7	0.548022599
		18.3	10	0.546448087
		18.6	10.5	0.564516129
	TCD.61012	19	9.5	0.5
	Zi4548	19.1	11	0.57591623
	L.10241a	19.2	11	0.572916667
		19.3	11.3	0.585492228
	NMING : F24480	19.3	10.8	0.559585492
		19.4	11	0.567010309
		19.4	10.1	0.520618557
		19.6	11.3	0.576530612
		19.6	11.2	0.571428571
		19.7	11.3	0.573604061
		20	11.4	0.57
		20	11.4	0.57
	Zi4548	20.1	11.4	0.567164179
	Zi4548	20.1	11.7	0.582089552
	Zi4548	20.4	12.8	0.62745098
	Zi4535	20.5	12.6	0.614634146
		20.7	11.5	0.555555556
		21.6	9.2	0.425925926
		22	11	0.5
		22.9	11.5	0.502183406
	Zi4537	22.9	12	0.524017467
		25	13.5	0.54
	Zi4548	25	15	0.6
	Zi4548	25.5	15.4	0.603921569
		27	15	0.555555556
	Zi4534	38	19	0.5

Table 6. Conch measurements for *Homoceras undulatum* (Brown, 1841). Measurements include: diameter (D), whorl width (WW) and (WW/D). Specimens were either collected from the Clare Shale Formation, Co. Clare, Ireland, or accessed in museum collections. Measurements of diameter (D) and whorl width (WW) are in mm. Where specimens don't have a specimen number, they are from Hodson's Southampton collection housed in Trinity College Dublin.

Species	Specimen Number	D	WW	WW/D
***Isohomoceras subglobosum* (Bisat, 1924)**	TCD.61021	4.4	3.6	0.818181818
	TCD.61022	11.1	7.4	0.666666667
		12.6	8.6	0.682539683

Table 7. Conch measurements for *Isohomoceras subglobosum* (Bisat, 1924). Measurements include: diameter (D), whorl width (WW) and (WW/D). Specimens were either collected from the Clare Shale Formation, Co. Clare, Ireland, or accessed in museum collections. Measurements of diameter (D) and whorl width (WW) are in mm. Where specimens don't have a specimen number, they are from Hodson's Southampton collection housed in Trinity College Dublin.

Species	Specimen Number	D	WW	WW/D
***Homoceratoides prereticulatus* (Bisat, 1924)**	LZ3034	3.4	1.9	0.558823529
		5	2	0.4
	LZ3034	6.5	3.9	0.6
	LZ3035	6.9	4.3	0.623188406
	LZ3034	6.9	4.3	0.623188406
		7.3	3.5	0.479452055
	LZ3034	7.5	5.2	0.693333333
	LZ3034	7.6	4.7	0.618421053
	LZ3034	7.7	5.2	0.675324675
	F24477/6	7.7	3.9	0.506493506
	LZ3034	7.8	4.3	0.551282051
	LZ3035	8	4.4	0.55
	TCD.61023	8.1	4.8	0.592592593
	LZ3034	8.1	4.8	0.592592593
	LZ3034	8.3	5.3	0.638554217
	LZ3034	8.4	4.9	0.583333333
	LZ3034	8.6	5.7	0.662790698
	LZ3035	8.6	4.8	0.558139535
	LZ3034	8.7	5.4	0.620689655
	LZ3034	9.2	5.5	0.597826087
	TCD.61026	9.5	5.2	0.547368421
	LZ3034	9.6	5.7	0.59375
		9.9	5.6	0.565656566
		10	5.8	0.58
	NMING : F24477/3	10	5.7	0.57
	LZ3034	10.1	5.7	0.564356436
	LZ3035	10.2	4.6	0.450980392
		10.3	6.1	0.59223301
		10.5	5.5	0.523809524
	LZ3035	11	5.9	0.536363636
	NMING : F24477/6	11	6.4	0.581818182
	NMING : F24477/6	11.2	6.2	0.553571429
		12	6	0.5
	LZ3034	12	6.2	0.516666667
		12.4	6.2	0.5
		13	8	0.615384615
	TCD.61029	13	7.7	0.592307692
	LZ3034	13.1	7.1	0.541984733
		13.5	5.5	0.407407407
		16	8.6	0.5375
	LZ3034	17.3	6.7	0.387283237
	TCD.61024	18	8.8	0.488888889
		20	8.5	0.425

Table 8. Conch measurements for *Homoceratoides prereticulatus* (Bisat, 1924). Measurements include: diameter (D), whorl width (WW) and (WW/D). Specimens were either collected from the Clare Shale Formation, Co. Clare, Ireland, or accessed in museum collections. Measurements of diameter (D) and whorl width (WW) are in mm. Where specimens don't have a specimen number, they are from Hodson's Southampton collection housed in Trinity College Dublin.

Species	Specimen Number	D	WW	WW/D
***Homoceratoides varicatus* Schmidt, 1934**	FOR1818	5.4	2.4	0.444444444
		6.5	4.3	0.661538462
	GSM.83139	6.9	4.8	0.695652174
	Zi4662	7.5	4.8	0.64
		7.7	5.5	0.714285714
	GSM.83140	8.4	5	0.595238095
		8.6	4.8	0.558139535
	Zi4663	8.6	5.5	0.639534884
	GSM.86930	9.1	5.8	0.637362637
		9.1	4.8	0.527472527
	GZG.INV.48188	9.2	5.3	0.576086957
	Zi4666	9.4	3.6	0.382978723
	Zi4664	9.4	4.8	0.510638298
		9.8	5.2	0.530612245
		10	5.6	0.56
		10.2	6	0.588235294
	Zi4684	10.6	5.8	0.547169811
	NMING : F24474	10.6	5.9	0.556603774
	Zi4661	10.9	4.4	0.403669725
		11.3	5	0.442477876
	LL.1181	11.5	6.2	0.539130435
	GSM.74168	11.5	5.5	0.47826087
	TCD.61007	11.5	5.9	0.513043478
	NMING : F24474	12.8	5.4	0.421875
	Zi4665	12.8	5.9	0.4609375
		13	7	0.538461538
	Zi4683	13.4	6.9	0.514925373
		14.2	7.4	0.521126761
	NMING : F24474	14.7	6.2	0.421768707
		15	6	0.4
		15.3	6.5	0.424836601
		15.7	7.1	0.452229299
		15.9	7.3	0.459119497
	NMING : F24474	16.4	9.5	0.579268293
		16.6	9.3	0.560240964
		17.5	7.6	0.434285714
	Zi4668	17.6	9.9	0.5625
	GSM.74170	18.2	7.5	0.412087912
	TCD.61008	18.6	9.1	0.489247312
		18.7	8.4	0.449197861
	Zi4669	22	10.1	0.459090909
	GZG.INV.48187	28	11.9	0.425

Table 9. Conch measurements for *Homoceratoides varicatus* Schmidt, 1934. Measurements include: diameter (D), whorl width (WW) and (WW/D). Specimens were either collected from the Clare Shale Formation, Co. Clare, Ireland, or accessed in museum collections. Measurements of diameter (D) and whorl width (WW) are in mm. Where specimens don't have a specimen number, they are from Hodson's Southampton collection housed in Trinity College Dublin.

Species	Specimen Number	D	WW	WW/D
***Vallites henkei* (Schmidt, 1925)**	TCD.61049	4.5	2.7	0.6
	TCD.61047	5.5	2	0.363636364
	TCD.61048	5.7	3	0.526315789
	TCD.61045	6.2	2.9	0.467741935
	TCD.61042	6.3	4.5	0.714285714
	TCD.61040	6.6	4.4	0.666666667
	TCD.61041	6.7	3.4	0.507462687
	TCD.61043	6.8	3.9	0.573529412
	TCD.61046	7	4.5	0.642857143
	GZG.INV.48185	7.1	4.4	0.61971831
	TCD.61038	7.3	5	0.684931507
	TCD.61044	8.2	4.7	0.573170732
		8.3	5.5	0.662650602
	GSM.81006	8.5	5	0.588235294
	TCD.61039	8.7	5	0.574712644
	TCD.61037	8.7	4.3	0.494252874
	NMING : F23971	9	4.8	0.533333333
	TCD.61034	9.1	5.7	0.626373626
	TCD.61035	9.5	5.4	0.568421053
	TCD.61036	9.6	5.3	0.552083333
	GSM.89946	10	6	0.6
	Zi4688	10.9	5.5	0.504587156
	Zi4690	11.5	6.9	0.6
	Zi4489	11.6	8.9	0.767241379
	GSM.86934	17.8	9.5	0.533707865
	GSM.86936	11.8	7.7	0.652542373
	TCD.61033	18.1	8.8	0.486187845
		18.5	9.7	0.524324324
	TCD.61032	18.9	10.8	0.571428571
	TCD.61031	20.1	10.7	0.532338308
	NMING : F23974	21.8	10.4	0.47706422
	GZG.INV.48186	21.9	8.6	0.392694064
		25	10.6	0.424
	GSM.86931	27.8	12.8	0.460431655
	GZG.INV.48184	30.7	14	0.456026059
		41	15	0.365853659

Table 10. Conch measurements for *Vallites henkei* (Schmidt, 1925). Measurements include: diameter (D), whorl width (WW) and (WW/D). Specimens were either collected from the Clare Shale Formation, Co. Clare, Ireland, or accessed in museum collections. Measurements of diameter (D) and whorl width (WW) are in mm. Where specimens don't have a specimen number, they are from Hodson's Southampton collection housed in Trinity College Dublin.

Species	Specimen Number	D	WW	WW/D
***Hudsonoceras proteus* (Brown, 1841)**	NMING : F24477	2.6	1.2	0.461538462
	NMING : F24475	3.8	1.5	0.394736842
	L.12240	4.9	2	0.408163265
	L.11797f	5.8	3	0.517241379
	NMING : F24475	6.6	3.4	0.515151515
	L.11797d	7.8	3.2	0.41025641
	L.11797c	8.5	3.8	0.447058824
	L.12241	8.5	3.5	0.411764706
	L.11797b	10.2	4	0.392156863
	L.11797a	11.6	4.4	0.379310345
	NMING : F24477	12	4.5	0.375
	NMING : F24478	13	4.8	0.369230769
	NMING : F24478	14.7	5.8	0.394557823
	NMING : F24477	15.7	6.9	0.439490446
	TCD.61050	18.5	5.3	0.286486486
	TCD.61051	26	6.9	0.265384615

Table 11. Conch measurements for *Hudsonoceras proteus* (Brown, 1841). Measurements include: diameter (D), whorl width (WW) and (WW/D). Specimens were either collected from the Clare Shale Formation, Co. Clare, Ireland, or accessed in museum collections. Measurements of diameter (D) and whorl width (WW) are in mm. Where specimens don't have a specimen number, they are from Hodson's Southampton collection housed in Trinity College Dublin.

Species	Specimen Number	D	WW	WW/D
***Hodsonites magistrorum* (Hodson, 1957)**	NMING : F20280/5	3.6	2.1	0.583333333
	NMING : F24476	3.8	1.7	0.447368421
		4	1.7	0.425
		4.3	6	0.558139535
	NMING : F20280/4	4.6	3.2	0.695652174
	TCD.61063	5	2.9	0.58
		5.4	3.2	0.592592593
	TCD.61062	6.2	4	0.64516129
	TCD.61060	6.3	4.2	0.666666667
	NMING : F20280/2	6.6	5.6	0.848484848
	NMING : F20280/3	6.7	4.4	0.656716418
	NMING : F24476	6.7	4.2	0.626865672
	TCD.61061	6.8	4	0.588235294
		6.9	3.7	0.536231884
	GSM.71456	7	5	0.714285714
	TCD.61059	7.2	5	0.694444444
	TCD.61058	7.3	5.1	0.698630137
	GSM.71461	7.3	4.3	0.589041096
	TCD.61056	7.6	4.9	0.644736842
		8	5.1	0.6375
	TCD.61055	8.1	5	0.617283951
	NMING : F20280/6	8.1	5.1	0.62962963
	NMING : F20275/4	8.4	5.4	0.642857143
		8.6	4.9	0.569767442
	TCD.61057	8.8	6.1	0.693181818
	TCD.61054	8.9	5	0.561797753
		9.2	5.2	0.565217391
	NMING : F20275/1	9.2	5.8	0.630434783
	NMING : F24476	9.3	5.7	0.612903226
	GSM.86935	9.4	6.6	0.70212766
	GSM.71460	9.4	5.7	0.606382979
		9.6	5.4	0.5625
	TCD.61053	9.7	5.7	0.587628866
		9.7	6.7	0.690721649
	NMING : F24476	10	5.4	0.54
	NMING : F24476	10.1	5.6	0.554455446
	GSM.86909	10.2	6.5	0.637254902
	NMING : F20276/1	10.3	7.1	0.689320388
		10.5	5.9	0.561904762
		11	7	0.636363636
		11.1	6.9	0.621621622
		11.1	6	0.540540541
	GSM.71455	11.4	6	0.526315789
		11.5	7.6	0.660869565
		11.5	5	0.434782609
	LL.1181	11.5	6.2	0.539130435
		11.7	6.5	0.555555556
	TCD.61052	11.7	6.9	0.58974359
	NMING : F24476	12.4	6.6	0.532258065
		12.9	7.8	0.604651163
	GSM.71458	13.5	8.7	0.644444444
		13.7	8.8	0.642335766
	GSM.71453	14.3	8.3	0.58041958
		15	9.7	0.646666667

	NMING : F20280/1	15	8	0.533333333
		15.2	9.9	0.651315789
	GSM.86913	15.5	10.5	0.677419355
	GSM.86912	15.7	8.2	0.522292994
		15.7	8	0.50955414
	GSM.86911	19.2	10.2	0.53125
	NMING : F24476	21.3	11.9	0.558685446
	GSM.86915	25	12.5	0.5
		27	12	0.444444444

Table 12. Conch measurements for *Hodsonites magistrorum* (Hodson, 1957). Measurements include: diameter (D), whorl width (WW) and (WW/D). Specimens were either collected from the Clare Shale Formation, Co. Clare, Ireland, or accessed in museum collections. Measurements of diameter (D) and whorl width (WW) are in mm. Where specimens don't have a specimen number, they are from Hodson's Southampton collection housed in Trinity College Dublin.

Appendix B:
Borehole Graphic Logs

Key to Graphic Logs:

Lithology:

Breccia (shale clasts)

Medium sand

Fine sand

Very-fine sand

Sand-rich siltstone (with rippled cross-lamination)

Siltstone

Shale (colour varying from black to dark grey to grey)

Clay-rich silt

Other:

Pyrite

Load structures

Lens (variable lithology)

Folding

Water-escape features

Paired pyrite tubes

Sand ball

Fossil material:

2D Ammonoid

3D Ammonoid

Nautiloid

Dunbarella sp.

Caneyella sp.

Undifferentiated bivalve material

Nodule

Ammonoid-bearing nodule

Plant material

Crinoid

Trilobite material

Sampled horizon

Legend for all borehole graphic logs

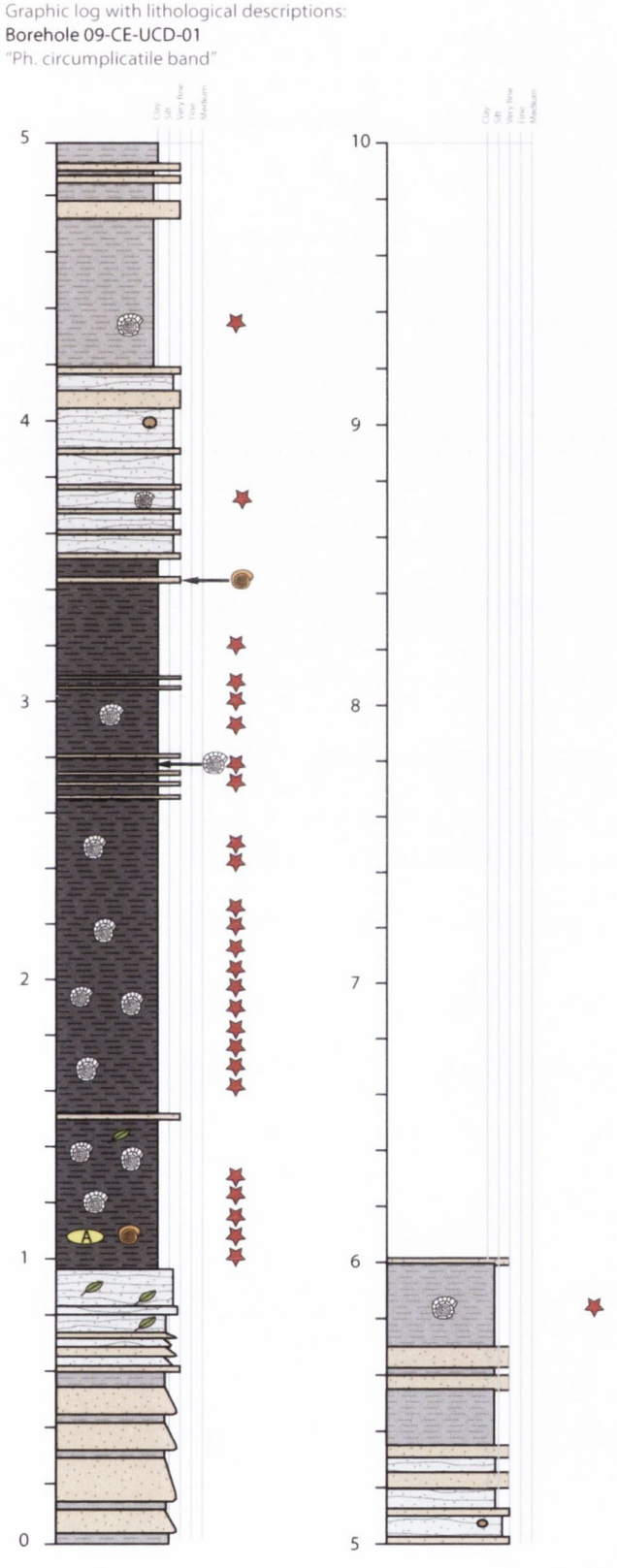

Log of "*Ph. circumplicatile* band" in 09-CE-UCD-01 (44 m to 50 m depth).

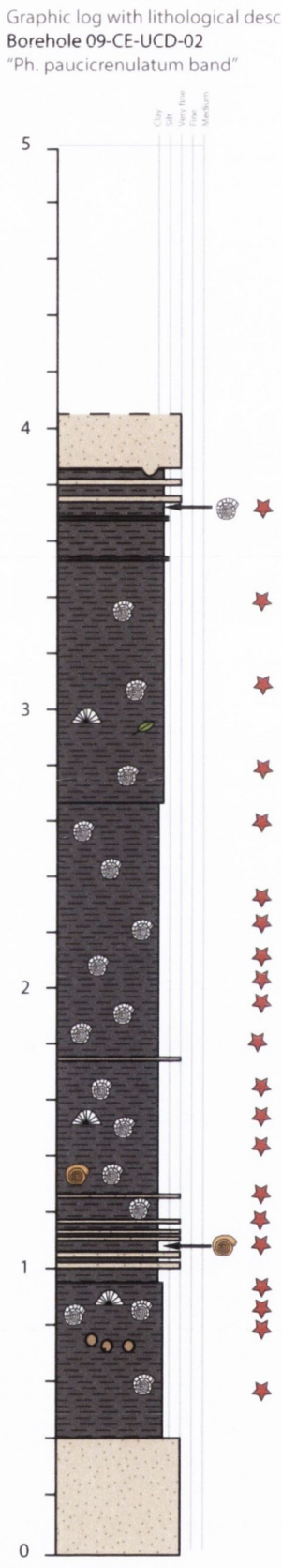

Log of "*Ph. paucicrenulatum* band" in 09-CE-UCD-02 (76 m to 72 m depth).

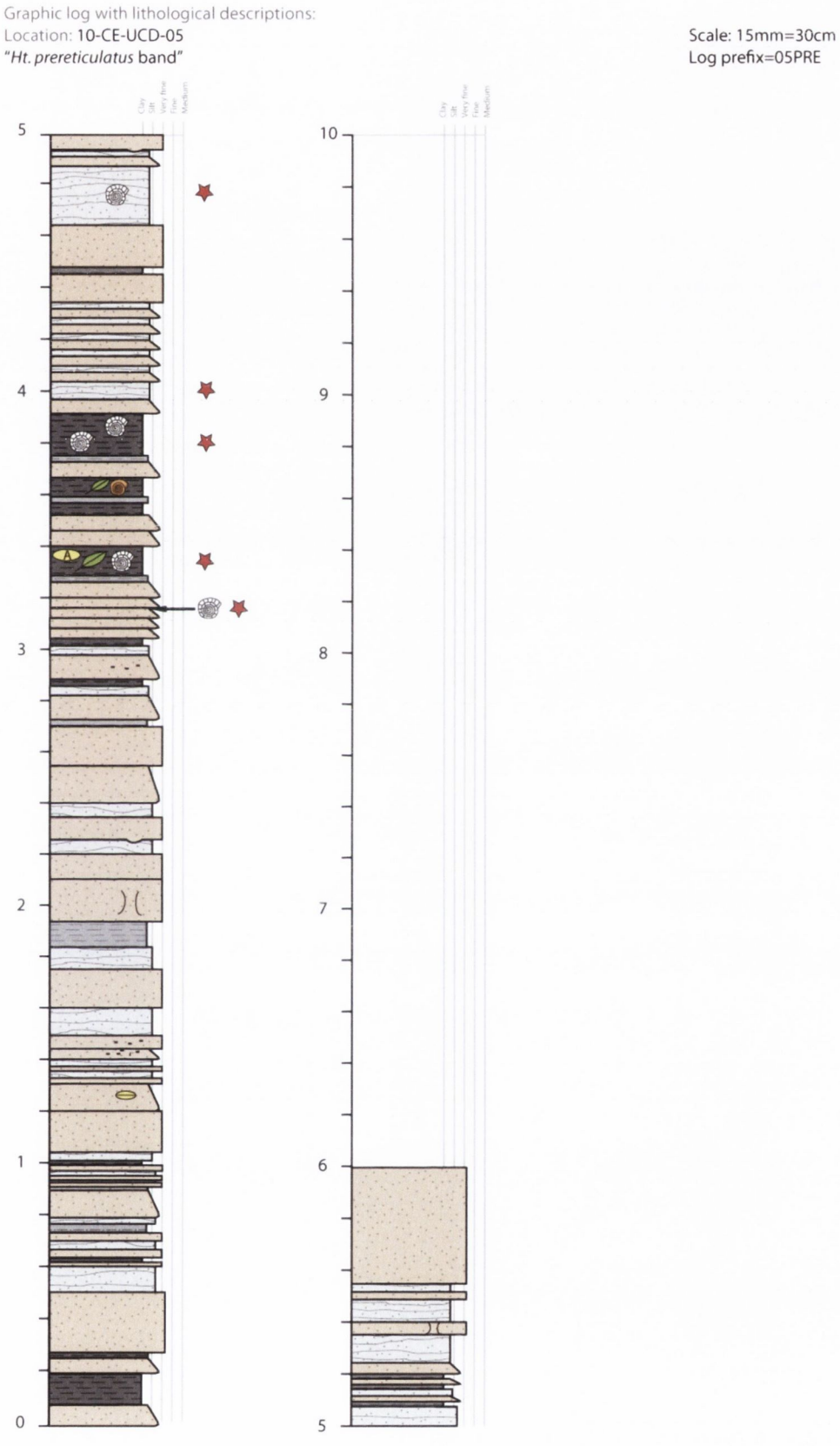

Log through "*Ht. prereticulatus* band" in 10-CE-UCD-05 (start at 24 m depth).

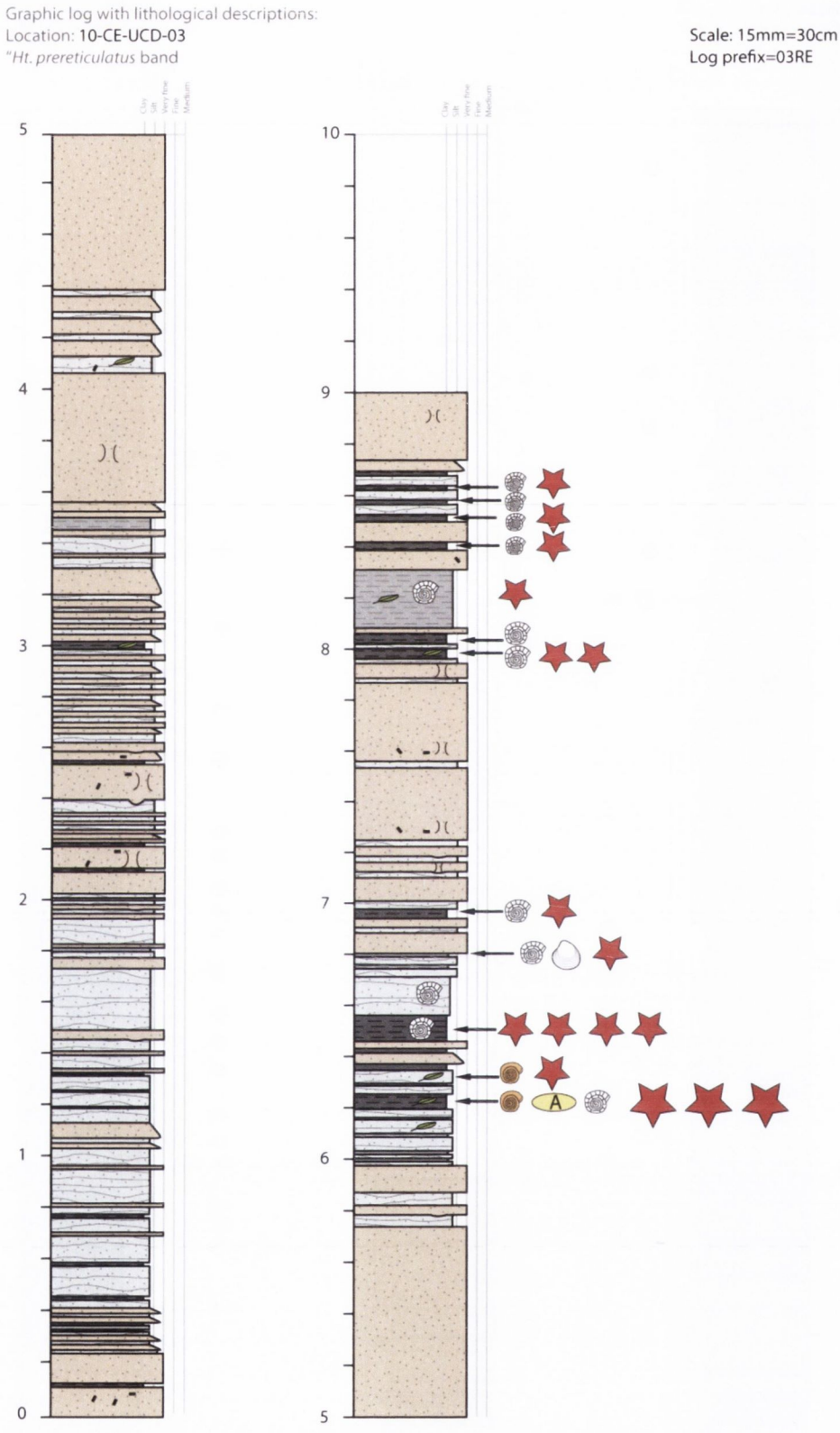

Log through "*Ht. prereticulatus* band" in 10-CE-UCD-03 (start at 62 m depth going up).

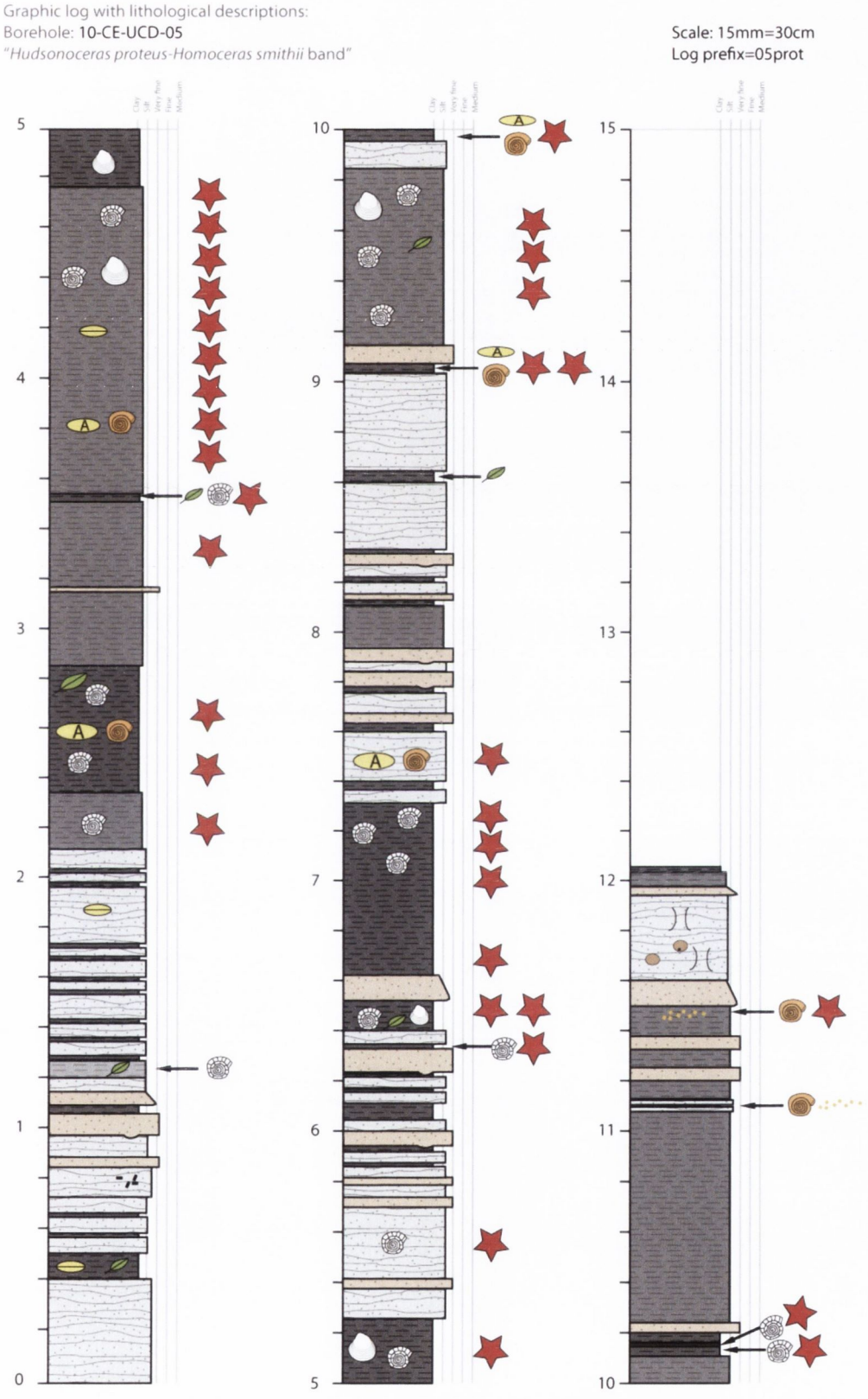

Log through "*Hud. proteus-Ho.smithii* band" in 10-CE-UCD-05 (start at 89 m depth going up).

Graphic log with lithological descriptions:
Borehole: 10-CE-UCD-03
"Hudsonoceras proteus-Homoceras smithii band"

Scale: 15mm=30cm
Log prefix=03prot

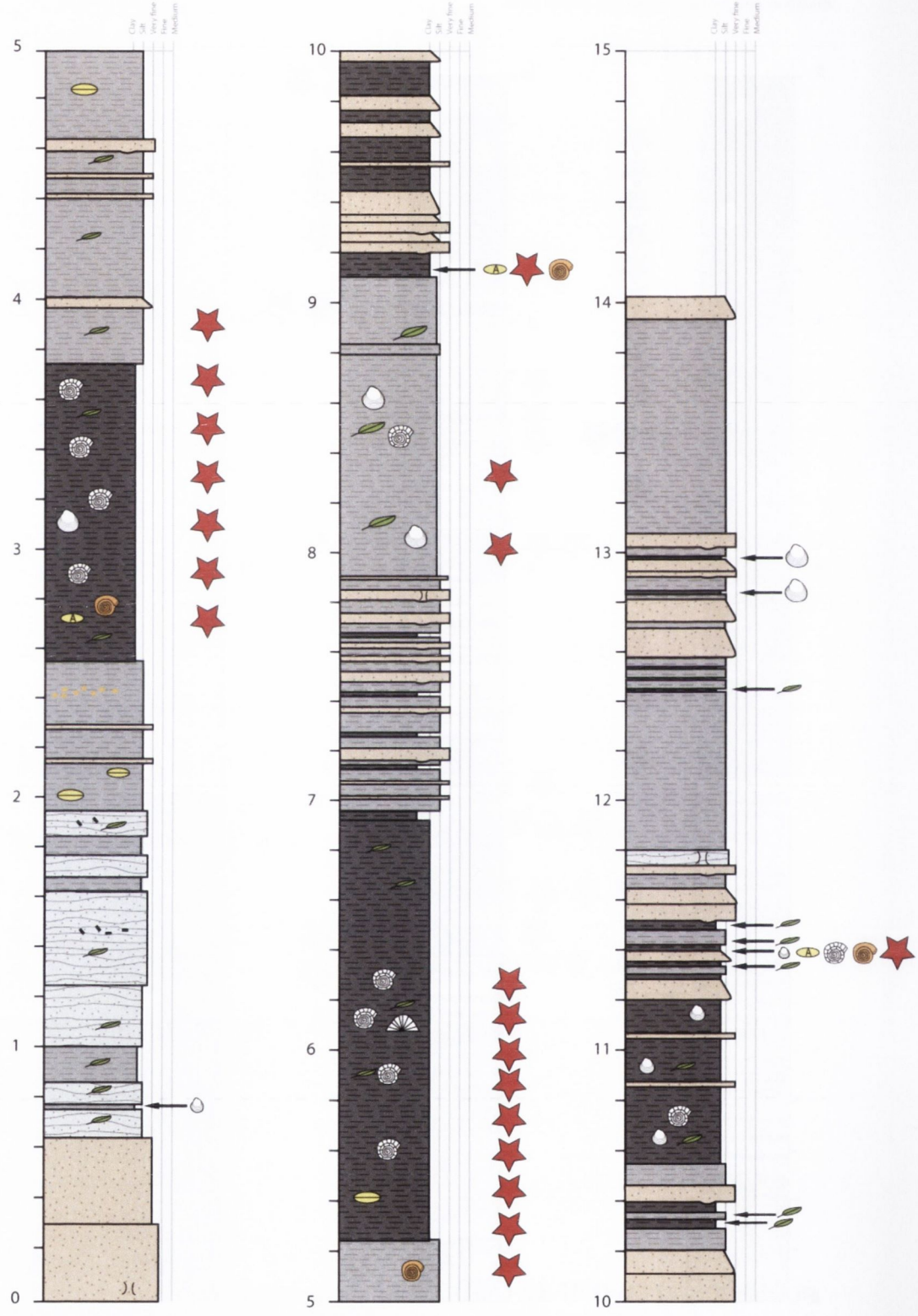

Log through " *Hud. proteus-Ho.smithii* band" in 10-CE-UCD-03 (start at 135 m, going up).

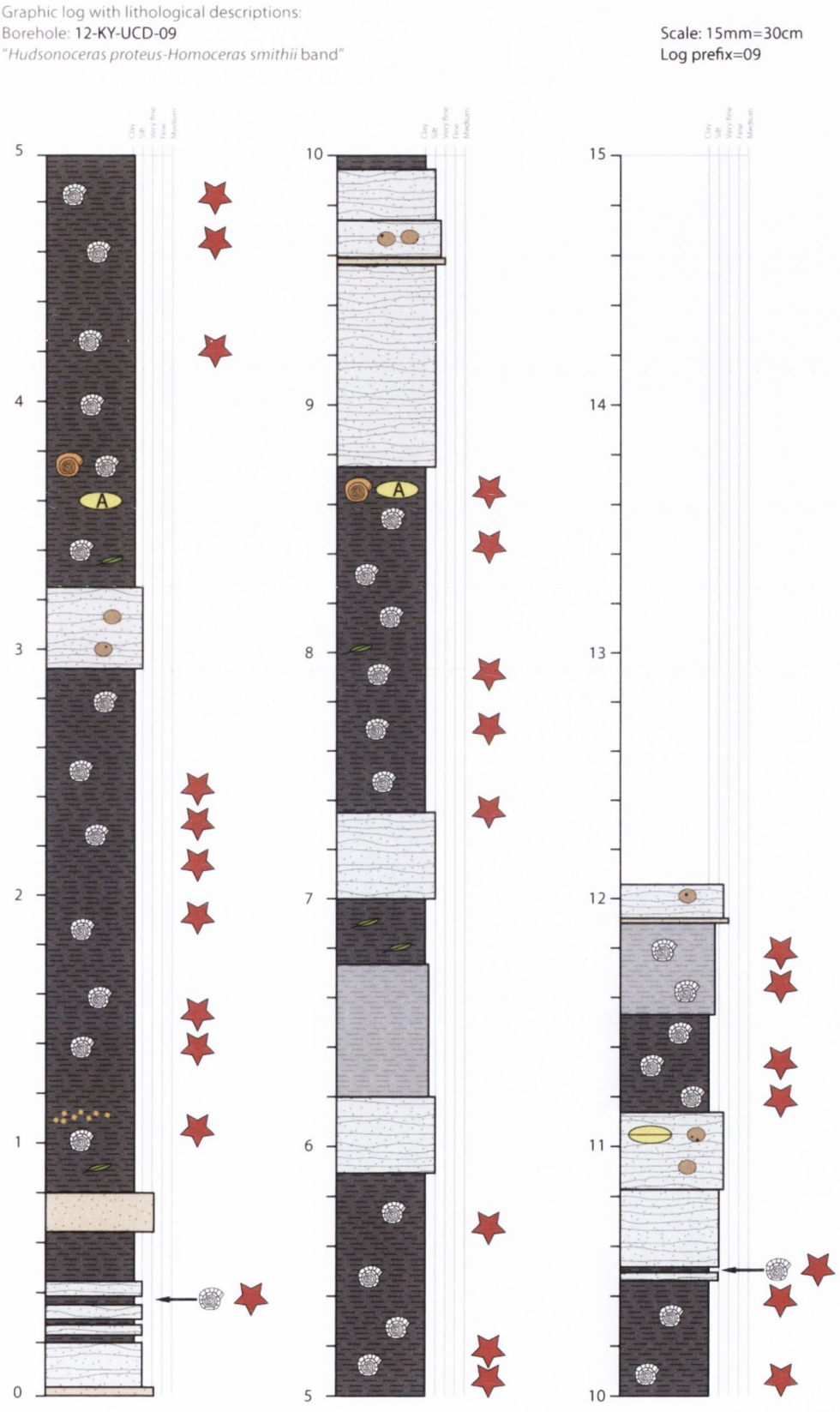

Log through the *"Hud. proteus-Ho.smithii* band" in 12-KY-UCD-09 (start at c. 70 m depth).

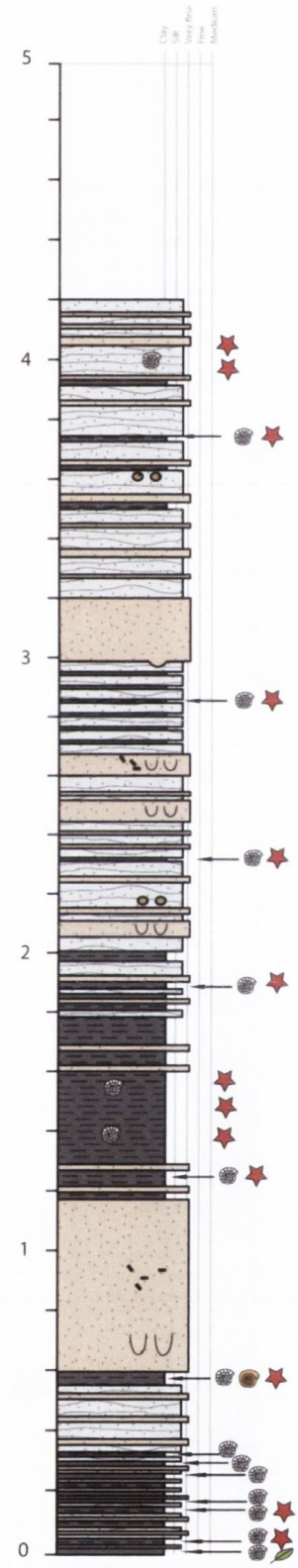

Log through "Dunmore Head west band" in 11-CE-UCD-08 (start at 60 m going up).

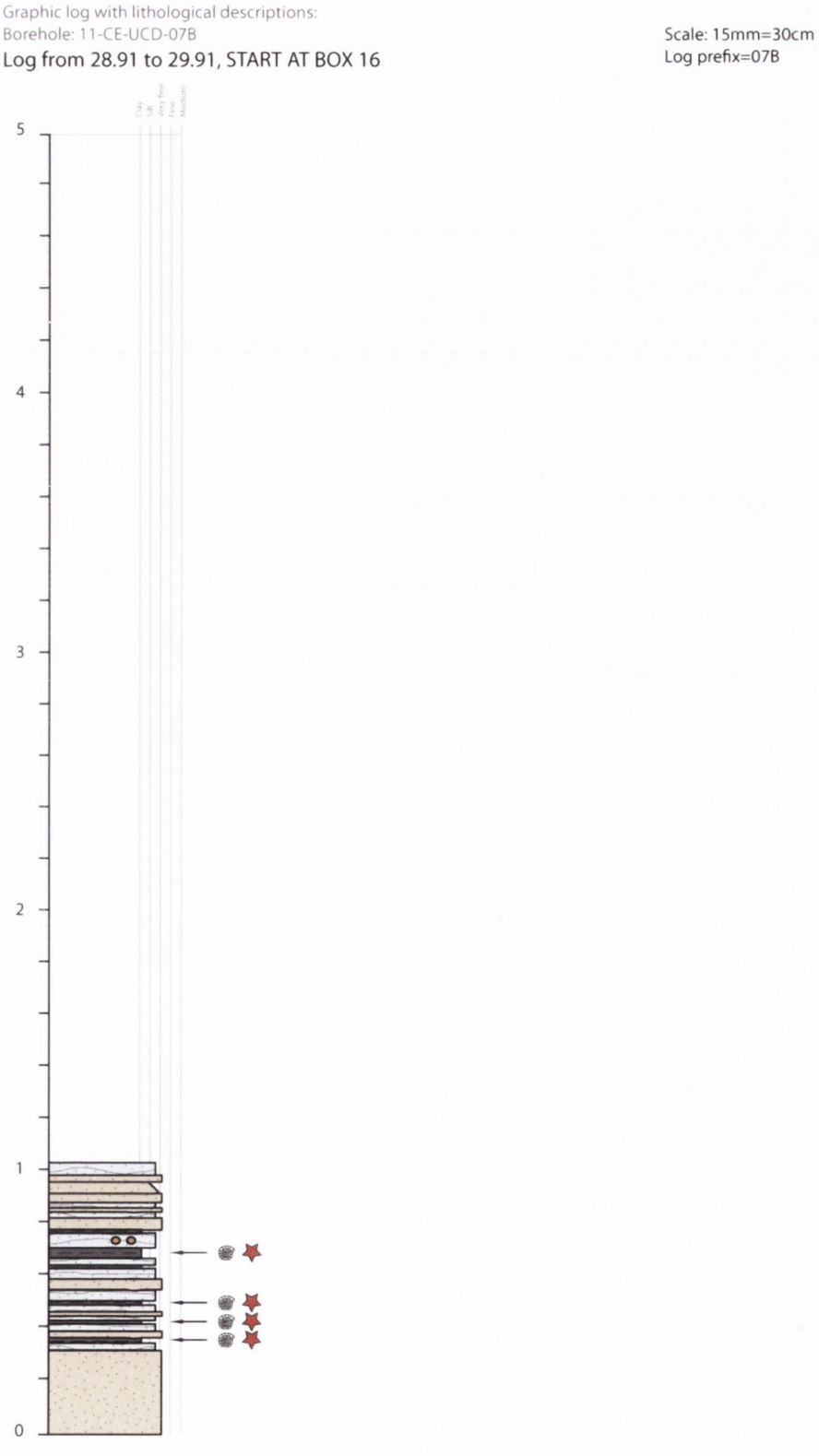

Log through fossiliferous band in 11-CE-UCD-07B (core box 16, 28-29 m depth).

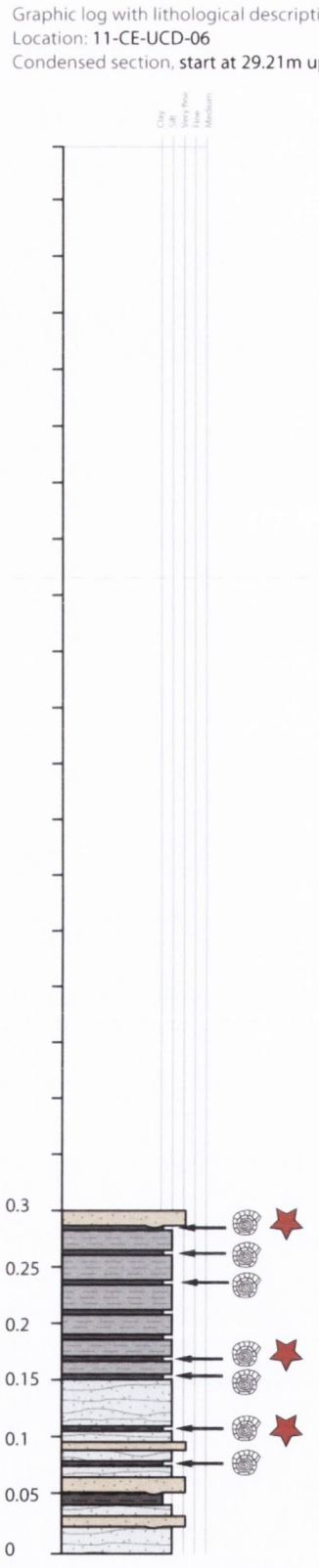

Log through fossiliferous band in 11-CE-UCD-06 (core box 14, 29-28 m depth).

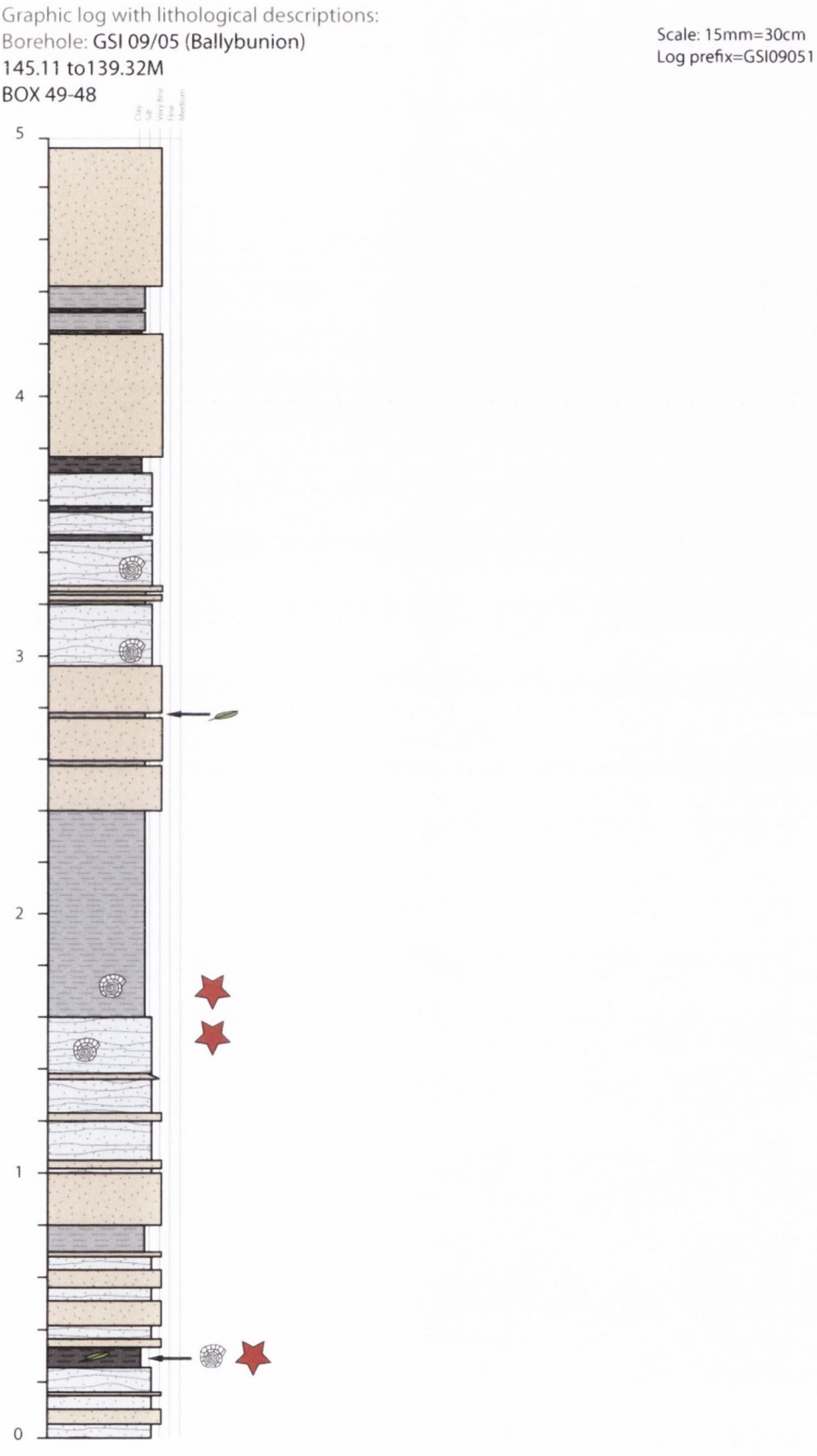

Log 1 through GSI09/05 (Ballybunion borehole) fossiliferous band (depth is indicated in the figure).

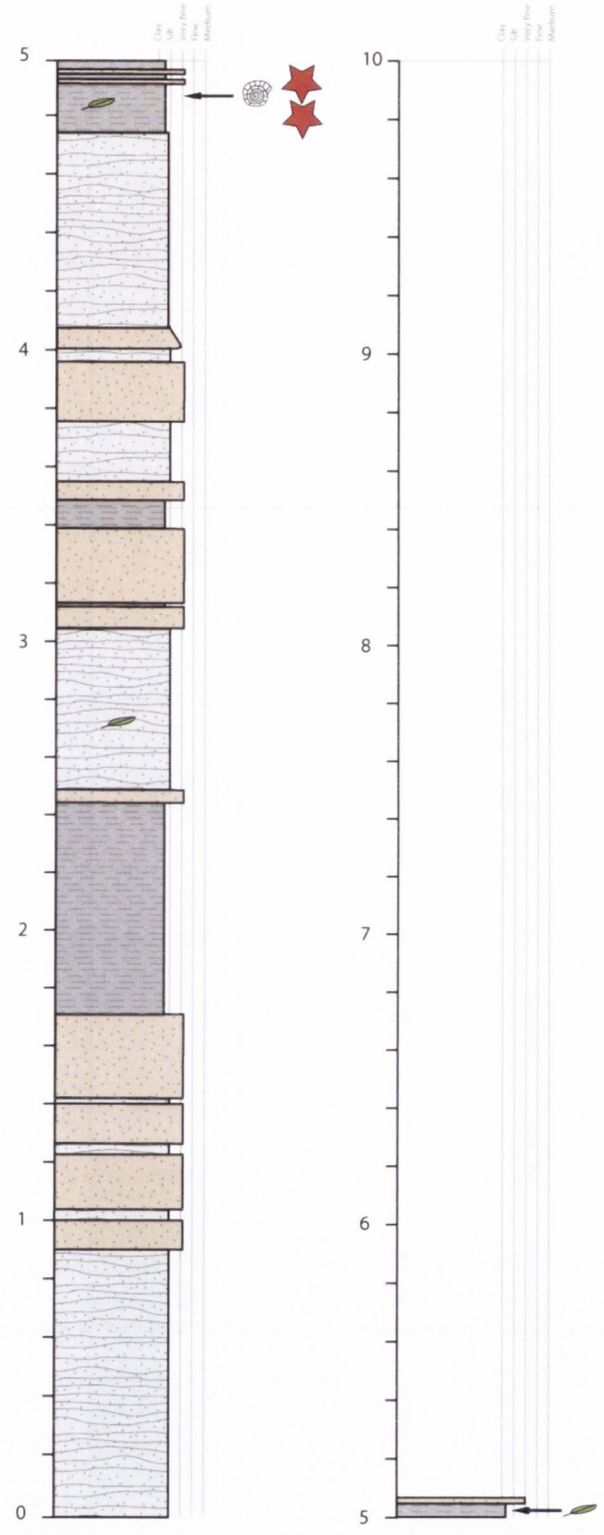

Log 2 through GSI09/05 (Ballybunion borehole) fossiliferous band. (depth is indicated in the figure)

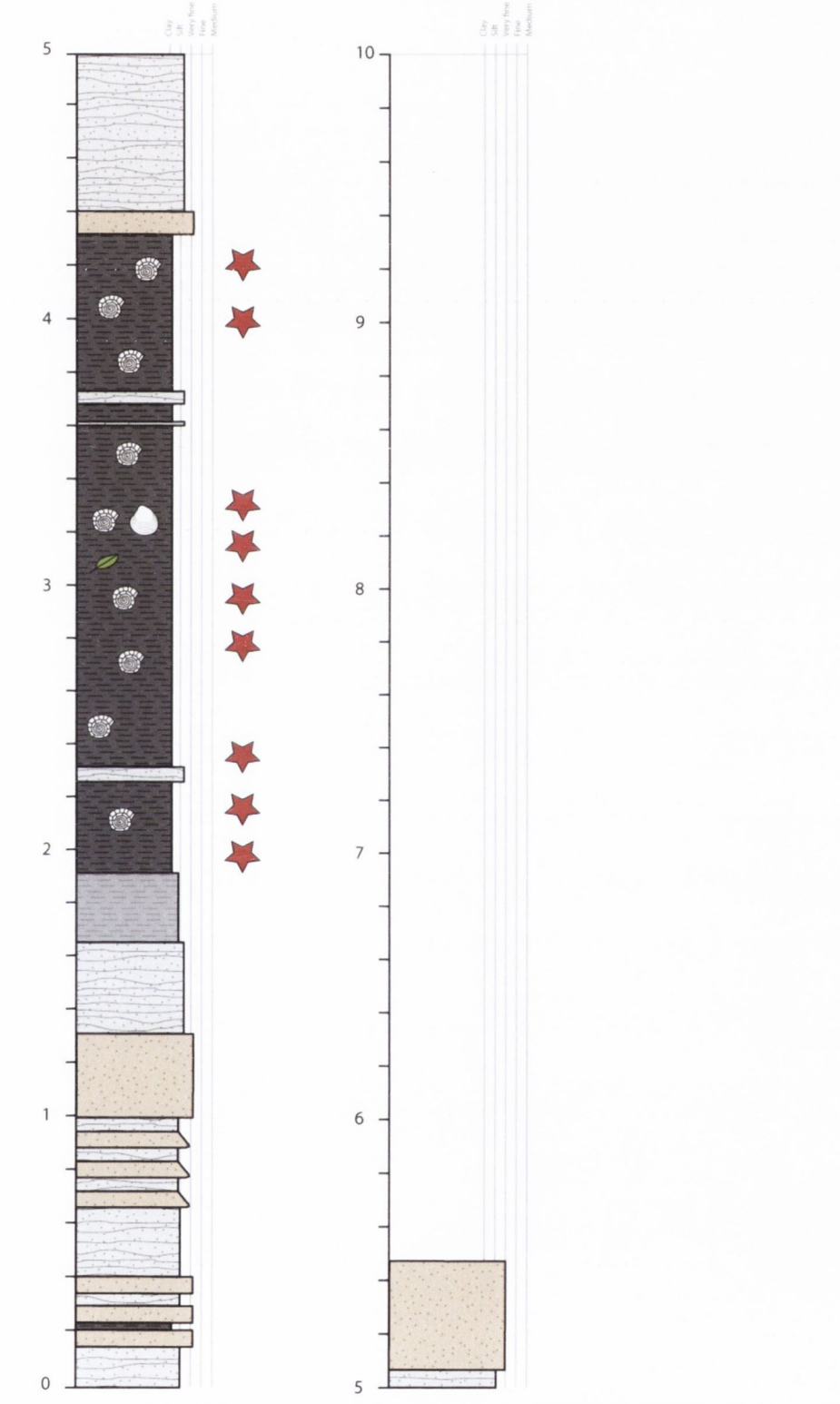

Log 3 through GSI09/05 (Ballybunion borehole) fossiliferous band band (depth is indicated in the figure).

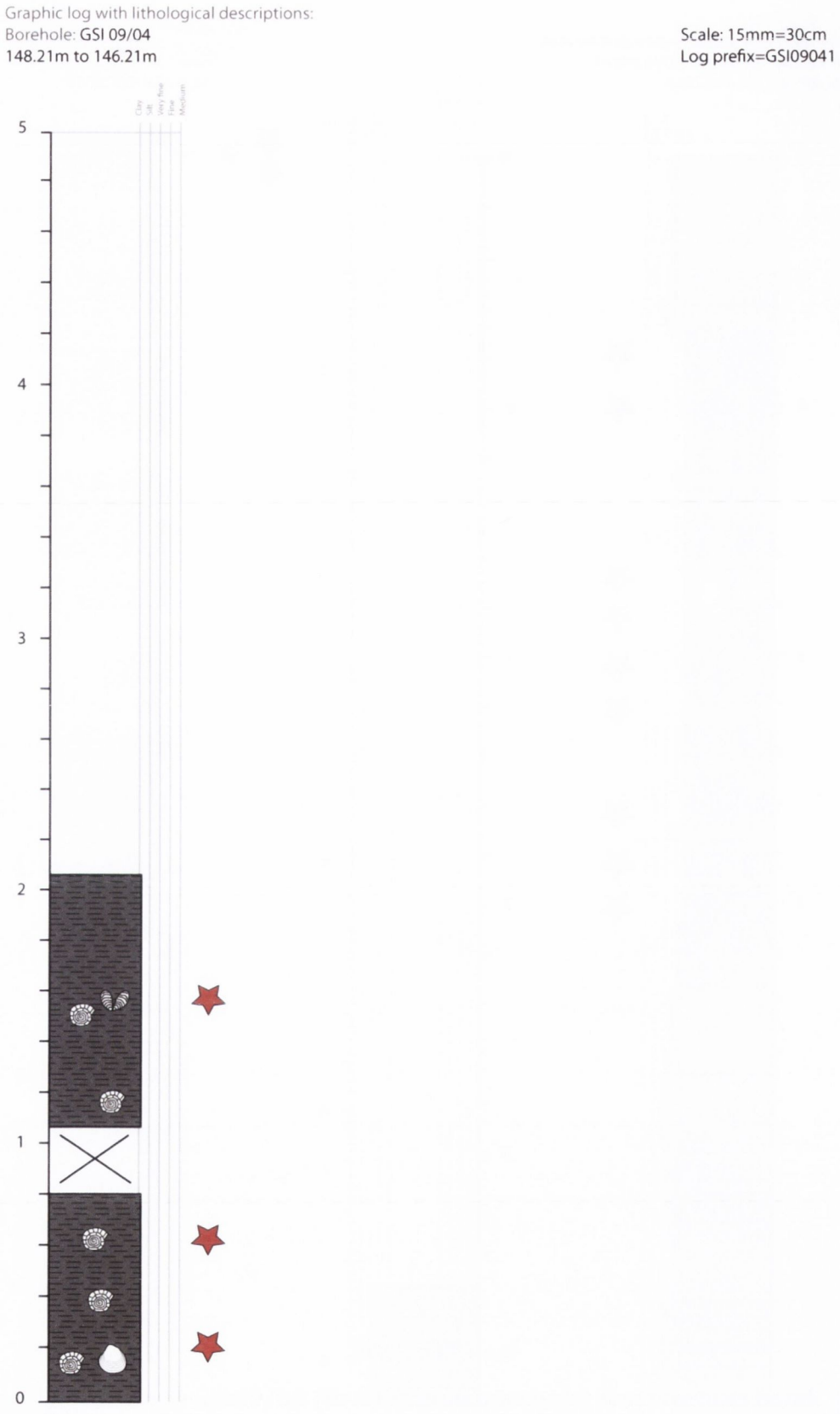

Log 1 through GSI09/04 (Kildysart borehole) fossiliferous band (depth is indicated in the figure).

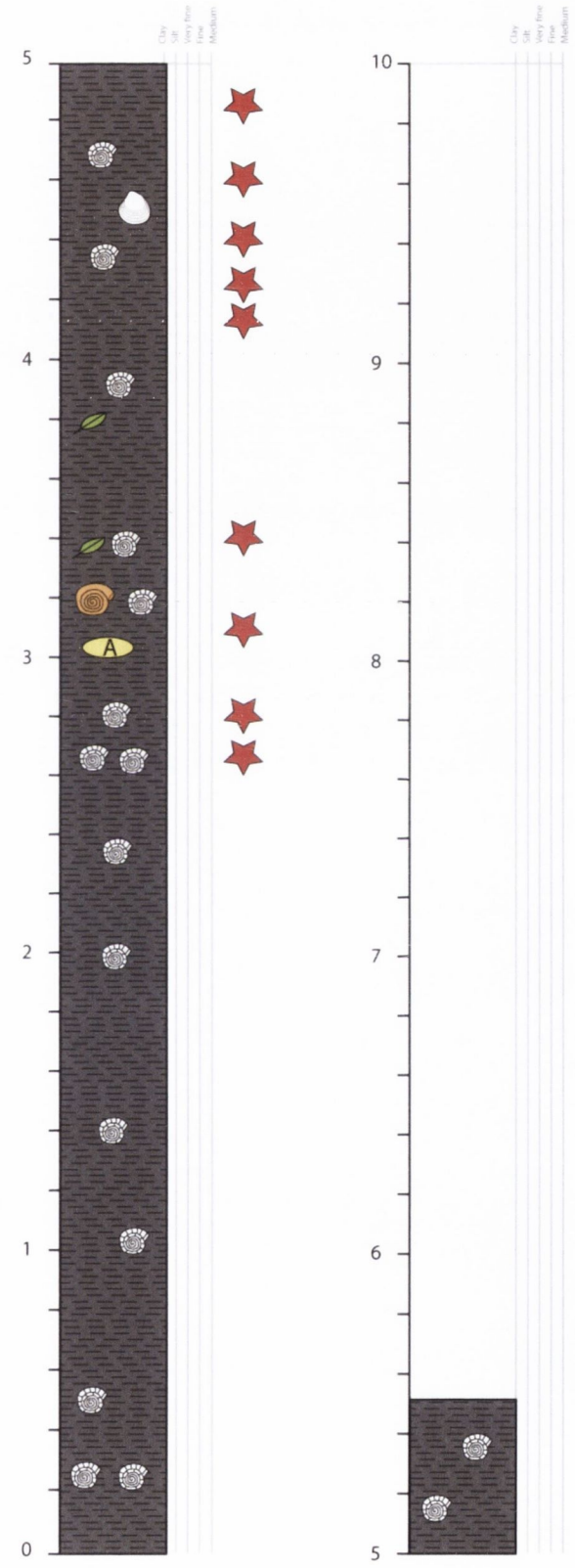

Log 2 through GSI09/04 (Kildysart borehole) fossiliferous band (depth is indicated in the figure).

Appendix C:
Palynology Data

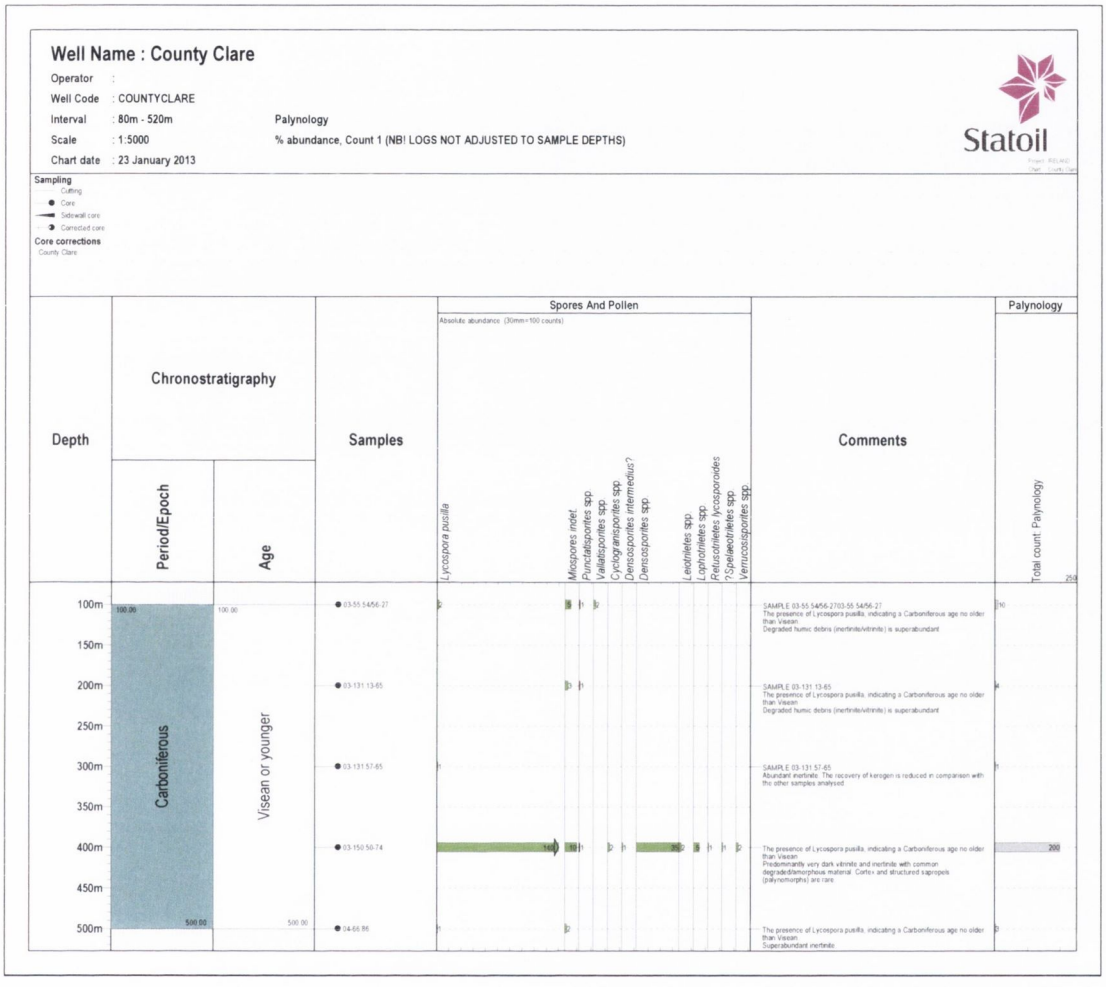

Above: Palynology results compiled by Statoil Labs. All of the samples can be dated as Carboniferous, with the presence of *Lycospora pusilla* indicating a Visean or younger age; a more refined dating was not possible due to the poor recovery and low diversity of taxa.

Appendix D:

XRD Results

a)

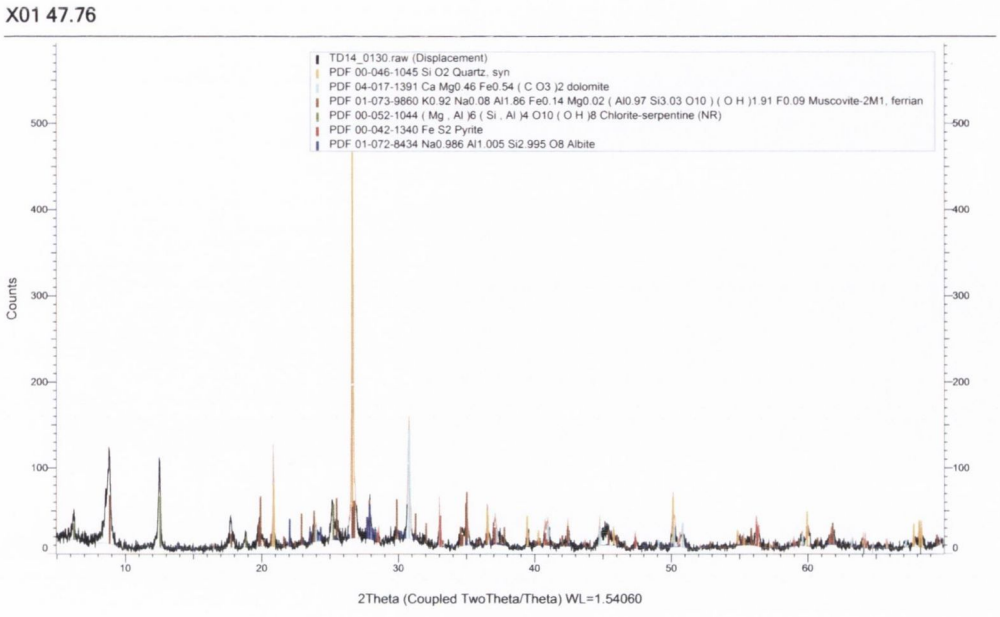
X01 47.76
TD14_0130.raw (Displacement)
PDF 00-046-1045 Si O2 Quartz, syn
PDF 04-017-1391 Ca Mg0.46 Fe0.54 (C O3)2 dolomite
PDF 01-073-9860 K0.92 Na0.08 Al1.86 Fe0.14 Mg0.02 (Al0.97 Si3.03 O10) (O H)1.91 F0.09 Muscovite-2M1, ferrian
PDF 00-052-1044 (Mg , Al)6 (Si , Al)4 O10 (O H)8 Chlorite-serpentine (NR)
PDF 00-042-1340 Fe S2 Pyrite
PDF 01-072-8434 Na0.986 Al1.005 Si2.995 O8 Albite
Counts
2Theta (Coupled TwoTheta/Theta) WL=1.54060

b)

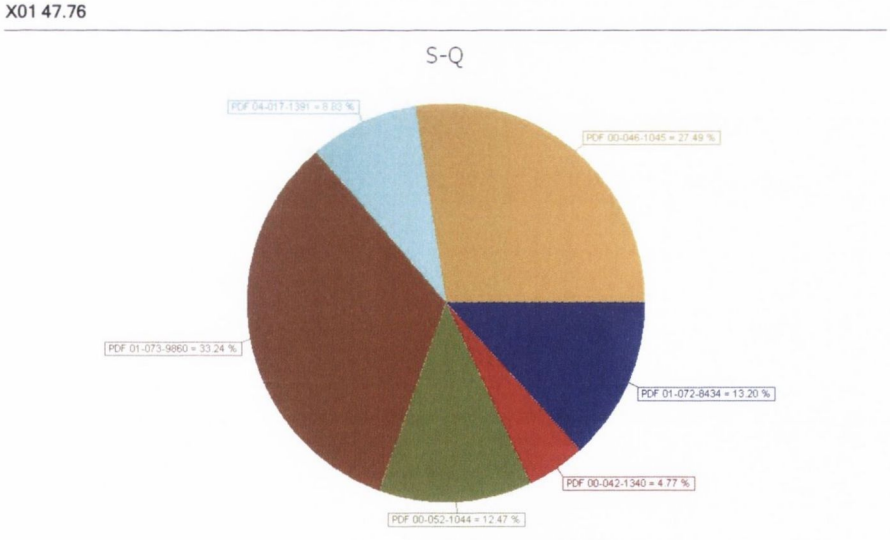
X01 47.76
S-Q
PDF 04-017-1391 = 8.82 %
PDF 00-046-1045 = 27.49 %
PDF 01-073-9860 = 33.24 %
PDF 01-072-8434 = 13.20 %
PDF 00-042-1340 = 4.77 %
PDF 00-052-1044 = 12.47 %

c)

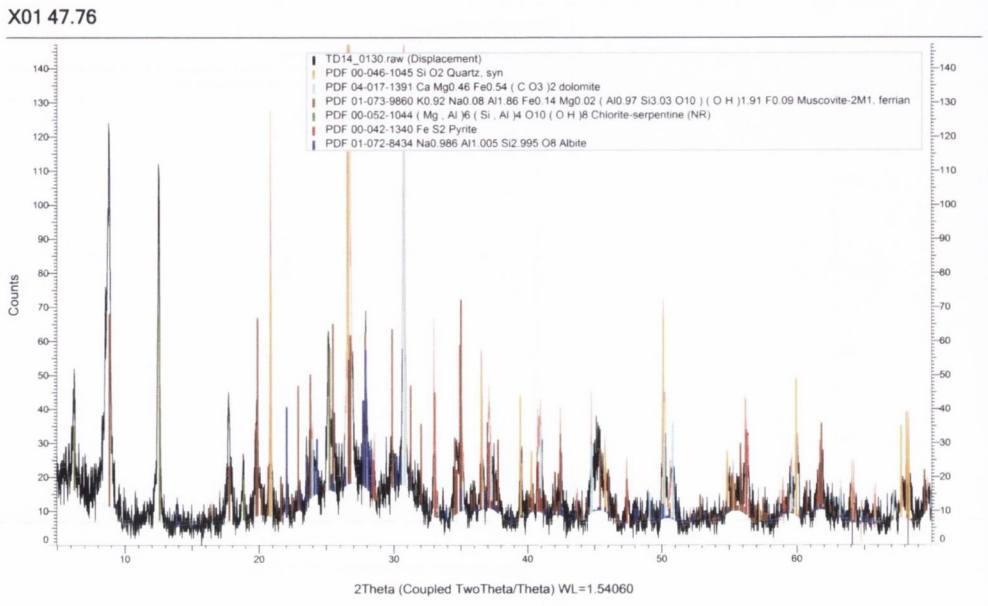

XRD Results Sample 1

a)

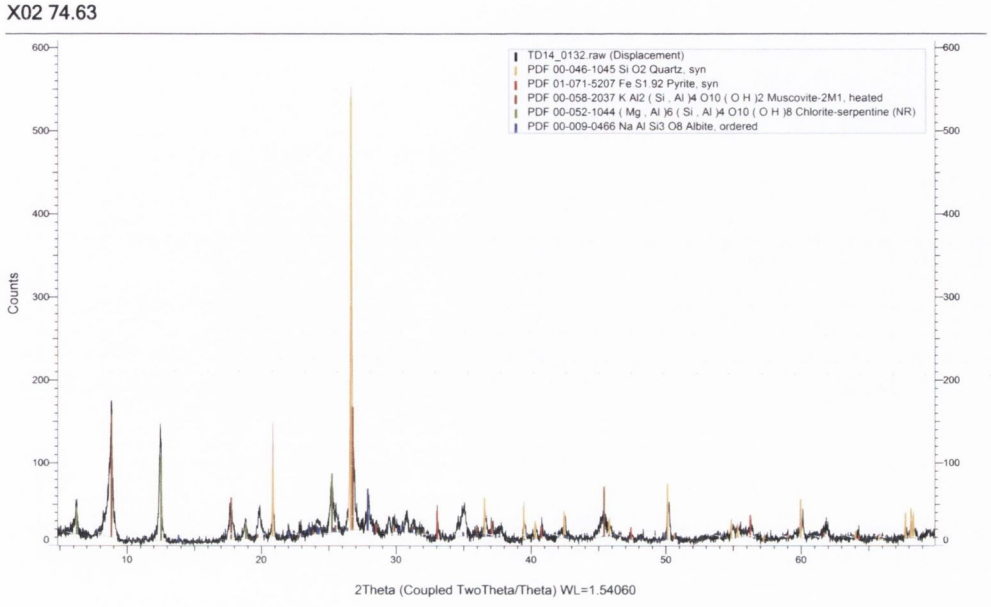
X02 74.63
TD14_0132.raw (Displacement)
PDF 00-046-1045 Si O2 Quartz, syn
PDF 01-071-5207 Fe S1.92 Pyrite, syn
PDF 00-058-2037 K Al2 (Si , Al)4 O10 (O H)2 Muscovite-2M1, heated
PDF 00-052-1044 (Mg , Al)6 (Si , Al)4 O10 (O H)8 Chlorite-serpentine (NR)
PDF 00-009-0466 Na Al Si3 O8 Albite, ordered
Counts
2Theta (Coupled TwoTheta/Theta) WL=1.54060

b)

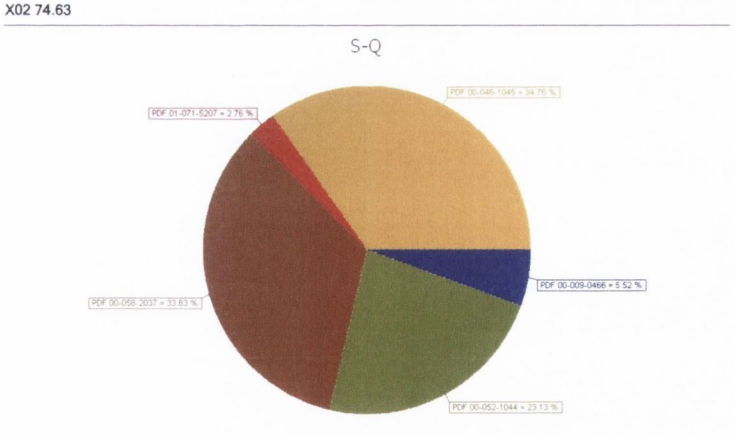
X02 74.63
S-Q
PDF 00-046-1045 = 34.75 %
PDF 01-071-5207 = 2.76 %
PDF 00-009-0466 = 5.52 %
PDF 00-058-2037 = 33.83 %
PDF 00-052-1044 = 23.13 %

c)

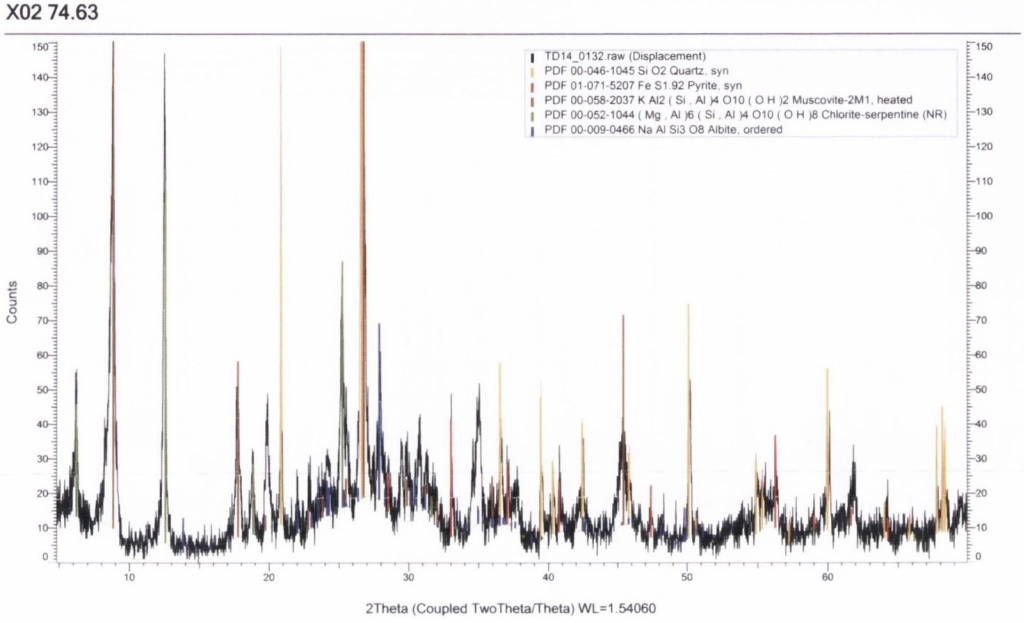

XRD Results Sample 2

a)

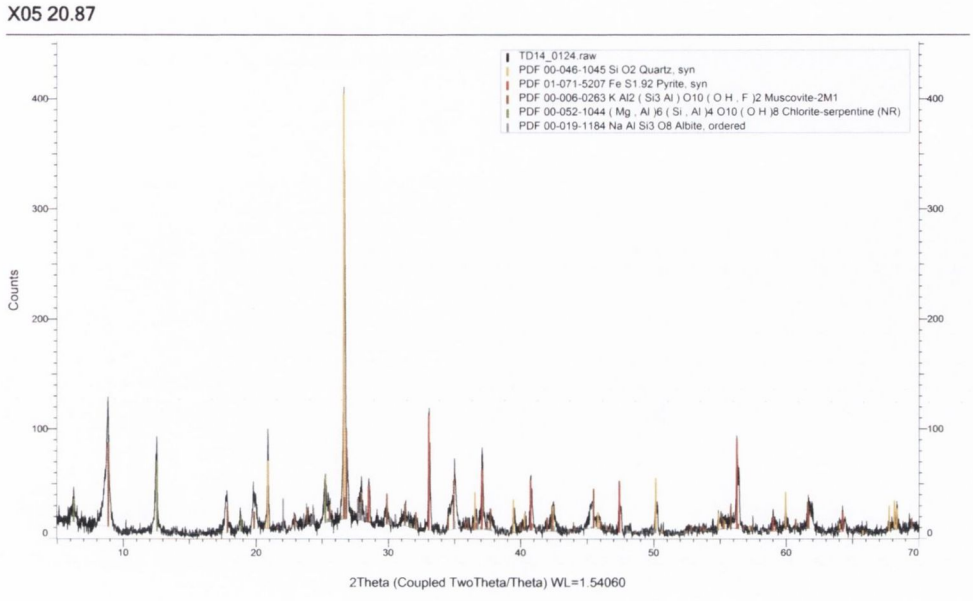
X05 20.87
TD14_0124.raw
PDF 00-046-1045 Si O2 Quartz, syn
PDF 01-071-5207 Fe S1.92 Pyrite, syn
PDF 00-006-0263 K Al2 (Si3 Al) O10 (O H , F)2 Muscovite-2M1
PDF 00-052-1044 (Mg , Al)6 (Si , Al)4 O10 (O H)8 Chlorite-serpentine (NR)
PDF 00-019-1184 Na Al Si3 O8 Albite, ordered
Counts
2Theta (Coupled TwoTheta/Theta) WL=1.54060

b)

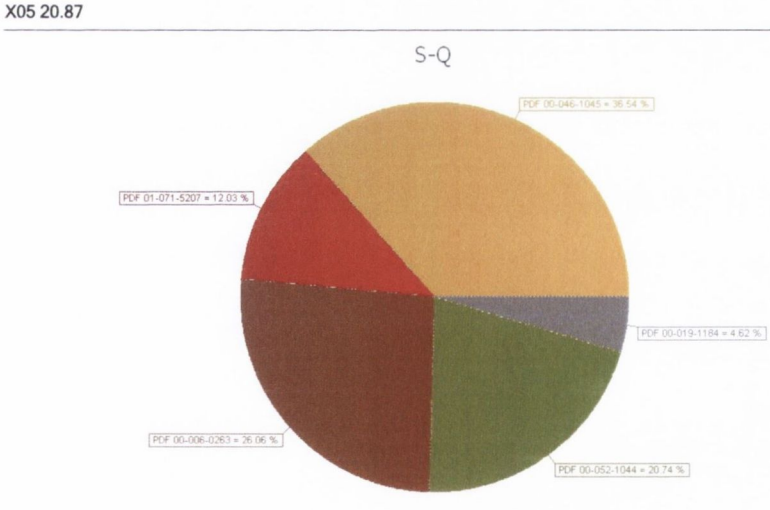
X05 20.87
S-Q
PDF 00-046-1045 = 36.54 %
PDF 01-071-5207 = 12.03 %
PDF 00-019-1184 = 4.62 %
PDF 00-006-0263 = 26.06 %
PDF 00-052-1044 = 20.74 %

c)

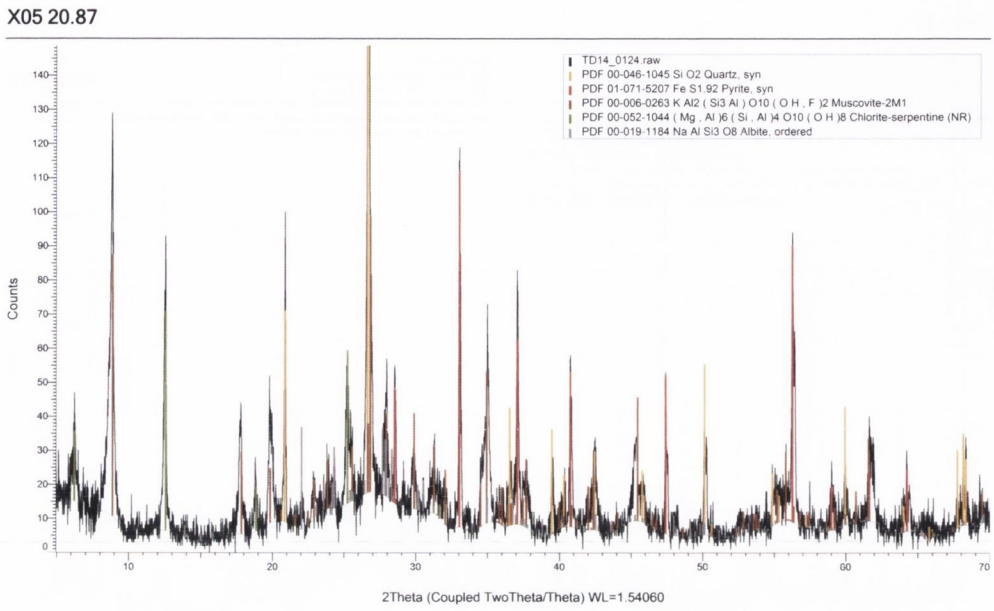

XRD Results sample 3

a)

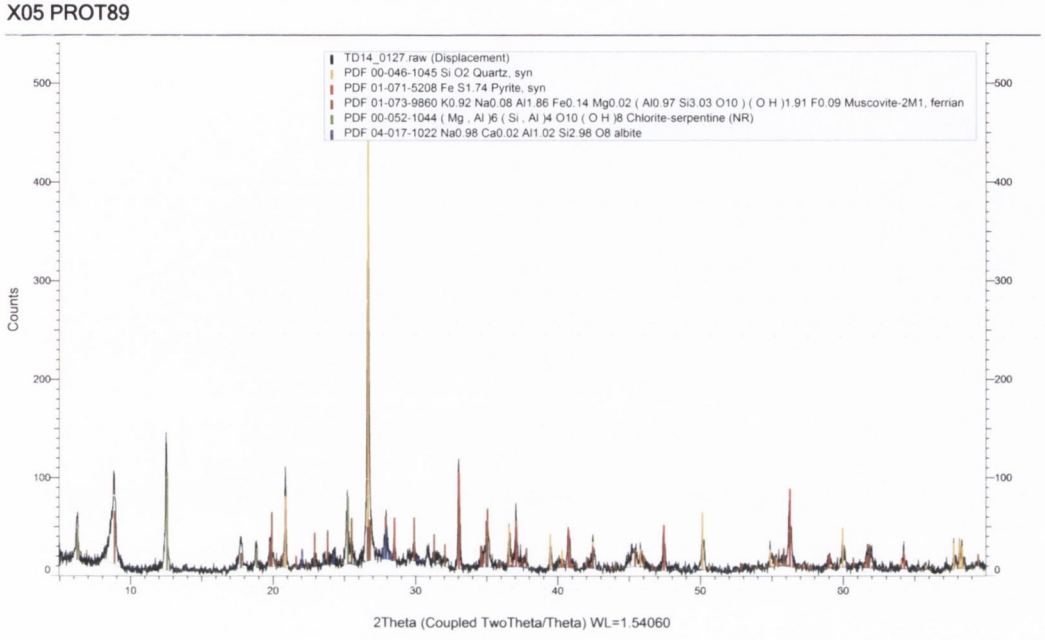
X05 PROT89
TD14_0127.raw (Displacement)
PDF 00-046-1045 Si O2 Quartz, syn
PDF 01-071-5208 Fe S1.74 Pyrite, syn
PDF 01-073-9860 K0.92 Na0.08 Al1.86 Fe0.14 Mg0.02 (Al0.97 Si3.03 O10) (O H)1.91 F0.09 Muscovite-2M1, ferrian
PDF 00-052-1044 (Mg , Al)6 (Si , Al)4 O10 (O H)8 Chlorite-serpentine (NR)
PDF 04-017-1022 Na0.98 Ca0.02 Al1.02 Si2.98 O8 albite
Counts
2Theta (Coupled TwoTheta/Theta) WL=1.54060

b)

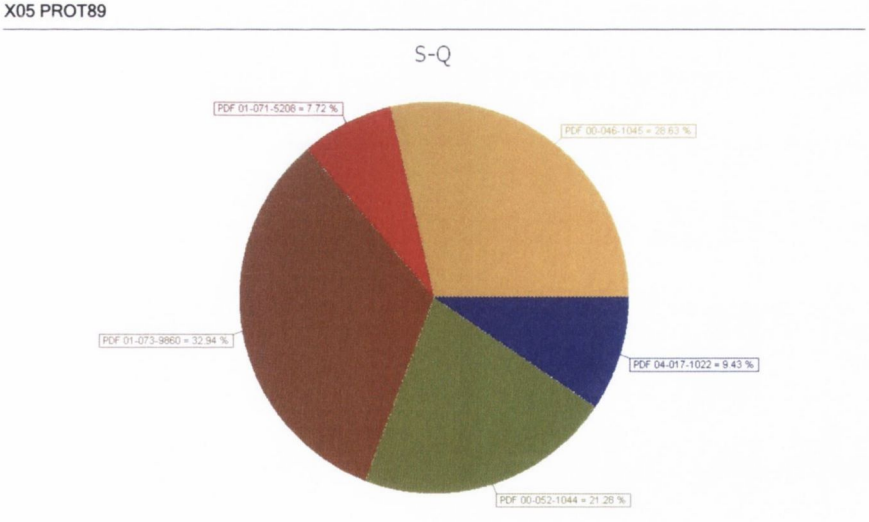
X05 PROT89
S-Q
PDF 01-071-5208 = 7.72 %
PDF 00-046-1045 = 28.63 %
PDF 01-073-9860 = 32.94 %
PDF 04-017-1022 = 9.43 %
PDF 00-052-1044 = 21.28 %

c)

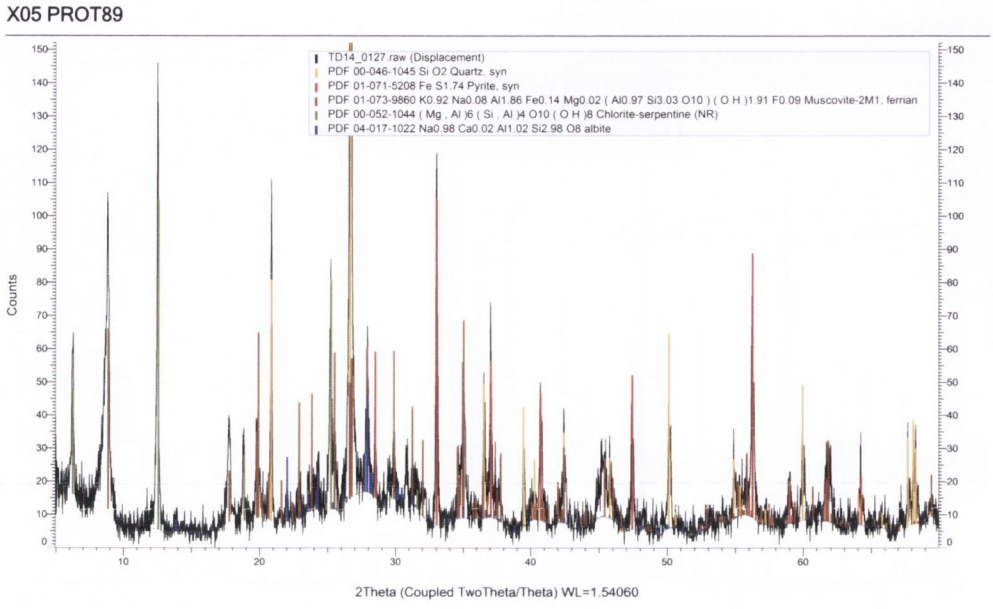

XRD Results Sample 4

a)

X08 55.97

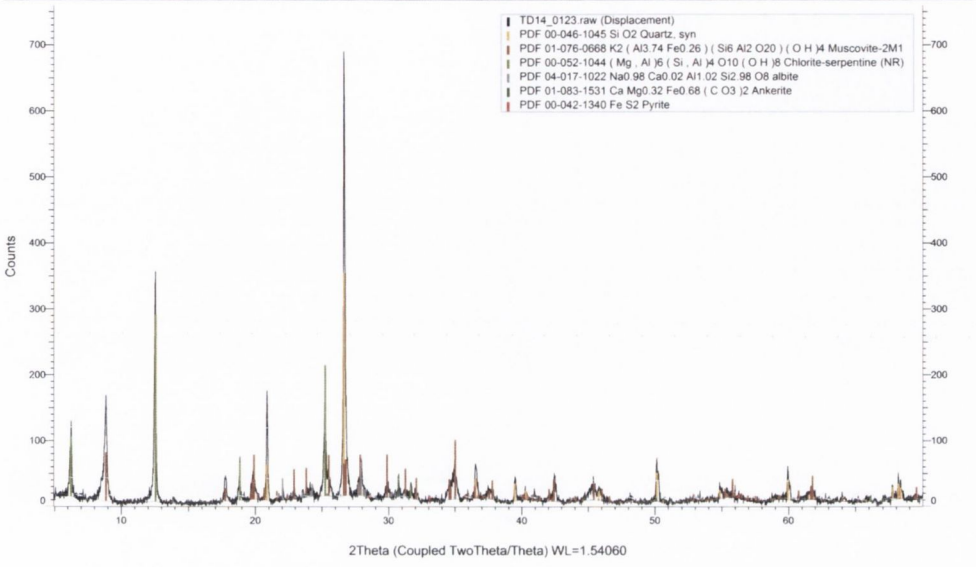

b)

X08 55.97

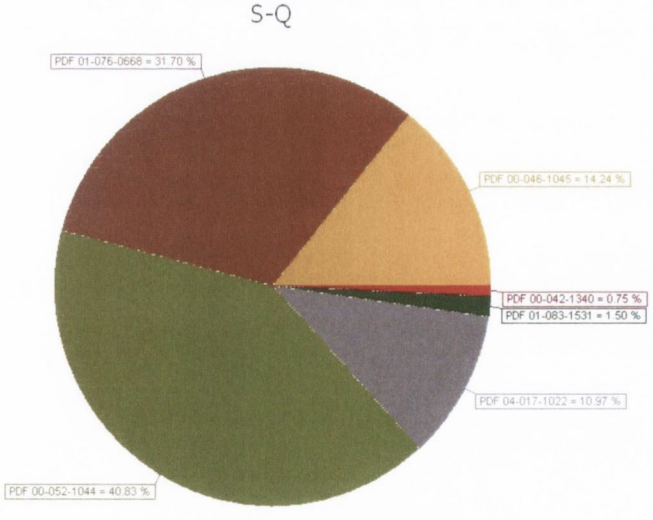

c)

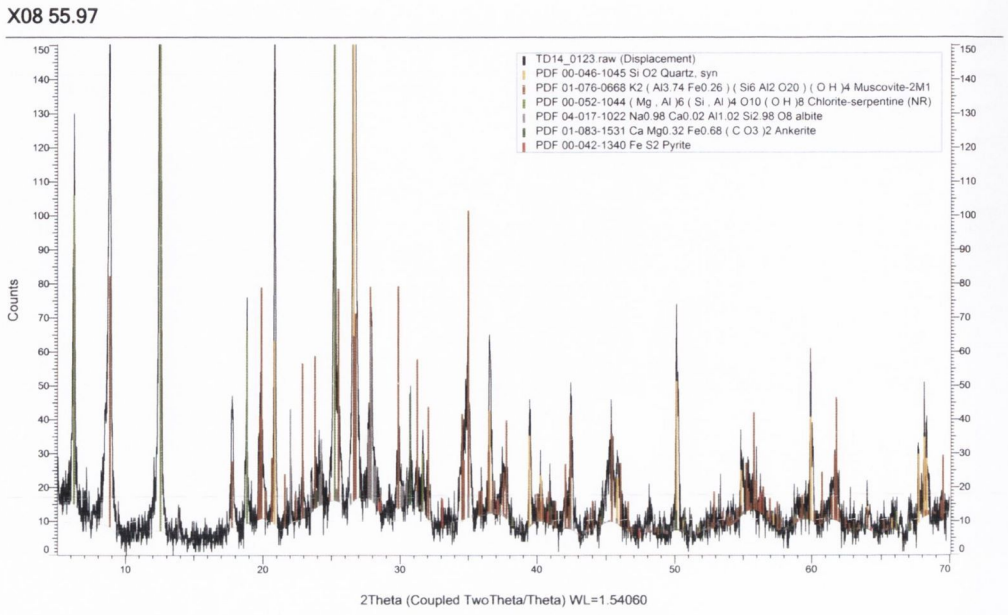

XRD Results Sample 5

a)

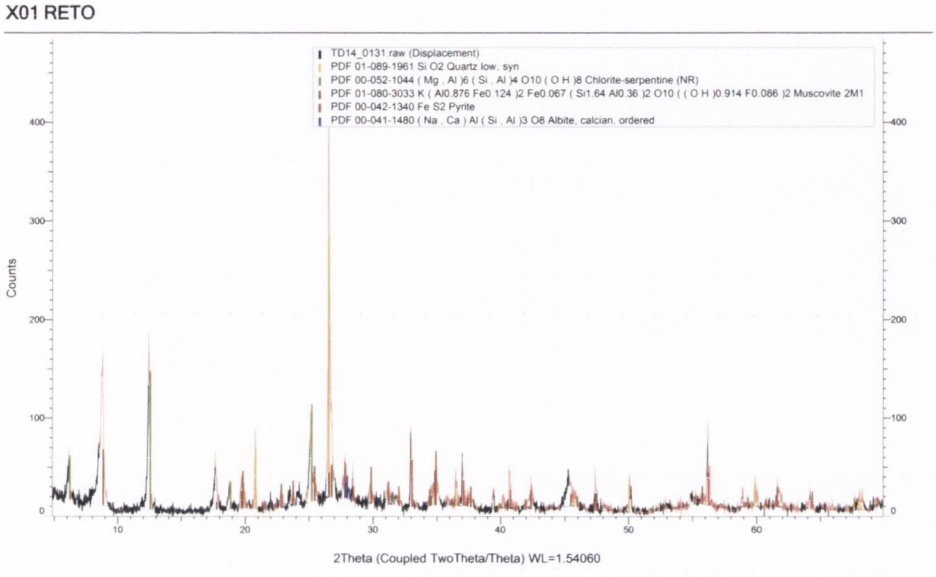
X01 RETO
TD14_0131.raw (Displacement)
PDF 01-089-1961 Si O2 Quartz low, syn
PDF 00-052-1044 (Mg , Al)6 (Si , Al)4 O10 (O H)8 Chlorite-serpentine (NR)
PDF 01-080-3033 K (Al0.876 Fe0.124)2 Fe0.067 (Si1.64 Al0.36)2 O10 ((O H)0.914 F0.086)2 Muscovite 2M1
PDF 00-042-1340 Fe S2 Pyrite
PDF 00-041-1480 (Na , Ca) Al (Si , Al)3 O8 Albite, calcian, ordered
Counts
2Theta (Coupled TwoTheta/Theta) WL=1.54060

b)

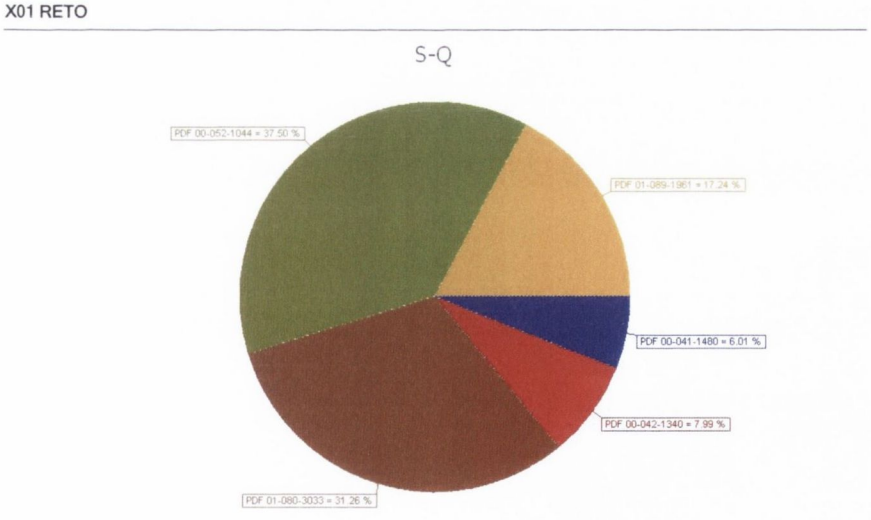
X01 RETO
S-Q
PDF 00-052-1044 = 37.50 %
PDF 01-089-1961 = 17.24 %
PDF 00-041-1480 = 6.01 %
PDF 00-042-1340 = 7.99 %
PDF 01-080-3033 = 31.26 %

c)

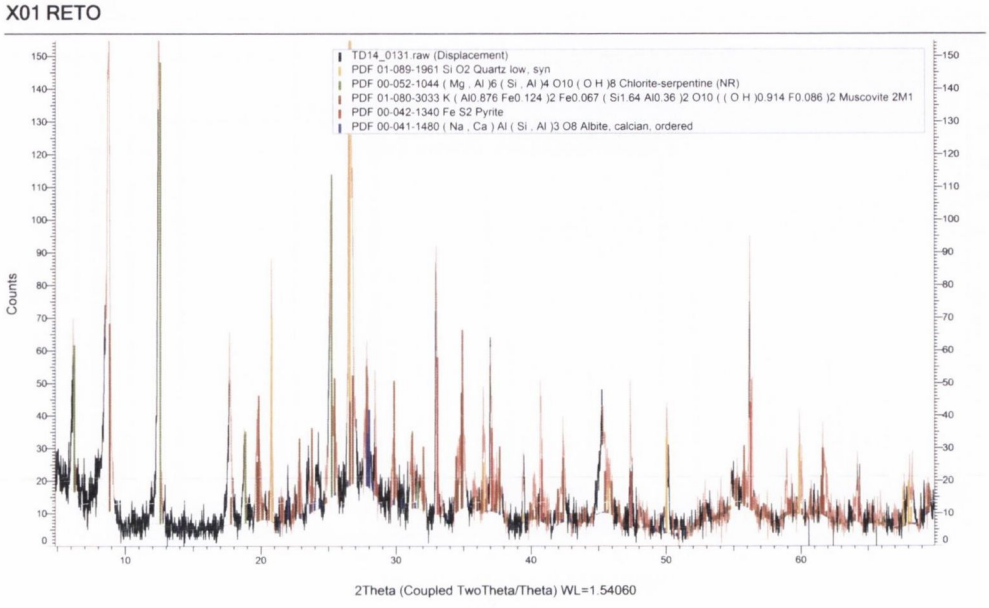

XRD Results Sample 6

a)

XO1RERV 187.38 m

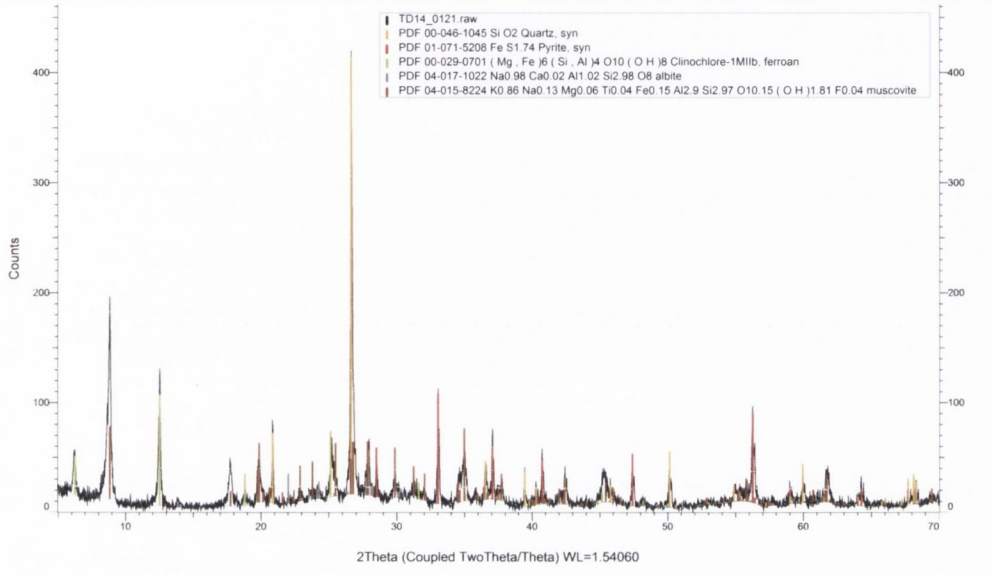

b)

XO1RERV 187.38 m

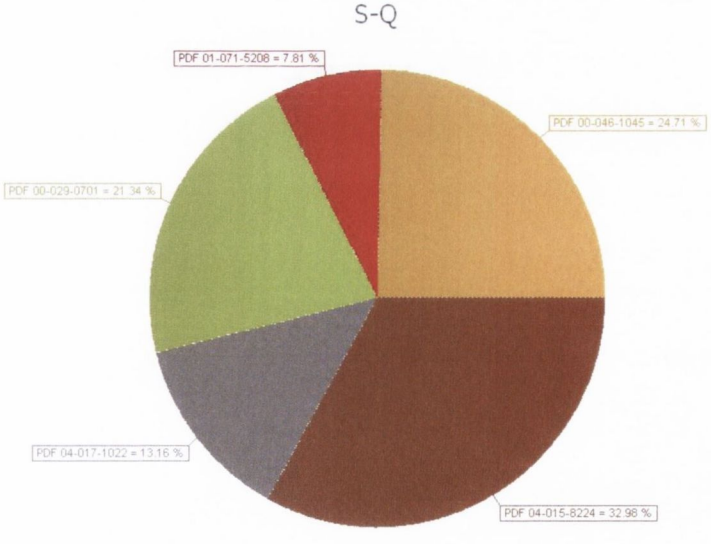

c)

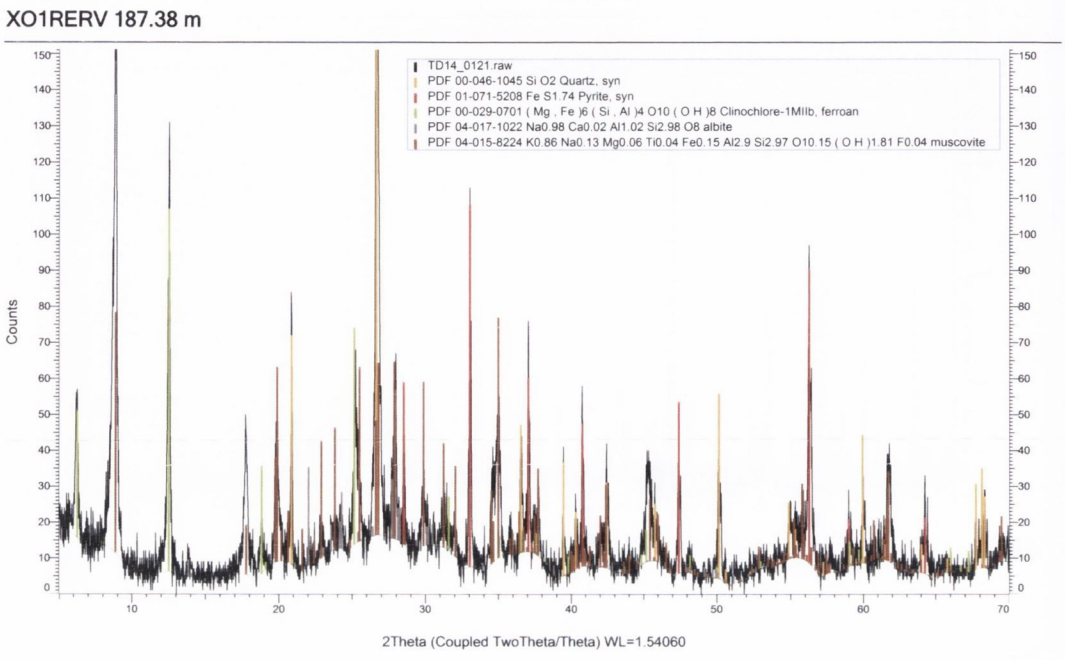

XRD Results Sample 7

a)

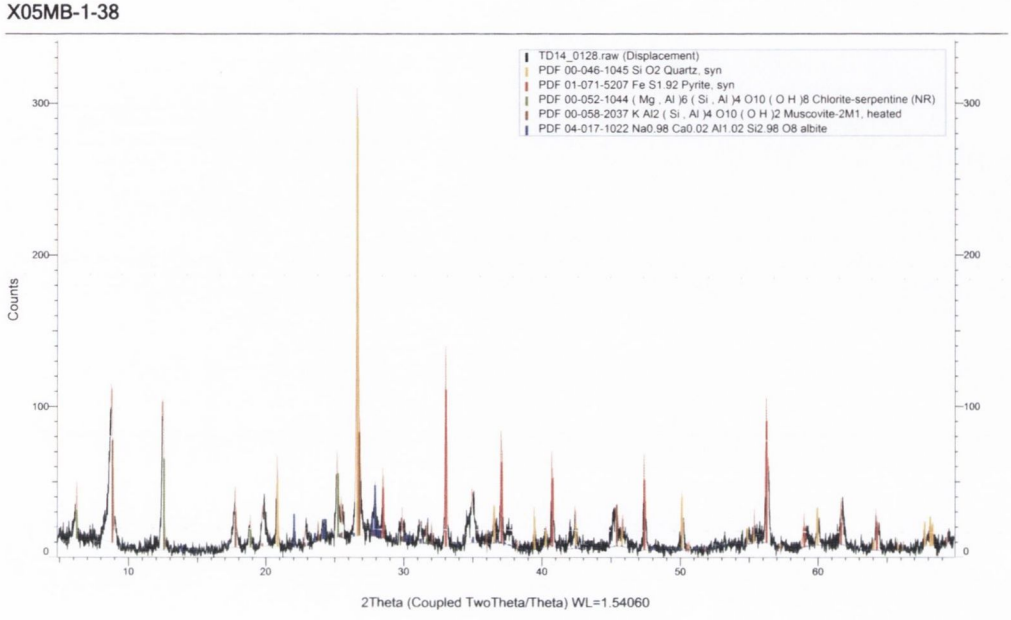
X05MB-1-38
TD14_0128.raw (Displacement)
PDF 00-046-1045 Si O2 Quartz, syn
PDF 01-071-5207 Fe S1.92 Pyrite, syn
PDF 00-052-1044 (Mg , Al)6 (Si , Al)4 O10 (O H)8 Chlorite-serpentine (NR)
PDF 00-058-2037 K Al2 (Si , Al)4 O10 (O H)2 Muscovite-2M1, heated
PDF 04-017-1022 Na0.98 Ca0.02 Al1.02 Si2.98 O8 albite
Counts
2Theta (Coupled TwoTheta/Theta) WL=1.54060

b)

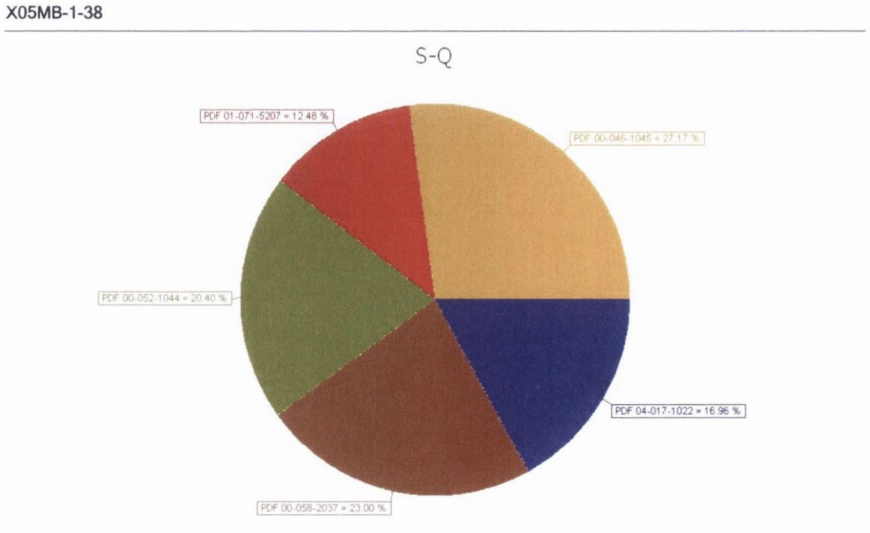
X05MB-1-38
S-Q
PDF 01-071-5207 = 12.48 %
PDF 00-046-1045 = 27.17 %
PDF 00-052-1044 = 20.40 %
PDF 04-017-1022 = 16.96 %
PDF 00-058-2037 = 23.00 %

c)

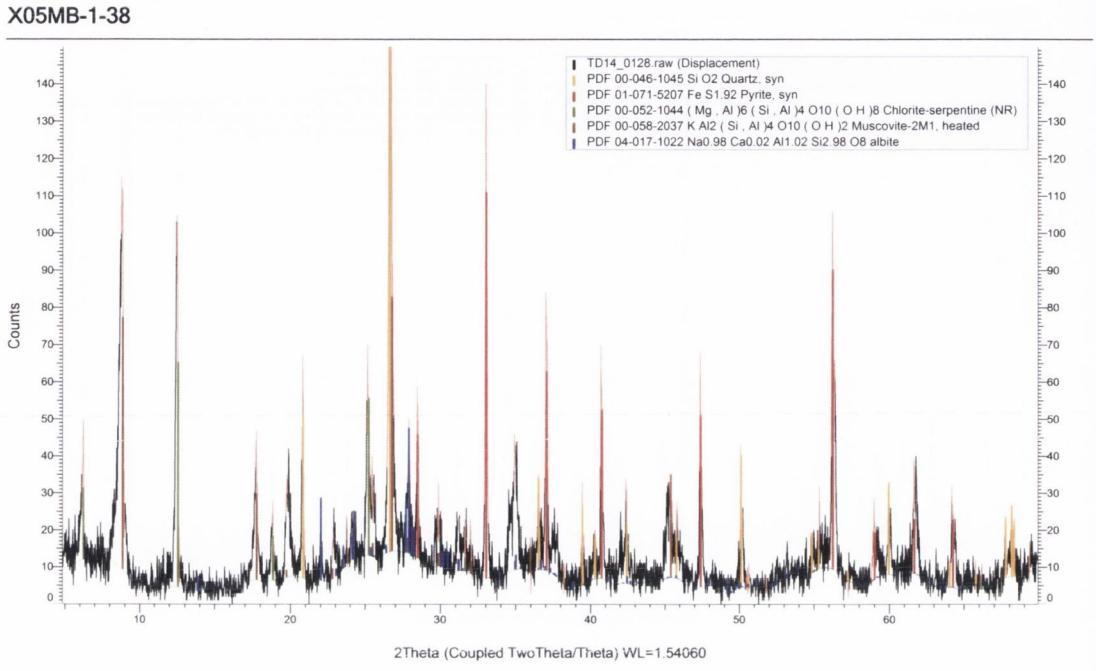

XRD Results Sample 8

a)

XQUILTYCP

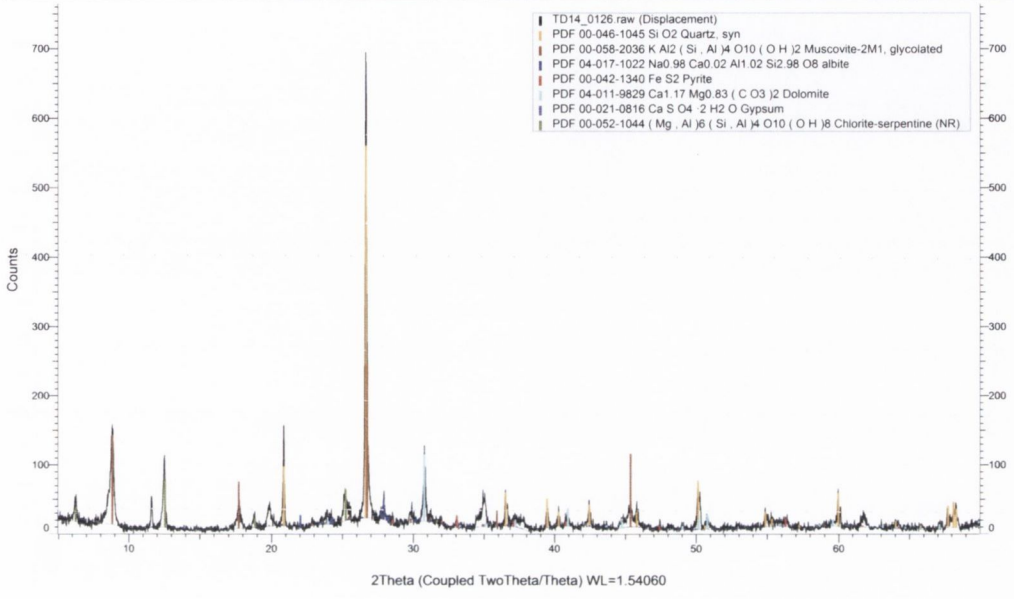

b)

XQUILTYCP

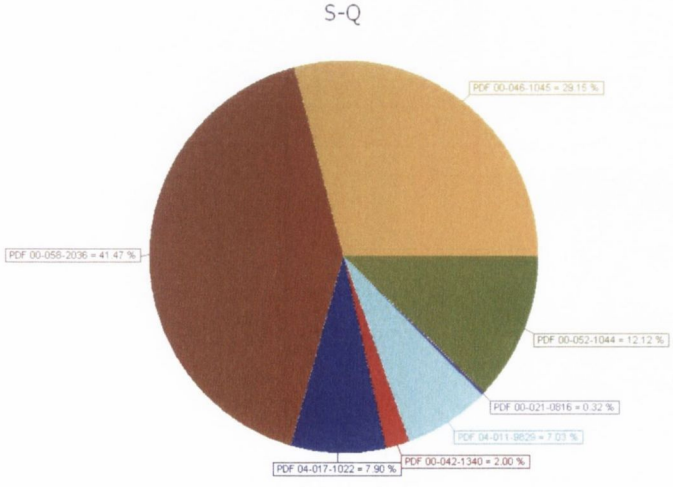

c)

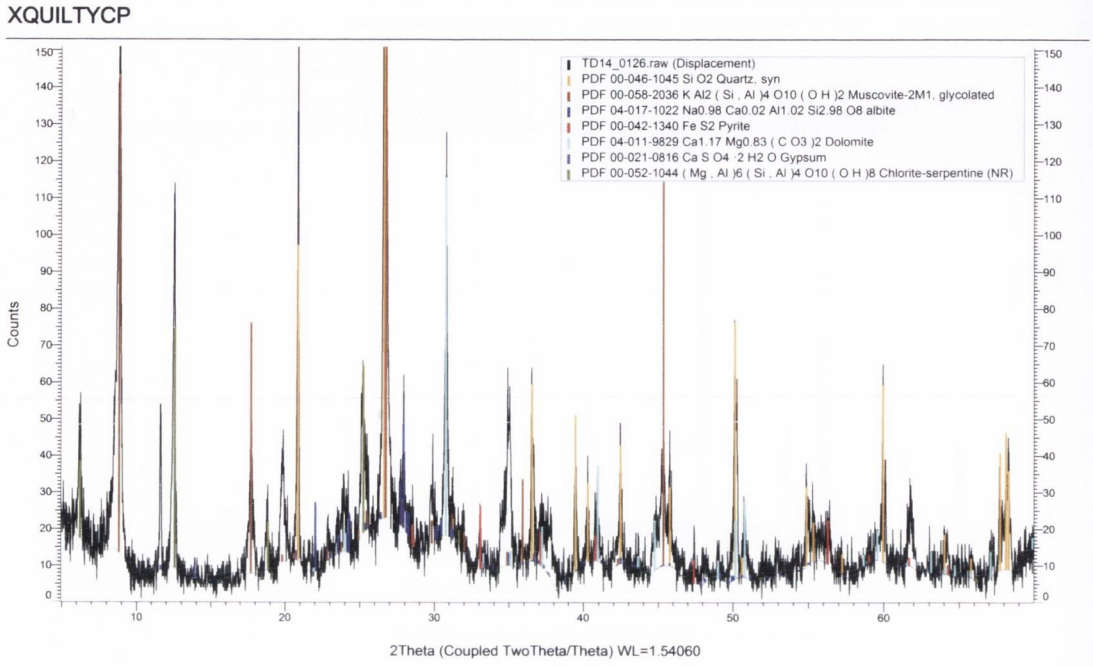

XRD Results Sample 9

a)

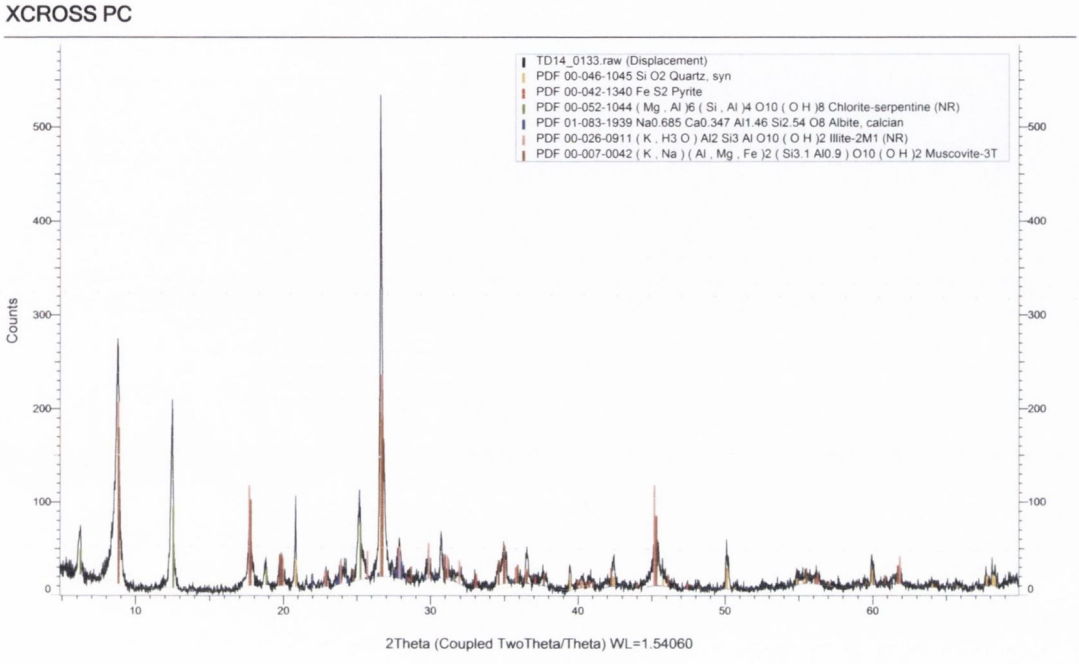
XCROSS PC
TD14_0133.raw (Displacement)
PDF 00-046-1045 Si O2 Quartz, syn
PDF 00-042-1340 Fe S2 Pyrite
PDF 00-052-1044 (Mg , Al)6 (Si , Al)4 O10 (O H)8 Chlorite-serpentine (NR)
PDF 01-083-1939 Na0.685 Ca0.347 Al1.46 Si2.54 O8 Albite, calcian
PDF 00-026-0911 (K , H3 O) Al2 Si3 Al O10 (O H)2 Illite-2M1 (NR)
PDF 00-007-0042 (K , Na) (Al , Mg , Fe)2 (Si3.1 Al0.9) O10 (O H)2 Muscovite-3T
Counts
0
100
200
300
400
500
10
20
30
40
50
60
2Theta (Coupled TwoTheta/Theta) WL=1.54060

b)

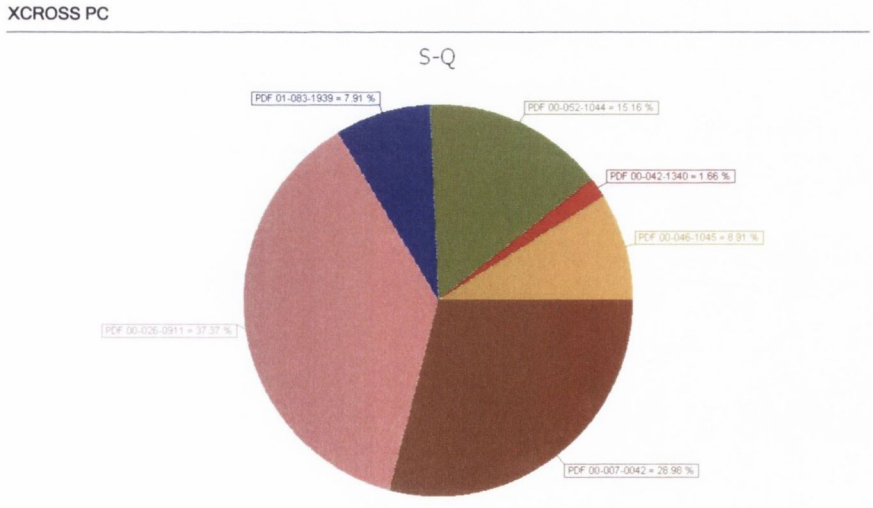
XCROSS PC
S-Q
PDF 01-083-1939 = 7.91 %
PDF 00-052-1044 = 15.16 %
PDF 00-042-1340 = 1.66 %
PDF 00-046-1045 = 8.91 %
PDF 00-026-0911 = 37.37 %
PDF 00-007-0042 = 28.96 %

c)

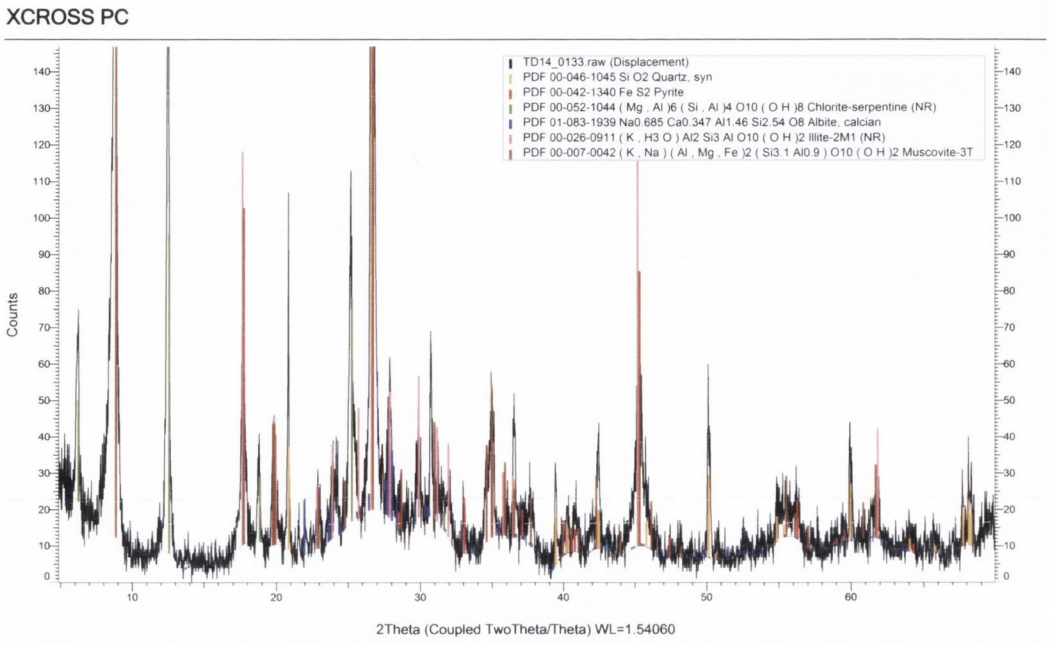

XRD Results Sample 10

a)

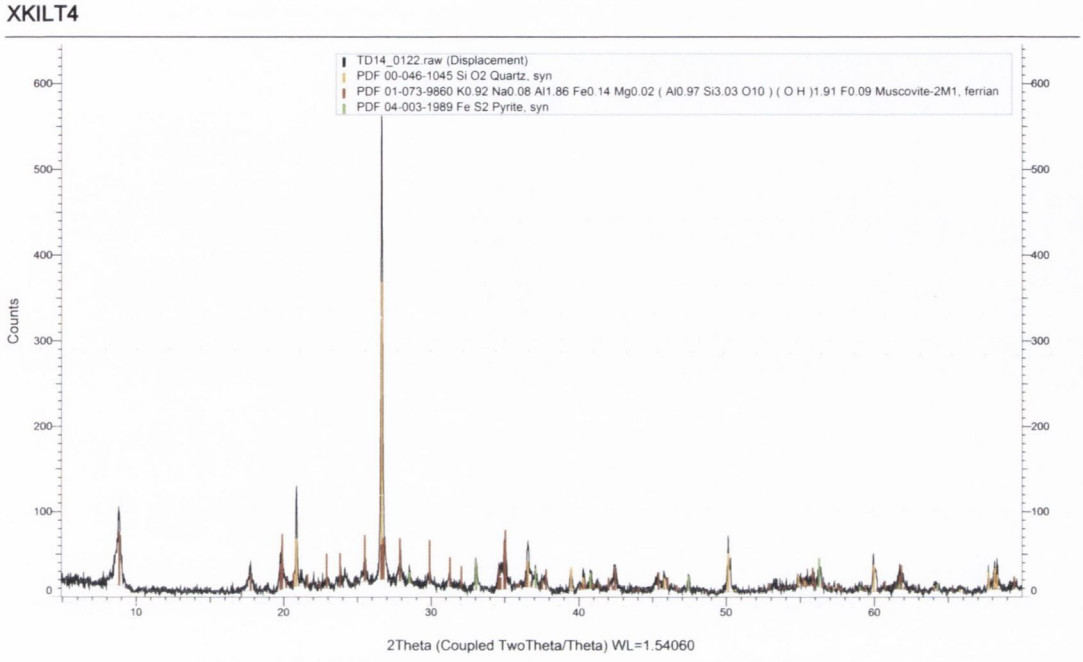

b)

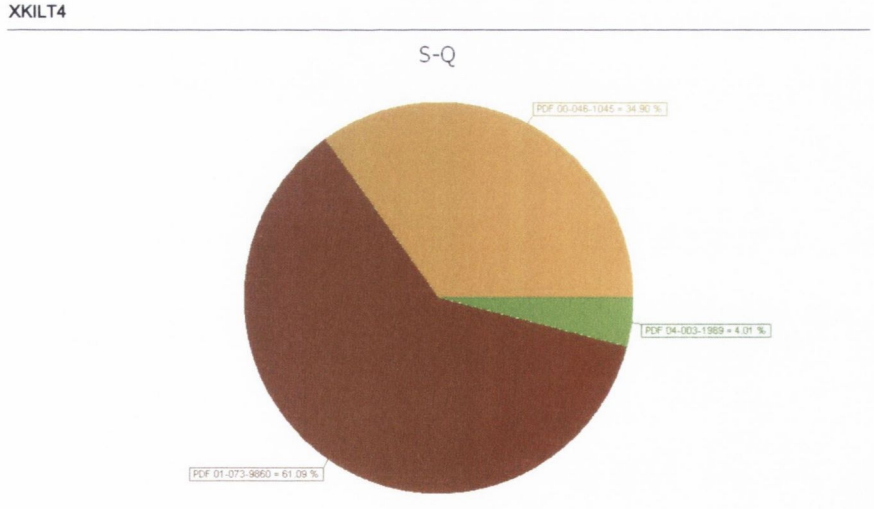

XRD Results Sample 11

a)

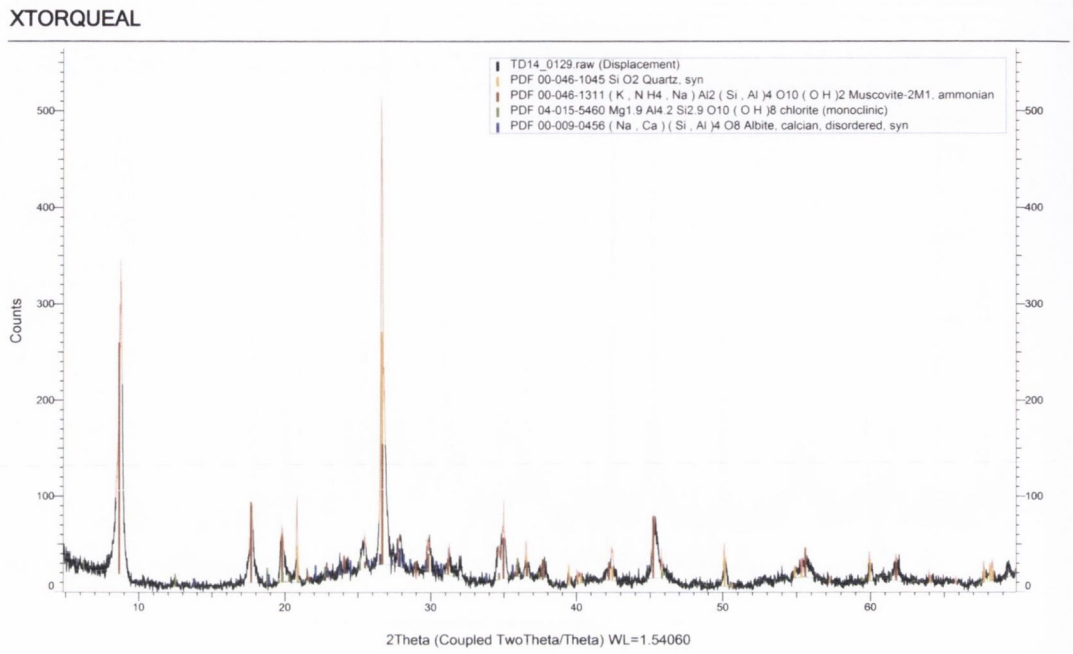
XTORQUEAL
TD14_0129.raw (Displacement)
PDF 00-046-1045 Si O2 Quartz, syn
PDF 00-046-1311 (K , N H4 , Na) Al2 (Si , Al)4 O10 (O H)2 Muscovite-2M1, ammonian
PDF 04-015-5460 Mg1.9 Al4.2 Si2.9 O10 (O H)8 chlorite (monoclinic)
PDF 00-009-0456 (Na , Ca) (Si , Al)4 O8 Albite, calcian, disordered, syn
Counts
0
100
200
300
400
500
10
20
30
40
50
60
2Theta (Coupled TwoTheta/Theta) WL=1.54060

b)

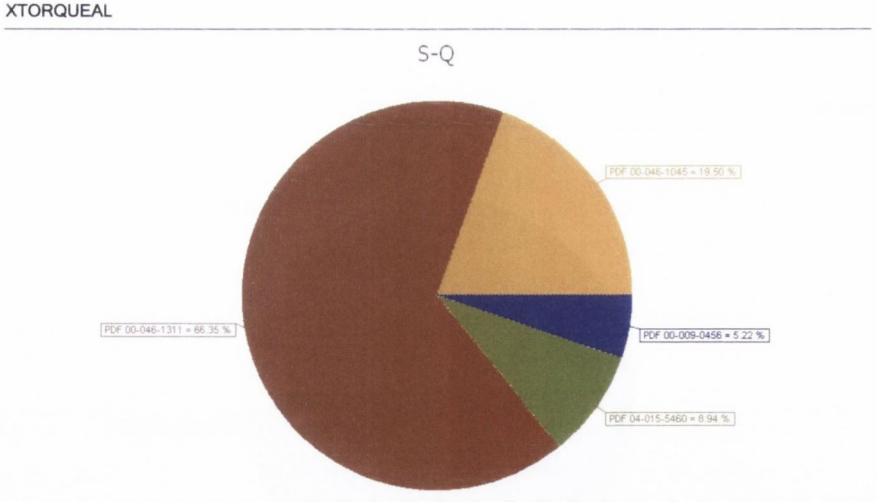
XTORQUEAL
S-Q
PDF 00-046-1045 = 19.50 %
PDF 00-009-0456 = 5.22 %
PDF 04-015-5460 = 8.94 %
PDF 00-046-1311 = 66.35 %

c)

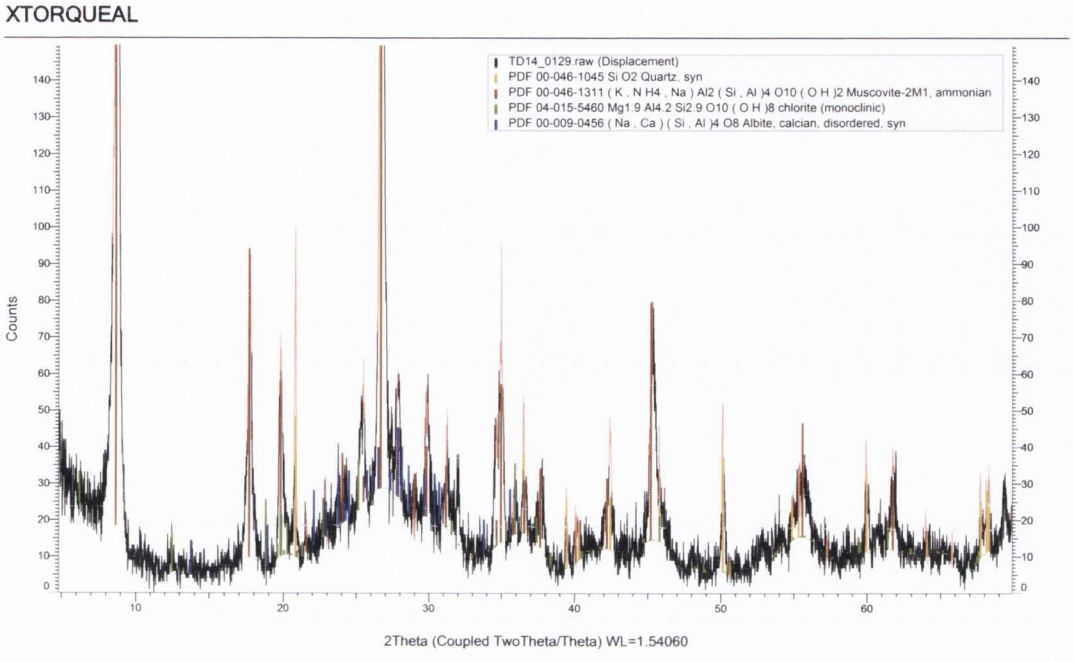

XRD Results Sample 12

a)

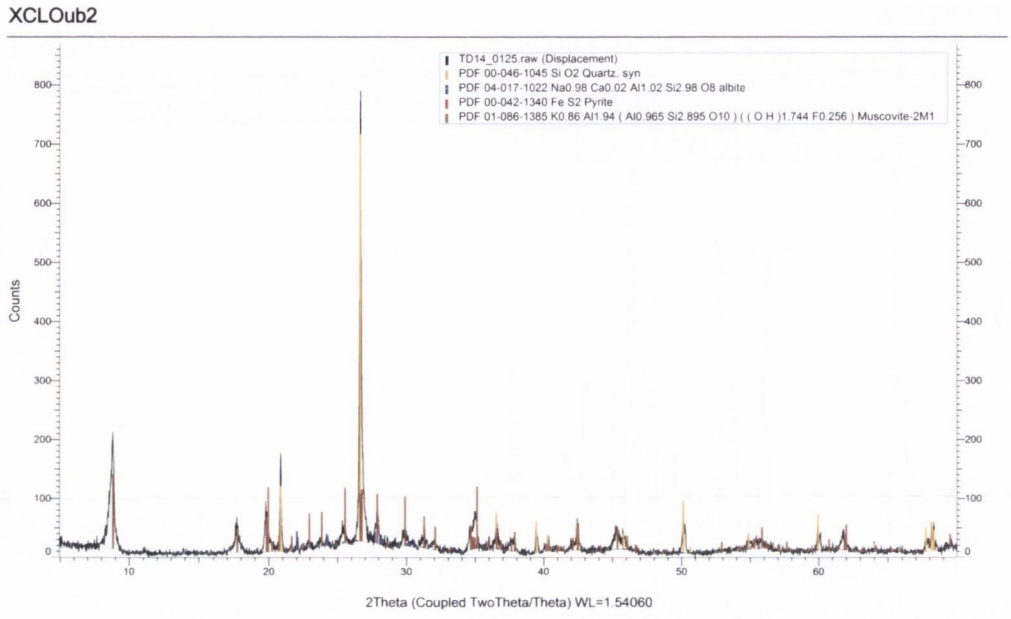
XCLOub2
TD14_0125.raw (Displacement)
PDF 00-046-1045 Si O2 Quartz, syn
PDF 04-017-1022 Na0.98 Ca0.02 Al1.02 Si2.98 O8 albite
PDF 00-042-1340 Fe S2 Pyrite
PDF 01-086-1385 K0.86 Al1.94 (Al0.965 Si2.895 O10) ((O H)1.744 F0.256) Muscovite-2M1
Counts
2Theta (Coupled TwoTheta/Theta) WL=1.54060

b)

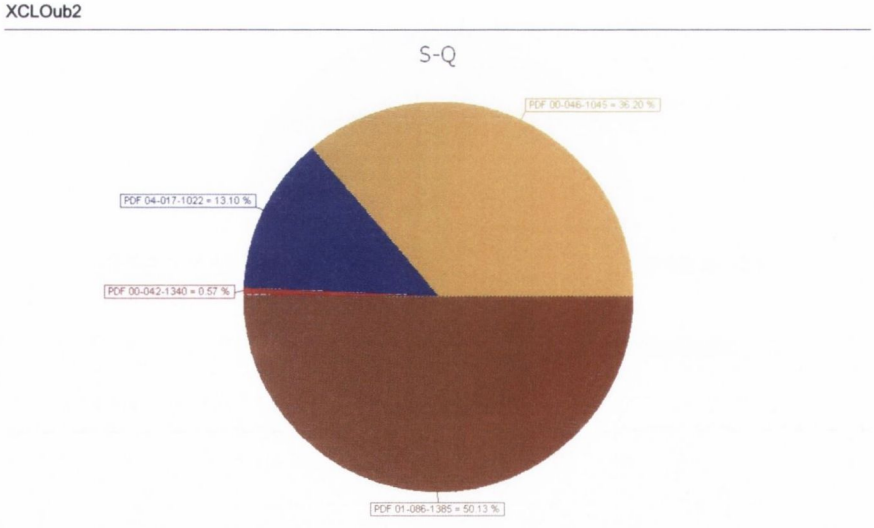
XCLOub2
S-Q
PDF 00-046-1045 = 36.20 %
PDF 04-017-1022 = 13.10 %
PDF 00-042-1340 = 0.57 %
PDF 01-086-1385 = 50.13 %

c)

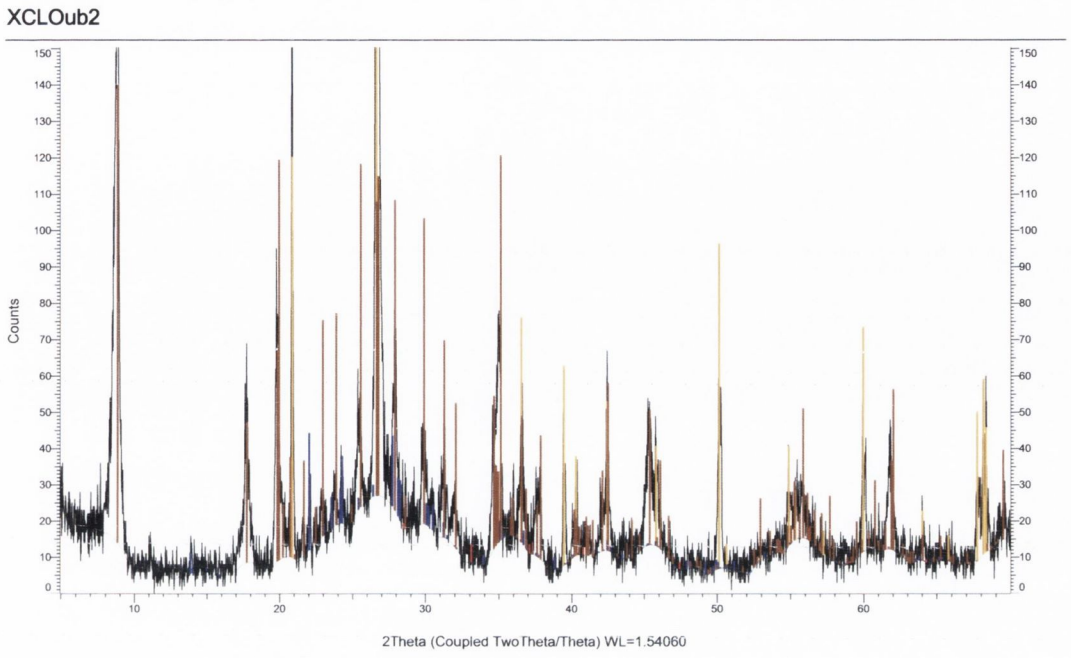

XRD Results Sample 13